DEVELOPMENT OF ACRYLIC NANOCOMPOSITES FOR OPTICAL APPLICATIONS

THESIS SUBMITTED TO THE
FACULTY OF TECHNOLOGY
UNIVERSITY OF DELHI
FOR THE AWARD OF THE DEGREE OF

DOCTOR OF PHILOSOPHY

BY

GUNJAN SURI

Under the supervision of

DR. R. K. KHANDAL & PROF. G. L. VERMA

DEPARTMENT OF APPLIED CHEMISTRY
DELHI COLLEGE OF ENGINEERING
UNIVERSITY OF DELHI
DELHI (INDIA)

CERTIFICATE OF SUPERVISORS

This is to certify that the thesis entitled **"*Development of acrylic nanocomposites for optical applications*"** submitted to the Faculty of Technology, Delhi College of Engineering, University of Delhi, Delhi, in fulfillment of the requirement for the award of the degree of Doctor of Philosophy in Applied Chemistry embodies the original research work carried out by Ms. Gunjan Suri under our supervision and that this work has not been submitted in part or full for any degree or diploma of this or any other University. It is further certified that the scholar has devoted more than two years, the minimum stipulated period, for the completion of this work.

DR. R. K. KHANDAL
(Supervisor)
Director
Shriram Institute for Industrial Research, 19, University Road, Delhi (India)

PROF. G. L. VERMA
(Supervisor)
Head
Department of Chemistry
Delhi College of Engineering, University of Delhi, Delhi (India)

Head of the Department
Applied Sciences
Delhi College of Engineering
University of Delhi, Delhi (India)

DECLARATION

This is to certify that the thesis entitled ***"Development of acrylic nanocomposites for optical applications"*** which is being submitted for the award of degree of Doctor of Philosophy in Applied Chemistry to the Delhi College of Engineering, University of Delhi, Delhi, is based on the experimental work carried out by me under the supervision of ***Dr. R. K. Khandal***, Director, Shriram Institute for Industrial Research, Delhi, India and ***Prof. G. L. Verma,*** Head, Department of Chemistry, Delhi College of Engineering, University of Delhi, Delhi, India. The results embodied in this thesis have not been submitted to any University or Institution for the award of any degree or diploma.

Place : Delhi **(Gunjan Suri)**

Date :

ACKNOWLEDGEMENTS

I take this opportunity to express a deep sense of gratitude to my esteemed supervisor, *Dr. R. K. Khandal,* Director, Shriram Institute for Industrial Research, (SRI), for his valuable guidance, profound expertise, inspiration, encouragement and motivation throughout the course of this work. He has played a very important role in motivating me for getting a higher degree. I will be always indebted to him for his kind and continued support behind successful completion of this work. He has been a very caring and motivating guide; no words are sufficient to thank him. His constant involvement in making every step perfect has enriched me at each and every stage. Without his unreserved guidance and supervision, this work could never have been completed.

I would like to express my sincere thanks and gratitude to my supervisor *Prof. G. L. Verma, Head, Department of Chemistry,* Delhi College of Engineering, University of Delhi, Delhi, for his valuable support, encouragement and guidance during the course of my work. I will always be thankful to him for providing valued supervision throughout my Ph. D. work.

I am highly thankful to *Prof. P. B. Sharma*, Vice-Chancellor, Delhi Technological University, for providing me the opportunity to pursue my Ph.D. I am also thankful to *Prof. Raj Senani*, Dean, Faculty of Technology, Delhi Technological University for his co-operation and support.

I am highly thankful to *Dr. U. K. Niyogi*, Joint Director (Material Science Division), SRI for his motivation and support.

I owe my special thanks to *Mrs. Sangita Khandal* for her continued support and motivation throughout this thesis work. I will always treasure her

love, care and encouragement provided to me. I am grateful to *Dr. Geetha Seshadri,* Sr. Scientist, SRI for providing me the technical guidance, moral courage and support during my work. She was always been there besides me in hour of need and her timely help would always be cherished by me. I express my heartfelt thanks to *Dr. Manjeet Aggarwal*, Sr. Asst. Director & Chief, SRI for her continued support and guidance throughout my thesis work.

I am thankful to the research scholars: *Dr. Mukti Tyagi, Mrs. Ruchi Aggarwal, Mrs. Pranshu Chhabra Kapoor, Mr. Neeraj Verma, Mr. Nilay Kanti Pramanik, Mr. Hemant Pal and Dr. Jay Pal Singh* of SRI, for their technical support and help. I also express my sincere thanks to all the staff members of Engineering Department, SRI and Shriram Applied Radiation Center (SARC) for helping me during the processing of the samples for my research work.

I am highly thankful to senior staff members of SRI with special mention of *Mr. V. Seth,* Deputy Director (EDP); for providing me with software facilities. *Dr. V. K. Verma,* Joint Director (EPD); *Dr. K. M. Chacko,* Joint Director (QAD); *Dr. P. K. Kaicker,* Joint Director (ASD); *Mr. P. Sharma,* Deputy Director (Coordination) *and Col. C. S. Ghosh,* Deputy Director (HR) for their moral support; *Dr. R. K. Diwan,* Sr. Asstt. Director & Chief*, Dr. A. K. Tyagi,* Asstt. Director & Chief, *Dr. R. S. Haldar,* Asstt. Director & Chief, *Dr. D. S. Mehra*, Scientist 'A' *and Ms. Meenu Talwar, Scientist 'C'* for their suggestions, Mr. Pushpendra, *Mr. Pushkar Singh, Mrs. Pooja Dalmia and Ms. Anju Upadhyay* for their kind help.

I am highly indebted to my esteemed institution, *Shriram Institute for Industrial Research* for providing me all the necessary facilities and permission for conducting the work.

I express deep gratitude to my parents, *Mrs. Saroj Suri* and *Mr. B. N. Suri,* who not only made me capable to achieve greater academic levels but also taught me the values of life. It is entirely because of their blessings that I have been able to complete this work. I would also like to express heartfelt gratitude to my sisters, *Mrs. Veneeta Arora and Mrs. Shefali M. Lamba* for their endless support, love and care*.*

Finally, my acknowledgements shall remain incomplete if I do not express sincere thanks to my uncle, *Dr. K. N. Sawhney, who* stood behind me in all my efforts and endeavors.

Gunjan Suri

ABSTRACT

Development of optical plastics happened solely because of the fact that the conventionally used materials i.e. glass has several drawbacks in spite of exhibiting the desired optical properties. A range of optical plastics with different characteristics have already been in the market for quite some time. When the issues like scratch resistance, mechanical strength, etc. go against the plastic materials, their optical properties plus their low density are the favorable parameters. At present, plastics have already become the preferred materials for several applications especially in the biomedical field. The users are able to use light weight optical lenses, thanks to the emergence of optical plastics.

The two major criteria i.e. refractive index and Abbe number are the ones based on which the optical plastics are evaluated for their suitability. Attempts have been made to maneuver the refractive index and Abbe number in a manner that materials of high Abbe number along with high refractive index can be designed. Of the materials being marketed so far, polythiourethanes are the best exhibiting a refractive index of 1.67. But the chemistry of polythiourethane does not allow the possibility of achieving a high Abbe number at the same time. On the other hand, there are optical plastics which show high Abbe number but they suffer from low refractive index.

To be able to develop new chemistries that meet with the requirements has been a difficult and time consuming task. The novel ways of producing low-weight optical plastics of high refractive index and at the same time optimum Abbe number are also being attempted. Methodologies like the hybrid materials involving organic matrix with the inorganic (dispersed) phase has been seen as the most prominent possibility to resolve such challenges.

This thesis is the research work on the very subject of incorporating the inorganic materials in an organic matrix to produce optical plastics materials of desired properties.

Taking cue from the experience of using metals of different types into glass to improve its optical and mechanical properties, the idea of incorporating same type of metals or metallic salts into monomers like acrylic acid has been pursued for the thesis work presented here.

An attempt has been made to transform a basic material like acrylic acid into a highly valuable optical plastic. Several metal salts (barium hydroxide, lanthanum oxide, titanium tetrachloride and organic titanates) have been incorporated in acrylic acid matrix to produce the optical plastics of desired properties. In order to achieve the mechanical as well as other related properties, certain monomers were also used along with the cross-linkers.

It has been a tough task especially in the case of incorporation of lanthanum and titanium in acrylic acid. The novelty of this work is the in-situ incorporation of these metals to produce optically clear materials having both Abbe number and refractive index within the desired limits. In fact the refractive index much higher than that of the most popular optical plastic i.e. polycarbonate has been achieved by using the methods described in this thesis. Use of co-monomers and cross-linkers were also found to be useful to produce optical plastics for ophthalmic applications.

The materials developed from this work were characterized and evaluated for the essential properties of an ophthalmic lens. The results are encouraging and they show the path forward for the optical industry to adopt the new kind of hybrid (nanocomposite) materials.

The thesis has been presented in 8 chapters. The brief about each chapter is given as follows:

Chapter 1: Chapter 1 is the Literature Survey which deals with the complete survey of literature about the research undertaken by various

national and international groups on developing nanocomposite materials for optical applications. State-of-the-art work pertaining to the incorporation of metals and metal salts (nanoscale) in organic polymer matrices has been thoroughly reviewed in this chapter. The development of materials for the use of optical industry has been the key focus highlighting the national and international status. The whole subject of literature survey is covered under the following headings:

a) Optical properties

b) Optical materials

c) Acrylate: their chemistry, structure and behavior

d) Acrylates for optical applications

e) Nanomaterials and nanocomposites

f) Challenges in making optical nanocomposites

g) Recent developments in metal-containing nanocomposites for optical applications

h) How metal-containing acrylate nanocomposites can be useful in resolving many of the existing drawbacks of the optical plastics

i) State-of-the-art and

j) Path forward

With the available knowledge so far, there are many gap areas which need to be covered and a lot more needs to be done. No doubt that plastics are considered as the most ideal materials for optical applications, and that the development of nanocomposites pave the way for meeting the challenges and growing demand of the present world, the technology is still far from the hands of a common user. With the potential of being one of the most promising technologies, nanotechnology is at a nascent stage and needs to be exploited further for optical applications

Chapter 2: Chapter 2 deals with the description of the materials used in the present thesis work. Use of various metal salts, dispersion matrices, co-

monomers and cross-linkers have been described in detail. Amongst the metal salts, barium hydroxide, titanium tetrachloride, organic titanates (tetraisopopyl titanate, triethanolamine titanate, titanium acetylacetonate, polybutyl titanate, tetrabutyl titanate and tetra 2-ethylhexyl titanate) and lanthanum oxide have been used to prepare metal-containing novel nanocomposites.

As dispersion matrices, acrylic acid and 2-hydroxyethylmethacrylate have been used for the dispersion of the above mentioned metal salts.

Cinnamic acid was added as a co-monomer to enhance the optical properties of metal acrylate compositions.

Styrene was used to achieve a cross-linked network structure of metal acrylate. Styrene has been used to impart hardness and clarity to the nanocomposites.

Chapter 3: Chapter 3 describes the methodology and various techniques adopted for the synthesis of metal-containing acrylic nanocomposites. Approaches followed for the preparation of barium-containing nanocomposites, titanium-containing nanocomposites and lanthanum-containing nanocomposites have been discussed in detail.

Salts of metals such as barium, titanium and lanthanum were dispersed in acrylate matrices using both in-situ and ex-situ approaches. It has been concluded during the discussion that in-situ synthesis and dispersion of nanoparticles of metal salts in the acrylate matrix is an ideal way to achieve clear and homogeneous metal-containing nanocomposites.

For the polymerization of metal-containing monomeric compositions, a gamma irradiation technology has been adopted and established as a novel and eco-friendly and processing techniques. Using this safe irradiation technology provides the advantage of eliminating the use of initiators during polymerization thus proving to be a cost effective and safe-to-use technology.

After polymerization, various instrumental state-of-the-art techniques have been used for the characterization of metal-containing nanocomposites. State-of-the-art instrumental techniques have been used for the analysis of basic parameters such as refractive index, Abbe number, transmittance (%), particle size etc to confirm the formation of nanocomposites.

Chapter 4: Chapter 4 pertains to the development of barium-containing nanocomposites based on acrylates and cinnamates for optical applications. Synthesis and dispersion of barium nanoparticles (in-situ) in acrylic matrix has been carried out in a novel and cost-effective manner. The chapter describes various approaches that have been followed to design barium acrylate nanocomposites for optical applications. It should be highlighted that the use of eco-friendly gamma irradiation technology leads to the formation of transparent and hard nanocomposites.

In the case of development of barium-containing nanocomposites, three approaches have been followed.

a) Preparation of barium acrylate nanocomposites by the dispersion of barium hydroxide in acrylic acid followed by its polymerization using styrene. The resulting nanocomposites were transparent and hard exhibiting high refractive index and Abbe number. They were also found to be better in terms of physico-mechanical properties when compared to conventionally available materials.

b) Preparation of barium cinnamate compositions by the dispersion of barium hydroxide in cinnamic acid. The compositions were characterised using different instrumental techniques. This was followed by polymerization using gamma irradiation.

c) Preparation of barium cinnamate-barium acrylate nanocomposites by the dispersion of barium cinnamate in barium acrylate. Varying amounts of barium cinnamate were dispersed in barium acrylate resulting in clear and uniform dispersions. This was followed by the

addition of styrene and polymerization by gamma irradiation. This resulted in transparent and high refractive index nanocomposites.

For the purpose of comparison of properties, cinnamic acid-acrylic acid polymer was prepared a standard reference material. Dispersion of varying amounts of cinnamic acid was carried out in acrylic acid followed by addition of styrene and polymerization using gamma irradiation.

Evaluation of the nanocomposites has been carried out with respect to key optical properties such as refractive index, Abbe number, transmittance, etc. Thermal stability and physico-mechanical properties has been studied and compared with the conventional optical plastic material. Overall, this chapter gives a description of developing high refractive index barium-containing nanocomposites for optical applications.

Chapter 5: Chapter 5 describes the preparation of titania acrylate nanocomposites using an inorganic salt of titanium. Titanium tetrachloride was used as a titanium precursor for dispersion in 2-hydroxyethyl methacrylate. The addition of titanium tetrachloride in 2-hydroxyethyl methacrylate led to the dispersion of nanoparticles of titania resulting from the hydrolysis of titanium tetrachloride. Titania acrylate compositions were studied for various parameters such as IR and UV-Visible spectroscopy, particle size, thermal stability, etc. Using the novel methodology of gamma irradiation, titania acrylate compositions were cast polymerized into lenses. The resulting nanocomposites were transparent, hard and exhibited high refractive index, higher than poly (2-hdroxyethyl methacrylate) as such. The physico-mechanical properties of titania acrylate nanocomposites were also improved.

It should be noted here that incorporation of titanium into polymer matrices for optical applications has been done for the first time. The nanocomposites exhibit better properties than the conventional optical plastic materials used so far. This paves the way for further exploitation of novel metal containing optical polymers.

Chapter 6: Chapter 6 details the development of novel titanium-containing nanocomposites using organic titanates. Acrylic acid has been used as the dispersion matrix and six different organic titanates have been used for the preparation of titanate acrylate compositions. Cinnamic acid as a co-monomer was added to improve the optical properties of the titanate acrylate compositions. Finally styrene was added as a cross-linker followed by polymerization through gamma irradiation. The nanocomposites obtained by the dispersion of titanates in acrylic acid and polymerization by gamma irradiation have been evaluated for key optical properties such as refractive index and Abbe number. Clear and transparent titanate acrylate nanocomposites were obtained having superior optical and physico-mechanical properties than the conventional optical polymers.

Chapter 7: Chapter 7 describes the development of lanthanum acrylate nanocomposites involving in-situ synthesis and dispersion of lanthanum oxide nanoparticles in acrylic acid. A novel methodology for the in-situ preparation and dispersion of nanoparticles in acrylic acid has been developed. Key optical properties such as refractive index and Abbe number have been improved. Use of cinnamic acid and styrene have helped to obtain transparent and clear high refractive index nanocomposites.

Chapter 8: In Chapter 8, conclusions of the present thesis work have been presented. The process technology for making lanthanum acrylate nanocomposites of varying refractive index by employing in-situ dispersion of nanoparticles of lanthanum has been developed. The technology developed for the preparation of lanthanum acrylate nanocomposites for making optical plastics of high refractive index is an indigenous, cost effective and novel technology with good potential for commercialization. The present work has great relevance for the growth of optical plastics industry in India as much as for the society looking for an indigenous product with an affordable cost. The outcome of this entire novel study has

been discussed and the path forward for several applications has been described.

The author has developed a novel technology for the incorporation of metals in acrylic acid and casting them into transparent and clear high refractive index lenses. Gamma irradiation has been used as a novel technique for cast polymerization of metal acrylate compositions. The work carried out by the author has resulted in two publications in international reputed journals, one chapter in an international reputed book and several awards at national and international platforms.

TABLE OF CONTENTS

S. No.	Contents	Page No.
	List of Tables	i-vii
	List of Figures	viii-xxii
	Abstract	xxiii-xxx
CHAPTER 1: LITERATURE REVIEW		**1-56**
1.0	INTRODUCTION	1
1.1	OPTICAL PROPERTIES	4
1.1.1	Refractive Index	4
1.1.2	Abbe Number	8
1.1.3	Transmittance	9
1.1.4	Reflectance	10
1.2	OPTICAL MATERIALS	12
1.3	ACRYLATES: THEIR CHEMISTRY, STRUCTURE & BEHAVIOUR	19
1.4	ACRYLATES FOR OPTICAL APPLICATIONS	22
1.5	NANOMATERIALS AND NANOCOMPOSITES	25
1.6	CHALLENGES IN MAKING OPTICAL NANOCOMPOSITES	31
1.7	RECENT DEVELOPMENTS IN METAL-CONTAINING NANO-COMPOSITES FOR OPTICAL APPLICATIONS	37
1.8	HOW METAL-CONTAINING ACRYLATE NANOCOMPOSITES CAN BE USEFUL FOR RESOLVING MANY OF THE DRAWBACKS OF THE EXISTING POLYMERS	47
1.9	STATE-OF-THE-ART	48
1.10	PATH FORWARD	55
CHAPTER 2: MATERIALS		**1-56**
2.0	INTRODUCTION	57
2.1	MATERIALS	57
2.1.1	Metal Salts	57
2.1.1.1	*Barium acrylate* nanocomposites	58
2.1.1.2	*Titania acrylate nanocomposites using inorganic titanium compounds*	59

S. No.	Contents	Page No.
	2.1.1.3 Titanate acrylate nanocomposites using organic compounds of titanium	59
	2.1.1.4 Lanthanum acrylate nanocomposites	61
	2.1.3 Carboxylic Acid	62
2.3	CONCLUSIONS	63
CHAPTER 3: TECHNIQUES ADOPTED		**64-89**
3.1	INTRODUCTION	64
3.2	METHODOLOGY ADOPTED	64
	3.1.1 Apparatus	64
	3.1.2 Dispersion of Metal Salts in Dispersing Media	64
	3.1.2.1 *Dispersion of Metal Salts*	64
	3.1.2.2 *Progress of the Reaction*	65
	3.1.3 Preparation of Cinnamic Acid Compositions	66
	3.1.3.1 *Dispersion* of cinnamic acid in metal acrylate compositions	66
	3.1.3.2 *Progress of the reaction*	66
	3.1.4 Cast Polymerization	66
	3.1.4.1 *Cast Polymerization*	66
3.2	SYNTHESIS OF METAL ACRYLATE COMPOSITIONS	68
	3.2.1 Synthesis of Barium Acrylate Nanocomposites	69
	3.2.1.1 *Preparation of barium acrylate nanocomposites*	69
	3.2.1.2 *Preparation of barium cinnamate nano-composites*	70
	3.2.1.3 *Preparation of barium cinnamate-barium acrylate-styrene nanocomposites*	70
	3.2.1.4 *Preparation of cinnamic acid-acrylic acid- styrene polymers*	72
	3.2.2 Synthesis of Titania Acrylate Nanocomposites	73
	3.2.2.1 *Ex- situ Synthesis and Dispersion of Nanoparticles of Titanium Dioxide into Acrylic acid to form Nanodispersed Titania Acrylate Compositions*	73

S. No.	Contents	Page No.
	3.2.2.2 *In-situ Synthesis and Dispersion of Nanoparticles of Titanium Dioxide into Acrylate Dispersion Media to form Titania Acrylate Nanocomposites*	76
	3.2.3 Synthesis of Titanate Acrylate Nanocomposites	77
	3.2.4 Synthesis of Lanthanum Acrylate Nanocomposites	78
3.3	CHARACTERIZATION AND EVALUATION OF ACRYLIC NANOCOMPOSITES	79
	3.3.1 Optical Properties	79
	3.3.1.1 Refractive index	79
	3.3.1.2 Abbe Number	80
	3.3.1.3 UV-Visible Spectroscopy	80
	3.3.2 Thermal Analysis	80
	3.3.2.1 Differential Scanning Calorimetry (DSC)	80
	3.3.2.2 Thermogravimetric Analysis (TGA)	81
	3.3.2.3 Vicat Softening Temperature	82
	3.3.3 Physico-mechanical Analysis	82
	3.3.3.1 Impact strength	82
	3.3.3.2 Scratch Resistance	82
	3.3.3.3 Shore–D hardness	83
	3.3.3.4 Machinability	83
	3.3.4 Minerological Study	83
	3.3.4.1 X-Ray Diffraction (XRD)	83
	3.3.5 Morphological study	84
	3.3.5.1 Scanning Electron Microscopy (SEM)	84
	3.3.5.2 Transmission Electron Microscopy (TEM)	85
	3.3.6 Spectroscopic Analysis	85
	3.3.6.1 Infra-red Spectroscopy	85
	3.3.7 Other properties	86
	3.3.7.1 Metal content	86
	3.3.7.2 Cross-link density	86
	3.3.7.3 Leachability	87
	3.3.7.4 Particle Size Analysis	87
	3.3.7.5 Acid value	87

S. No.	Contents	Page No.
CHAPTER 4: BARIUM–CONTAINING NANOCOMPOSITES BASED ON ACRYLATES & CINNAMATES		**90-158**
4.0	INTRODUCTION	
4.1	PREPARATION OF BARIUM ACRYLATE NANOCOMPOSITES	93
	4.1.1 Dispersion of Barium Hydroxide in Acrylic Acid	93
	4.1.2 Cast Polymerization of barium acrylate	93
4.2	PREPARATION OF BARIUM CINNAMATE NANOCOMPOSITES	93
	4.2.1 Dispersion of barium hydroxide in cinnamic acid	93
	4.2.2 Cast Polymerization of barium cinnamate	94
4.3	PREPARATION OF BARIUM CINNAMATE-BARIUM ACRYLATE NANOCOMPOSITES	94
	4.3.1 Synthesis of barium acrylate and barium cinnamate	94
	4.3.2 Dispersion of barium cinnamate in barium acrylate	94
	4.3.3 Cast polymerization of barium acrylate-barium cinnamate	95
4.4	PREPARATION OF CINNAMIC ACID-ACRYLIC ACID POLYMERS	95
	4.4.1 Dispersion of cinnamic acid in acrylic acid	95
	4.4.2 Cast Polymerization of cinnamic acid-acrylic acid compositions	95
RESULTS & DISCUSSION		95
4.5	CONCLUSIONS	152
CHAPTER 5: TITANIA ACRYLATE NANOCOMPOSITES USING INORGANIC TITANIUM COMPOUNDS		**159-190**
5.0	INTRODUCTION	159
5.1	SYNTHESIS OF NANODISPERSED TITANIA ACRYLATE COMPOSITIONS	163
5.2	CAST POLYMERIZATION OF NANODISPERSED TITANIA ACRYLATE COMPOSITIONS	163
RESULTS & DISCUSSION		164
5.3	CONCLUSIONS	189

S. No.	Contents	Page No.
CHAPTER 6: TITANATE ACRYLATE NANOCOMPOSITES USING ORGANIC TITANATES		**191-230**
6.0	INTRODUCTION	191
6.1	STEP I: DISPERSION OF ORGANIC TITANATES IN ACRYLIC ACID	192
6.2	STEP II: INCORPORATION OF CINNAMIC ACID AND STYRENE IN TITANATE-ACRYLIC ACID COMPOSITIONS	192
6.3	STEP III: CAST POLYMERIZATION OF TITANATE ACRYLATE-STYRENE COMPOSITIONS	193
RESULTS & DISCUSSION		193
6.4	CONCLUSIONS	227
CHAPTER 7: LANTHANUM ACRYLATE NANOCOMPOSITES		**231-263**
7.0	INTRODUCTION	231
7.1	STEP I: DISPERSION OF LANTHANUM OXIDE IN ACRYLIC ACID	232
7.2	STEP II: INCORPORATION OF CINNAMIC ACID AND STYRENE IN LANTHANUM ACRYLATE COMPOSITIONS	233
7.3	STEP III: CAST POLYMERIZATION OF LANTHANUM CONTAINING COMPOSITION-STYRENE	233
RESULTS & DISCUSSION		234
7.4	CONCLUSIONS	260
CHAPTER 8: CONCLUSIONS		**264-266**
REFERENCES		**267-306**
PUBLICATIONS		
AWARDS		
BIODATA OF THE STUDENT		

LIST OF TABLES

Table 1.1 : Classification of materials based on refractive index

Table 1.2 : Composition and optical properties of different types of optical glasses. The refractive index of the glass depends upon the nature and types of metal oxide dispersed in the glass matrix.

Table 1.3 : Evolution of polymers for optical applications

Table 1.4 : Optical properties of polymers and their uses in various optical devices

Table 1.5 : Different types of acrylate and methacrylate based polymers

Table 1.6 : Different classes of nanomaterials employing different materials. Their structure can be three, two or one dimensional

Table 2.1 : Properties of various metals used for the preparation of metal acrylate nanocomposites

Table 4.1 : Effect of addition of barium hydroxide on the refractive index of acrylic acid. The maximum amount of barium hydroxide that could be dispersed in acrylic acid is 16% which leads to 0.8 % increase in refractive index of acrylic acid. The increase in refractive index confirms the formation of barium hydroxide-acrylic acid composition by the reaction between acrylic acid and barium hydroxide.

Table 4.2 : Weight loss (%) due to thermal decomposition of barium hydroxide, acrylic acid and barium acrylate

Table 4.3 : Effect of addition of barium hydroxide on the acid value of acrylic acid. As the amount of barium hydroxide increases, the acid value decreases

Table 4.4 : Particle size analysis of barium acrylate compositions indicates that the dispersion of barium hydroxide takes place in the nanoscale dimension.

Table 4.5 : Results of effect of styrene on polymerization indicating that 150% (by weight of barium acrylate) of styrene is required for polymerization of barium acrylate. The nanocomposites obtained were hard and transparent which were easily released from the molds.

Table 4.6 : Effect of gamma irradiation on the polymerization of bariumacrylate-styrene composition. 20 kGy was found to be the optimum dose for barium acrylate-styrene nanocomposites.

Table 4.7 : Weight loss due to thermal decomposition of acrylic acid-styrene polymer and barium acrylate-styrene nanocomposite indicates higher thermal stability of barium acrylate-styrene nanocomposite due to formation of nanoparticles of barium

Table 4.8 : Addition of different amounts of barium hydroxide to cinnamic acid. Addition of upto 0.4 moles of barium hydroxide in 2 moles cinnamic acid led to the formation of homogeneous compound. Beyond 0.4 moles, phase separation takes place

Table 4.9 : Results of barium (% by weight) and barium oxide (% by weight) in barium cinnamate. As expected, the percentage content of barium increases with increase in the addition of barium hydroxide.

Table 4.10 : Weight loss (%) due to decomposition of barium hydroxide, cinnamic acid and barium cinnamate

Table 4.11 : Effect of dispersion of barium cinnamate on refractive index of barium acrylate. Refractive index increases with increase in the concentration of barium cinnamate in barium acrylate

Table 4.12 : Weight loss of barium cinnamate, barium acrylate and barium cinnamate-barium acrylate composition due to thermal decomposition

Table 4.13 : Effect of styrene on polymerization of barium cinnamate-barium acrylate compositions indicating that 150% (by weight of barium cinnamate-barium acrylate) of styrene is optimum amount required to obtain clear, transparent and hard nanocomposites which are easily released from the mold

Table 4.14 : Results of effect of gamma irradiation on the polymerization of barium cinnamate-barium acrylate nanocomposites. The styrene content for all the cases is kept at 150% (by weight of barium cinnamate-barium acrylate compositions)

Table 4.15 : Refractive index and Abbe number of barium-cinnamate-barium acrylate nanocomposites

Table 4.16 : Weight loss due to thermal decomposition of acrylic acid-styrene polymer and barium cinnamate-acrylate-styrene nanocomposite

Table 4.17 : Effect of dispersion of cinnamic acid on clarity and refractive index of acrylic acid. Cinnamic acid is soluble upto a concentration of 13% (by weight). Beyond 13%, cinnamic acid could not be dispersed in acrylic acid. Maximum refractive index achieved by the dispersion of cinnamic acid in acrylic acid is 1.448.

Table 4.18 : Acid value of cinnamic acid-acrylic acid compositions indicate that the acid value do not change significantly due to acidic character of both the components

Table 4.19 : Weight loss due to thermal decomposition of acrylic acid, cinnamic acid and cinnamic acid-acrylic acid composition

Table 4.20 : Effect of styrene on polymerization indicating that 150% of styrene (by weight of cinnamic acid-acrylic acid composition) is sufficient to obtain clear, transparent and hard polymers which are easily released from mold

Table 4.21 : Effect of gamma irradiation on the polymerization of cinnamic acid-acrylic acid polymers. 20 kGy was found to be the optimum dose for cinnamic acid-acrylic acid polymers

Table 4.22 : Refractive index and Abbe number of acrylic acid-cinnamic acid polymers show that the refractive index of acrylic acid increases as content of cinnamic acid is increased

Table 4.23 : Weight loss due to thermal decomposition of acrylic acid-styrene polymer and acrylic acid-cinnamic acid polymer

Table 4.24 : Properties of barium containing acrylic nanocomposites which show improved performance as compared to the conventionally available optical materials

Table 5.1 : Dispersion of nanoparticles of titanium dioxide in HEMA and acrylic acid

Table 5.2 : Preparation of fusion mixture with titanium dioxide

Table 5.3 : Effect of acid hydrolysis on the particle size. The pH was varied from 1.2-2.0. The size of the particles obtained was different at different pH

Table 5.4 : Effect of base hydrolysis on the particle size. The pH was varied from 10-13. The size of the particles obtained was different at different pH.

Table 5.5 : Dispersion of synthesized nanoparticles of titanium dioxide in acrylic acid. The nanoparticles settled down indicating that the density of the particles is very high

Table 5.6 : Observations related to dispersion of titanium tetrachloride in HEMA and acrylic acid

Table 5.7 : Determination of titanium content in nano dispersed titania acrylate compositions indicates that upto 4% titanium could be dispersed homogeneously in the matrix

Table 5.8 : Acid value of titania dispersed HEMA compositions indicates that acid value of HEMA increases with increase in content of titanium precursor due to its acidic character

Table 5.9 : Weight loss (%) due to thermal decomposition of HEMA and titania acrylate composition

Table 5.10 : Cross-link density results of titanium-containing nanocomposites

Table 5.11 : Effect of gamma irradiation on hardness of titania acrylate nanocomposites

Table 5.12 : Weight loss (%) at various temperatures due to thermal decomposition of pHEMA and titania acrylate nanocomposite

Table 5.13 : Water absorption studies of titania acrylate nanocomposites

Table 6.1 : Titania (%) content and refractive index of various titanates used for the preparation of titanate-acrylic acid compositions. Polybutyl titanate exhibits the highest refractive index due to the highest amount of titania present

Table 6.2 : Results of effect of addition of organic titanates on refractive index of acrylic acid. Maximum refractive index of 1.463 was achieved by the addition of 25% polybutyl titanate in acrylic acid

Table 6.3 : Results of effect of addition of titanates on acid value of acrylic acid. Acid value of acrylic acid decreases on the addition of titanate indicating that reaction between acrylic acid and titanate is taking place at the carboxylic acid group of acrylic acid

Table 6.4 : Determination of particle size distribution of titanate-acrylic acid compositions. Particle size of the compositions was found to be less than 0.8 nm indicating the formation of homogeneous solution of titanate-acrylic acid

Table 6.5 : Weight loss (%) due to thermal decomposition of acrylic acid, titanates and titanate-acrylic acid compositions. The results indicate that due to addition of titanate, the thermal stability of acrylic acid increases

Table 6.6 : Effect of cinnamic acid on refractive index of titanate acrylate compositions shows that highest refractive index achieved is 1.489 due to 14% incorporation of cinnamic acid to polybutyl titanate acrylate composition

Table 6.7 : Weight loss due to thermal decomposition of polybutyl titanate acrylate-cinnamic acid composition and triethanolamine titanate acrylate-cinnamic acid composition. The results indicate that the loss in weight at initial temperatures is more in the case of polybutyl titanate acrylate-cinnamic acid composition which becomes comparable to triethanolamine titanate acrylate-cinnamic acid composition at higher temperatures

Table 6.8 : Effect of styrene (% by weight of titanate acrylate-cinnamic acid composition) on polymerization of titanate acrylate-cinnamic acid compositions

Table 6.9 : Cross-link density results of titanate acrylate-styrene nanocomposites indicate that 90 kGy is the optimum dose required to result in hard polymers

Table 6.10 : Effect of gamma irradiation on titanate acrylate-styrene nanocomposites

Table 6.11 : Effect of gamma irradiation on titanate acrylate-cinnamic acid-styrene nanocomposites

Table 6.12 : Refractive index and Abbe number of titanate acrylate nanocomposites

Table 6.13 : Weight loss (%) due to thermal decomposition of acrylic acid-styrene polymer and titanate acrylate-cinnamic acid-styrene nanocomposites

Table 7.1 : Effect of dispersion of lanthanum oxide on transmittance of acrylic acid was observed from 200-800 nm. The results show that upto 20% lanthanum oxide can be dispersed into acrylic acid retaining optical clarity and transparency of the composition

Table 7.2 : Results of the dispersion of lanthanum oxide on refractive index of acrylic acid. Data indicate that the dispersion of 17% lanthanum oxide in acrylic acid increases the refractive index to 1.466 from 1.424 to begin with.

Table 7.3 : Results of dispersion of lanthanum oxide on acid value and pH of acrylic acid. Acid value decreases with increase in percentage of lanthanum oxide in acrylic acid. pH value increases to 2.21 in the case of 17% dispersion of lanthanum oxide as lanthanum gets reacted with acrylic acid. The change in the acid value and pH is due to the reaction between lanthanum oxide and acrylic acid

Table 7.4 : Determination of particle size distribution of lanthanum oxide-acrylic acid compositions. Particle size of the compositions was found to be less than 0.8 nm indicating the formation of homogeneous solution of lanthanum oxide-acrylic acid

Table 7.5 : Weight loss (%) due to thermal decomposition of acrylic acid, lanthanum oxide and lanthanum oxide-acrylic acid composition. The theoretical weight loss indicates that the lanthanum oxide-acrylic acid composition formed is thermally stable

Table 7.6 : Effect of addition of cinnamic acid on lanthanum acrylate composition indicates that upto 10% cinnamic acid can be dispersed in lanthanum acrylate resulting in transparent and clear compositions

Table 7.7 : Effect of cinnamic acid on refractive index of 17% lanthanum acrylate composition shows that maximum refractive index achieved is 1.478

Table 7.8 : Weight loss (%) due to thermal decomposition of acrylic acid, lanthanum oxide and lanthanum acrylate composition. Theoretical loss in weight of lanthanum acrylate-cinnamic acid composition is also presented.

Table 7.9 : Effect of styrene (% by weight of lanthanum acrylate-cinnamic acid) on polymerization of lanthanum acrylate-cinnamic acid compositions

Table 7.10 : Cross-link density results of lanthanum acrylate-cinnamic acid-styrene polymers indicate that 10 kGy is the optimum dose required for the polymerization

Table 7.11 : Weight loss (%) due to thermal decomposition of polyacrylate and lanthanum acrylate-cinnamic acid-styrene nanocomposite

LIST OF FIGURES

Figure 1.1 : Phenomenon of refraction of light when light moves from medium A to medium B. The light moving at speed V_A in the medium A when enters into the medium B, the speed of the light changes to V_B. At the same time, the direction of the movement of light also changes; the angle of incidence (i) in the case of medium A changes to an angle of refraction (r) in medium B. The change in its angle is always seen with respect to the perpendicular axis (normal) drawn on the interface of the media.

Figure 1.2 : Transmittance of a beam of light as it travels through a material of thickness‘t’

Figure 1.3 : Complete reflectance of light beam from the surface of a material. ‘i’ is the angle of incidence made by the incident light with the normal and ‘r’ is the angle of reflection made by the reflected light with the normal; example of any metal where incident light is reflected from its surface leading to opacity in the metal.

Figure 1.4 : Scattering of a beam of light after striking a material. Extent of light scattered is dependent on the crystal structure arrangement of a material. It also depends upon the overall thickness of the material.

Figures 1.5 : Structure of acrylic acid (1.5a) and acrylate (1.5b). Acrylic acid gets esterified with an alcohol to form alkyl acrylate.

Figure 1.6a) : Methacrylic acid formation due to substitution of α-H of acrylic acid by methyl group.

Figure 1.6b) : Methyl methacrylate formation due to the esterification reaction of methacrylic acid with methanol.

Figure 1.7 : Polymerization of methyl methacrylate to form polymethyl methacrylate (PMMA). Polymethyl methacrylate is an important polymer used for optical applications exhibiting excellent optical clarity.

Figure 1.8 : Structure of metal-containing acrylate polymer formed by bonding of metal atom to the carboxylic acid group of acrylic acid

Figures 1.9a-c : Change of specific area by miniaturization of a macro system (1.9a) to micro system (1.9b) to nano system (1.9c). The number of particles increases extraordinarily when the size of the particles is reduced while moving from macro to micro to nano scale. As a result, volume fraction ratio of particles of nano-based systems is the highest.

Figure 1.10 : Structure of metal-polymer nanocomposites where metal nanoparticles or metal oxide nanoparticles act as dispersion phase and polymer matrix such as polyacrylate matrix act as continuous phase. Homogeneous dispersion of nanoparticles in the matrix gives rise to nanocomposites. Example, dispersion of nanoparticles of titanium dioxide (TiO_2) into polymethyl methacrylate (PMMA) gives TiO_2-PMMA nanocomposite suitable for optical applications such as coatings, etc.

Figure 2.1 : (a) Structure of barium hydroxide octahydrate used to prepare barium containing nanocomposites and (b) Structure of cinnamic acid used as co-monomer to prepare barium containing nanocomposites

Figure 2.2 : Structure of titanium tetrachloride used to prepare titanium acrylate nanocomposites

Figure 2.3 : Structure of a) Titanium acetylacetonate b) Tetra 2-ethylhexyl titanate c) Tetraisopropyl titanate d) Tetrabutyl titanate e) Polybutyl titanate and f) Triethanolamine titanate. These organic precursors were used to prepare titanate acrylate nanocomposites

Figure 2.4 : Structure of lanthanum oxide used to prepare lanthanum acrylate nanocomposites

Figure 2.5 : Structure of a) Acrylic acid and b) 2-Hydroxyethyl methacrylate (HEMA) used as dispersion media for metal compounds for the preparation of metal containing nanocomposites

Figure 2.6 : Structure of cinnamic acid used to prepare metal containing nanocomposites

Figure 2.7 : Structure of styrene used as a co-monomer for polymerization

Figure 3.1 : Schematic diagram of reaction assembly showing a) Motorized overhead stirrer, b) Thermometer, c) Addition funnel, d) Three-necked round bottom flask, e) Platform and f) Stand

Figure 3.2 : Mold assembly with gasket and clamp

Figure 3.3 : Casting and filling unit of lenses including (a) Steel container (b) Nitrogen cylinder (c) Filter and (d) Rotator

Figure 3.4 : Methodology for the preparation and evaluation of barium acrylate nanocomposites. The methodology involved the dispersion of barium hydroxide in acrylic acid to form barium acrylate nanocomposites.

Figure 3.5 : Methodology for the preparation and evaluation of barium cinnamate nanocomposites

Figure 3.6 : Methodology for the preparation and evaluation of barium cinnamate-barium acrylate nanocomposites. The methodology involved two steps, first is the preparation of barium acrylate composition and simultaneously, preparation of barium cinnamate. The second step involves their mixing and addition of styrene followed by radiationpolymerization to form barium cinnamate-barium acrylate nanocomposite

Figure 3.7 : Methodology for the preparation and evaluation of cinnamic acid-acrylic acid- styrene polymer. The methodology involved the dispersion of cinnamic acid in acrylic acid to form cinnamic acid-acrylic acid- styrene polymer.

Figure 3.8 : Methodology for the preparation of nanodispersed titanium acrylate compositions. The methodology involved fusion of nanoparticles of titanium dioxide to bring them into solution form before dispersion in acrylic acid.

Figure 3.9 : Methodology for the preparation of nanodispersed titania acrylate compositions. The methodology involved acid hydrolysis of titanium isopropoxide resulting in the formation of nanoparticles of titanium dioxide.

Figure 3.10 : Methodology for the preparation of nanodispersed titania acrylate compositions. The methodology involved base hydrolysis of titanium isopropoxide resulting in the formation of nanoparticles of titanium dioxide

Figure 3.11 : Methodology for the preparation of titania acrylate nanocomposites. The methodology involved in-situ preparation and dispersion of nanoparticles of titanium dioxide in HEMA.

Figure 3.12 : Methodology for the preparation of titanate acrylate-cinnamic acid-styrene nanocomposites. The methodology involved dispersion of organic titanates in acrylic acid to yield titanate-containing nanocomposites.

Figure 3.13 : Methodology for the preparation and evaluation of lanthanum acrylate-cinnamic acid-styrene nanocomposites. The methodology involved single step dispersion and formation of nanoparticles of lanthanum oxide in acrylic acid to form lanthanum-containing nanocomposites.

Figure 3.14 : Abbe refractometer

Figure 3.15 : Schematic diagram of UV-Visible Spectrophotometer

Figure 3.16 : DSC instrument (DSC-2910) and sample chamber

Figure 3.17 : Thermogravimetric analyzer instrument (SDT-2960)

Figure 3.18 : Impact tester

Figure 3.19 : Shore-D Hardness Tester

Figure 3.20 : X-Ray Diffraction instrument

Figure 3.21 : Scanning Electron Microscope Instrument

Figure 3.22 : Transmission Electron Microscope

Figure 3.23 : Infra-red Spectrophotometer

Figure 3.24 : Inductively Coupled Plasma-Optical Emission Spectrometer (ICP-OES)

Figure 3.25 : Particle Size Analyzer

Figure 4.1 : TGA thermograms of barium hydroxide, acrylic acid and barium hydroxide-acrylic acid composition indicate increased thermal stability of acrylic acid due to incorporation of barium

Figure 4.2 : DTG thermograms of barium hydroxide, acrylic acid and barium hydroxide-acrylic acid indicate formation of new peaks

Figure 4.3 : DTA thermograms of barium hydroxide, acrylic acid and barium hydroxide-acrylic acid composition indicate completely different behaviour than acrylic acid and barium hydroxide forming a new compound (barium acrylate)

Figure 4.4 : Reaction between barium hydroxide and acrylic acid. 2 moles of acrylic acid react with 1 mole of barium hydroxide forming barium acrylate

Figure 4.5 (a-e) : UV-Visible spectra of acrylic acid and barium hydroxide-acrylic acid composition (varying concentrations). The λ_{max} value of acrylic acid does not change with the dispersion of barium hydroxide and hence it can be said that the reaction between barium hydroxide and acrylic acid is taking place at the carboxylic acid group of acrylic acid.

Figure 4.6 : IR analysis of acrylic acid, barium hydroxide and barium hydroxide-acrylic acid composition. Absence of band pertaining to carboxylic acid and presence of band pertaining to ester group confirms the formation of new compound as barium acrylate after the reaction between barium hydroxide and acrylic acid

Figure 4.7 : Barium acrylate nanocomposites a) without styrene and b) with styrene indicating that addition of styrene as co-monomer is essential for obtaining clear and transparent nanocomposites.

Figure 4.8 : Effect of barium hydroxide on refractive index of acrylic acid. The refractive index increases as the percentage of barium hydroxide is increased

Figure 4.9 : Effect of barium hydroxide on Abbe number of barium acrylate. No significant changes in Abbe number was observed as the percentage of barium hydroxide was increased. Abbe number lies in the well desired limit for optical applications

Figure 4.10 : TGA thermograms of polyacrylate and cast polymerized barium acrylate-styrene nanocomposite indicate stability due to addition of barium and formation of nanoparticles of barium

Figure 4.11 : DTG thermograms of acrylic acid-styrene polymer and barium acrylate-styrene nanocomposite indicate stability due to addition of barium and formation of nanoparticles of barium

Figure 4.12 : DTA thermograms of polyacrylate and barium acrylate-styrene nanocomposite indicate stability due to addition of barium and formation of nanoparticles of barium.

Figure 4.13 : XRD pattern of barium hydroxide, cinnamic acid and barium hydroxide-cinnamic acid. The peaks of barium hydroxide and cinnamic acid are absent in the case of higher amount of barium hydroxide indicating complete reaction between barium hydroxide and cinnamic acid

Figure 4.14 : IR analysis of cinnamic acid, barium hydroxide and barium cinnamate. Appearance of new band at 1538 cm^{-1} in the case of barium cinnamate confirm its formation

Figure 4.15 : Structure of barium cinnamate formed as a result of the reaction between cinnamic acid and barium hydroxide

Figure 4.16 : DSC thermograms of barium hydroxide, cinnamic acid and the reaction product barium cinnamate. The endothermic peaks in barium hydroxide are absent in barium cinnamate indicating the reaction to take place between the two starting materials. The endothermic peak due to cinnamic acid is absent in the case where higher content of barium hydroxide is incorporated, indicating the complete reaction of cinnamic acid with barium hydroxide to form barium cinnamate.

Figure 4.17 : TGA thermogram of barium hydroxide, cinnamic acid and barium cinnamate. The thermograms indicate higher stability of barium cinnamate as compared to cinnamic acid due to the presence of barium in it.

Figure 4.18 : DTA thermogram of barium hydroxide, cinnamic acid and barium cinnamate. The thermograms show new peaks in the case of product of reaction between barium hydroxide and cinnamic acid confirming the formation of new compound i.e. barium cinnamate

Figure 4.19 : DTG thermogram of barium hydroxide, cinnamic acid and barium cinnamate. The thermograms show new peaks in the case of barium cinnamate indicating the formation of new compound

Figure 4.20 : TGA thermograms of barium cinnamate, barium acrylate and barium cinnamate-barium acrylate composition. The thermograms show that the barium cinnamate-barium acrylate composition is stable at high temepratures

Figure 4.21 : DTA thermograms of barium cinnamate, barium acrylate and barium cinnamate-barium acrylate composition show that the peaks pertaining to barium cinnamate and barium acrylate are absent in the case of barium cinnamate-barium acrylate composition indicating the formation of new compound.

Figure 4.22 : DTG thermograms of barium cinnamate, barium acrylate and barium cinnamate-barium acrylate composition. Absence of some peaks of the starting materials indicate that there is a formation of new compound by the reaction of barium cinnamate and barium acrylate

Figure 4.23 (a-d): UV-Visible spectra of barium cinnamate-barium acrylate (varying concentrations). The λ_{max} value of vinyl group of barium acrylate does not change with the dispersion of barium cinnamate

Figure 4.24 : IR spectra barium cinnamate- barium acrylate compositions of varying percentages indicate the formation of homogeneous solution

Figure 4.25 : Appearance of barium cinnamate-barium acrylate nanocomposites a) without styrene and b) with styrene. In the absence of styrene, inhomogeneous and foamy polymers are formed while in the presence of styrene, transparent, clear and hard nanocomposites suitable for optical applications are obtained.

Figure 4.26 : TGA thermograms of polyacrylate and barium cinnamate-barium acrylate nanocomposite indicating higher thermal stability of barium containing nanocomposites as compared to polyacrylates as such

Figure 4.27 : DTA thermograms of barium cinnamate- barium acrylate nanocomposites indicate better thermal stability than polyacrylate

Figure 4.28 : DTG thermograms of acrylic acid-styrene polymer and barium cinnamate- barium acrylate nanocomposite indicating the formation of a new compound as evident from the absence of peaks in acrylic acid-styrene polymer

Figure 4.29 : Effect of cinnamic acid on refractive index of acrylic acid. Refractive index of acrylic acid increases as the amount of dispersion of cinnamic acid in acrylic acid is increased.

Figure 4.30 a-f): UV-Visible spectra of acrylic acid, cinnamic acid and cinnamic acid-acrylic acid compositions. Acrylic acid exhibits λ_{max} at 210 nm and cinnamic acid exhibits λ_{max} at 273 nm. In the case of cinnamic acid-acrylic acid compositions, 2 peaks are observed; at 210 nm (characteristic of acrylic acid) and 273 nm (characteristic of cinnamic acid). Presence of peaks indicates that vinyl group of acrylic acid and cinnamic acid is intact

Figure 4.31 : IR analysis of acrylic acid, cinnamic acid and cinnamic acid-acrylic acid composition

Figure 4.32 : TGA thermograms of acrylic acid, cinnamic acid & cinnamic acid-acrylic acid composition indicate lower thermal stability of the cinnamic acid-acrylic acid composition

Figure 4.33 : DTA thermograms of acrylic acid, cinnamic acid & cinnamic acid-acrylic acid composition shows absence of peaks in final composition and hence formation of new compound

Figure 4.34 : DTG thermograms of acrylic acid, cinnamic acid & cinnamic acid-acrylic acid composition. Thermogram indicates that new peaks are absent in the starting materials thereby indicating the formation of new compound.

Figure 4.35 : Cinnamic acid-acrylic acid polymer a) without styrene and b) with styrene indicating that the presence of styrene is essential to obtain polymers suitable for optical applications

Figure 4.36 : Effect of cinnamic acid on refractive index of cinnamic acid-acrylic acid-styrene polymer. Refractive index increases with the increasing content of cinnamic acid in the polymer

Figure 4.37 : Effect of cinnamic acid on Abbe number of cinnamic acid-acrylic acid-styrene polymer.

Figure 4.38 : TGA thermograms of cinnamic acid-acrylic acid-styrene polymer indicates higher thermal stability than the polyacrylate

Figure 4.39 : DTG thermograms of polyacrylate and cinnamic acid-acrylic acid polymer showing absence of peaks in the case of acrylic acid-cinnamic acid polymer thereby indicating the formation of a new compound

Figure 4.40 : DTA thermograms of polyacrylate and cinnamic acid-acrylic acid polymer shows the formation of a new compound

Figure 5.1 : Occurrence of titanium in its various forms, both natural and synthetic

Figure 5.2a) : XRD pattern of nanoparticles of titanium dioxide prepared via acidic hydrolysis shows the formation of crystalline titanium dioxide

Figure 5.2b) : XRD pattern of nanoparticles of titanium dioxide prepared via base hydrolysis shows the formation of crystalline titanium dioxide

Figure 5.3 : TEM analysis of prepared nanoparticles of titanium dioxide in a) acidic medium and b) basic medium

Figure 5.4 : TEM analysis of as such a) HEMA and b) nano dispersed titania composition in HEMA by hydrolysis of titanium tetrachloride indicating that the size of the nanoparticles is 8-14 nm

Figure 5.5 : IR spectra of HEMA and titanium tetrachloride dispersed in HEMA at various concentrations. The spectra of titania acrylate compositions is similar to HEMA indicating that no chemical reaction takes place between the two and hence, it is only the nanodispersion of titanium dioxide in HEMA resulting from the hydrolysis of HEMA.

Figure 5.6a) : TGA thermogram of HEMA and nanodispersed titania acrylate composition indicates higher stability of the latter due to the incorporation of titanium

Figure 5.6b) : DTA thermogram of HEMA and nanodispersed titania acrylate composition

Figure 5.6c) : DTG thermogram of HEMA and nanodispersed titania acrylate composition

Figure 5.7 (a-e) : UV-Visible spectra of HEMA and titania acrylate compositions. The results show no change in the spectra of HEMA indicating that the vinyl group in HEMA remains intact.

Figure 5.8 : Effect of gamma irradiation on the crosslink density of titania acrylate nanocomposites

Figure 5.9 : Refractive index titania acrylate nanocomposites increases with increase in titanium content

Figure 5.10 : Tailor–making of Abbe number has been achieved by varying the content of titanium in the matrix.

Figure 5.11 : FTIR analysis of acrylate polymer matrix (pHEMA) (before dispersion) and titania acrylate nanocomposite

Figure 5.12 : Specific gravity increases with increase in titanium content. As can be seen from the graph, the experimental values are lower than the theoretical values indicating that the titanium containing composites are lightweight which is an added advantage

Figure 5.13a) : TGA thermograms of pHEMA and titania acrylate nanocomposites indicates higher thermal stability of the nanocomposites due to titanium

Figure 5.13b) : DTA thermograms of pHEMA and titania acrylate nanocomposites shows absence of peaks in the case of titanium containing nanocomposite

Figure 5.13c) : DTG thermograms of pHEMA and titania acrylate nanocomposite shows shift of the peak towards right side of the thermogram indicating higher stability

Figure 5.14 : SEM images of a) Acrylate matrix (before dispersion) b) Acrylate matrix (after dispersion). The images confirm the presence of nanoparticles. Such homogeneous dispersion led to the formation of clear and transparent nanocomposites

Figure 5.15 : XRD analysis of (a) pHEMA and (b) titania acrylate nanocomposite indicates amorphous nature of the nanocomposite

Figure 6.1 : Structure of a) Titanium acetylacetonate b) Tetra 2-ethylhexyl titanate c) Tetraisopropyl titanate d) Tetrabutyl titanate e) Polybutyl titanate and f) Triethanolamine titanate. These organic precursors were used to prepare titanium- containing nanocomposites

Figure 6.2 : Results of effect of addition of titanates on refractive index of acrylic acid. With the addition of upto 20% titanates, the refractive index of acrylic acid increases gradually. The maximum refractive index for all titanates is obtained at 25% incorporation in acrylic acid except for tetra 2-ethylhexyl titanate where a maximum refractive index of 1.433 is obtained with 20% addition.

Figure 6.3a) : TGA thermograms of acrylic acid, polybutyl titanate, polybutyl titanate-acrylic acid composition, triethanolamine titanate and triethanolamine titanate-acrylic acid composition indicate that transitions are taking place when titanates are added to acrylic acid

Figure 6.3b) : DTA thermograms of acrylic acid, polybutyl titanate, polybutyl titanate-acrylic acid composition, triethanolamine titanate and triethanolamine titanate-acrylic acid composition

Figure 6.3c) : DTG thermograms of acrylic acid, polybutyl titanate, polybutyl titanate-acrylic acid composition, triethanolamine titanate and triethanolamine titanate-acrylic acid composition. Shift in the DTG peaks indicate that thermal transitions are taking place as an effect of reaction between acrylic acid and titanates

Figure 6.4 (a-e) : UV-Visible spectra of acrylic acid and polybutyl titante-acrylic acid composition (varying concentrations). The λ_{max} value of acrylic acid does not change with the dispersion of polybutyl titanate and hence it can be said that the vinyl group of acrylic acid remains intact.

Figure 6.5 (a-e) : UV-Visible spectra of acrylic acid and triethanolamine titante-acrylic acid composition (varying concentrations). The λ_{max} value of acrylic acid does not change with the dispersion of triethanolamine titanate and hence it can be said that that the vinyl group of acrylic acid remains intact

Figure 6.6 : Infrared spectra of a) acrylic acid, triethanolamine titanate and triethanolamine titanate-acrylic acid compositions and b) acrylic acid, polybutyl titanate and polybutyl titanate-acrylic acid compositions. The band at 1544-1550 cm^{-1} confirms the presence of COO^- group suggesting that new compounds (polybutyl titanate acrylate and triethanolamine titanate acrylate) have been formed by the reaction between acrylic acid and titanates

Figure 6.7 : Effect of dispersion of cinnamic acid on refractive index of titanate acrylate compositions. The increase in refractive index is more in the case of polybutyl titanate acrylate composition

Figure 6.8 a) : TGA thermogram of triethanolamine titanate acrylate-cinnamic acid composition shows higher stability than polybutyl titanate acrylate-cinnamic acid composition

Figure 6.8b) : DTA thermogram of polybutyl titanate acrylate-cinnamic acid composition and triethanolamine titanate acrylate-cinnamic acid composition

Figure 6.8c) : DTG thermogram of polybutyl titanate acrylate-cinnamic acid composition and triethanolamine titanate acrylate-cinnamic acid composition

Figure 6.9 (a-d) : UV-Visible spectra of cinnamic acid and polybutyl titanate acrylate-cinnamic acid compositions. Cinnamic acid exhibits λ_{max} at 273 nm. In the case of polybutyl titanate acrylate-cinnamic acid compositions, 2 peaks are observed; at 210 nm (characteristic of acrylic acid) and 273 nm (characteristic of cinnamic acid). Presence of peak at λ_{max} : 273 nm indicates that vinyl group of the cinnamic acid is intact

Figure 6.10 (a-d): UV-Visible spectra of cinnamic acid and triethanolamine titanate acrylate-cinnamic acid compositions. Cinnamic acid exhibits λ_{max} at 273 nm. In the case of triethanolamine titanate acrylate-cinnamic acid compositions, 2 peaks are observed; at 210 nm (characteristic of acrylic acid) and 273 nm (characteristic of cinnamic acid). Presence of peak at λ_{max} : 273 nm indicates that vinyl group of the cinnamic acid is intact.

Figure 6.11a: Infrared spectra of polybutyl titanate acrylate-cinnamic acid compositions. The band pertaining to C=O stretch in -C=C-COOH at 1683 cm^{-1} is present in the spectra of cinnamic acid. In the case of titanate acrylate-cinnamic acid compositions, band at 1683 cm^{-1} has shifted towards the higher frequency

Figure 6.11b: Infrared spectra of polybutyl titanate acrylate-cinnamic acid compositions and b) triethanolamine titanate acrylate-cinnamic acid compositions. The band pertaining to C=O stretch in -C=C-COOH at 1683 cm^{-1} is present in the spectra of cinnamic acid. In the case of titanate acrylate-cinnamic acid compositions, band at 1683 cm^{-1} has shifted towards the higher frequency

Figure 6.12 : Results of effect of titanates on refractive index of acrylate-styrene nanocomposites (without cinnamic acid and with cinnamic acid). Refractive index is almost comparable for both the nanocomposites in both cases

Figure 6.13 : Effect of titanium on Abbe number of titanate acrylate nanocomposites a) without cinnamic acid and b) with cinnamic acid. Abbe number is higher in the case of polybutyl titanate acrylate-styrene nanocomposites

Figure 6.14a) : TGA thermograms of polybutyl titanate-acrylate-cinnamic acid-styrene nanocomposites, triethanolamine titanate acrylate-cinnamic acid-styrene nanocomposites indicating higher thermal stability than Acrylic acid-styrene polymer due to incorporation of titanium

Figure 6.14b) : DTA thermograms of polybutyl titanate-acrylate nanocomposites, triethanolamine titanate acrylate nanocomposites and acrylic acid-styrene polymer

Figure 6.14c) : DTG thermograms of polybutyl titanate-acrylate nanocomposites, triethanolamine titanate acrylate nanocomposites and acrylic acid-styrene polymer

Figure 6.15 a): SEM picture of acrylic acid-styrene polymer and b) SEM picture of polybutyl titanate acrylate-styrene nanocomposite indicates change in surface morphology on addition of titanate

Figure 7.1 : Effect of dispersion of lanthanum oxide on refractive index of acrylic acid. The value of refractive index increases with the increase in percentage of lanthanum oxide in acrylic acid. Beyond 15% of lanthanum oxide, the change is not significant.

Figure 7.2 a) : TGA thermograms of acrylic acid, lanthanum oxide and the composition of lanthanum oxide-acrylic acid. Results indicate higher thermal stability of the lanthanum containing composition than acrylic acid.

Figure 7.2 b) : DTA thermograms of acrylic acid, lanthanum oxide and the composition of lanthanum oxide-acrylic acid. Results indicate that the thermal transitions are taking place due to the addition of lanthanum oxide to acrylic acid

Figure 7.2 c) : DTG thermograms of acrylic acid, lanthanum oxide and the composition of lanthanum oxide-acrylic acid. Results indicate that new compound is being formed due to the interactions between acrylic acid and lanthanum oxide

Figure 7.3 (a-e) : UV-Visible spectra of acrylic acid and lanthanum oxide-acrylic acid composition (varying concentrations). The λ_{max} value of acrylic acid does not change with the dispersion of lanthanum oxide and hence it can be said that the reaction between lanthanum oxide and acrylic acid is taking place at the carboxylic acid group of acrylic acid.

Figure 7.4 : Infrared spectra of acrylic acid and lanthanum oxide-acrylic acid composition. The band at 1544-1550 cm^{-1} confirms the presence of COO^- group suggesting that a new compound (lanthanum acrylate) has been formed by the reaction between acrylic acid and lanthanum oxide.

Figure 7.5 : Effect of 10% cinnamic acid on refractive index of lanthanum acrylate compositions. The refractive index increase from 1.468 to 1.478 by the incorporation of 10% cinnamic acid in 17% lanthanum acrylate composition

Figure 7.6 a) : TGA thermograms of lanthanum acrylate and lanthanum acrylate-cinnamic acid composition indicate low thermal stability of lanthanum acrylate-cinnamic acid composition as compared to lanthanum acrylate as such

Figure 7.6 b) : DTA thermograms of lanthanum acrylate and lanthanum acrylate-cinnamic acid composition

Figure 7.6c) : DTG thermograms of lanthanum acrylate and lanthanum acrylate- cinnamic acid composition show the presence of new peaks indicating chemical interactions are taking place between lanthanum acrylate and cinnamic acid.

Figure 7.7 (a-f): UV-Visible spectra of cinnamic acid and lanthanum acrylate-cinnamic acid compositions. Cinnamic acid exhibits λ_{max} at 273 nm. In the case of lanthanum acrylate-cinnamic acid compositions, 2 peaks are observed; at 210 nm (characteristic of acrylic acid) and 273 nm (characteristic of cinnamic acid). Presence of peak at λ_{max} : 273 nm indicates that vinyl group of the cinnamic acid is intact.

Figure 7.8 : Infrared spectra of lanthanum acrylate-cinnamic acid compositions. The band pertaining to C=O stretch in -C=C-COOH at 1683 cm^{-1} is present in the spectra of cinnamic acid. In the case of lanthanum acrylate-cinnamic acid compositions, band at 1683 cm^{-1} has shifted towards higher frequency.

Figure 7.9 : Effect of lanthanum oxide on refractive index of lanthanum acrylate-cinnamic acid-styrene nanocomposites. Refractive index increases with the increase in amount of lanthanum oxide in the nanocomposite. The refractive index increases to 1.58 from 1.50 (acrylic acid-styrene polymer) to start with.

Figure 7.10 : Effect of lanthanum oxide on Abbe number of lanthanum acrylate-cinnamic acid-styrene nanocomposites. Abbe number increases with increase in the amount of lanthanum oxide in the nanocomposite

Figure 7.11a) : TGA thermograms of lanthanum acrylate-cinnamic acid-styrene nanocomposite indicates higher thermal stability than acrylic acid-styrene polymer due to the formation of cross-linked matrix due to the presence of lanthanum

Figure 7.11b) : DTA thermograms of acrylic acid-styrene polymer and lanthanum acrylate-cinnamic acid-styrene nanocomposites. The acrylic acid-styrene polymer shows an exotherm at 520 ºC which is not present in the case of lanthanum-containing polymer.

Figure 7.11c) : DTG thermograms of lanthanum acrylate-cinnamic acid-styrene nanocomposite shows presence of new peaks due to the formation of new cross-links as compared to acrylic acid-styrene polymer

Chapter 1
Literature Survey

CHAPTER 1
LITERATURE SURVEY

1.0 INTRODUCTION

Optical applications, as the term suggests, means all those applications where the laws and rules of optics are exploited for a given purpose. It encompasses all those devices used for the purpose as also all the materials employed to fabricate those devices. In order to develop a particular device, taking advantage of the principles of optics, it is essential therefore, to first understand the basic requirements for which the device is to be designed. Once that is done, the next most important step involves the development of the materials (also referred as optical materials) for the purpose. This is completely in line with the adage that for success of a novel device, it is utmost imminent to design an innovative material full of novelty. In other words, unless there are materials available to deliver the desired performance, the new devices cannot be introduced. This is an evolutionary exercise where one event follows the other in a continuous manner. By the time a new device is introduced, it runs the risk of getting obsolete within a short period because of the pace at which science and technology has been improving with time. Thus, the need for novel materials with improved properties is always in existence. In the area of optical applications, it is perhaps more challenging because many of the devices are also being used for biomedical applications. For biomedical applications, especially for implants, the choice of materials that can be chosen for the purpose is quite limited and hence, the challenge for the material scientists is even tougher.

The optical devices take advantage of basic optical phenomena such as reflection, refraction, transmission, dispersion, etc. Depending upon the applications, the devices are designed to cover the possible ranges of each parameter. Accordingly, the optical materials are to be designed. The basic properties to be maneuvered while designing optical materials can be listed as: (i) refractive index, (ii) transmission, (iii) dispersion (Abbe number),

(iv) reflection and (iv) haze. It must be noted that the most basic criteria for selection of optical materials are its clarity and refractive index.

After this, the other properties are checked to ascertain the suitability of materials. Of course, the preference is given to low density materials. For implants, the bio-compatibility of materials becomes the most essential criteria.

Designing optical materials has been quite evolutionary. To begin with, glass was the material which served almost all purposes. As understanding of optics became clear with time, the requirements of new materials were met by the development of a variety of glass materials. Several types of innovative approaches became a reality and as a result, glass materials with unique features came into existence. One such example which can be used to explain this aspect relates to the incorporation of various types of metals into glass matrix. Not only did it provide glass materials of varying optical properties, it also enabled to produce optical materials with varying tintability. While such developments leading to the emergence of different type of devices, example given telescopes, on the one hand and spectacle lenses on the other hand became a reality, all along there has always been a need to come up with alternative materials. Glass being inorganic, amorphous and a hard material, always posed the problem when it came to density and other physico-mechanical properties of the material. The goal has always been to design materials that are amorphous with desired optical behavior on the one hand and strong physico-mechanical characteristics with low inherent density on the other hand. To meet this requirement, several attempts were made to design polymeric materials to replace glass which resulted in the introduction of optical plastics for this purpose.

Optical plastics are the materials, as the name suggests, which possess the optical behaviour making them suitable for optical applications plus they are plastic in nature, so that they can be cast or molded. To begin with, homopolymers based on different monomers were developed following which

co-polymers came into existence. Every time high refractive index, high Abbe number and high transmittance were targeted and different types of monomers were tried to design the desired optical materials. Today there exist the materials of following features:

i. High refractive index, low Abbe number for materials such as polythiourethanes, polycarbonates, etc and

ii. Low refractive index, high Abbe number for materials such as diethylene glycol bis allyl carbonate (CR-39), etc

The latest developments suggest that composite materials can solve many of the problems faced by the optical industry. One of the newly emerging type of materials are based on nanocomposites. The term nanocomposite describes a two-phase material; here one of the phases has at least one dimension in the nanometer range. The most widely studied nanocomposite system pertains to the one based on polymers as the base materials.

The present chapter deals with a complete survey of literature on the subject of nanocomposite materials for optical applications. It aims to bring out the development on different aspects of nanocomposite materials for optical applications as available in the literature. Based on this literature survey, an attempt has been made to list out the gap areas while describing the developments leading to the emergence of novel materials. In other words, this literature survey highlights the state-of-the-art in the subject field of nanocomposites for optical applications. The whole subject of literature survey is covered here with the following outline:

1.1 Optical properties

1.2 Optical materials

1.3 Acrylates; their chemistry, structure and behaviour

1.4 Acrylates for optical applications

1.5 Nanomaterials and Nanocomposites

1.6 Challenges in making optical nanocomposites

1.7 Recent developments in metal-containing nanocomposites for optical applications

1.8 How metal-containing acrylate nanocomposites can be useful in resolving many of the existing drawbacks of the optical plastics

1.9 State-of-the-art and

1.10 Path forward

1.1 OPTICAL PROPERTIES

One of the most studied natural phenomena by mankind pertains to light or optics. The behavior of the material towards light decides the suitability of that particular material for optical applications. The ability of the material to reflect, refract and transmit light in all directions is important for optical applications. There are five main optical properties namely (i) Refractive index, (ii) Abbe number, (iii) Transmittance (iv) Reflectance and (v) Haze, which are essential for the materials to be used for optical applications. Let us discuss each of these properties one-by-one.

1.1.1 Refractive Index

It is a fact that the speed of light is constant in a given medium but it varies depending upon the nature of medium through which it passes. Light travels more slowly through air than it does through vacuum or empty space, more slowly through water than air, slower still through quartz and slowest through materials like diamond. As soon as the light crosses the interface between two different media, it get refracted. The path of light changes when it enters into a different medium. The phenomenon of refraction is dependent upon the nature and type of medium through which the light is to pass.

In order to understand the behavior of light through different media, a parameter called refractive index is used. The refractive index is a measure of

how much light is bent or refracted as it passes through a substance from air. It is defined **[1]** by Equation 1 (Snell's equation) given below:

$$n = \frac{\sin i}{\sin r} \qquad \text{(Equation 1)}$$

where "n" is the refractive index; "i" and "r" are the angles of incidence and refraction respectively as can be seen in Figure 1.1.

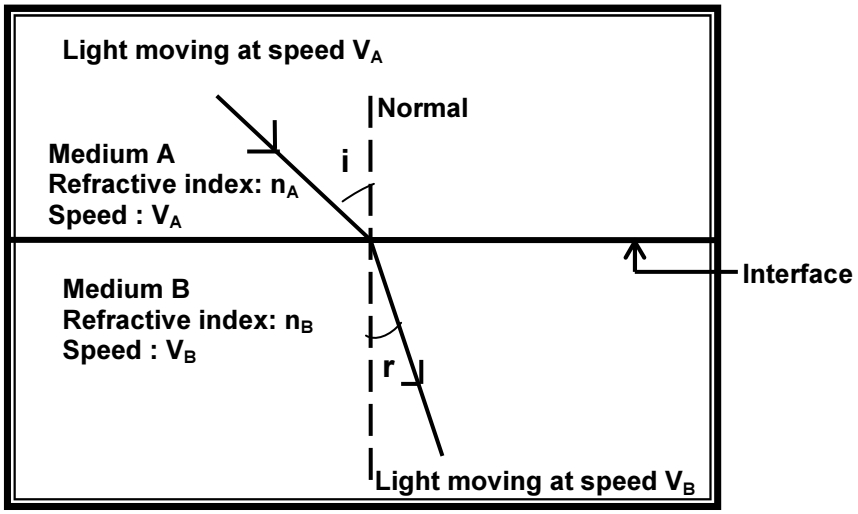

Figure 1.1: Phenomenon of refraction of light when light moves from medium A to medium B. The light moving at speed V_A in the medium A when enters into the medium B, the speed of the light changes to V_B. At the same time, the direction of the movement of light also changes; the angle of incidence (i) in the case of medium A changes to an angle of refraction (r) in medium B. The change in its angle is always seen with respect to the perpendicular axis (normal) drawn on the interface of the media.

The most important property of an optical material is the refractive index and its dispersion behavior. If light enters a non-absorbing homogeneous material, reflection and refraction occur at the boundary surface. When the light travels through the material, it changes its path with a different speed and this phenomenon is called refraction. Practically speaking, the refractive index is a

measure of the deflection occurring at the boundary surface due to the refraction of light beam. Refraction phenomenon as shown in Figure 1.1 can be attributed to the fact that the composition and structure of the two materials being different from each other would affect the velocity of light passing through them. Hence, the refractive index of a material becomes significant while selecting the material for optical applications.

The refractive index is also defined as the ratio of the velocity of light in vacuum to the velocity of light in any medium **[2]**. It may be noted that the presence of atoms in a matter serve as obstacles and would slow down the speed of light. Hence, the value of refractive index is always greater than 1 as velocity of light while travelling through matter would always be less than that in vacuum. By the way, the index of refraction varies with wavelength of light. As the light passes through different media, its frequency remains constant and wavelength changes. This change of wavelength causes speed of light to change at the interface between two mediums and cause light to refract. Thus, refractive index decreases as wavelength increases and the rate of decrease is less in the case of longer wavelengths. This rate of change of refractive index with wavelength is called dispersion and is defined by Equation 2 **[3]**.

$$\mathbf{D} = \frac{\Delta \mathbf{n}}{\Delta \lambda} \qquad \text{(Equation 2)}$$

where, n : refractive index of a material at wavelength λ . The refractive index is used to calculate the dispersive power, D.P. of a prism given in Equation 3..

$$\mathbf{D.\ P} = \frac{\mathbf{n_F - n_C}}{\mathbf{n_D - 1}} \qquad \text{(Equation 3)}$$

$\mathbf{n_D}$: Refractive index of the material at λ_d = 587.56 nm; d=587.56nm (Sodium)

$\mathbf{n_F}$: Refractive index of the material at λ_f = 486.13 nm; f= 486.13 nm (Helium)

$\mathbf{n_C}$: Refractive index of the material at λ_c = 656.27 nm; c= 656.27 nm (Mercury)

Refractive index can be used to design devices. High refractive index materials can yield thinner lenses with the same focal distance as that of low refractive index materials. Refractive index is generally estimated in terms of molar refraction R which quantifies the intrinsic refractive power of the structural units constituting the materials and is represented as Equation 4.

$$n = \sqrt{\frac{V + 2R_{LL}}{V - R_{LL}}} \qquad \text{(Equation 4)}$$

Where, n is refractive index, V is molar volume and R_{LL} is molar refraction of the structural units. For two materials having identical molar volume (V), the one with a higher intrinsic molar refraction will have higher refractive index value than the other **[4-5]**.

The value of refractive index increases with the amount of material per unit volume. As discussed earlier, the atoms act as obstacles to a beam of light passing through a material. If two materials have identical molar refraction (R), then the material with smaller molar volume (V) will represent a larger number of obstacles and will therefore have a larger value of refractive index (n).

Refractivity is determined by the polarizabilities of the combined groups in a molecule. For obtaining a high refractive index, element should have a high mean polarizability and low molar volume. It is well known that the refractive index of a material depends on the polarizability of its constituents; movements of electron cloud of the atoms forming the constituents **[6-17]**. Based on the molar refraction and molar dispersion, sulfur and oxygen containing optical materials have high refractive index values **[18-19]**.

Based on refractive index, existing materials suitable for optical applications are generally classified as low, mid and high refractive index **[20-23]**. Some of the materials used for optical applications are shown in Table-1.1.

Table 1.1: Classification of materials based on refractive index

Grades	Range of refractive index	Materials (refractive index)
Low refractive index	1.3-1.5	• Sodium-Calcium Glass (1.50) • Polymethyl methacrylate (1.49) • Dimethyl siloxane (1.41) • Dimethyl diphenyl siloxane (1.43) • Poly (2-hydroxyethyl methacrylate) (1.45)
Mid refractive index	1.5 - 1.6	• Polyacrylates (1.56) • Polycarbonates (1.58) • Borosilicate glass (1.60)
High refractive index	>1.6	• Polythiourethane(1.66 - 1.68) • Polynaphthalene (1.68) • Polyether ketone(1.65) • Polyvinyl carbazole (1.68) • Titanium-Lanthanum glass (1.70) • Lanthanum-Niobium glass (1.80)

1.1.2 Abbe Number

The variation of refractive index with the wavelength of light causes the phenomenon of chromatic dispersion of white light upon refraction. To characterize the dispersive power of the material, a quantity called Abbe number is used with the formula as given in Equation 5 **[24-25]**:

$$\nu_d = \frac{n_d - 1}{n_f - n_c} \qquad \text{(Equation 5)}$$

$\mathbf{n_d}$: Refractive index of the material at λ_d = 587.56 nm; d=587.56nm (Sodium)

$\mathbf{n_f}$: Refractive index of the material at λ_f = 486.13 nm; f= 486.13 nm (Helium)

$\mathbf{n_c}$: Refractive index of the material at λ_c = 656.27 nm; c= 656.27 nm (Mercury)

Abbe number which is a key property for refractive index dispersion is also an important parameter for optical materials used. The larger Abbe number

corresponds to a lower dispersion in the refractive index **[26]**. Highly refractive materials generally exhibit a small Abbe number **[27]**. The Abbe number is inversely proportional to chromatic dispersion of the material. The Abbe number varies between 60 for the materials with least chromatic dispersion and 20 for the materials with the highest chromatic dispersion **[28].** The Abbe number is important in certain specialized applications such as the design of achromatic lenses, which are required to focus a range of wavelengths to the same spot.

1.1.3 Transmittance

Materials having the ability to let the light pass through completely are termed transparent materials; those which absorb a part of the light and let the remaining light pass through are termed translucent and materials which absorb all the light without letting it pass through are termed opaque **[29-31]**.

As a beam of light falls on a material, it interacts with the molecules of the material and passes out (Figure 1.2). The intensity with which a beam of light is incident on a material may change after interaction with the matter. Transmittance is defined as the ratio of intensity of light coming out from a material to the intensity of light falling on it (Equation 6). It depends upon the optical homogeneity of the polymer both in bulk and at the surface. Transmittance of a material is sometimes given as a percentage value.

$$T = \frac{I}{I_o} \qquad \text{(Equation 6)}$$

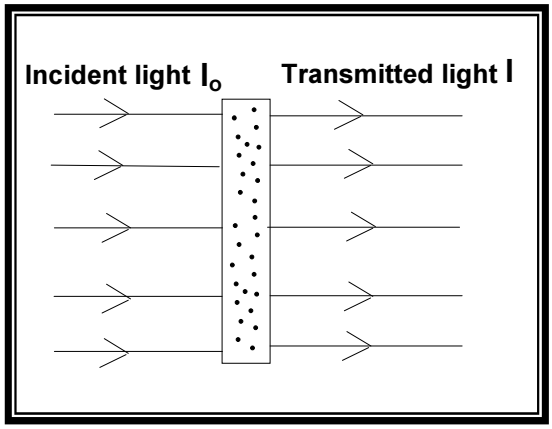

Figure 1.2: Transmittance of a beam of light as it travels through a material of thickness‘t’

As a general rule, a material with 85% transmission of light is considered as transparent. The transparency is also termed as optical clarity and is dependent on the thickness of the sample used for assessment; it decreases with increase in thickness. Maximum transmittance is achieved by minimizing the size of the scattering centers.

1.1.4 Reflectance

When the incident light on the surface of the material returns back after hitting the surface, the phenomenon is called as reflection. Reflectance is the ability of the sample to reflect light. It is defined as the ratio of intensity of reflected light (I_r) to incident light (I) as can be presented as Equation 7.

$$R = \frac{I_r}{I} \qquad \text{(Equation 7)}$$

Unlike transmission, reflectance does not change with the thickness of the material. At the same time as refraction, the phenomenon of reflection of light also occurs at the surface of optical materials (Figure 1.3).

Reflectance leads to reduced transparency due to undesirable reflections from the lens surface because of the reduction in the intensity of light that enters the lens. This unwanted reflection can be completely eliminated by applying an efficient anti-reflection coating **[32]**.

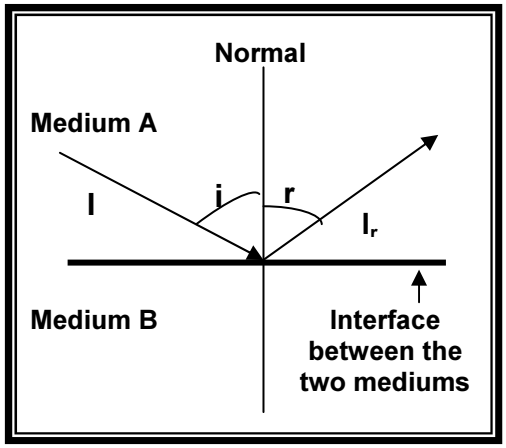

Figure 1.3: Complete reflectance of light beam from the surface of a material. 'i' is the angle of incidence made by the incident light with the normal and 'r' is the angle of reflection made by the reflected light with the normal; example of any metal where incident light is reflected from its surface leading to opacity in the metal.

1.1.5 Haze

Haze is defined as the percentage of transmitted light which on passing through the sample deviates from incident beam by forward scattering. It tells how cloudy a sample appears. Haze is dependent on the thickness of the material, its crystal structure, voids, bubbles, impurities, etc. For example, the more quickly a material is cooled after it is shaped, the less hazy it is likely to be due to the fact that polymer chains have less time to rearrange into crystalline structures. Surface roughness also cause light deviation and contributes to haze value **[33]**.

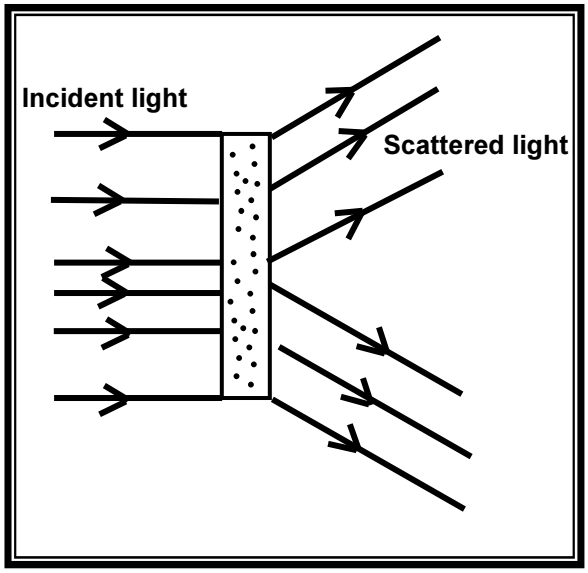

Figure 1.4: Scattering of a beam of light after striking a material. Extent of light scattered is dependent on the crystal structure arrangement of a material. It also depends upon the overall thickness of the material.

Through the above discussion, it can be seen that the key parameters for optical materials are refractive index, Abbe number, transmittance, reflectance and haze. All the above-mentioned properties are important and should be kept in mind while designing materials for optical applications. It is the nature of the bonds that decides the refractive index of the material. Similarly, Abbe number is related to the scattering of light when it passes through a material. It is very important for a material to exhibit transparency and clarity for optical applications. Less is the reflectance, more is the transparency and hence

better clarity. In order to understand all the above-mentioned basic phenomena of light, let us discuss about materials that shows various transitions when they are subjected to interaction with light.

1.2 OPTICAL MATERIALS

Selection of a material for optical applications is done on the basis of (a) physico-chemical properties (b) processability and machinability characteristics and (c) properties having direct bearing on the performance behavior of the product for a given application for which the material is to be selected.

The material is selected based on the fact that the physical properties of the material are compatible with the environment in which it is to operate and it exhibits the optical properties consistent with the desired level of performance. The physical properties to be considered for optical applications include density, hardness, rigidity, stability at service temperature conditions, thermal expansion, electrical and thermal conductivity, affinity to absorb and retain water and radiation resistance. The desired limits for various properties would vary with the requirements of given application for which the material is to be selected.

As already mentioned earlier, glass has been the inorganic material of choice for optical applications due to its excellent clarity and hardness. Optical glasses are usually described in terms of their refractive index and their Abbe number. Glasses with refractive index less than 1.60 and Abbe number value of 55 or above are termed as crown glass. Those optical glasses which have refractive index value greater than 1.60 and Abbe number value of less than 50 are termed as flint glasses. For those optical glasses where value of refractive index is greater than 1.60 are also termed as crown glasses provided they exhibit high Abbe number of greater than 50. Crown glasses are usually alkali silicate glasses and flint glasses are lead alkali silicates. Other than flint glass and crown glass, various other types of glasses have been used for optical applications with varying contents and compositions of

additives such as metal oxides. The optical properties change with the change of the type of metal or metal composition incorporated in glass. Table 1.2 gives a description of various glasses being used for optical applications. The refractive index range of the available glasses lies between 1.50-1.90. As the percentage of metal oxides, such as lanthanum oxide and niobium pentoxide in the case of lanthanum niobium glass, is increased, the refractive index increases correspondingly **[34]**.

Although glass has been a preferred choice of optical material for optical industries, one of the major drawbacks associated with glass is that glass is very heavy in weight. As the power of the optical lens increases, the thickness of the lens also increases resulting in an overall increase in weight of the lens leading to poor aesthetics. The limits of glass for optical applications in terms of processability, fragility and heavy-weight raised the need for alternative materials such as polymeric materials or optical plastics.

Table 1.2: Composition and optical properties of different types of optical glasses. The refractive index of the glass depends upon the nature and types of metal oxide dispersed in the glass matrix.

S. No.	Glass	Composition	Metal oxide (%)	Refractive index
1.	Crown	Alkali silicates	100	1.52
2.	Flint	Lead oxide	30-70	1.6-1.8
3.	Sodium-calcium	Sodium oxide Calcium oxide	11 9	1.50
4.	Borosilicate	Boric oxide	15	1.60
5.	Titanium	Titanium dioxide	15	1.60
6.	Lanthanum-Titanium	Lanthanum oxide Titanium dioxide	14 6	1.70
7.	Lanthanum-Niobium	Lanthanum oxide Niobium pentoxide	21-24 15-21	1.80-1.90

Until the 19th century, variety of conventional materials like metals, wood, stone, etc. were used to make articles. With the expansion of organic and synthetic polymer chemistries, an outcome of several challenges overcome by development of various types of materials during World War II, polymers were discovered to be good materials for optical applications. With this, the product called plastic lens or optical plastic came into existence. With the advent of plastic materials for optical applications, the optical devices have become much lighter than before. In earlier times, spectacle lenses made out of glass were very heavy for the users. For optical applications, polymers as the base materials offer profound advantages over traditionally used inorganic glass in terms of light weight, impact resistance and better control of focal length. Since refractive index is an important criteria to decide the suitability of the material for optical applications, plastics gets prominence. Optical plastics are also superior in shock resistance, lightness, processability and are more commonly used in the field of optical applications in place of glass.

Major growth of plastics industry has mainly been from 1930 onwards. Initial attempts to lower the weight of a given lens were carried out in the late 1930s, using Polymethyl methacrylate (PMMA). During World War II, PMMA was used for submarine periscopes, windshields, canopies, and gun turrets for airplanes. The material exhibits excellent clarity and good processability. It is often preferred because of its excellent properties, easy handling, processing and low cost. Inspite of these advantages, one major drawback of the material was its inability to resist scratches. To overcome this drawback, development of PMMA was followed by the discovery of the thermosetting resin diethylene glycol bisallyl carbonate, commonly known as CR-39 in the late 1940s. The inherent scratch resistance, impact resistance and low density of this material were superior compared with other materials known at that time. Polycarbonates to be used as optical plastics were developed in 1950s and became as one of the widely used optical plastics by the late 1980s.

Another material to be discovered and developed in late 1980s was of polythiourethane chemistry. Polythiourethanes are high refractive index

materials. The development of high refractive index optical plastics is quite recent. In fact, until the beginning of 1990s, the only high refractive index materials available for ophthalmic use were dense barium flint, or extra dense flint glasses or titanium dioxide based glasses with the refractive index in the range of 1.65-1.70. The lens cast using polythiourethanes as monomer provided a refractive index of 1.71. The chronology of developments in the area of polymers for optical applications has been listed in the Table 1.3.

Table 1.3: Evolution of polymers for optical applications [35]

Year	Material	Applications	Processing
1937	Poly (methyl methacrylate)	Lenses; windshields, sunglasses	• Cast molding • Injection molding • Compression molding • Extrusion
1942	Poly (diethylene glycol bis allyl carbonate) (CR-39)	Lenses (prescription & non-prescription),	• Cast molding
1955	Polycarbonate	Sun glasses, Lenses (prescription & non-prescription), headlights, visors	• Extrusion • Injection molding
1987	Polythiourethane	Prescription lenses, progressive lenses, aspheric lenses	• Cast molding

As can be seen from Table 1.3, four major classes of optical plastics are poly (methyl methacrylate), poly (diethylene glycol bisallyl carbonate), polycarbonates and polythiourethanes. These materials are very novel in a way that they possess inherent characteristics of being light-weight. Poly (methyl methacrylate) amongst all can be processed through almost all techniques and hence is a viable option to easily work with. A range of monomers with functional groups of varying refractive index have been exploited for achieving a high refractive index polymer. Table 1.4 lists some of the major polymers and their building blocks (monomers) for optical

applications. The major application areas include spectacle lenses, intraocular lenses and contact lenses.

The polymeric backbone of optical materials generally consists of C, H, N, S and O along with halogen atoms such as chloro, bromo, iodo, etc **[36-39]**. Unsaturated acids and systems such as divinyl benzene, styrene and phthalic acid have also been used to produce high refractive index materials **[40-41]**. Replacement of acid by a salt and depending upon the extent of dispersion, transparent or non-transparent films could be obtained. The incorporation of aromatic rings containing chloro, bromo or iodo groups can increase the refractive index of the system **[42-52]**. The synthesis of such compounds is extremely difficult and expensive. Also bromo, iodo and chloro groups normally lead to colour in the system thus, restricting their use for optical applications is desired. Introduction of heavy metals that have high polarizability and low ionic radius (like barium, lead, lanthanum, titanium, strontium, etc.) into materials has been traditional used principle to increase the refractive index values of the inorganic glass materials being prepared **[53-57]**.

The refractive index and Abbe number value of the polymer changes with the change in the functionality of the monomer. Thiol group (SH) containing sulfur exhibits the highest refractive index. Benzene ring (aromaticity) also contributes for achieving high refractive index polymer. PMMA or Diethylene glycol bis allyl carbonate have the lowest refractive index amongst all the commonly used polymers. Optical plastics are used for a variety of applications such as prescription and non-prescription lenses, windows, sport masks, goggles, camera lenses, aircraft and automobile applications.

It can be summarized that even though glass had all the properties essential for a material to be used for optical applications, its high density and cumbersome processing led to the need for materials with improved optical properties. The evolution of plastics as optical material came as a boon for optical industry. The nature and type of constituent composing an optical plastic is responsible for its behavior towards light.

Table 1.4: Optical properties of polymers and their uses in various optical devices

S.No.	Building block (Monomer)	Polymer	Refractive index	Abbe Number	Applications
1.	Methyl methacrylate 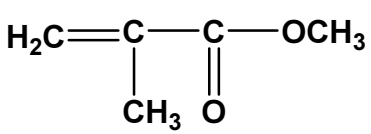	Polymethyl methacrylate	1.49	61	• Spectacle lenses • Intraocular lenses • Contact lenses • Telescope lenses • Magnifying lenses • Optical fibers • Liquid Crystal Displays
2.	Thiol 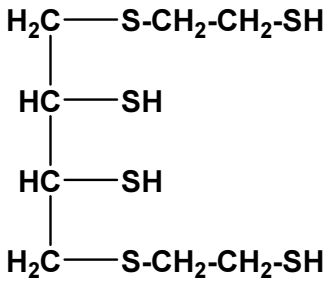	Polythiourethane	1.67	32	• Spectacle lenses • Magnifying lenses • Aspheric lenses
3.	Bis-phenol A 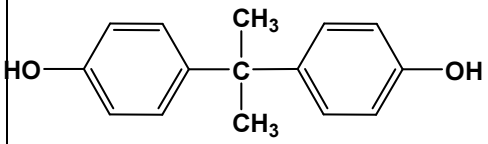	Polycarbonate	1.59	34	• Spectacle lenses • Telescope lenses • Magnifying lenses • Binocular lenses • Sunglasses • Automotive headlights

S.No.	Building block (Monomer)	Polymer	Refractive index	Abbe Number	Applications
4.	Diethylene glycol bis allyl carbonate 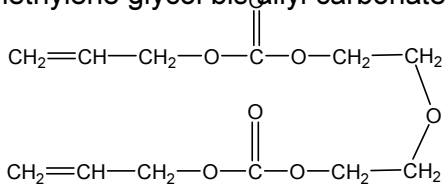	Poly (diethylene glycol bis allyl carbonate)	1.49	56	• Spectacle lenses • Sunglasses
5.	2-Phenyl ethyl acrylate 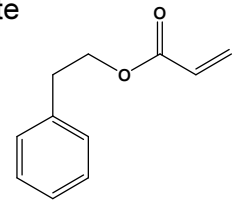	Poly (phenyl ethyl acrylate)	1.55	34.3	• Raw material for IOL
6.	2-Phenyl ethyl methacrylate 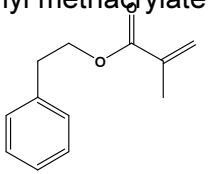	Poly (phenyl ethyl methacrylate)	1.55	35.2	• Raw material for IOL
7.	2-hydroxyethyl methacrylate 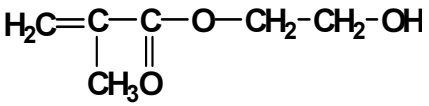	Poly (2-hydroxy ethyl methacrylate)	1.45	57	• Contact lenses • Intraocular lenses

The incorporation of metals and halogen atoms having high polarizability impart necessary features to the polymer matrices. Amongst the various polymeric materials, polyacrylates are the principal optical materials with good moldability, optical clarity and thermal stability. Before discussing different types of acrylates used for optical applications, let us first understand the chemistry, structure and behavior of acrylates.

1.3 ACRYLATES: THEIR CHEMISTRY, STRUCTURE & BEHAVIOUR

Acrylic acid is a carboxylic acid consisting of a vinyl group and a carboxylic group. Acrylic acid undergoes the typical reactions of a carboxylic acid such as esterification with the alcohols to form alkyl esters, generally known as alkyl acrylates **[58-60]**. The structures of the acrylic acid (Figure 1.5 a) and alkyl acrylates (Figure 1.5 b) are represented below.

The most common esters of acrylic acid are methyl acrylate, ethyl acrylate, butyl acrylate and 2-ethyl hexyl acrylate. Acrylate esters show a wide range of properties **[61-62]** depending upon the type of monomer used and reaction conditions for the synthesis. The alkyl (R) group in the acrylate (ester of acrylic acid) determines many key properties of the polymers formed such as glass transition temperature, hydrophobicity, hydrophilicity, film-making properties due to change in flexibility, etc **[63]**.

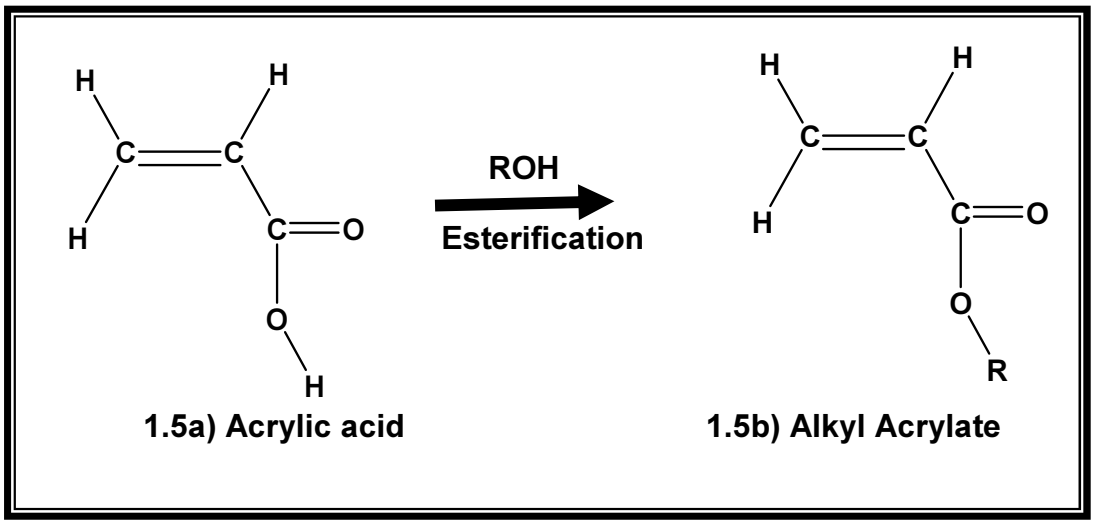

Figures 1.5: Structure of acrylic acid (1.5a) and acrylate (1.5b). Acrylic acid gets esterified with an alcohol to form alkyl acrylate.

Besides esterification, acrylic acid can also be modified by the replacement of the α- hydrogen atom with an alkyl group, example methyl group to form methacrylic acid (Figure 1.6a). This molecule further undergoes esterification to form methyl methacrylate (Figure 1.6b).

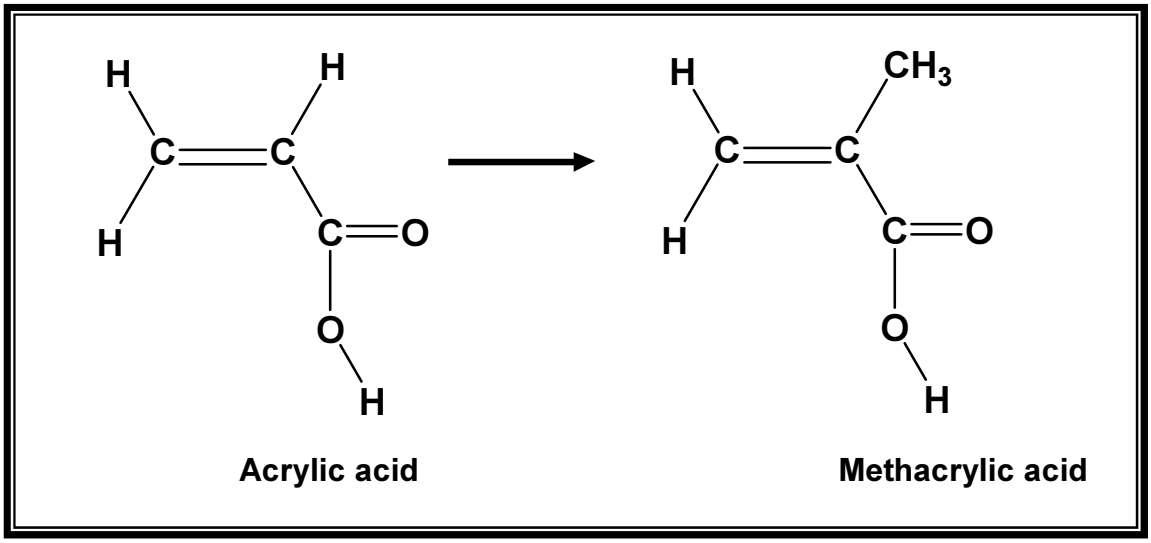

Figure 1.6a): Methacrylic acid formation due to substitution of α-H of acrylic acid by methyl group.

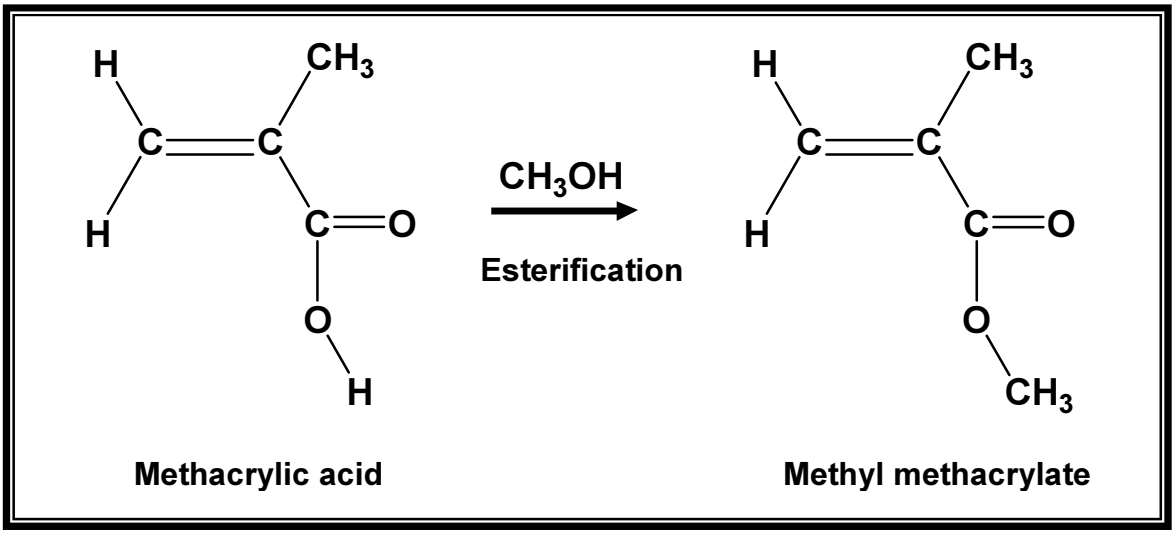

Figure 1.6b): Methyl methacrylate formation due to the esterification reaction of methacrylic acid with methanol.

Acrylic acid and its esters undergo the reaction at the double bond which readily combine with themselves or co-monomers to form homo-polymers or co-polymers **[64-67],** which are used in the production of optical lenses, paints

and coatings **[68-78]**, adhesives **[79-82]**, elastomers, super absorbent polymers, flocculants, etc. Acrylates and methacrylates are the common monomers in forming acrylate polymers **[83-85]** such as phenyl ethyl acrylate, polymethyl methacrylate, etc. Figure 1.7 represents the polymerization reaction of methyl methacrylate monomer to polymethyl methacrylate.

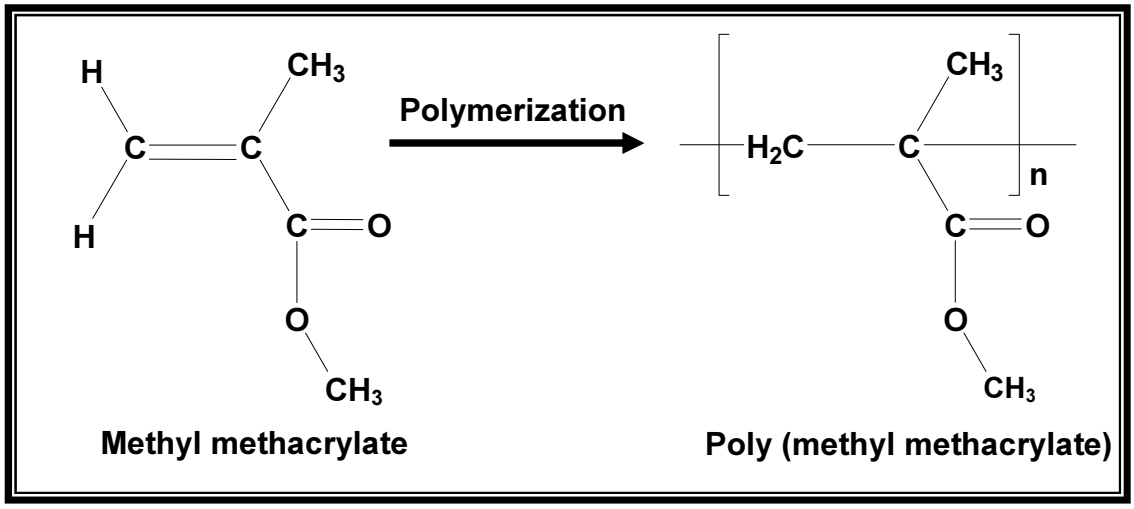

Figure 1.7: Polymerization of methyl methacrylate to form polymethyl methacrylate (PMMA). Polymethyl methacrylate is an important polymer used for optical applications exhibiting excellent optical clarity.

Polymethyl methacrylate **[86-87]** is a clear, transparent plastic with high softening point, good impact strength and weatherability. The outstanding property of PMMA is its optical clarity which makes it highly useful for applications where light transmission is important **[88]**. Since the chemistry of acrylic acid is very versatile, it is used as a raw material in many of the industries. Because of the fact that acrylic acid has a high reactivity, it becomes an ideal choice as a starting material for many synthetic products. Its tendency to readily polymerize to form homo- or co-polymers makes it a preferred material for many applications. Due to its easy availability and cost-effectiveness, it would be worth-while to consider acrylic acid for optical applications. Let us now see various types of polyacrylates used for optical applications

1.4 ACRYLATES FOR OPTICAL APPLICATIONS

Polyacrylates form an important class of materials which are used in all major optical applications such as contact lenses, intraocular lenses and spectacle lenses. Poly (methyl methacrylate) (PMMA) and poly (2-hydroxyethyl methacrylate) (PHEMA) are two polymers, which have been commercially exploited for optical applications to a great extent. Various polymers based on acrylates and methacrylates are listed in Table 1.5 along with their key properties such as refractive index, glass transition (Tg) temperature and density.

Table 1.5: Different types of acrylate and methacrylate based polymers [89]

Polymer	Tg (°C)	Density (g/cm³)	Refractive index
Poly(methyl acrylate)	6	1.22	1.479
Poly(ethyl acrylate)	-24	1.12	1.464
Poly(n-butyl acrylate)	-55	1.08	1.474
Poly(methyl methacrylate)	105	1.190	1.490
Poly(ethyl methacrylate)	65	1.119	1.485
Poly(n-propyl methacrylate)	35	1.085	1.484
Poly(isopropyl methacrylate)	81	1.033	1.552
Poly(n-butyl methacrylate)	20	1.055	1.483
Poly(sec-butyl methacrylate)	60	1.052	1.480
Poly(isobutyl methacrylate)	53	1.045	1.477
Poly(t-butyl methacrylate)	107	1.022	1.4638
Poly(n-hexyl methacrylate)	-5	1.007	1.4813
Poly(lauryl methacrylate)	-65	0.929	1.474
Poly(benzyl methacrylate)	54	1.179	1.568

From the data on refractive index, glass transition temperature and density of various types of polymers based on methacrylates and derivatives of methacrylates, it is evident that the refractive index of all the acrylates falls within the low refractive index range of 1.4-1.5. However, the glass transition (Tg) temperature, an important characteristic of a polymer, varies significantly with the change in substituent group of the acrylate or methacrylate monomer. The Tg of a polymer is the deciding factor for selecting a suitable polymer for a given application. For example, one would need a very low Tg (<20°C) for applications such as intraocular lenses whereas a Tg (>50°C) would be preferred for contact lenses and spectacle lenses.

Inspite of having various advantages of being a promising optical material, polyacrylates suffer from drawbacks such as low refractive index and poor impact resistance, which limit their use for optical applications. To overcome these drawbacks, materials with improved refractive index and toughness are needed. This can be achieved by modifying either the structure or the chemistry of the polyacrylates with suitable functional groups. The scope of the applications of polyacrylates can be widened, by suitable modifications, to take care of the drawbacks. One of the ways by which the improvement is possible is by incorporation of additives containing halogen atoms, aromatic rings and heavy metals in the monomer for improving the refractive index, hardness and thermal stability of polyacrylates. Incorporation of suitable metals for desired results has been considered as novel idea, in this regard. It has been reported **[90-91]** that the dispersion of salts of metal having high polarizability and low ionic radii bring tremendous improvements in the overall optical properties of polymers. Incorporation of various metal atoms into polyacrylates leads to positive results and helps in getting materials with refractive index in the range of 1.62-1.65 **[92-95]**. One should keep in mind that the percentage loading of the metal introduced in the polymer matrix should be enough to bring about changes in the inherent properties of the base polymer used.

Transition metal complexes and metal-containing materials are well studied and the presence of metal centers has shown to give rise to a diverse range of interesting and useful properties **[96]**. In addition, metal centers have shown to play pivotal role with respect to both the structure and function of many polymers. The incorporation of metals into the structures of synthetic polymers (Figure 1.8) clearly offers considerable potential for the processable materials with properties that differ significantly from those of conventional organic polymers.

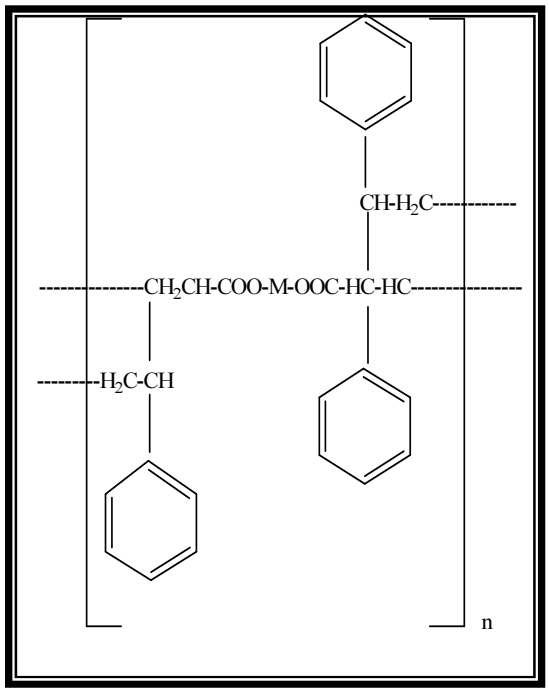

Figure 1.8: Structure of metal-containing acrylate polymer formed by bonding of metal atom to the carboxylic acid group of acrylic acid.

Acrylates thus, exhibit properties suitable for use as optical material. But several drawbacks limit their application. Thus, a need arises for modifying the acrylates to be used as materials for optical applications. However, not much work has been carried out on the modification of acrylates for optical applications **[97-98]**. Due to several favourable characteristics of acrylates, it would be meaningful if they can be modified to take care of the drawbacks. In this regard, metals play a key role in designing novel acrylate materials with improved properties for optical applications. Metals, due to their high polarizability and high refractive index, prove to be ideal materials for incorporation in polymer matrices. Therefore, the development of metal-containing polymers should create exciting new dimensions for polymer materials. Since, inorganic metal and organic polymer are two separate phases; incongruence between them would always lead to non-homogeneous products. Thus, a novel process methodology needs to be designed to overcome this gap. For this, preparation of composite materials would provide lead so as to how a bridge between the organic and the inorganic phases should be made.

1.5 NANOMATERIALS AND NANOCOMPOSITES

Composite materials are basically the materials made out of a combination of two or more materials to form desired structures so as to take advantage of the synergistic effect by which the desirable properties of one component complement those of the other. Composites always have two phases: one of them being the dispersed phase or the load-bearing phase while the other one is the dispersing phase or the load-transferring phase. The dispersed phase is also called as reinforcement as it is always hard and brittle providing strength to the composite. The dispersing phase is also called as matrix and is soft and ductile. Composites involving inorganic materials and organic polymers have become the subject of intense interest because of the fact that the composites exhibit better electrical, optical, catalytic and mechanical properties than the individual neat polymer **[99-107]**. This is due to the quantization effect due to the dispersed particles in the polymeric matrices in a composite material **[108]**.

Designing composite materials having the desired properties is a challenging task. Several polymeric composites have been known and many of them are being developed to meet the requirements of varying types. The composites for optical applications is relatively a new area and the aim is mainly to achieve certain optical properties in the already existing optical polymers by forming composites; especially nanocomposites **[109]**.

For the development of composites for optical applications, nanotechnology holds a lot of promise. During the late 20^{th} century it was realized that the behavior of materials depended on the size of the particles constituting the material and that the dependence was most evident when the size of the constituents was that of nanometers. The term “Nanotechnology” is increasingly employed to describe the process technologies and analytical techniques for materials in the ultrafine range of the order of a millionth of a millimeter. As the size of a particle decreases in the order of one millionth of a millimeter, the number of particles increases extraordinarily for a given volume of material. As a result of this, the volume fraction increases as one goes from

macro to micro to nanosystems (Figures 1.9a-c) **[110-111]**. The dimensions of inter-particle interactions become so huge and meaningful that the complete physico-mechanics of the structure gets transformed when a nano-engineered system is designed. At this state, the fundamental physical properties of the system change drastically.

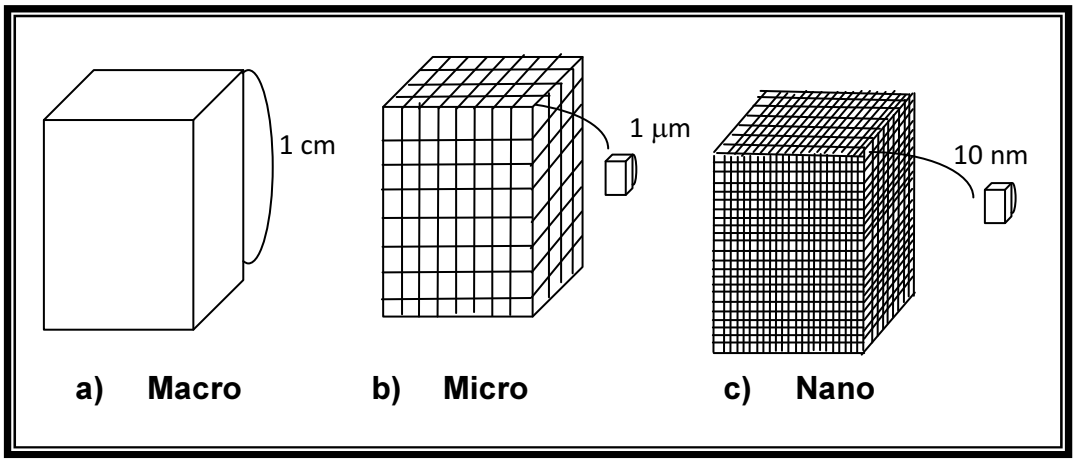

Figures 1.9a-c: Change of specific area by miniaturization of a macro system (1.9a) to micro system (1.9b) to nano system (1.9c). The number of particles increases extraordinarily when the size of the particles is reduced while moving from macro to micro to nano scale. As a result, volume fraction ratio of particles of nano-based systems is the highest.

Also, as particles get smaller than the wavelength of visible light, they not only become transparent but also emit special light by plasma absorption. They show completely different electromagnetic or physico-chemical properties from their bulk counterparts, although they are made out of the same materials. Materials consisting of dimensions in nanometer range are termed as nanomaterials. Nanomaterials have been the target for various applications, especially when the special effects like optical are desired alongside the mechanical strength **[112]**. Transparent materials can be obtained due to the small size of the nanoparticles, which prevents excessive light scattering. There are basically two routes to prepare nanoparticles: a top-down approach and a bottom-up approach. The concept behind the top-down approach is designing and controlling the properties at a macroscale to few

times smaller in size. This process of reducing the scale continues until a nanosize is produced. The top-down approach is not a friendly and rapid way of producing nanostructures. The concept of a bottom-up approach is that one starts with atoms or molecules, which build to form larger structures. Therefore, a bottom-up approach needs to be considered.

There is a lot of interest in low-dimensional structures, especially 1D array of metals and semiconductor nanoparticles and their potential applications in optical and electronic sensors, nanoscale electronics and catalysis. Table 1.6 lists out various one, two or three dimensional nanomaterials **[113]**. Different types of materials are used to design such nanomaterials depending upon the requirement.

The introduction of inorganic nanomaterials into organic matrix systems results in nanocomposites (Figure 1.10) exhibiting multi-functional, high-performance matrices; characteristics different from the conventional materials. Nanocomposites offer ultra-large interfacial surface area per volume and the distances between the host matrix and filler components are extremely short. One can easily maneuver the properties and behaviour of the nanocomposites by control of size of materials at the nanoscale level. Since, the researchers are now exploiting quick and better ways to invent a product, the latter approach through preparation of nanocomposites seems ideal, avoiding long processes and conditions for preparation of the composite material **[114]**.

The ideal materials for designing high refractive index nanocomposites are metals. Metal nanoparticles have half-filled conduction band and the associated electrons have the ability to move almost freely in case of particles as large as a few tens of nanometers **[115-116]**. When the particle diameter becomes smaller than the electronic mean – free path in the bulk metal (~ 10 nm), the scattering of free electrons at the particle surface should be taken into account.

Table 1.6: Different classes of nanomaterials employing different materials. Their structure can be three, two or one dimensional

	Size (nm)	Materials
1D nanocrystals and clusters (quantum dots)	1-10 (diameter)	Metals, semiconductors, magnetic materials
Nanoparticles	1-100 (diameter)	Ceramic oxides
Nanowires	1-100 (diameter)	Metals, semiconductors, oxides, sulfides, nitrides
Nanotubes	1-100 (diameter)	Carbon, layered metal, chalcogenides
2D arrays (of nanoparticles)	Few nm^2	Metals, semiconductors, magnetic materials, polymer films
Surfaces and thin films	1-100 (thickness)	Varied materials
3D structures (superlattices)	Few nm in all directions	Metals, semiconductors, magnetic materials, nanostructured materials
Nanoparticles in polymers	1-100	Metal-polymer nanocomposites

Such small clusters demonstrate a molecular type behavior with optical properties very different from those for metal nanoparticles of bigger size **[117]**. Apart from increasing the refractive index, the inorganic material would improve the hardness of the polymer, resulting in an optical material with good clarity suitable for applications such as lenses and coatings **[118]**. For the effective incorporation of metal in the organic phase and the achievement of optimum performance, dispersion of metal in the nano form is an important criterion **[119]**.

An ideal way to harness the special properties of metal nanoparticles is by incorporating them into polymer matrices **[120-121]**. In recent years, metal nanoparticles have been used towards the fabrication of high refractive index nanocomposites **[122]**. Also the unique features provided by metals to the polymer remain intact and both the mediums continue to complement each other. Suitable way to incorporate metals into polymers for the purpose of

improving optical properties is the dispersion (both in-situ and ex-situ) **[123-128]** of the metal atoms/ salts having high refractive index in nano size directly into acrylates.

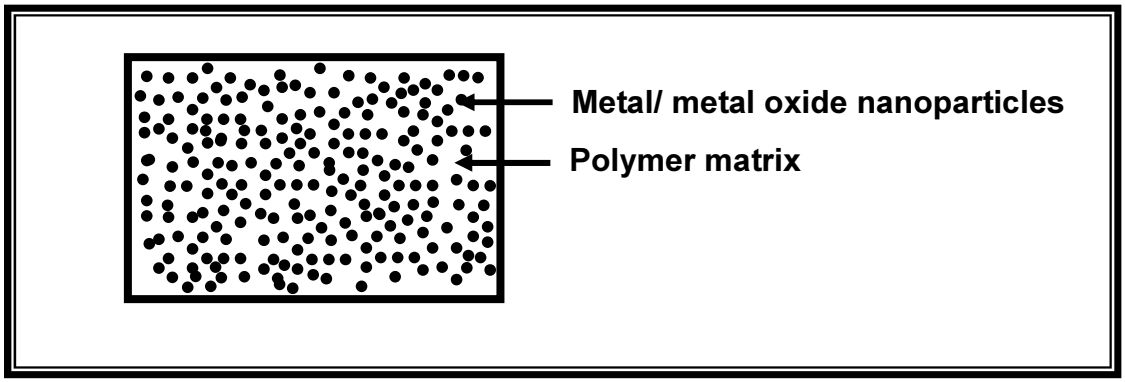

Figure 1.10: Structure of metal-polymer nanocomposites where metal nanoparticles or metal oxide nanoparticles act as dispersion phase and polymer matrix such as polyacrylate matrix act as continuous phase. Homogeneous dispersion of nanoparticles in the matrix gives rise to nanocomposites. Example, dispersion of nanoparticles of titanium dioxide (TiO_2) into polymethyl methacrylate (PMMA) gives TiO_2-PMMA nanocomposite suitable for optical applications such as coatings, etc.

Designing nanocomposite materials is not always as easy as it appears to be mainly because of the fact that one has to deal with completely different materials to bring them into one cohesive structure to deliver the desired performance. A number of different classes of hybrid inorganic-organic polymeric systems may be prepared depending upon the nature of the organic functional groups, which are incorporated within the structure of the polymer. The polymeric compound tends to act as a base matrix material with the inorganic phase dispersed throughout. The fundamental knowledge on the preparation and nature of metal-polymer nanocomposites has a long history. The oldest technique for the preparation of metal-polymer nanocomposites was described in 1835. Gold salt was reduced in the presence of gum arabic yielding a nanocomposite **[129]**. Metals undergo property change by size

reduction and their composites with polymers are very interesting for functional applications **[130]**.

The precursors for the preparation of nanoparticles are reduced chemically **[131-132]**, thermally **[133]** or by UV irradiation **[134-135]**. Existing in-situ techniques include condensation of metal vapour into liquid monomer prior to polymerization **[136]**, simultaneous metal evaporation and plasma polymerization **[137]**, ion exchange/ implantation **[138-139]**, and the mixing of metal precursors into polymer substrates followed by decomposition **[140-141]**.

Incorporation of inorganic nanoparticles into organic polymer matrix can significantly affect the properties of the polymer matrix due to their high surface to bulk ratio **[142-143]**. The composite and assembly of nanoparticles has been the research focus for scientists during the past decade **[144-148]**. The polymer-nanocomposites with functionality and high performance have attracted more attention due to their optical, electrical, magnetic, electronic & enhanced mechanical properties **[149-156]**. In particular, the composite optical materials with high refractive index, find potential applications in filters, lenses, reflectors, optical waveguides, optical adhesives, and anti-reflection films and have been studied extensively **[157]**. Incorporating inorganic nano-domains into a polymer matrix is an effective way to fabricate high refractive index nanocomposite materials **[158-159]**. However, the size must be less than one-tenth of the wavelength of visible light (400-800 nm) in order to avoid scattering & obtain transparent polymer nanocomposites.

It is known that the hardness of a material generally increases with the decreasing size, and that the mechanical strength of the materials considerably increases by micronizing the structure of the metal and ceramic material or composing them in nano range **[160-161]**. Furthermore, with the ceramic material having particle size less than several hundred nanometers, the unique super-plastic phenomenon is seen that it is extended several hundred to several thousand times from the original size at the elevated

temperature over 50% of the melting point **[162]**, which may provide the possibility of forming and processing of ceramics like metallic materials.

Thus, nanomaterials show completely different properties as compared to their macro counterpart. They can be used to provide different functionalities to the already existing polymers. Polymer nanocomposites offer tremendous versatility by combining two or more materials on a sub-microscopic, microscopic and even at macroscopic level to obtain properties, which are not available for the individual component. As a result, nanocomposites are always in demand for a much greater variety of applications as they allow controlled manipulation and optimization of properties. While preparing metal-containing nanocomposites for optical applications, several problems are encountered pertaining to dispersion of nanoparticles into polymer matrix and retaining the optical properties of the nanocomposite material. To overcome the challenges faced in the process of preparation of nanocomposites, several ways need to be adopted.

1.6 CHALLENGES IN MAKING OPTICAL NANOCOMPOSITES

Although, the idea of preparation of metal-containing nanocomposites is novel, the challenges involved in its preparation are numerous. High refractive index optical materials pose a challenge to exploit nanocomposites for such applications as countries like India depend totally on the import of high refractive index materials. Development of indigenous technology to synthesize such materials remains still a challenge, which needs to be worked upon using new areas such as nanotechnology.

As mentioned above, polymeric materials have a limitation where the refractive index cannot go beyond 1.7; materials having high refractive index need to be incorporated. Metals have an intrinsically high refractive index in the range of 2.0-4.0 and are thus, promising candidates for the development of composites for optical applications. Optical properties of metal nanocomposites are studied over a decade **[163]**. Metal oxide nanoparticles can be used in thin film polymer systems to engineer specific material

properties while maintaining visible transparency. High loading of nanoparticles in a polymer can manipulate refractive index and UV absorbance over a wide range.

Some of the challenges listed below make working with metals in its purest form a huge challenge:

1. Rarity of the pure metal
2. Low thermal conductivity of metals leading to high manufacturing cost.
3. Adhesion with other metals
4. Loss of strength at temperatures > 400 $^{\circ}$C

It is due to these reasons that metal dispersion in polymers are achieved through the fine particles or nanoparticles of metals or metal salts. Organic dispersions are those in which both polar & non-polar organic fluids and non-ionic steric stabilizers or dispersants are used to prevent the particles from forming larger aggregate ions **[164]**. Generally the dispersion in polymeric materials has proven to be difficult and frequently results in phase separation due to agglomeration. Typical specific surface free energies of inorganic solids amount to 500-2000 mJ/m^2 **[165-166]** compared to 20-50 mJ/m^2 for polymers **[167]**. As a result of such high values for the inorganic compounds, nanocomposites can be far from equilibrium **[168]** if the interfacial energy in the system is not compensated by interactions between the polymer and the inorganic particles. As a consequence, agglomeration of inorganic colloids can be a problem in the synthesis of nanocomposites **[169-170]**.

Once the nanocomposites are formed, the activation energy required to reach the equilibrium is too high. Powders, which contain base nanoparticles often observe a problem of agglomeration. This is due to the fact that the inorganic particles have high surface energies which tend primary particles to agglomerate to secondary particles. The common method to prepare a composite by just mixing the particles with the polymer is not successful because the agglomerates do not break easily into their primary particles during the procedure applied for the

nanocomposite preparation. Thus, the agglomeration makes the nanocomposite preparation difficult. The agglomerates act as larger particles that may scatter or reflect light. So for transparency, the small particles must be highly dispersed (non-agglomerated) in the polymer to avoid light scattering **[171].** To obtain transparent dispersions is a huge challenge where the transparency of a polymer depends on the size and refractive index of the metal oxide particles **[172]**.

Dispersion of metal oxide particles in polymers is possible by avoiding agglomeration through a) adopting in-situ synthesis and dispersion of inorganic nanoparticles into organic matrix, b) coating of the metal oxide particles with an organic acid or a surfactant to create an organophilic surface and c) electrostatic stabilization by the creation of an aqueous colloid.

The in-situ synthesis of lead sulfide nanocomposites, using water soluble lead salts such as lead acetate or lead nitrate and hydrogen sulfide (H_2S) is reported **[173-175]**. Hydrolysis is a preferred reaction for the in-situ synthesis of nanoparticles **[176-178]**. While many inorganic salts which are suited as starting materials for the synthesis of nanoparticles are better soluble in water but there exist numerous inorganic compounds which are soluble in organic media, thus allowing in-situ preparation of nanoparticles in the non-aqueous media as well **[179-180]**. As an alternative to the in-situ preparation of the inorganic particles, colloids with a strongly bound surface layer of organic molecules may be used if they can be isolated and if the primary particles can be re-dispersed. Here, the agglomeration can be suppressed by the surface free energy and therefore tends to decrease the attraction between the particles. The modification of the surface of the particles improves the interfacial interaction between the particles and the polymer matrix **[181-182]**.

In-situ preparation of inorganic nanoparticles in polyelectrolytic multi-layer film (PEM) has been reported **[183]**. PEM composed of weak electrolytes such as polyacrylic acid (PAA) and poly (allylamine hydrochloride) (PAH) are particularly employed **[184]**. Multi-layer processing conditions control the size and overall metal concentration of the films **[185]**. Metal nanoparticles were

prepared by the reduction of dissolved metal ions or metal complexes **[186-188]** and semiconductors by combination of dissolved metal ions or metal complexes and the respective ionic counterparts **[189-190]**. The intensity of lost light transmitted through dispersions of coloured gold particles with diameters below 50 nm originates mainly from absorption and not from scattering **[191-192]** while scattering of light becomes more prominent for larger particles **[193]**. Therefore, the nanocomposites appear transparent whereas composites with larger particles are opaque. Opaqueness may also be due to agglomeration of the nanoparticles. A matrix with a refractive index of 1.5 was selected and for that of the metals were selected as 0.608 for gold, 1.12 for copper, 1.71 for nickel, 2.03 for platinum, 3.45 for tungsten and 5.10 for osmium. It was observed that the intensity loss by scattering becomes pronounced for particle diameters above ~ 5-20 nm, depending on the refractive index difference between the particles and the matrix **[194]**. On the other hand, the transmittance in the above examples is essentially zero at particle diameters of 35-135 nm. Hence, composites with very small particles are exceedingly transparent and that the particle diameter plays an important role if the refractive index difference between the matrix and the particles is pronounced. However, polymers containing sulfides of lead, silicon and iron and gold nanoparticles showed extraordinary refractive indices of 2.5 to 3 or ~1 (with gold) **[195-198]**. For lead sulfide, particles larger than 25 nm exhibit scattering losses **[199]**.

Inorganic particles are hydrophilic and the surface has to be functionalized to avoid aggregation when the nanoparticles are integrated in a hydrophobic matrix. The key issue is the development of synthesis methods allowing for particle generation in solution without aggregation and subsequent functionalization and transfer into the hydrophobic matrix without isolation of the particles **[200]**.

Authors **[201]** describe the use of several nanoscale inorganic particles to create molded articles for varying refractive indices; limitation being the compatibility between the organic and the inorganic phase. Issues of

agglomeration of the particles can be addressed through chemical surface reactions. Inorganic particles were surface treated with hydrolysable silane containing atleast one polymerizable or polycondensable group.

One of the promising metal candidate ideal for the purpose of improving the properties of optical polymers is titanium. Titanium has found its niche in many industries owing to its unique properties of high corrosion resistance and good mechanical strength **[202-206]**. It finds wide use in various industries in its many forms of existence, which are titanium metal, organic titanates and titanium dioxide **[207-209]**. Titanium dioxide or titania is used in almost every field as a white pigment for manufacture of paint and paper, as a filler in rubber and plastics due to its exceptionally high refractive index; higher than that of diamond in the visible region of the electromagnetic spectrum. While large crystals of titanium dioxide are transparent and do not refract, fine particles scatter light very strongly **[210]**. It is due to these reasons that titanium dispersions in polymers are achieved through the fine particles or nanoparticles of titanium dioxide.

The rutile form of titania is the most desirable form due to hardness and refractive index **[211]**. Owing to very high refractive index of titania (2.45), it serves the purpose of obtaining high refractive index metal nanocomposites. Besides being optimum for contributing to the preparation of high refractive index nanocomposites, the major problems with titanium dioxide, particularly the rutile crystalline phase include: long process times, need to use additional stabilizing counter ions which must be laboriously removed prior to use, extreme pH conditions and limited stability **[212]**. It would be desirable to have quick and easy methods for preparing the stable colloidal dispersions of inorganic particles containing titanium where the particles have properties comparable to the rutile form of titania. Fine particles of titania (TiO_2) having narrow particle size distribution and little aggregation have been produced by the hydrolysis of the metal halide in the presence of an organic solvent **[213]**.

The major challenge with dispersion of titanium dioxide particles is the inability to suitably stabilize suspensions of the nanoparticles. It would be desirable to have stable suspensions of nanoparticles that could be used days later or preferably even weeks or months later. Existing titania (TiO_2) particles and solutions are often too unstable to be economically feasible for use in suspension form. The challenge is to use particles with controlled particle size, shape and stability and methods for economic production. The use of dispersing agents give stable dispersion of nanoparticles of titanium dioxide with more uniform shape, size and more stability than titanium nanoparticles formed without the use of a dispersing agent. Dispersing agents are used to influence the average size of the titanium dioxide nanoparticles **[214-217]**. Dispersing agents can be alkoxyorganosilanes, carboxylic acids or combination of both. Examples of alkoxyorganosilanes are octyltriethoxysilane, octadecyltrimethoxy silane, hexadecyltrimethoxy silane or combination of all. Carboxylic acids having C_3-C_{18} carbon chain length are also preferred as dispersing aids.

It is preferable to use highly dispersed colloidal titanium dioxide or sols. The particles dispersed in a sol are spherical or pseudospherical agglomerates, non-uniform in particle diameter leading to opacity and poor transparency **[218-219]**. The sol is stable only in the acid region in a pH of less than 3; its limitations are that it forms precipitates or gels under neutral or alkaline conditions. When the sol is mixed with an organic solvent, it becomes unstable and precipitates out thus making it difficult to be used as a hard coating material to be applied to the surface of plastics **[220-223]**.

Particles in a sol assume a spherical or pseudospherical configuration, when it is used as a coating, by mixing it with a base resin. The titania (TiO_2) particles are not present densely in the coating and leave spaces among the particles. The density of the particles cannot be enhanced, thus giving a coating, which is poor in characteristics and strength as desired for the coatings for optical plastics **[224-225]**.

Titania (TiO_2) particles though can be made in very small particle sizes of 50 Å they can seldom be applied as such due to the fact that the particles are always highly coagulated. Such nanoclusters appear to be indefinitely stable at room temperature in highly acidic solutions. Heating or dilution of such particles results either in flocculation, precipitation or formation of an elastic gel. Titania (TiO_2) based sols and gels in which the size of the nanoclusters is made much smaller than the wavelength of visible light are the characteristics of a good dispersion **[226]**.

From the above experiences of researchers, it may be noted that many methods have been employed to achieve high refractive index nanocomposites. The idea of incorporation of metals such as titanium, lead, gold, etc. into polymeric substances is very novel to achieve modified polymer with improved properties. Metals undergo considerable property change by size reduction and their composites with polymers are very interesting for functional applications. Both ex-situ and in-situ dispersion of nanoparticles have been carried to prepare novel nanocomposites. While ex-situ method leads to unstable dispersion, use of dispersing aids are recommended. But one has to keep in mind that while dealing with additives in the matrix, essential optical properties should not be lost. In-situ method proves to be an ideal method for preparation of nanocomposites. For a simple reason that in-situ preparation and dispersion leads to homogeneous matrix, it is found to be the most promising technique for the preparation of nanocomposites. Apart from the techniques adopted by the scientists so far for the preparation of nanocomposites for optical applications, more innovative approaches should be followed for the development of novel nanocomposites.

1.7 RECENT DEVELOPMENTS IN METAL-CONTAINING NANOCOMPOSITES FOR OPTICAL APPLICATIONS

The search for new optical materials for device applications has inspired recent developments in the creation of nanostructured molecular architectures

[227-230]. The types of materials range from organic polymers **[231]** to nanoparticles **[232]**. The creation of metal particles with definite geometries and sizes (diameter) has also allowed for the systematic investigation of the fundamental optical excitation in metal objects **[233-236]**. A well established methodology used for the formation of metal nanoparticles is to use micelles of molecules, either surfactants or amphiphilic block copolymers where precursors are solubilized inside a self-assembled template **[237-238]**. Polymer assisted synthesis of metal nanoparticles have received substantial attention because of a) very low concentration of homopolymer or co-polymer capable of stabilizing nanoparticles by steric stabilization, b) polymer containing appropriate functional group serving as both reducing and capping/ stabilizing agent, c) possibility of controlling the size, morphology of nanoparticles by varying the polymer/ metal salt ratio and d) offers to prepare novel metal-polymer nanocomposites **[239]**.

Researchers reported synthesis of optical polymers by the radical polymerization of 2,5 bis-(2-thia-3-butenyl)-1,4-dithiane and the polyaddition of oligo [2,5-bis (thiomethyl)-1,4-dithiane] or di-or tri-isocyanates **[240]**. Authors have also reported episulfide type copolymers exhibiting high refractive index and high Abbe number values **[241]**. In recent years, transparent hybrid materials have attracted interest, particularly in optical applications **[242]**. Integrating inorganic fillers into polymer matrices provides new materials combining properties like luminescence **[243-245]**, UV absorption **[246-249]** and high refractive index **[250-254]** with the transparency of the organic polymer matrices.

As discussed in the earlier sections, metal-containing polymers provide an alternative to even the specialty glass materials conventionally used for optical applications. Metals such as lead, lanthanum, barium and titanium have been used to improve the optical properties such as refractive index and mechanical properties such as hardness of the optical plastics **[255]**. The metal containing optical plastic materials with improved refractive index of as

much as 1.60 along with the Abbe number of more than 30 have been successfully designed **[256-259]**.

Significant contributions have been made in the area of controlled and tunable refractive index materials. Using sol-gel chemistry, silica (SiO_2) – titania (TiO_2) mixed oxide glasses have been prepared which show a composition dependent refractive index from 1.4 to 2.4 **[260]**. These materials are particularly useful as anti-reflective coatings for various optical devices. High refractive index materials for index matched adhesives have been prepared using brominated and iodinated carbazole rings on a methacrylate backbone **[261]**. Refractive index was controlled from 1.67 to 1.77 by varying the level of bromination of the homopolymers. In another study, the authors have synthesized a polymer matrix material using copolymerization of chromium-forsterite with refractive index targeted at 1.652. Four co-monomers were selected viz. pentabromophenyl methacrylates (PBPM), tribromophenyl methacrylates (TBPM), pentabromobenzyl acrylate (PBBA) and tribromostyrene (TBS). The refractive indices of the composites prepared by incorporation of chromium-forsterite ranged between 1.66 to 1.71 **[262]**.

The polymerization rate and uniformity of acrylates with multi-functionality are three to seven times faster than that of their corresponding methacrylates **[263]**. The researchers have tried to develop shape-memory polymers based on methacrylates for minimal invasive surgeries **[264]**. Such materials hold a great potential for ophthalmic applications; especially for intraocular lenses (IOLs) **[265]**. The shape memory properties of the prepared polymer networks were studied through free-strain recovery test which is defined as unconstrainted polymer shape change as a function of temperature. The chain motion becomes less restricted as the temperature approaches T_{onset} and rapid recovery is only induced at the temperatures near or above T_{onset} when the polymer has been deformed.

Temperature dependence of the optical properties such as refractive index is presented at a reference temperature of 22 °C as per USA Standard **[266]**.

Temperature dependence of refractive characteristics of five plastic materials viz. polymethyl methacrylate (PMMA), S-low styrene, Zeonex, Optorez and Bayer, has been investigated in the interval between 10-50 °C **[267]**. A decrease of refractive index with increase in temperature was established for all the optical plastics. This change in property due to change in service temperature cannot be neglected while designing the optical elements and devices. This dependence is specific for each optical polymer and is attributed to two factors: a) the change in density caused by positive coefficient of thermal expansion and b) increase in polarizability with temperature. The variation of refractive index also altered the dispersion characteristics of optical plastics. Lowest variation in Abbe number was observed in Bayer whereas the highest in the case of PMMA.

A novel strategy to synthesize hybrid metal-polymer nanocomposites has been achieved based on in-situ free radical suspension and bulk polymerization. An organometallic precursor complex is dissolved in a liquid monomer phase prior to polymerization, where the precursor molecules are immobilized inside the polymer matrix during its formation **[268]**. The precursor molecules can be naturally trapped inside the polymer matrix and converted into nanoparticles via reduction mechanism. Through this method, very high concentration of metal precursor can be added. In this study, silver was chosen for dispersion of nanoparticles, azo isobutyronitrile (AIBN) as initiator and the polymers polyvinyl chloride (PVC) and methyl methacrylate (MMA) as the polymer matrices. The inorganic silver precursor that was chosen was (1,5-cyclooctadiene)(1,1,1,5,5,5-hexa fluoroacetylacetonato) silver (I). The reaction between the polymer, inorganic precursor and catalyst was carried out at 70 °C for 8 hrs. The average particle size of silver nanoparticles obtained by this method was found to be 10 nm. Thermogravimetric analysis showed approximately 1% by wt. uptake of silver in the nanocomposites.

Thin films (100 nm) of silver containing poly (ethylene terphthalate) (Ag-PET) have been synthesized that exhibit features suitable for applications like

filters, absorbers, etc. The narrow transmission at 320 nm arises due to the absorption edge of the polymer and metals and broad band absorption is attributed to the metal nanostructures of various shapes and sizes arising due to the coalescence of two or more particles giving rise to small interactions at short range between the metal aggregates **[269]**.

The influence of silver nanoparticles on the glass transition temperature as well as on the thermal and thermo-oxidative stability of polymethyl methacrylate (PMMA) matrix was studied. It has been reported that the optical properties of metal atoms are the consequences of the electromagnetic field induced collective oscillations of the conduction band electrons and is known as surface plasmon **[270-271]**.

Uniform spherical silver nanoparticles were embedded in polymethyl methacrylate (PMMA) matrix by in-situ radical polymerization of methyl methacrylate (MMA) using azo isobutyronitrile (AIBN) to initiate polymerization process. The thermal degradation behavior of the composite material was studied and it was found that the presence of silver nanoparticles improved the thermal properties of the overall nanocomposite **[272]**.

A method is described for the preparation of new nanocomposites based on poly (ethylene terphthalate) (PET), poly (vinyl chloride) (PVC) and polypropylene (PP) on the one hand and the noble metals (silver and platinum) on the other hand **[273]**. The method comprises of the formation of nanoporous polymer matrices by incorporation of noble metal precursors into the matrices. In-situ reduction of the precursors yields the metal-polymer nanocomposites. The nanoparticles of silver with average size of about 4.6 nm were homogeneously dispersed in PET polymer. The polymers were annealed and were put into the metal-precursor solutions where the polymer gets deformed, thereby indicating the filling of pores of the polymer by the metal. The incorporation of a second component into a nanoporous structure of the polymer automatically led to the formation of nanocomposites because the particle size of the metal incorporated could not exceed the porosity size

of the polymer matrix. Similarly, PP and PVC-Pt nanocomposites were prepared. The estimated size of the nanoparticles was ~40 nm.

Authors, in a study, reported the preparation of transparent composites with high solid loading (> 5 vol%) by matching the refractive index of the inorganic particle with low cost polymers like polymethyl methacrylate (PMMA), so as to circumvent the use of any complex processing techniques or particle surface modification. It was observed that the transparency of the PMMA composites was largely affected due to the increase in solid loading (> 10 vol%) and higher refractive index mismatch of PMMA composites was observed **[274]**.

By using sol-gel method, amorphous form of titania was introduced into epoxy polymers to prepare a series of high refractive index titanium resin nanocomposite films. To increase the refractive index of the hybrid films, triethoxy silane capped trimercapto- thioethylamine was synthesized. Refractive index was tailor-made from 1.61 to 1.797 with the increasing content of titania from 0% to 65 % **[275]**.

A novel synthetic route is developed by the authors **[276]** to prepare polyimide-nanocrystalline-titania hybrid optical films with a high titania content (upto 50 wt%) and thickness (20-30 μm) from soluble polyimides containing hydroxyl groups. The hydroxyl groups on the backbone of the polyimides could provide the organic-inorganic bonding resulting in the homogeneous hybrid solutions. The flexible hybrid films could be obtained with tunable refractive index and high optical clarity. The maximum refractive index achieved was 1.92. Mixing or spin coating and casting a suspension of nanoparticles in appropriate organic solvents can be used to prepare nanocomposites. Reverse micelles technology has been used to prepare UV curable, transparent, acrylic resin and titania compositions by controlled hydrolysis of titanium tetrabutoxide **[277]**.

Nanoparticles of titania were successfully prepared **[278]** by the sol-gel method employing organic tetrabutyl titanate as precursor in acidic media. Titania/ acrylate nanocomposite emulsions were prepared by in-situ emulsion

polymerization. The particle diameter of titania nanoparticles was approximately 10.2 nm and its dispersion in polyacrylate matrix was homogeneous. This preparation technique will give rise to application of titania in various industries like automobile, waste water treatment, self-cleaning coatings, etc.

In another study **[279]**, sol-gel derived poly (methyl methacrylate)-titania hybrid materials were synthesized by using acrylic acid as a coupling agent. Titanium butoxide modified with acrylic acid was hydrolyzed to produce a titania network and then polymethyl methacrylate (PMMA) chains, formed in-situ through a radical polymerization were chemically bound to the titania network to synthesize a hybrid material. The products changed from yellow to red in colour as the content of titania was increased. The thermal stability of the hybrid materials was considerably improved as compared to pure PMMA.

Methyl methacrylate-butyl acrylate-methacrylic acid co-polymer was used to prepare titania containg hybrid material. Emulsion polymerization was used to prepare hybrid composite. Surfactants were used to increase the stability of titania dispersion and upto 79% dispersion of titania was achieved **[280]** in this study.

Titania nanoparticles were generated in-situ in polymethyl methacrylate (PMMA) polymer matrix by using electro-spinning technique along with sol-gel method **[281]**. The synthesis process involved the hydrolysis of tetrabutyl titanate in a solvent mixture of tetrafluoro acetic acid and dichloromethane followed by the incorporation of this solution into the PMMA solution. With this technique, complete hydrolysis of the titanate precursor was achieved. Electro-spinning method was employed to prepare the fibers of PMMA composite. There was a strong hydrogen bonding interaction between titania precursor and PMMA matrix. It is well known that when metal oxide reacts with water, the metal ion increases its co-ordination by employing its vacant d-orbitals to accept oxygen lone pairs from ligands such as –OH groups **[282]**. This is further confirmed by thermogravimetric analysis which showed 3 peaks

revealing the dehydration of water, hydroxyl groups in Ti-OH **[283]** and hydroxyl groups on the surface of titania **[284]**. The actual content of titania varied from 2.3 – 9.7 wt% in the TiO_2/ PMMA nanohybrids. The pure PMMA exhibits a glass transition temperature of 109.2 °C whereas those incorporating titania showed a higher glass transition temperature of around 118-135 °C. This was attributed to the hydrogen bonding of titania with the polymer.

Development of a process to tailor-make the refractive index of polymethyl methacrylate (PMMA) using a UV curable reactive resin and ceramic nanopowders (Al_2O_3) has been studied. The dispersion of nanoscale inorganic filler in reactive polymer resins allowed the modification of a polymer's refractive index to vary, depending on the filler type. The properties of the composites depend upon the type of incorporated nanoparticles, their size, shape, concentration and interaction with polymer matrix. Refractive index and optical transparency were improved by using more sophisticated dispersion methods with high shear forces in the homogenization process. A refractive index of 1.4968 was achieved using Al_2O_3-C **[285]**.

Authors have prepared lead containing methacrylates (MA), obtaining transparent co-polymers of lead methacrylate ($Pb(MA)_2$)/ styrene/ methacrylate (MA) with upto 30 wt% lead methacrylate. The refractive index of the polymer was found to lie in the range of 1.554-1.563 depending upon the content of lead methacrylate incorporated.

Researchers have used 86 wt% ZnS as a high refractive index material for poly (urethane-methacrylate macromer) increasing the refractive index from 1.645 to 1.796 at 632 .8 nm **[286]**. Gold/ gelatin composites were prepared with as high loading upto 90 wt%, lowering the refractive index of the material to 1, offering the lowest refractive index known ever for a polymer composite material **[287]**.

In a study, graphite based nanocomposites were prepared in which the monomer was introduced into the pores of graphite layer followed by

polymerization **[288]**. The graphite maintained the layered structure **[289-292]** with large layered spacings. The overall aim of this study was to design a carbon nanocomposite whose properties were comparable to those of carbon nanotubes. It was reported that lower fractions of graphite introduction showed the electrical conductivity in polymers like nylon 6, polystyrene and polymethyl methacrylate (PMMA) nanocomposites by in-situ polymerization of polymer matrices **[293-296]**. With as little as 0.5 wt% graphite, the relative permittivity increased drastically. With increase in temperature from 30 °C to 150 °C, the value of permittivity also increased from ~ 25 to 150.

The thermal behavior of zinc (Zn), cobalt (Co), nickel (Ni) and copper (Cu) acrylates and their polymers were investigated **[297]**. These metal acrylates were synthesized by the reaction of acrylic acid and metal salts in toluene suspensions at 40-50 °C. The reactions were carried out for 5 hrs with gradual addition of reactants and with constant stirring. After reaction, the products were dried and thermal analysis was performed on them. The curves of Zn and Cu acrylates showed that there occurred a thermal polymerization and decomposition reactions while those of Co and Ni acrylates revealed dehydration process. The polymers followed the following pattern of thermal stability: Zn> Co> Ni> Cu. The polymers of Zn, Co and Ni contained 9-27% unreacted double bonds. During polymerization reactions, the double bonds reacted leading to cross-linked products. Cu acrylate on the other hand showed low ability of polymerization and thus lowest cross-linking.

The thermal behavior of several metal acrylates and methacrylates was investigated **[298]** and the temperature characteristics were determined. Thermal behaviour of acrylates with salts of sodium (Na), calcium (Ca), magnesium (Mg) & zinc (Zn) have been studied **[299]**. Divalent metal acrylates were thermally more stable than their corresponding methacrylates. It has been reported that polymers of lithium (Li), sodium (Na), potassium (K) and cesium (Cs) salts of methacrylic acid **[300]** are stable up to 350 °C. Metals used for the study were those from alkali and alkaline earth metal series. The metals were being reacted with acrylic acid and methacrylic acid

to form corresponding acrylates and methacrylates. Dehydration of the metal acrylates or methacrylates were observed in the case of alkaline earth metal series. The thermal polymerization temperature was observed to be lowest for strontium methacrylate and highest for potassium methacrylate. The sodium salts were the most stable of the alkali metal acrylates and methacrylates.

The authors have reported the synthesis of Hf (Ta, Nb) containing polymers with methacrylate and fumarate groups **[301]**. The pyrolysis of the composition leads to the formation of metal-polymer nanocomposites consisting of crystalline Hf (Ta, Nb) – containing nanoparticles stabilized by the polymer matrix. This was achieved by thermal transformation of metal-containing monomers and their thermolysis to obtain stabilized polymers. These nanocomposites have potential scope to be used as refractory materials.

In a study **[302]**, silica (SiO_2) nanoparticles having a diameter 10-50 nm were used together with UV and electron beam curable acrylates to produce transparent coatings with improved mechanical properties. For a higher amount of nanoparticles to be incorporated into polymer matrix without any agglomeration, the modification of the surface of the nanoparticles is done using trialkoxysilanes **[303-305]**. The incorporation of nano silica into polymer matrix resulted in better hardness (~ 260 N/mm^2) as compared to neat acrylate (200 N/mm^2). The weatherability test was performed on the silica containing nanocomposites where it was seen that the acrylate nanocomposite coatings can withstand more than 3000 hrs of accelerated weathering conditions.

Sol-gel method is considered to be a useful approach to design nanocomposites for optical applications. Silver and other rare earth metal's nanoparticles are synthesized using sol-gel method and dispersed in acrylate materials to get nanocomposites. Nature and type of metal has shown to have effect on the overall thermal stability of the synthesized metal acrylates. Apart

from optical properties, metals have proven to improve the mechanical properties of the nanocomposites.

1.8 HOW METAL-CONTAINING ACRYLATE NANOCOMPOSITES CAN BE USEFUL FOR RESOLVING MANY OF THE DRAWBACKS OF THE EXISTING POLYMERS

As described earlier, the polarizability of the substituent groups can increase the refractive index of the polymers **[306-307].** This approach can be tried for modification of polyacrylates. To achieve this, there can be two obvious ways, either using copolymers having desired atomic bonds or incorporating high refractive index metals **[308]**.

By blending nanoparticles with materials such as acrylate plastics, significant changes and improvements in material properties can be realized. One of the advantages that polymer nanocomposites offer when compared with other conventionally filled polymers is the theoretically possible optical clarity and improved refractive index because of the negligible intensity loss by light scattering of nanosized particles and their refractive index. Acrylate nanocomposites also exhibit several unique material properties making them suitable for a wide variety of optical applications. First the addition of nanoparticles into the polymer matrix can improve the tribological properties such as wear and tear, scratch resistance, etc. Second, the large surface area to volume ratio of nanoparticles allows significant improvements and modifications of material properties with only a small number of nanoparticles. Finally, certain nanoparticles have a high rate of UV absorption, which prevents UV degradation of the resulting nanocomposites **[309]**.

In–situ synthesis and dispersion of titania by sol-gel method has been used for the preparation of optical films where trialkoxysilane capped polymethyl methacrylate (PMMA)-titania hybrid optical thin films have been prepared using spin coating and multi-step baking. Titanium butoxide was used for the preparation of titania network in acrylic monomers. FTIR showed good bonding between organic and inorganic moieties. DSC results also showed

good dispersion of the PMMA segment in the titania network. Variation of titania content not only tuned the refractive index but also the position of absorption maxima **[310-311]**.

Hybrid composites were synthesized using titanium tetrapropoxide and multifunctional acrylate or methacrylate. 3-(methacryloyloxypropyl)trimethoxy silane has been used as the dispersant in this case. The organic and inorganic networks interpenetrate together to form a transparent composite. The composites with enhanced refractive index of 1.68 and potential applications in photonics has been reported **[312]**.

Uniform dispersions of titania were obtained by the use of organosilane coupling agents. Such dispersions have been used for the coating of polymer, wood and metal surfaces. Such ceramers have been used on articles for abrasion resistance and high gloss appearance for traffic signs, pavement markers, lenses for glasses & microwave oven doors **[313-314]**.

As can be seen from the work carried out so far, there is a lot of emphasis being given on the preparation of hybrid materials involving titania. Because of the high refractive index of titania (2.45), it is a preferred choice for every material scientist to use it for novel applications like optical. It appears to be obvious to use nanoparticles of metals to obtain desired optical materials. Thus, metal-polymer nanocomposites are useful for overcoming any drawbacks exhibited currently by the optical polymers.

1.9 STATE-OF-THE-ART

As have already highlighted, one efficient way to incorporate inorganic domains into a polymer matrix is by using sol-gel method **[315-318]**. Out of the available inorganic materials, titania has been widely used to achieve high refractive index transparent materials **[319-326]**. A series of hybrid materials were prepared **[327]** by incorporation of titania (TiO_2) into polymer matrix by using sol-gel process. The dispersed phase of titania was reported to be of amorphous nature and the refractive index of the polymer could be increased

upto 2.0 by dispersing titania. By using in-situ sol-gel method, hybrid films of PMMA consisting of titania nanoparticles were being prepared. To obtain a stable dispersion, the titania nanoparticles were capped by trialkoxy silane. These films exhibited a refractive index between 1.51 and 1.87, depending upon the content of titania incorporated.

Novel nanocomposite films of titania nanoparticles and hydrophobic polymers having polar groups, poly (bisphenol A and epichlorohydrin) or copolymer of styrene and maleic anhydride were prepared. The composites exhibited high refractive indices, high transparency and no colour. They were solvent resistant, thermally stable and have good mechanical properties. In the process of preparing colloidal solution of titania nanoparticles, severe aggregation of particles were reduced by surface modification using carboxylic acid and long chain alkyl amine. These titania nanoparticles dispersed in the solvent were not found to aggregate after mixing with the polymer solutions. Transparent, colorless, homogeneous films were obtained by drying a mixture of titania colloidal particle solutions in polymer solutions in vacuum. Transmission electron microscopic studies of the films suggested that the titania nanoparticles of 3-6 nm in diameter were dispersed in polymer matrices. Thermogravimetric analysis indicated that the nanocomposite film had good thermal stability and the weight fraction of the dispersed titania nanoparticles in the film was in good accordance with that of the theoretical calculations. The refractive index of nanocomposite films of titania and poly (bis phenol A and epichlorohydrin) was in the range of 1.58-1.81 at 589 nm, which linearly increased with the content of titania nanoparticles from 0-80 wt% **[328]**.

Transparent organic-inorganic nanocomposites were successfully synthesized from sulphonic acid modified poly (bisphenol A carbonate) and titania or zirconia nanoparticles. The dispersibility of nanoparticles was significantly improved by both surface treatment of nanoparticles with phosphoric acid 2-ethyl hexyl ester and introduction of sulphonic acid moiety into the polycarbonate chain. Efficient dispersion of nanoparticles and the absence of

crystallization resulted in highly transparent nanocomposites with upto 42% titania and 50% zirconia. The refractive index of the nanocomposites increased linearly with increasing amount of nanoparticles **[329]**. The same behavior was observed with polyamide-nanocrystalline-titania hybrid materials with titania contents from 20 wt% to 90 wt% **[330]**.

Change of refractive index through the range 1.39-1.65 was achieved by varying the ratio between SiO_2 and titania concentrations in polyvinyl pyrrolidone matrix to form nanocomposites. Precursor solutions of alkoxides such as silicon alkoxide or titanium alkoxide were used to produce high refractive index particles of SiO_2 and titania, which were reacted with water containing an acid or a base catalyst. titania is known for its high refractive index; titanium isopropoxide was used to produce it along with acetylacetone which prevented hydrolysis leading to precipitation of titania. A hydrolysis reaction took place followed by polycondensation resulting in a 3-D oxide network. PVP is an ideal pre-polymerized material due to its solubility in polar solvents and its thermal cross-linking characteristics **[331]**. By using titanium ethyl hexoxide together with acetic acid and 2-propanol as solvent, the precipitation up to 30% by wt. dispersion of titania was avoided. The sol-gel processing is one approach because of the high quality of optical materials produced and the freedom to impregnate them with a variety of additives to modify their optical characteristics.

The synthesis of a nanocomposite material based on polyvinyl pyrrolidone with tunable refractive index, luminescence properties and versatile processing behavior has been described **[332]**. An interesting alternative to titania colloids is represented by layered titanates **[333-337]**. Titanate nanosheets were synthesized and used as refractive index enhancers while CdSe-ZnS quantum dots were properly functionalized. This approach brought the refractive index to 1.8 and stable luminescence properties.

High refractive index inorganic domain such as titania (TiO_2) **[338]**, zirconia (ZrO_2), tin oxide (SnO_2), cadmium sulfide (CdS), zirconium sulfide (ZrS) and

lead sulfide (PbS) **[339-342]** have been introduced into polymer matrices. The inorganic domain in the composite obtained using sol-gel method was amorphous form and the refractive index was too low.

A series of nanoparticles-polymer nanocomposites with high refractive index have been recently prepared. A research work highlights the preparation of high refractive index and highly transparent nanocomposites consisting of titania-zirconia nanoparticles. Zirconia was used as an outer layer of titania nanoparticles to depress the photoctalytic activity of titania. In addition, the surface of the nanoparticles was modified by using acrylic acid to control the aggregation of the nanoparticles and then UV curing was used to prepare the nanocomposites. The refractive index of the nanocomposite blocks was determined to be in the range of 1.54-1.65 **[343]**.

Authors have reported the preparation of titania / epoxy nanocomposites coatings with high refractive index and optical transparency. Highly dispersed titania nanoparticles were synthesized by sol-gel method at room temperature. The titania nanoparticles can be dispersed directly into the polymer without the use of organic surfactant. Nanocomposite coating with refractive index of 1.668 can be obtained by the addition of 30 wt% titania nanoparticles into the polymer matrix. All coatings with different amount of titania exhibit excellent optical transparency of more than 90%. Cracks appear at the surface of the coating when the amount of titania is increased **[344]**.

Authors have modified titania nanoparticles first with polybutylene succinimide diethyltriamine and then dispersed 5 wt% of the hydrophobized particles in styrene **[345-347]**. Incorporation of acrylic acid as a co-monomer increased the interaction between titania and polymer cores, and addition of a hydrophobic agent effectively prevented monomer diffusing into the aqueous phase **[348]**. Authors have successfully synthesized polystyrene/ titania nanocomposite spheres by microemulsion technique with both organic monomer and inorganic precursor **[349]**. Recent developments of organic-inorganic nanocomposites synthesized via miniemulsion polymerization has

been described in detail **[350]**. The preparation and characterization of nanocomposite materials based on the incorporation of titania in PMMA has also been reported.

Some semi-conductor nanoparticles of metal sulfides have a high refractive index & can be introduced into polymer matrix to prepare high refractive index nanocomposites. The nanoparticles of lead sulfide & iron sulfide were introduced into poly (ethylene oxide) or gelatin to produce nanocomposites with high refractive index. The polymer matrices used in these studies are water-soluble polymers and there was no chemical bonding between nanoparticles and the polymer matrices. So the application of such composite materials is restrained in many fields where the materials with water insolubility, good thermal stability and mechanical properties are needed **[351-353]**.

A novel method for in-situ incorporation of lead sulfide (PbS) nanoparticles into water-insoluble polymer matrix to fabricate high refractive index nanocomposites has been reported **[354]**. The nanocomposites consisting of lead sulfide (PbS) nanoparticles with average diameter of 26 Å and polyvinyl alcohol (PVA) were synthesized using colloidal chemistry methods. The PbS/PVA nanocomposites were characterized using optical, structural, thermal and mechanical techniques. No difference between infrared spectra and no difference between glass transition temperatures after incorporation of the lead sulfide nanoparticles in the polyvinyl alcohol matrix indicated weak interaction between nanofiller and polymer. Due to weak interaction between nanofiller and polymer a slight improvement of the mechanical properties of the PbS/PVA nanocomposite was observed compared to the neat PVA. On the other hand, the presence of the lead sulfide nanoparticles in the matrix induced the increase of the crystallization temperature and enthalpy of crystallization. Also, the thermal decomposition of the polyvinyl alcohol shifted towards higher temperature for about 15 °C in the presence of the lead sulfide **[355]**.

Metal oxide nanoparticles can be used in thin film polymer systems to engineer specific material properties while maintaining transparency. Both particle size and loading influenced the overall refractive index of the nanocomposite. Very small particles showed reduced refractive index as compared to that of particles with diameter $\geq$ 25nm. Cerium dioxide (CeO_2), zinc oxide (ZnO) and silica (SiO_2) were successfully incorporated into PMMA thin films with loadings upto 60% by volume. The effect of the nanoparticles on the refractive index and transparency of the polymeric nanocomposites were studied **[356]**.

Various methods can be used to produce metal nanoparticles within the polymeric matrix **[357-359]**. A novel method was developed to synthesize metal/polymer nanocomposite material by photo-initiated polymerization of di-functional acrylates containing small amount of bismuth nanoparticles. These were generated by the reduction of bismuth chloride with t-BuONa. The visco-elastic properties of the bismuth containing acrylate matrix was considerably improved as compared to the neat polymer matrix **[360]**.

A number of modified particles have been isolated; gold (Au), silver (Ag) or cadmium sulfide (CdS) nanoparticles surrounded by a layer of organic thiols, where the thiol groups were attached to the particle surfaces and the organic residues were exposed to the ambient conditions **[361-363]**. An organic shell lowers the specific surface free energy of the inorganic particles. If chemical interactions between the shells were little pronounced and the chemical nature of the modified inorganic surface and the polymer allowed a miscibility of particles and polymer, the particle-polymer interactions can be lower than the sum of the particle-particle or polymer-polymer interactions, which would result in a thermodynamically stable system with individually dispersed primary particles.

Metal containing compositions were prepared by combining discrete metal containing functional precursors with a pre-polymer in solution **[364]**. The metals were selected out of zirconium (Zr), hafnium (Hf), germanium (Ge),

titanium (Ti), lead (Pb), zinc (Zn), tin (Sn), etc, whereas the prepolymer was diurethane dimethacrylate. The refractive index varied from 1.49 to 1.70 depending upon the metal used.

Two novel types of bulk zinc sulfide-polymer nanocomposites with high refractive index and high inorganic nanophase content have been designed **[365]**. Authors have used a method to prepare 2-mercaptoethanol capped zinc sulfide nanoparticles and then immobilizing them into polymer matrix to prepare high refractive index bulk material **[366]**. The refractive index achieved by the authors was 1.64. The nanocomposites were prepared by curing episulfide and HEMA. The results showed that the zinc sulfide polymer obtained from episulfide compounds have good optical, thermal, mechanical properties, etc. The refractive index of the zinc sulfide polymer nanocomposites could be regulated in the range from 1.59 to 1.65 by the content of zinc sulfide nanoparticles. The introduction of Me-Zn can improve surface hardness and cross-linking degree of the system. The zinc sulfide - polymer system had highest pencil hardness of about 5H-6H. These nanocomposites with well balanced properties have potential applications in fabricating optical materials with tunable refractive index and high abrasion resistance.

As a result of the latest methodologies developed, status of the metal-polymer nanocomposites used for optical applications, as of today, is not very appreciable. With the available knowledge so far, there are many areas yet to be covered to fill the gaps and lot more needs to be done. No doubt that plastics are considered as ideal materials for optical applications, and that the development of nanocomposites pave the way for meeting the challenges and growing demand of the present world, the technology is still far from the hands of a common user. With the potential of being one of the most promising technologies, nanotechnology still needs to be exploited further for optical applications.

1.10 PATH FORWARD

Optical plastics, regarded as a wonder material of the 20th century, has successfully proven itself to be a good replacement for the conventional material, glass. Optical plastics have replaced glass in all major areas of optical applications. With the inherent advantages of being light-weight due to low density, optical plastics provide more comfort and better aesthetics to the user. They have thus, become the most preferred material for optical applications.

Polyacrylates, the earliest optical material to be discovered followed by polycarbonates and polythiourethanes were able to provide a wide range of options both for aesthetic purposes and prescription to the user, especially for spectacle lenses.

Optical devices such as contact lenses and intraocular lenses were made possible only because of the presence of polymeric materials like PHEMA, PVP, etc. Optical polymers have helped design contact lenses of day-to-day wear, extended wear, cosmetic, tinted, etc. and foldable intraocular lenses. It is only because of optical plastics that the contact lenses and intraocular lenses industry is a thriving industry today.

Homopolymers such as PMMA, CR-39, pHEMA, etc. and co-polymers like MMA-NVP, etc have been exploited so far for optical applications. The refractive index of all the polymers developed so far lies in the range of 1.3-1.7. Such materials were found to be most appropriate for applications such as contact lenses, IOLs and spectacle lenses. Structural features of such polymeric materials do not allow a refractive index beyond 1.7. For more advanced applications, such as fiber optics, photonics, etc, where dispersion power, focusing power, etc. are major requirements, refractive index plays a key role. Therefore, there is a growing need for high refractive index materials having refractive index > 2.0.

Inorganic materials are known to exhibit a refractive index greater than 2.0 and are found to be an ideal choice for the advanced optical applications. Incorporation of high refractive index materials into plastic matrices would

lead to the development of materials with interesting optical properties. The unique features of organic materials, say polymers and inorganic materials, say metals and minerals, when brought together, can result in the development of composites with synergistic features. The concept is a highly challenging one, since incorporation of the materials is to be done in such a way that the transparency and clarity of the material are not affected. For this, it is essential to bring down the particle size of the inorganic particles to a size which is less than the wavelength of visible light i.e. 50 nm.

Composites based on nanomaterials will surely represent a solution to all technological demands as they exhibit novel properties and combinations. The special characteristics of nano-sized materials can be exploited for a number of advanced functional applications. Amongst the polymers known so far, polyacrylates because of their excellent optical clarity, easy availability and easy processing prove to be the most ideal materials to be used further for advanced optical applications.

Seeing the demands, the need for optical materials with high refractive index and transparency in the fields of anti-reflection coating, ophthalmic lenses **[367]**, optical waveguides **[368]**, and adhesives for optical components will increase tremendously. For sustainable growth all over the world, nanoscale science and technology will have to be prioritized in the areas of optical research. New matrices will be exploited so as to broaden the understanding of the subject. The following objectives should be kept in mind while carrying out research work on metal containing nano optical plastics:

1. Use of cost-effective and easily available material
2. Increased productivity during manufacturing
3. Minimize the use of harmful additives while preparing nanocomposites
4. Better efficiency with maximum output
5. Moving towards more green technologies for manufacturing or processing of nanomaterials

Chapter 2
Materials

CHAPTER 2
MATERIALS

2.0 INTRODUCTION

In this chapter, the materials used for the studies involved in the preparation of metal acrylate polymers covered in this thesis have been compiled. The materials required for experimental studies include:

- Metal salts
- Dispersion media
- Carboxylic acids
- Co-monomers for polymerization

2.1 MATERIALS

The raw materials used in each step for the preparation of metal acrylate polymers have been described here as follows:

2.1.1 Metal salts

Salts of metals were selected based on the ionic size and polarizability of the metals. Elements of group II A, III B and IV B of the periodic table were selected for dispersion. Amongst the II A group of elements, barium was selected; from the III B group of elements, lanthanum was selected and from the IV B group, titanium was selected for the preparation of metal containing acrylates. Also, the selection was done on the basis of easy availability of the metal salts. The ionic size and the polarizability of various metal atoms are as shown in Table 2.1. The inorganic compounds of these metals were used to prepare the following:

- Barium acrylate nanocomposites
- Titania acrylate nanocomposites using inorganic titanium compounds
- Titanate acrylate nanocomposites using organic compounds of titanium
- Lanthanum acrylate nanocomposites

Table 2.1: Properties of various metals used for the preparation of metal acrylate nanocomposites

S. No.	Properties	Barium	Titanium	Lanthanum
1.	Group	IIA	IVB	IIIB
2.	Period	VI	IV	VI
3.	Atomic radius (Å)	2.24	1.4	1.69
4.	Ionic radius (Å)	1.36	0.81	1.032
5.	Polarizability ($Å^3$)	39.7	14.6	31.1

2.1.1.1 Barium acrylate nanocomposites

Barium hydroxide octahydrate [Ba $(OH)_2.8H_2O$] of 99.9% purity having a melting point of 86 °C, procured from Qualigens, India was used for the experimental studies to prepare barium acrylate polymers.

Cinnamic acid of laboratory grade having purity of 99% and melting point of 133°C was procured from LOBA Chemie, India and was used to prepare barium cinnamate.

The structure of barium precursor and cinnamic acid used for the preparation of barium cinnamate is given in Figure 2.1(a) and 2.1 (b).

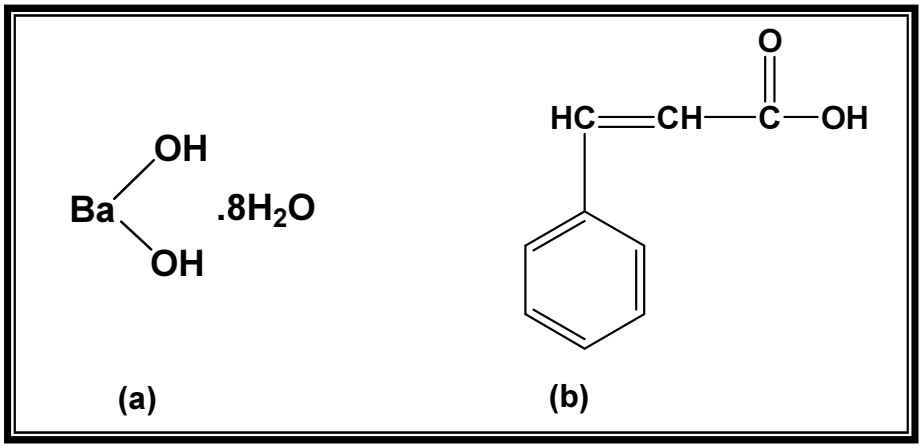

Figure 2.1: (a) Structure of barium hydroxide octahydrate used to prepare barium containing nanocomposites and (b) Structure of cinnamic acid used as co-monomer to prepare barium containing nanocomposites

2.1.1.2 Titania acrylate nanocomposites using inorganic titanium compounds

For the preparation of titania acrylate nanocomposites, titanium dioxide of particle size < 25 nm was procured from Aldrich, USA. Isopropanol from Qualikems, India was used as a solvent for the preparation of nanoparticles of titanium dioxide. Hydrochloric acid (35% assay), Sulfuric acid (98% assay) and Ammonia (25% assay) were procured from Rankem, India which were used for adjusting the pH of the solutions for the preparation of nanoparticles of titanium.

Potassium hydrogen sulfate (purity: 99%) was procured from s.d. Fine Chemicals, India and Acetone of LR grade was procured from Qualikems, India for the preparation of titanium dioxide nanoparticles. Titanium tetrachloride from Spectrochem, India as an inorganic compound of titanium with 98% purity was used. Titanium tetrachloride exhibited a boiling point of 135 °C. Structure of titanium tetrachloride is given in Figure 2.2.

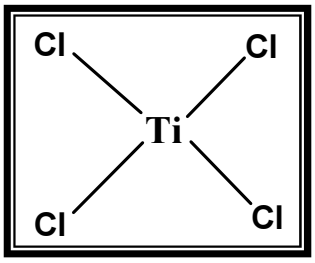

Figure 2.2: Structure of titanium tetrachloride used to prepare titanium acrylate nanocomposites

2.1.1.3 Titanate acrylate nanocomposites using organic compounds of titanium

Organic metal compounds of titanium (titanates) were used to prepare titanate acrylate nanocomposites. Following six organic titanium compounds were used for the preparation:

a) Titanium acetylacetonate (boiling point= 188 °C)

b) Tetra 2-ethylhexyl titanate (boiling point = 185 °C)

c) Tetraisopropyl titanate (boiling point=232 °C)

d) Tetrabutyl titanate (boiling point=310 °C)

e) Polybutyl titanate (boiling point >2000 °C)

f) Triethanolamine titanate (boiling point = 85°C)

The above-mentioned titanium compounds were procured from Synthochem Pvt Ltd., India with >99% purity and were used as such without any further purification. The structure of organic compounds of titanium are given in Figures 2.3 (a-f).

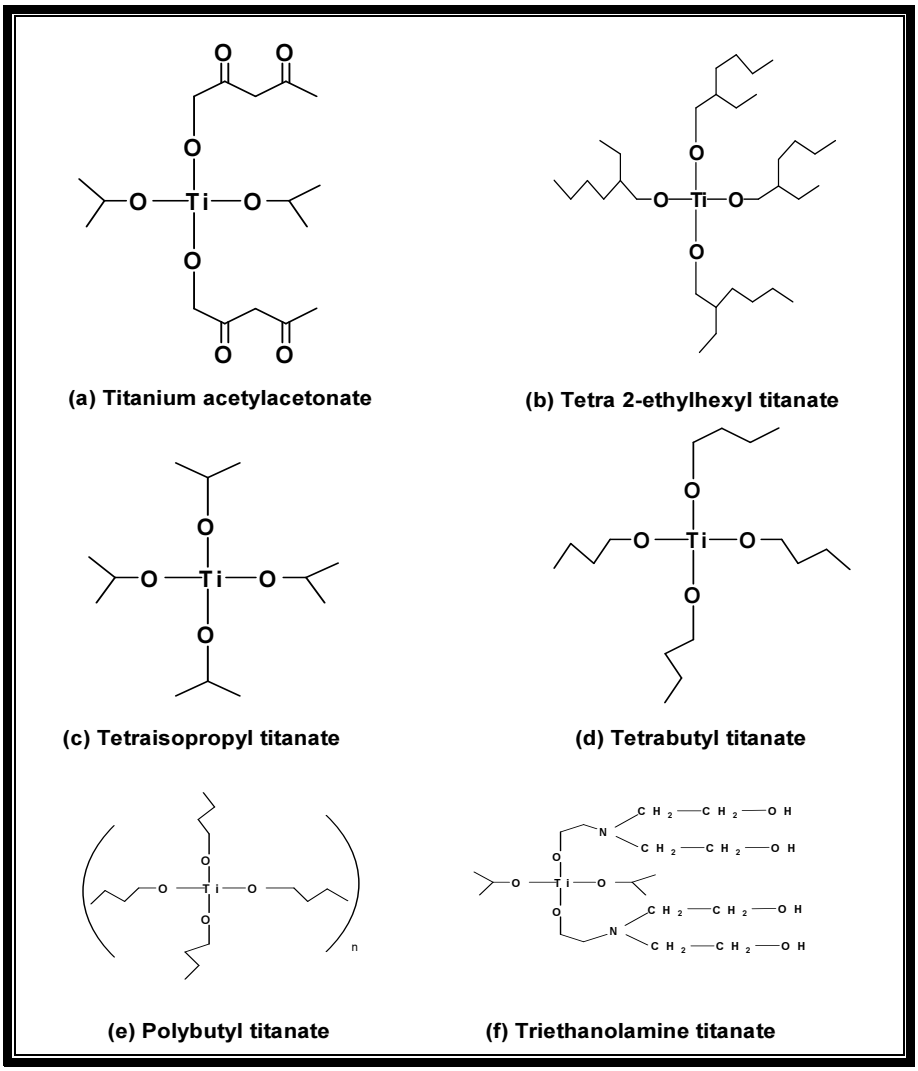

Figure 2.3: Structure of a) Titanium acetylacetonate b) Tetra 2-ethylhexyl titanate c) Tetraisopropyl titanate d) Tetrabutyl titanate e) Polybutyl titanate and f) Triethanolamine titanate. These organic precursors were used to prepare titanate acrylate nanocomposites

2.1.1.4 Lanthanum acrylate nanocomposites

For the preparation of lanthanum acrylate nanocomposites, lanthanum compound used for the experimental work was lanthanum oxide [La_2O_3] having a melting point of 2315 °C and purity of 99.9% and was procured from Central Drug House (P) Ltd, India. The structure of lanthanum oxide used is given in Figure 2.4.

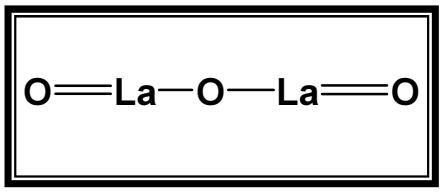

Figure 2.4: Structure of lanthanum oxide used to prepare lanthanum acrylate nanocomposites

2.1.2 Dispersion media

Two different monomers were tried for the dispersion of metal compounds to prepare nanocomposites.

(i) Acrylic acid having a boiling point of 141°C was procured from s.d.Fine Chemicals, India and

(ii) 2-hydroxyethyl methacrylate having a boiling point of 205 °C was procured from Acros Organics, USA

The monomers were used as such. The structures of monomers are given in Figure 2.5 (a-b).

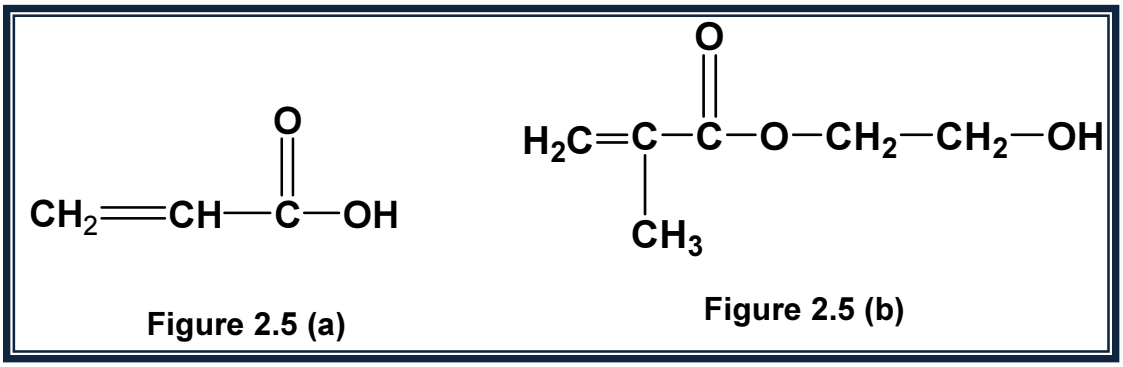

Figure 2.5 (a) **Figure 2.5 (b)**

Figure 2.5: Structure of a) Acrylic acid and b) 2-Hydroxyethyl methacrylate (HEMA) used as dispersion media for metal compounds for the preparation of metal containing nanocomposites

2.1.3 Carboxylic Acid

Cinnamic acid, a carboxylic acid having a melting point of 133 °C was procured from LOBA Chemie, India and was used for the experimental studies to prepare metal containing nanocomposites. The carboxylic acid was of laboratory grade and used as such for the studies without any further processing or treatment. The structure of the carboxylic acid used is given in Figure 2.6.

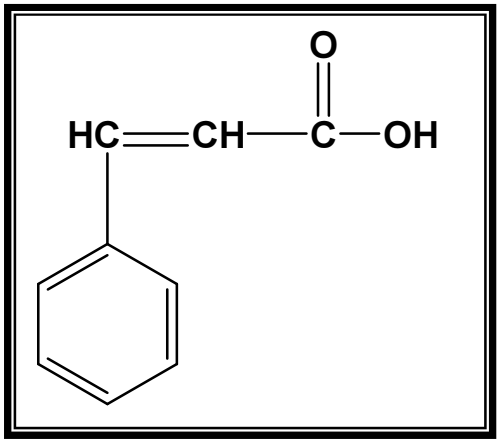

Figure 2.6: Structure of cinnamic acid used to prepare metal containing nanocomposites

2.1.4 Co-monomer for polymerization

The co-monomer used for polymerization of metal containing compositions was styrene having a boiling point of 142-146°C and purity of > 99%. Styrene was procured from G.S. Chemical Testing Lab & Allied Industries and was used as such without any further purification. The structure of the co-monomer used for polymerization is given in Figure 2.7.

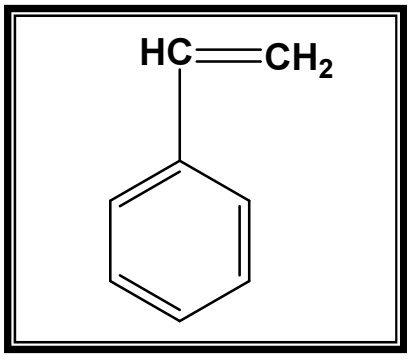

Figure 2.7: Structure of styrene used as a co-monomer for polymerization

2.2 CONCLUSIONS

From the above discussions, following conclusions can be drawn:

a) Amongst the metals, barium, titanium and lanthanum were selected for the preparation of metal containing nanocomposites based on their ionic size and polarizability.

b) Inorganic metal compounds of barium i.e. barium hydroxide, titanium i.e. titanium tetrachloride and lanthanum i.e. lanthanum oxide were selected for dispersion based on their easy availability.

c) Organic metal compounds of titanium i.e. titanium acetylacetonate, Tetra 2-ethylhexyl titanate, tetraisopropyl titanate, tetrabutyl titanate, polybutyl titanate and triethanolamine titanate were selected for the preparation of titanate acrylate polymers based on their easy availability.

d) Acrylic acid and 2-hydroxyethyl methacrylate were selected as the dispersing media for metal compounds due to their low cost, easy availability and good optical properties.

e) Cinnamic acid, a carboxylic acid, was used for improving the optical properties of the metal acrylate nanocomposites.

f) To achieve a cross-linked structure, styrene was used as the co-monomer for polymerization.

Chapter 3
Techniques Adopted

CHAPTER 3
TECHNIQUES ADOPTED

3.0 INTRODUCTION

In this chapter, the methodologies used for the preparation of acrylic nanocomposites have been compiled. The experimental work involving the synthesis of metal containing compositions and metal containing polymers has been covered by a detailed experimental plan covering the following aspects:

- Methodology adopted
- Synthesis of metal acrylate compositions
- Characterization and evaluation of acrylate nanocomposites

3.1 METHODOLOGY ADOPTED

3.1.1 Apparatus

A three-necked round bottom (RB) flask fitted with (i) thermometer, (ii) stirrer and (iii) funnel was used for the synthesis of metal containing compositions. A schematic diagram of the apparatus is presented in Figure 3.1**.**

3.1.2 Dispersion of Metal Salts in Dispersing Media

The selected dispersing medium for the dispersion of metal salts was taken in the reaction flask. The metal compounds used in the preparation of nanodispersed metal acrylate compositions are inorganic compounds of barium, lanthanum, titanium and organic compounds of titanium. The materials, as per the methodology, were added to the reaction flask fitted as indicated in the reaction set up shown in Figure 3.1.

The procedure for the dispersion of metal salts into the dispersing media involved the following steps:

3.1.2.1 Dispersion of Metal Salts

Monomers used as the dispersing medium were taken in a three-necked R.B flask. Metal compounds of barium, lanthanum and titanium were added using a funnel. The metal salts were gradually added to the monomer under

continuous stirring at room temperature. The reaction mixture was stirred continuously using an overhead stirrer for the nanodispersion of the metal compounds in the monomer.

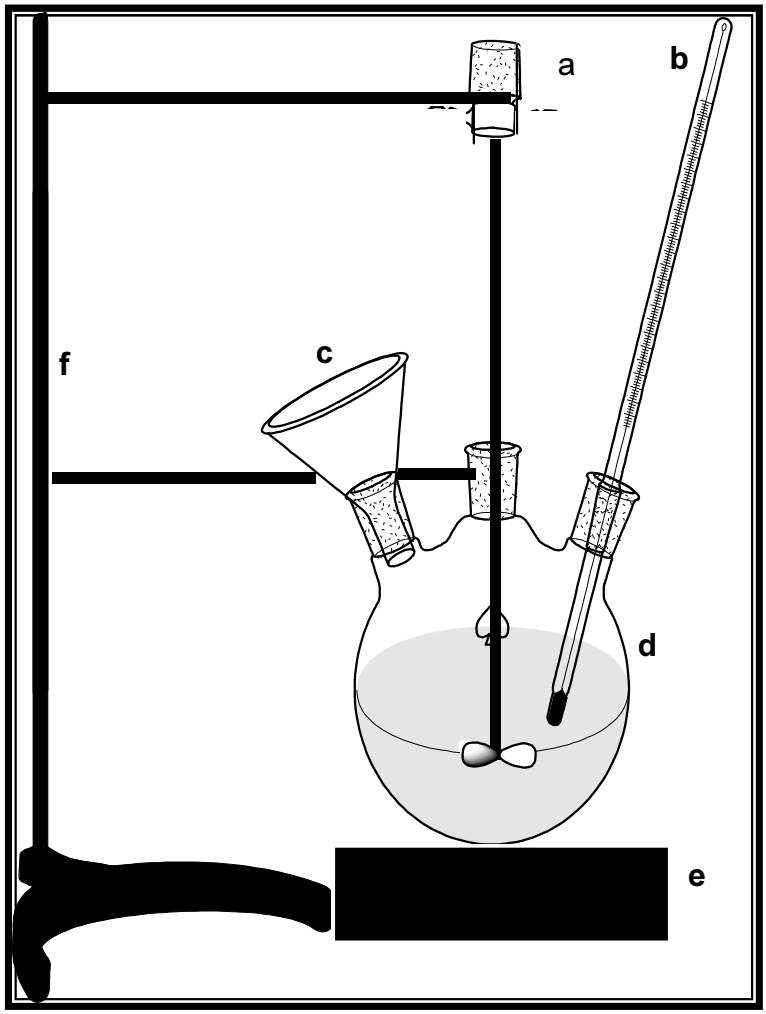

Figure 3.1: Schematic diagram of reaction assembly showing a) Motorized overhead stirrer, b) Thermometer, c) Addition funnel, d) Three-necked round bottom flask, e) Platform and f) Stand

3.1.2.2 Progress of the Reaction

The formation of nano dispersions were studied by analyzing the samples at regular intervals. The samples were analyzed for refractive index, transmittance and thermal stability to confirm the formation of metal acrylate compositions.

3.1.3 Preparation of Cinnamic Acid Compositions

Preparation of cinnamic acid compositions involves the addition of cinnamic acid, a carboxylic acid in metal acrylate compositions of lanthanum and organic titanium. The steps involved are as follows:

3.1.3.1 Dispersion of cinnamic acid in metal acrylate compositions

Cinnamic acid was added gradually to the lanthanum acrylate and titanate acrylate compositions under continuous stirring at ambient temperature. The reaction mixture was stirred continuously for the complete dispersion of cinnamic acid at room temperature. The addition of the cinnamic acid was done gradually till the point where dispersion of cinnamic acid stops which is indicated by settling down of the cinnamic acid.

3.1.3.2 Progress of the reaction

Effect of cinnamic acid on lanthanum acrylate and titanate acrylate compositions was studied by determining the refractive index, transmittance and thermal analysis of the samples obtained at regular intervals.

3.1.4 Cast Polymerization

Styrene was used as a co-monomer in the final step of polymerization of monomer compositions prepared in the above sections. Addition of styrene to the acrylic based compositions containing barium, lanthanum and titanium in various percentages was carried out. Gamma irradiation was used for carrying out the cast polymerization of monomer compositions into lenses.

3.1.4.1 Cast Polymerization

The monomer compositions were cast polymerized into lenses involving the following steps:

a) Preparation of gasket
b) Fitting of molds
c) Filling of molds and
d) Polymerization of monomer compositions

3.1.4.1.1 Preparation of gasket

A polyvinyl chloride (PVC) gasket consisting of grooves of 2mm thickness into which the lens blanks were fitted was prepared from plastisol. For the preparation of plastisol, PVC powder (grade –SR 10A) was homogeneously mixed with plasticizer, poured into a stainless steel mold and kept in the oven at 180^0C for 30 minutes. The mold was cooled and the gasket was removed from the mold.

3.1.4.1.2 Fitting of molds

Clean, dry and polished glass molds were fitted into the grooves of the gasket and were held by a clamp as given in Figure 3.2.

Figure 3.2: Mold assembly with gasket and clamp

3.1.4.1.3 Filling of Molds

The monomer compositions were injected into a glass mold using the casting apparatus as shown in Figure 3.3. Metal acrylate composition was taken in a steel container as shown in Figure 3.3a. Nitrogen gas was used to pressurize the cylinder (Figure 3.3b) to allow the flow of the monomer composition through a filter of 2 μm (Figure 3.3c). After passing through the filter, the dispersion was filled into the mold assembly using a rotator (Figure 3.3d).

3.1.4.1.4 Polymerization of Monomer Compositions

Gamma irradiation technique was used for the polymerization of metal acrylate compositions. During polymerization by gamma irradiation, monomer compositions were polymerized into acrylic polymers. The minimum dose required for maximum polymerization was optimized by evaluating the polymer subjected to various doses of gamma irradiation through hardness, cross-link density, etc.

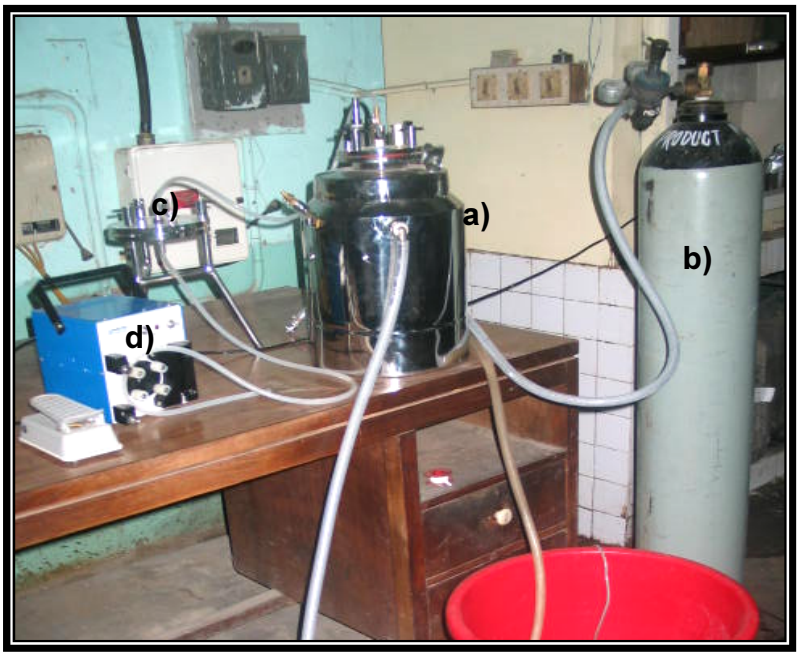

Figure 3.3: Casting and filling unit of lenses including (a) Steel container (b) Nitrogen cylinder (c) Filter and (d) Rotator.

3.2 SYNTHESIS OF METAL ACRYLATE COMPOSITIONS

The experimental work involving the synthesis of metal acrylate compositions and metal acrylate polymers have been covered by a detailed experimental plan.

a) Preparation of barium acrylate nanocomposites

b) Preparation of titania acrylate nanocomposites

c) Preparation of titanate acrylate nanocomposites

d) Preparation of lanthanum acrylate nanocomposites

3.2.1 Synthesis of Barium acrylate nanocomposites

The methodology involves the dispersion of barium precursor in the acrylate matrix and cinnamic acid as dispersing media. The evaluation of barium cinnamate and barium acrylate compositions was carried out for various properties. Preparation of barium containing nanocomposites involved various steps:

3.2.1.1 Preparation of barium acrylate nanocomposites

The first approach (Figure 3.4) pertains to the incorporation of inorganic form of barium as barium hydroxide into acrylic acid forming barium acrylate. The metal-acrylic acid compositions were polymerized using styrene as a co-monomer by gamma irradiation technology to obtain transparent and clear nanocomposites.

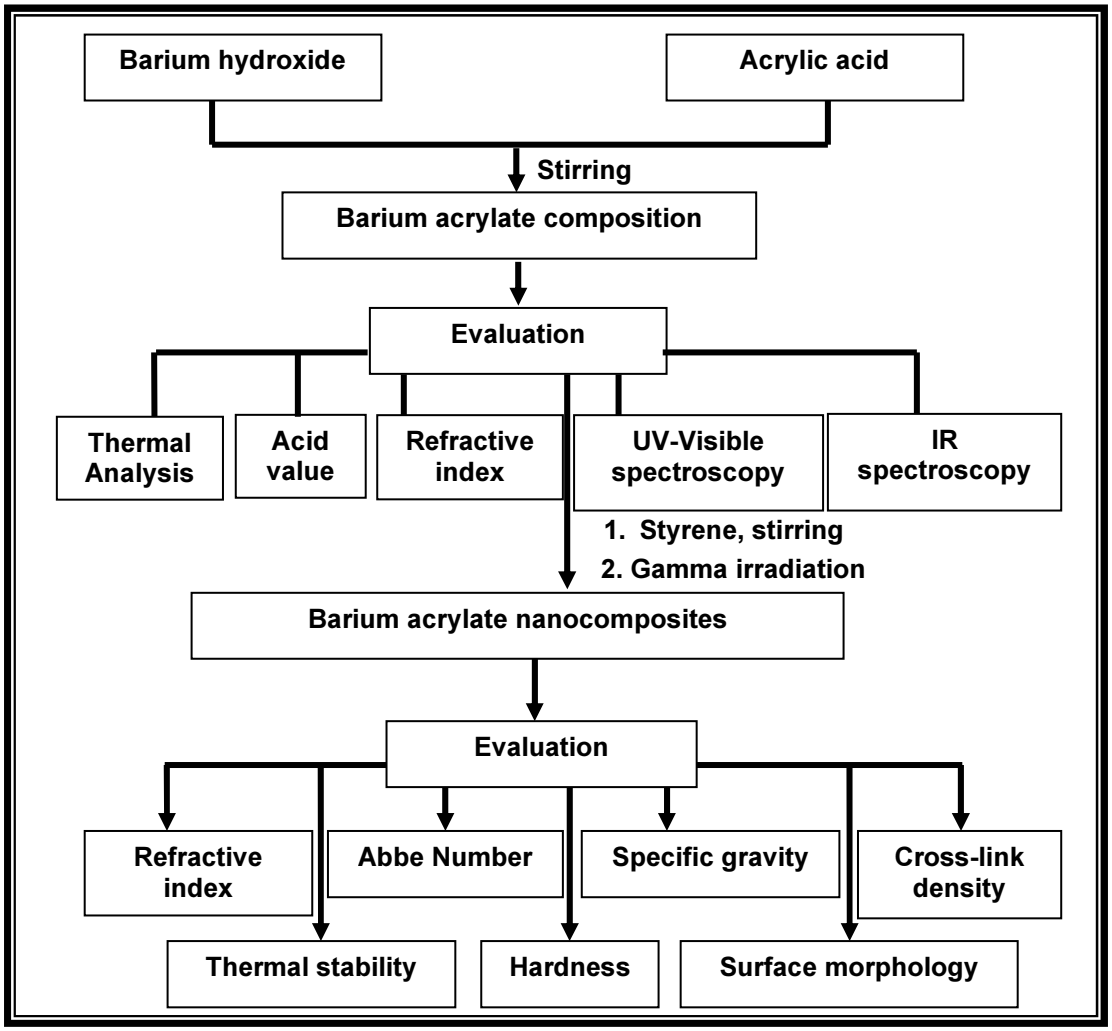

Figure 3.4: Methodology for the preparation and evaluation of barium acrylate nanocomposites. The methodology involved the dispersion of barium hydroxide in acrylic acid to form barium acrylate nanocomposites.

3.2.1.2 Preparation of barium cinnamate nanocomposites

The second approach (Figure 3.5) relates to the preparation of nanocomposites utilizing organic form of barium. Barium hydroxide is reacted with cinnamic acid in different molar ratios to yield barium cinnamate. The prepared barium cinnamate compositions were evaluated for various properties such as acid value, spectroscopic analysis, barium content (%), etc

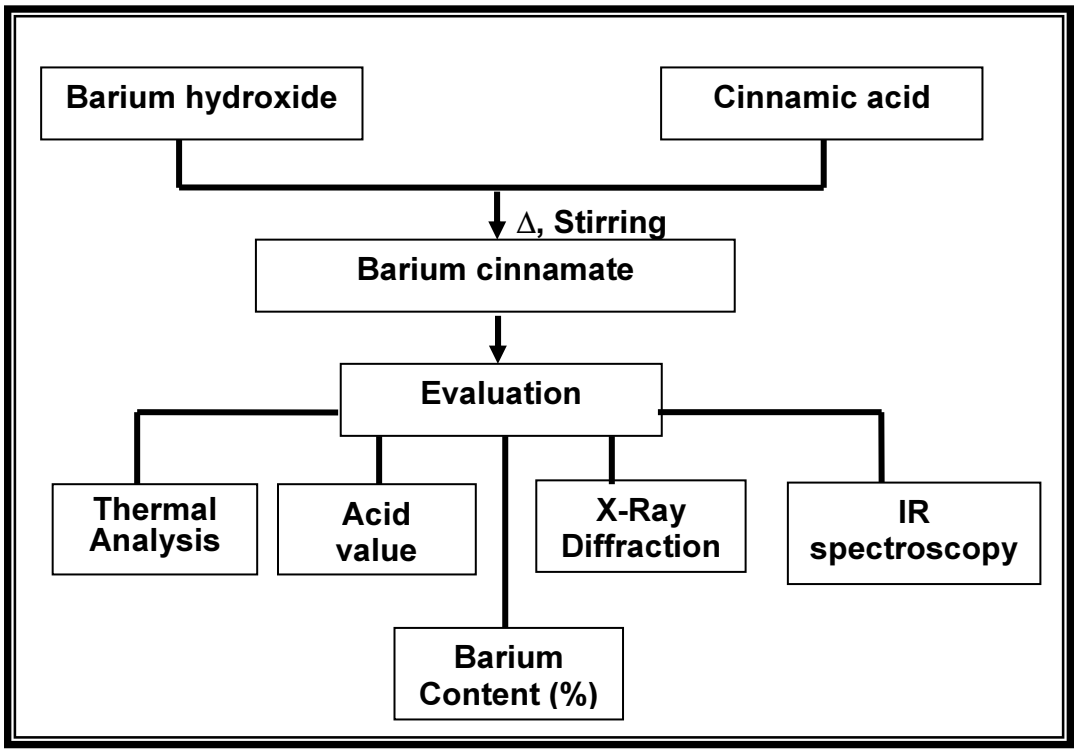

Figure 3.5: Methodology for the preparation and evaluation of barium cinnamate nanocomposites.

3.2.1.3 Preparation of barium cinnamate-barium acrylate-styrene nanocomposites

The third approach (Figure 3.6) followed to prepare barium containing nanocomposites was the simultaneous synthesis of barium acrylate and barium cinnamate and mixing the two in different ratios to achieve maximum dispersion of barium in acrylic acid. This was followed by polymerization through gamma irradiation using styrene as a co-monomer to obtain transparent and clear nanocomposites.

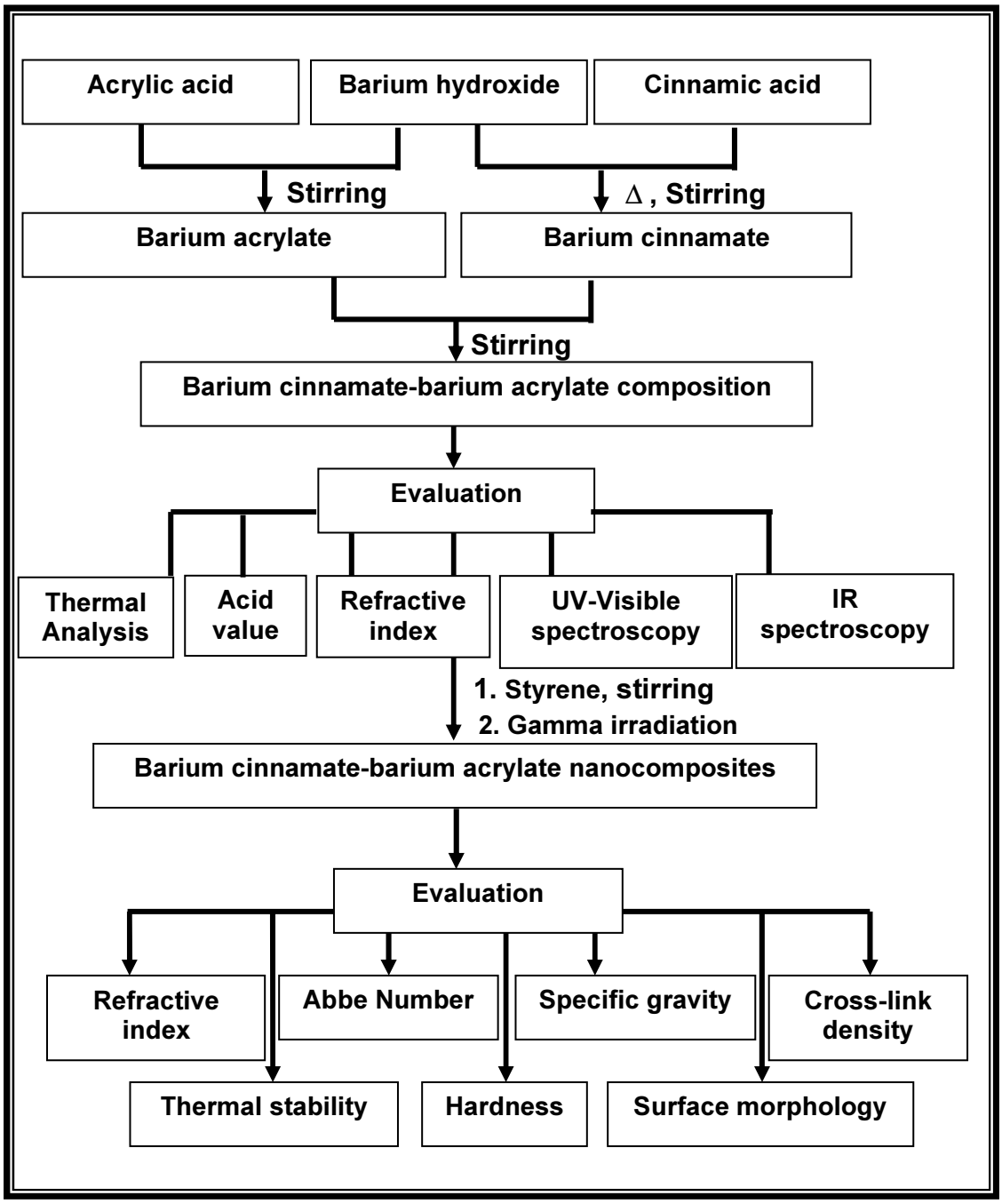

Figure 3.6: Methodology for the preparation and evaluation of barium cinnamate-barium acrylate nanocomposites. The methodology involved two steps, first is the preparation of barium acrylate composition and simultaneously, preparation of barium cinnamate. The second step involves their mixing and addition of styrene followed by radiation polymerization to form barium cinnamate-barium acrylate nanocomposite.

3.2.1.4 Preparation of cinnamic acid-acrylic acid- styrene polymers

The preparation of cinnamic acid-acrylic acid- styrene polymers as reference materials Figure 3.7 was carried out as per methodology described in Figure 3.7. It was carried out by the dispersion of cinnamic acid in acrylic acid. The cinnamic acid-acrylic acid compositions prepared were polymerized in the presence of styrene by gamma radiation technique.

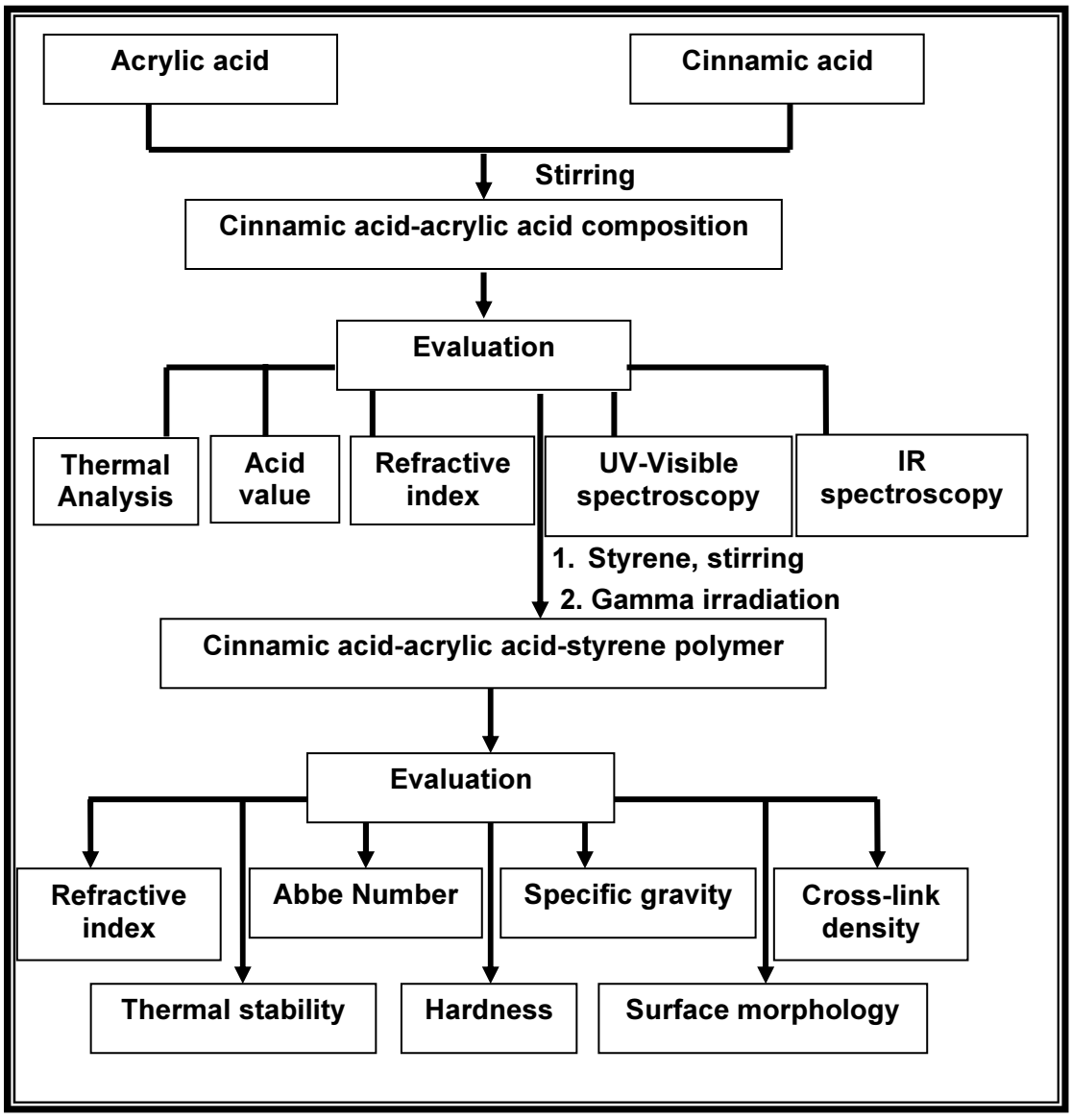

Figure 3.7: Methodology for the preparation and evaluation of cinnamic acid-acrylic acid- styrene polymer. The methodology involved the dispersion of cinnamic acid in acrylic acid to form cinnamic acid-acrylic acid- styrene polymer.

3.2.2 Synthesis of Titania Acrylate Nanocomposites

Dispersion of inorganic titanium compound was carried out in acrylic acid and 2-hydroxyethyl methacrylate (HEMA) as dispersing media to obtain nanodispersed titania acrylate compositions. Titanium in the form of titania (TiO_2) was dispersed in the dispersing media. Both ex-situ and in-situ methods were employed to disperse nanoparticles of titania in the dispersing media to prepare nanodispersed titania acrylate compositions.

3.2.2.1: Ex- situ Synthesis and Dispersion of Nanoparticles of Titanium Dioxide into Acrylic acid to form Nanodispersed Titania Acrylate Compositions

Ex-situ synthesis of nanoparticles of titania were carried out by acid and base hydrolysis of titanium precursor. The effect of pH on the particle size of titania was studied by carrying out the hydrolysis of titanium precursor in the presence of an acid and a base. Nanoparticles of titania were analyzed for various parameters. Fusion of titania was also carried out to bring titania into solution form before dispersing it in acrylic acid. The methodology followed for the preparation of nanoparticles of titania and their dispersion is presented in Figures 3.8, 3.9 and 3.10.

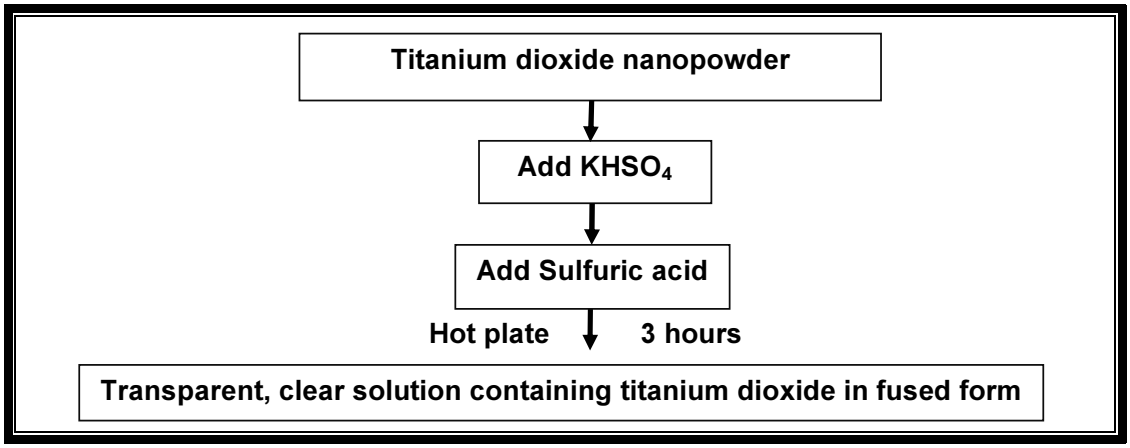

Figure 3.8: Methodology for the preparation of nanodispersed titanium acrylate compositions. The methodology involved fusion of nanoparticles of titanium dioxide to bring them into solution form before dispersion in acrylic acid.

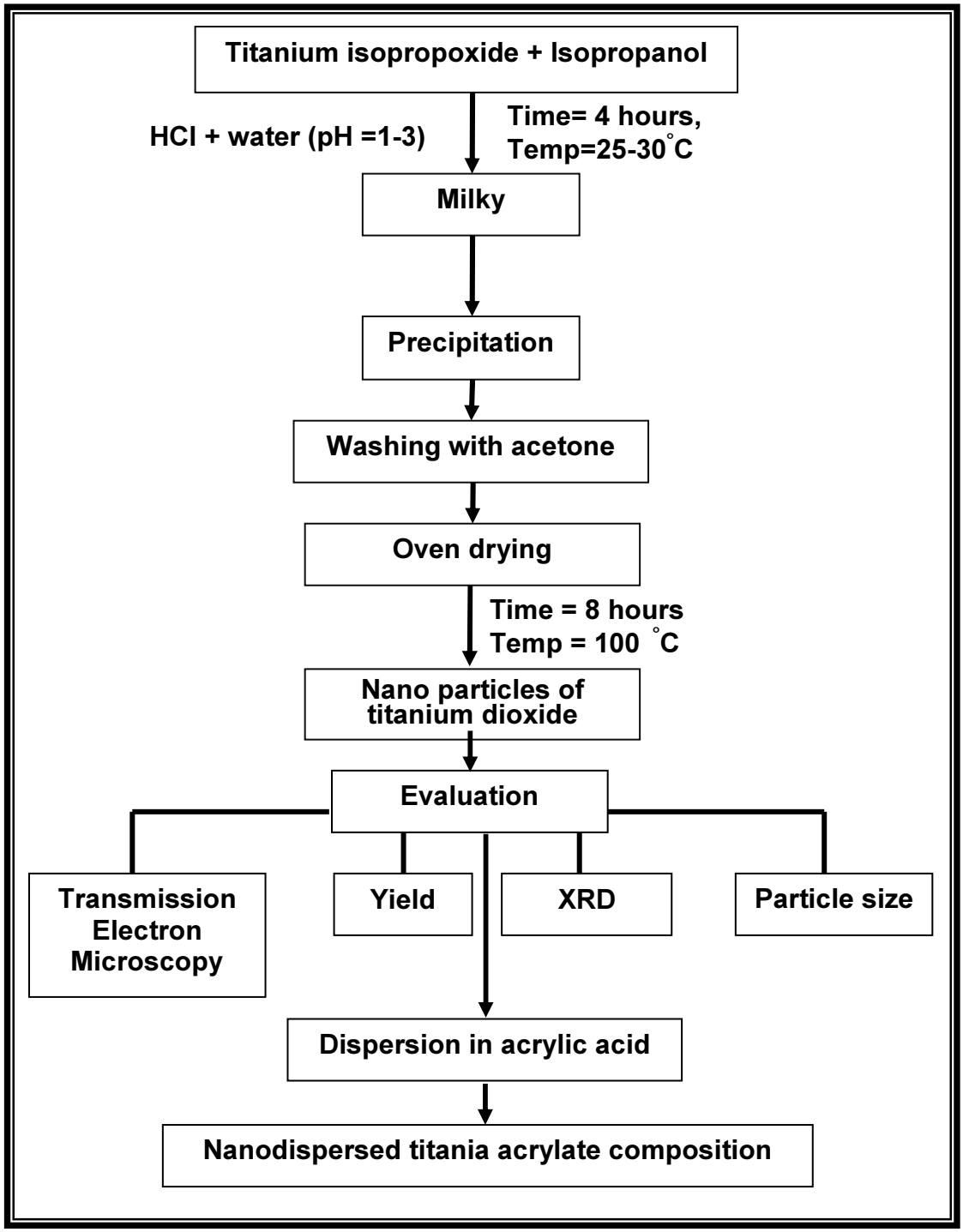

Figure 3.9: **Methodology for the preparation of nanodispersed titania acrylate compositions. The methodology involved acid hydrolysis of titanium isopropoxide resulting in the formation of nanoparticles of titanium dioxide.**

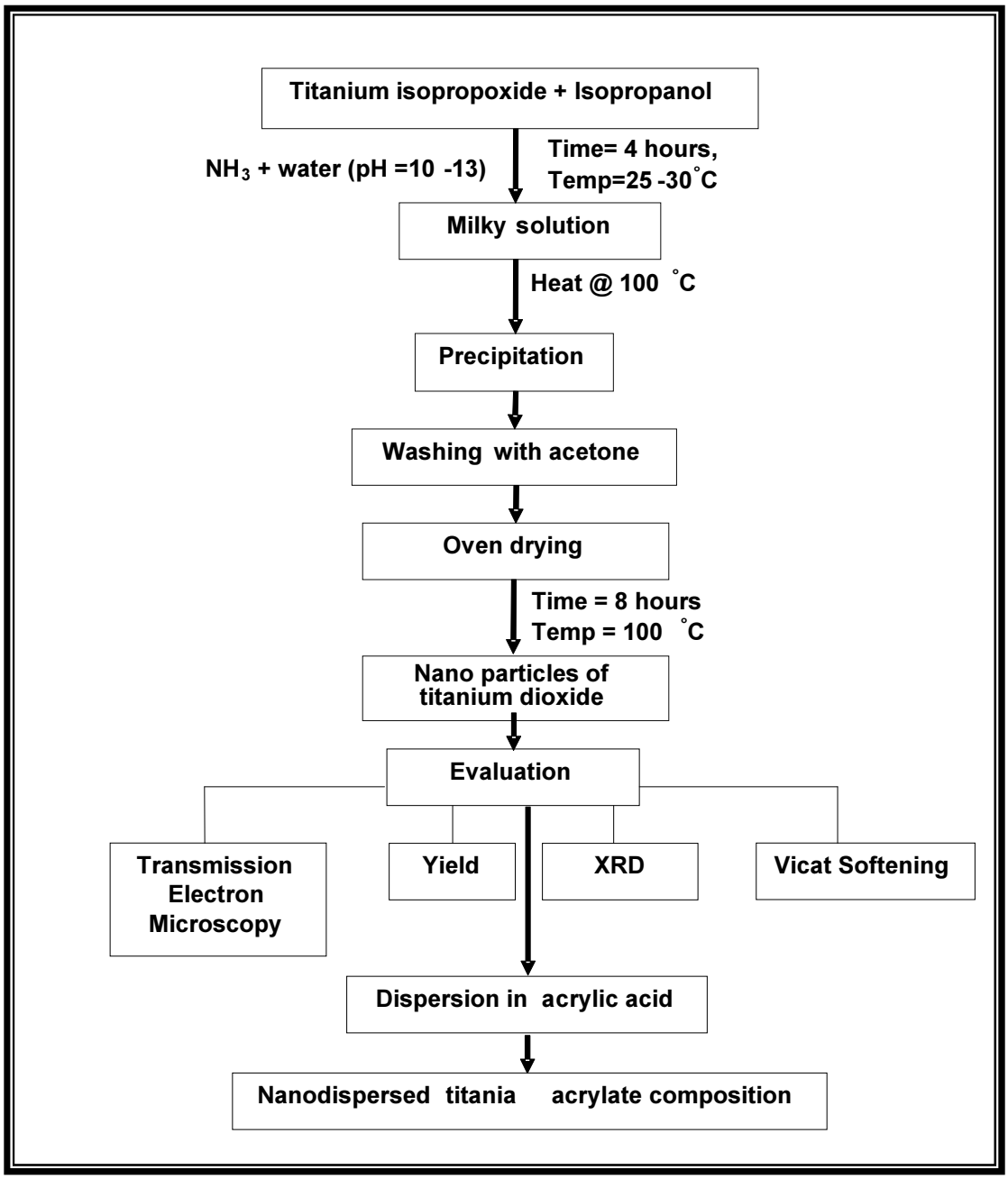

Figure 3.10: Methodology for the preparation of nanodispersed titania acrylate compositions. The methodology involved base hydrolysis of titanium isopropoxide resulting in the formation of nanoparticles of titanium dioxide

3.2.2.2 In-situ Synthesis and Dispersion of Nanoparticles of Titanium Dioxide into Acrylate Dispersion Media to form Titania Acrylate Nanocomposites

In-situ synthesis of nanoparticles of titanium dioxide was carried out by the dispersion of titanium tetrachloride in HEMA as dispersing media. The in-situ preparation and dispersion of nanoparticles of titanium dioxide was done in single step. The prepared nanodispersed titania acrylate compositions were evaluated for various properties. The methodology for the preparation of nanodispersed titania acrylate compositions is shown in Figure 3.11.

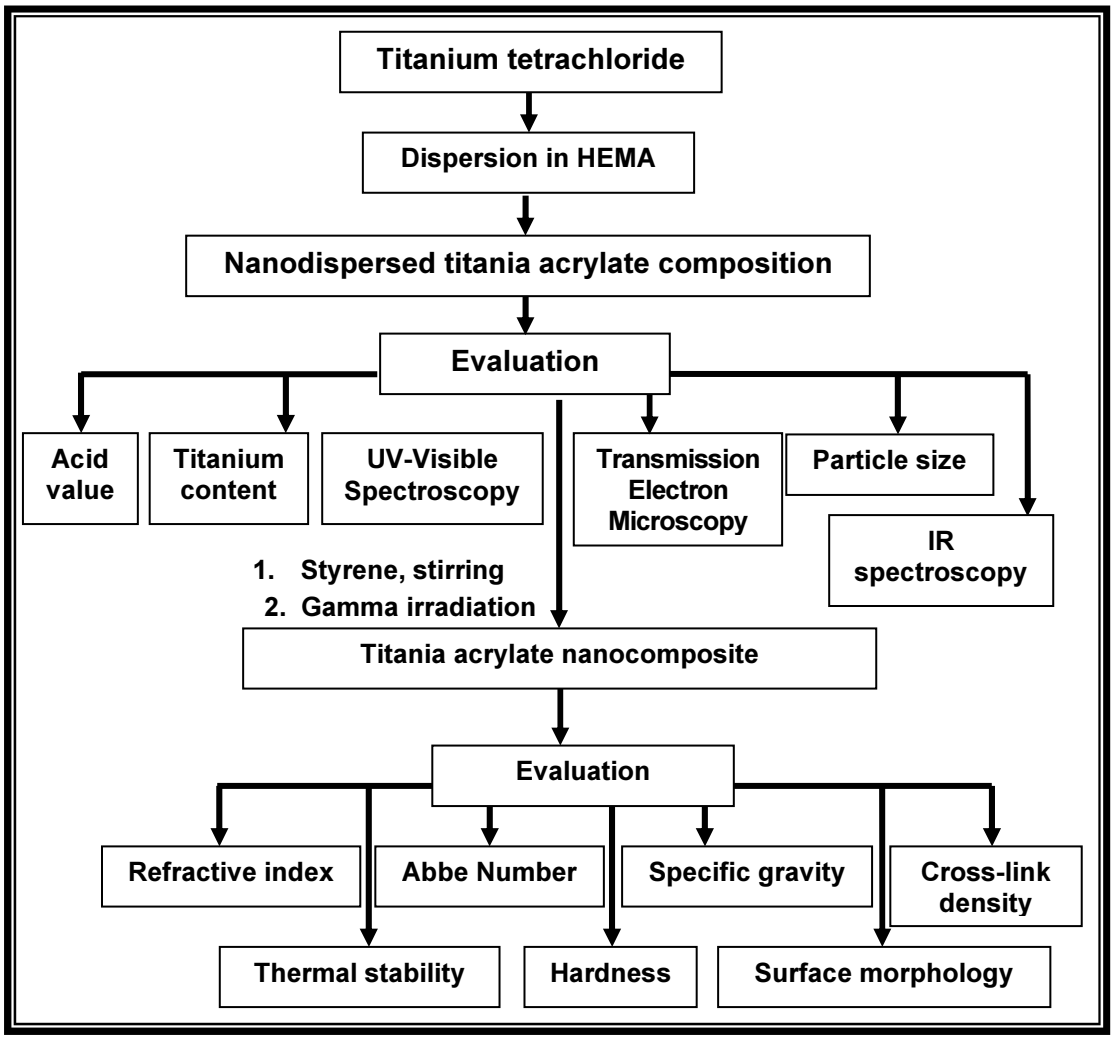

Figure 3.11: Methodology for the preparation of titania acrylate nanocomposites. The methodology involved in-situ preparation and dispersion of nanoparticles of titanium dioxide in HEMA.

3.2.3 Synthesis of Titanate Acrylate Nanocomposites

The dispersion of organic titanium compounds in acrylic acid was carried out as dispersing medium to obtain nanodispersed titanate acrylate compositions. Six organic titanates were dispersed in acrylic acid to prepare nanodispersed titanate acrylate compositions followed by polymerization. The methodology adopted for the synthesis of titanate acrylate nanocomposites is given in Figure 3.12.

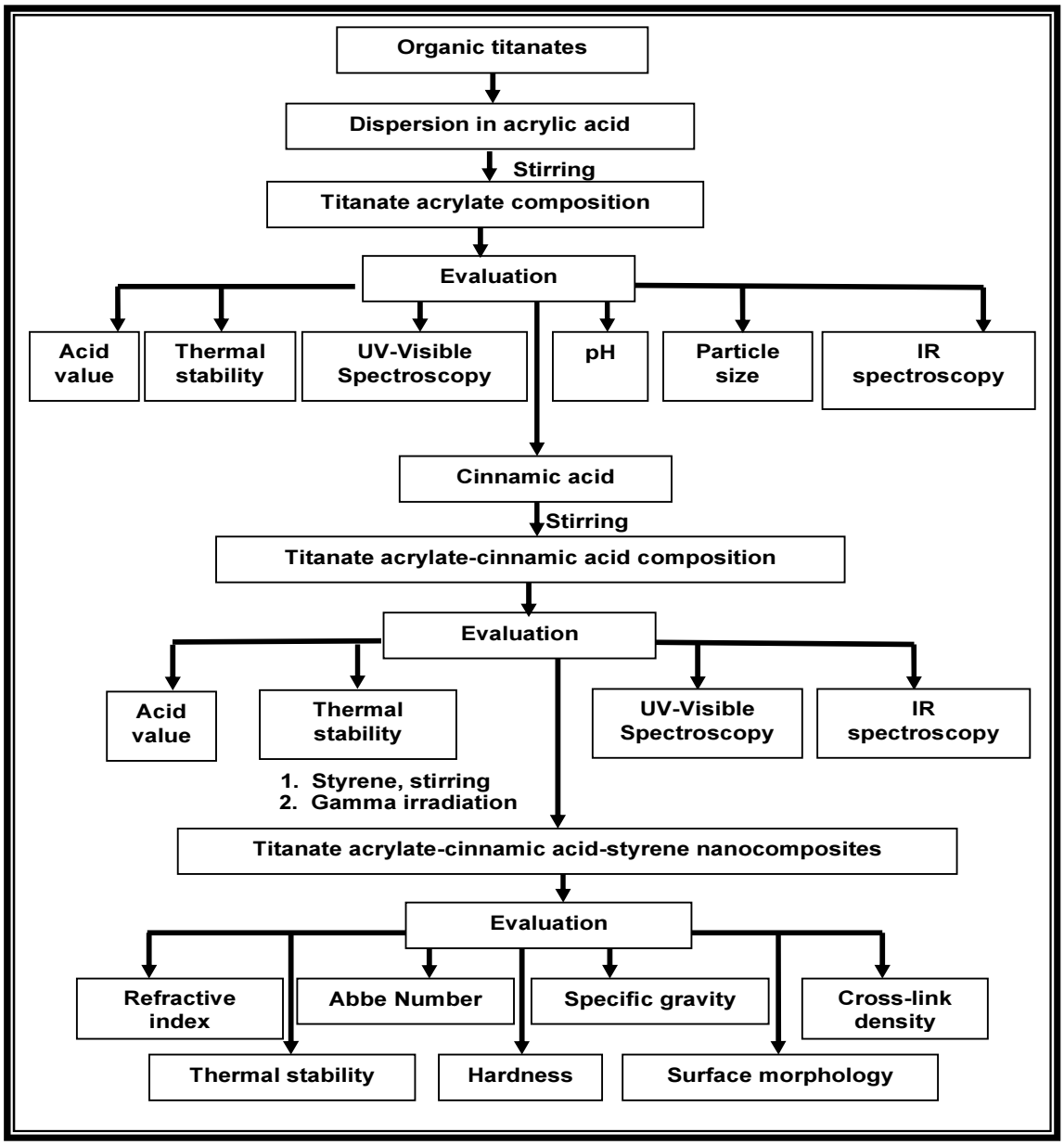

Figure 3.12: Methodology for the preparation of titanate acrylate-cinnamic acid-styrene nanocomposites. The methodology involved dispersion of organic titanates in acrylic acid to yield titanate-containing nanocomposites.

3.2.4 Synthesis of Lanthanum Acrylate Nanocomposites

The methodology pertains to the dispersion of lanthanum compound in acrylic acid as a dispersing medium to obtain nanodispersed lanthanum acrylate compositions (Figure 3.13). The in-situ preparation and dispersion of nanoparticles of lanthanum was done in single step.

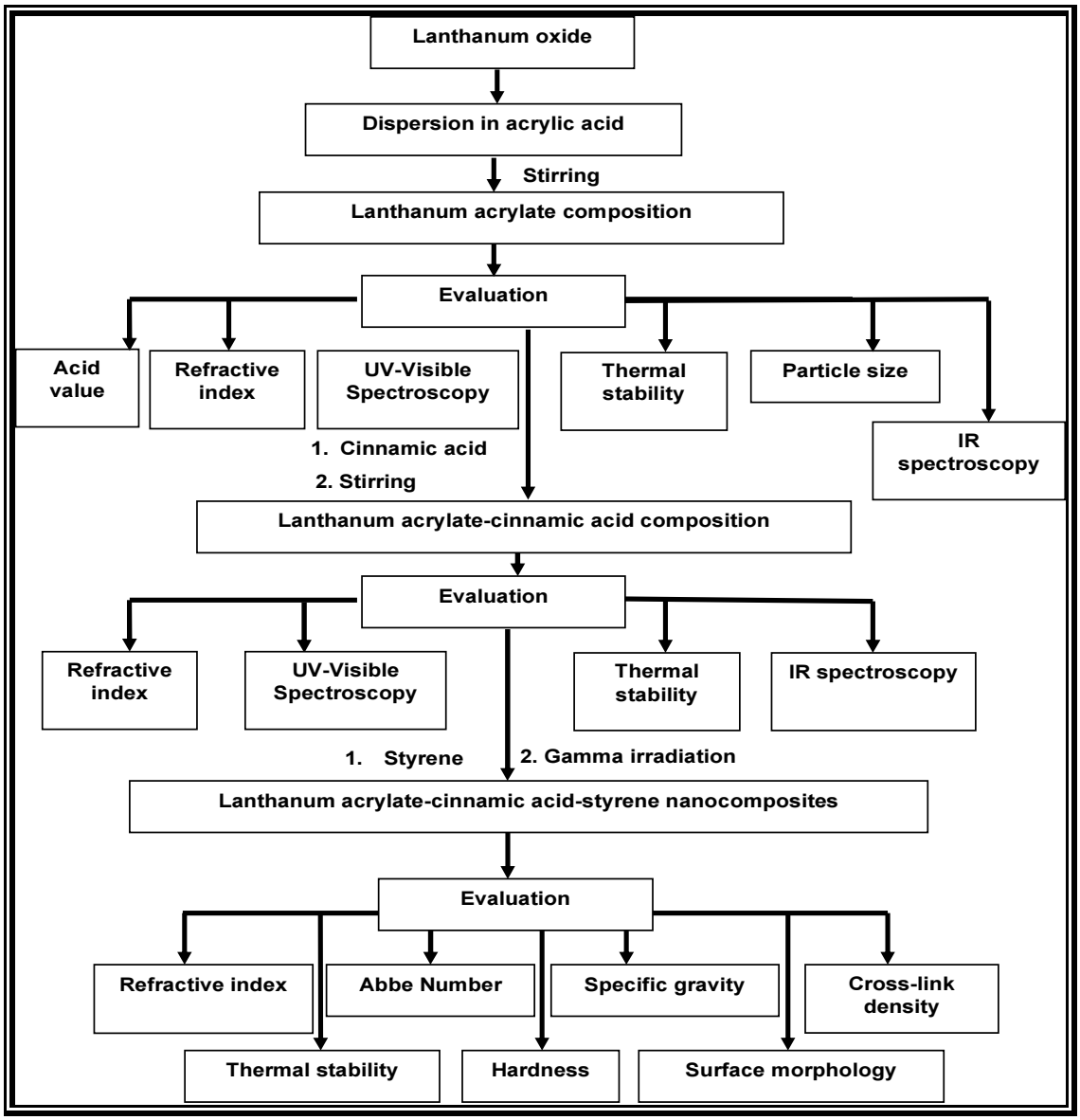

Figure 3.13: Methodology for the preparation and evaluation of lanthanum acrylate-cinnamic acid-styrene nanocomposites. The methodology involved single step dispersion and formation of nanoparticles of lanthanum oxide in acrylic acid to form lanthanum-containing nanocomposites.

The prepared nanodispersed lanthanum acrylate compositions were evaluated for various properties. Further, these compositions were cast polymerized by gamma irradiation into clear and transparent nanocomposites.

3.3 CHARACTERIZATION AND EVALUATION OF ACRYLIC NANOCOMPOSITES

Acrylic polymers were characterized by using various methods and instruments. The analysis of optical properties, thermal properties and physico-mechanical properties of the systems described above was carried out. The methods adopted for analysis and the instruments used are described as follows:

3.3.1 Optical Properties

3.3.1.1 Refractive index

Refractive index **[369]** was determined by using Abbe refractometer as shown in Figure 3.14. Refractive index (n) was calculated using the following formula as given in Equation 1:

$$n = \frac{\sin i}{\sin r} \qquad \text{(Equation 1)}$$

where, n = refractive index; i = angle of incidence ; r = angle of refraction.

Figure 3.14: Abbe refractometer

3.3.1.2 Abbe Number

Abbe number **[369]** was determined by using Abbe refractometer as shown in Figure 3.14. Abbe number was calculated using the following formula in Equation 2:

$$\nu_d = \frac{n_D - 1}{n_F - n_C} \qquad \text{(Equation 2)}$$

where ν_d = Abbe number

n_D = Refractive index for λ_d = 589.2 nm

n_F = Refractive index for λ_f = 486.10 nm

n_C = Refractive index for λ_c = 656.3 nm

3.3.1.5 UV-Visible Spectroscopy

The UV-Visible spectroscopy of the cast lenses in the UV-Visible region of 200nm to 800 nm was determined on the UV-Visible spectrophotometer (Model no. UV-1700) procured from Shimadzu **[370-371]**.The schematic diagram of the UV-Visible spectrophotometer is described in Figure 3.15.

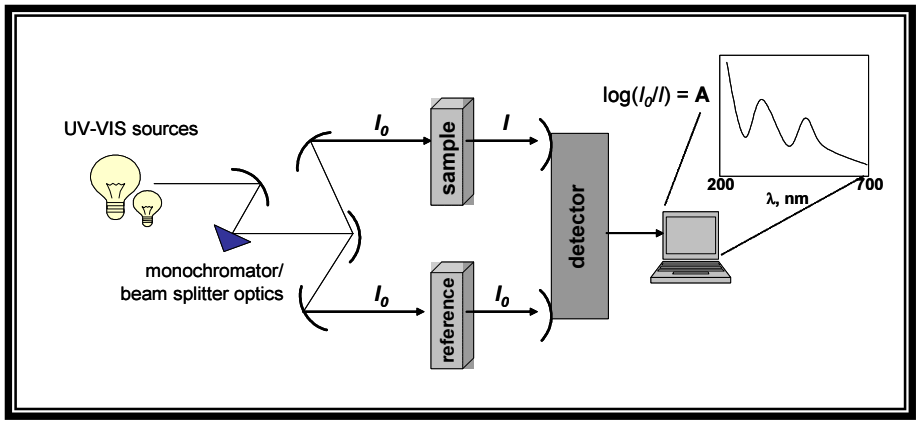

Figure 3.15: Schematic diagram of UV-Visible Spectrophotometer

3.3.2 Thermal Analysis

3.3.2.1 Differential Scanning Calorimetry (DSC)

DSC was used to characterize the nature of interactions between the various constituents of the metal containing polymers and to determine

the thermal stability of compositions used for polymerization. For DSC studies, model 2910 (Figure 3.16) of TA Instruments, USA was used.

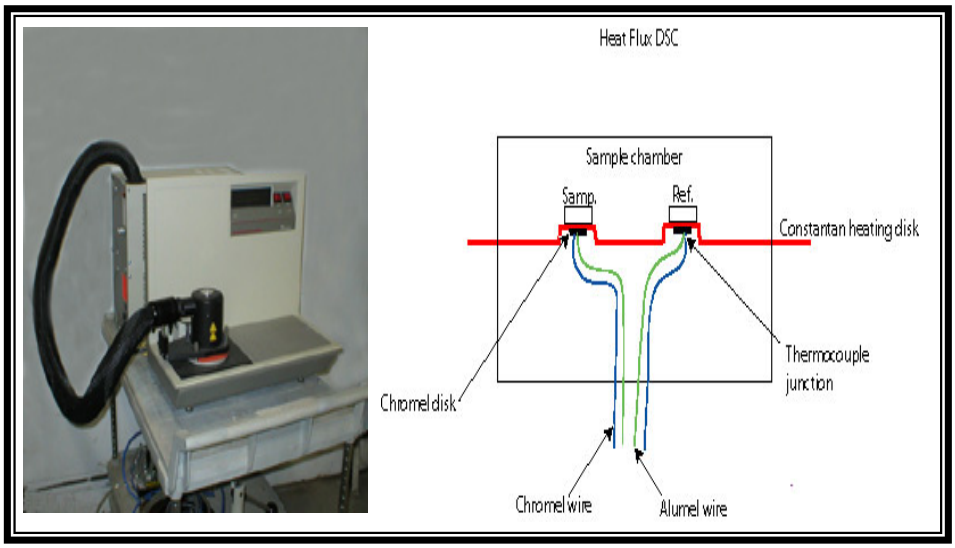

Figure 3.16: DSC instrument (DSC-2910) and sample chamber

3.3.2.2 Thermogravimetric Analysis (TGA)

For TGA, DTA and DTG studies, model 2960 (Figure 3.17) of TA Instruments, USA was used. TGA was used to study the thermal stability of metal dispersed compositions and metal containing polymers. The TGA studies were carried out in nitrogen atmosphere with operating temperature ranging from room temperature to 700 $^{\circ}$C.

Figure 3.17: Thermogravimetric analyzer instrument (SDT-2960)

3.3.2.3 Vicat Softening Temperature

Vicat softening temperature was determined to find out the working temperature of the sample by ASTM D-1525 **[372].**

3.3.3 Physico-mechanical Analysis

3.3.3.1 Impact strength

Impact strength was determined using impact tester (Figure 3.18) fabricated as per FDA 21 CFR 801.410 **[373],** where a steel ball weighing 16.2 g was dropped from a height of 127 cm upon the horizontal upper surface of the lens. Lenses which did not crack or break were taken to be impact resistant.

Figure 3.18: Impact tester

3.3.3.2 Scratch Resistance

Scratch resistance was determined as per ASTM D-3363 **[374].** Pencils of different hardness were used to scratch the surface of the lens. This process was started with the hardest pencil and continued down. The scale of hardness where it left no scratch mark on the tested specimen was noted down as scratch hardness.

3.3.3.3 Shore–D hardness

Shore-D hardness of the acrylic polymers were measured using the Durometer (Figure 3.19) of Hiroshima Instruments, Japan as per ASTM D-2240 **[375].** The hardness value was determined by the penetration of the indenter of the Durometer into the sample.

Figure 3.19: Shore-D Hardness Tester

3.3.3.4 Machinability

Machinability, i.e. ability to cut and grind, of acrylic polymers was carried out on a lathe cutting machine. Polishing of lens blanks was carried out by rubbing the surface of polymers on emery paper of various grades. Polishing was done on a rotating wheel fitted with a velvet cloth in the presence of micropolished alumina powder (0.3 micron) procured from Buehler (USA).

3.3.4 Minerological Study

3.3.4.1 X-Ray Diffraction (XRD)

XRD analysis yields the atomic structure of materials and is based on the elastic scattering of X-rays from the electron clouds of the individual atoms in the sample. It is used to characterize the crystallographic structure and size (Figure 3.20).

Figure 3.20: X-Ray Diffraction instrument

XRD studies of acrylic polymers were carried out on Phillips Analytical X-ray.

3.3.5 Morphological study

3.3.5.1 Scanning Electron Microscopy (SEM)

The SEM analysis of the acrylic polymers was carried out to analyze the surface morphology of the polymer. SEM model Leo 435 VP was used to carry out the study (Figure 3.21).

Figure 3.21: Scanning Electron Microscope Instrument

3.3.5.2 Transmission Electron Microscopy (TEM)

Monomer compositions and prepared nanoparticles have been evaluated by TEM using Morgagni 268D to study the magnitude of the nanoparticles formed in the composition (Figure 3.22).

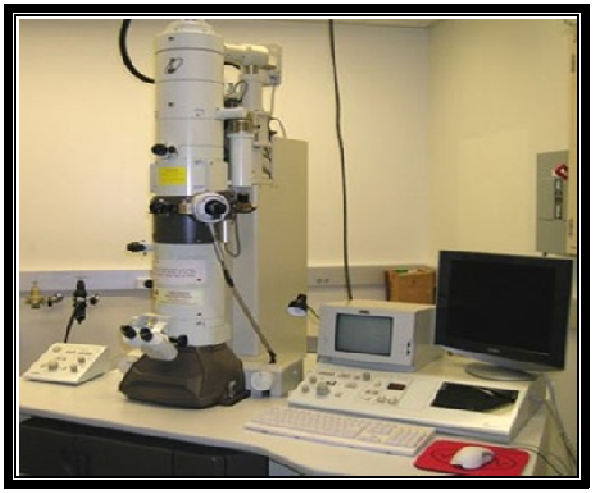

Figure 3.22: Transmission Electron Microscope

3.3.6 Spectroscopic Analysis

3.3.6.1 Infra-red Spectroscopy

Metal containing acrylate compositions were studied under infrared radiation to understand the structural changes taking place between the functional groups and metals. The results could be manifested on the basis of the characteristic of the bond formed. The FTIR Spectrophotometer FTIR-ATR BOMEM (FTLA 2000) in transmittance mode from 4000–400 cm^{-1} was used (Figure 3.23).

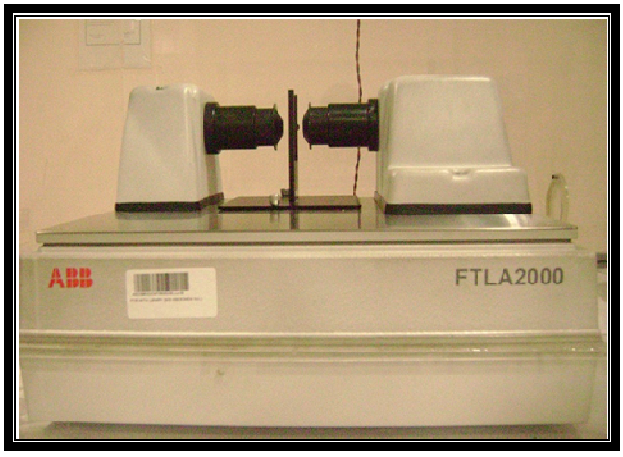

Figure 3.23: Infra-red Spectrophotometer

3.3.7 Other properties

3.3.7.1 Metal content

Content of metals such as barium, titanium and lanthanum in acrylic polymers was analyzed by Inductively Coupled Plasma (ICP-OES, VISTA-MPX ELO6033904) of Varian, Australia (Figure 3.24).

Figure 3.24: Inductively Coupled Plasma-Optical Emission Spectrometer (ICP-OES)

3.3.7.2 Cross-link density

Cross-link density is used to determine the extent of crosslinking in a polymer. It is determined by ASTM D-2765 **[376]**. Chloroform was used as a solvent for extraction studies. In this method, swell ratio and extract percentage was evaluated to determine the percentage of cross-link density as given in Equation 3-4.

$$\text{Extract \%} = C / D \times 100 \quad \text{(Equation 3)}$$

Where, C=weight (in grams) of solvent entrapped in gel
D= weight (in grams) of original sample

$$\text{Cross link density (\%)} = 100 - \text{Extract \%} \quad \text{(Equation 4)}$$

3.3.7.3 Leachability

Leachability tests were carried out in acids such as nitric acid and sulfuric acid. The samples were dipped in acid for 12 hrs; SO_2 and NO_2 were removed by diluting the solution with water and boiling the solution. The presence of barium, titanium and lanthanum was analyzed by Inductively Coupled Plasma (ICP). The presence of free barium, titanium and lanthanum in the nanocomposites was analyzed by Inductively Coupled Plasma (ICP-OES, VISTA-MPX ELO6033904) of Varian, Australia (Figure 3.24).

3.3.7.4 Particle Size Analysis

Particle size and particle size distribution were analyzed by Particle Size analyzer nano-sizer by Metrohm Inc. (Figure 3.25).

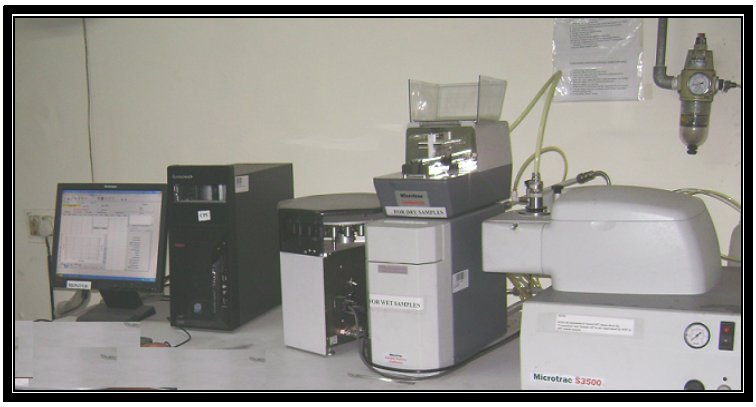

Figure 3.25: Particle Size Analyzer

3.3.7.5 Acid value

Acid value is determined by directly titrating the material in an alcoholic medium with aqueous sodium or potassium hydroxide solution as per IS 548 (Part I):1964 **[377]**. Acid value is determined by Equation 5.

$$\textbf{Acid value} = (56.1 \times V \times N) / W \quad \text{(Equation 5)}$$

Where V = Volume of standard KOH or NaOH used (in ml)
N = Normality of standard KOH or NaOH prepared
W = Weight of the sample (in grams)

3.3.7.6 Water absorption

Water absorption studies of acrylic nanocomposites were carried out by soaking the sample in water for 72 hrs for complete absorption of water. The percentage of water absorbed was calculated as given in Equation 6.

$$\text{Water absorption (\%)} = [(W_2 - W_1) / W_1] \times 100 \quad \text{(Equation 6)}$$

Where W_1 = Weight of the sample before water absorption (in grams)

W_2 = Weight of the sample after water absorption (in grams)

3.4 CONCLUSIONS

From the above discussion, the following conclusions can be drawn:

a) Novel methodologies for the synthesis of barium, titanium and lanthanum containing polymers have been developed.

b) The basic parameters such as refractive index, acid value, particle size, etc. will be useful to confirm the formation of monomer compositions.

c) Particle size analysis will be useful for determining the particle size of the dispersions.

d) Transmission Electron Microscopy (TEM) is useful to study the presence and dispersion of the nanoparticles of metals in the monomer compositions.

e) Instrumental techniques such as TGA/DTA and DSC are useful to study the thermal properties of the acrylic polymers. These parameters will be used to study the interactions involved in the formation of the acrylic polymers.

f) Vicat softening temperature is useful to determine the working temperature of the acrylic polymers.

g) Cross-link density is useful to determine the extent of cross-linking in the acrylic polymers.

h) The extent of polymerization and dose optimization was studied by carrying out leachability studies of the acrylic polymers in various acids.

i) XRD analysis is useful to study the crystal structure of the acrylic polymers.

j) Infra-red spectroscopic analysis is useful for structural elucidation of the polymers by studying the various bonds that are formed in the acrylic polymers.

k) Scanning Electron Microscope (SEM) is useful to study the surface morphology of the acrylic polymers.

Chapter 4

Barium–Containing Nanocomposites based on Acrylates & Cinnamates

CHAPTER 4
BARIUM–CONTAINING NANOCOMPOSITES BASED ON ACRYLATES & CINNAMATES

4.0 INTRODUCTION

Acrylic acid and cinnamic acid are an important class of compounds which form the building blocks for the production of some of the commonly used industrial and consumer products. Acrylic acid and acrylates are essential ingredients in paints, coatings, textiles, adhesives, plastics and other applications. The unique attributes of the structure of acrylic acid are due to the fact that it is a molecule of small size having a carboxylic acid for derivatization and a double bond for linkages of monomers.

One of the most well known applications of acrylates is in the optical industry where polyacrylates such as polymethyl methacrylates, phenyl ethyl acrylate, phenyl ethyl methacrylate are some of the acrylates used for optical applications and are obtained by the esterification of acrylic acid with alcohols having varying alkyl chain length. This means that one can design the polyalkyl acrylates by varying the alcohol structure. A large range of polyacrylates have already been in use for various applications. Here, it must be noted that the whole range has yet to be developed.

Cinnamic acid has been widely studied because of its very specific structure. The carboxylic acid group is separated from the aromatic ring by a double bond and causes conjugation between the C=C bond and the π-electron system. It has two different donor sites to form bonds with the metal ions: the double bond between the carbon atoms and the oxygen atoms of the carboxylic acid group **[378-380]**. Cinnamic acid has two different donor sites for forming bonds with metal ions: the double bond between the carbon atoms and the oxygen atoms of the carboxylic acid group **[381]**. Cinnamic acid and cinnamates are used in flavours and pharmaceutical industries.

Exploitation of cinnamates for optical applications has not been reported as far as the literature review conducted by us. This is so, inspite of the fact that the presence of an aromatic ring in the structure of cinnamic acid is characterized by a high intrinsic molar refraction which is responsible for the high refractive index (1.555). The only reason for this could be the fact that cinnamic acid exists in solid form at room temperature. Besides its use as a co-monomer for the synthesis of various industrial products, they are also an important raw material for food industry **[382]**. If not as such, can cinnamates be used along with other monomers like acrylic acid, was the idea considered worth trying and hence, this study.

While all the essential properties of polyacrylates are in order to make them suitable for optical applications, the main limitation hindering their use pertains to the inferior refractive index of acrylic acid. In order to exploit the potential of polyacrylates, it is utmost essential that the basic structure of acrylic acid is modified. This can be done by way of introducing moieties that can enhance the refractive index. Since carboxylic acid group can be used for this purpose, there can be two possible ways to achieve this objective. First, derivatize acrylic acid with molecules having groups like hydroxyl molecules. Secondly, the carboxylic acid group can be attached (reacted) with entities like metal ions to achieve the desired results.

In the present work, novel cinnamates have been synthesized and their use for high refractive index optical plastics has been studied.

Modification of low refractive index polymers for high refractive index applications can be done by the introduction of moieties having a high bond refraction value. Amongst the organic moieties, benzene ring is characterized by a high intrinsic molar refraction (26.14). Therefore, modification of acrylic acid and acrylates with the introduction of such organic groups is desirable. Cinnamic acid belonging to the group of aromatic carboxylic acids is a candidate for the modification of refractive index of acrylic acid; it is expected that the refractive index of acrylic acid will increase significantly by the introduction of benzene ring.

Another methodology followed for the improvement of refractive index is the introduction of metal atoms having a low ionic size and high polarizability which would lead to a high refractive index. Such metals are dispersed in the polymer matrix to form nanocomposites having good transparency and clarity desired for optical applications.

The challenging task of modifying the refractive index of acrylic acid and converting it into high refractive index material was taken up in the present study. The novelty of the present work lies in the fact that high refractive index metals as well as the aryl functional group (benzene ring) were introduced in acrylic acid.

Nanocomposites of metal containing acrylates and metal containing cinnamates were developed and their suitability for optical applications was studied in detail. Barium belongs to group II A of the periodic table having an ionic size of 1.36 Å and polarizability of 39.7$Å^3$. It was dispersed in the form of barium hydroxide in acrylic acid to form barium acrylate and in cinnamic acid to form barium cinnamate. Barium cinnamate was, in turn, dispersed in acrylic acid to form barium cinnamate-acrylate and barium acrylate to form barium cinnamate barium acrylate compositions. These were then polymerized to form cross-linked structure of poly (barium cinnamate-barium acrylate).

The study was carried out with the experimental plan as described below:

a. Preparation of barium acrylates and converting them into cast polymerized lenses. Characterization of the base material as well as the final product (lenses) was carried out.

b. Preparation of barium cinnamates and converting them into cast-polymerized lenses. Characterization of the base material as well as the final product was carried out.

c. Preparation of cast polymerized lenses using the combination of barium acrylate and barium cinnamates and their characterization.

d. Preparation of cast polymerized lenses of acrylic acid-cinnamic acid-styrene without barium was done to use it as a reference for the study.

The description of each part of the study as listed above is given in the following section:

4.1 PREPARATION OF BARIUM ACRYLATE NANOCOMPOSITES

4.1.1 Dispersion of barium hydroxide in acrylic acid

Effect of dispersion of barium hydroxide on the properties of acrylic acid were studied at regular intervals. Acrylic acid (a weight amount) was taken in a round bottom flask fitted with overhead stirrer and condenser as described in Chapter 3. Under constant stirring, barium hydroxide was added gradually to it at ambient temperature. The compositions with clear and transparent dispersions of barium hydroxide were studied for various properties such as refractive index, transparency, thermal stability, etc.

4.1.2 Cast Polymerization of barium acrylate

Cast polymerization of above prepared dispersions into lenses using gamma irradiation was carried out. For this, styrene was used as a co-monomer for polymerization to obtain transparent and clear lenses. Styrene was added in varying amounts and the effect of addition of styrene on polymerization was studied by the physico-chemical evaluation of the compositions prepared. Various essential parameters for refractive index, Abbe number, hardness, specific gravity and transparency were evaluated for the final product (lenses). The dose of gamma irradiation was optimized by subjecting the compositions to gamma irradiation from 10 kGy-30 kGy.

4.2 PREPARATION OF BARIUM CINNAMATE NANOCOMPOSITES

4.2.1 Dispersion of barium hydroxide in cinnamic acid

Infact as described for acrylic acid, dispersion of barium hydroxide was done in cinnamic acid. Because of the fact that cinnamic acid was a solid at room temperature, the incorporation of barium hydroxide was done in molten cinnamic acid. Barium hydroxide was added gradually to cinnamic acid in

liquid state maintaining the temperature 140 °C – 145 °C resulting in the formation of barium cinnamate.

Barium hydroxide dispersed cinnamic acid composition of varying contents of barium was characterized for barium content, acid value, thermal stability and structure elucidation.

4.2.2 Cast Polymerization of barium cinnamate

Cast polymerization of barium cinnamate into lenses using gamma irradiation was carried out. For this, styrene was used as a co-monomer for polymerization to obtain transparent and clear lenses. Styrene was added in varying amounts and the effect of addition of styrene on polymerization was studied by the physico-chemical evaluation of the compositions prepared. The dose of gamma irradiation was optimized by subjecting the compositions to gamma irradiation from 10 kGy-30 kGy.

4.3 PREPARATION OF BARIUM CINNAMATE-BARIUM ACRYLATE NANOCOMPOSITES

4.3.1 Synthesis of barium acrylate and barium cinnamate

Barium acrylate and barium cinnamate were synthesized as described in above Sections 4.1.1 and 4.2.1 respectively.

4.3.2 Dispersion of barium cinnamate in barium acrylate

Barium cinnamate was added gradually to barium acrylate till the point where no separation of barium cinnamate took place. The transparent and clear solutions obtained were evaluated for various properties such as refractive index, thermal stability, particle size, etc.

4.3.3 Cast polymerization of barium acrylate-barium cinnamate

Cast polymerization of barium acrylate-barium cinnamate compositions was carried out by the addition of styrene as a co-monomer and cast polymerized into nanocomposites by gamma irradiation. The effect of styrene and dose of radiation on the nanocomposites were studied. The nanocomposites were evaluated for various properties such as refractive index, Abbe number, surface morphology, specific gravity, etc.

4.4 PREPARATION OF CINNAMIC ACID-ACRYLIC ACID POLYMERS

4.4.1 Dispersion of cinnamic acid in acrylic acid

Cinnamic acid was dispersed in acrylic acid by the gradual addition of cinnamic acid to acrylic acid under continuous stirring at room temperature. Cinnamic acid was dispersed in acrylic acid till no precipitation of cinnamic acid takes place. The compositions obtained after the dispersion of cinnamic acid were clear and transparent and were evaluated for various properties such as refractive index, transmittance, acid value, etc.

4.4.2 Cast Polymerization of cinnamic acid-acrylic acid compositions

Compositions of cinnamic acid-acrylic acid were cast polymerized into lenses using styrene as co-monomer, by gamma irradiations. The effect of amount of styrene on the polymerization of compositions was studied. Optimization of the dose of gamma irradiation was carried out. Transparent, hard and clear polymers were obtained which were evaluated for refractive index, Abbe number, hardness, specific gravity, etc.

RESULTS & DISCUSSION

Results of various studies performed during the preparation of barium-containing nanocomposites are presented in this section. Observations for various parameters at different stages of the study are discussed.

Following studies were performed during the preparation of barium-containing nanocomposites

- Transmittance and clarity of dispersion
- Acid value
- UV-Visible spectroscopy
- Infrared spectroscopy
- Shore-D hardness
- Refractive index
- Thermal analysis
- Pencil hardness
- Transmittance
- Refractive index
- pH
- Particle size distribution
- Thermal analysis
- Cross-link density
- Abbe number
- Machinability
- Vicat Softening temperature
- X-ray diffraction

Preparation of Barium Acrylate Nanocomposites

Dispersion of Barium Hydroxide in Acrylic Acid

The first step involved the synthesis of barium hydroxide-acrylic acid composition. Addition of barium hydroxide to acrylic acid was done gradually. Barium hydroxide was added at ambient temperature to acrylic acid taken in a round bottom flask, gradually under constant stirring and compositions were prepared with varying content (0%-20% by weight) of barium hydroxide. The effect of addition of barium hydroxide to acrylic acid was monitored by studying the effect of barium hydroxide on the refractive index of acrylic acid after each addition. The results of refractive index of addition of barium hydroxide in acrylic acid are tabulated in Table 4.1.

The formation of barium hydroxide-acrylic acid composition results in an increase in refractive index of acrylic acid from 1.424 to 1.431 in the case of 4 % addition of barium hydroxide. Further addition upto 8 % and then upto 12 % barium hydroxide to acrylic acid leads to a refractive index of 1.433 and 1.436 in the case of addition of 16 % barium hydroxide to acrylic acid. Dispersion of barium hydroxide beyond 16% in acrylic acid leads to no change in refractive index as can be seen from Table 4.1. Beyond 16%, refractive index of barium acrylate composition remains constant. This shows that 16% is the optimum concentration of barium hydroxide to bring about maximum improvement in the refractive index of acrylic acid. Here it may be noted that the addition of barium hydroxide beyond 18% resulted into a hazy dispersion indicating that for optical applications, the incorporation of barium hydroxide will have to be restricted to 16% by weight.

Table 4.1: Effect of addition of barium hydroxide on the refractive index of acrylic acid. The maximum amount of barium hydroxide that could be dispersed in acrylic acid is 16% which leads to 0.8 % increase in refractive index of acrylic acid. The increase in refractive index confirms the formation of barium hydroxide-acrylic acid composition by the reaction between acrylic acid and barium hydroxide.

S. No.	Amount (% by wt)	Refractive index
1.	0.0	1.424
2.	4.0	1.431
3.	8.0	1.433
4.	12.0	1.433
5.	16.0	1.436
6.	18.0	1.436
7.	20.0	--

Refractive index is a property which is dependent upon the molar refractivity of the bonds constituting the compound. The change in refractive index of acrylic acid is a confirmation of the fact that the addition of barium hydroxide to acrylic acid results in the formation of a compound such as barium acrylate with higher intrinsic molar refraction than the reactants. Barium belongs to the sixth group of the periodic table; ionic size of barium is 1.36 Å. This causes the change in refractive index of the acrylic acid when barium is incorporated into it.

To study the thermal behavior of barium hydroxide-acrylic acid compositions, TGA/DTA/DTG analysis were carried out. The differential thermograms obtained from TGA analysis clearly indicate the changes in the thermal behavior of acrylic acid as a result of interactions between acrylic acid and barium hydroxide (Figures 4.1 to 4.3).

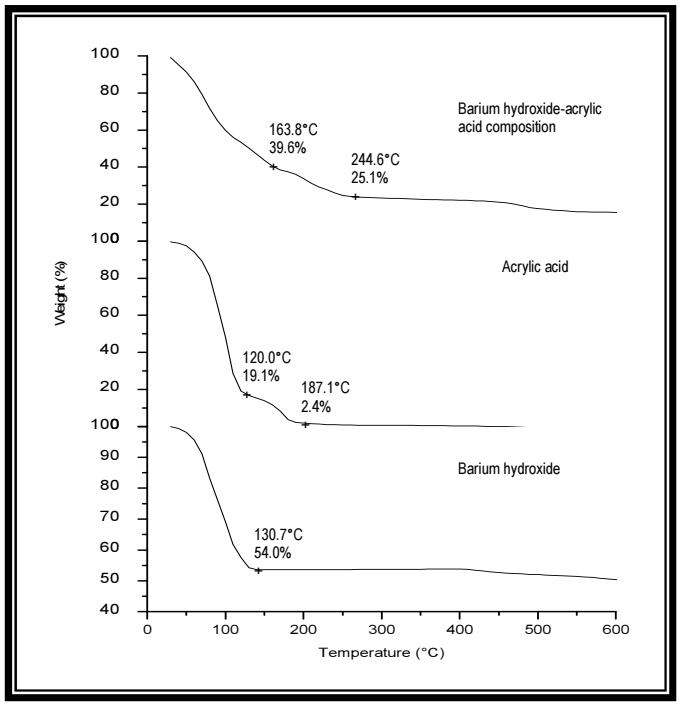

Figure 4.1: TGA thermograms of barium hydroxide, acrylic acid and barium hydroxide-acrylic acid composition indicate increased thermal stability of acrylic acid due to incorporation of barium

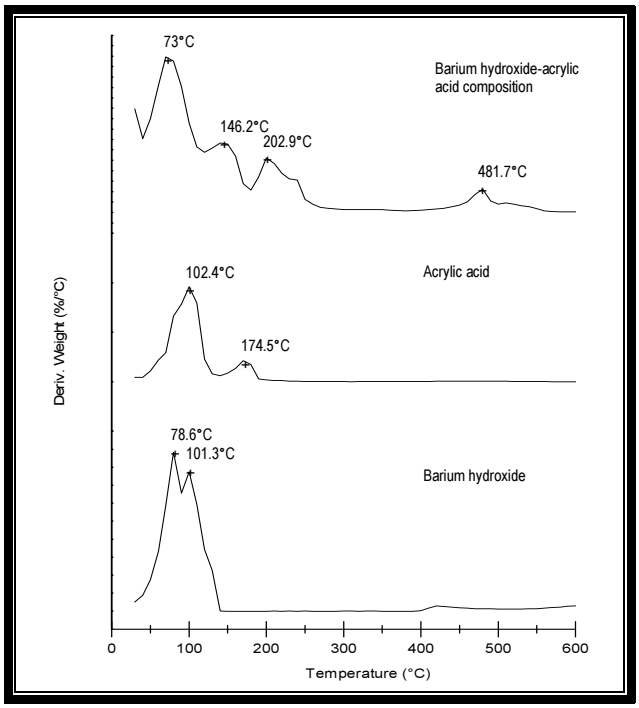

Figure 4.2: DTG thermograms of barium hydroxide, acrylic acid and barium hydroxide-acrylic acid indicate formation of new peaks

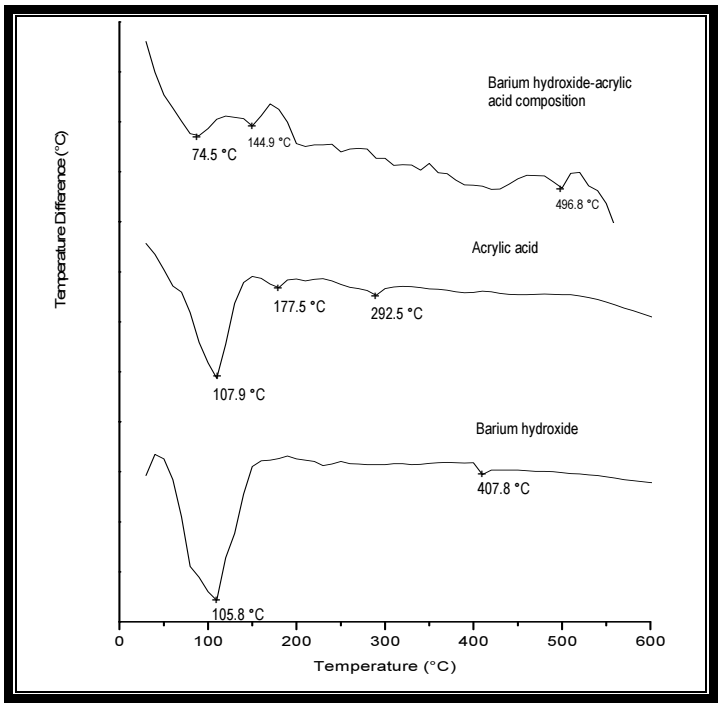

Figure 4.3: DTA thermograms of barium hydroxide, acrylic acid and barium hydroxide-acrylic acid composition indicate completely different behaviour than acrylic acid and barium hydroxide forming a new compound (barium acrylate)

For better understanding, the TGA results have been further examined as per the weight loss percentage due to thermal decomposition as presented in Table 4.2.

Table 4.2: Weight loss (%) due to thermal decomposition of barium hydroxide, acrylic acid and barium acrylate

Product	Weight loss (%)					
	100 °C	**200 °C**	**300 °C**	**400 °C**	**500 °C**	**600 °C**
Barium hydroxide	31.0	46.43	46.3	46.4	48.0	49.7
Acrylic acid	52.2	98.2	100	100	100	100
Barium hydroxide-acrylic acid	40.2	66.1	76.7	77.9	82.3	84.4
Theoretical loss in weight of barium hydroxide-acrylic acid	48.8	89.9	91.4	91.4	91.7	92.0

TGA analysis of barium hydroxide, acrylic acid and barium hydroxide-acrylic acid composition clearly show the following:

a) TGA thermogram of barium hydroxide shows that the thermal decomposition process occurs in a well-defined large step in the temperature range of 30 to 130.7 ºC with a weight loss of 46%, defined by a sharp DTA peak at 105.8 ºC and DTG peaks at 78.6 ºC and 101.3 ºC, which is attributed to the loss of water molecules from the compound. Following the initial decomposition, barium hydroxide does not loose weight. The decomposition of barium hydroxide is ascribed to the formation of inorganic barium oxide which is 48.6% by weight of barium hydroxide. This is also evident from the residue due to barium oxide (47.9%) left in the case of thermal decomposition of barium hydroxide.

b) TGA of acrylic acid shows that the thermal decomposition process of acrylic acid occurs in a well-defined large step in the temperature range from 47.3 ºC to 120.0 ºC with a weight loss of 80 %, defined by a sharp DTG peak at 102.4 ºC and DTA peak at 107.9 ºC attributed to the loss of water. This is followed by a second decomposition from 119.9 ºC to

187.1 ºC with a maximum decomposition rate at 174.5 ºC and weight loss of 17%. This DTG peak corresponds to the DTA peak at 177.5 ºC and corresponds to the formation of anhydride of acrylic acid.

c) Thermal decomposition of barium hydroxide-acrylic acid composition takes place in two steps. First decomposition starts at 30 °C and goes upto 163.8 °C with a total weight loss of 61 %. A sharp DTG peak at 73°C is ascribed to the loss of water from the composition. Later a small decomposition takes place till 244.6 °C with approximately 14% loss in weight. Maximum decomposition rate in this temperature range occur at 202.9 ºC as is evident from the corresponding DTG peak. This is due to the decomposition of barium hydroxide-acrylic acid composition.

d) The TGA of barium hydroxide-acrylic acid has substantially shifted towards the right side of the graph indicating that the composition is more thermally stable than acrylic acid which is an obvious observation, very much on the expected lines.

Weight loss due to decomposition in the case of barium hydroxide-acrylic acid is much less as compared to acrylic acid, simply because of the fact that there is a formation of a strong bond between barium and acrylic acid. Upto 200 ºC, theoretical weight loss of acrylic acid and barium hydroxide is 90%. On the other hand, upto 200 ºC, weight loss in the case of barium hydroxide-acrylic acid composition is 66%. This indicates that the product obtained after the reaction between acrylic acid and barium hydroxide is not just a mixture but a solution consisting of strong bonds between barium and acrylic acid. The results obtained with acrylic acid matched well with the already reported data. The observed weight loss upto 600 ºC in the case of barium hydroxide-acrylic acid composition is much less than the calculated one. Thus, barium hydroxide-acrylic acid exhibits higher stability which is due to the fact that barium is not just mixed in acrylic acid but bonded to it resulting in a new compound (barium acrylate).

The reaction product of barium hydroxide with acrylic acid was analyzed for acid value. Acrylic acid has a pH value of less than 1 and an acid number of

626 which is indicative of the acidic character of acrylic acid. Acid value was determined to study the interactions between the acid and metal salt. The acid value is taken as an indication of the presence of free acrylic acid and the results are tabulated in Table 4.3.

Table 4.3: Effect of addition of barium hydroxide on the acid value of acrylic acid. As the amount of barium hydroxide increases, the acid value decreases.

S.No.	Barium hydroxide (% by wt)	Acid number	pH
1	0.0	626	< 1
2	4.0	596	1.53
3	8.0	542	1.79
4	12.0	502	1.96
5	16.0	477	2.12

As can be seen from Table 4.3, acid value of acrylic acid decreases with increase in the dispersion of barium hydroxide. With 4% addition of barium hydroxide, the acid number of acrylic acid decreases to a value of 596. With 8 % addition of barium hydroxide, the acid number decreases to 542, 502 with 12 % addition of barium hydroxide and to 477 with 16 % addition of barium hydroxide. This clearly indicates that barium hydroxide is reacting with acrylic acid, resulting in the formation of barium hydroxide-acrylic acid composition as depicted in Figure 4.4. From the data, it is evident that the reaction takes place involving one atom of barium and two molecules of acrylic acid.

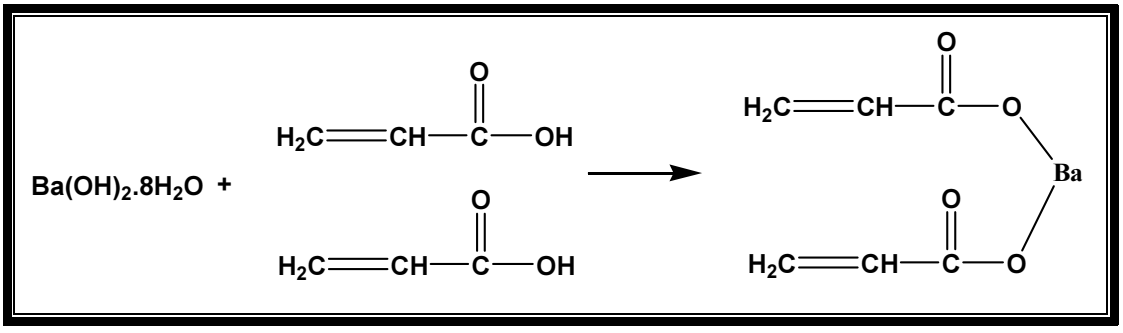

Figure 4.4: Reaction between barium hydroxide and acrylic acid. 2 moles of acrylic acid react with 1 mole of barium hydroxide forming barium acrylate

As can be seen from Figure 4.4, 2 moles of acrylic acid undergo reaction with 1 molecule of barium hydroxide to give barium acrylate.

In order to understand the interactions taking place between barium hydroxide and acrylic acid, UV-Visible spectroscopy was performed from 200-800 nm on the compositions of barium hydroxide-acrylic acid in ethanol as a solvent (Figure 4.5 a-e).

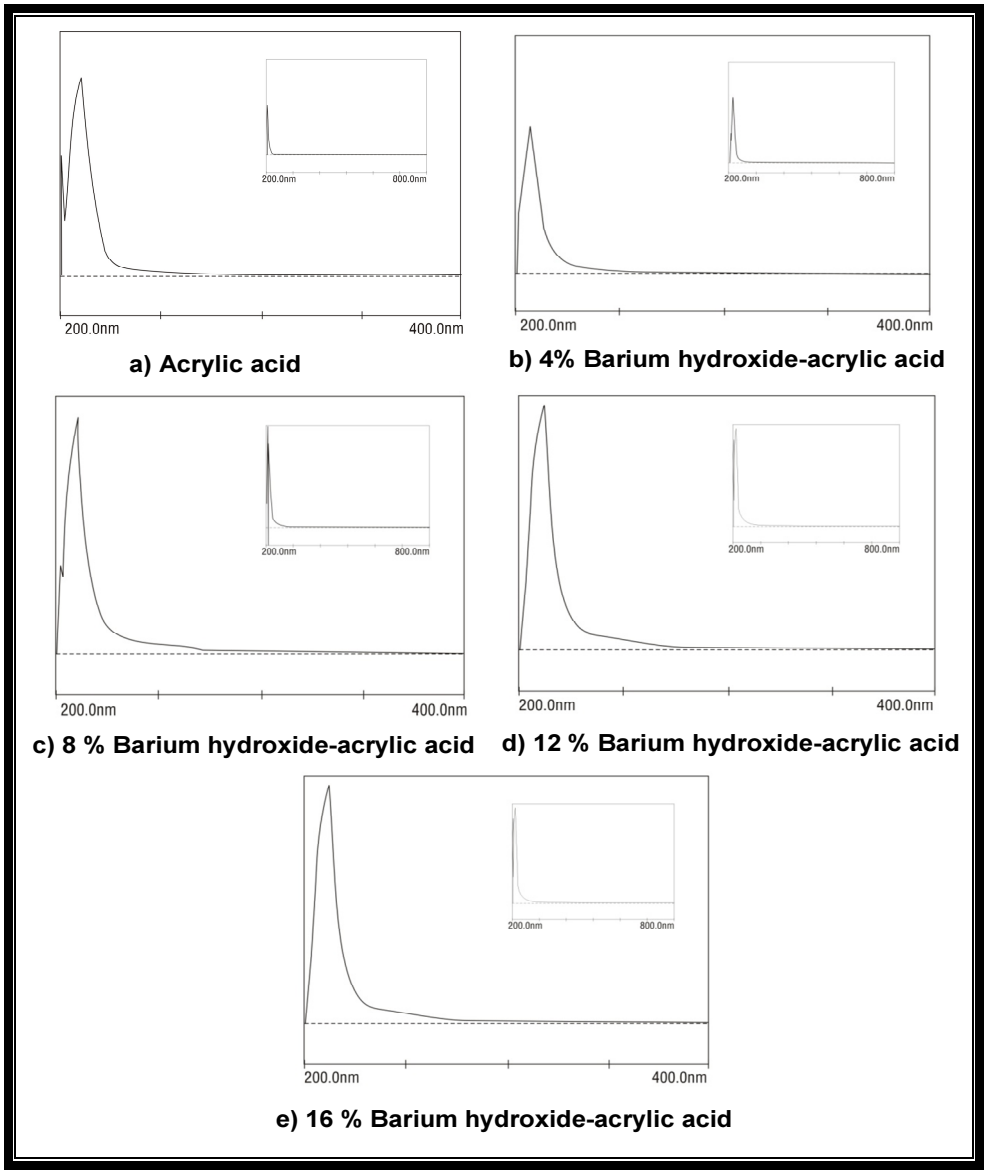

Figure 4.5 (a-e): UV-Visible spectra of acrylic acid and barium hydroxide-acrylic acid composition (varying concentrations). The λ_{max} value of acrylic acid does not change with the dispersion of barium hydroxide and hence it can be said that the reaction between barium hydroxide and acrylic acid is taking place at the carboxylic acid group of acrylic acid.

The maximum absorption peak (λ_{max}) of acrylic acid was observed at 210 nm. As can be seen from Figure 4.5, there is no change in the λ_{max} value of acrylic acid with increase in the amount of barium hydroxide dispersed in acrylic acid. This confirms that the vinyl group of acrylic acid remains intact and hence the only site for the reaction of barium hydroxide is the carboxylic acid group.

IR analysis was carried out to study the reaction occurring between acrylic acid and barium hydroxide. The IR spectrum analysis is presented in Figure 4.6.

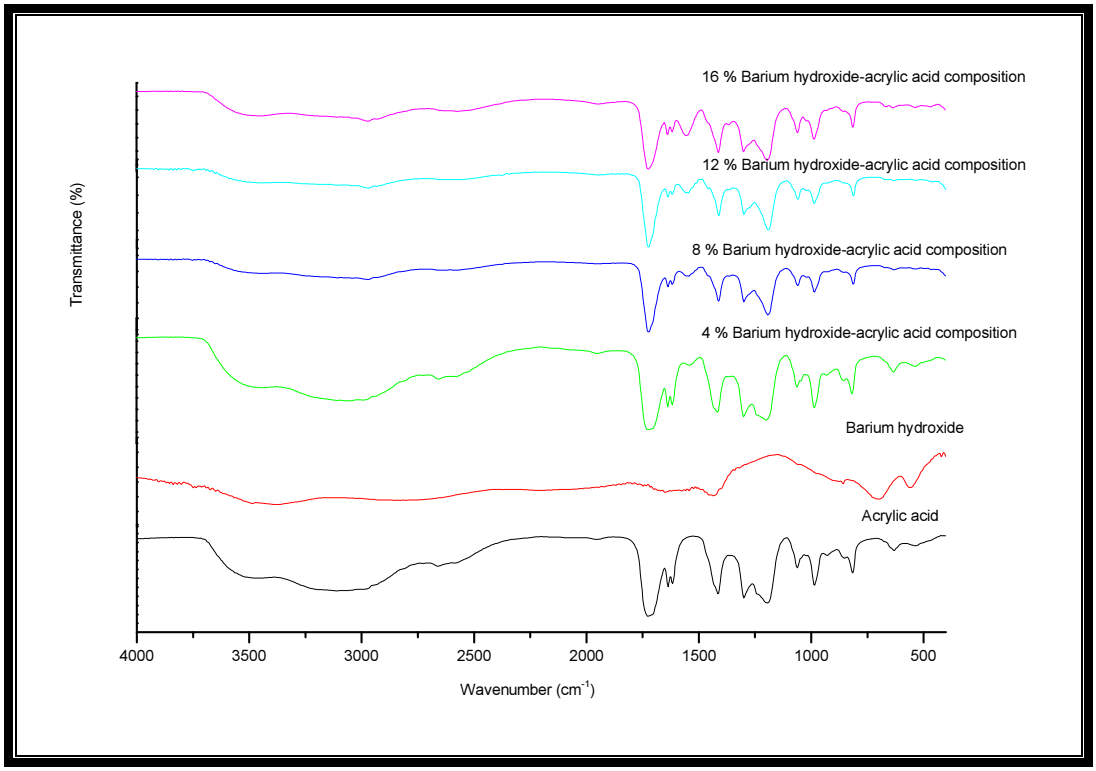

Figure 4.6: IR analysis of acrylic acid, barium hydroxide and barium hydroxide-acrylic acid composition. Absence of band pertaining to carboxylic acid and presence of band pertaining to ester group confirms the formation of new compound as barium acrylate after the reaction between barium hydroxide and acrylic acid

As can be seen from the IR spectrum, acrylic acid exhibits a characteristic band at 3100 cm^{-1} ascribed to C-H group of -C=C-H group and C=O stretch at 1725 cm^{-1}. C=C stretching due to the presence of vinyl group appears at 1640 cm^{-1} **[387]**. Barium hydroxide on the other hand shows a broad band due to the

presence of -OH at 3600 cm^{-1} and 2850 cm^{-1}. IR spectrum of barium acrylate shows the presence of bands due to C=O and C=C. This indicates that during the reaction of barium hydroxide with acrylic acid, reaction is not taking place at the vinyl group. Absence of O-H band and presence of C=O band in the case of barium acrylate shows that the addition of barium hydroxide takes place at the carboxylic group of acrylic acid to forming an acrylate. Presence of a sharp peak at 1555 cm^{-1} is due to the presence of $–COO^-$ group.

Particle size of the compositions were evaluated on Particle size analyzer. The result are tabulated in Table 4.4.

Table 4.4: Particle size analysis of barium acrylate compositions indicates that the dispersion of barium hydroxide takes place in the nanoscale dimension.

S.No.	Barium hydroxide (% by wt)	Particle size (nm)
1	0.0	< 0.8
2	4.0	< 0.8
3	8.0	< 0.8
4	12.0	< 0.8
5	16.0	< 0.8

The results of the particle size analysis show that the dispersed particles of barium hydroxide are in the range much lower than nanometer size and that is why no particles could be observed in the particle size analyzer (nanosizer). The dispersion in this scale is responsible for overall improvement of the properties of acrylic acid. The clarity and transparency of the compositions of the barium hydroxide-acrylic acid also suggests the same.

Cast Polymerization of barium acrylate compositions

The attempt was made to polymerize the composition of acrylic acid and barium hydroxide containing 16% by weight of barium hydroxide to obtain the optical lenses. It was observed that on polymerization, the material turned into

a solid product with full of foam and hence, it could not be considered suitable for making lenses. In order to convert the composition of barium hydroxide and acrylic acid into optical products, therefore, further work was done for the incorporation of styrene as a co-monomer for the purpose of obtaining lenses.

On addition of styrene, how the final product changed in its form and appearance can be seen in Table 4.5. It may be noted here that with the incorporation of styrene, the composition of barium hydroxide and acrylic acid could be transformed into clear and transparent lenses on polymerization. The amount of styrene needed for this purpose was found to be 150% by weight. The composites consisting of barium hydroxide, acrylic acid and styrene were made and then characterized for various essential parameters of optical plastics. It must be mentioned here that styrene alone does not get polymerized at gamma irradiation doses 10 kGy to 30 kGy.

Table 4.5: Results of effect of styrene on polymerization indicating that 150% (by weight of barium acrylate) of styrene is required for polymerization of barium acrylate. The nanocomposites obtained were hard and transparent which were easily released from the molds.

S. No.	Styrene (% by weight)	Shore-D Hardness	Transmittance (%)	Appearance, etc.
1.	0	40	*	Foamy and opaque, Brittle
2.	30	*	*	Sticky could not be released
3.	60	*	*	Sticky could not be released
4.	90	*	*	Sticky, could not be released
5.	120	90	77	Hazy at the surface, hard
6.	150	90	90	Clear, transparent, easily released

*: Shore-D hardness and Transmittance could not be determined as the nanocomposites were foamy or sticky in nature

From the results presented in Table 4.5, it may be seen that in the absence of styrene, the nanocomposite obtained was foamy and opaque with shore-D hardness of 40. With 30% to 90% styrene (by weight of barium acrylate), the nanocomposite obtained was soft and sticky which could not be released from the molds. With 150% styrene (by weight of barium acrylate), the shore-D hardness achieved was between 90 and the nanocomposites were easily released from the mold. Clear and transparent nanocomposites suitable for optical applications were obtained. This indicates that 150% styrene (by weight of barium acrylate) was sufficient for polymerization. The appearance of polymers with and without styrene is depicted in Figure 4.7.

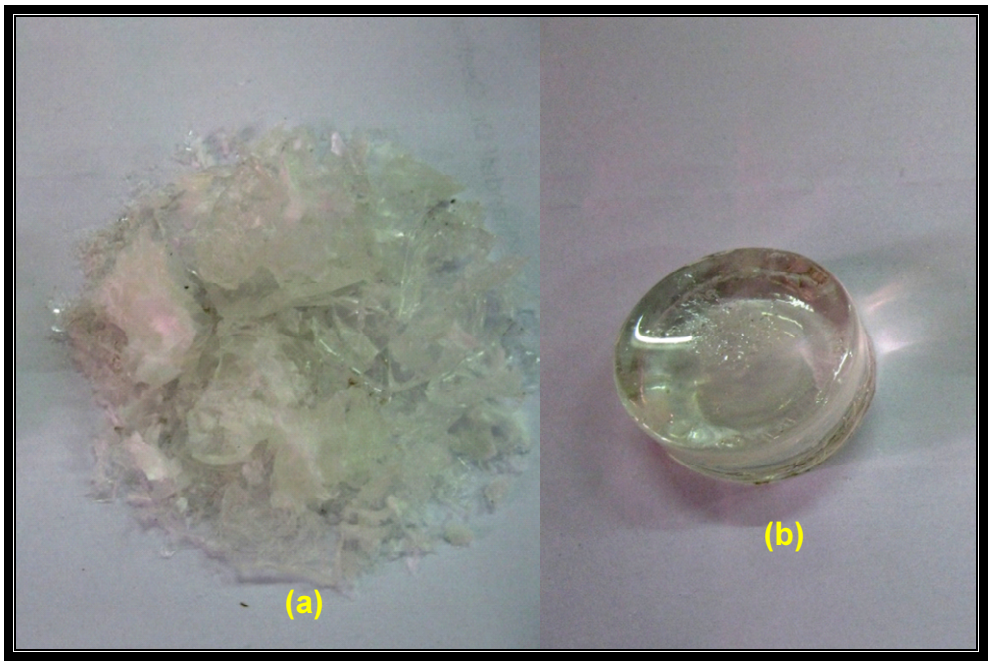

Figure 4.7: Barium acrylate nanocomposites a) without styrene and b) with styrene indicating that addition of styrene as co-monomer is essential for obtaining clear and transparent nanocomposites.

It can be very clearly seen that the presence of styrene as a co-monomer for polymerization of barium acrylate compositions is very important to obtain clear, transparent and hard nanocomposites.

In the case of polymerization of acrylic acid, the beta carbon atom, polarized by the carbonyl group, behaves as an electrophile. This favors the addition of

nucleophile and active hydrogen compounds to the vinyl group. Moreover, the carbon–carbon double bond undergoes radical–initiated addition reactions, Diels-Alder reactions with dienes and polymerization reactions **[383-386].**

The results of the effect of gamma irradiation on polymerization of barium acrylate-styrene nanocomposites are presented in Table 4.6. Polymerization of barium acrylate-styrene compositions was carried out at various doses of 10 kGy, 15 kGy, 20 kGy, 25 kGy and 30 kGy. Results of the polymerization studies are shown in Table 4.6.

Table 4.6: Effect of gamma irradiation on the polymerization of barium acrylate-styrene composition. 20 kGy was found to be the optimum dose for barium acrylate-styrene nanocomposites.

S.No.	Dose (kGy)	Shore-D Hardness	Cross-link density (%)	Appearance
1	10	*	72	Soft, sticky, unpolymerized liquid at the surface
2	15	*	84	Transparent, sticky at the surface
3	20	90	95	Transparent, hard and easily released
4	25	90	95	Transparent, hard and easily released
5	30	90	96	Transparent, hard and easily released

*: Shore-D hardness could not be measured due to sticky nature of nanocomposites

As seen from the results in Table 4.6, barium acrylate-styrene compositions when subjected to a dose of 10 kGy-15 kGy, soft and sticky nanocomposites were obtained. At doses of 20 kGy and higher, transparent and hard nanocomposites with a shore-D hardness of 90 and cross-link density of 95% were obtained. It can be seen that as the dose of irradiation increases further, the shore-D hardness of samples does not change. The suitable dose for polymerization by gamma radiation was optimized as 20 kGy for barium acrylate-styrene compositions. It may be noted here that compositions without styrene at all the irradiation doses of 10-30 kGy led to the formation of brittle and foamy polymer.

Having cast polymerized the lenses using various compositions of acrylic acid and barium hydroxide plus styrene, the lenses were evaluated for various parameters. The results are discussed in the following section.

Refractive index and Abbe number of the nanocomposites were determined on the Abbe refractometer. The results are presented in Figures 4.8-4.9.

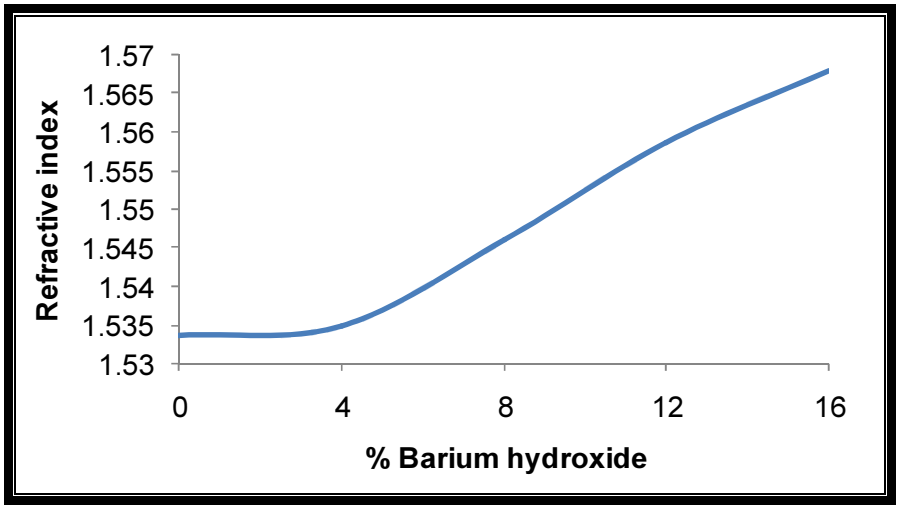

Figure 4.8: Effect of barium hydroxide on refractive index of acrylic acid. The refractive index increases as the percentage of barium hydroxide is increased

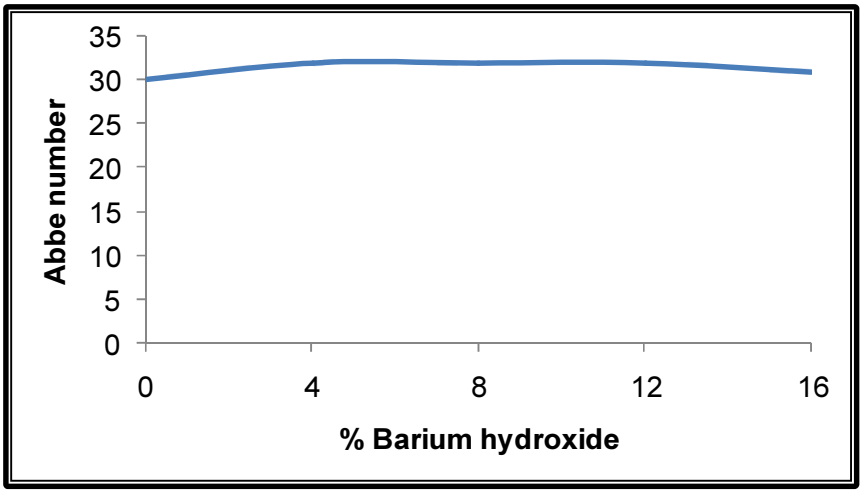

Figure 4.9: Effect of barium hydroxide on Abbe number of barium acrylate. No significant changes in Abbe number was observed as the percentage of barium hydroxide was increased. Abbe number lies in the well desired limit for optical applications.

As can be seen from the figures, polyacrylate-styrene polymer has a refractive index of 1.5336 and Abbe number of 30. A refractive index of 1.5348 and an Abbe number of 32 was obtained for barium acrylate-syrene nanocomposites with 4 % dispersion of barium hydroxide in acrylic acid. A refractive index of 1.5459 and an Abbe number of 32 was obtained with 8 % of barium hydroxide and a refractive index of 1.5587 and Abbe number of 32 was obtained with 12% of barium hydroxide. The refractive index further increases to 1.5681 and Abbe number of 31 with the dispersion of 16% barium hydroxide. It is found to be better than commercially available polyacrylates i.e. Polymethyl methacrylate, a commercial grade of acrylate polymer for various optical applications, which has a refractive index of 1.491.

Thermal analysis of barium acrylate-styrene nanocomposites by TGA/DTA/DTG was studied. Thermal studies (Figure 4.10 – 4.12) of the acrylate nanocomposites indicate the formation of a highly cross-linked, thermally stable structure. The weight loss of the nanocomposites was recorded at various temperatures, which is given in Table 4.76. The heat stability of the barium containing nanocomposite systems is found to be much higher than the polyacrylates due to the formation of a cross-linked structure.

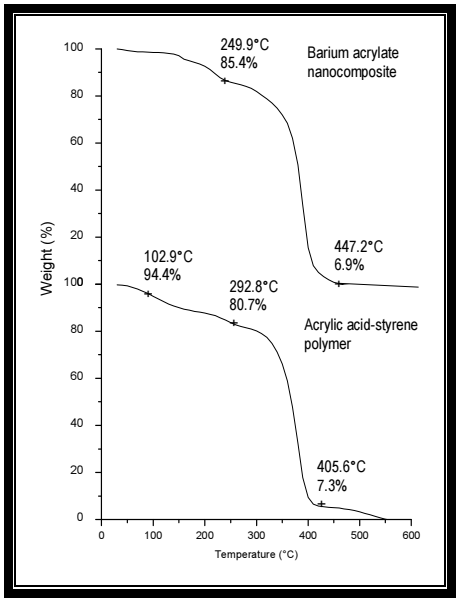

Figure 4.10: TGA thermograms of polyacrylate and cast polymerized barium acrylate-styrene nanocomposite indicate stability due to addition of barium and formation of nanoparticles of barium.

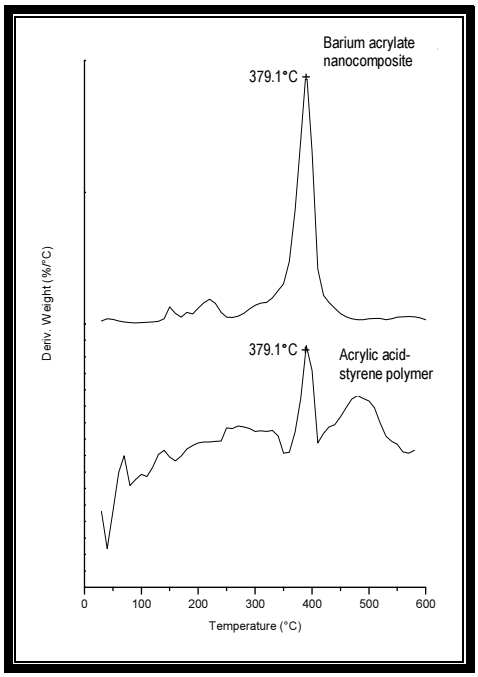

Figure 4.11: DTG thermograms of acrylic acid-styrene polymer and barium acrylate-styrene nanocomposite indicate stability due to addition of barium and formation of nanoparticles of barium.

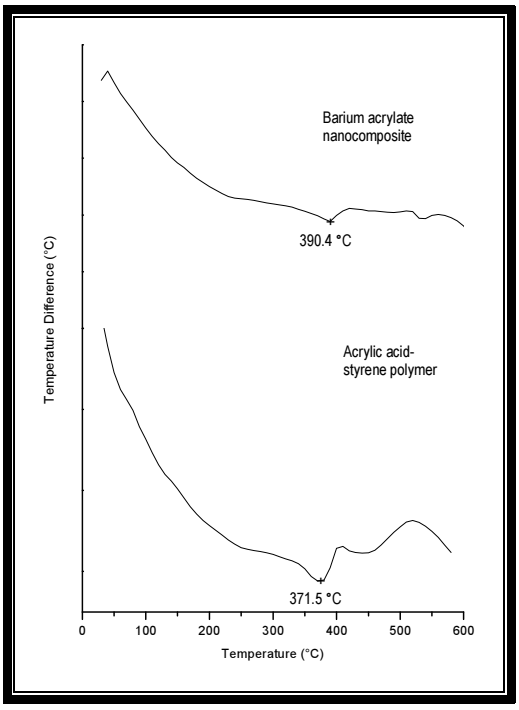

Figure 4.12: DTA thermograms of polyacrylate and barium acrylate-styrene nanocomposite indicate stability due to addition of barium and formation of nanoparticles of barium.

Table 4.7: Weight loss due to thermal decomposition of acrylic acid-styrene polymer and barium acrylate-styrene nanocomposite indicates higher thermal stability of barium acrylate-styrene nanocomposite due to formation of nanoparticles of barium

Product	Weight loss (%)					
	100 °C	200 °C	300 °C	400 °C	500 °C	600 °C
Acrylic acid-styrene polymer	5.2	12.3	19.9	90.6	96.7	100
Barium acrylate-styrene nanocomposite	2.7	7.4	18.1	72.0	89.8	93.1

As can be seen from the thermograms presented in Figures 4.10-4.12, it is very clear that the acrylic acid-styrene polymer matrices with and without barium behave completely different from each other. The acrylic acid-styrene polymer shows decomposition in two steps, similar to barium acrylate-styrene nanocomposite which also shows decomposition in two steps. The first decomposition in the case of acrylic acid-styrene polymer takes place upto 292.8 °C with a weight loss of 20% and is ascribed to moisture and volatile organic compounds which are lost upto this temperature. After this, there is a well-defined loss in weight of 73% upto 406°C which is evident from a DTG peak at 379 °C and DTA peak at 371.5 °C. This is attributed to the chain scissioning of the acrylic acid-styrene polymer leading to smaller fragments.

In the case of barium acrylate-styrene nanocomposites, the first decomposition step is upto 249.9 °C with a weight loss of 15% which is attributed to loss of moisture and volatiles. Second decomposition step is upto 447.2 °C with a weight loss of 79 % leaving behind a residue of 6.9%. A sharp DTG peak at 392.7 °C indicates the polymer chain scission. The thermograms clearly show that barium acrylate-styrene nanocomposites have enhanced thermal stability as compared to polyacrylate without barium. The DTG peak shifts towards higher temperature

indicating that the acrylate polymer has gained stability after the incorporation of barium into it.

The transmittance of the samples as determined by UV-Visible spectroscopy was found to be 90%. The nanocomposites were found to be impact resistant as per FDA regulations.

Machinability was checked by subjecting the samples to grinding and machining. Machinability of the nanocomposites was found to be good. The hardness of the lenses was checked by determining the shore-D hardness by Shore-D Durometer and scratch resistance power of the nanocomposite. Shore-D hardness of the nanocomposites was found to be 90. Pencil hardness and scratch resistance of barium acrylate-styrene nanocomposites was found to be higher than PMMA. PMMA has a scratch resistance of “C” grade and a pencil hardness of 4H while barium acrylate-styrene nanocomposites have scratch resistance of “B” and pencil hardness of 6H. Barium acrylate-styrene nanocomposites are superior in hardness to PMMA due to the dispersion of metal atoms.

For barium acrylate-styrene nanocomposites, specific gravity of 1.19 was obtained. The specific gravity of PMMA is 1.26. This suggests that metal-containing nanocomposites are much lighter in weight as compared to the conventional optical material used. This is an achievement where low weight polymers are required especially for high diopter lenses.

The Vicat softening temperature of 120 °C for barium acrylate-styrene nanocomposites indicate that the working temperature of barium acrylate-styrene nanocomposites is much higher than PMMA which has a working temperature of 109 °C. This clearly indicates that barium acrylate-styrene nanocomposites can be used for applications where high temperatures are required.

Preparation of Barium Cinnamate Nanocomposites

Dispersion of barium hydroxide in cinnamic acid

Barium cinnamate was synthesized by the reaction of barium hydroxide and cinnamic acid. The molar ratios of barium hydroxide and cinnamic acid were varied where the synthesis of barium cinnamate was carried out by adding barium hydroxide to cinnamic acid in different molar ratios of barium hydroxide: cinnamic acid i.e. 0.2:2, 0.4:2, 0.6:2, 0.8:2 and 1:2. It was observed that 0.2:2 (Ba/0.2/CA/2) and 0.4:2 (Ba/0.4/CA/2) molar ratios were successful for the preparation of a homogeneous compound while beyond a molar ratio 0.4: 2, phase separation takes place (Table 4.8).

Table 4.8: Addition of different amounts of barium hydroxide to cinnamic acid. Addition of upto 0.4 moles of barium hydroxide in 2 moles cinnamic acid led to the formation of homogeneous compound. Beyond 0.4 moles, phase separation takes place

S.No.	$Ba(OH)_2$ (moles)	Cinnamic acid (moles)	Observations
1.	0.2	2	Homogeneous compound
2.	0.4	2	Homogeneous compound
3.	0.6	2	Phase separation
4.	0.8	2	Phase separation
5.	1.0	2	Phase separation

The reaction between barium hydroxide and cinnamic acid was established by evaluating barium hydroxide-cinnamic acid composition for various parameters such as acid value, barium content (%), structure elucidation and thermal analysis.

Barium content and barium oxide content present in the composition was evaluated by ICP-OES and the results are tabulated in Table 4.9.

Table 4.9: Results of barium (% by weight) and barium oxide (% by weight) in barium cinnamate. As expected, the percentage content of barium increases with increase in the addition of barium hydroxide.

Sample	Ba (%)	BaO (%)	Acid value
Barium hydroxide octahydrate	45.8	48.6	0
Cinnamic acid	0.0	0.0	368
Ba/0.2/CA/2	6.4	7.42	264
Ba/0.4/CA/2	13.5	15.7	150

It can be seen from Table 4.9 that with increasing molar ratios of barium hydroxide : cinnamic acid, the amount of barium (%) in the resulting product increases. Similarly, amount of barium oxide in the compositions increases by increasing the percentage of barium hydroxide added from Ba/0.2/CA/2 to Ba/0.4/CA/2. As barium reacts with cinnamic acid, percentage of barium present in the compound increases. Table 4.9 shows various percentages of barium that has reacted with cinnamic acid. The results show that 13.5 % of barium could be incorporated successfully to form barium hydroxide-cinnamic acid composition as can be seen from Table 4.9.

To confirm the reaction between cinnamic acid and barium hydroxide, acid value of the product was determined. The results of acid value are tabulated in Table 4.9. At the initial point of the reaction, acid value of cinnamic acid was determined to be 368. As can be seen from Table 4.9, acid value decreases to 264 when 0.2 moles of barium hydroxide is added to 2 moles of cinnamic acid. The acid value further decreases to 150 when 0.4 moles of barium hydroxide is added to 2 moles of cinnamic acid. The decrease in acid value is a clue to the reaction taking place between barium hydroxide and cinnamic acid resulting in the formation of barium cinnamate.

The reaction taking place between barium hydroxide and cinnamic acid was further understood by crystallographic studies. X-ray diffraction pattern was

studied for barium hydroxide, cinnamic acid and barium hydroxide-cinnamic acid composition from Figure 4.13.

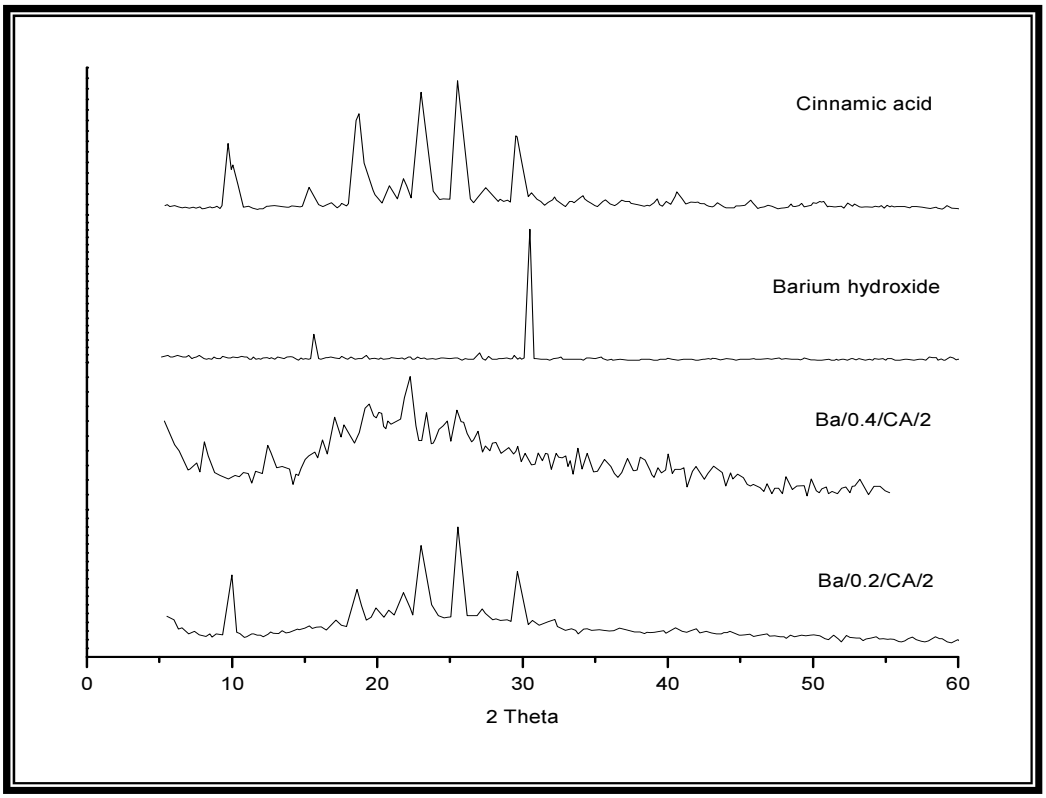

Figure 4.13: XRD pattern of barium hydroxide, cinnamic acid and barium hydroxide-cinnamic acid. The peaks barium hydroxide and cinnamic acid are absent in the case of higher amount of barium hydroxide indicating complete reaction between barium hydroxide and cinnamic acid

As can be seen from the XRD pattern, the peaks pertaining to cinnamic acid at 2θ value 9.73, 18.76, 23.00 and 25.4 and barium hydroxide at 2θ values of 15.6 and 30.4 are completely absent in Ba/0.4/CA/2. This indicates the completion of the reaction between cinnamic acid and barium hydroxide to form a new compound i.e. barium cinnamate. The XRD pattern is also a confirmation of the amorphous nature of barium cinnamate, as no sharp peaks due to crystalline nature is observed.

IR analysis (Figure 4.14) of cinnamic acid, barium hydroxide and barium cinnamate was very helpful to arive at the structure of barium cinnamate (Figure 4.15).

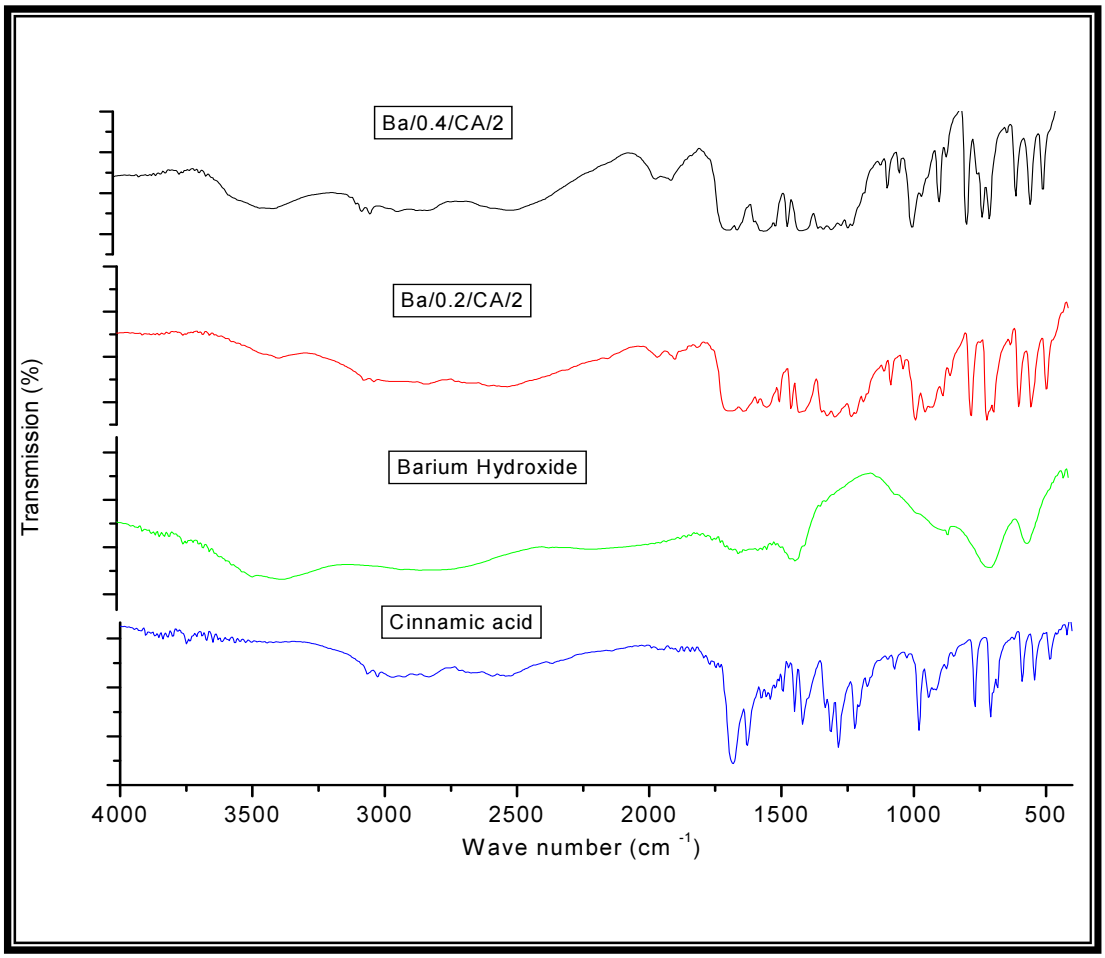

Figure 4.14: IR analysis of cinnamic acid, barium hydroxide and barium cinnamate. Appearance of new band at 1538 cm^{-1} in the case of barium cinnamate confirm its formation

The reaction between cinnamic acid and barium hydroxide is indicated by the absence of characteristic band of conjugated C=O stretch at 1683 cm^{-1}. This means that the carboxylic acid group is taking part in the reaction with barium hydroxide to form barium cinnamate. Further, a characteristic band of ester group at 1540 cm^{-1} indicates that –COOH group in cinnamic acid has been converted to –COOBa **[387]**.

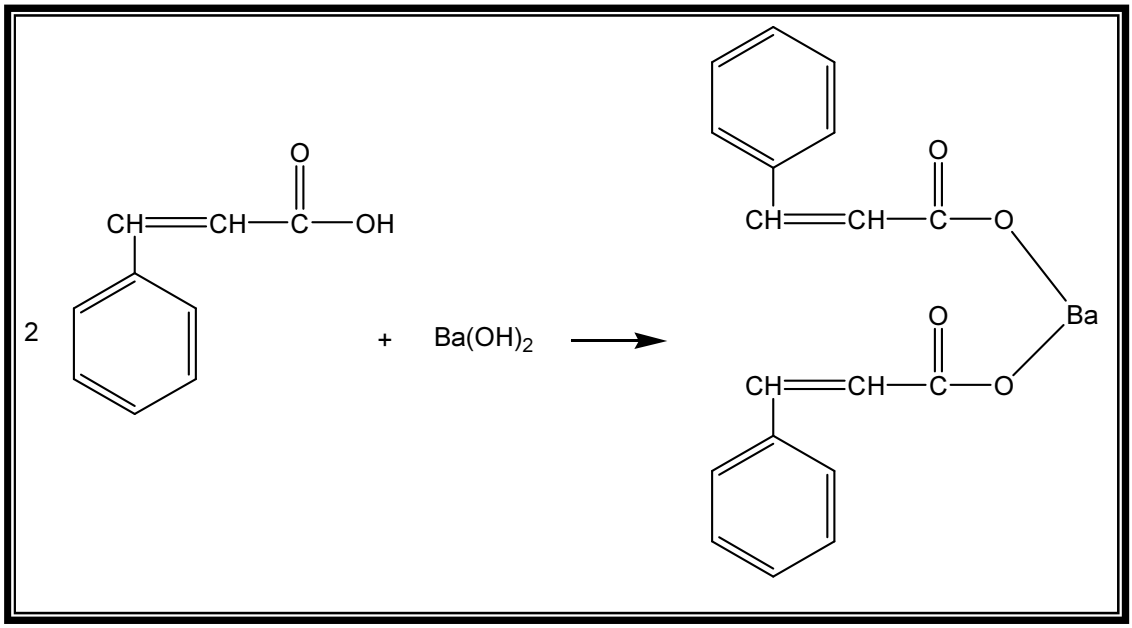

Figure 4.15: Structure of barium cinnamate formed as a result of the reaction between cinnamic acid and barium hydroxide

The thermal stability of barium cinnamate was analyzed by DSC, TGA, DTA & DTG. The thermograms are presented as Figure 4.16 for DSC analysis and Figures 4.17 to 4.19 for TGA, DTA and DTG analysis

The DSC curve of cinnamic acid shows a sharp endothermic peak at 135.2 ºC corresponding to the melting event, characteristic of a pure substance. The onset temperature of the melting peak is 133.5 ºC and ∆H fusion is 142.7 J/g. The DSC curve of barium hydroxide shows two sharp endothermic peaks at 84.6 ºC, corresponding to the melting event and 114.4 ºC due to loss of water molecules. The onset temperature of the melting peak is 81.6 ºC and ∆H fusion is 241.4 J/g.

While, the DSC curve of Ba/0.2/CA/2 shows a sharp endothermic peak at 130.2 ºC, with corresponding peak in DTA at 128.5 ºC, ascribed to the melting point of cinnamic acid, the DSC curve of Ba/0.4/CA/2, on the other hand shows a sharp endothermic peak at 98.66 ºC corresponding to DTA peak at 104.3 ºC, which is ascribed to the loss of moisture. A sharp peak at 153.0ºC, with corresponding peak in DTA at 152.7 ºC is ascribed to the melting of the compound. The onset temperature of the melting peak is 147.7 ºC and ∆H

fusion is 18.12J/g. It is evident from the DSC analysis that cinnamic acid is left unreacted in the case of Ba/0.2/CA/2 and complete reaction between barium hydroxide and cinnamic acid takes place at molar ratio 0.4:2 (barium hydroxide:cinnamic acid) to form barium cinnamate

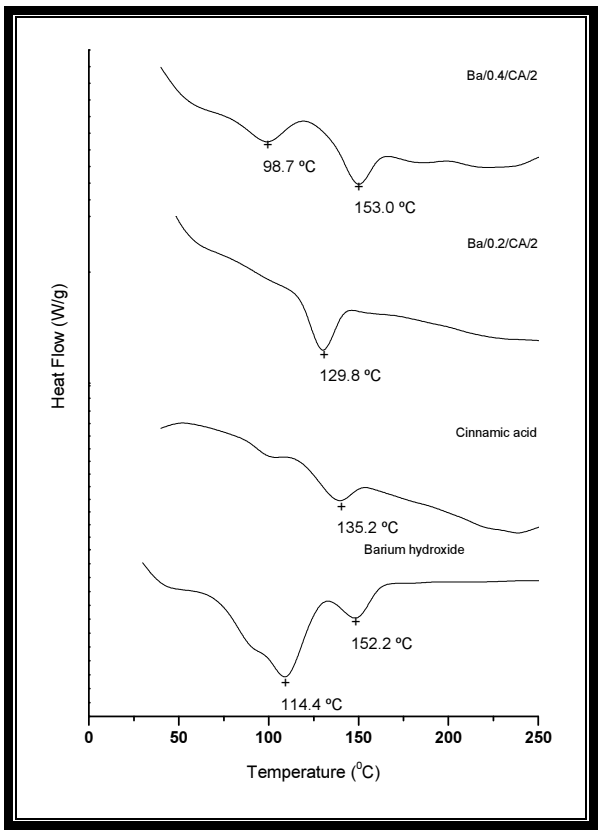

Figure 4.16: DSC thermograms of barium hydroxide, cinnamic acid and the reaction product barium cinnamate. The endothermic peaks in barium hydroxide are absent in barium cinnamate indicating the reaction to take place between the two starting materials. The endothermic peak due to cinnamic acid is absent in the case where higher content of barium hydroxide is incorporated, indicating the complete reaction of cinnamic acid with barium hydroxide to form barium cinnamate.

The DSC data combined with TG, shows that barium hydroxide is thermally stable upto 30 ºC. The thermal decomposition process occurs in a well-defined large step in the temperature range from 30 to 130ºC with a weight loss of 46%, defined by a sharp DTA peak at 106 ºC, which is attributed to the

loss of water molecules from barium hydroxide octahydrate. Later, barium hydroxide remains thermally stable at a temperature above 130 ºC as can be seen by the absence of peaks.

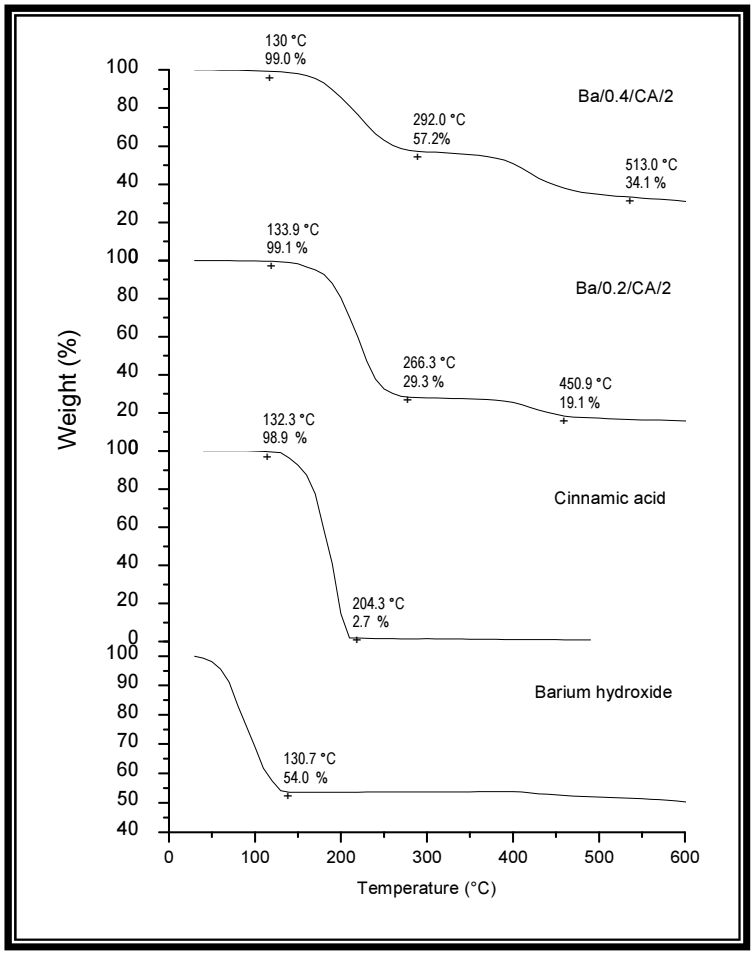

Figure 4.17: TGA thermogram of barium hydroxide, cinnamic acid and barium cinnamate. The thermograms indicate higher stability of barium cinnamate as compared to cinnamic acid due to the presence of barium in it.

The DSC data combined with TGA, shows that cinnamic acid is thermally stable upto 133 ºC after which melting of cinnamic acid takes place at 135 ºC. The thermal decomposition process occurs in a well-defined large step in the temperature range from 133 to 204.3 ºC with a weight loss of 96.0 %, defined by a DTG peak at 198.6 ºC, which is attributed to its decomposition. Presence of DTA peaks at 110.9 ºC, 139.3 ºC, 175.3 ºC and 204.3 ºC confirm the loss of components from cinnamic acid at these temperatures.

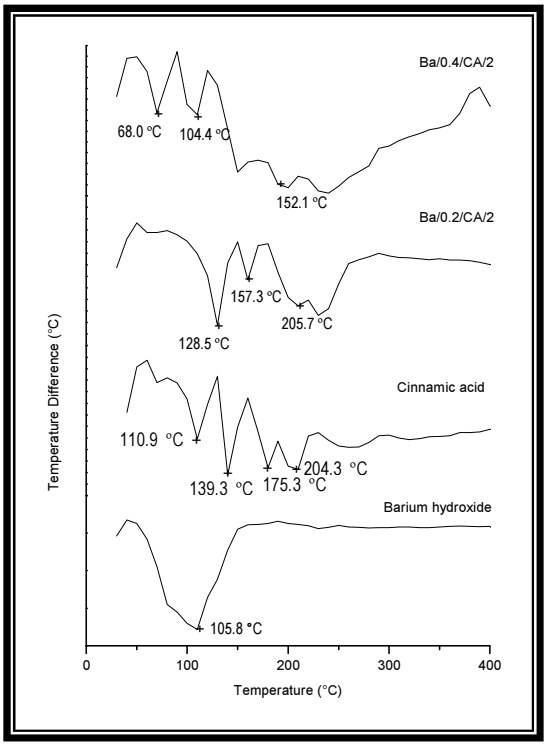

Figure 4.18: DTA thermogram of barium hydroxide, cinnamic acid and barium cinnamate. The thermograms show new peaks in the case of product of reaction between barium hydroxide and cinnamic acid confirming the formation of new compound i.e. barium cinnamate

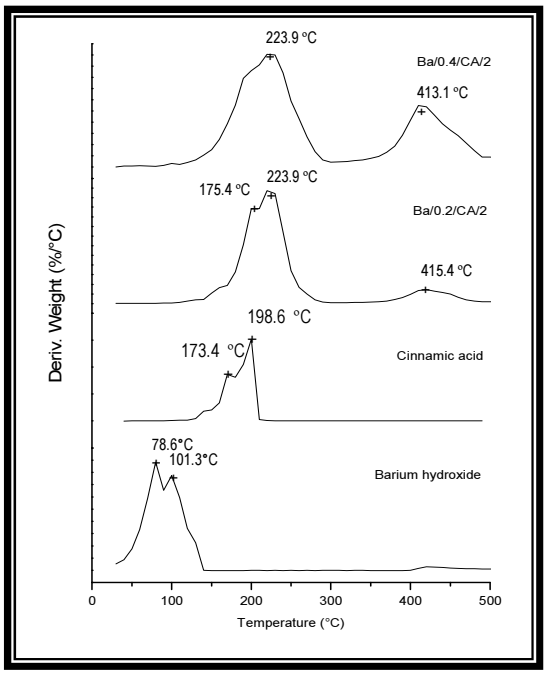

Figure 4.19: DTG thermogram of barium hydroxide, cinnamic acid and barium cinnamate. The thermograms show new peaks in the case of barium cinnamate indicating the formation of new compound

The DSC data combined with TGA, shows that barium cinnamate Ba/0.2/ CA/2 decomposes in two steps. Barium cinnamate Ba/0.2/CA/2 is thermally stable upto 134.0 ºC. The thermal decomposition process occurs in a well-defined large step in the temperature upto 266.0 ºC with a weight loss of 70 %, defined by a sharp DTG peak at 224.0 ºC, at which maximum decomposition rate is observed. Later, barium cinnamate Ba/0.2/CA/2 decomposes in a second step in temperature range upto 450.9 ºC as can also be seen in DSC, with a weight loss of 10%. Maximum decomposition rate is observed at 415.4 ºC as is evident by a small DTG peak corresponding to its decomposition.

TGA of Ba/0.4/CA/2 shows that it decomposes in two steps. Barium cinnamate Ba/0.4/CA/2 is thermally stable upto 130 ºC. The thermal decomposition process occurs in a well-defined large step in the temperature range from 130 ºC to 292 ºC corresponding to a weight loss of 42.0 % which is defined by a sharp DTG peak at 224 ºC, corresponding to its decomposition. The DTA peaks at 68 ºC and 104 ºC are ascribed to the weight loss due to removal of water molecules. DTA peak at 152 ºC is attributed to the melting of barium cinnamate as is evident from DSC also. Later, barium cinnamate decomposes in a second step in the temperature upto 450.9 ºC with a weight loss of 19 %. A DTG peak at 413 ºC and an exotherm at 446 ºC prove the rapid decomposition of barium cinnamate at this temperature.

Table 4.10: Weight loss (%) due to decomposition of barium hydroxide, cinnamic acid and barium cinnamate

Product	Weight loss (%)					
	100 °C	**200 °C**	**300 °C**	**400 °C**	**500 °C**	**600 °C**
Barium hydroxide	31.0	46.4	46.3	46.4	48.0	49.7
Cinnamic acid	0	98.3	100	100	100	100
Ba/0.2/CA/2	0.2	19.5	72.1	74.5	82.8	84.2
Ba/0.4/CA/2	0.5	14.5	43	49	65.3	68.9

As can be seen from the table, the thermal stability of barium cinnamates lie between that of barium hydroxide and cinnamic acid. Barium cinnamate with more amount of barium exhibit lower weight loss and hence higher thermal stability as compared to the one having less amount of barium. Weight loss in the case of barium cinnamate takes place very gradually. Initial weight loss upto 100 ºC is more in the case of barium hydroxide due to the loss of water of crystallization. This is not present in the case of barium cinnamates as weight loss upto 100 ºC is negligible. Also for barium cinnamate which has less amount of barium or more amount of organic cinnamic acid (in the case of Ba/0.2/CA/2), decomposes fast as compared to the other.

The thermograms obtained from TGA analysis clearly indicate the changes in the thermal behavior of barium cinnamate as a result of interactions between barium hydroxide and cinnamic acid.

The thermal stability of barium cinnamates lie between that of barium hydroxide and cinnamic acid. Barium cinnamate with more amount of barium exhibits higher thermal stability as compared to the one having less amount of barium. Weight loss in the case of barium cinnamate takes place very gradually. Initial weight loss upto 100 ºC is more in the case of barium hydroxide due to the loss of water of crystallization. The same is not observed in the case of barium cinnamate where weight loss upto 100 ºC is negligible. Barium cinnamate which has less amount of barium decomposes faster than the one with more amount of barium, confirming the higher thermal stability of Ba/0.4/CA/12.

Cast Polymerization of barium cinnamate compositions

An attempt was made to polymerize barium cinnamate compositions to obtain the optical lenses. The compositions were subjected to various doses of gamma irradiation from 10 kGy to 30 kGy. Visual observations indicated that there is no change in the appearance of the compositions before and after irradiation. Further confirmation was obtained by DSC analysis of the compositions before and after irradiation. The melting point of 152 ºC was obtained for both. Thus this clearly indicates that barium cinnamate as such does not undergo polymerization.

To facilitate the polymerization of barium cinnamate, effect of co-monomer such as styrene on its polymerization was studied. It was observed that barium cinnamate does not form homogeneous composition with styrene at any concentration. Thus, it was not possible to co-polymerize barium cinnamate.

Preparation of barium cinnamate-barium acrylate nanocomposites

Synthesis of barium cinnamate and barium acrylate

Barium cinnamate and barium acrylate were synthesized as described previously in the above sections.

Dispersion of barium cinnamate in barium acrylate

Barium cinnamate was dispersed in barium acrylate (16 %) in different percentages (by weight) to study the effect of incorporation of barium cinnamate on properties of barium acrylate. Transparent and clear compositions were obtained by the dispersion of upto 12% by weight of barium cinnamate in barium acrylate. Beyond 12% by weight, barium cinnamate was found to settle down to the bottom of the composition.

Barium cinnamate-barium acrylate compositions were evaluated for various properties such as refractive index, transmittance, thermal stability, etc.

The results of the effect of dispersion of barium cinnamate on the refractive index of barium acrylate is given in Table 4.11. As the percentage of barium cinnamate in barium acrylate increases, refractive index increases. A maximum refractive index of 1.457 is obtained in the case of dispersion of 12% by weight of BA/0.2/CA/2 in barium acrylate. On the other hand, a refractive index of 1.464 is obtained by the dispersion of 12% by weight of Ba/0.4/CA/2 in barium acrylate. This shows that there is formation of new bonds between barium cinnamate and barium acrylate taking place which is responsible for the improvement in refractive index of barium acrylate.

Table 4.11: Effect of dispersion of barium cinnamate on refractive index of barium acrylate. Refractive index increases with increase in the concentration of barium cinnamate in barium acrylate.

S. No.	Barium cinnamate (%)	Refractive index		Transmittance (%)
		Ba/0.2/CA/2	Ba/0.4/CA/2	
1.	0	1.436	1.436	94
2.	2	1.443	1.442	94
3.	4	1.447	1.445	94
4.	6	1.448	1.447	94
5.	8	1.451	1.454	94
6.	10	1.454	1.458	94
7.	12	1.457	1.464	94

Thermal stability of barium cinnamate-barium acrylate compositions was evaluated through TGA/DTA/DTG analysis. The thermograms are presented in Figures 4.20 to 4.22.

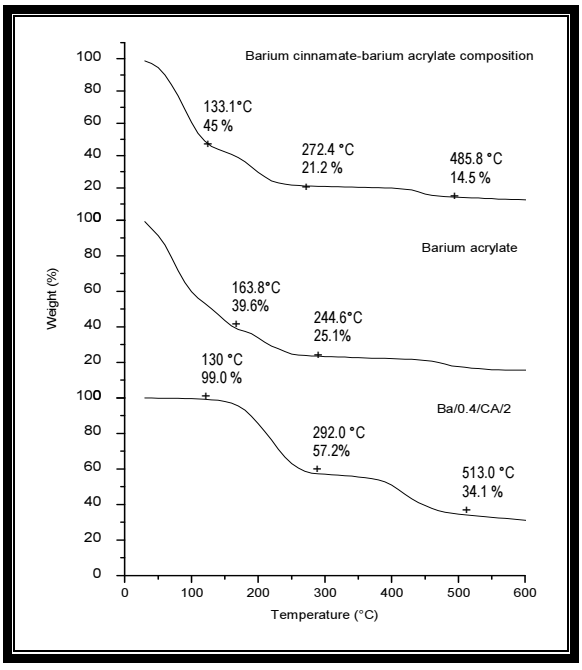

Figure 4.20: TGA thermograms of barium cinnamate, barium acrylate and barium cinnamate-barium acrylate composition. The thermograms show that the barium cinnamate-barium acrylate composition is stable at high temepratures.

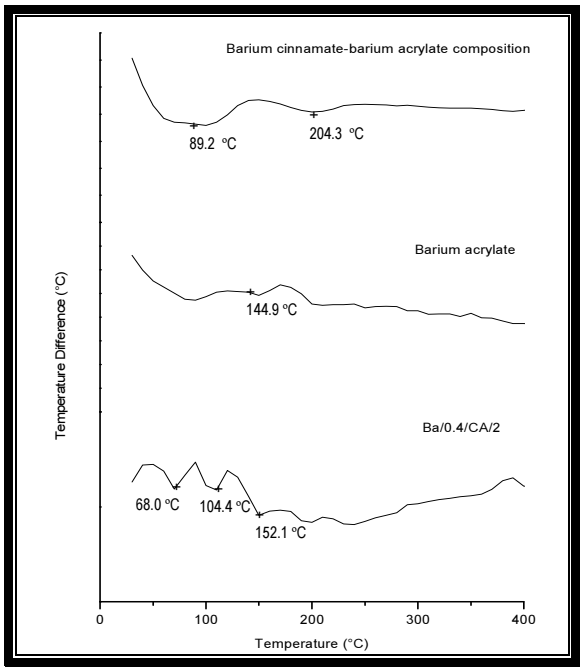

Figure 4.21: DTA thermograms of barium cinnamate, barium acrylate and barium cinnamate-barium acrylate composition show that the peaks pertaining to barium cinnamate and barium acrylate are absent in the case of barium cinnamate-barium acrylate composition indicating the formation of new compound.

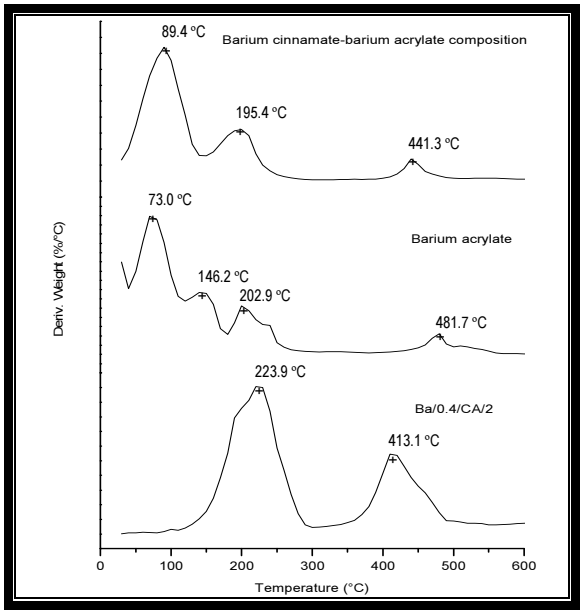

Figure 4.22: DTG thermograms of barium cinnamate, barium acrylate and barium cinnamate-barium acrylate composition. Absence of some peaks of the starting materials indicate that there is a formation of new compound by the reaction of barium cinnamate and barium acrylate.

The thermal stability of the compositions containing barium cinnamate is found to be comparable to barium acrylate indicating that the presence of barium affects the overall stability of the composition. Values of weight loss, both observed and calculated are presented in Table 4.12.

Thermal decomposition of barium cinnamate-barium acrylate composition takes place in three steps. Thermal decomposition of the composition starts immediately after 40 °C and goes upto 133 °C with 55% loss in weight. Maximum rate of decomposition occur at 89.4 °C as is evident by a sharp DTG peak ascribed to loss of water. Next decomposition occurs upto 292.4 °C with 29% loss in weight. This is ascribed to the decomposition of barium cinnamate-barium acrylate composition. Next weight loss of 7% occurs upto 485.8 °C with a DTG peak at 441.3 °C.

Table 4.12: Weight loss of barium cinnamate, barium acrylate and barium cinnamate-barium acrylate composition due to thermal decomposition

Product	Weight loss (%)					
	100 °C	200 °C	300 °C	400 °C	500 °C	600 °C
Barium cinnamate (Ba/0.4/CA/2)	0.5	14.5	43	49	65.3	68.9
Barium-acrylate	40.2	66.1	76.7	77.9	82.3	84.4
Barium cinnamate-barium acrylate composition	39.5	70.4	79.1	80.1	85.8	87.4
Theoretical loss in weight in Barium cinnamate- barium acrylate composition	35.3	59.9	72.7	74.5	80.2	82.6

The loss in weight calculated is in close agreement with the observed values indicating that the mechanism of the reaction occurs as expected.

To understand the reaction taking place between barium cinnamate and barium acrylate, UV-Visible spectroscopy was performed (Figure 4.23 a-d).

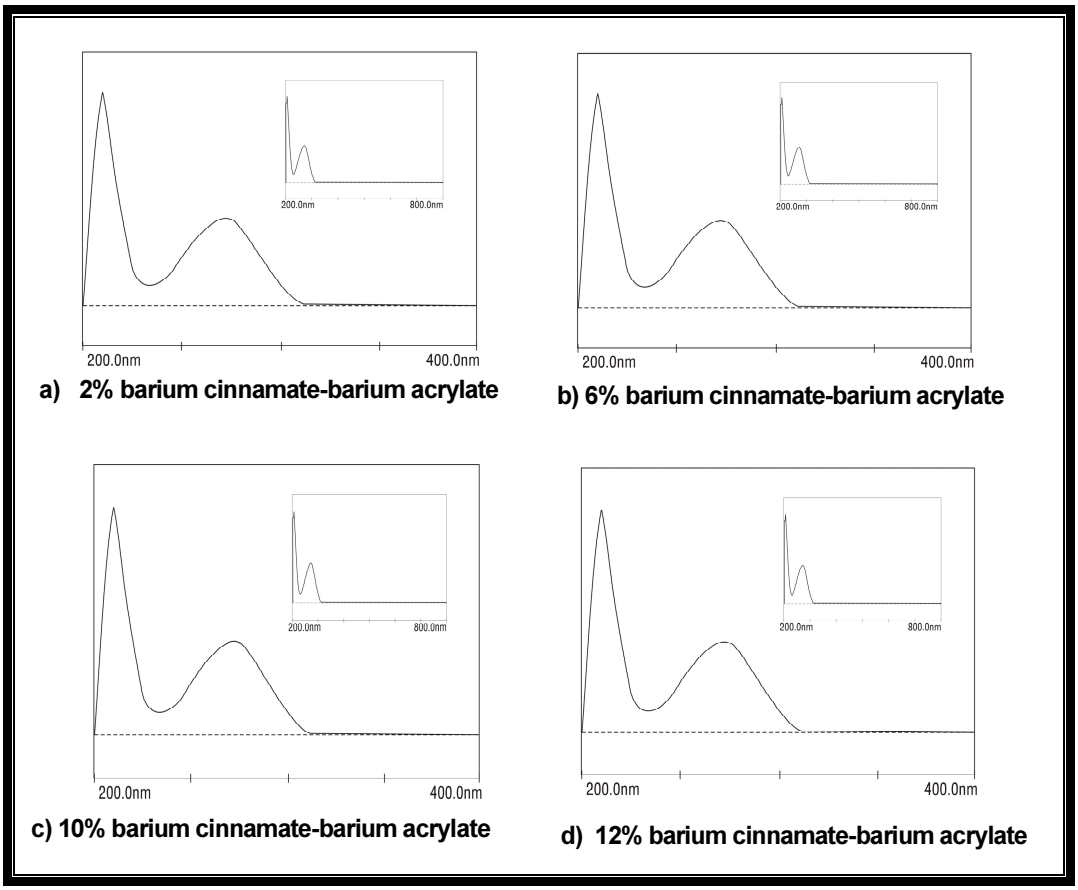

Figure 4.23 (a-d): UV-Visible spectra of barium cinnamate-barium acrylate (varying concentrations). The λ_{max} value of vinyl group of barium acrylate does not change with the dispersion of barium cinnamate.

The maximum absorption peak (λ_{max}) of barium acrylate was observed at 210 nm. As can be seen from Figure 4.23, there is no change in the λ_{max} value of barium acrylate with increase in the amount of barium cinnamate dispersed in barium acrylate. This confirms that the vinyl group of barium acrylate remains intact.

In order to understand the interactions taking place between barium cinnamate and barium acrylate, IR analysis was carried out and presented in Figure 4.24.

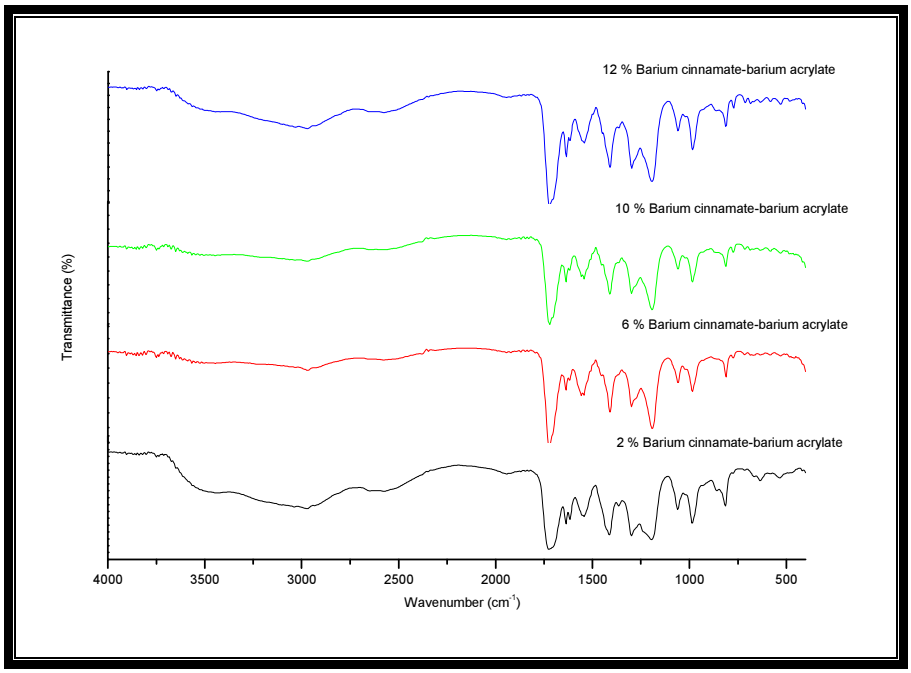

Figure 4.24: IR spectra barium cinnamate- barium acrylate compositions of varying percentages indicate the formation of homogeneous solution

Presence of bands of strong intensity at 1725 cm^{-1} and 1550 cm^{-1} indicates the presence of esters. Similar bands were also observed in individual components, i.e. barium cinnamate and barium acrylate. This indicates that no reaction is taking place between barium cinnamate and barium acrylate and thus, they appear to be in solution form homogeneously.

Cast Polymerization of Barium cinnamate-barium acrylate compositions

Barium cinnamate-barium acrylate compositions were subjected to gamma irradiation for polymerization using styrene as a co-monomer. The effect of addition of amount of styrene and gamma irradiation at doses 10-30 kGy, were studied. The dose of gamma irradiation required for complete polymerization was optimized and the effect of styrene on polymerization was studied by varying percentages of styrene (by weight of barium acrylate-barium cinnamate).

The results of the effect of styrene (percentage by weight of barium cinnamate-barium acrylate) on the polymerization of barium cinnamate-barium acrylate composition by gamma irradiation are presented in Table 4.13.

Table 4.13: Effect of styrene on polymerization of barium cinnamate-barium acrylate compositions indicating that 150% (by weight of barium cinnamate-barium acrylate) of styrene is optimum amount required to obtain clear, transparent and hard nanocomposites which are easily released from the mold

S. No.	Styrene (% by weight of barium cinnamate-barium acrylate)	Shore-D Hardness	Transmittance (%)	Appearance, etc.
1.	0	40	*	Foamy and opaque, Brittle
2.	30	*	*	Sticky could not be released
3.	60	*	*	Sticky could not be released
4.	90	*	*	Sticky, could not be released
5.	120	90	77	Hazy at the surface, hard
6.	150	90	90	Clear, transparent, easily released

*: Shore-D hardness and transmittance could not be determined due to the incomplete polymerization of the sample.

As can be seen from Table 4.13, polymerization with 30% to 90% styrene (by weight of barium cinnamate-barium acrylate), soft, sticky and brittle polymer was obtained due to insufficient amounts of styrene for polymerization. The polymer could not be released from the mold, which limits the processing characteristics of the polymer. At 120% addition of styrene (% by weight of barium acrylate-barium cinnamate), hazy polymer was obtained. Further, at 150% addition of styrene (% by weight of barium acrylate-barium cinnamate), hard, transparent and clear polymers which were easily released from the mold were obtained. This indicates that 150% (by weight) of styrene is

sufficient for polymerization of barium cinnamate-barium acrylate compositions.

To understand the role of styrene in giving hard and clear nanocomposites suitable for optical applications, let us have a look at the appearance of polymers with and without styrene (Figure 4.25).

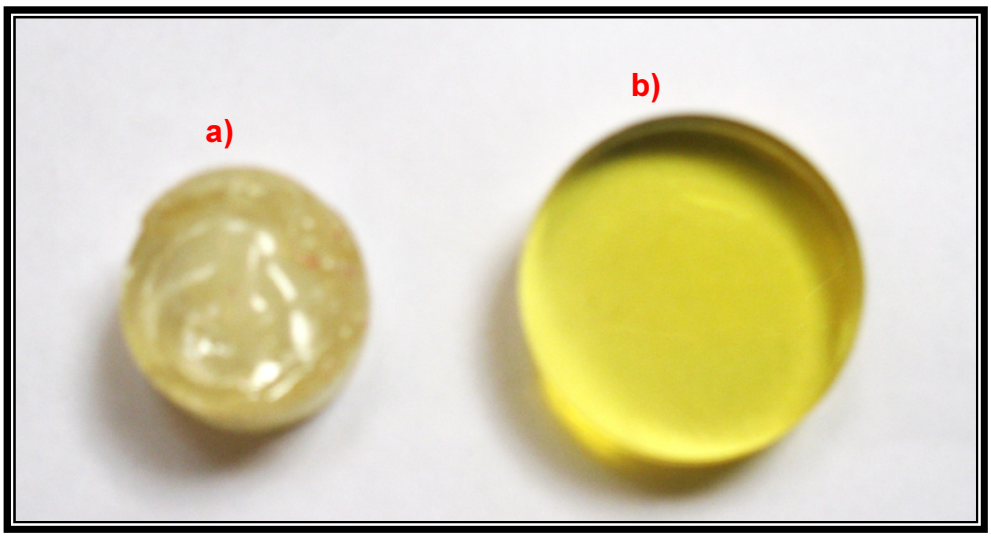

Figure 4.25: Appearance of barium cinnamate-barium acrylate nanocomposites a) without styrene and b) with styrene. In the absence of styrene, inhomogeneous and foamy polymers are formed while in the presence of styrene, transparent, clear and hard nanocomposites suitable for optical applications are obtained.

From the figure, it is evident that the presence of styrene is essential for the preparation of nanocomposites ideal for optical applications.

Polymerization of barium cinnamate-barium acrylate-styrene compositions was carried out at various doses from 10 kGy-30 kGy. Results of polymerization are shown in Table 4.14. The results of the polymerization vary with the molar ratio of barium cinnamate added i.e. Ba/0.2/CA/2 and Ba/0.4/CA/2.

Table 4.14: Results of effect of gamma irradiation on the polymerization of barium cinnamate-barium acrylate nanocomposites. The styrene content for all the cases is kept at 150% (by weight of barium cinnamate-barium acrylate compositions)

Dose	Barium Cinnamate				
	Ba/0.2/CA/2			Ba/0.4/CA/2	
	2%	4%, 6%, 8%	10%, 12%	2%	4%, 6%, 8%, 10%,12%
10	Viscous Liquid	Viscous Liquid	Viscous Liquid	Viscous liquid	Viscous liquid
15	Foamy	Foamy	Foamy	Sticky	Sticky
20	Foamy	Transp., clear	Foamy	Foamy	Transp., clear and hard
25	Foamy	Transp,, clear	Foamy	Foamy	Transp., clear and hard
30	Foamy	Transp., clear	Foamy	Foamy	Transp., clear and hard

As seen from the results in Table 4.14, it is clear that compositions at 10-15 kGy doses are viscous liquid to sticky in nature. Beyond 15 kGy, transparent, hard and clear nanocomposites are obtained for compositions containing 4-8% Ba/0.2/CA/2 while in the case of Ba/0.4/CA/2 maximum percentage of barium cinnamate that could be dispersed in barium acrylate is 12 %. This clearly indicates that with varying percentages of barium, different interactions take place resulting in the nanocomposite.

Refractive index and Abbe number of the nanocomposites were determined on the Abbe refractometer. The results are tabulated in Table 4.15.

Table 4.15: Refractive index and Abbe number of barium-cinnamate-barium acrylate nanocomposites

S. No.	Barium Cinnamate (%)	Refractive index		Abbe number	
		Ba/0.2/CA/2	Ba/0.4/CA/2	Ba/0.2/CA/2	Ba/0.4/CA/2
1.	0	1.5681	31	1.5681	31
2.	2	N.D	N.D	N.D	N.D
3.	4	1.5655	33.4	N.D	N.D
4.	6	1.5608	34.6	1.5538	31.5
5.	8	1.5623	32.8	1.5669	34.6
6.	10	N.D	N.D	1.5641	32.3
7.	12	N.D	N.D	1.5629	31.0

As can be seen from Table 4.15, addition of barium cinnamate to barium acrylate does not bring much change in the optical properties of the final complex nanocomposite. The refractive index of barium cinnamate-barium acrylate nanocomposites lie in the range of 1.5538-1.5669 and Abbe number in the range of 31-35.

Thermal stability of barium cinnamate-barium acrylate-styrene nanocomposite was studied by TG/DTA/DTG. The TGA studies of the barium cinnamate-barium acrylate-styrene nanocomposite indicate that the thermal stability is higher than the polyacrylates without barium (Figure 4.26-4.28).

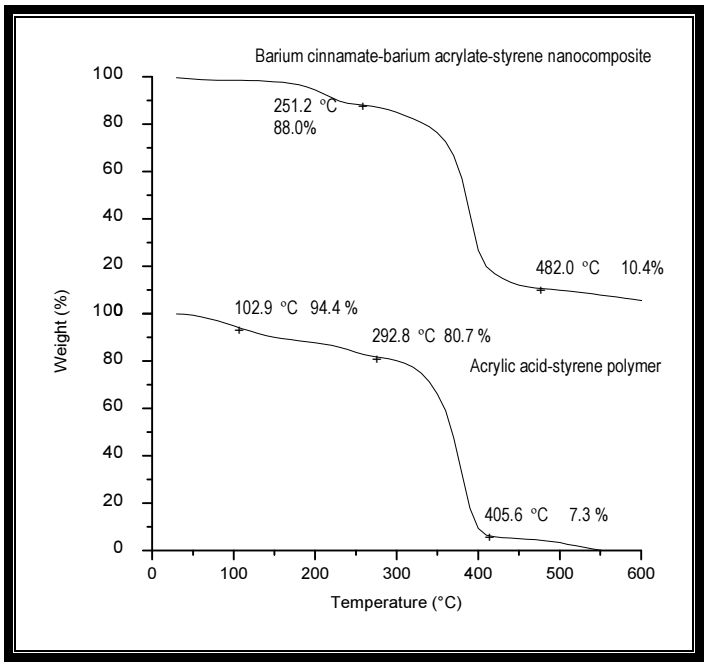

Figure 4.26: TGA thermograms of polyacrylate and barium cinnamate-barium acrylate nanocomposite indicating higher thermal stability of barium containing nanocomposites as compared to polyacrylates as such

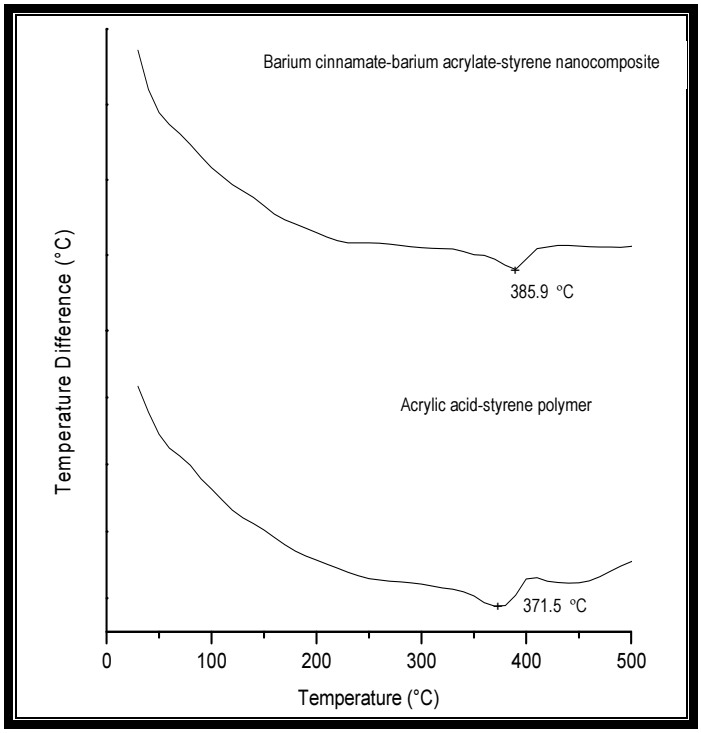

Figure 4.27: DTA thermograms of barium cinnamate- barium acrylate nanocomposites indicate better thermal stability than polyacrylate

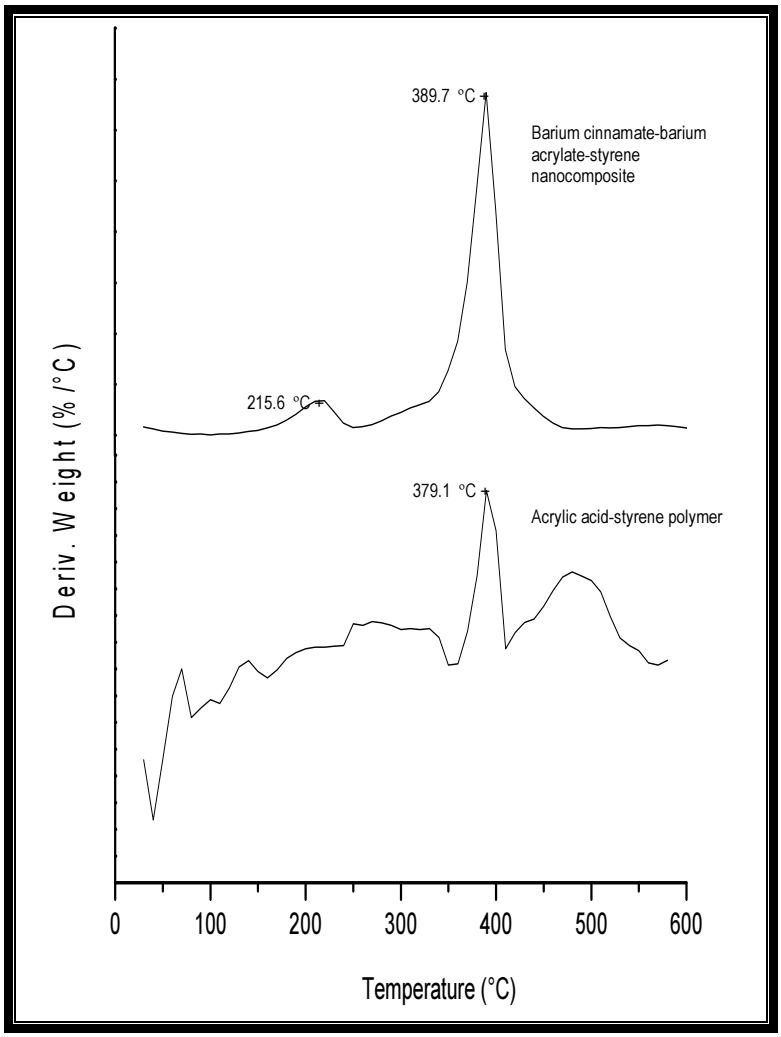

Figure 4.28: DTG thermograms of acrylic acid-styrene polymer and barium cinnamate- barium acrylate nanocomposite indicating the formation of a new compound as evident from the absence of peaks in acrylic acid-styrene polymer

Barium cinnamate-barium acrylate-styrene nanocomposites 251.2 °C with weight loss of 12% and DTG peak at 215.6 °C. Second decomposition occur upto 482 °C with 78% weight loss and DTG peak at 289.7 °C. The thermogram of barium cinnamate-barium acrylate-styrene nanocomposite shows higher thermal stability than polyacrylate as such due to the addition of barium cinnamate. The reason is greater amount of barium in the nanocompositess which imparts the stability. Polyacrylate on the other hand without barium is thermally less stable. Loss in weight due to thermal

decomposition of acrylic acid-styrene polymer and barium cinnamate-barium acrylate-styrene nanocomposites is presented in Table 4.16.

Table 4.16: Weight loss due to thermal decomposition of acrylic acid-styrene polymer and barium cinnamate-acrylate-styrene nanocomposite

Product	Weight loss (%)					
	100 °C	200 °C	300 °C	400 °C	500 °C	600 °C
Acrylic acid-styrene polymer	5.2	12.3	19.9	90.6	96.7	100
Barium cinnamate barium-acrylate-styrene nanocomposite	1.5	1.4	15.1	73.3	90.1	94.4

It is clearly visible from Table 4.16 that barium cinnamate-barium acrylate-styrene nanocomposite is thermally stable as compared to polyacrylate as such. This is due to the fact that the presence of barium in the nanocomposite builds a strong network resulting in high thermal stability of the final product.

The transmittance of the samples as determined by UV-Visible spectroscopy was found to be 90%. The lenses were found to be impact resistant as per FDA regulations.

Machinability of the nanocomposites was checked by subjecting the samples to grinding. No odour was observed during the machining and the samples were easily machined into various shapes. The hardness of the lenses was checked by determining the shore-D hardness and scratch resistance. Shore-D hardness of the nanocomposites was found to be 94. In the case of barium cinnamate-barium acrylate-styrene nanocomposite, specific gravity of 1.19 was obtained. This would help in designing of light-weight optical devices.

The Vicat softening temperature of 123 $^{\circ}$C for barium cinnamate-barium acrylate-styrene nanocomposite indicates that the working temperature is much higher than PMMA which has a working temperature of 109 $^{\circ}$C. This brings scope for the barium nanocomposites to be used in extreme conditions.

Preparation of cinnamic acid-acrylic acid polymers

Synthesis of cinnamic acid-acrylic acid composition

Synthesis of cinnamic acid-acrylic acid composition was done by gradual addition of cinnamic acid to acrylic acid in a round bottom flask (assembly shown in Chapter 3) at ambient temperature. Cinnamic acid was added to acrylic acid in varying percentages under vigorous stirring. The observations related to the dispersion of cinnamic acid to acrylic acid are tabulated in Table 4.17. For understanding the changes taking place during the reaction of acrylic acid and cinnamic acid, cinnamic acid-acrylic acid compositions were evaluated for refractive index. The results of the refractive index values are given in Table 4.17 and Figure 4.29.

Table 4.17: Effect of dispersion of cinnamic acid on clarity and refractive index of acrylic acid. Cinnamic acid is soluble upto a concentration of 13% (by weight). Beyond 13%, cinnamic acid could not be dispersed in acrylic acid. Maximum refractive index achieved by the dispersion of cinnamic acid in acrylic acid is 1.448.

S. No.	Cinnamic acid (%)	Observations	Refractive index
1.	0	Transparent, clear solution	1.424
2.	2	Transparent, clear solution	1.431
3.	4	Transparent, clear solution	1.435
4.	6	Transparent, clear solution	1.438
5.	8	Transparent, clear solution	1.441
6.	10	Transparent, clear solution	1.442
7.	12	Transparent, clear solution	1.445
8.	13	Transparent, clear solution	1.448
9.	14	Could not be dispersed	*

*: Refractive index could not be determined as cinnamic acid was not homogeneously dispersed

It was being observed that upto 13% (by weight) addition of cinnamic acid to acrylic acid resulted in clear and transparent solutions. Beyond 13%, cinnamic acid could not be dispersed in acrylic acid. It can be seen from the results presented in Table 4.17 that the addition of cinnamic acid to acrylic acid brings an improvement in the refractive index of acrylic acid. The refractive index of acrylic acid increases from 1.424 to 1.448 by the dispersion of 13% (by weight) of cinnamic acid to acrylic acid. Here, it may be noted that the aromatic ring of cinnamic acid which is characterized by a high intrinsic molar refraction (26.14) is responsible for bringing an improvement in the refractive index of acrylic acid.

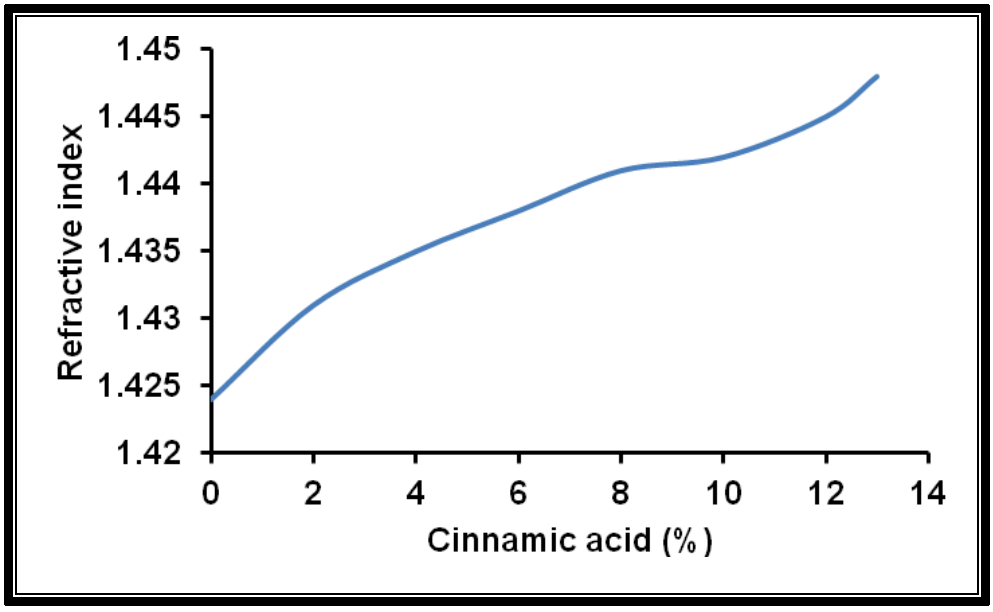

Figure 4.29: Effect of cinnamic acid on refractive index of acrylic acid. Refractive index of acrylic acid increases as the amount of dispersion of cinnamic acid in acrylic acid is increased.

Acid value of cinnamic acid-acrylic acid compositions was determined and is presented in Table 4.18.

Table 4.18: Acid value of cinnamic acid-acrylic acid compositions indicate that the acid value do not change significantly due to acidic character of both the components

S. No.	Cinnamic acid (%)	Acid value
1.	0	626
2.	2	616
3.	4	608
4.	6	596
5.	8	582
6.	10	575
7.	12	568
8.	13	560

As can be seen from Table 4.18, there is a decrease in the acid value of acrylic acid as cinnamic acid is added to it. Acrylic acid has an acid value of 626. Cinnamic acid being acidic possess an acid value of 368. On addition of 2% cinnamic acid to acrylic acid, the acid value of acrylic acid decreases to 616, 608 with 4% addition of cinnamic acid, 596 with 6% addition, 582 with 8% addition of cinnamic acid, 575 with 10% addition, 568 with 12% addition and 560 with 13% addition of cinnamic acid to acrylic acid. It is clear that the acid value does not change much as both the components are acidic in nature.

In order to understand the reaction between acrylic acid and cinnamic acid, UV-Visible spectroscopy was performed (Figure 30 a-f).

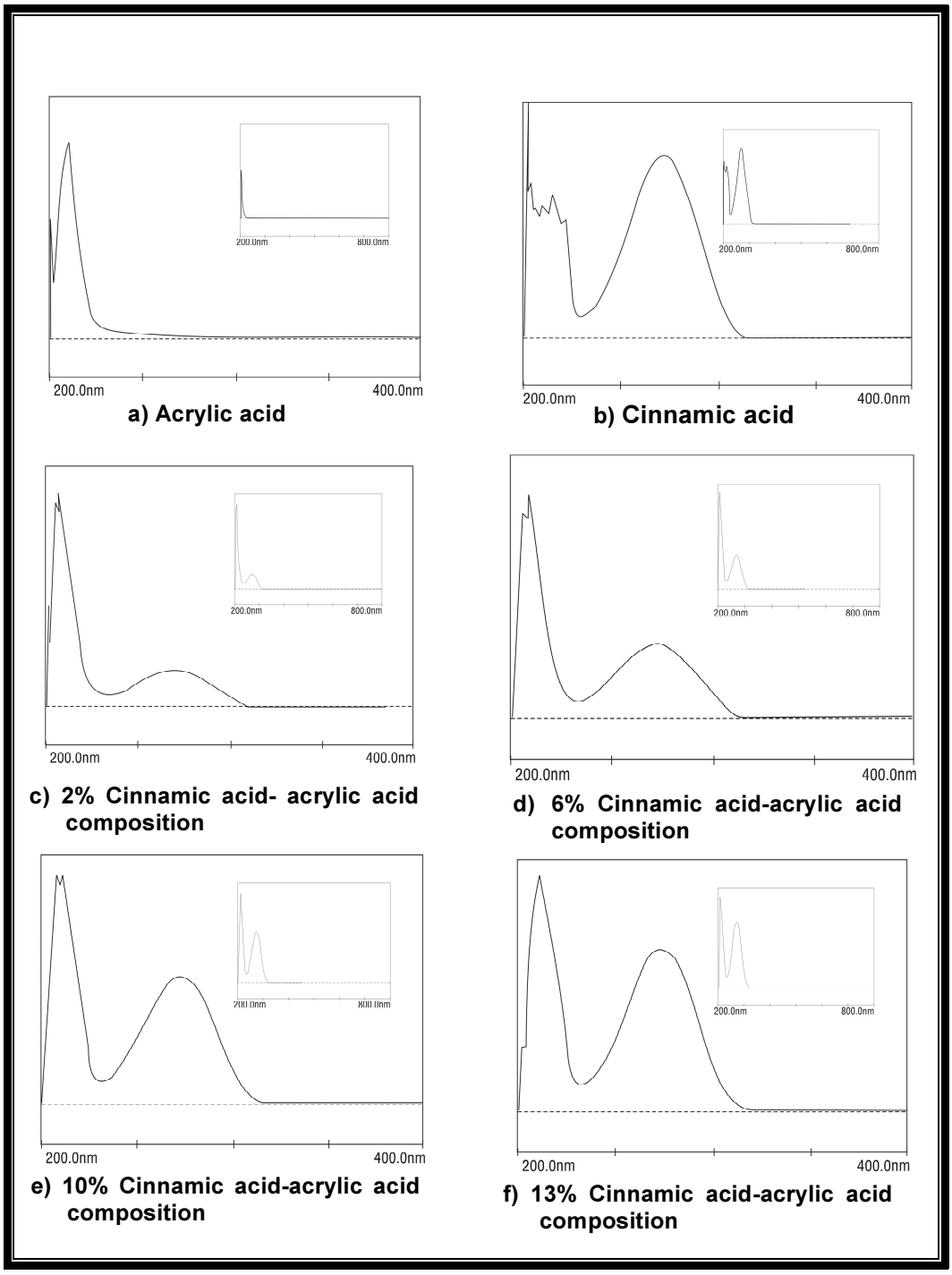

Figure 4.30 a-f): UV-Visible spectra of acrylic acid, cinnamic acid and cinnamic acid-acrylic acid compositions. Acrylic acid exhibits λ_{max} at 210 nm and cinnamic acid exhibits λ_{max} at 273 nm. In the case of cinnamic acid-acrylic acid compositions, 2 peaks are observed; at 210 nm (characteristic of acrylic acid) and 273 nm (characteristic of cinnamic acid). Presence of peaks indicates that vinyl group of acrylic acid and cinnamic acid is intact.

As can be seen from Figure 30 a-f, cinnamic acid-acrylic acid composition exhibit a peak at 210 nm, characteristic of acrylic acid and 273 nm which is a characteristic peak of cinnamic acid, at all concentrations. This shows that the reaction between cinnamic acid and acrylic acid do not take place at the vinyl group of cinnamic acid or lanthanum acrylate; the vinyl group remains intact. To understand the interactions taking place between acrylic acid and cinnamic acid, IR analysis was performed and the results are presented in Figure 4.31.

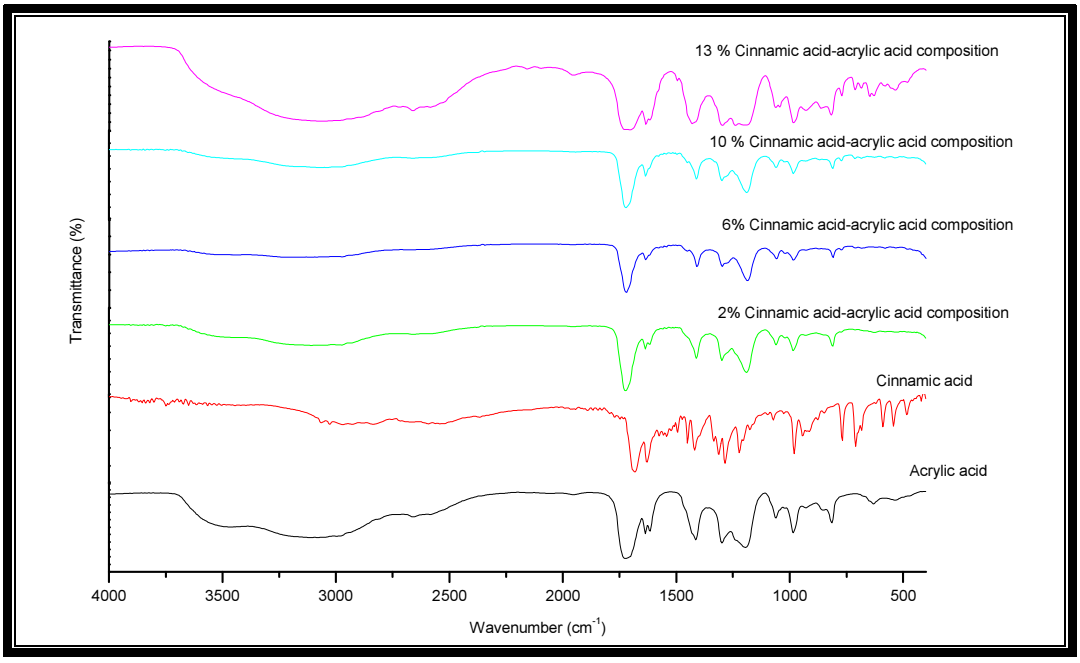

Figure 4.31: IR analysis of acrylic acid, cinnamic acid and cinnamic acid-acrylic acid composition

As can be seen from Figure 4.31, cinnamic acid exhibits an aryl C=C stretching at 1629 cm^{-1}. In the case of cinnamic acid -acrylic acid composition, band at 1634 cm^{-1} is ascribed to vinyl C=C vibration. Spectra also confirm the presence of free carboxylic acid groups. It is suggested that the co-ordination take place between the π-electron system of the cinnamic acid as the change to lower frequency of 1625 to 1617 cm^{-1} is observed.

Thermal stability of cinnamic acid- acrylic acid compositions was evaluated through TGA/ DTA/DTG. The thermogram of the same is presented in Figures 4.32 to 4.34.

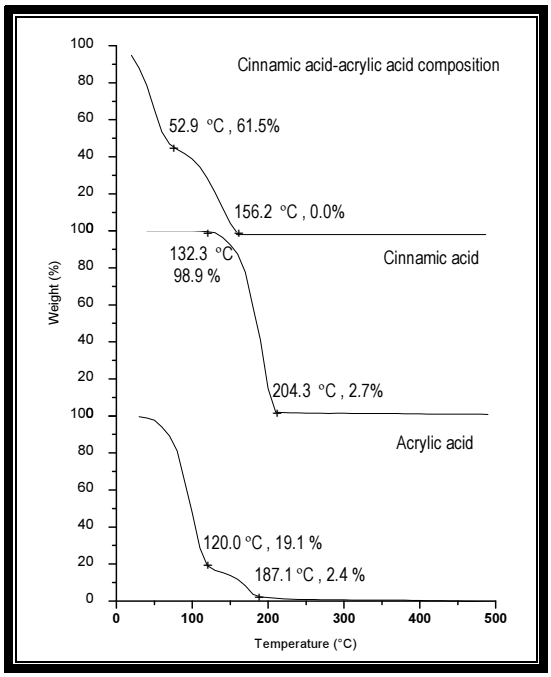

Figure 4.32: TGA thermograms of acrylic acid, cinnamic acid & cinnamic acid-acrylic acid composition indicate lower thermal stability of the cinnamic acid-acrylic acid composition

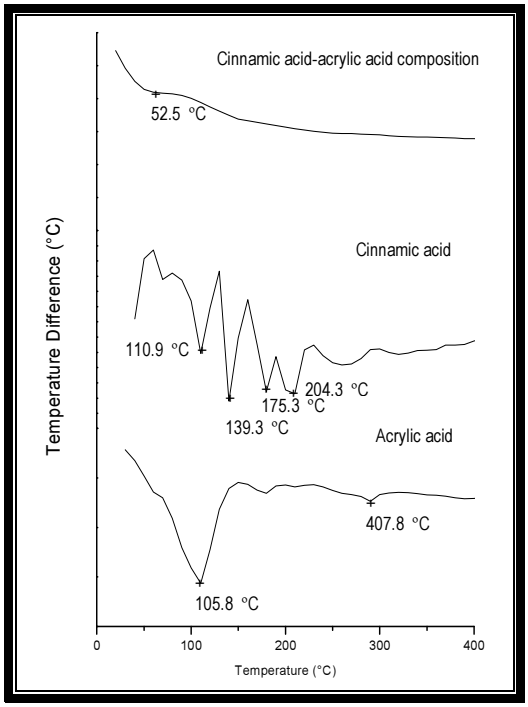

Figure 4.33: DTA thermograms of acrylic acid, cinnamic acid & cinnamic acid-acrylic acid composition shows absence of peaks in final composition and hence formation of new compound

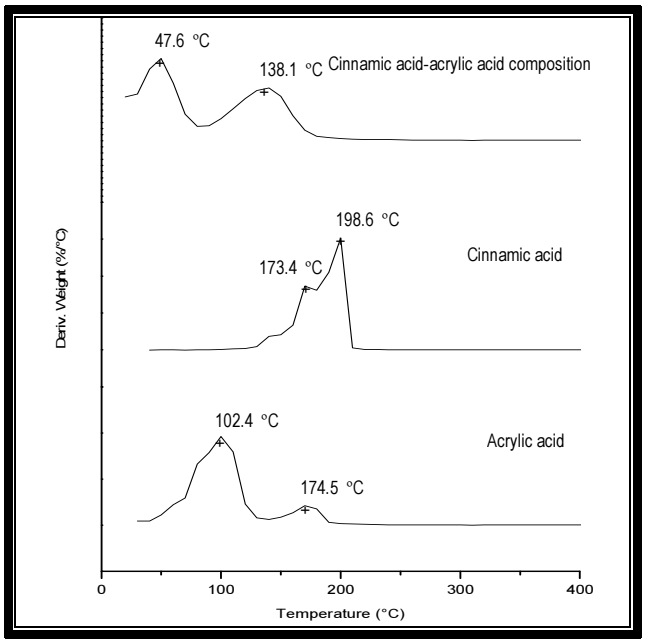

Figure 4.34: DTG thermograms of acrylic acid, cinnamic acid & cinnamic acid-acrylic acid composition. Thermogram indicates that new peaks are absent in the starting materials thereby indicating the formation of new compound.

TGA of cinnamic acid shows single step decomposition. Cinnamic acid starts decomposing after 133 ºC. At 133 ºC, cinnamic acid melts and undergoes phase change. The thermal decomposition process occurs in a well-defined large step upto 204.9 ºC with a weight loss of 96.5 %, defined by DTG peaks at 172.9 ºC and 199.0 ºC. Both the peaks are ascribed to the decomposition of cinnamic acid. Both cinnamic acid and acrylic acid show maximum weight loss upto 200 °C. In all the cases, maximum decomposition take place upto 200 ºC. Acrylic acid-cinnamic acid composition is found to undergo complete decomposition before 200 ºC.

Cinnamic acid-acrylic acid composition decomposes completely before 200 °C. It consists of 2 sharp DTG peaks corresponding to two decomposition steps. The first decomposition occur upto 52.9 °C with a weight loss of 39%. The DTG peak at 47.6 ºC is ascribed to the decomposition of the newly formed complex. The second decomposition results in complete weight loss

of the composition upto 156.2 °C and shows a DTG peak at 138.1 °C. Weight loss due to second decomposition is 43 %.

The results of weight loss due to thermal decomposition of acrylic acid, cinnamic acid and cinnamic acid-acrylic acid compositions are given in Table 4.19.

Table 4.19: Weight loss due to thermal decomposition of acrylic acid, cinnamic acid and cinnamic acid-acrylic acid composition

Product	Weight loss (%)					
	100 °C	**200 °C**	**300 °C**	**400 °C**	**500 °C**	**600 °C**
Acrylic acid	52.2	98.2	100	100	100	100
Cinnamic acid	0	98.5	100	100	100	100
Cinnamic acid-acrylic acid composition	61.2	100	100	100	100	100
Theoretical loss in weight of Cinnamic acid- acrylic acid composition	45.4	98.2	100	100	100	100

As can be seen from Table 4.19, the thermal decomposition behaviour of cinnamic acid-acrylic acid composition is similar to the individual raw materials used to prepare it. The weight loss (%) is on the same lines as expected and calculated theoretically.

Cast Polymerization of cinnamic acid-acrylic acid compositions

Cinnamic acid-acrylic acid compositions were subjected to different doses of gamma irradiation for polymerization. Styrene was used as a co-monomer for polymerization. The effect of addition of styrene and gamma irradiation dose on polymerization of acrylic acid-cinnamic acid compositions was studied. The polymers were evaluated for various properties based on which optimization of process parameters was carried out.

The effect of amount of styrene (% by weight of cinnamic acid-acrylic acid composition) on the polymerization of cinnamic acid-acrylic acid composition by gamma irradiation was studied and the results are presented in Table 4.20.

Table 4.20: Effect of styrene on polymerization indicating that 150% of styrene (by weight of cinnamic acid-acrylic acid composition) is sufficient to obtain clear, transparent and hard polymers which are easily released from mold

S. No.	Styrene (moles)	Shore-D Hardness	Transmittance (%)	Appearance, etc.
1.	0	*	*	Foamy and opaque, Brittle
2.	30	*	*	Sticky could not be released
3.	60	*	*	Sticky could not be released
4.	90	*	*	Sticky, could not be released
5.	120	92	71	Hazy at the surface, hard
6.	150	94	90	Clear, transparent, easily released

*: Shore-D hardness and Transmittance could not be determined due to foamy or sticky nature of the polymers

From the results presented in Table 4.20, it may be seen that polymerization of cinnamic acid-acrylic acid composition by gamma irradiation results in foamy and brittle polymer in the absence of styrene (Figure 4.35a). In the presence of styrene, clear, transparent and hard polymers suitable for optical applications were obtained (Figure 4.35b).

With the addition of 30%-90% (by weight of cinnamic acid-acrylic acid composition) of styrene, soft and sticky polymers were obtained due to insufficient amounts of styrene. The polymer, being soft and sticky could not be released from the molds, which limits the processing characteristics of the polymer. With 120% addition of styrene (by weight of cinnamic acid-acrylic acid composition), hazy polymer is obtained. With 150% (by weight of cinnamic acid-acrylic acid composition) of styrene, the shore-D hardness increased to 94 and the polymers were easily released from the mold. Transmittance was maximum for 150% (by weight of cinnamic acid-acrylic acid composition) of styrene used. Clear and transparent polymers were obtained.

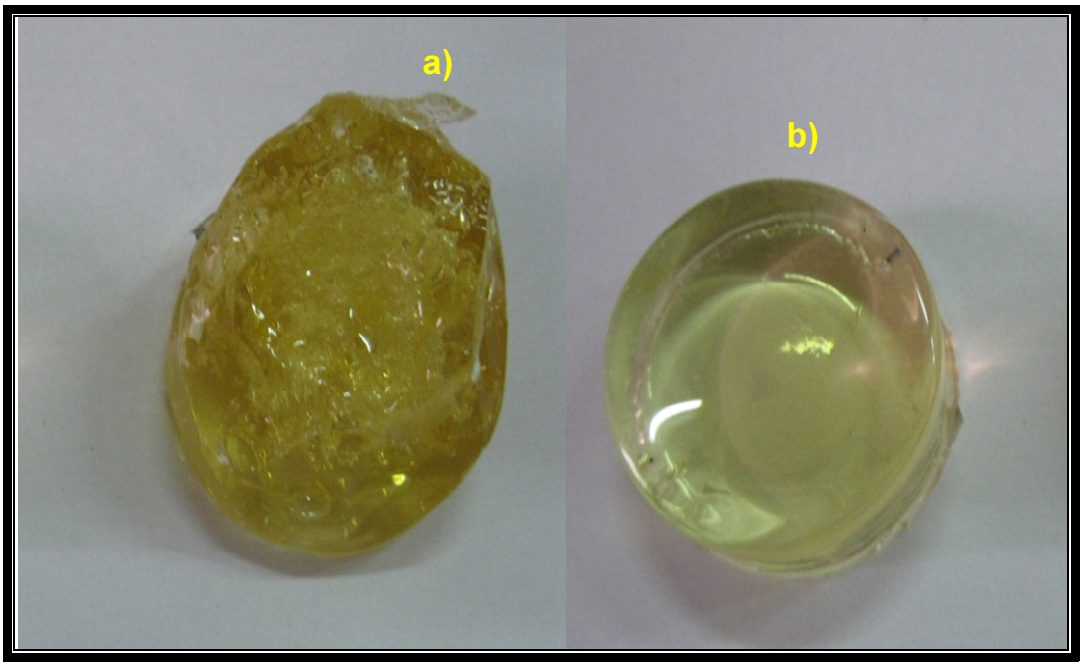

Figure 4.35: Cinnamic acid-acrylic acid polymer a) without styrene and b) with styrene indicating that the presence of styrene is essential to obtain polymers suitable for optical applications

The results of the effect of dose from 10 kGy to 30 kGy of gamma irradiation on the polymerization of cinnamic acid-acrylic acid -styrene compositions are presented in Table 4.21.

Table 4.21: Effect of gamma irradiation on the polymerization of cinnamic acid-acrylic acid polymers. 20 kGy was found to be the optimum dose for cinnamic acid-acrylic acid polymers.

S.No.	Dose (kGy)	Shore-D Hardness	Cross-link density (%)	Appearance
1	10	*	*	Viscous liquid
2	15	*	84	Transparent, sticky at the surface
3	20	94	95	Transparent, hard and easily released
4	25	94	95	Transparent, hard and easily released
5	30	94	96	Transparent, hard and easily released

*: Shore-D hardness and cross-link density of the polymers could not be determined due to viscous liquid sticky nature of the polymer

As seen from the results in Table 4.21, cinnamic acid-acrylic acid-styrene compositions when subjected to a dose of 10 kGy gave a viscous liquid. Dose of 15 kGy gave a sticky polymer which was very soft and difficult to process. A dose of 20 kGy and higher led to transparent and hard polymers with a shore-D hardness of 94. It can be seen that the dose of radiation does not affect the shore-D hardness of samples beyond 20 kGy. The suitable dose for polymerization by gamma irradiation was optimized as 20 kGy for cinnamic acid-acrylic acid-styrene polymers.

Refractive index and Abbe number of the polymers were determined on the Abbe refractometer. The results are tabulated in Table 4.22 and presented in Figures 4.36-4.37.

Table 4.22: Refractive index and Abbe number of cinnamic acid-acrylic acid polymers show that the refractive index of acrylic acid increases as content of cinnamic acid is increased

S.No	Cinnamic acid (% by wt)	Cinnamic acid-acrylic acid polymers	
		Refractive index	Abbe number
1.	0	1.5336	32
2.	2	1.5352	32
3.	4	1.5492	31
4.	6	1.5528	33
5.	8	1.5536	32
6.	10	1.5530	32
7.	12	1.5589	32
8.	13	1.5624	32

As can be seen from Table 4.22, maximum refractive index of 1.5624 was obtained with 13% (by weight) dispersion of cinnamic acid in polymer with Abbe number of 32. It is found to be better than commercially available polyacrylates i.e. polymethyl methacrylate, a commercial grade of acrylate polymer for various optical applications, which has a refractive index of 1.491.

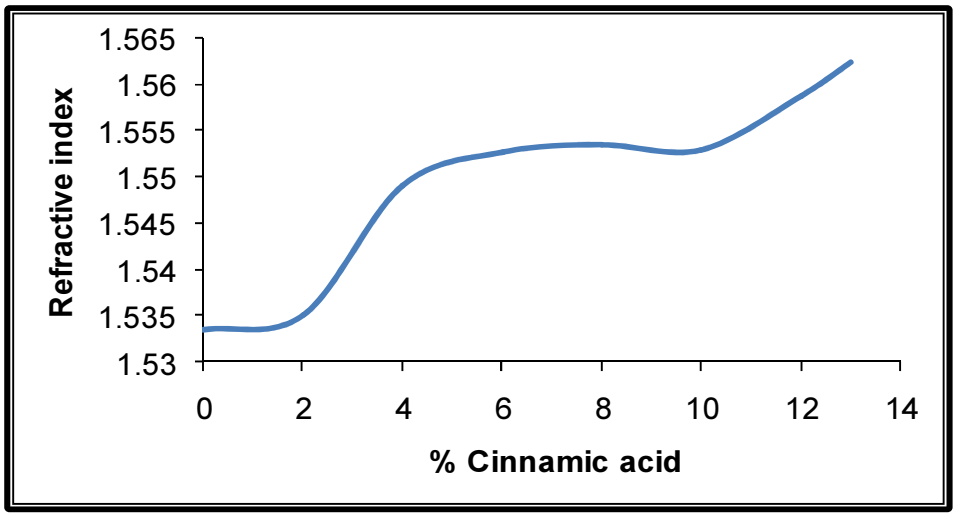

Figure 4.36: Effect of cinnamic acid on refractive index of cinnamic acid-acrylic acid-styrene polymer. Refractive index increases with the increasing content of cinnamic acid in the polymer

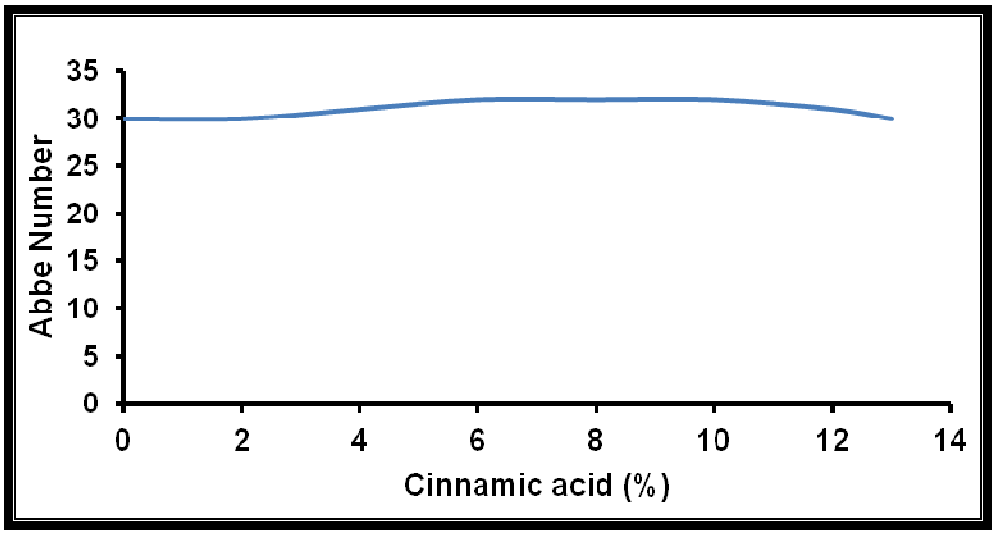

Figure 4.37: Effect of cinnamic acid on Abbe number of cinnamic acid-acrylic acid-styrene polymer.

Thermal analysis of cinnamic acid-acrylic acid polymers was studied by TG/DTA/DTG. The TGA studies of the cinnamic acid-acrylic acid-styrene polymer indicate the formation of a highly cross-linked, thermally stable structure as can be seen from Figures 4.38 to 4.40.

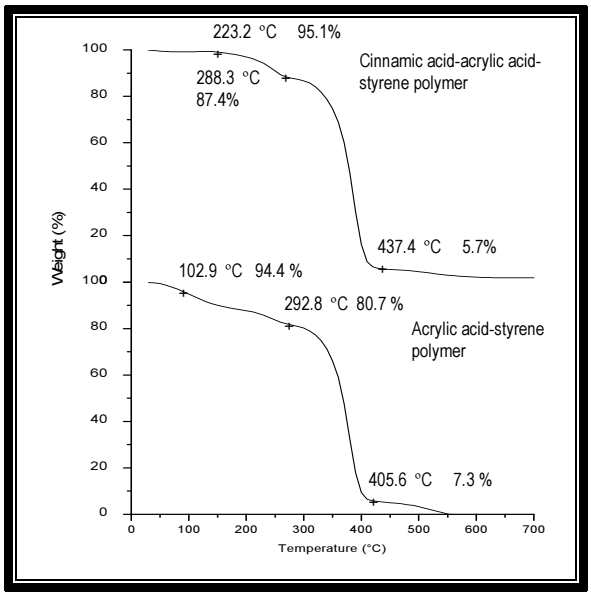

Figure 4.38: TGA thermograms of cinnamic acid-acrylic acid-styrene polymer indicates higher thermal stability than the polyacrylate

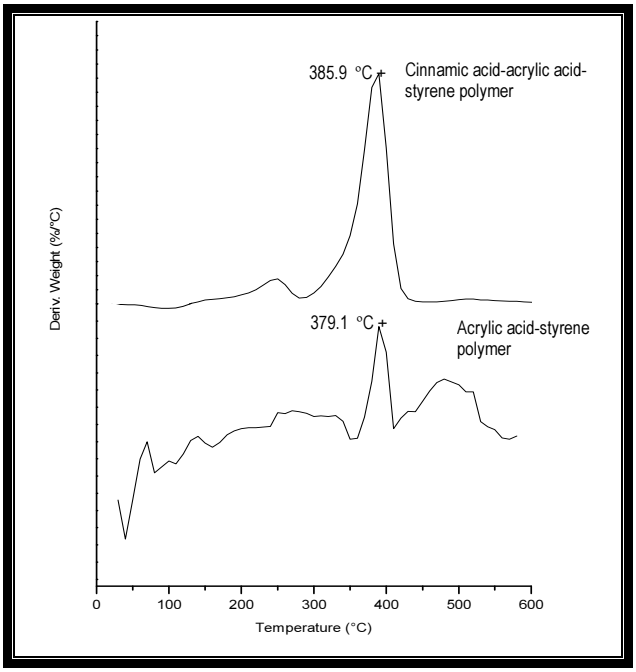

Figure 4.39: DTG thermograms of polyacrylate and cinnamic acid-acrylic acid polymer showing absence of peaks in the case of acrylic acid-cinnamic acid polymer thereby indicating the formation of a new compound

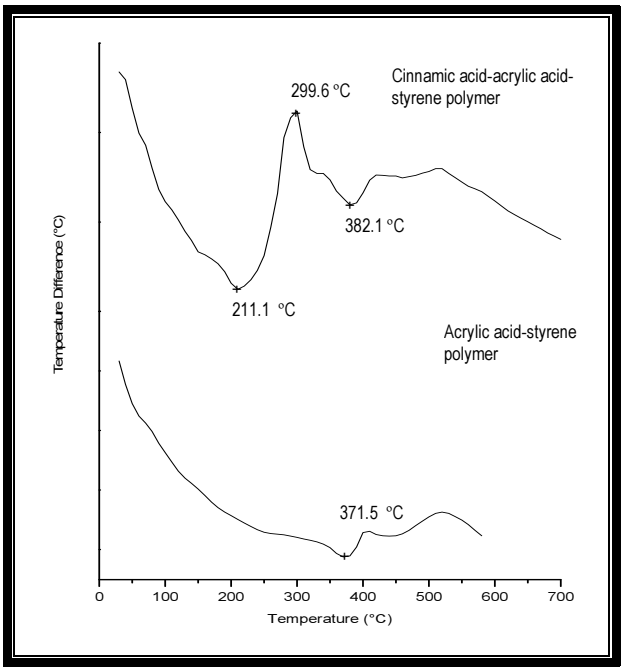

Figure 4.40: DTA thermograms of polyacrylate and cinnamic acid-acrylic acid polymer shows the formation of a new compound

The weight loss of the polymers was recorded at various temperatures, which is given in Table 4.23. The heat stability of the polymer system is found to be much higher than that of the acrylic acid-styrene polymer, which is possible only due to the formation of a cross-linked structure.

Table 4.23: Weight loss due to thermal decomposition of acrylic acid-styrene polymer and cinnamic acid-acrylic acid polymer

Product	Weight loss (%)					
	100 °C	200 °C	300 °C	400 °C	500 °C	600 °C
Acrylic acid-styrene polymer	5.2	12.3	19.9	90.6	96.7	100
Acrylic acid-cinnamic acid-styrene polymer	1.2	6.4	16.1	76.4	91.4	95.4

The cinnamic acid-acrylic acid-styrene polymer shows decomposition in two steps with a weight loss of approximately 13% by weight upto 288.3 °C which could be due to the presence of moisture and volatiles. Second weight loss of

82% occur upto 437.4 °C; DTG peak at 385.9 °C and corresponding DTA peak at 382.1 °C. An exotherm at 299.6 °C is also observed which is attributed to the decomposition of the complex. It can also be seen that the acrylic acid-cinnamic acid polymer is much thermally stable at 600 ºC as compared to acrylic acid-styrene polymer which do not contain cinnamic acid. Hence, cinnamic acid-acrylic acid-styrene polymers can be used for high temperature applications.

The transmittance of the samples as determined by UV-Visible spectroscopy was found to be 90%. The polymers were found to be impact resistant as per FDA regulations.

Machinability was checked by subjecting the samples to grinding and machining. It was observed that the polymers possessed good machinability characteristics. The hardness of the polymers was checked by determining the shore-D hardness using a shore-D Durometer and scratch resistance. Shore-D hardness of the polymers was found to be 94 for acrylic acid-cinnamic acid polymer. Pencil hardness and scratch resistance of acrylic acid-cinnamic acid polymers was found to be better than PMMA. PMMA has a scratch resistance of grade “C” and a pencil hardness of 4H while cinnamic acid-acrylic acid-styrene polymer have scratch resistance of grade “B” and pencil hardness of 6H. Acrylic acid-cinnamic acid polymer is superior in hardness to PMMA.

In the case of cinnamic acid-acrylic acid-styrene polymer, specific gravity of 1.16 was obtained. The specific gravity of PMMA is 1.26. This indicates that the cinnamic acid-acrylic acid-styrene polymers prepared by gamma irradiation are much lighter as compared to the conventional polymer system.

The Vicat softening temperature of 100 °C for cinnamic acid-acrylic acid polymer indicate that the working temperature of cinnamic acid-acrylic acid polymer is much lower than PMMA which has a working temperature of 109 °C.

4.5 CONCLUSIONS

In this chapter, novel nanocomposites based on acrylates and cinnamates of barium metal have been prepared. The achievements of the present study are as follows:

1. Three methodologies have been adopted to prepare barium-containing nanocomposites
2. Preparation of barium-containing nanocomposites has been done using acrylic acid and cinnamic acid.
3. Out of the many compounds of barium tried for dispersion in acrylic acid, the most suitable was barium hydroxide.
4. The modification of an important monomer, acrylic acid, for optical applications, has been done in a novel and cost-effective manner.
5. The effect of dispersion of barium In acrylic acid was monitored by studying the changes taking place in the refractive index, acid value and thermal stability of acrylic acid.
6. The effect of dispersion of barium hydroxide on the transmittance of acrylic acid was studied and was found to have 99% transmittance in the visible range. Thus, the solutions obtained after the reaction of barium hydroxide and acrylic acid were transparent and clear in appearance and suitable for optical applications.
7. Dispesion of barium hydroxide in acrylic acid resulted in an increase in refractive index to 1.436 from 1.424 to start with.
8. The acidity of acrylic acid decreases from 626 to 477 by the addition of barium hydroxide. This fact was supported by the change in pH values from < 1 to 2.12 of acrylic acid. This clearly indicates that the reaction is taking place between barium hydroxide and acrylic acid.
9. Particle size analysis of barium hydroxide-acrylic acid compositions show that the particles are of the size of less than 0.8 nm confirming

that the dispersion of barium hydroxide in acrylic acid leads to the formation of homogeneous and clear solution.

10. The thermal analysis of the composition was carried out and the observed loss in weight of the composition was less than the theoretical data. Acrylic acid as such looses its weight completely upto 300 $^{\circ}$C. It was found that the observed loss in weight was less as compared to the calculated one. This indicates high thermal stability of acrylic acid on addition of barium to it.

11. In order to further confirm the interactions taking place between barium hydroxide and acrylic acid, UV-Visible spectroscopy and infrared spectroscopy was performed. The results show that the vinyl group of acrylic acid remains intact during the dispersion of barium hydroxide and the reaction is taking place at the carboxylic acid group as is evident by the presence of characteristic band of ester group (1544 cm^{-1}-1550 cm^{-1}) leading to the formation of barium acrylate.

12. Polymerization of such compositions into transparent and clear lenses for optical applications would be a breakthrough in the optical industry.

13. To facilitate the cross-linking of the groups during polymerization, styrene as a co-monomer was added to barium acrylate. Styrene was added in varying percentages (by weight) to barium acrylate to obtain clear and transparent solutions.

14. Gamma irradiation has been used as a novel technique for the polymerization of barium acrylate. Addition of 150 % styrene (by weight of barium acrylate) resulted in clear and transparent lenses with shore-D hardness of 90.

15. Optimization of irradiation dose was done based on cross-link density. Compositions were subjected to gamma irradiation dose from 10 kGy to 30 kGy and the optimum dose of 20 kGy was decided based on maximum cross-link density of the nanocomposite (i.e. 95%).

16. The resulting nanocomposites were clear and transparent. The maximum refractive index of the nanocomposite obtained was 1.568 and Abbe number was 31. The optical properties can be tailor-made by varying the content of the metal salt.

17. The physico-mechanical properties such as specific gravity, hardness, machinability, etc are better than the properties of conventional available polymers.

18. The second approach followed for the preparation of barium-containing nanocomposites pertains to the dispersion of barium in cinnamic acid.

19. A detailed study of the properties of barium cinnamate, an aspect never investigated before has been done successfully. Barium was incorporated upto an extent of 14% to prepare barium cinnamate.

20. XRD analysis showed that formation of a new compound (barium cinnamate) takes place by the reaction of barium hydroxide and cinnamic acid.

21. The infrared spectra also showed the formation of new compound on the reaction of barium hydroxide and cinnamic acid.

22. Thermal analysis studies showed that barium cinnamate is thermally more stable than cinnamic acid. This is due to the fact that barium forms strong bonds with cinnamic acid resulting in higher thermal stability.

23. An attempt to polymerize barium cinnamate was carried out. It was observed that barium cinnamate does not get polymerized as such.

24. Third novel approach for preparation of barium-containing nanocomposites was followed by the dispersion of barium cinnamate in barium acrylate.

25. Upto 12% (by weight) barium cinnamate could be dispersed in barium cinnamate yielding clear and transparent compositions.

26. By the dispersion of barium cinnamate in barium acrylate, refractive index of barium acrylate could be improved to 1.464.

27. UV-Visible and Infrared spectroscopy was carried out to confirm the reaction between barium cinnamate and barium acrylate. It was seen that all the bands of barium acrylate were intact after dispersion of barium cinnamate in barium acrylate, thereby suggesting the formation of a mixture.

28. Styrene was used as a co-monomer for the cast polymerization of barium cinnamate-barium acrylate compositions into lenses.

29. Barium cinnamate-barium acrylate nanocomposites were synthesized using gamma irradiation technology and the essential properties were tailor-made.

30. The physico-mechanical properties of barium cinnamate-barium acrylate-styrene nanocomposites were fund to be better as compared to the conventional available optical plastics.

31. Refractive index of the nanocomposites were found to lie between 1.55 and 1.57 whereas Abbe number lie between 31 and 35.

32. Barium cinnamate-barium acrylate nanocomposites were found to be thermal more stable than the conventional optical materials used.

33. Preparation of reference material without barium metal i.e. cinnamic acid-acrylic acid polymer has been developed by varying the concentration of cinnamic acid in acrylic acid.

34. Upto 13% (by weight) cinnamic acid could be dispersed in acrylic acid to obtain clear and transparent compositions exhibiting 99% transmittance.

35. UV-Visible and Infrared spectroscopy suggested that no new bands are present in the composition, thereby suggesting the formation of a mixture rather than a chemical reaction taking place.

36. Change in the acid number of acrylic acid after the dispersion of cinnamic acid was found to be insignificant as acid character of cinnamic acid contributes to the overall acid value of the compositions.

37. UV-Visible spectroscopy and Infrared spectroscopy does not show the presence of any new bands in the compositions, indicating the cinnamic acid-acrylic acid compositions to be homogeneous mixtures.

38. Thermal stability of the cinnamic acid-acrylic acid compositions was found to be comparable with the individual components and very low as compared to barium-containing nanocomposites.

39. Styrene was used as a co-monomer for the cast polymerization of cinnamic acid-acrylic acid compositions into lenses.

40. Cinnamic acid-acrylic acid nanocomposites were synthesized using gamma irradiation technology.

41. Refractive index and Abbe number was found to lie between 1.53- 1.56 and 31-33 respectively.

The properties obtained while designing barium-containing nanocomposites are given in Table 4.24. Properties of the conventional available materials are also listed which shows that incorporation of barium leads to an improvement in the properties an thus, overall performance of the optical polymers.

Table 4.24: Properties of barium containing acrylic nanocomposites which show improved performance as compared to the conventionally available optical materials

S. No.	Property	Barium acrylate-styrene nanocomposite	Barium cinnamate-barium acrylate styrene nanocomposite	cinnamic acid - Acrylic acid styrene polymer	CR-39	PMMA	PTU
1.	Machinability	Good	Good	Good	Good	Good	Good
2.	Specific gravity	1.19	1.19	1.16	1.26	1.26	1.36
3.	Shore-D hardness	90	94	94	87	85	75
4.	Pencil hardness	6H	6H	6H	4H	4H	6H
5.	Vicat softening ($^{\circ}$C)	120	123	129	100	109	100
6.	Scratch resistance	B	B	B	C	C	B

Through these studies, the process technology for making barium acrylate nanocomposites employing in-situ synthesis and dispersion of nanoparticles has been developed. The technology developed for the preparation of barium acrylate nanocomposites for making optical plastics of high refractive index are materials having a high potential for commercialization. The present work has great relevance for the growth of optical plastics industry in India as much as for the society looking for an indigenous product with an affordable cost.

Chapter 5

Titania Acrylate Nanocomposites using Inorganic Titanium Compounds

CHAPTER 5
TITANIA ACRYLATE NANOCOMPOSITES USING INORGANIC TITANIUM COMPOUNDS

5.0 INTRODUCTION

Acrylates are derivatives of acrylic acid and are regarded as important components of polymer industries. They are extremely resistant to oxygen and decompose very slowly at high temperatures. They are largely resistant to acid and alkaline hydrolysis. From applications in paints and coatings to textile and leather industries, polyacrylates have been used extensively due to their outstanding properties. Polyacrylates have been recognized as a natural choice for optical applications, for many decades due to their excellent optical clarity and light-weight **[388-391]**. Their suitability as an optical material is a boon for many optical devices such as spectacle lenses, intraocular lenses, contact lenses, etc. Besides having several advantages, applications of polyacrylates is limited by a medium refractive index between 1.42 to 1.49. In order to overcome the drawbacks of being a medium refractive index material, one of the options available is the incorporation of high refractive index compounds such as inorganic metals and metal salts in the polyacrylate matrix to form hybrid materials.

The preparation of organic-inorganic hybrid materials exhibits wide interest for applications where high refractive index materials are required. Incorporation of metals in glass has been known for years for improving the properties of glass as per the requirements of the end user. Examples of the incorporation of metals like lanthanum, barium, lead, zirconium, zinc, niobium, etc. in glass are the prominent ones amongst the many to achieve unique properties of glass. The metals like titanium and niobium have been known for the manufacture of specialty glasses. If some of the characteristics exhibited by metals in glass could be achieved in plastics by making metal-containing optical plastics, a novel material with best of both the organic polymer and the inorganic metal can be obtained.

The metals provide physico-mechanical properties to the matrix whereas the continuous phase, i.e. plastic, binds them together providing a uniform distribution of reinforced material, i.e. metals. Such composite materials involving inorganic materials and organic polymers exhibit better electrical, optical, catalytic and mechanical properties than the individual pure polymers. The preparation of materials consisting of metals in plastics, yet retaining the optical properties is a challenge!

The studies reported on plastics have shown that incorporation of metals like lanthanum, barium and lead in plastics has resulted in an improved plastic material with desired optical as well as mechanical properties **[119]**. However, not much work has been carried out in the incorporation of titanium in plastics. Incorporation of titanium into plastics is not an easy task.

Titanium is a lustrous, light and strongly metallic white colored metal recognized for its ductile nature **[392]**, high melting point of 1650 °C and density of 4.05 g/cm^3, high refractive index **[393]**, inertness and colourability **[394-395]**.

The high refractive index (2.45) and high hardness of titanium make it a desirable metal for dispersion in optical plastics to obtain high refractive index polymer composites. Titanium belongs to group IV B of the periodic table having an ionic size of 0.81 Å and polarizability of 14.6 Å^3. Due to its low ionic radii and high polarizability, titanium **i**s an ideal choice for dispersion in polymer matrices to prepare high refractive index composite materials.

Titanium finds wide use in various industries in its many forms of existence, which are titanium metal, organic titanates and titanium dioxide. Titanium metal due to its unique properties of being light-weight, temperature and corrosion resistant is a preferred material for applications in industries such as aerospace, marine, medical manufacturing equipment. Organic titanates, which include basic titanates, polymerized titanates and chelated titanates find wide applications in surface coatings, printing inks and paint industry **[396]**. The most abundant form (titanium dioxide) is the one preferably used to

acquire the attributes of titanium in various products instead of using the pure metal, wherever possible, mainly due to the high cost of extraction of titanium.

Both inorganic and organic compounds are formed synthetically using various industrial processes. Titanates and salts of titanium are synthetic forms of titanium. The occurrence of titanium in its various forms is as depicted in Figure 5.1.

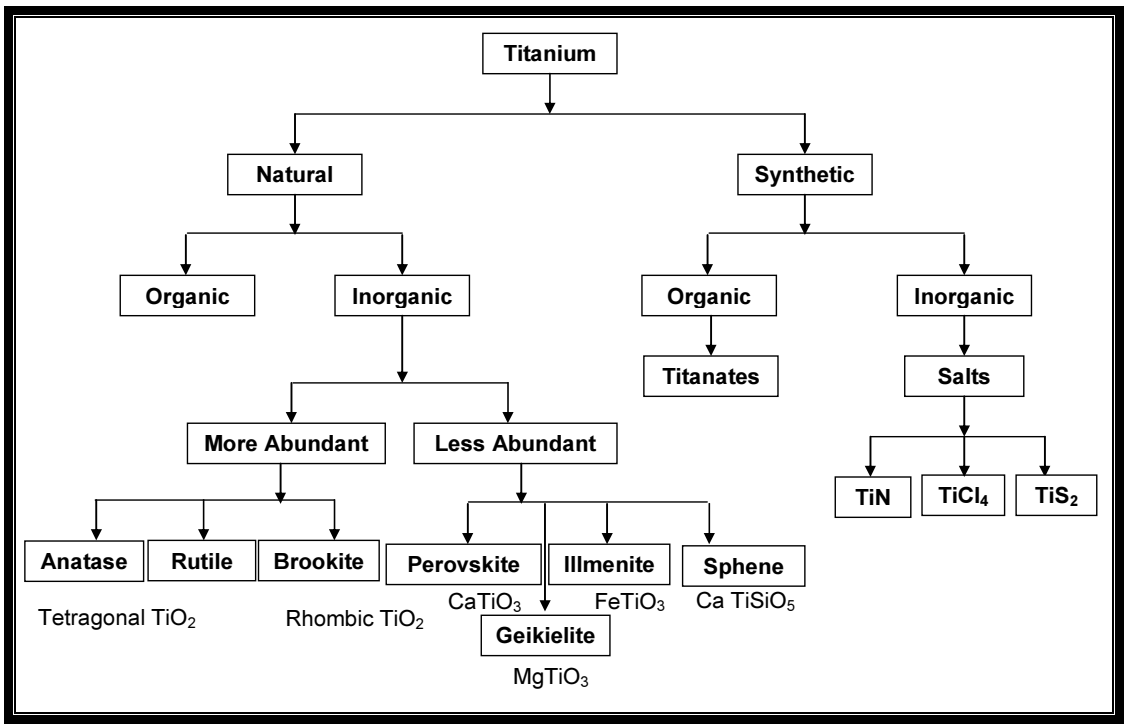

Figure 5.1: Occurrence of titanium in its various forms, both natural and synthetic

Titanium metal is considered to be physiologically inert. Titanium forms a protective oxide coating (leading to increased corrosion-resistance) when exposed to elevated temperatures in air. This protective layer is only 1–2 nm thick but continues to slowly grow; reaching a thickness of 25 nm with time. Titanium burns in air when heated to 1200 °C and in pure oxygen when heated to 610 °C or higher, forming titanium dioxide. This results in the fact that it is not possible to melt the metal in open air as it burns well before its melting point is reached, so melting is possible only in an inert atmosphere or in vacuum. It is also one of the few elements that burn in pure nitrogen gas (it

burns at 800 °C and forms titanium nitride which causes embrittlement). Titanium is resistant to dilute sulfuric acid and hydrochloric acid along with chlorine gas, chloride solutions and most organic acids.

Titanium dioxide or titania is used in almost every field as a white pigment for manufacture of paint and paper and as filler in rubber and plastics due to its exceptionally high refractive index which is higher than that of diamond in the visible region of the electromagnetic spectrum. While large crystals of titanium dioxide are transparent and do not refract, fine particles scatter light very strongly. This is due to the fact that light directed at the polymer containing large metal oxide particles would be reflected back to the light source or deflected to the side, reducing the apparent transparency of the polymer.

Titanium halides such as titanium tetrachloride are also well known. Titanium tetrachloride ($TiCl_4$) **[397-398]** is the basic raw material from which all the organic titanium compounds are made and are readily converted to titanium esters (tetra alkyl titanates) **[399]**. The unique properties of titanium tetra chloride make it a very popular chemical to be used for several applications. Due to the presence of titanium, its attributes are imparted to the host matrix in which it is incorporated and is readily hydrolyzed to form titanium dioxide (Equation 1).

(Equation 1)

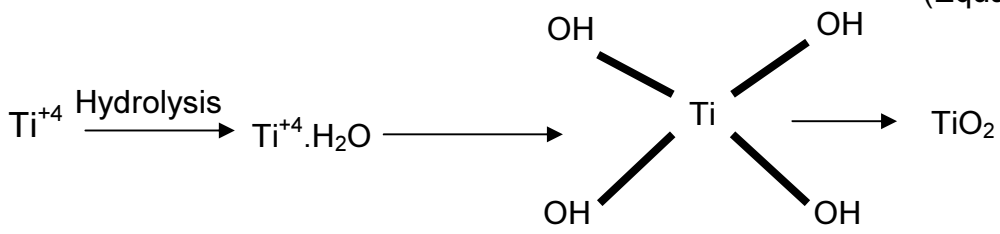

In the present study, an attempt has been made to disperse titanium in acrylate matrix to design high refractive index composite materials. The approach followed for the preparation of titanium-containing polymers is the dispersion of inorganic salts such as titania. Titania was dispersed both ex-situ and in-situ in acrylate monomers to prepare nanodispersed titania acrylate compositions. The developed compositions were cast polymerized

into clear and bubble free lenses for optical applications. By varying the amount of titanium tetrachloride in acrylate monomer, a new range of acrylate polymers with unique features of high refractive index and high Abbe number have been developed. Besides this, the refractive index and Abbe number can also be tailor-made.

A uniform dispersion of the oxide within the plastic matrix is needed to impart maximum transparency without causing loss of physical and mechanical properties.

In order to incorporate titanium into acrylate polymer for the preparation of high refractive index titania acrylate nanocomposites, the following methodology has been adopted:

5.1 SYNTHESIS OF NANODISPERSED TITANIA ACRYLATE COMPOSITIONS

Both ex-situ and in-situ dispersion of titanium dioxide in acrylate matrices was carried out to prepare titania acrylate compositions. Titanium dioxide nanoparticles of size < 25 nm were procured from the market and dispersed in the acrylate matrices in varying concentrations. For in-situ dispersion, titanium tetrachloride was dispersed in the acrylate matrix in varying concentrations for the simultaneous conversion and dispersion of titanium tetrachloride into titanium dioxide. The dispersions were evaluated for acid number, thermal stability, particle size, etc.

5.2 CAST POLYMERIZATION OF NANODISPERSED TITANIA ACRYLATE COMPOSITIONS

For polymerization of nanodispersed titania acrylate compositions, gamma irradiation technique was adopted. The compositions were sent at varying doses from 10kGy to 500 kGy for polymerization. The extent of polymerization was studied through cross-link density and hardness of the polymers. The prepared titania acrylate nanocomposites were evaluated for various optical, mechanical and thermal properties.

RESULTS & DISCUSSION

Results of various studies performed during the preparation of titania acrylate nanocomposites are presented in this section. Observations for various parameters at different stages of the study are discussed. First the studies on titanium-containing compositions were performed for the following parameters:

- Transmittance and clarity of dispersion
- Acid value
- UV-Visible spectroscopy
- Infrared spectroscopy
- Transmission Electron Microscopy
- X-ray diffraction
- pH
- Particle size distribution
- Thermal analysis

Followed by the above step, cast polymerization of the titania acrylate was carried out using gamma irradiation. The studies for the following parameters were carried out:

- Shore-D hardness
- Refractive index
- Thermal analysis
- Pencil hardness
- Leachability of the metal ions
- Scanning Electron Microscopy
- Infrared spectroscopy
- Cross-link density
- Abbe number
- Machinability
- Vicat Softening temperature
- Transmittance
- X-ray Diffraction

Synthesis of nanodispersed titania acrylate compositions

Ex-situ dispersion of titanium dioxide was carried out. Nanoparticles of titanium dioxide having a particle size of less than 25 nm were procured from the market. The concentration of titanium dioxide nanoparticles was varied from 0.1% to 2% to observe the dispersion of titanium dioxide. Table 5.1 gives

the results of dispersion of titanium dioxide in 2-hydroxyethyl methacrylate (HEMA) and acrylic acid.

Table 5.1: Dispersion of nanoparticles of titanium dioxide in HEMA and acrylic acid

S. No.	TiO_2 (%)	Observations	
		HEMA	Acrylic acid
1.	0	Colorless and transparent	Colorless and transparent
2.	0.1	Salt settled down	Salt settled down
3.	0.5	Salt settled down	Salt settled down
4.	1.0	Salt settled down	Salt settled down
5.	1.5	Salt settled down	Salt settled down
6.	2.0	Salt settled down	Salt settled down

Even though the particle size of the nanoparticles was reported to be 25nm, it could not be dispersed in the acrylate matrix and settled down. It is also due to the fact that the nanoparticles of titanium dioxide obtained from the market are highly polydispersed having very few nanoparticles of size less than 25 nm. Therefore, in order to disperse titanium dioxide in the matrix, it was necessary to bring it in the solution form and for this fusion of titanium dioxide was carried out with sulfuric acid. Titanium dioxide was added in various percentages to potassium hydrogen sulfate and sulfuric acid and heated strongly till a transparent and clear fusion mixture is obtained. Later, this fusion mixture was dispersed in acrylic acid. The results of the experiments are tabulated in Table 5.2.

Table 5.2: Preparation of fusion mixture with titanium dioxide

S.No.	TiO_2 (%)	Fusion mixture	Dispersion in Acrylic acid
1.	0	---	Clear and transparent liquid
2.	0.25	Clear transparent solution	Pink colour, layer separation takes place
3.	0.50	Clear transparent solution	Pink colour, layer separation takes place
4.	1.0	Clear transparent solution	Pink colour, layer separation takes place

As can be seen from Table 5.2, the fusion mixtures when dispersed in acrylic acid, led to the formation of layers of acrylic acid and fused titanium dioxide, indicating the incompatibility between with fusion mixture and acrylic acid.

Ex-situ synthesis of nanoparticles of titanium dioxide were carried out by acid and base hydrolysis of titanium precursor which are well reported in the literature **[400]**. The effect of pH of the solution on particle size of titanium dioxide was studied by carrying out the hydrolysis of titanium precursors in the presence of an acid and a base. Ex-situ preparation and dispersion of nanoparticles of titanium dioxide was analyzed for various parameters.

The nanoparticles synthesized by ex-situ methods were analyzed for particle size before dispersion in acrylic acid. Results of the characterization of particle size is summarized in Table 5.3 and Table 5.4.

Table 5.3: Effect of acid hydrolysis on the particle size. The pH was varied from 1.2-2.0. The size of the particles obtained was different at different pH

S.No.	pH	Size (nm)	Yield (%)
1	1.20	85-86	40
2	1.30	80	41
3	1.50	84	40
4	1.60	90	39
5	1.90	94-95	42-44
6	2.00	100	40

Table 5.4: Effect of base hydrolysis on the particle size. The pH was varied from 10-13. The size of the particles obtained was different at different pH.

S. No.	pH	Size (nm)	Yield (%)
1	10.70	85-86	40
2	10.80	80	41
3	11.00	90-94	39-42
4	12.00	95-250	40-44
5	13.00	377	38

As can be seen from Table 5.3 and 5.4, formation of nanoparticles in acid and basic pH results in different particle sizes. In the case where acidic pH of 1-2 was maintained, the size of the titanium dioxide nanoparticles was found to be between 86-100 nm. The yield of the nanoparticles was approximately 40%. In the case of preparation of titanium dioxide nanoparticles under basic pH of 10-13, the size of the particles was found to be 80-377 nm. The yield of the nanoparticles was approximately 40%. The results indicate that nanoparticles synthesized under acidic conditions have lower particle size as compared to the particles synthesized in basic medium.

XRD analysis of the synthesized nanoparticles was carried out to study the nature of the nanoparticles. The graphs indicated the crystalline nature of the synthesized nanoparticles as presented in Figures 5.2a) and b).

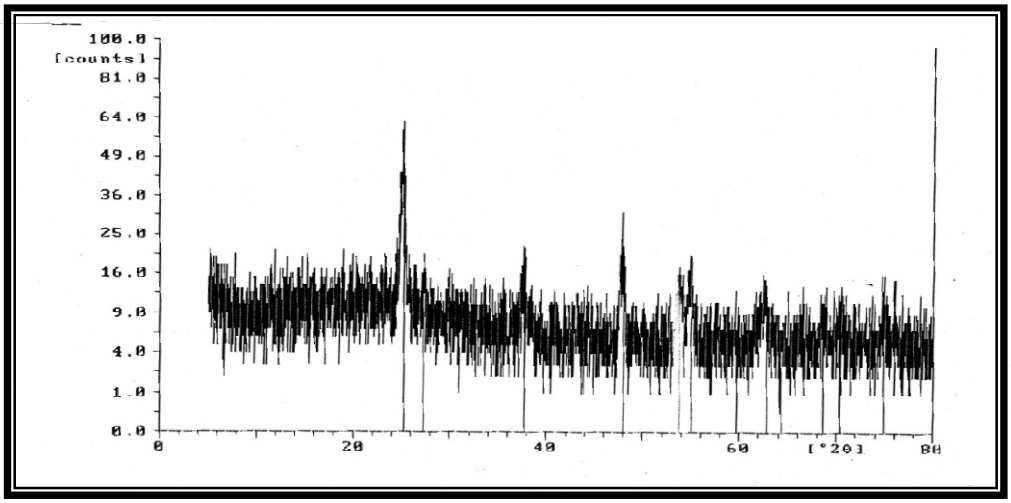

Figure 5.2a): XRD pattern of nanoparticles of titanium dioxide prepared via acidic hydrolysis shows the formation of crystalline titanium dioxide

XRD analysis of the nanoparticles prepared via acidic and basic hydrolysis of titanium precursor shows the presence of peaks at 25.38° and 25.26° which confirms the presence of rutile form of titanium dioxide.

TEM analysis (Figures 5.3a and 5.3b) of the prepared nanoparticles in both acidic and basic medium showed that the particles were spherical in shape.

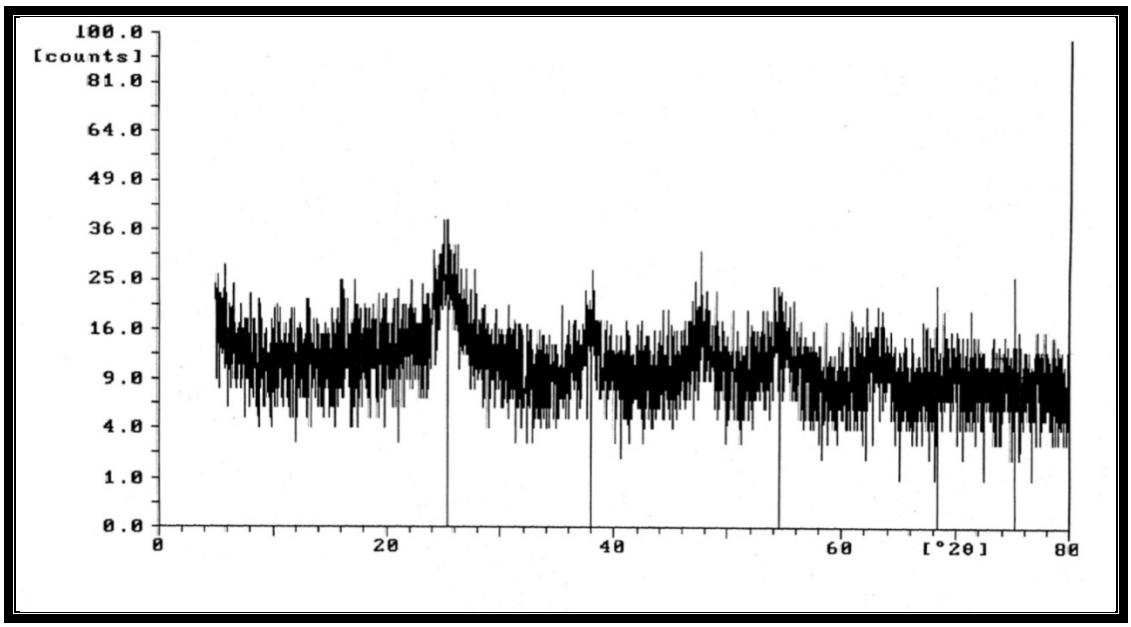

Figure 5.2b): XRD pattern of nanoparticles of titanium dioxide prepared via base hydrolysis shows the formation of crystalline titanium dioxide

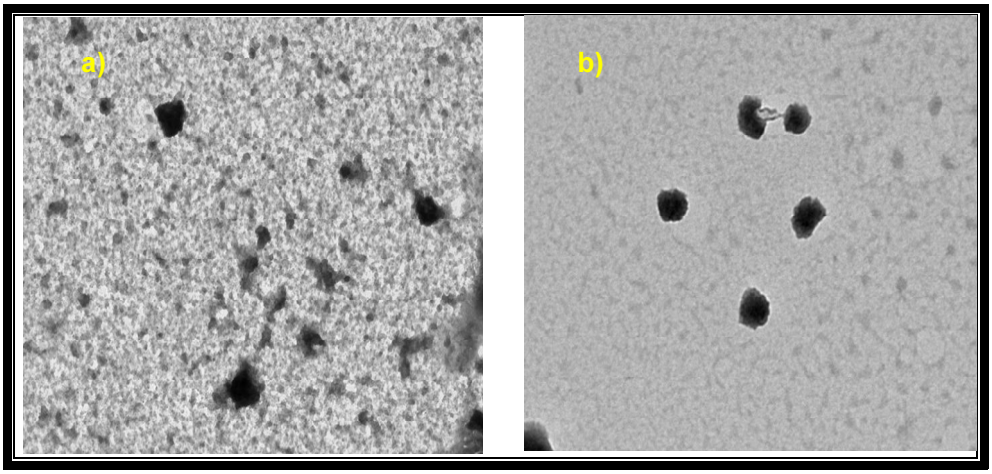

Figure 5.3: TEM analysis of prepared nanoparticles of titanium dioxide in a) acidic medium and b) basic medium

The nanoparticles of varying particle sizes synthesized via acidic and basic hydrolysis were dispersed in acrylic acid. The particles were found to settle down to the bottom leading to non-uniform dispersion. The results of the dispersion are shown in Table 5.5.

Table 5.5: Dispersion of synthesized nanoparticles of titanium dioxide in acrylic acid. The nanoparticles settled down indicating that the density of the particles is very high.

S.No.	Titanium dioxide (%)	Size (nm)	Observation
1	0.01	70	Salt settled at the bottom
2	0.01	80	Salt settled at the bottom
3	0.01	190	Salt settled at the bottom
4	0.01	200	Salt settled at the bottom

As can be seen from Table 5.5, nanoparticles of titanium dioxide of different sizes settled down to the bottom of acrylic acid leading to non-homogeneous dispersion. Since, homogeneous and uniform compositions could not be obtained by ex-situ dispersion of titanium dioxide; in-situ methods for dispersion of titanium dioxide were adopted.

In-situ dispersion

In-situ synthesis and dispersion of nanoparticles of titanium dioxide were carried out simultaneously by dispersing titanium tetrachloride in HEMA and acrylic acid.

Titanium tetrachloride was dispersed by the gradual addition of titanium tetrachloride in HEMA and acrylic acid under vigorous stirring at room temperature. The results are tabulated in Table 5.6.

From the results, it can be seen that colour formation takes place when titanium tetrachloride is added with the intensity of the color increasing as the concentration of titanium tetrachloride is increased.

Table 5.6: Observations related to dispersion of titanium tetrachloride in HEMA and acrylic acid

S. No.	$TiCl_4$ (%)	Observations		Transm. (%)
		HEMA	Acrylic acid	
1.	0	Colourless and transparent	Colourless and transparent	90
2.	2	Transparent, light yellow coloured solution	Transparent, Dark red coloured solution	90
3.	5	Transparent, light yellow coloured solution	Transparent, Dark red coloured solution	90
4.	9	Transparent, yellow coloured solution	Transparent, Dark red coloured solution	90
5.	13	Transparent, yellow-orange coloured solution	Transparent, Dark red coloured solution	90
6.	17	Transparent, orange coloured solution	Transparent, Dark red coloured solution	90
7.	20	Transparent, orange coloured solution	Transparent, Dark red coloured solution	90
8.	25	Transparent, viscous dark orange coloured solution	Transparent, viscous dark red coloured solution	90
9.	30	Transparent, viscous dark orange-red coloured solution	Transparent, viscous dark red coloured solution	90
10.	35	Transparent, viscous dark orange-red colored solution	Transparent, viscous dark red coloured solution	90
11.	40	Transparent, viscous dark orange-red colored solution	Transparent, viscous dark red coloured solution	90
12.	45	Transparent, viscous dark orange-red colored solution	Transparent, viscous dark red coloured solution	90
13.	50	Transparent, viscous dark orange-red colored solution	Transparent, viscous dark red coloured solution	90

At a concentration of 2% and 5% of titanium tetrachloride in HEMA, the solutions were transparent and very pale yellow. While in the case of acrylic acid, dark coloured solutions were obtained. The formation of transparent solutions as indicated by the transmittance values of 90% also show that

titanium tetrachloride was dispersed homogeneously in both HEMA and acrylic acid. Since the colour of acrylic acid dispersions were very dark and therefore, not suitable for optical applications, further work was carried out with HEMA.

The solutions of HEMA containing titanium tetrachloride were analyzed further for the presence of nanoparticles of titanium dioxide. The solutions were subjected to TEM analysis as shown in Figures 5.4a) and 5.4b). From the TEM analysis, it can be seen that the particles of approximately 20 nm in size were homogeneously dispersed in HEMA during the dispersion of titanium tetrachloride. This confirms the formation of nanoparticles of titanium dioxide during dispersion of titanium tetrachloride due to its hydrolysis in the presence of HEMA.

TEM analysis show the presence of finely dispersed nanoparticles of titanium dioxide. The particles are spherical in shape and have a particle size of approximately 20 nm.

The amount of titania dispersed in HEMA as a result of the in-situ formation and dispersion of titanium dioxide was determined and the results are tabulated in Table 5.7.

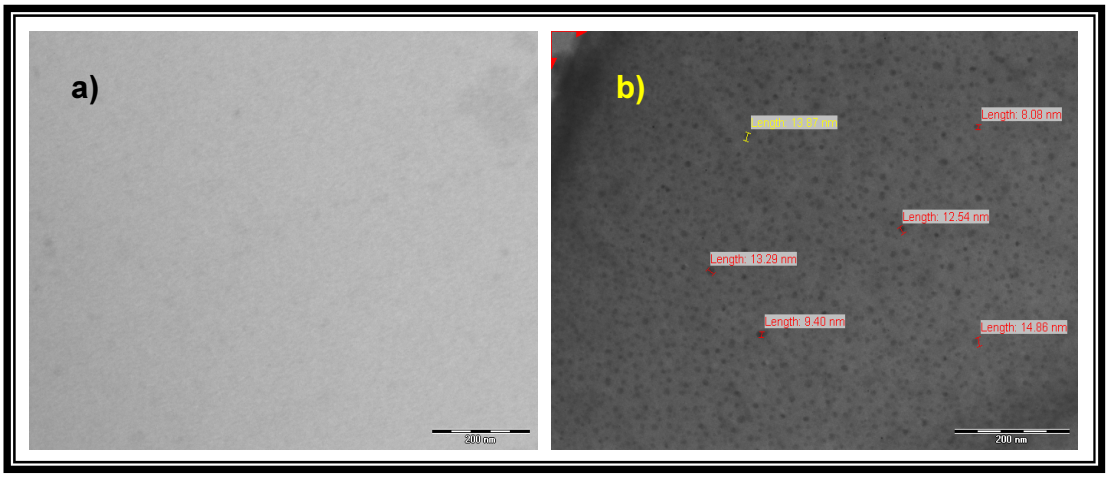

Figure 5.4: TEM analysis of as such a) HEMA and b) nano dispersed titania composition in HEMA by hydrolysis of titanium tetrachloride indicating that the size of the nanoparticles is 8-14 nm

Table 5.7: Determination of titanium content in nano dispersed titania acrylate compositions indicates that upto 4% titanium could be dispersed homogeneously in the matrix

S. No.	$TiCl_4$ (%)	Ti (%) observed	Ti (%) theoretical
1.	2	0.50	0.50
2.	5	1.30	1.30
3.	9	2.60	2.30
4.	13	3.20	3.30
5.	17	4.00	4.30

The amount of titanium dispersed was determined experimentally with the help of ICP-OES instrument and compared with the theoretical values. There was a very close similarity between the experimental and theoretical values. It was seen that 17% dispersion of titanium tetrachloride in HEMA which is the maximum percentage of titanium tetrachloride that could be dispersed, lead to 4% dispersion of titanium metal in HEMA. Thus, upto 4% of titanium could be dispersed into the matrix. Beyond 4%, agglomeration of titanium dioxide occurred leading to non-homogeneous dispersion.

Nano dispersed titania-acrylate compositions were evaluated for acid value. The results are tabulated in Table 5.8

Acid value increases due to the formation of hydrochloric acid while hydrolysis of titanium tetrachloride to titanium dioxide as can be seen from Equation 2. Acid value of HEMA as such is 6.1 indicating the absence of acid. As the amount of titanium tetrachloride in HEMA is increased, acid value increases due to the increase in hydrochloric acid content in the dispersed nano titania acrylate composition.

$$TiCl_4 + H_2O \longrightarrow TiO_2 + HCl \qquad \text{(Equation 2)}$$

Table 5.8: Acid value of titania dispersed HEMA compositions indicates that acid value of HEMA increases with increase in content of titanium precursor due to its acidic character

S. No.	$TiCl_4$ (%)	Acid value
1.	0	6.1
2.	2	11.9
3.	5	16.5
4.	9	19.7
5.	13	43.0
6.	17	53.3
7.	100	925.0

To understand the mechanism between the reaction of HEMA and titanium tetrachloride, IR spectroscopy was done. The IR spectra is presented in Figure 5.5.

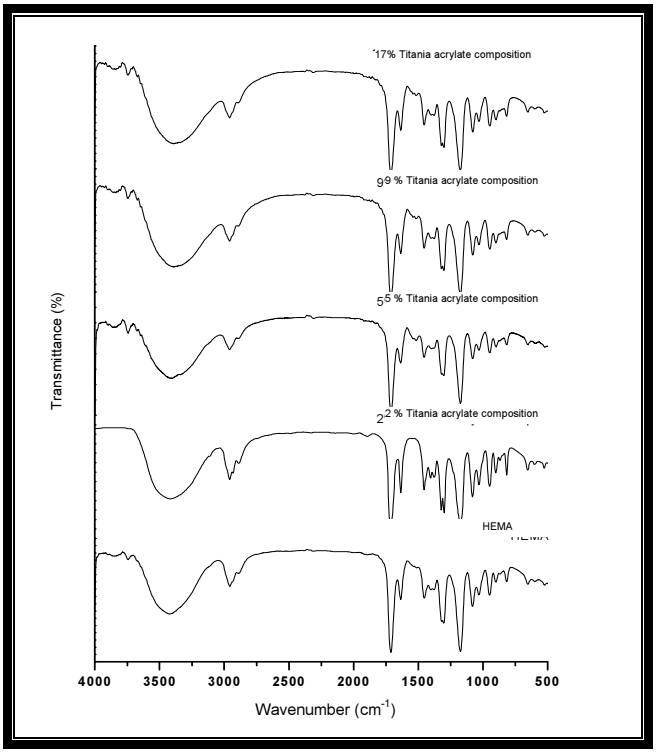

Figure 5.5: IR spectra of HEMA and titanium tetrachloride dispersed in HEMA at various concentrations. The spectra of titania acrylate compositions is similar to HEMA indicating that no chemical reaction takes place between the two and hence, it is only the nanodispersion of titanium dioxide in HEMA resulting from the hydrolysis of HEMA.

As can be clearly seen in IR spectra, no new band is observed in the case of compositions when titanium tetrachloride is added to HEMA. This indicates that no chemical reaction is taking place between titanium tetrachloride and HEMA. It is in fact the formation and dispersion of titanium dioxide nanoparticles in HEMA formed as a result of hydrolysis of titanium tetrachloride in the presence of HEMA. Thermal stability of titania acrylate composition was studied by TGA and the results are shown in Figure 5.6 a - c.

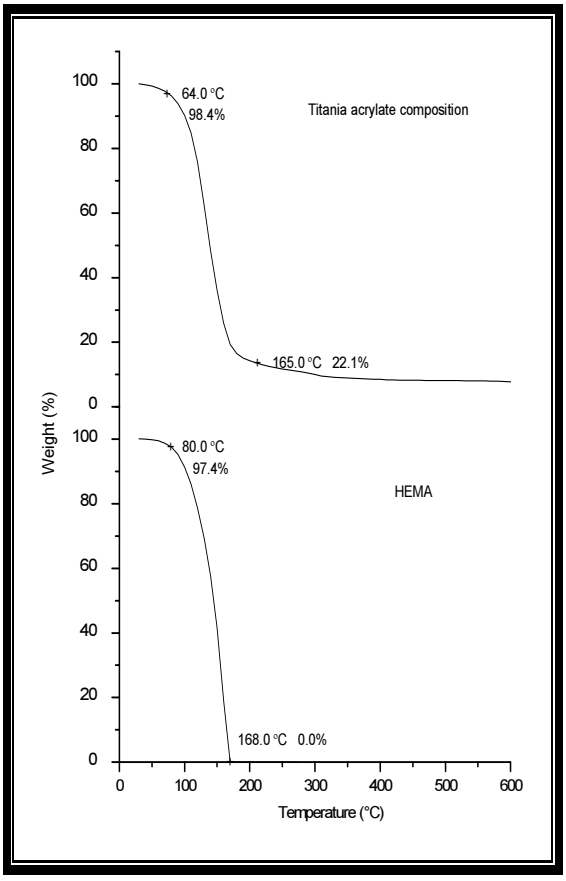

Figure 5.6a): TGA thermogram of HEMA and nanodispersed titania acrylate composition indicates higher stability of the latter due to the incorporation of titanium

Nanodispersed titania acrylate composition is thermally more stable as compared to pure HEMA. Thermogram of titania acrylate composition shows the presence of two step decomposition.

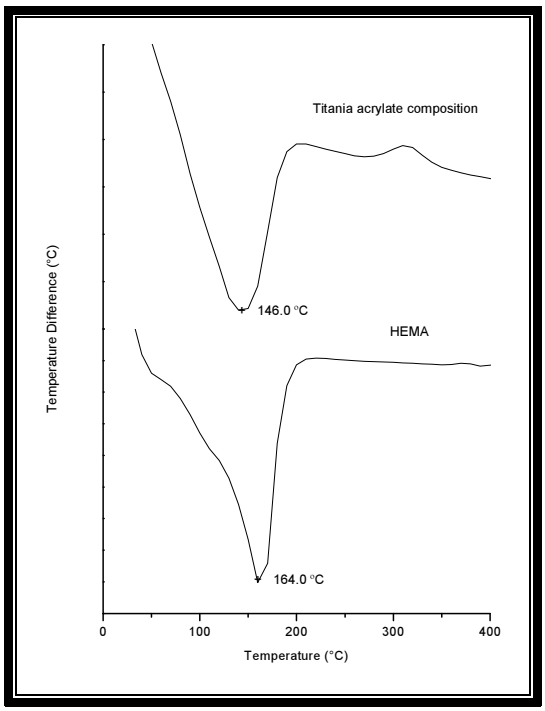

Figure 5.6b): DTA thermogram of HEMA and nanodispersed titania acrylate composition

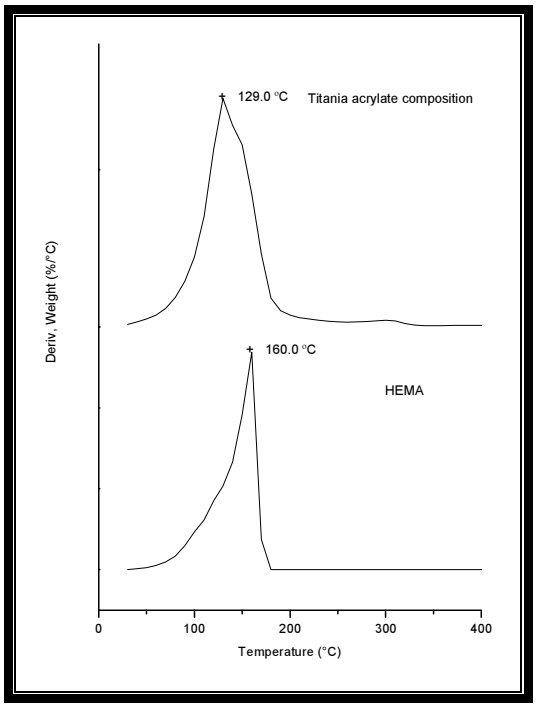

Figure 5.6c): DTG thermogram of HEMA and nanodispersed titania acrylate composition

Titania acrylate is stable up to a temperature of 64 ºC and starts decomposing after that. 76% weight loss is observed in temperature range between 64 ºC and 165 ºC with maximum loss at 129 ºC as can be seen by a DTG peak. DTA shows a corresponding peak at 146 ºC. The second step starts at a temperature of about 165 ºC up to 353 ºC which is ascribed to the introduction of Ti-O network **[401]**. Further, titania acrylate composition remains stable with 6.5% residue which is ascribed to the formation of titanium dioxide.

Table 5.9 tabulates the weight loss (%) in HEMA and titania acrylate composition due to thermal decomposition.

Table 5.9: Weight loss (%) due to thermal decomposition of HEMA and titania acrylate composition

Product	Weight loss (%)					
	100 °C	**200 °C**	**300 °C**	**400 °C**	**500 °C**	**600 °C**
HEMA	8.7	100	100	100	100	100
Titania acrylate composition	9.7	85.8	90	91.5	91.8	92.3

It can be seen from Table 5.9, that titania acrylate is thermally more stable than pure HEMA monomer. As can be seen that HEMA decomposes completely before 200 ºC. On the other hand, after 200 ºC, there is still 10% residue left in the case of titania acrylate. The titania acrylate composition remains thermally stable after 200 ºC showing not much loss in weight. This clearly shows that it is titanium in the form of titania which is responsible for the overall stability of the acrylate composition. In-situ formation and dispersion of titania in acrylate matrix forms a network which imparts thermal stability to HEMA.

UV-Visible spectroscopy (Figure 5.7) was performed on the samples to understand the interaction taking place between HEMA and titanium tetrachloride.

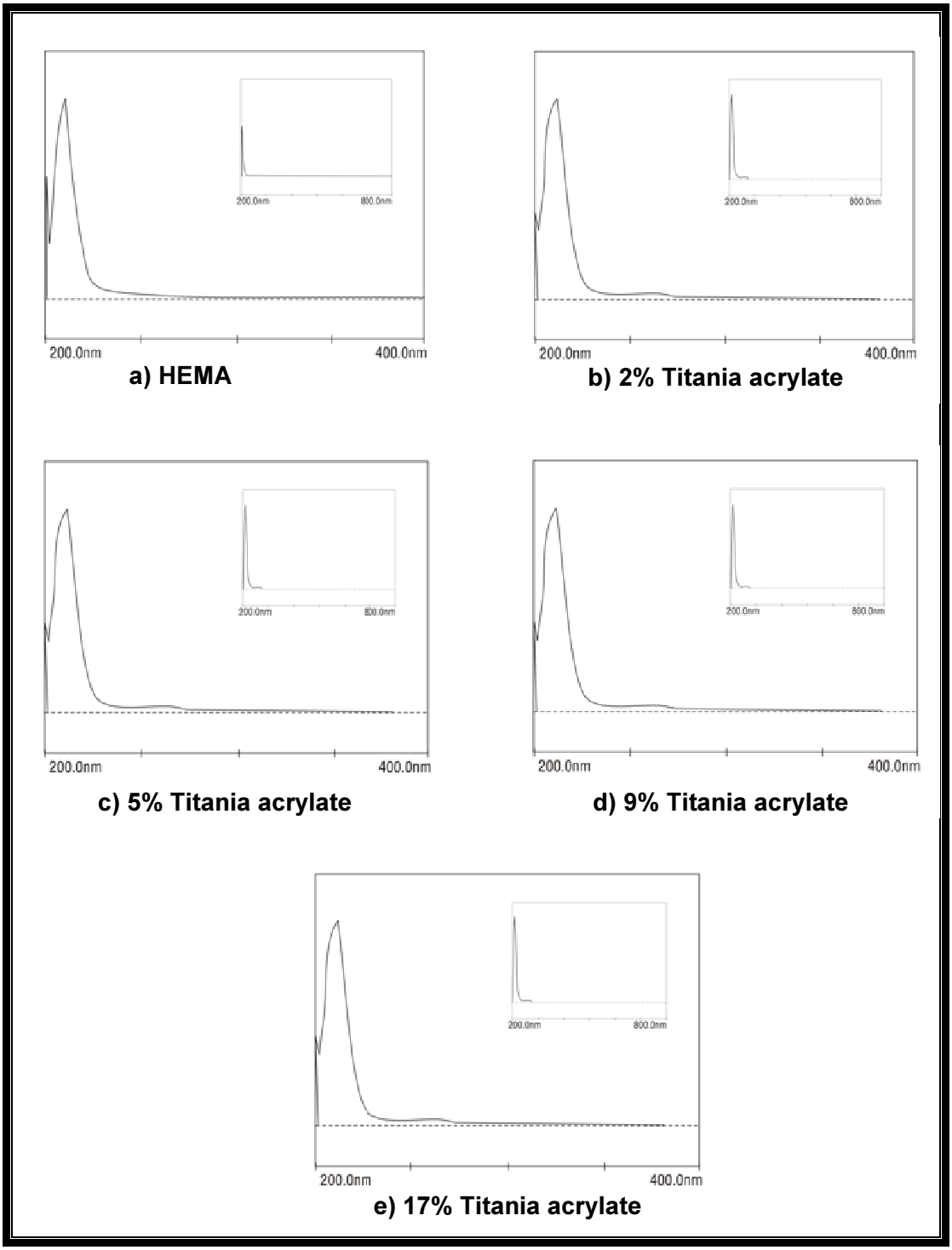

Figure 5.7 (a-e): UV-Visible spectra of HEMA and titania acrylate compositions. The results show no change in the spectra of HEMA indicating that the vinyl group in HEMA remains intact.

UV-Visible spectra of the compositions confirm that no change is taking place at the vinyl group in HEMA. Thus, the vinyl group remains intact and no reaction takes place at vinyl group.

Cast polymerization of titania acrylate compositions

The effect of gamma irradiation on the polymerization of titania acrylates was carried out by subjecting the nano dispersed titania acrylate compositions to radiation doses from 10 kGy to 500 kGy. Optimization of dose was carried out by evaluating the cross-link density of titania acrylate nanocomposites at each dose. The results of cross-link density are tabulated in Table 5.10 and depicted in Figure 5.8.

Table 5.10: Cross-link density results of titanium-containing nanocomposites

% Ti	Dose (kGy)								
	5	10	20	50	100	200	300	400	500
0.0	94.4	96.3	97.8	99.8	99.5	99.6	98.7	94.3	94.5
0.50	99.1	99.4	98.9	99.8	98.7	96.4	97.8	91.8	91.4
1.30	90.6	91.7	94.8	95.3	98.2	98.1	95.8	91.9	95.4
2.60	87.8	94.6	94.1	98.3	98.7	91.0	91.8	93.8	93.8
3.20	32.9	53.4	87.1	88.4	90.3	91.7	86.8	91.3	91.6
4.00	29.7	50.5	77.6	84.5	91.3	91.8	87	84.6	87.7

From the results obtained in Table 5.10, it can be seen that a dose of 50-100 kGy is required for complete cross-linking of polymers. For HEMA polymer and titania acrylate nanocomposite (0.5% Ti), a dose of 50 kGy gave highest cross-link density indicating complete polymerization. For nanocomposites containing titanium more than 0.5% i.e. 1.3 – 4%, radiation dose of 100 kGy is required to achieve complete cross-linking.

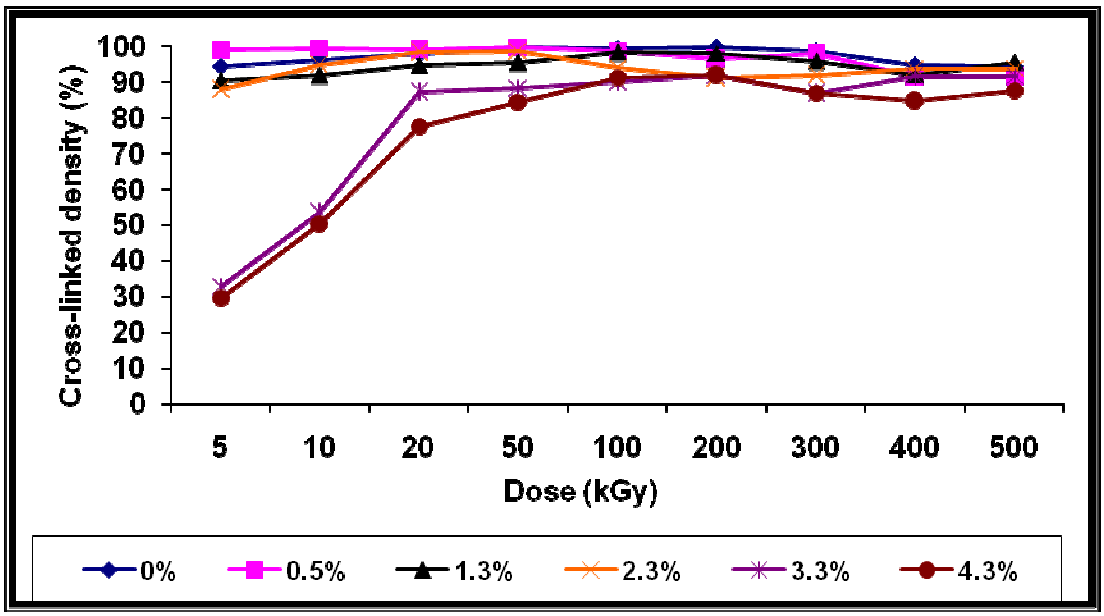

Figure 5.8: Effect of gamma irradiation on the crosslink density of titania acrylate nanocomposites

The effect of gamma irradiation on the hardness of the polymer was evaluated. The results of hardness of the nanocomposites are tabulated in Table 5.11.

Table 5.11: Effect of gamma irradiation on hardness of titania acrylate nanocomposites

S. No.	Ti (%) in HEMA	Hardness
1.	0	84
2.	0.5	90
3.	1.3	91
4.	2.6	92
5.	3.2	92
6.	4.0	90

From the results, it can be seen that the nanocomposites are extremely hard having a value of shore-D hardness of greater than or equal to 90. This property is attributed to the presence of titanium as titanium dioxide in the polymer.

The effect of titania on the optical properties such as refractive index and Abbe number were determined for the titania acrylate nanocomposites. The refractive index was measured using Abbe refractometer, with increasing content of titanium in the polymer matrix. The result is presented in Figure 5.9.

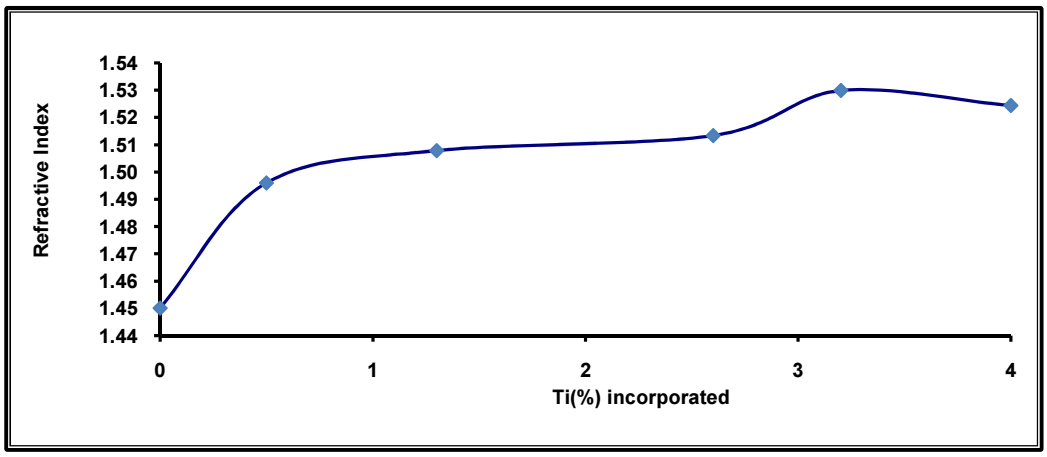

Figure 5.9: Refractive index titania acrylate nanocomposites increases with increase in titanium content

From Figure 5.9 it can be seen that the refractive index of HEMA increases gradually as the dispersion of titanium increases from 0.5-3.2%. Beyond 3.2% dispersion of titanium in HEMA, refractive index remains constant. The refractive index of the pHEMA i.e. without any dispersion of nanoparticles of titania had a refractive index of 1.45. The refractive index increases as the percentage incorporation of titanium increased. Maximum refractive index achieved was 1.53 with 3.2% incorporation of titanium. Besides, this also demonstrates the possibility of tailor-making the refractive index by varying the concentration of the nanodispersed titanium dioxide in the acrylate matrix.

Similarly, Abbe number was measured and the result of Abbe number determination is presented in Figure 5.10.

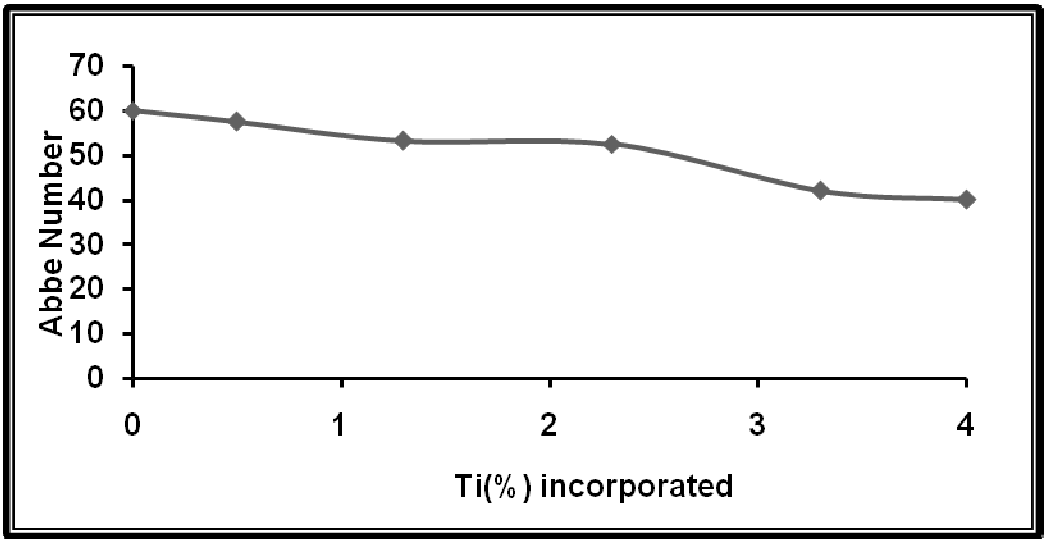

Figure 5.10: Tailor–making of Abbe number has been achieved by varying the content of titanium in the matrix.

From Figure 5.10, it can be seen that the Abbe number of pHEMA is quite high i.e. 60 which is in agreement with the equation that Abbe number and refractive index are inversely proportional to each other. pHEMA has a low dispersive power as indicated by the high value of Abbe number. As the percentage dispersion of titanium dioxide in pHEMA is increased, the Abbe number decreases from a maximum value of 60 to a minimum value of 40 with the dispersion of 4% dispersion of titanium. The values of Abbe number though less than the initial value of 60 are still within the required limits of Abbe number for optical applications. By varying the amount of dispersion of titanium in acrylate matrix, tailor-making of refractive index and Abbe number is possible.

To understand the reactions taking place during dispersion of titanium tetrachloride, IR analysis of pHEMA and titania acrylate nanocomposites were carried out (Figure 5.11).

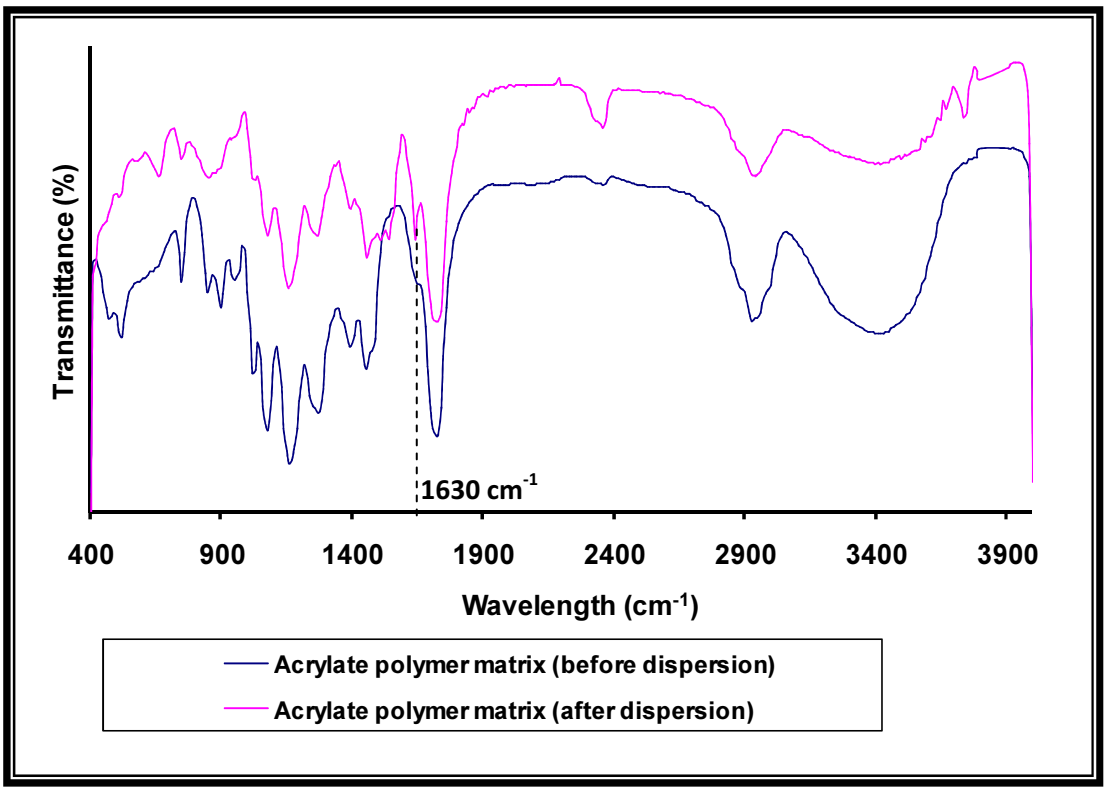

Figure 5.11: FTIR analysis of acrylate polymer matrix (pHEMA) (before dispersion) and titania acrylate nanocomposite

As can be seen from Figure 5.11, the appearance of peak at 1630 cm^{-1} in titania acrylate nanocomposite, which was absent in HEMA polymer is due to the presence of titanium dioxide **[402]**. This indicates that the hydrolysis of titanium tetrachloride takes place in the presence of HEMA leading to the formation of titanium dioxide nanoparticles.

The specific gravity of titania acrylate nanocomposites were evaluated (Figure 5.12). The experimental value was compared with the theoretical values using the law of mixtures as given in Equation 3.

$$\rho_c = \rho_x V_x + \rho_y V_y \qquad \text{(Equation 3)}$$

Where, ρ; density, c: composite, x : component 1, y: component 2 and V: volume fraction of components

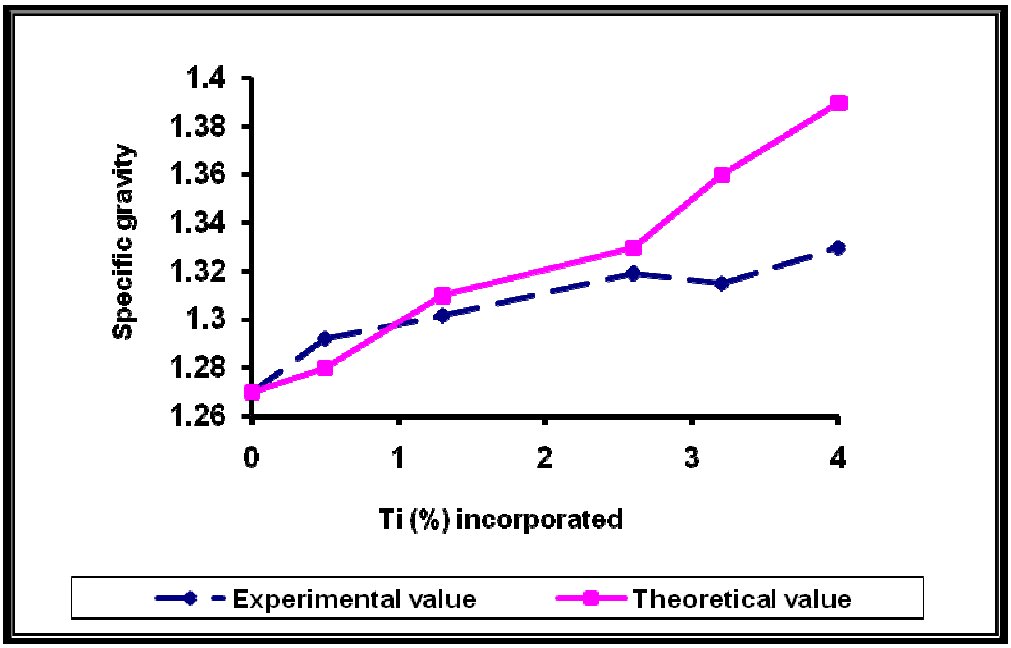

Figure 5.12: Specific gravity increases with increase in titanium content. As can be seen from the graph, the experimental values are lower than the theoretical values indicating that the titanium containing composites are lightweight which is an added advantage

It can be seen from the results that the specific gravity of pHEMA does not vary significantly with even up to 4% dispersion of titanium, in contrary to the theoretical values. This can be attributed to the effect of the nanoparticles where the reduced size has not affected the specific gravity. The specific gravity of the nanocomposites prepared in this way is comparable to the specific gravity of commercial optical polymers, which is an added advantage of the nanocomposites prepared in this way.

The thermal degradation of poly(*n*-alkyl methacrylates) has been investigated by several authors **[403-405]**. The thermal degradation of these polymers proceeds via a depolymerization mechanism with formation of the monomer as the only product. Besides the thermal degradation of alkyl methacrylates having hydroxyl side group, studies were carried out by authors **[406-409]**. Poly(2-hydroxyethyl methacrylate), poly(HEMA), is an important polymer having hydrophilic properties and good compatibility with skin and tissue **[410-**

415]. A number of studies on thermal degradation of pHEMA have been reported in literature **[416-417]**. Thermal stability of titania acrylate nanocomposites prepared in this study was evaluated. The TGA analysis was carried out and the results are shown as Figures 5.13a)- c).

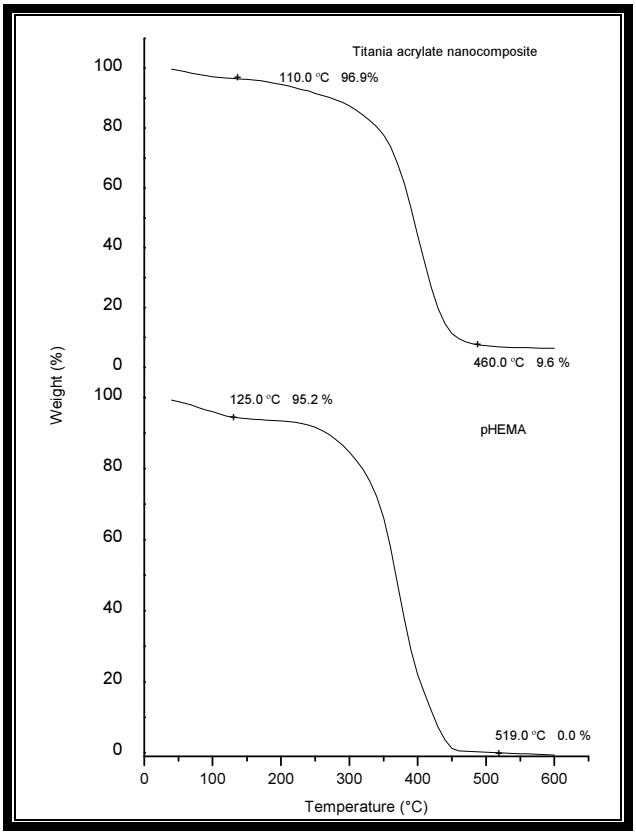

Figure 5.13a): TGA thermograms of pHEMA and titania acrylate nanocomposites indicates higher thermal stability of the nanocomposites due to titanium

From Figure 5.13, it can be clearly seen that the titania acrylate nanocomposite is thermally more stable than the pHEMA. Decomposition in the case of pHEMA starts right after 35 ºC. First decomposition of pHEMA takes place up to 125 ºC with a weight loss of 5%. DTA shows two small peaks; one at 60 ºC which is attributed to random chain scission and another at 100 ºC ascribed to loss of moisture from the polymer. Next decomposition occurs at a temperature up to 519 ºC and the maximum weight loss is observed at a temperature of 370 ºC as indicated by the DTG.

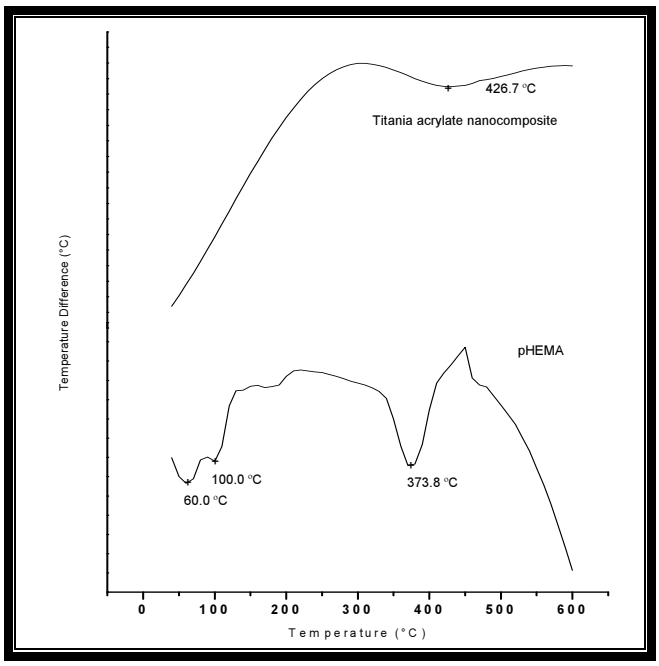

Figure 5.13b): DTA thermograms of pHEMA and titania acrylate nanocomposites shows absence of peaks in the case of titanium containing nanocomposite

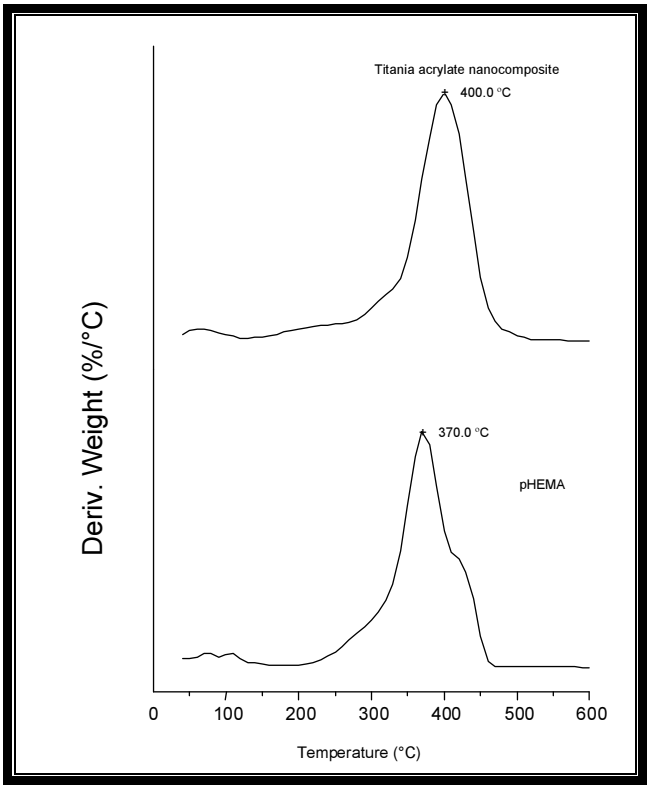

Figure 5.13c): DTG thermograms of pHEMA and titania acrylate nanocomposite shows shift of the peak towards right side of the thermogram indicating higher stability

In the case of titania acrylate nanocomposites, initial decomposition takes place at 110 ºC with the addition of titanium. There is a single step weight loss up to 460 ºC where 85 % decomposition takes place with major loss at 400 ºC as confirmed by the DTG peak. Thus, the stability of the pHEMA has shifted towards the right side of the thermogram indicating the titania acrylate nanocomposite to be more stable thermally. The role of titania is worth mentioning here which is responsible for the increased stability of the nanocomposite.

The values of weight loss (%) of pHEMA and titania acrylate nanocomposites due to thermal decomposition are given in Table 5.12.

Table 5.12: Weight loss (%) at various temperatures due to thermal decomposition of pHEMA and titania acrylate nanocomposites

Product	Weight loss (%)					
	100 °C	**200 °C**	**300 °C**	**400 °C**	**500 °C**	**600 °C**
pHEMA	4.0	6.6	15.4	77.9	99.8	100
Titania acrylate nanocomposite	2.8	5.4	12.6	55.8	92.7	93.6

As can be clearly seen from Table 5.12, percentage weight loss is higher in the case of pHEMA. This is simply because of the fact that cross-linking of pHEMA is very weak as compared to the nanocomposite of titania acrylate. Titania provides an overall stability to the nanocomposite, thereby, responsible for higher thermal stability

SEM analysis was carried out to study the surface morphology of the nanocomposites as shown in Figures 5.14 a) and b).

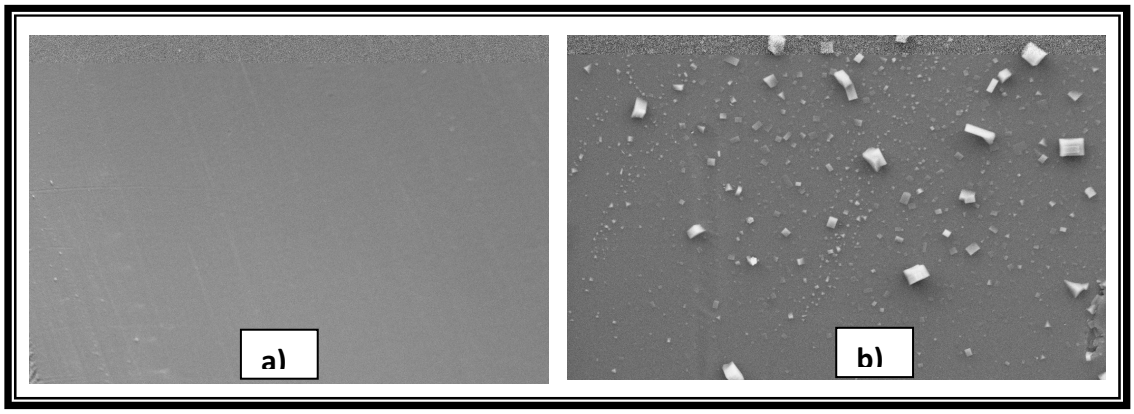

Figure 5.14: SEM images of a) Acrylate matrix (before dispersion) b) Acrylate matrix (after dispersion). The images confirm the presence of nanoparticles. Such homogeneous dispersion led to the formation of clear and transparent nanocomposites.

The presence of nanoparticles in the polymerized nanocomposites were confirmed by SEM analysis. SEM analysis of acrylate polymer matrix after dispersion of titania confirms the formation of cubical shaped nanoparticles. This is very much in agreement with the fact that the mechanical properties such as hardness, of the polymer are increased due to the presence of metal oxide nanoparticles. XRD analysis was carried out to compare the crystal structure of pHEMA and titania acrylate nanocomposite. The patterns are shown in Figure 5.15.

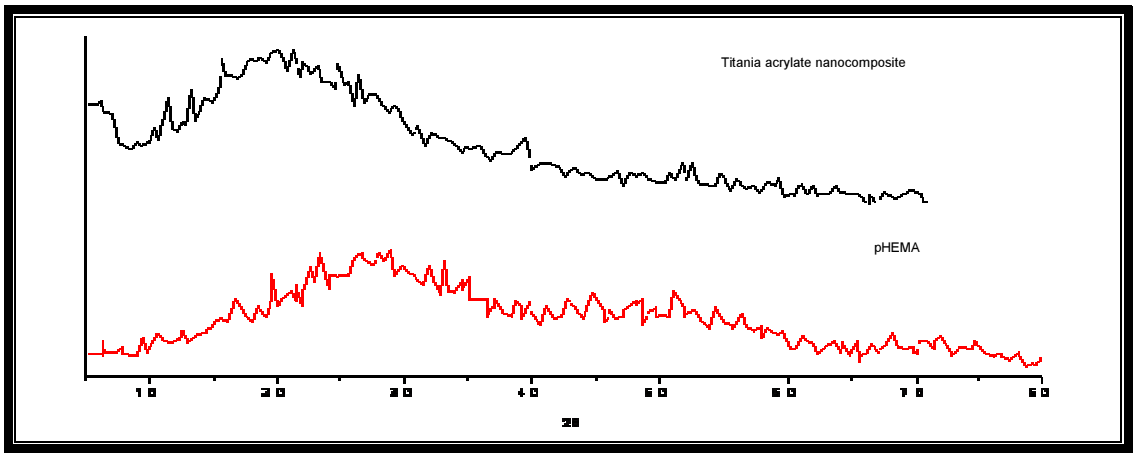

Figure 5.15: XRD analysis of (a) pHEMA and (b) titania acrylate nanocomposite indicates amorphous nature of the nanocomposite

XRD analysis was undertaken to understand the nature of nanocomposites. As can be seen from the XRD graphs, the absence of peaks indicates the amorphous nature of the polymer.

Water absorption studies of pHEMA were carried out to study the effect of dispersion of nanoparticles on the water absorption capacity of HEMA. The results are tabulated in Table 5.13.

Table 5.13: Water absorption studies of titania acrylate nanocomposites

S. No.	Ti (%)	Water absorption (%)
1.	0	34.6
2.	0.5	27.7
3.	1.3	22.5
4.	2.6	18.5
5.	3.2	18.2
6.	4.0	17.1

pHEMA is known for its high hydrophilic nature having a water absorption capacity of 35%. As seen from Table 5.13, with the dispersion of titanium tetrachloride in HEMA leading to the formation of titanium dioxide nanoparticles, the water absorption decreases due to the incorporation of the nanoparticles in the highly cross-linked polymer matrix.

Leachability was determined as per method described in Chapter 3. Leachability of titanium metal was observed in concentrated nitric acid and concentrated hydrochloric acid and analyzed through ICP-OES instrument. Leachability of 14 ppm of titanium was obtained in concentrated hydrochloric acid and 10 ppm of titanium in concentrated nitric acid, indicating that the metal atoms are not free. Titanium dioxide is very tightly bound by the polymeric network of HEMA and is therefore not affected in the presence of acids.

5.3 CONCLUSIONS

In this chapter, novel titania acrylate nanocomposites using inorganic compounds of titanium have been prepared. Dispersion of nanoparticles of titanium dioxide was carried out by adopting in-situ and ex-situ methods. The achievements of the studies carried out are as follows:

1. Synthesis of nanoparticles of titanium dioxide was carried out by both ex-situ and in-situ methods.
2. Nanoparticles having a particle size of less than 10nm were synthesized and dispersed simultaneously from titanium tetrachloride in HEMA leading to the formation of homogeneous and transparent nano dispersions of titania acrylate. Upto 17% of $TiCl_4$ or 4% titanium was successfully dispersed in HEMA.
3. The modification of an important monomer, HEMA, for optical applications, has been done in a novel and cost-effective manner, thanks to the attributes provided by titanium dioxide nanoparticles formed in-situ.
4. TEM analysis of nanodispersed titania acrylate composition confirms the formation of cube shaped titanium dioxide nanoparticles having a particle size of less than 10nm
5. Gamma irradiation has been used as a novel technique for the polymerization of nanodispersed titania acrylate compositions. Dose optimization has been carried out to obtain transparent and clear nanocomposites of polyacrylates suitable for optical applications.
6. By varying the concentration of titanium in nanocomposites, refractive index can be tailor-made from 1.450 to 1.530 and Abbe number can be tailor-made from 40-60.
7. Nanocomposites formed by the dispersion of nanoparticles of titanium dioxide are amorphous in nature.

8. Water absorption capacity, an inherent characteristic of HEMA has been reduced from 32% to17% by the incorporation of nanoparticles.
9. The developed acrylic nanocomposites are thermally stable having good machinability and impact resistance.
10. Light-weight nanocomposites, where the specific gravity of the nanocomposites is lighter or similar to the conventional optical plastics have been developed.

At the end of this work, the process technology for making titania acrylate nanocomposites employing in-situ preparation and dispersion of nanoparticles of titanium dioxide, with varying refractive index and other important properties has been developed. Novel feature of tailor-making of properties achieved in this work is not available with conventional optical plastic materials. Thus, this achievement would be a breakthrough in the optical industry where, for the first time, titanium has been successfully incorporated into an optical polymer at concentrations upto 4 %.

Chapter 6

Titanate Acrylate Nanocomposites using Organic Titanium Compounds

CHAPTER 6
TITANATE ACRYLATE NANOCOMPOSITES USING ORGANIC TITANATES

6.0 INTRODUCTION

Organic titanium compounds also known as titanates are an important class of compounds well known in the polymer and paint industry where they are used as catalysts and cross-linking agents. Titanium tetrachloride is the basic raw material from which all organic compounds of titanium are made. A variety of compounds are produced depending on whether the chlorine atoms in titanium tetrachloride are partially or fully replaced by other groups. Accordingly four classes of compounds are formed; a) tetra alkoxides ($Ti(OR)_4$), b) chelates ($Ti\ (OR)_2\ (OR'X)_2$), c) acylates ($Ti\ (OR)_x(OC(O)R')_{4-x}$) and d) alkoxy halides ($Ti(OR)_xCl_{4-x}$). Titanium tetra alkoxides are formed by the complete replacement of chlorine atoms by the alkyl group and are regarded as alkyl esters of orthotitanic acid ($Ti(OH)_4$). These are, therefore, referred to as alkyl titanates. When the alkyl radical contains another functional group, such as amino or carboxyl groups capable of co-coordinating with titanium, chelated esters are formed.The structure of organic titanium compounds involves a covalent bond between titanium and another atom bonded to a carbon-based group.

The rate of hydrolysis of tetra alkyl titanates is governed by the nature of alkoxy groups in the lower titanium alkoxides, with the exception of tetramethyl titanates which are rapidly hydrolyzed by water giving a series of condensed titanoxanes ($Ti\text{-}O\text{-}Ti\text{-}O\text{-})_x$. As the chain length of alkyl group increases, the rate of hydrolysis decreases.

Reaction with Acids

Organic acids form acrylates when heated with tetra alkyl titanates. Best results are obtained using only 1 or 2 mole of acid, as attempts to force the reaction with 3 or 4 mole of acid can yield polymers. Review of the literature on titanates show

that a number of studies have been conducted on the chemistry and reactions of titanates. Exploitation of titanates as catalysts, etc. for the polymer industry is done widely. But not much work has been carried out on their applications for high refractive index polymers. These novel compounds pave way for the designing of high refractive index metal containing polymers. Besides improving their optical properties, mechanical properties of the polymers can also be improved by incorporating titanium in the form of organic titanates.

In the present chapter, the organic form of titanium i.e. organic titanates has been dispersed in acrylic acid to form titanate acrylate polymers. The choice of using acrylic acid is mainly because of the fact that acrylates exhibit properties which are very well suited for the optical industry. Keeping the above concept in mind, the entire study has been carried out as follows:

6.1 STEP I: DISPERSION OF ORGANIC TITANATES IN ACRYLIC ACID

For dispersion of titanium in acrylic acid, six different titanates were chosen viz. tetraisopropyl titanate, tetrabutyl titanate, tetra 2-ethylhexyl titanate, polybutyl titanate, triethanolamine titanate and titanium acetylacetonate. These titanates were selected based on their refractive index. Titanates were added gradually to acrylic acid taken in a round bottom flask fitted with a condenser and stirred vigorously at room temperature to find out the maximum amount of titanate going into solution without adversely affecting its transparency. After knowing this concentration, specimens of varying amount (% by weight) of titanates in acrylic acid were prepared covering a range of 0% to 30% (by weight) of titanates.

6.2 STEP II: INCORPORATION OF CINNAMIC ACID AND STYRENE IN TITANATE-ACRYLIC ACID COMPOSITIONS

Aryl carboxylic acid such as cinnamic acid was dispersed in titanate-acrylic acid compositions in varying amounts to study the effect of cinnamic acid on the optical properties of titanate-acrylic acid compositions.

The dispersion of cinnamic acid in titanate-acrylic acid composition was followed by cast polymerization in the presence of styrene. For the purpose of creating the three-dimensional network of structure, styrene was used as a co-monomer for polymerizing titanate-acrylic acid-cinnamic acid compositions. Styrene undergoes addition at the double bond of the vinyl group and is therefore used as cross-linking agent to form networks. Hence it was expected to produce a transparent optical polymer.

6.3 STEP III: CAST POLYMERIZATION OF TITANATE ACRYLATE-STYRENE COMPOSITIONS

Styrene as a co-monomer was used for polymerization of titanate acrylate compositions. Gamma irradiation technique was adopted for polymerization of titanate acrylate-cinnamic acid-styrene compositions. The dose of gamma irradiation was optimized to prepare hard, transparent and clear lenses.

RESULTS & DISCUSSION

Results of various studies performed during the preparation of titanate acrylate nanocomposites are presented in this section. Observations for various parameters at different stages of the study are discussed. First the studies on titanium-containing compositions were performed for the following parameters:

- ❖ Transmittance and clarity of dispersion
- ❖ Refractive index
- ❖ Acid value
- ❖ pH
- ❖ UV-Visible spectroscopy
- ❖ Particle size distribution
- ❖ Infrared spectroscopy
- ❖ Thermal analysis

Then, the studies pertaining to the incorporation of cinnamic acid as a co-monomer were carried out for the following parameters:

- ❖ Transmittance and clarity of dispersion
- ❖ Refractive index

- ❖ UV-Visible spectroscopy
- ❖ Infrared spectroscopy
- ❖ Thermal analysis

Followed by the above step, cast polymerization of the titanate acrylate-cinnamic acid-styrene was carried out using gamma irradiation at different doses. The studies for the following parameters were carried out:

- ❖ Shore-D hardness
- ❖ Cross-link density
- ❖ Refractive index
- ❖ Abbe number
- ❖ Thermal analysis
- ❖ Machinability
- ❖ Pencil hardness
- ❖ Vicat Softening temperature
- ❖ Leachability of the titanium ions
- ❖ Transmittance

Dispersion of organic titanates in acrylic acid

Six different organic compounds of titanium i.e. tetraisopropyl titanate (IPT), tetrabutyl titanate (TBT), polybutyl titanate (PBT), tetra 2-ethylhexyl titanate (TEHT), triethanolamine titanate (TEAT) and titanium acetylacetonate (TAA) were dispersed in acrylic acid at various concentrations at room temperature under continuous stirring. The structure of each organic titanate that has been used in this study is shown in Figure 6.1 a) – f).

The organic titanates used for the present study were evaluated for refractive index and percentage titania before their dispersion in acrylic acid. The results are tabulated in Table 6.1.

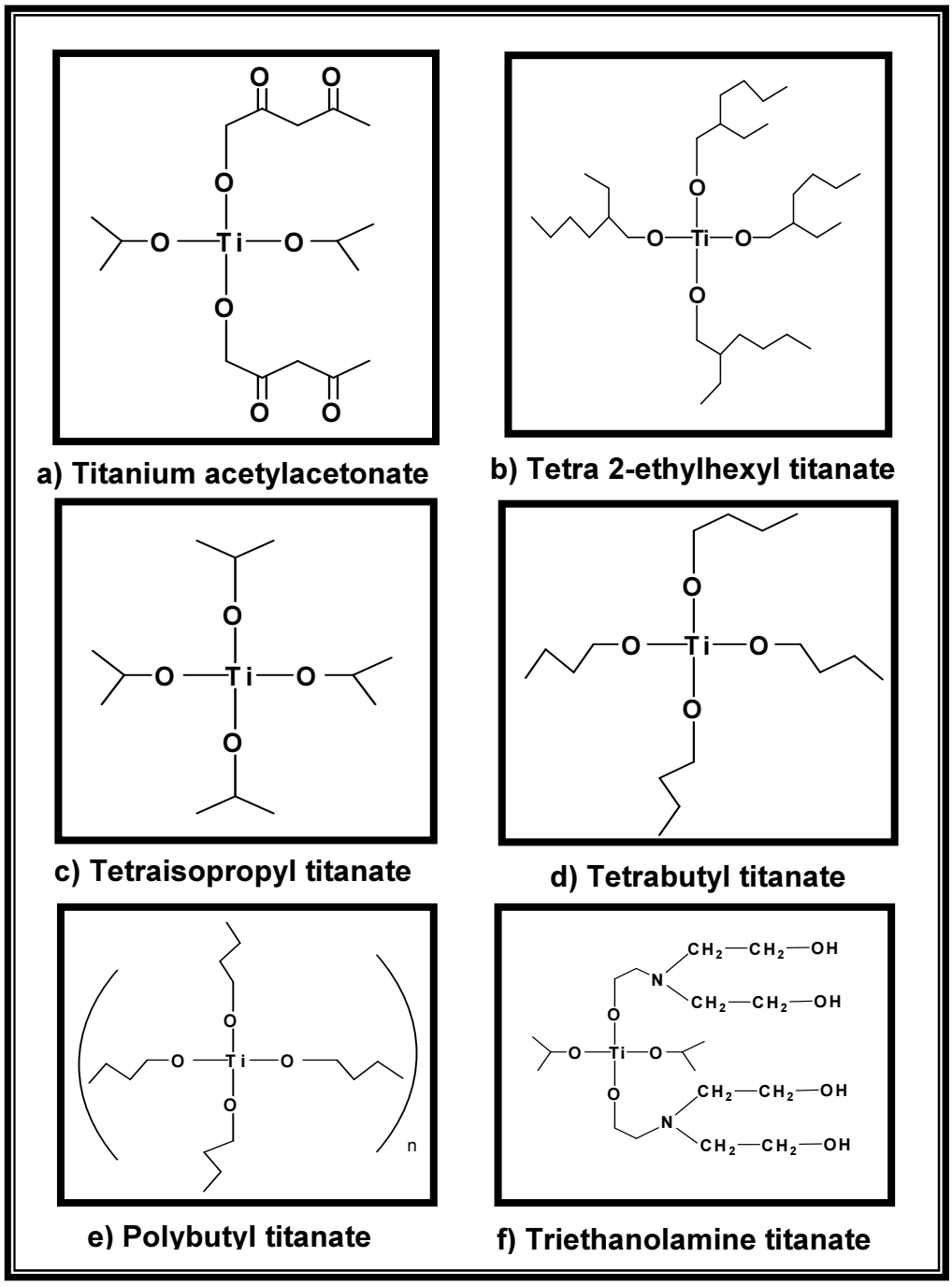

Figure 6.1: Structure of a) Titanium acetylacetonate b) Tetra 2-ethylhexyl titanate c) Tetraisopropyl titanate d) Tetrabutyl titanate e) Polybutyl titanate and f) Triethanolamine titanate. These organic precursors were used to prepare titanium-containing nanocomposites

Table 6.1: Titania (%) content and refractive index of various titanates used for the preparation of titanate-acrylic acid compositions. Polybutyl titanate exhibits the highest refractive index due to the highest amount of titania present

S. No.	Titanate	% Titania (observed)	% Titania (reported)	Refractive index
1.	Triethanolamine titanate	12.18	13.97	1.493
2.	Tetra 2-ethylhexyl titanate	13.21	14.1	1.483
3.	Titanium acetylacetonate	15.63	16.27	1.507
4.	Tetrabutyl titanate	22.81	23.42	1.492
5.	Tetraisopropyl titanate	26.72	28.01	1.486
6.	Polybutyl titanate	30.61	34.5	1.516

As can be seen from Table 6.1, there is good agreement between the observed and reported values of titania. The highest percentage of titania amongst the six titanates was found to be present in polybutyl titanate (30.6%). Polybutyl titanate was also found to have the highest refractive index of 1.516, amongst all the titanates used for the study.

The above mentioned organic titanates were dispersed in acrylic acid, taken in a round bottom flask, by the addition of different titanates in varying amounts at regular intervals. The addition of titanates to acrylic acid was done under vigorous stirring at room temperature. To evaluate the change in optical properties, refractive index of titanate-acrylic acid compositions was determined at regular intervals to determine the maximum amount of titanate to be added to acrylic acid so as to bring a maximum increase in refractive index. The refractive index obtained by the addition of different titanates to acrylic acid is given in Table 6.2 and depicted in Figure 6.2.

Table 6.2: Results of effect of addition of organic titanates on refractive index of acrylic acid. Maximum refractive index of 1.463 was achieved by the addition of 25% polybutyl titanate in acrylic acid

S.No.	Concentration (%)	TAA	TEAT	TBT	TEHT	IPT	PBT
1.	0	1.424	1.424	1.424	1.424	1.424	1.424
2.	5	1.431	1.434	1.432	1.429	1.435	1.436
3.	10	1.432	1.444	1.435	1.430	1.444	1.444
4.	15	1.438	1.445	1.438	1.432	1.444	1.445
5.	20	1.442	1.455	1.440	**1.433**	1.448	1.458
6.	25	**1.445**	**1.461**	**1.445**	1.433	**1.453**	**1.463**
7.	30	1.445	1.461	1.445	1.433	1.453	1.463

As can be seen from Table 6.2, the addition of different organic titanates leads to a gradual increase in the refractive index of acrylic acid. Dispersion of 20% tetra 2-ethylhexyl titanate in acrylic acid exhibited a maximum refractive index of 1.433. Beyond 20% addition, there is no change observed in refractive index. Similarly in the case of titanium acetylacetonate, 25% addition of titanate to acrylic acid increases the refractive index to 1.445 from 1.424 to start with. In the case of triethanolamine titanate, incorporation of 25% titanate in acrylic acid results in a refractive index of 1.461. There is no change in refractive index of acrylic acid beyond the incorporation of 25% triethanolamine titanate. In the case of tetrabutyl titanate, refractive index of 1.445 is obtained by dispersion of 25% titanate in acrylic acid. In the case of tetraisopropyl titanate, 25% incorporation of titanate in acrylic acid results in a refractive index of 1.453 and 1.463 in the case of 25% dispersion of polybutyl titanate. Thus, it can be seen that amongst all the titanates used, maximum refractive index is imparted by polybutyl titanate to acrylic acid i.e. 1.463. The

increase in refractive index is attributed to the presence of Ti-O bond. Presence of more number of Ti-O bonds in the case of polybutyl titanate gives rise to higher refractive index as compared to other titanate-acrylic acid compositions.

The reaction between titanate and acrylic acid is shown in Equation 1. The formation of acrylates is taking place by the reactivity of organic titanates with acrylic acid.

$$n\ RCOOH + Ti(OR')_4 \longrightarrow (R\ COO)_nTi(OR')_{4-n} + n\ R'OH$$

where n= 1 to 4 (Equation 1)

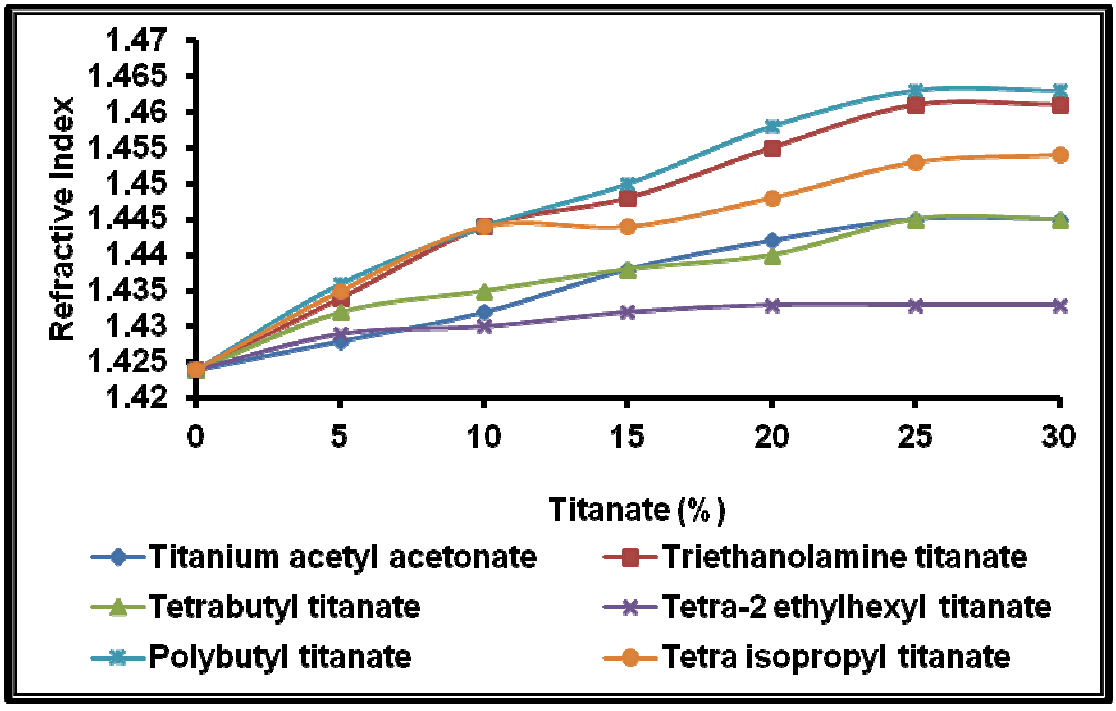

Figure 6.2: Results of effect of addition of titanates on refractive index of acrylic acid. With the addition of upto 20% titanates, the refractive index of acrylic acid increases gradually. The maximum refractive index for all titanates is obtained at 25% incorporation in acrylic acid except for tetra 2-ethylhexyl titanate where a maximum refractive index of 1.433 is obtained with 20% addition.

To study the reactivity of titanates with acrylic acid, acid number of titanate-acrylic acid compositions was determined. The result of change in acid number of acrylic acid on incorporation of titanate to it is given in Table 6.3.

Acid value of acrylic acid is 626 which decrease with the gradual addition of titanates confirming the reactivity of acrylic acid with titanates to form titanate acrylate. This is also an indication of the fact that reactions are taking place between carboxylic acid and titanates.

Table 6.3: Results of effect of addition of titanates on acid value of acrylic acid. Acid value of acrylic acid decreases on the addition of titanate indicating that reaction between acrylic acid and titanate is taking place at the carboxylic acid group of acrylic acid

S. No.	Titanate	Titanate (% by weight of acrylic acid)	Acid value
1.	-	0	626
2.	TAA	25	508
3.	TEAT	25	471
4.	TBT	25	492
5	TEHT	20	500
6.	IPT	25	510
7.	PBT	25	498

Keeping the improvement in key optical property i.e. refractive index in mind, selection of two matrices, viz. polybutyl titanate-acrylic acid composition and triethanolamine titanate-acrylic acid composition were made and further work was carried out on these two compositions.

Particle size analysis was carried out for titanates-acrylic acid compositions. The results of particle size analysis are tabulated in Table 6.4.

Table 6.4: Determination of particle size distribution of titanate-acrylic acid compositions. Particle size of the compositions was found to be less than 0.8 nm indicating the formation of homogeneous solution of titanate-acrylic acid

S. No.	Polybutyl titanate- acrylic acid (%)	Particle size (nm)	Triethanolamine titanate- acrylic acid (%)	Particle size (nm)
1.	0	0	0	0
2.	5	<0.8	5	<0.8
3.	10	<0.8	10	<0.8
4.	15	<0.8	15	<0.8
5.	20	<0.8	20	<0.8
6.	25	<0.8	25	<0.8

It can be seen from Table 67.4 that with the dispersion of titanates in acrylic acid, particle size of less than 0.8 nm was obtained. This is also reflected in the formation of clear and transparent compositions. This is the confirmation of the fact that titanates get reacted with acrylic acid to form homogeneous solutions rather than dispersion and that is why the compositions are clear and transparent.

To study the thermal stability of titanate-acrylic acid compositions, TGA, DTA and DTG analysis was carried out on 25% polybutyl titanate-acrylic acid composition and 25% triethanolamine titanate-acrylic acid composition. The thermograms are shown in Figure 6.3 (a-c).

TGA of acrylic acid is explained in Chapter 4. Thermogram of polybutyl titanate shows two-step decomposition. A sharp DTG peak at 215.9 ºC shows maximum rate of weight loss upto 244.6 °C with total weight loss of 43%. DTG peak at 108.7 °C and DTA peak at 151.3 °C are ascribed to the loss of volatiles from the compound. Next decomposition takes place upto 332.9 ºC with a weight loss of 27% with maximum decomposition rate at 326 ºC as exhibited by a sharp DTG peak. DTA shows a corresponding endothermic peak at 327.8 ºC. This is ascribed to the loss of organic moiety from th titanate after which there is no further loss in weight.

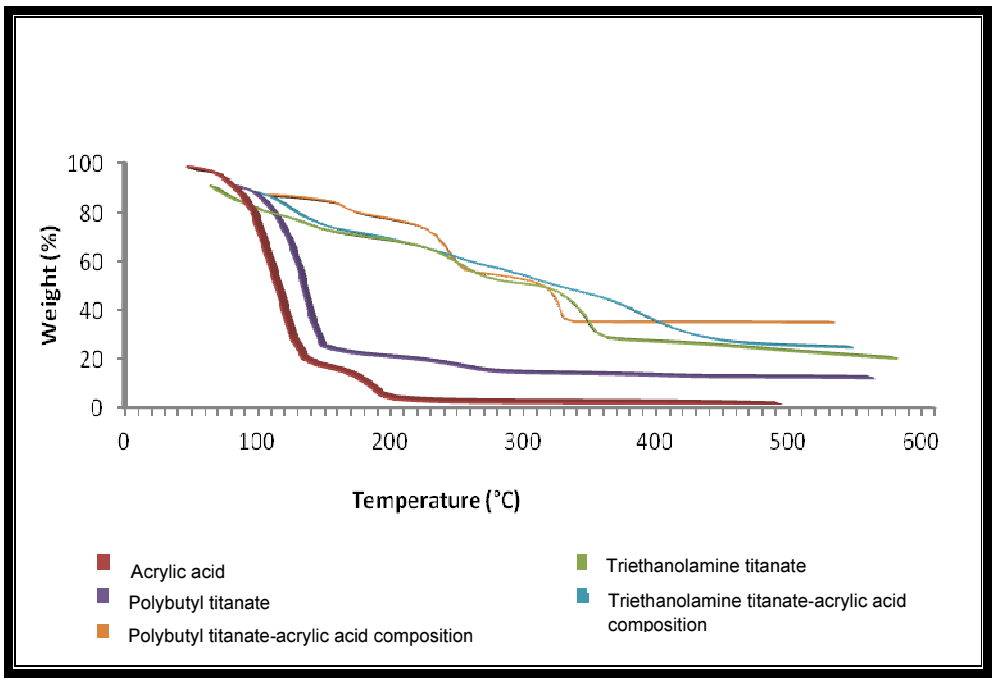

Figure 6.3a): TGA thermograms of acrylic acid, polybutyl titanate, polybutyl titanate-acrylic acid composition, triethanolamine titanate and triethanolamine titanate-acrylic acid composition indicate that transitions are taking place when titanates are added to acrylic acid

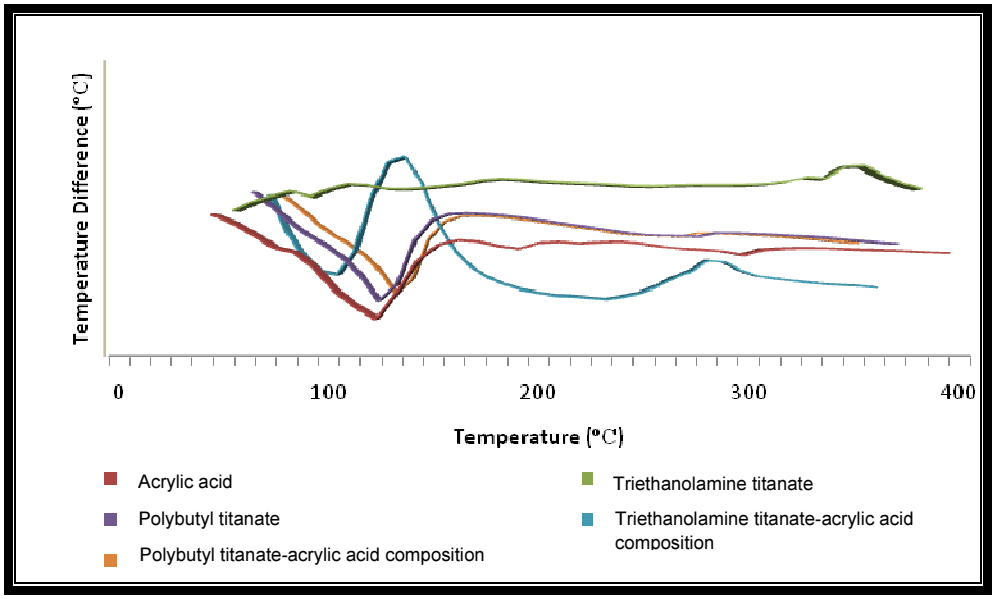

Figure 6.3b): DTA thermograms of acrylic acid, polybutyl titanate, polybutyl titanate-acrylic acid composition, triethanolamine titanate and triethanolamine titanate-acrylic acid composition

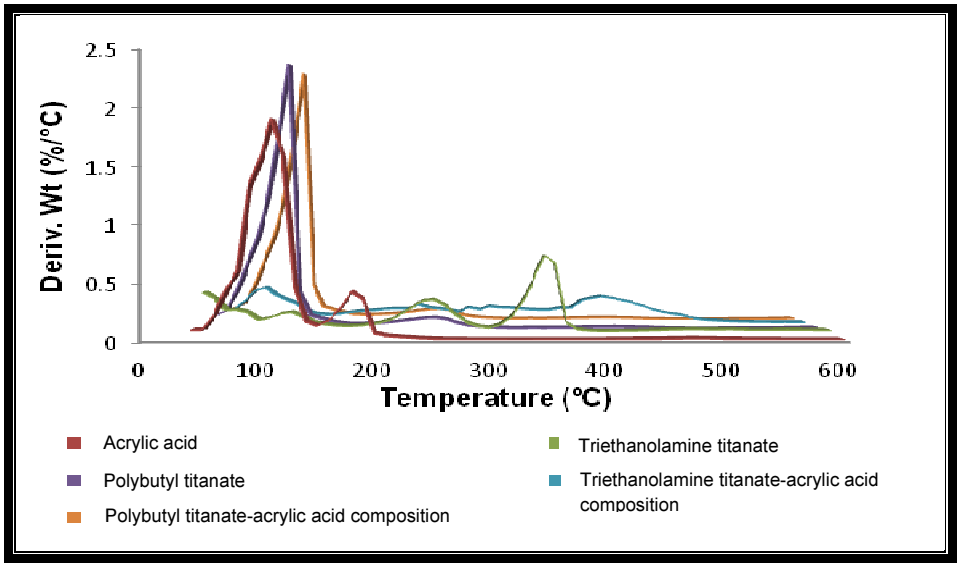

Figure 6.3c): DTG thermograms of acrylic acid, polybutyl titanate, polybutyl titanate-acrylic acid composition, triethanolamine titanate and triethanolamine titanate-acrylic acid composition. Shift in the DTG peaks indicate that thermal transitions are taking place as an effect of reaction between acrylic acid and titanates

Thermogram of polybutyl titanate acrylate shows single step decomposition corresponding to a weight loss of 80%. Both DTA and DTG show a sharp peak at 102.8 ºC and 99.1 ºC respectively. This behavior very well indicates that there is a reaction taking place between acrylic acid and polybutyl titanate leading to such thermal transitions.

Thermogram of triethanolamine titanate showed two-step decomposition. The sample starts decomposing immediately after 30 °C indicating the volatile nature of triethanolamine titanate. DTA peak at 69.5 ºC is ascribed to the loss of solvent and further at 116.4 ºC is ascribed to the loss of volatiles present in the titanate with corresponding DTG peaks at 106 °C and 110 °C. The decomposition from 116 ºC till 263.2 ºC with a weight loss of 47% is ascribed to the decomposition of the titanate. Maximum decomposition rate takes place at 236 ºC as is evident from a DTG peak. Further, decomposition takes place upto 368.3 ºC with a weight loss of 28%, maximum being at 344.6 ºC as is evident from a sharp DTG peak. Also presence of an exotherm at 354 ºC indicates the decomposition of the titanate.

Thermogram of triethanolamine titanate acrylate shows single-step decomposition and presence of many components as is evident by a number of DTG peaks. The sample starts decomposing immediately after 30 °C indicating the volatile nature of the composition. Maximum rate of weight loss observed at 68 ºC as is evident from DTG peak is ascribed to the loss of ethanol from the titanate. Corresponding DTA peak at 68 ºC confirms the loss of material. Total weight loss observed is 80% till 488 °C. The thermogram is accompanied with small DTG peaks at 221.7 ºC, 273.0 ºC and 293.6 ºC. An exotherm in DTA is observed at 293 ºC which is ascribed to the decomposition of the acrylate composition.

The loss in weight due to thermal decomposition of acrylic acid, titanates and titanate-acrylic acid compositions are listed in Table 6.5.

Table 6.5: Weight loss (%) due to thermal decomposition of acrylic acid, titanates and titanate-acrylic acid compositions. The results indicate that due to addition of titanate, the thermal stability of acrylic acid increases.

Product	Weight loss (%)					
	100 °C	**200 °C**	**300 °C**	**400 °C**	**500 °C**	**600 °C**
Acrylic acid	52.2	98.2	100	100	100	100
Triethanolamine titanate	20.0	31.5	50.0	75.3	79.0	83.0
Triethanolamine titanate-acrylic acid composition	18.7	31.0	46.6	64.4	79.6	81.9
Polybutyl titanate	4.5	22.3	48.0	70.0	70.1	70.2
Polybutyl titanate- acrylic acid composition	64.7	86.0	92.2	93.4	94.3	94.8
Theoretical weight loss of triethanolamine titanate-acrylic acid composition	44.2	81.6	87.5	93.8	94.8	95.8
Theoretical weight loss of polybutyl titanate-acrylic acid composition	20.1	79.3	87.0	92.5	92.5	92.5

As can be seen from Table 6.5, major weight loss in the case of acrylic acid takes place upto 200 ºC. In contrast, titanates are quite stable thermally due to the presence of titanium in them. This stability is reflected in the case of titanate-acrylic acid compositions which are thermally more stable than acrylic acid. In the case of triethanolamine titanate, weight loss at different temperatures is more as compared to triethanolamine titanate-acrylic acid composition. This is due to the bonding between titanate and acrylic acid leading to a stable network than the individual components. The synergistic effect of both the components plays a vital role in bringing the stability in the composition. On the other hand, in the case of polybutyl titanate, the weight loss due to decomposition is much lower as compared to when it is incorporated into acrylic acid to form polybutyl titanate-acrylic acid composition. This lower thermal stability in the composition may be attributed to the weaker interactions between acrylic acid and polybutyl titanate. But it should be noted here that the titanate-acrylic acid composition is much thermally stable as compared to acrylic acid alone, which is ascribed to the presence of titanium in the acrylic network that binds with the functional groups in acid leading to a stronger matrix.

As can be seen from Table 6.5, theoretical weight loss in the case of dispersion of triethanolamine titanate in acrylic acid is more than the observed value. This means that the triethanolamine titanate-acrylic acid composition is thermally more stable than expected. The calculated loss in weight due to decomposition in the case of polybutyl titanate-acrylic acid composition is less than the observed values at the initial temperatures. This indicates that the thermal loss in the composition is due to the presence of volatiles. Later at higher temperatures, the calculated and observed values of weight loss becomes comparable and hence shows expected pattern of decomposition.

In order to understand the interactions taking place between titanates and acrylic acid, UV-Visible spectroscopy was carried out from 200-800 nm. The spectra are presented in Figure 6.4 a-e (for polybutyl titanate-acrylic acid compositions) and 6.5 a-e (for triethanolamine titanate-acrylic acid compositions).

The maximum absorption peak (λ_{max}) of acrylic acid was observed at 210 nm. As can be seen from Figure 6.4, there is no change in the λ_{max} value of acrylic acid with increase in the amount of titanates dispersed in acrylic acid. This confirms that the vinyl group of acrylic acid remains intact and hence the only site for the reaction of titanates is the carboxylic acid group.

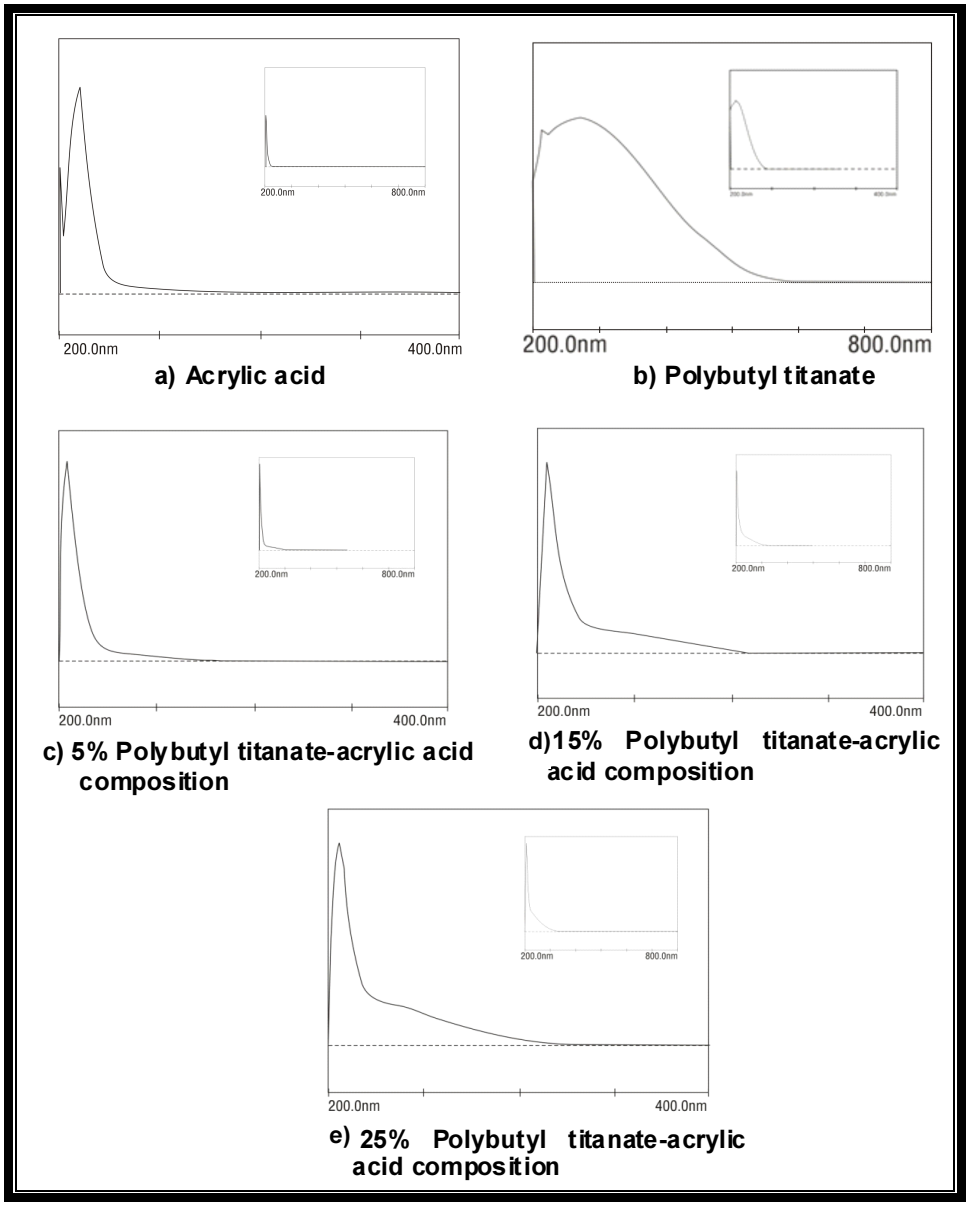

Figure 6.4 (a-e): UV-Visible spectra of acrylic acid and polybutyl titante-acrylic acid composition (varying concentrations). The λ_{max} value of acrylic acid does not change with the dispersion of polybutyl titanate and hence it can be said that the vinyl group of acrylic acid remains intact.

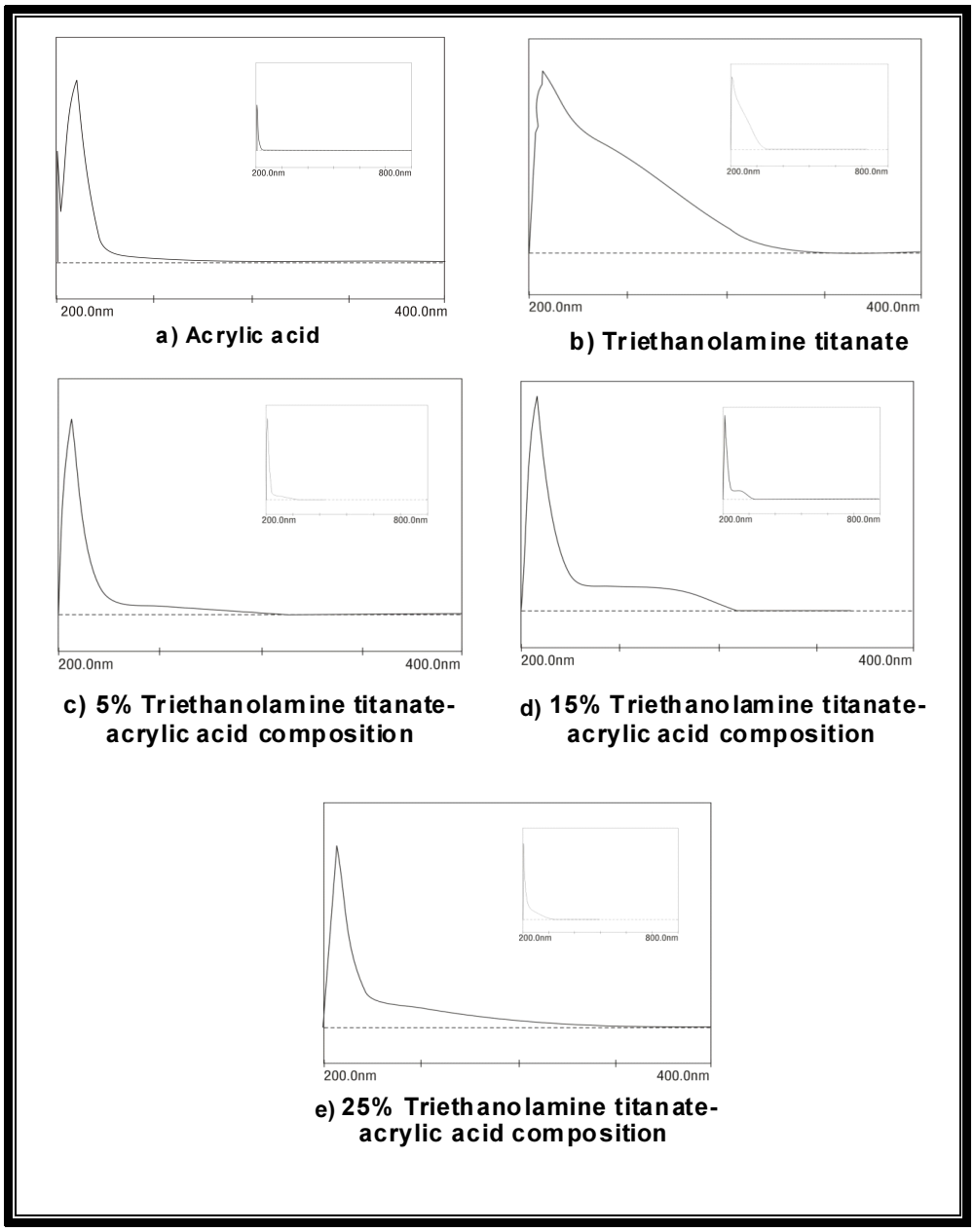

Figure 6.5 (a-e): UV-Visible spectra of acrylic acid and triethanolamine titante-acrylic acid composition (varying concentrations). The λ_{max} value of acrylic acid does not change with the dispersion of triethanolamine titanate and hence it can be said that that the vinyl group of acrylic acid remains intact

To understand the reaction between titanates and acrylic acid, infrared spectroscopy was performed on the samples. Infrared spectra were taken from 4000 to 400 cm^{-1} in transmittance mode (Figure 6.6 a and b).

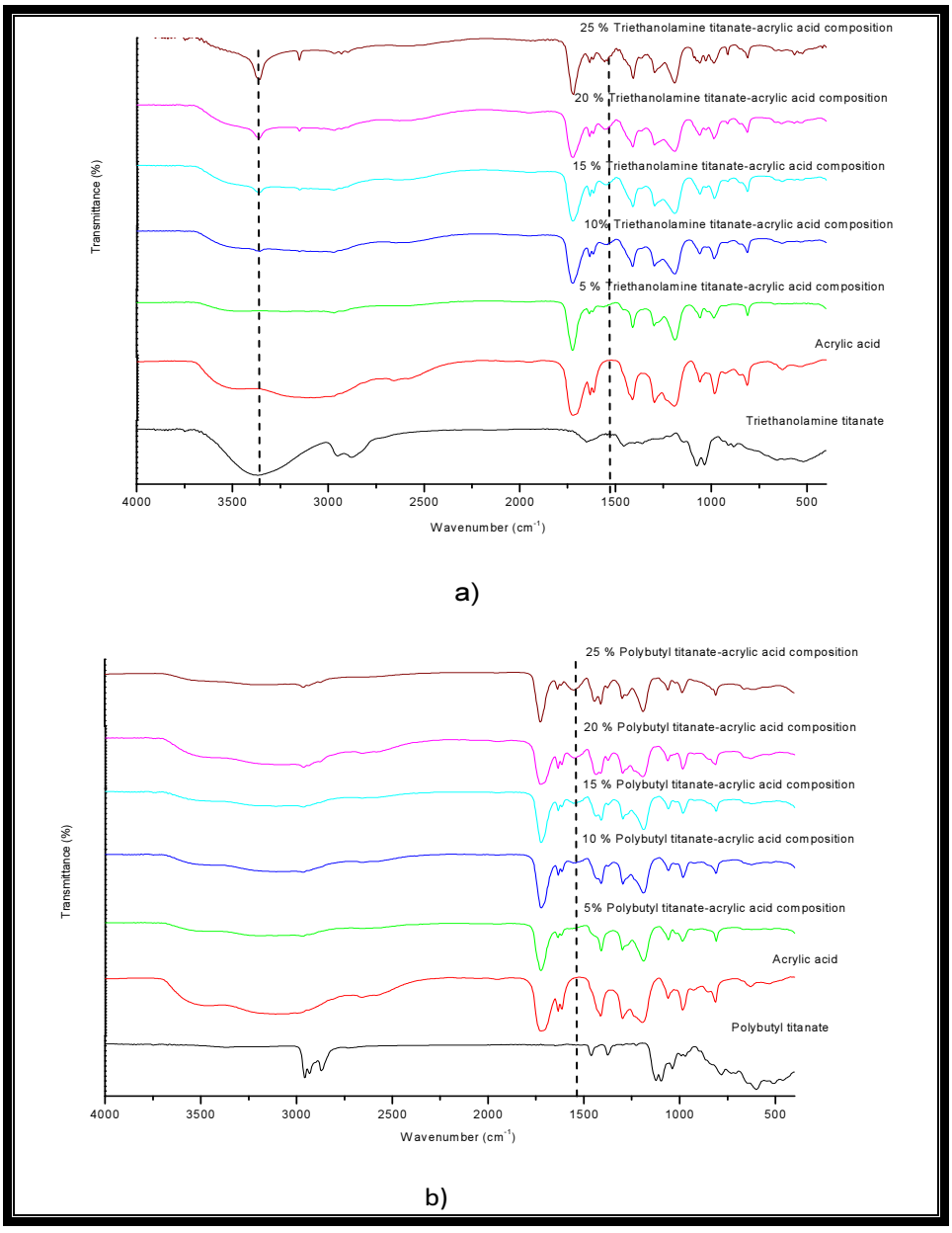

Figure 6.6: Infrared spectra of a) acrylic acid, triethanolamine titanate and triethanolamine titanate-acrylic acid compositions and b) acrylic acid, polybutyl titanate and polybutyl titanate-acrylic acid compositions. The band at 1544-1550 cm^{-1} confirms the presence of COO^- group suggesting that new compounds (polybutyl titanate acrylate and triethanolamine titanate acrylate) have been formed by the reaction between acrylic acid and titanates

As can be seen from Figure 6.6 a and b, the band pertaining to carboxylic acid group is absent in the case of titanates-acrylic acid composition. On the contrary, band at 1544-1550 cm^{-1} is present and is ascribed to the presence of COO band of the ester group. The intensity of this band also increases as the amount of titanates in acrylic acid increases. This indicates that titanates reacts with acrylic acid and forms titanate acrylate.

Dispersion of cinnamic acid and styrene in titanate acrylate compositions

To increase the refractive index of the titanate acrylates further, cinnamic acid having a refractive index of 1.555 was added to titanate acrylate composition. Cinnamic acid was added to titanate acrylates in varying concentrations and its effect on refractive index was measured at each step. The results are tabulated in Table 6.6 and presented in Figure 6.7.

It can be seen from the table that addition of cinnamic acid to titanate acrylate composition leads to a significant change in the refractive index of acrylic acid. The maximum increase in refractive index obtained in the case of triethanolamine titanate-acrylate composition was 1.484 and 1.489 in the case of polybutyl titanate-acrylate composition. Here again it may be noted that refractive index increase is higher in the case of dispersion of cinnamic acid in polybutyl titanate-acrylate composition.

Table 6.6: Effect of cinnamic acid on refractive index of titanate acrylate compositions shows that highest refractive index achieved is 1.489 due to 14% incorporation of cinnamic acid to polybutyl titanate acrylate composition

S.No.	Cinnamic acid (%)	Triethanol amine titanate-acrylate composition	Polybutyl titanate titanate-acrylate composition
1.	0	1.461	1.463
2.	2	1.472	1.471
3.	4	1.472	1.475
4.	6	1.475	1.478
5.	8	1.477	1.481
6.	10	1.480	1.485
7.	12	1.483	1.489
8.	14	1.484	1.489
9.	16	*	*

*: Cinnamic acid did not dissolve

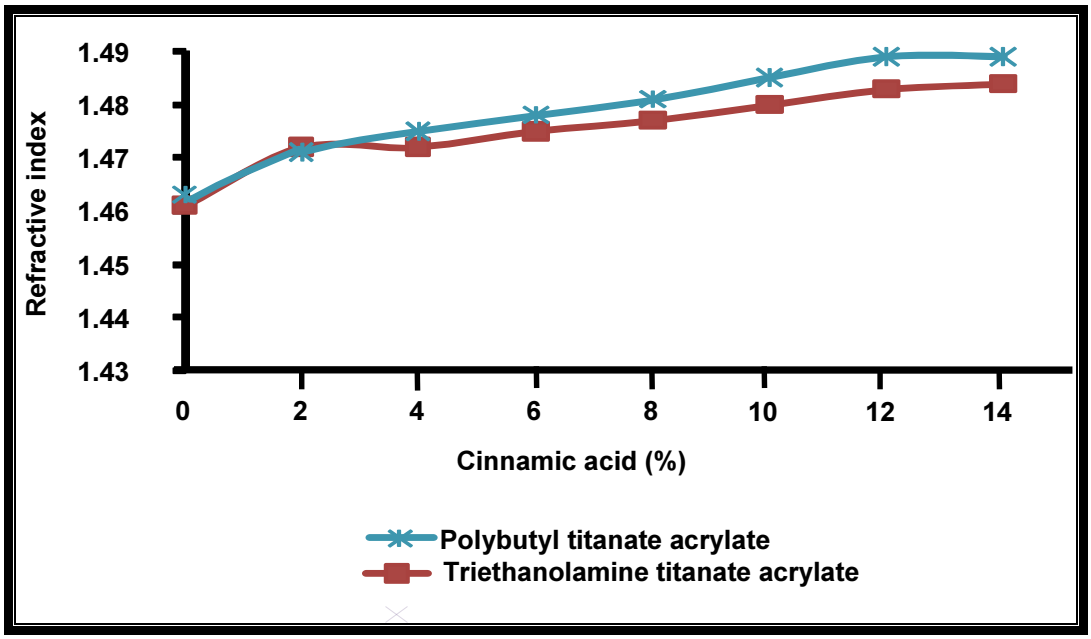

Figure 6.7: Effect of dispersion of cinnamic acid on refractive index of titanate acrylate compositions. The increase in refractive index is more in the case of polybutyl titanate acrylate composition

The compositions of titanate acrylate with the dispersion of cinnamic acid were evaluated for thermal analysis. The thermograms are presented in Figure 6.8 a-c.

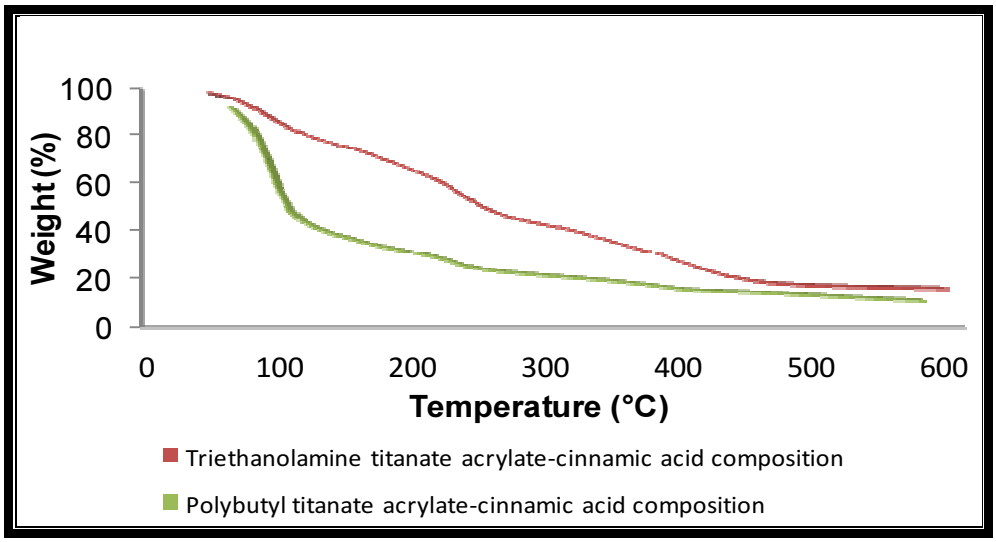

Figure 6.8a): TGA thermogram of triethanolamine titanate acrylate-cinnamic acid composition shows higher stability than polybutyl titanate acrylate-cinnamic acid composition

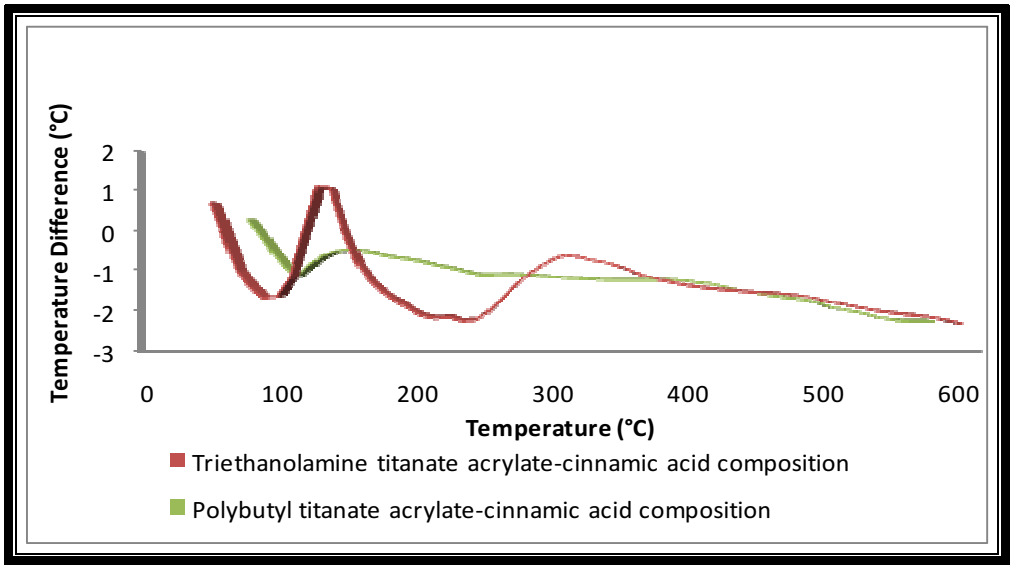

Figure 6.8b): DTA thermogram of polybutyl titanate acrylate-cinnamic acid composition and triethanolamine titanate acrylate-cinnamic acid composition

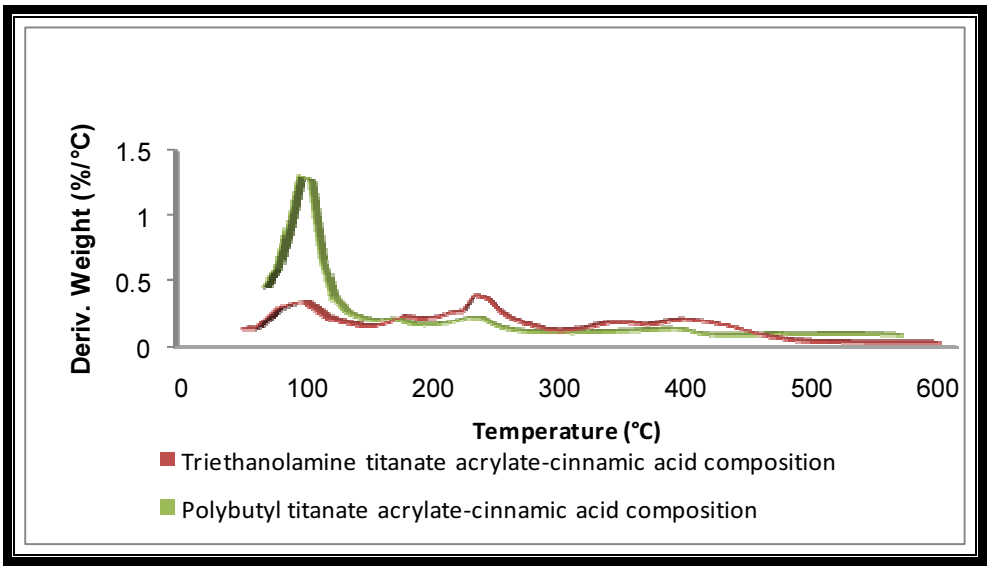

Figure 6.8c): DTG thermogram of polybutyl titanate acrylate-cinnamic acid composition and triethanolamine titanate acrylate-cinnamic acid composition

Thermograms of triethanolamine titanate acrylate-cinnamic acid composition showed three-step decomposition. The first step corresponds to a weight loss of 21% upto 118.6 °C and is reflected in both the DTA peak at 73.3 ºC and DTG peak at 81.7 ºC. Maximum decomposition rate is observed at 81.7 ºC as evident from DTG peak and is ascribed to the loss of ethanol from the titanate-composition corresponding to a DTA peak at 73.3 ºC. Further, the second decomposition step till 249.7 ºC is observed with a weight loss of 31 %, with maximum decomposition rate at 218.7 ºC confirmed by a DTG peak. The third decomposition takes place upto 459.3 ºC with a weight loss of 31% ascribed to the decomposition of the titanate acrylate-cinnamic acid composition.

Thermogram of polybutyl titanate acrylate-cinnamic acid composition showed two-step decomposition. Decomposition starts at 35 ºC till 98.2 ºC with maximum rate of weight loss at 74.3 ºC as is evident from DTG and DTA .Total weight loss observed at this stage is 56%. Further, the second decomposition step till 402.2 ºC is observed with a weight loss of 31.4 %, with

a small DTG peak at 224.4 ºC. This loss in weight is ascribed to the decomposition of polybutyl titanate acrylate-cinnamic acid composition.

Weight loss due to thermal decomposition of polybutyl titanate acrylate-cinnamic acid composition and triethanolamine titanate acrylate-cinnamic acid composition is shown in Table 6.7.

Table 6.7: Weight loss due to thermal decomposition of polybutyl titanate acrylate-cinnamic acid composition and triethanolamine titanate acrylate-cinnamic acid composition. The results indicate that the loss in weight at initial temperatures is more in the case of polybutyl titanate acrylate-cinnamic acid composition which becomes comparable to triethanolamine titanate acrylate-cinnamic acid composition at higher temperatures

Product	Weight loss (%)					
	100 °C	200 °C	300 °C	400 °C	500 °C	600 °C
Triethanolamine titanate acrylate - cinnamic acid composition	17.4	36.2	57.9	74.2	83.6	84.9
Triethanolamine titanate- acrylic acid composition	18.7	31.0	46.6	64.4	79.6	81.9
Polybutyl titanate acrylate-cinnamic acid composition	55.89	71.4	81.1	86.5	89.6	92.4
Polybutyl titanate-acrylic acid composition	64.7	86.0	92.2	93.4	94.3	94.8
Cinnamic acid	0	98.5	100	100	100	100
Theoretical loss in weight in Triethanolamine titanate acrylate - cinnamic acid composition	16.1	40.5	54.1	69.4	82.5	84.4
Theoretical loss in weight in Polybutyl titanate acrylate - cinnamic acid composition	55.6	86.0	83.7	88.4	95.1	95.5

As can be seen from Table 6.7, addition of cinnamic acid to the titanate acrylate compositions has brought an effect on thermal stability of the compositions. The thermal stability in the case of both the titanate acrylate-cinnamic acid composition is different from each other. In the case of triethanolamine titanate acrylate-cinnamic acid, the composition exhibited higher thermal stability than polybutyl titanate acrylate-cinnamic acid composition. But the thermal stability of polybutyl titanate acrylate has increased after the incorporation of cinnamic acid to it.

In order to understand the transitions taking place between titanate acrylate and cinnamic acid, UV-Visible spectroscopy was performed on the solutions from 200-800 nm (Figure 6.9 a-d).

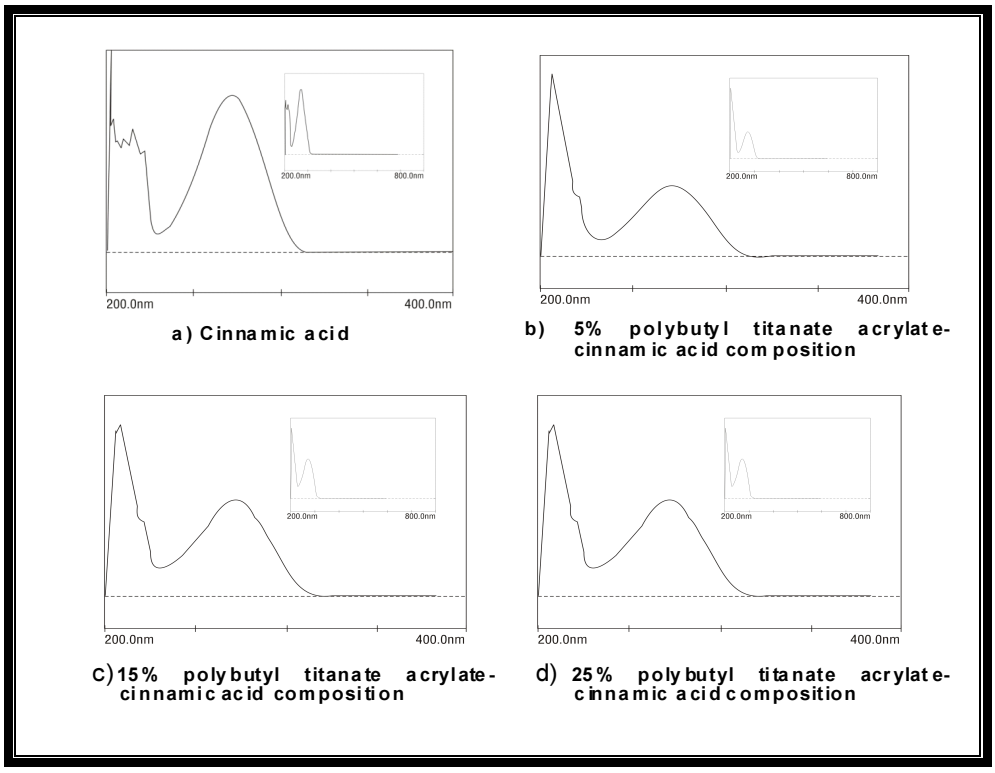

Figure 6.9 (a-d): UV-Visible spectra of cinnamic acid and polybutyl titanate acrylate-cinnamic acid compositions. Cinnamic acid exhibits λ_{max} at 273 nm. In the case of polybutyl titanate acrylate-cinnamic acid compositions, 2 peaks are observed; at 210 nm (characteristic of acrylic acid) and 273 nm (characteristic of cinnamic acid). Presence of peak at λ_{max} : 273 nm indicates that vinyl group of the cinnamic acid is intact.

As can be seen from Figure 6.6 (a-d), polybutyl titanate acrylate-cinnamic acid composition exhibit a peak at 210 nm, characteristic of acrylic acid and 273 nm which is a characteristic peak of cinnamic acid, at all concentrations. The peak in UV-Visible spectra of cinnamic acid appears at λ_{max} = 273 nm. This shows that the vinyl group remains intact.

Similarly, UV-Visible spectroscopy was performed on triethanol amine acrylate-cinnamic acid compositions (Figure 6.10 a-d).

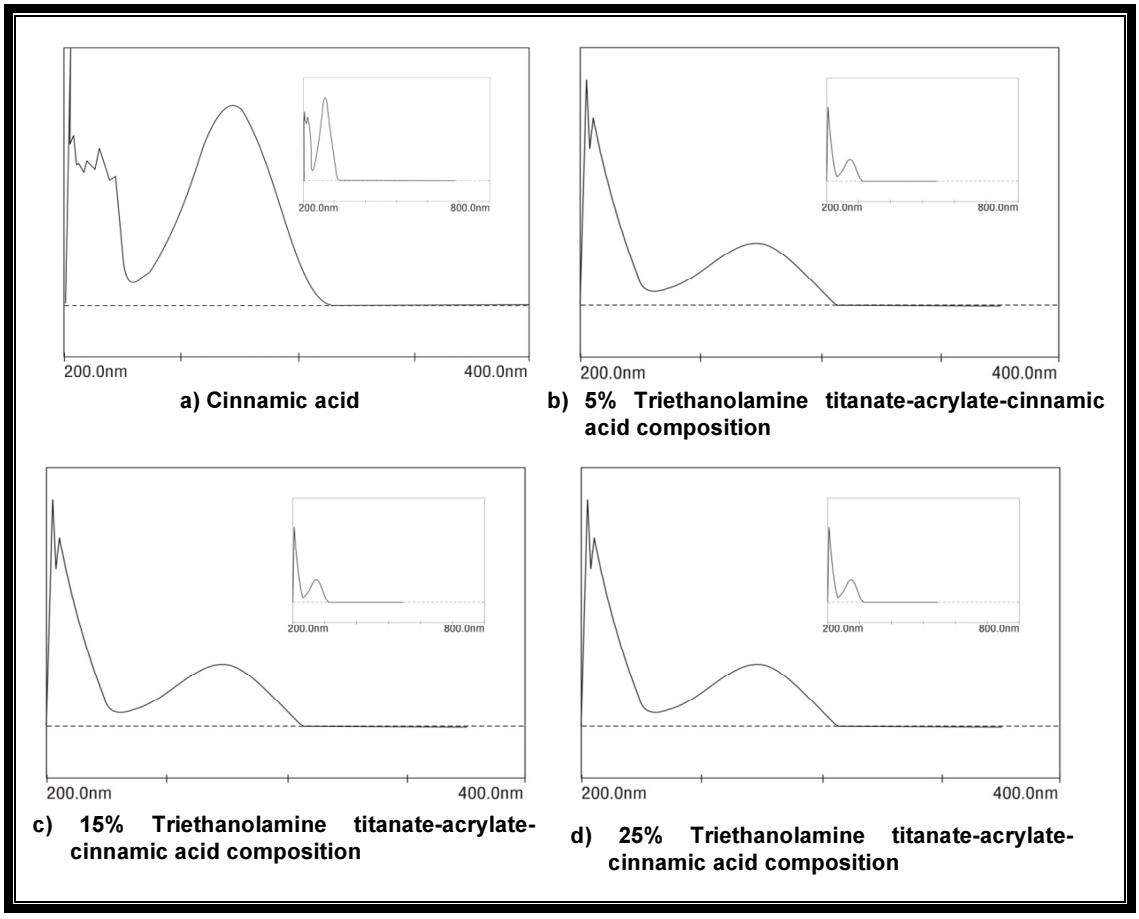

Figure 6.10 (a-d): UV-Visible spectra of cinnamic acid and triethanolamine titanate acrylate-cinnamic acid compositions. Cinnamic acid exhibits λ_{max} at 273 nm. In the case of triethanolamine titanate acrylate-cinnamic acid compositions, 2 peaks are observed; at 210 nm (characteristic of acrylic acid) and 273 nm (characteristic of cinnamic acid). Presence of peak at λ_{max} : 273 nm indicates that vinyl group of the cinnamic acid is intact.

As can be seen from Figure 6.10 (a-d), triethanolamine titanate acrylate-cinnamic acid composition exhibit a peak at 210 nm, characteristic of acrylic acid and 273 nm which is a characteristic peak of cinnamic acid, at all concentrations. This shows that the vinyl group remains intact.

Infrared spectroscopy was performed on the compositions (Figure 6.11a and b) to understand the interactions taking place between polybutyl titanate acrylate and cinnamic acid.

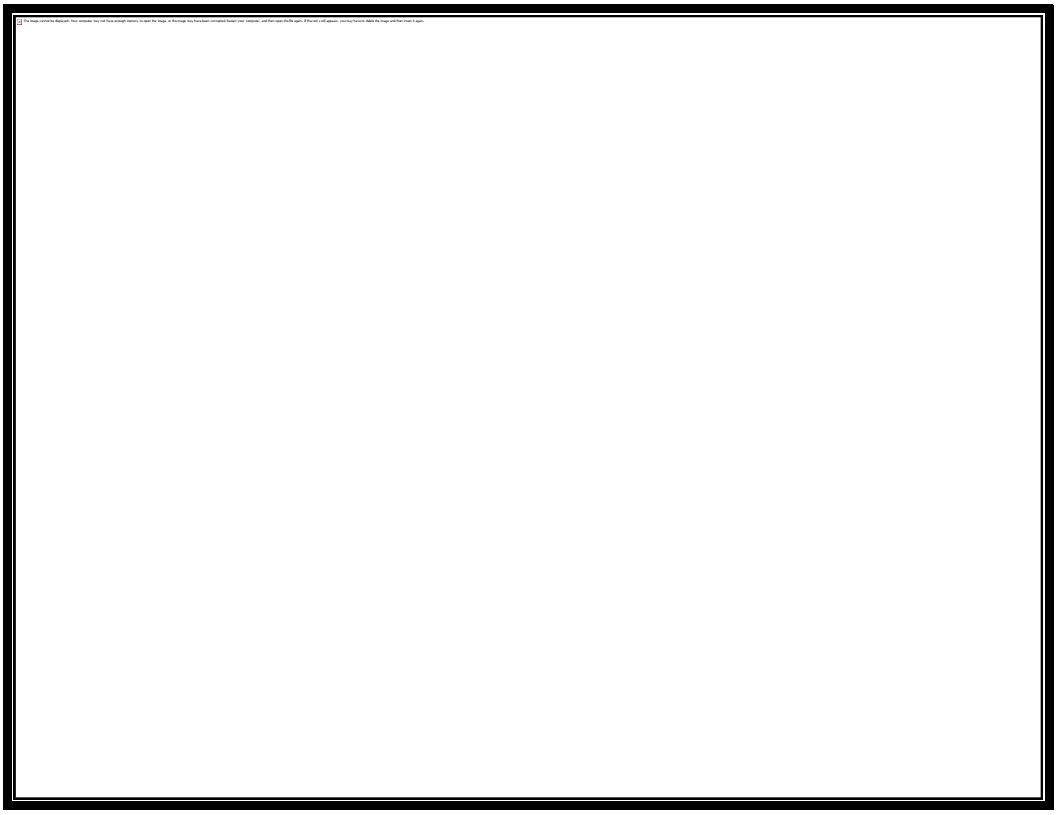

Figure 6.11a): Infrared spectra of polybutyl titanate acrylate-cinnamic acid compositions. The band pertaining to C=O stretch in -C=C-COOH at 1683 cm^{-1} is present in the spectra of cinnamic acid. In the case of titanate acrylate-cinnamic acid compositions, band at 1683 cm^{-1} has shifted towards the higher frequency.

It can be seen from Figure 6.11a and Figure 6.11b that the reaction between cinnamic acid and titanate acrylate is indicated by the shift of characteristic band of conjugated C=O stretch to higher frequencies. Thus, cinnamic acid is responsible for the changes in the properties of titanate acrylate compositions.

Styrene, a co-monomer, was used for polymerization of titanate acrylate-cinnamic acid compositions. Styrene was added in different percentages by weight to titanate acrylate-cinnamic acid compositions and stirred continuously to produce transparent and clear titanate acrylate-cinnamic acid-styrene compositions.

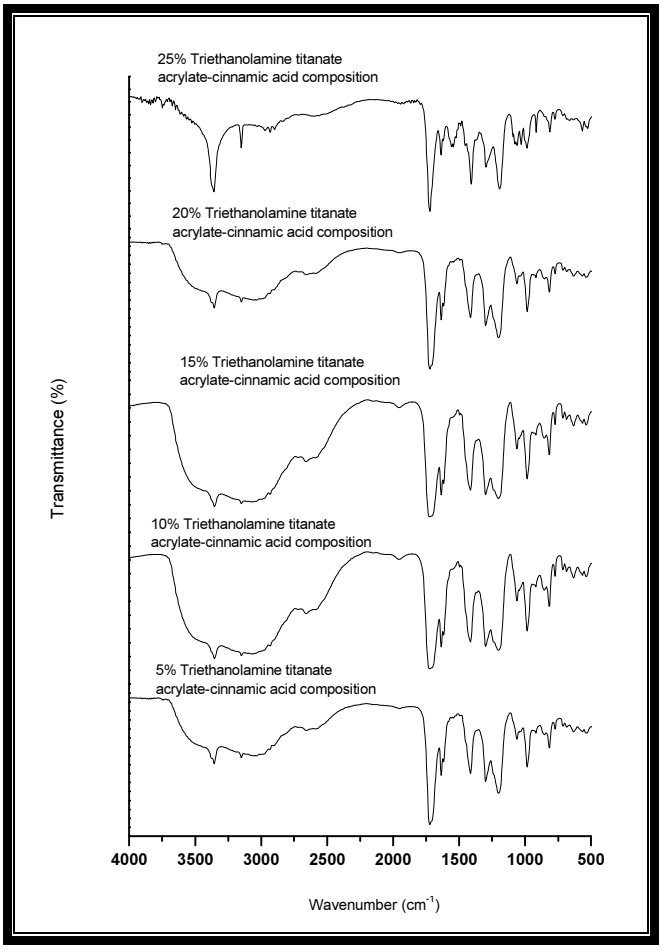

Figure 6.11b): Infrared spectra of polybutyl titanate acrylate-cinnamic acid compositions and b) triethanolamine titanate acrylate-cinnamic acid compositions. The band pertaining to C=O stretch in -C=C-COOH at 1683 cm^{-1} is present in the spectra of cinnamic acid. In the case of titanate acrylate-cinnamic acid compositions, band at 1683 cm^{-1} has shifted towards the higher frequency.

Cast polymerization of titanate acrylate-cinnamic acid-styrene compositions

Cast polymerization of titanate acrylate-cinnamic acid-styrene compositions into lenses was carried out by subjecting the compositions to polymerization by gamma irradiation. The effect of amount of styrene (% by weight of titanate acrylate) was studied and the results are tabulated in Table 6.8.

Table 6.8: Effect of styrene (% by weight of titanate acrylate-cinnamic acid composition) on polymerization of titanate acrylate-cinnamic acid compositions

S. No.	Styrene (% by weight)	Observations	Shore-D hardness
1.	25	Soft, sticky sample, could not be released from the mold	40
2.	50	Soft, sticky sample, could not be released from the mold	50
3.	65	Brittle and semi-hard sample, could not be released from the mold	75
4.	85	Transparent sample, released easily from the mold	91
5.	100	Semi-transparent sample, released easily from the mold	90
6.	120	Slightly hazy sample, released easily from the mold	90

It may be seen that with 25-65 % (by weight of titanate acrylate-cinnamic acid composition) of styrene, the polymer is soft, sticky and brittle due to insufficient amount of styrene for polymerization. The shore-D hardness of the polymer is 40 for 25% (by weight of lanthanum acrylate-cinnamic acid composition) of styrene, 50 for 50% (by weight of titanate acrylate-cinnamic acid composition) of styrene and 75 for 65% (by weight of titanate acrylate-cinnamic acid composition) of styrene. The polymer could not be released from the mold, which limits the processing characteristics of the polymer. With 85% (by weight of titanate acrylate-cinnamic acid composition) of styrene,

shore-D hardness increased to 91 and the polymers were easily released from the mold. This indicates that 85% (by weight of titanate acrylate-cinnamic acid composition) of styrene is sufficient for polymerization of titanate acrylate nanocomposites. Clear and transparent polymers were obtained. Styrene if used at 100% (by weight of titanate acrylate-cinnamic acid composition) or above, gave colored and hazy polymer. From these observations, it is clear that 85% (by weight of titanate acrylate-cinnamic acid composition) of styrene is required for the complete polymerization to form transparent titanate acrylate nanocomposites. Similar results were obtained with titanate acrylate-styrene compositions (without cinnamic acid).

The compositions of titanates with and without cinnamic acid were subjected to gamma irradiation for polymerization. Polymerization was achieved by subjecting the compositions to various doses of gamma irradiation from 10 kGy to 90 kGy. The optimum dose required for complete polymerization was arrived at by analysis of cross-link density of the nanocomposites. The results of cross-link density are tabulated in Table 6.9.

Table 6.9: Cross-link density results of titanate acrylate-styrene nanocomposites indicate that 90 kGy is the optimum dose required to result in hard polymers

S. No.	Dose (kGy)	Cross-link density (%)
1.	10	55.9
2.	30	62.1
3	50	74.9
4.	70	82.2
5.	90	97.2
6.	100	94.3

As can be seen from Table 6.9, 10 kGy of gamma irradiation dose led to a cross-link density of nanocomposites of only 56%, indicating incomplete polymerization. Similarly, gamma irradiation dose of 30-70 kGy resulted in the cross-link density between 62% - 82%. Maximum cross-link density of 97% was obtained at 90 kGy and hence titanate acrylate nanocomposites were prepared at a radiation dose of 90 kGy.

Effect of gamma irradiation on appearance of the nanocomposites, with and without cinnamic acid, was studied and the results are tabulated in Table 6.10 and Table 6.11.

From the results of Table 6.10, triethanolamine titanate-acrylate-styrene nanocomposites, presence of up to 10% of titanate gave hard and transparent nanocomposites. Beyond 10%, the nanocomposites were opaque and not suitable for optical applications. Similarly in the case of polybutyl titanate-acrylate nanocomposites, up to 10% titanate showed transparent polymers.

As can be seen from Table 6.11, polymerization of 10% triethanolamine titanate acrylate-cinnamic acid-styrene compositions resulted in hard and transparent polymers. Beyond 10%, the polymers were opaque and not suitable for optical applications. In the case of polybutyl titanate, 5% - 25% incorporation of titanate resulted in completely transparent polybutyl titanate acrylate-cinnamic acid-styrene nanocomposites.

The effect of titanates on the optical properties such as refractive index and Abbe number of titanate acrylate-styrene nanocomposites was determined. Tailor-making of the refractive index and Abbe number is possible and are presented in Table 6.12. The results of the maximum refractive index and Abbe number values achieved in each case is presented in Figure 6.12.

Table 6.10: Effect of gamma irradiation on titanate acrylate-styrene nanocomposites

S. No.	Conc. (%)	Triethanolamine titanate	Polybutyl titanate
1.	0	Brittle and foamy polymer	Brittle and foamy polymer
2.	5	Hard, transparent	Hard, transparent
3.	10	Hard, transparent	Hard, transparent
4.	15	Opaque	Opaque
5.	20	Opaque	Opaque
6.	25	Opaque	Opaque

Table 6.11: Effect of gamma irradiation on titanate acrylate-cinnamic acid-styrene nanocomposites

S.No.	Conc. (%)	Triethanolamine titanate	Polybutyl titanate
1.	0	Brittle and foamy polymer	Brittle and foamy polymer
2.	5	Hard, transparent	Hard, transparent
3.	10	Hard, transparent	Hard, transparent
4.	15	Opaque	Hard, transparent
5.	20	Opaque	Hard, transparent
6.	25	Opaque	Hard, transparent

Having cast polymerized the lenses using various compositions of titanate acrylate-cinnamic acid plus styrene, the lenses were evaluated for various parameters. The results are discussed in the following section.

As can be seen from Figure 6.12, the maximum refractive index of the nanocomposites is achieved by the addition of triethanolamine titanate. Maximum refractive index of 1.561 is exhibited by triethanolamine titanate acrylate-titanate nanocomposites with 10% titanate addition. In the case of polybutyl titanate acrylate-styrene nanocomposites, refractive index obtained was 1.554.

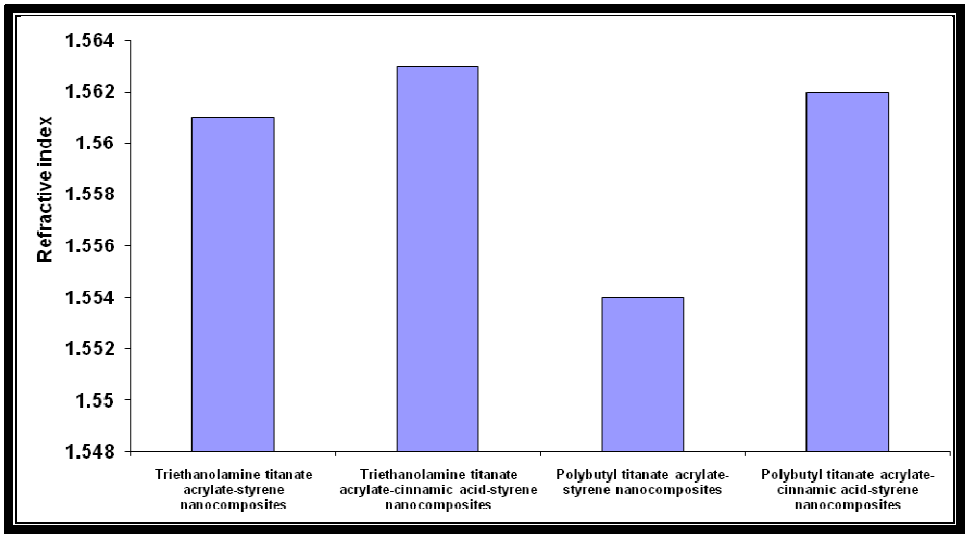

Figure 6.12: Results of effect of titanates on refractive index of acrylate-styrene nanocomposites (without cinnamic acid and with cinnamic acid). Refractive index is almost comparable for both the nanocomposites in both cases

In the case of cinnamic acid dispersed nanocomposites, the polymers show more or less the same behavior like in the case of nanocomposites without cinnamic acid. Maximum refractive index is exhibited by triethanolamine titanate acrylate-cinnamic acid nanocomposites with a value of 1.563. For polybutyl titanate acrylate-cinnamic acid nanocomposites, the refractive index achieved was 1.547 to 1.562 depending upon the concentration of titanate used.

Similarly, Abbe number of the polymers, with and without cinnamic acid, were evaluated and the results are presented in Figure 6.13

Table 6.12: Refractive index and Abbe number of titanate acrylate nanocomposites

S. No.	Nanocomposites	Without Cinnamic acid		With Cinnamic acid	
		Refractive index	Abbe number	Refractive index	Abbe number
1.	Triethanol amine titanate acrylate-styrene	5%: 1.555 10%: 1.561	30 32	1.558 1.563	34 33
2.	Polybutyl titanate acrylate-styrene	5%: 1.542 10%: 1.554 15%: -- 20%: -- 25%: --	36 37 -- -- --	1.547 1.554 1.558 1.560 1.562	36 36 35 34 34

As can be seen from Figure 6.13, maximum Abbe number is obtained in the case of addition of polybutyl titanate. Abbe number of 31-32 is obtained with the addition of triethanolamine titanate, which is the lowest. It is in trend with the refractive index value, as the refractive index of triethanolamine titanate-acrylate nanocomposites is the highest amongst all.

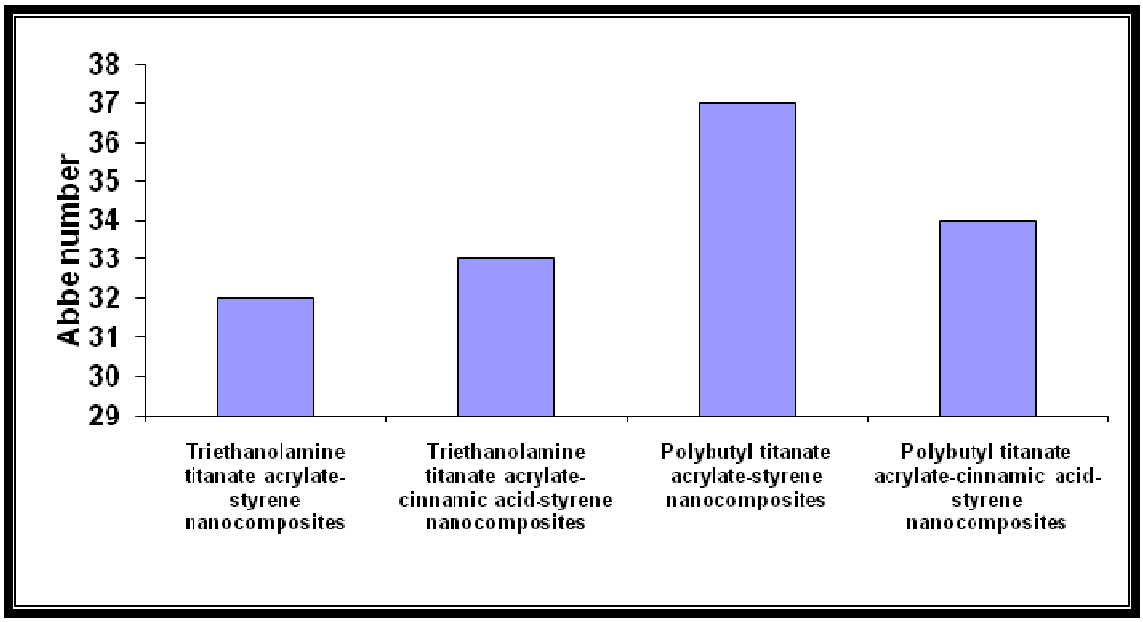

Figure 6.13: Effect of titanium on Abbe number of titanate acrylate nanocomposites a) without cinnamic acid and b) with cinnamic acid. Abbe number is higher in the case of polybutyl titanate acrylate-styrene nanocomposites

The specific gravity of the nanocomposites lies in the range of 1.30-1.32, which is comparable to the conventional optical polymers used for optical applications (1.28 for PMMA).

TGA-DTA-DTG of titanate acrylate nanocomposites with cinnamic acid was carried out to study the thermal stability and phase transitions of acrylic polymers containing titanium. The thermograms are shown in Figures 6.14a)-c).

The thermal decomposition of acrylic acid-styrene polymer takes place in two steps. First decomposition takes place up to 222.4 $^{\circ}$C with 10% weight loss attributed to loss of moisture and volatile components. A well-defined weight loss of 80% is observed between 222.4 $^{\circ}$C and 423.7 $^{\circ}$C, with a maximum decomposition rate at 384 $^{\circ}$C as evident from a sharp DTG peak. Further decomposition occurs leading to complete weight loss before 550 $^{\circ}$C indicated by a sharp exotherm in DTA at 537.3 $^{\circ}$C.

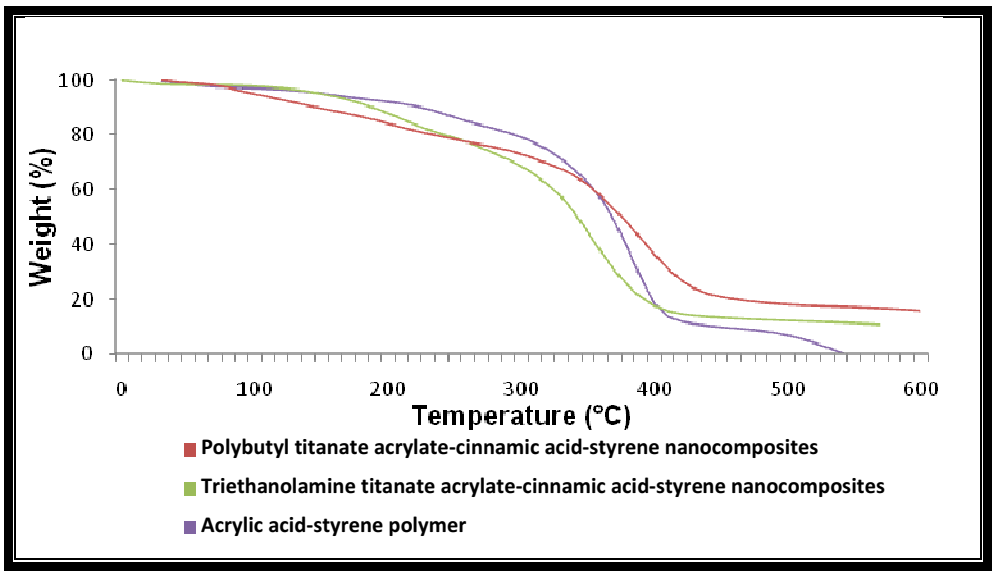

Figure 6.14a): TGA thermograms of polybutyl titanate-acrylate-cinnamic acid-styrene nanocomposites, triethanolamine titanate acrylate-cinnamic acid-styrene nanocomposites indicating higher thermal stability than Acrylic acid-styrene polymer due to incorporation of titanium

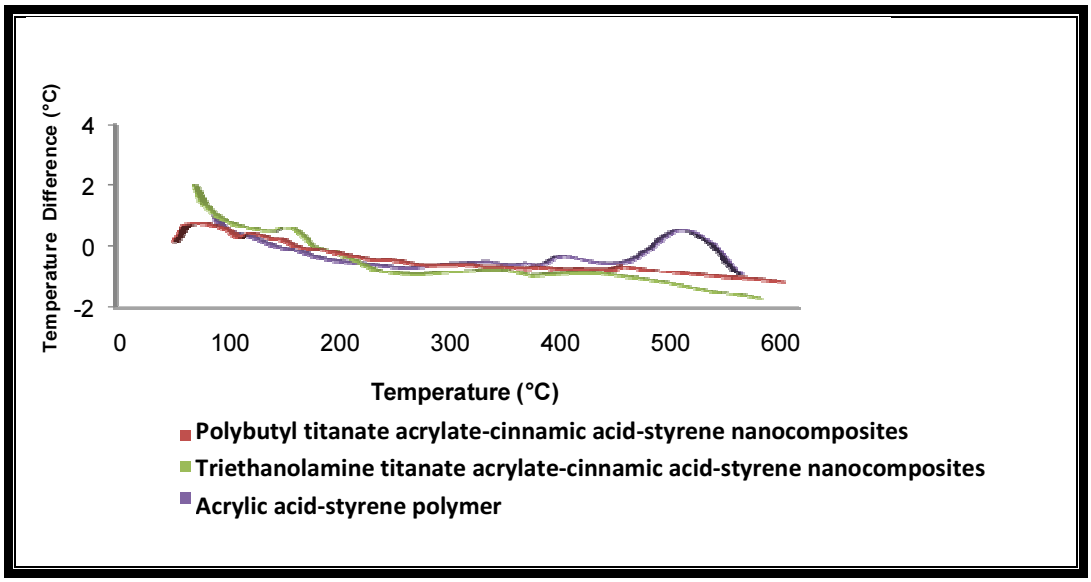

Figure 6.14b): DTA thermograms of polybutyl titanate-acrylate nanocomposites, triethanolamine titanate acrylate nanocomposites and acrylic acid-styrene polymer

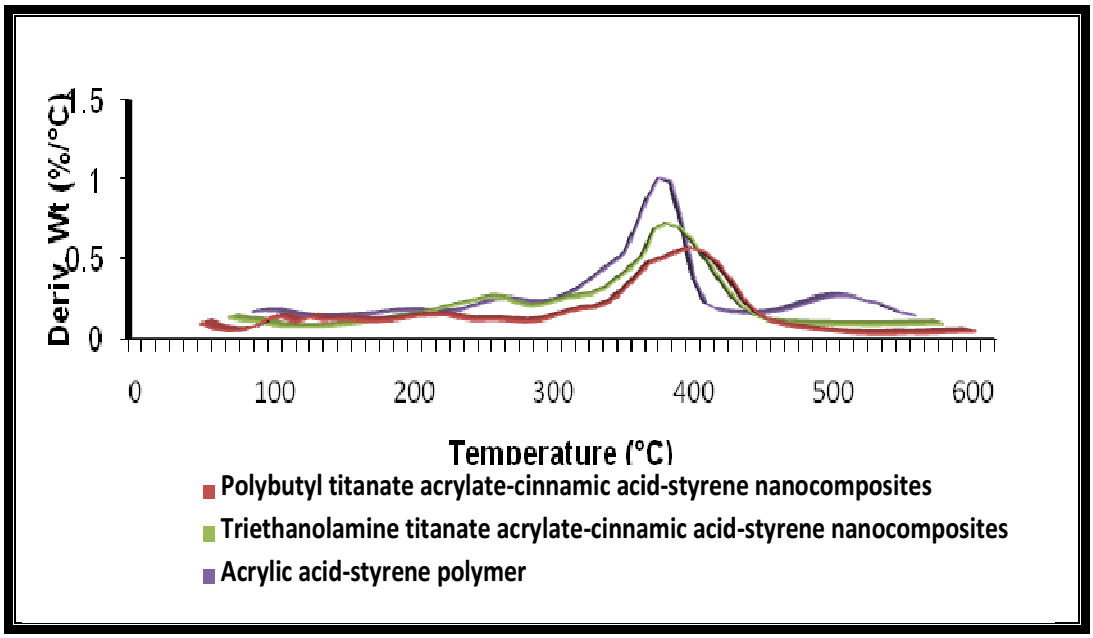

Figure 6.14c): DTG thermograms of polybutyl titanate-acrylate nanocomposites, triethanolamine titanate acrylate nanocomposites and acrylic acid-styrene polymer

In the case of triethanolamine titanate acrylate-cinnamic acid-styrene nanocomposites, the polymer shows single step decomposition upto 453.3 ºC with approximately 86% loss in weight. A sharp DTG peak at 382.1 ºC appears which is ascribed to the maximum decomposition rate at this temperature due to the polymer chain scissioning of the titanate acrylate-cinnamic acid-styrene nanocomposites.

In the case of polybutyl titanate acrylate-cinnamic acid-styrene nanocomposites, incorporation of 25% polybutyl titanate gave transparent and clear nanocomposites. The nanocomposites experiences one step weight loss. A loss in weight of 80% is observed up to 449.5 ºC. DTA peak at 88.5 ºC shows the loss of moisture from the nanocomposites. Further maximum loss in weight at 389 ºC was observed as is evident by a sharp DTG peak. This is ascribed to the decomposition of the nanocomposites.

The weight loss of polyacrylate and titanate acrylate-styrene nanocomposites is shown in Table 6.13.

Table 6.13: Weight loss (%) due to thermal decomposition of acrylic acid-styrene polymer and titanate acrylate-cinnamic acid-styrene nanocomposites

Product	Weight loss (%)					
	100 °C	200 °C	300 °C	400 °C	500 °C	600 °C
Acrylic acid-styrene polymer	3.2	8.1	21	81.6	93.3	0
Triethanolamine titanate acrylate-cinnamic acid-styrene nanocomposites	2.0	7.4	24.9	69.6	87.4	89.43
Polybutyl titanate acrylate-cinnamic acid-styrene nanocomposites	5.3	16.1	27.3	63.7	82.0	84.3

As can be seen from Table 6.13, initial weight loss of titanate acrylate-styrene nanocomposites is more than the acrylic acid-styrene polymer due to the presence of volatile components in the titanate acrylate nanocomposites. Similar trend is observed till 300 ºC. At 400 ºC, acrylic acid-styrene polymer indicate a greater weight loss of 82% is observed. In the case of titanate acrylate nanocomposites, weight loss of 63-70% is observed. This higher stability of titanate acrylate nanocomposites is ascribed to the presence of titanium in the system which makes the nanocomposites more thermally stable as compared to the one without titanium. Major decompositions in the case of titanate acrylate compositions took place well before 400 ºC. After polymerization of the components, the stability is increased as observed by weight loss after 400 ºC. The thermal studies indicate the formation of a highly cross-linked, stable structure with no free acrylic acid and cinnamic acid.

Leachability was determined as per method described in Chapter 3 using ICP-OES instrument. Leachability of titanium metal was observed in concentrated nitric acid and concentrated hydrochloric acid. Zero leachability of titanium was obtained in concentrated hydrochloric acid and 60 ppm of

titanium in concentrated nitric acid, indicating that titanium is not present in free form.

Transmittance of titanium-containing nanocomposites was evaluated to be 90%. The polymers which were cast into lenses were found to be impact resistant (method described in Chapter 3) as per FDA regulations.

Vicat softening temperature was determined for titanium-containing nanocomposites. Vicat softening temperature was determined to be 54 °C indicating that the working temperature of titanium nanocomposites is lower than PMMA which has a working temperature of 109 °C.

Shore-D hardness of all nanocomposites lies in the range of 90-92. Transmittance was evaluated and was found to be 85-90% for all titanium nanocomposites.

SEM analysis was carried out to study the surface morphology of the titanate acrylate-styrene nanocomposites. As can be seen from Figure 6.15, SEM picture of titanate acrylate-styrene nanocomposites (Figure 6.15b) is completely different from the SEM of polyacrylate (Figure 6.15a).

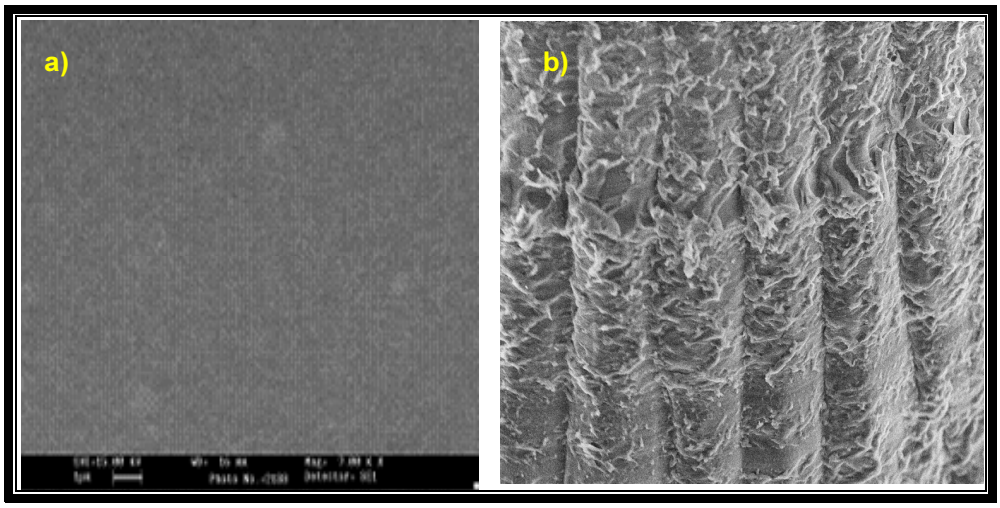

Figure 6.15: a) SEM picture of acrylic acid-styrene polymer and b) SEM picture of polybutyl titanate acrylate-styrene nanocomposite indicates change in surface morphology on addition of titanate

As can be seen from Figure 6.15 a) and b), that the surface of acrylic acid-styrene polymer is absolutely clear and homogeneous. In the case of titanate acrylate-styrene nanocomposites, continuous domains are bound to a polymeric network and are uniformly dispersed. This may be ascribed to the bonding taking place between the titanate and the acrylate matrix.

6.4 CONCLUSIONS

In this chapter, novel titanate acrylate-styrene nanocomposites using organic titanates have been prepared for optical applications for the first time. The achievements of titanate acrylate-styrene nanocomposites are as follows:

1. Novel methodology for the incorporation of titanium in acrylate matrix is being developed.
2. Six organic titanates namely tetraisopropyl titanate, tetrabutyl titanate, tetra 2-ethylhexyl titanate, polybutyl titanate, triethanolamine titanate and titanium acetylacetonate were used to prepare titanate acrylate nanocomposites.
3. Dispersion of organic titanates into acrylic matrix has been carried out successfully where upto 25% titanates (by weight) have been dispersed in acrylic acid.
4. The modification of an important monomer, acrylic acid, for optical applications, has been done in a novel and cost-effective manner, thanks to the attributes provided by titanium.
5. The effect of dispersion of titanates on acrylic acid was monitored by studying the changes taking place in the refractive index, acid value and thermal stability of acrylic acid.
6. The formation of titanate-acrylic acid compositions results in an increase in refractive index from 1.424 to 1.463 in the case of addition of 25% polybutyl titanate, 1.461 in the case of addition of 25% triethanolamine titanate, 1.453 in the case of addition of 25% tetraisopropyl titanate, 1.445 in the case of addition of 25% tetrabutyl titanate and 25% titanium acetylacetonate and 1.433 in the case of addition of 25% tetra 2-ethylhexyl titanate.

7. Acid value of titanate-acrylic acid compositions were being evaluated and acid number of acrylic acid was found to decrease from 626 to 471 with the addition of titanates. This result indicates the interactions are taking place between titanate and acrylic acid.
8. Particle size analysis of titanate-acrylic acid compositions show that the dispersion of titanate in acrylic acid is in nanometer scale resulting in clear and transparent compositions.
9. Since, maximum refractive index amongst the titanates were achieved by the dispersion of polybutyl titanate and triethanolamine titanate in acrylic acid, further studies were carried out using these titanates only.
10. Titanate-acrylic acid compositions are thermally more stable as compared to acrylic acid due to the synergistic combination of titanate and acrylic acid. This shows that new compound (titanate acrylate is being formed by the reaction between acrylic acid and titanates).
11. UV-Visible spectroscopy of titanate acrylates was performed and it was found that the vinyl group of acrylic acid remains intact and does not undergo reaction with titanates.
12. Infrared spectroscopy showed that the band pertaining to the carboxylic acid group of acrylic acid is absent as titanates are added to it. This indicates that the reaction of titanates is taking place at the carboxylic acid group of acrylic acid forming ester.
13. To further improve the properties of titanate acrylate compositions, cinnamic acid was added to it. Dispersion of cinnamic acid in titanate acrylate led to the formation of clear and transparent high refractive index titanate acrylate-cinnamic acid compositions.
14. Cinnamic acid was added to titanate-acrylate compositions to give transparent composition with refractive index ranging between 1.461 (in the case of triethanolamine titanate acrylate-cinnamic acid composition) to 1.489 (in the case of polybutyl titanate acrylate-cinnamic acid composition).

15. Thermal analysis of titanate acrylate-cinnamic acid compositions showed that they are comparable in terms of thermal stability with the compositions before addition of cinnamic acid. This shows that addition of cinnamic acid in titanate acrylate compositions results in the formation of a mixture.
16. UV-Visible spectroscopy and Infrared spectroscopy also confirmed that no chemical reaction is taking place between cinnamic acid and titanate acrylate compositions.
17. Styrene was added to titanate acrylate-cinnamic acid compositions as a co-monomer for polymerization into lenses.
18. Gamma irradiation has been used as a novel technique for the polymerization of titanate acrylate compositions, with and without cinnamic acid. Optimization of irradiation dose was done based on the cross-link density.
19. Tailor-making of important optical properties such as refractive index and Abbe number has been possible. Refractive index can be maneuvered between 1.542-1.561 in the case of titanate acrylate polymers without cinnamic acid and 1.536-1.563 in the case of titanate acrylate nanocomposites with cinnamic acid. Similarly, Abbe number can be tailor-made between 30-37, in the case of titanate acrylate nanocomposites without cinnamic acid and 33-37 in the case of titanate acrylate polymers with cinnamic acid.
20. The developed titanate acrylate nanocomposites are thermally stable having good machinability and impact resistance. They are extremely hard and very light-weight as compared to the conventional optical plastics in use.

At the end of this work, the process technology for making titanate acrylate nanocomposites using in-situ dispersion of titanium with varying refractive index and other important properties has been developed. The technology

developed for the preparation of titanate acrylate polymers for making optical plastics of high refractive index has the novelty as well as the potential for commercialization. The present work has great relevance for the growth of optical plastics industry in India as much as for the society looking for an indigenous product with an affordable cost.

Chapter 7
Lanthanum Acrylate Nanocomposites

CHAPTER 7
LANTHANUM ACRYLATE NANOCOMPOSITES

7.0 INTRODUCTION

The traditional optical material, glass, is characterized by a low refractive index of 1.35. The inorganic materials of high refractive index were found to help enhance the refractive index of glass. Thus, to increase the refractive index and thereby the scope of its applications, salts of high refractive index such as lanthanum oxide (lanthal glass), lead oxide (flint glass), barium nitrate (barium glass), etc. have been incorporated in glass during its processing. This way, glass materials of high refractive index have been in use for different types of optical applications for quite some time. It must be mentioned here that this was not good enough because of the fact that the inherent drawbacks like inferior physico-mechanical properties were limiting the use of glass in all applications. That is why, there has always been the need for the development of optical plastics as the alternative material for glass. Lanthanum-containing glass is used in camera and telescope lenses because of its high refractive index and low dispersion indices. Lanthanum oxide (La_2O_3) is used in manufacturing of high transparency and high refractive index glass. The end application is precision optics like microscope and telescope lenses and camera components. Lanthanum oxide is also used for polishing glass and gemstones. The idea of incorporating lanthanum oxide in glasses besides leading to an improvement in optical properties, the presence of inorganic moiety in an organic matrix would also lead to an enhancement of mechanical properties.

Optical plastics have already been accepted as the prominent alternative to glass. However, plastics also suffer from certain drawbacks, especially related to their optical properties. One of the challenges that remain unresolved so far pertains to the balancing of refractive index and Abbe number. High refractive index and high Abbe number is a difficult target to achieve. Learning from the

experiences of enhancing the refractive index of glass by incorporating inorganic compounds of high refractive index, one would be tempted to replicate this in plastics. There have been references which show that it is feasible. Various metallic salts including lanthanum have been used to increase the refractive index. Use of such an approach in the synthesis of polymeric optical materials in most of the cases have been reported to exhibit positive results and helps in getting materials with refractive index values of as high as 1.65. Metal matrices have also been shown to offer high temperature stability, mechanical strength and stiffness when incorporated in polymers **[418]**.

The present chapter includes the studies wherein lanthanum acrylate nanocomposites have been prepared by the dispersion of inorganic lanthanum oxide in acrylic acid. The lanthanum acrylate nanocomposites has then been further co-polymerized by dispersion of a co-monomer to obtain a transparent, hard and clear polymer suitable for optical applications. For all this, gamma radiation technology has been used. The preparation of lanthanum-based polymers has been described earlier in Chapter 3 and consists of the following steps:

7.1 STEP I: DISPERSION OF LANTHANUM OXIDE IN ACRYLIC ACID

Lanthanum belongs to group III B of periodic table having an ionic size of 1.032 Å and polarizability of 31.1 $Å^3$. Among the lanthanum salts, lanthanum nitrate, lanthanum oxide and lanthanum chloride were identified for dispersion in acrylic acid based on their easy availability. Lanthanum oxide was selected for dispersion in acrylic acid, since it was highly soluble in acrylic acid. Due to insolubility in acrylic acid, lanthanum nitrate and lanthanum chloride were not considered suitable for preparation of optical polymers **[418].** Lanthanum oxide was added gradually to acrylic acid taken in a round bottom flask fitted with a condenser and stirred vigorously at room temperature to find the maximum amount of lanthanum going into solution without adversely affecting

its transparency. After knowing this concentration, specimens of varying amount (% by weight) of lanthanum in acrylic acid were prepared covering a range of 0% to 20% (by weight) of lanthanum oxide.

7.2 STEP II: INCORPORATION OF CINNAMIC ACID AND STYRENE IN LANTHANUM ACRYLATE COMPOSITIONS

Cinnamic acid was taken as a co-monomer for dispersion in lanthanum acrylate composition to prepare high refractive index compositions. Cinnamic acid in varying amounts was added to lanthanum acrylate compositions of varying concentration of lanthanum to prepare high refractive index lanthanum acrylate-cinnamic acid compositions.

Cinnamic acid is known for its high intrinsic molar refraction due to the presence of an aromatic benzene ring. Cinnamic acid was thus, taken as a co-monomer for dispersion in lanthanum acrylate composition to improve its optical properties.

The dispersion of cinnamic acid in lanthanum acrylate composition was followed by cast polymerization in the presence of styrene. For the purpose of creating the three-dimensional network of structure, styrene was used as a co-monomer for polymerizing lanthanum acrylate-cinnamic acid compositions. Styrene undergoes addition at the double bond of the vinyl group and is therefore used as cross-linking agent to form networks. Hence it was expected to produce a transparent optical polymer.

7.3 STEP III: CAST POLYMERIZATION OF LANTHANUM CONTAINING COMPOSITION-STYRENE

Lanthanum acrylate-cinnamic acid-styrene compositions were polymerized and cast into lenses using gamma irradiation technique. The dose of the gamma irradiation was optimized to prepare hard, transparent and clear lenses.

RESULTS & DISCUSSION

Results of various studies performed during the preparation of lanthanum acrylate nanocomposites are presented in this section. Observations for various parameters at different stages of the study are discussed. First the studies on lanthanum-containing compositions were performed for the following parameters:

- ❖ Transmittance and clarity of dispersion
- ❖ Refractive index
- ❖ Acid value
- ❖ pH
- ❖ UV-Visible spectroscopy
- ❖ Particle size distribution
- ❖ Infrared spectroscopy
- ❖ Thermal analysis

Then the studies pertaining to the incorporation of cinnamic acid as a co-monomer were carried out for the following parameters:

- ❖ Transmittance and clarity of dispersion
- ❖ Refractive index
- ❖ UV-Visible spectroscopy
- ❖ Infrared spectroscopy
- ❖ Thermal analysis

Followed by the above step, cast polymerization of the lanthanum acrylate-cinnamic acid-styrene was carried out using gamma irradiation. The studies for the following parameters were carried out:

- ❖ Shore-D hardness
- ❖ Cross-link density
- ❖ Refractive index
- ❖ Abbe number
- ❖ Thermal analysis
- ❖ Machinability
- ❖ Pencil hardness
- ❖ Vicat Softening temperature
- ❖ Leachability of the lanthanum ions
- ❖ Transmittance

Dispersion of lanthanum oxide in acrylic acid

Dispersion of lanthanum oxide was carried out in acrylic acid at various concentrations from 0% - 25%, to prepare lanthanum oxide-acrylic acid compositions. Refractive index and acid number of compositions of varying content of lanthanum were studied and plotted against the concentration of lanthanum oxide in acrylic acid. As lanthanum oxide was dispersed in acrylic acid, observations were noted and are tabulated in Table 7.1.

Table 7.1: Effect of dispersion of lanthanum oxide on transmittance of acrylic acid was observed from 200-800 nm. The results show that upto 20% lanthanum oxide can be dispersed into acrylic acid retaining optical clarity and transparency of the composition

S.No.	Lanthanum oxide (%)	Observations	Transmittance (%)			
			200 nm	400 nm	600 nm	800 nm
1.	5	Clear and transparent solution	17	98	99	99
2.	10	Clear and transparent solution	39	97	98	99
3.	15	Clear and transparent solution	20	99	99	99
4.	17	Clear and transparent solution	18	95	98	99
5.	20	Clear and transparent solution	15	95	98	99
6.	25	Hazy solution	10	65	70	70

As can be seen from Table 7.1, dispersion of upto 20% lanthanum oxide in acrylic acid yields transparent and clear solutions as evident from the value of transmittance as 99% in the visible region. The transmittance at all percentages of lanthanum oxide dispersion in acrylic acid was 99% indicating that the solutions are absolutely transparent and clear. At wavelength of 400 nm and 600 nm, the compositions exhibit transmittance of 95-98%. Transmittance of the

composition decreases to 10%-39% in the UV region. Beyond 20% dispersion of lanthanum oxide, however, the compositions were observed to be hazy initially but turning opaque at concentrations higher than 25%.

Change in properties of lanthanum oxide-acrylic acid composition was observed also through the measurement of refractive index. Refractive index increases with increase in the concentration of lanthanum oxide in the compositions (Figure 7.1). The results are tabulated in Table 7.2.

As can be seen from Figure 7.1, refractive index of acrylic acid increases gradually on the addition of lanthanum oxide in acrylic acid. The refractive index of acrylic acid is 1.424 which increased to 1.441 on addition of 5% lanthanum oxide to it. Further addition of 10% lanthanum oxide to acrylic acid resulted in an increase of refractive index to 1.451. The refractive index increases to 1.464 in the case of 15% dispersion of lanthanum oxide in acrylic acid and 1.466 in the case of 17% addition of lanthanum oxide to acrylic acid. Beyond 17% addition of lanthanum oxide to acrylic acid, the refractive index remains constant and does not show any change. Hence, 17% is the optimized percentage of lanthanum oxide that could be incorporated into acrylic acid to yield lanthanum acrylate compositions without loosing transparency while enhancing the refractive index.

Table 7.2: Results of the dispersion of lanthanum oxide on refractive index of acrylic acid. Data indicate that the dispersion of 17% lanthanum oxide in acrylic acid increases the refractive index to 1.466 from 1.424 to begin with.

S. No.	Lanthanum oxide in acrylic acid (%)	Refractive index
1.	0	1.424
2.	5	1.441
3.	10	1.451
4.	15	1.464
5.	17	1.466
6.	20	1.467

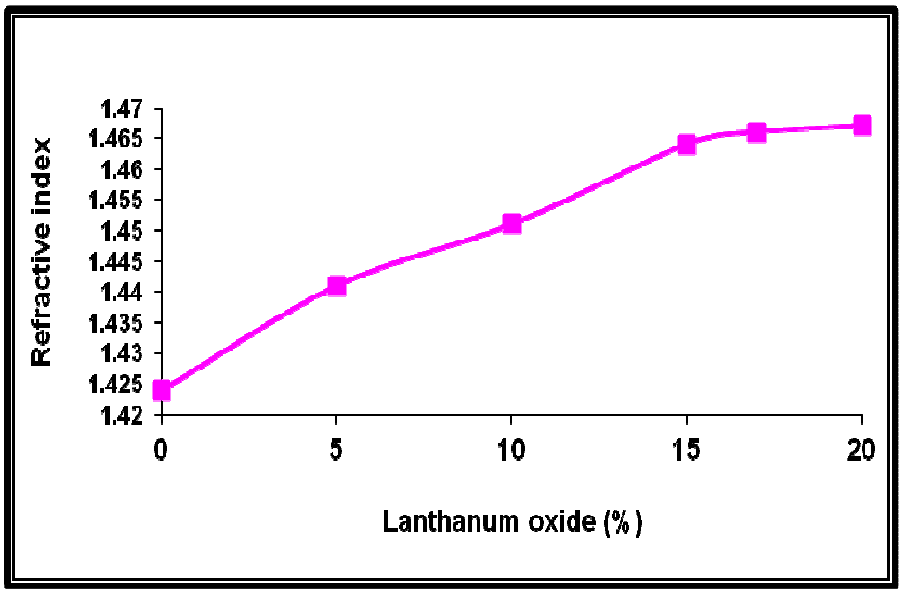

Figure 7.1: Effect of dispersion of lanthanum oxide on refractive index of acrylic acid. The value of refractive index increases with the increase in percentage of lanthanum oxide in acrylic acid. Beyond 15% of lanthanum oxide, the change is not significant.

Acid value of lanthanum acrylate compositions was determined as per the method described in Chapter 3, with varying concentration of lanthanum oxide in acrylic acid was varied. The results are tabulated in Table 7.3.

Table 7.3: Results of dispersion of lanthanum oxide on acid value and pH of acrylic acid. Acid value decreases with increase in percentage of lanthanum oxide in acrylic acid. pH value increases to 2.21 in the case of 17% dispersion of lanthanum oxide as lanthanum gets reacted with acrylic acid. The change in the acid value and pH is due to the reaction between lanthanum oxide and acrylic acid

S. No.	Lanthanum Oxide (%)	Acid value	pH
1.	0	626	< 1
2.	5	549	1.03
3.	10	443	1.66
4.	15	364	1.80
5.	17	358	2.21
6.	100	0.0	--

At the initial point of the reaction, acid value of acrylic acid was determined to be 626. As can be seen from Table 7.3, acid value decreases to 549 in the case of 5% dispersion of lanthanum oxide in acrylic acid. The acid value further decreases to 443 in the case of 10% dispersion and 364 in the case of 15% dispersion of lanthanum oxide in acrylic acid. The acid value of 17% dispersion of lanthanum oxide in acrylic acid is 358. The decrease in acid value is taken as a confirmation of the reaction taking place between lanthanum oxide and acrylic acid. Similarly, the acidity of acrylic acid decreases from < 1 to 2.21 as indicated by the pH value by increasing the amount of dispersion of lanthanum oxide.

Particle size analysis was carried out for lanthanum oxide-acrylic acid compositions. The results of particle size analysis are tabulated in Table 7.4.

Table 7.4: Determination of particle size distribution of lanthanum oxide-acrylic acid compositions. Particle size of the compositions was found to be less than 0.8 nm indicating the formation of homogeneous solution of lanthanum oxide-acrylic acid

S. No.	Lanthanum oxide in acrylic acid (%)	Particle size (nm)
1.	0	0
2.	5	<0.8
3.	10	<0.8
4.	15	<0.8
5.	17	<0.8

It can be seen from Table 7.4 that with the dispersion of lanthanum oxide in acrylic acid, particle size of less than 0.8 nm was obtained. This is also reflected in the formation of clear and transparent compositions. This is the confirmation of the fact that lanthanum oxide gets reacted with acrylic acid to form homogeneous solution rather than a dispersion and that is why the compositions are clear and transparent.

Results of thermal analysis i.e. thermogravimetric analysis (TGA), differential thermal analysis (DTA) and differential thermogravimetry (DTG) of the components (acrylic acid, lanthanum oxide and lanthanum oxide-acrylic acid

composition having 17% of lanthanum oxide) are presented in this section. Thermal decomposition of lanthanum oxide-acrylic acid composition was evaluated and the results are shown in Figure 7.2 a)-c).

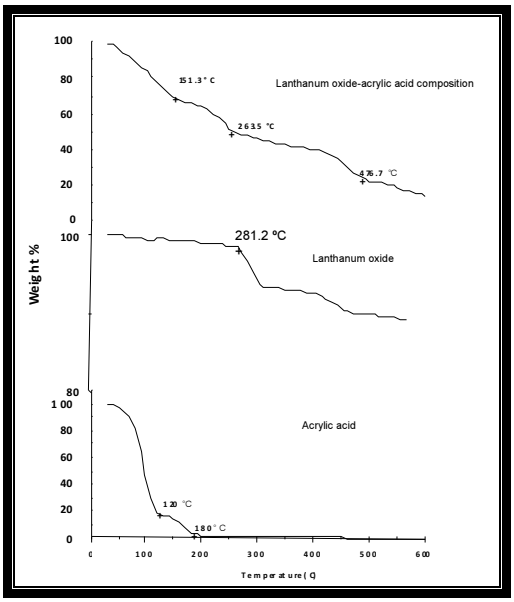

Figure 7.2 a): TGA thermograms of acrylic acid, lanthanum oxide and the composition of lanthanum oxide-acrylic acid. Results indicate higher thermal stability of the lanthanum containing composition than acrylic acid.

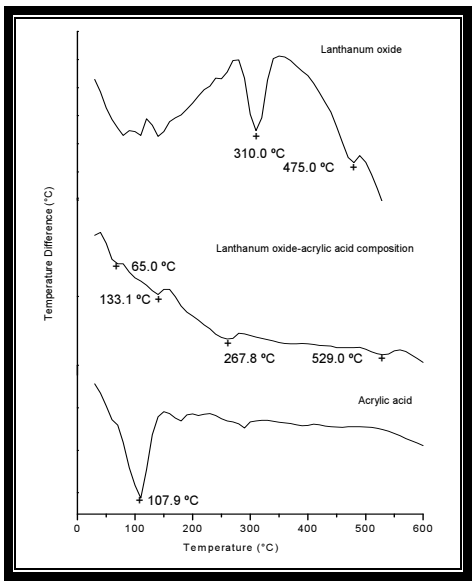

Figure 7.2 b): DTA thermograms of acrylic acid, lanthanum oxide and the composition of lanthanum oxide-acrylic acid. Results indicate that the thermal transitions are taking place due to the addition of lanthanum oxide to acrylic acid

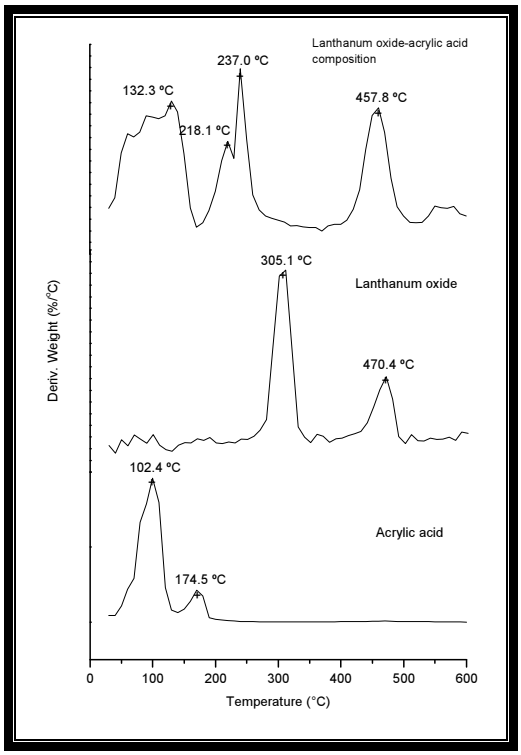

Figure 7.2 c): DTG thermograms of acrylic acid, lanthanum oxide and the composition of lanthanum oxide-acrylic acid. Results indicate that new compound is being formed due to the interactions between acrylic acid and lanthanum oxide

TGA of acrylic acid has already been described in Chapter 4. The TGA pattern of lanthanum oxide (Figure 7.2 b) indicates weight-loss in two steps. The total loss in weight is to the extent of approximately 11 % when the specimen is heated upto 600 ºC. Peaks at 305.1 ˚C and 470.4 ˚C are present in DTG. Corresponding DTA peaks at 310 ˚C and 475 ˚C are due to the weight loss due to decomposition of lanthanum oxide. Lanthanum oxide being inorganic possesses good thermal stability as can be seen from the thermogram. The lanthanum oxide-acrylic acid composition showed initial loss in weight of 32% upto 151.3 ºC due to the loss of moisture and volatile substances. This is followed by 20% further weight loss upto 263.5 ºC. Small DTA endotherms are observed at 65 ˚C and 133 ˚C which are ascribed to the weight loss due to moisture and volatiles. The lanthanum oxide-acrylic acid composition shows a DTG peak at 132.3 ºC, 218.1 ºC and 237.0 ºC. Next, the material gets decomposed upto 476.7 ºC with 23% weight loss. Sharp DTG

peaks at 237.0 ˚C and 457.8 ˚C describe the decomposition with corresponding peaks in DTA at 267.8 ˚C and 529 ˚C. However, there are clear-cut differences in the TGA pattern of the lanthanum oxide-acrylic acid composition and the one for acrylic acid. The TGA of the lanthanum oxide-acrylic acid composition has substantially shifted towards the right side of the graph indicating that the lanthanum oxide-acrylic acid composition has gained thermal stability as compared to acrylic acid. The peaks in DTA thermogram of lanthanum oxide and acrylic acid as such are not present in the lanthanum oxide-acrylic acid composition. This clearly shows the formation of a new compound (lanthanum acrylate).

The boiling point of acrylic acid is 141 ºC. Therefore, it is expected that well before 150 ºC, evaporation of entire amount of acrylic acid should have taken place. From the thermogram, it is evident that the loss in weight of acrylic acid has taken place in two distinct stages; first weight loss of approximately 80% upto 125 ºC and the rest upto approximately 300 ºC. Maximum weight loss of acrylic acid is observed up to 200 ºC; beyond 200 ºC, there is a formation of polymeric form during the heating of acrylic acid which is responsible for a small amount of weight loss at temperatures higher than 200 ºC.

Weight loss due to thermal decomposition of acrylic acid, lanthanum oxide and lanthanum acrylate composition is given in Table 7.5. It may be concluded that acrylic acid as such looses its complete weight by approx. 300 ºC whereas lanthanum oxide losses approx. 10% by 500 ºC. In a composition having 17% by weight of lanthanum oxide and 83% by weight of acrylic acid, it is expected (theoretically) that the composition should have lost its weight as presented in Table 7.5.

The loss in weight of 11% on heating lanthanum oxide is an indication of its high thermal stability. In the case of lanthanum oxide-acrylic acid, the composition loses 50% its weight at 300 ºC indicating the formation of a new compound (lanthanum acrylate) different from lanthanum oxide and acrylic acid by the dispersion of lanthanum oxide to acrylic acid.

Table 7.5: Weight loss (%) due to thermal decomposition of acrylic acid, lanthanum oxide and lanthanum oxide-acrylic acid composition. The theoretical weight loss indicates that the lanthanum oxide-acrylic acid composition formed is thermally stable

Product	Weight loss (%)					
	100 °C	200 °C	300 °C	400 °C	500 °C	600 °C
Acrylic acid	52.2	98.2	100	100	100	100
Lanthanum oxide	0.4	0.9	3.3	7.2	9.9	10.8
Lanthanum oxide-acrylic acid	16.7	36.2	54.3	60.3	77.7	86.2
Theoretical weight loss of Lanthanum oxide-acrylic acid	43.4	81.7	83.6	84.2	84.7	84.8

Weight loss due to decomposition in the case of lanthanum acrylate is much less as compared to acrylic acid, simply because of the fact that lanthanum acrylate formation is accompanied by a strong bond between lanthanum and acrylic acid. Upto 200 ºC, total weight loss of acrylic acid and lanthanum oxide is 99%. On the other hand, upto 200 ºC, weight loss in the case of lanthanum acrylate is 36%. This indicates that the product obtained after the reaction between acrylic acid and lanthanum oxide is not just a mixture but a solution consisting of strong bonds between lanthanum and acrylic acid. The results obtained with acrylic acid matched well with the already reported data. The thermal decomposition pattern in the case of acrylic acid and lanthanum oxide-acrylic acid is quite similar but with a delayed weight loss in the case of lanthanum oxide-acrylic acid as evident from the shift in DTG peaks to the right side of the thermogram. As can also be seen from the theoretical values presented in Table 7.5, lanthanum oxide-acrylic acid exhibits higher stability. This is due to the fact that lanthanum is not just mixed in acrylic acid but bonded to it resulting in a new compound (lanthanum acrylate).

In order to further confirm the formation of lanthanum acrylate, UV-Visible spectroscopy was performed (Figure 7.3 a-e). The UV-Visible spectra of the compositions was measured in ethanol as a base solvent in the range of 200-800 nm.

The maximum absorption peak (λ_{max}) of acrylic acid was observed at 210 nm. As can be seen from Figure 7.3, there is no change in the λ_{max} value of acrylic acid with increase in the amount of lanthanum oxide dispersed in acrylic acid. This confirms that the vinyl group of acrylic acid remains intact and hence the only site for the reaction of lanthanum oxide is the carboxylic acid group.

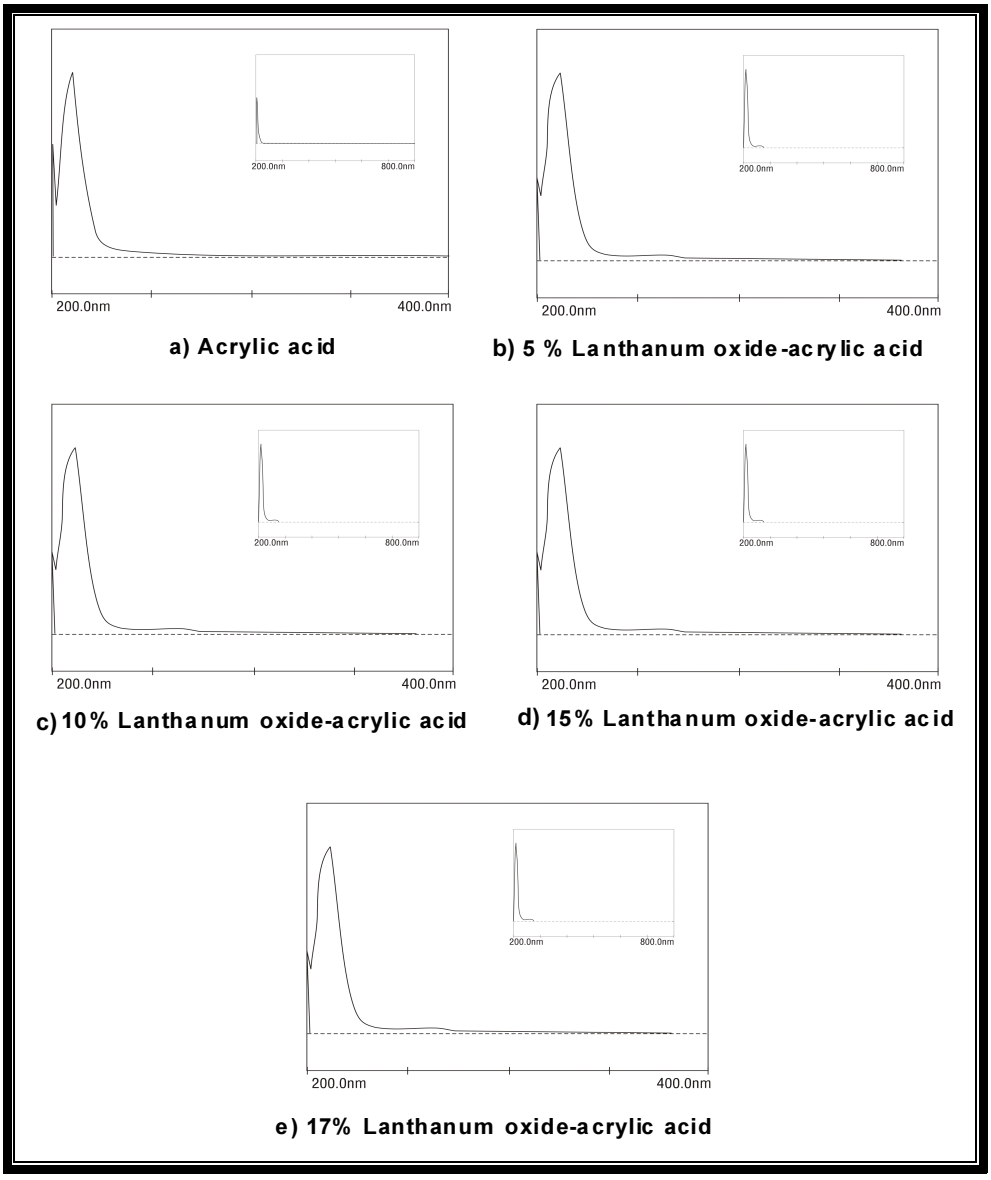

Figure 7.3 (a-e): UV-Visible spectra of acrylic acid and lanthanum oxide-acrylic acid composition (varying concentrations). The λ_{max} value of acrylic acid does not change with the dispersion of lanthanum oxide and hence it can be said that the reaction between lanthanum oxide and acrylic acid is taking place at the carboxylic acid group of acrylic acid.

To understand the interactions taking place between lanthanum oxide and acrylic acid, infrared spectroscopy was carried out. Infrared spectra were taken from 4000 to 400 cm^{-1} in transmittance mode (Figure 7.4).

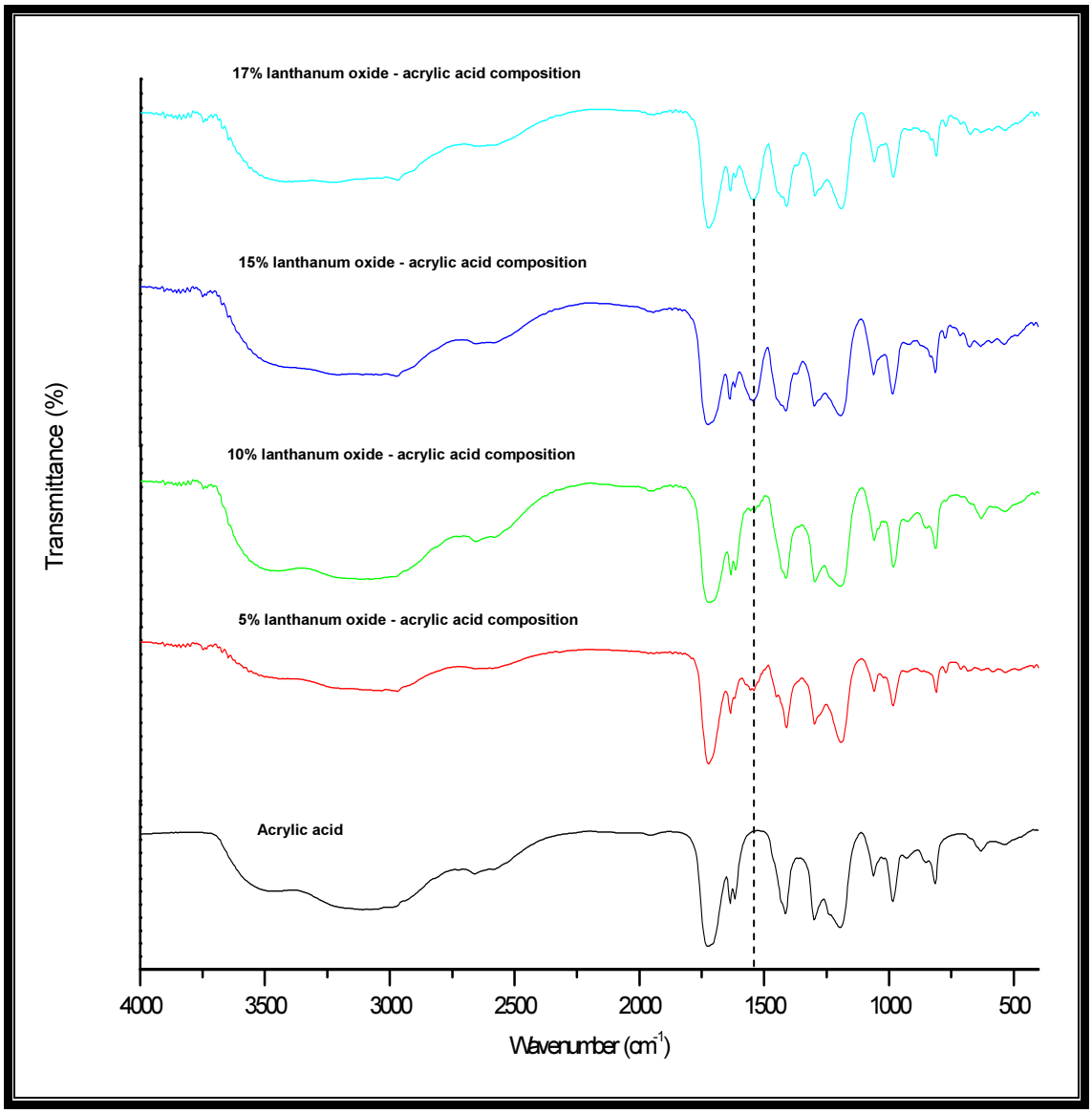

Figure 7.4: Infrared spectra of acrylic acid and lanthanum oxide-acrylic acid composition. The band at 1544-1550 cm^{-1} confirms the presence of COO^- group suggesting that a new compound (lanthanum acrylate) has been formed by the reaction between acrylic acid and lanthanum oxide.

As can be seen from Figure7.4, the band pertaining to carboxylic acid group is absent in the case of lanthanum oxide-acrylic acid composition. On the contrary, band at 1544-1550 cm^{-1} is present and is ascribed to the presence of COO^- band of the ester group. The intensity of this band also increases as the amount of lanthanum oxide in acrylic acid increases. This indicates that lanthanum oxide reacts with acrylic acid and forms lanthanum acrylate.

Incorporation of cinnamic acid and styrene in lanthanum acrylate compositions

Cinnamic acid, as a co-monomer, was incorporated in lanthanum acrylate composition prepared in Step I at various concentrations to improve the optical properties of lanthanum acrylate. Table 7.6 lists observations of lanthanum acrylate-cinnamic acid compositions as cinnamic acid is added gradually.

Table 7.6: Effect of addition of cinnamic acid on lanthanum acrylate composition indicates that upto 10% cinnamic acid can be dispersed in lanthanum acrylate resulting in transparent and clear compositions

S.No.	Cinnamic acid (%)	Observations	Transmittance (%)
1.	0	Clear and transparent solution	99
2.	2	Clear and transparent solution	99
3.	4	Clear and transparent solution	99
4.	6	Clear and transparent solution	99
5.	8	Clear and transparent solution	99
6.	10	Clear and transparent solution	99
7.	12	Does not dissolve	--

As can be seen from Table 7.6, addition of upto 10% cinnamic acid gave transparent and clear compositions. Beyond 10%, cinnamic acid does not dissolve and leads to a non-homogeneous composition.

Lanthanum acrylate-cinnamic acid compositions were evaluated for refractive index and the results are tabulated in Table 7.7.

Table 7.7: Effect of cinnamic acid on refractive index of 17% lanthanum acrylate composition shows that maximum refractive index achieved is 1.478

S. No.	Cinnamic acid (%)	Refractive index
1.	0.0	1.466
2.	2.0	1.468
3.	4.0	1.469
4.	6.0	1.471
5.	8.0	1.475
6.	10.0	1.478

As can be seen from Table 7.7, addition of cinnamic acid leads to the formation of clear and transparent solutions having a refractive index of 1.478.

Percentage of cinnamic acid was kept constant (10% by weight of lanthanum acrylate) in all the compositions containing lanthanum oxide. Effect of constant amount of cinnamic acid on lanthanum acrylate containing different percentages of lanthanum oxide is presented in Figure 7.5.

The increase in refractive index is due to the presence of an aromatic ring in the structure of cinnamic acid.

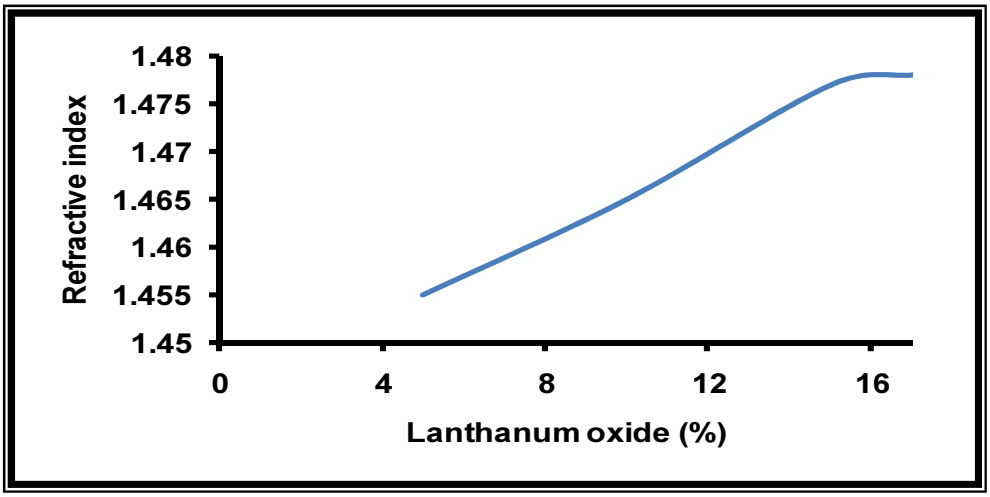

Figure 7.5: Effect of 10% cinnamic acid on refractive index of lanthanum acrylate compositions. The refractive index increase from 1.468 to 1.478 by the incorporation of 10% cinnamic acid in 17% lanthanum acrylate composition

Hence, 10% cinnamic acid was dispersed in lanthanum acrylate compositions having varying amount of lanthanum oxide. As can be seen from Figure 7.5, there is a gradual increase in refractive index of compositions containing a fixed 10% by weight of cinnamic acid in acrylic acid but with varying amount of lanthanum oxide. Refractive index of cinnamic acid dispersed lanthanum acrylate compositions lies between 1.468-1.478. This is a very novel feature as this suggests the possibility of the tailor-making of refractive index, an essential property of optical materials. The increase in refractive index is due to the incorporation of new organic moieties such as a benzene ring of cinnamic acid, whose molar refraction contributes to the refractive index of the composition.

Thermal stability of cinnamic acid dispersed lanthanum acrylate compositions was also evaluated. The thermogram is presented as Figure 7.6 a)-c).

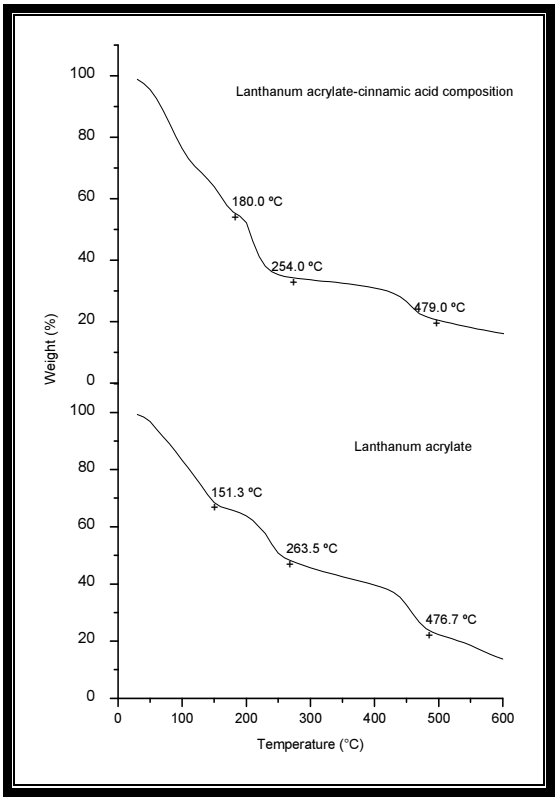

Figure 7.6 a): TGA thermograms of lanthanum acrylate and lanthanum acrylate-cinnamic acid composition indicate low thermal stability of lanthanum acrylate-cinnamic acid composition as compared to lanthanum acrylate as such

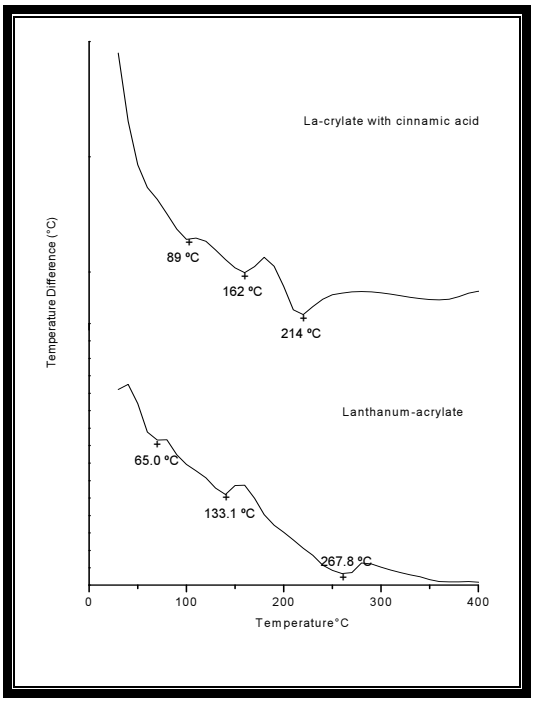

Figure 7.6 b): DTA thermograms of lanthanum acrylate and lanthanum acrylate-cinnamic acid composition

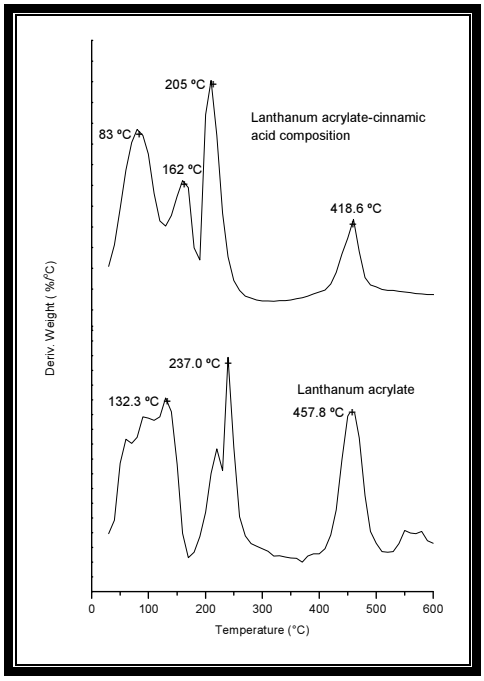

Figure 7.6 c): DTG thermograms of lanthanum acrylate and lanthanum acrylate- cinnamic acid composition show the presence of new peaks indicating chemical interactions are taking place between lanthanum acrylate and cinnamic acid.

Thermograms show TGA-DTA-DTG pattern of cinnamic acid dispersed lanthanum acrylate composition. Decomposition takes place in three major steps accompanied by the presence of four DTG peaks. First decomposition takes place upto 180 ºC with a weight loss of 45%. Two DTG peaks; one at 83 ºC, ascribed to the loss of moisture from the composition and another one at 162 ºC, ascribed to the loss of free acrylic acid, are observed. Corresponding DTA peaks at 89 ºC and 162 ºC suggests that the weight loss is due to decomposition. The next decomposition is observed upto 254 ºC showing further weight loss of 20%, maximum being at 205 ºC as is evident by a DTG peak and a corresponding DTA peak at 214 ºC. Further decomposition takes place upto 479 ºC with maximum at 418.6 ºC, as is evident by a DTG peak. Lanthanum acrylate-cinnamic acid composition further decomposes and loses weight with 16% residue left at 600 ºC. As can be seen from the thermograms, the DTG peaks in the case of lanthanum acrylate-cinnamic acid composition have shifted towards lower side of the temperature as compared to lanthanum acrylate composition (as such); indicating that the thermal decomposition of lanthanum acrylate-cinnamic acid has taken place before that of lanthanum acrylate composition as such. It is thus, quite evident from the thermal studies that the new bonds formed due to the dispersion of cinnamic acid and release of water and other volatiles takes place leading to the appearance of DTG peaks at lower temperature.

Weight loss at different temperatures due to thermal decomposition of lanthanum acrylate composition and cinnamic acid dispersed lanthanum acrylate composition is given in Table 7.8.

The observed weight loss is in close agreement with theoretically calculated weight loss. This shows that the loss of moisture and volatiles is taking place.

Table 7.8: Weight loss (%) due to thermal decomposition of acrylic acid, lanthanum oxide and lanthanum acrylate composition. Theoretical loss in weight of lanthanum acrylate-cinnamic acid composition is also presented.

Product	Weight loss (%)					
	100 °C	**200 °C**	**300 °C**	**400 °C**	**500 °C**	**600 °C**
Lanthanum acrylate	16.7	36.2	54.3	60.3	77.7	86.2
Cinnamic acid	0	98.5	100	100	100	100
Lanthanum acrylate- Cinnamic acid composition	23.7	47.9	66.4	69.1	79.6	83.9
Weight loss (theoretical) of lanthanum acrylate-cinnamic acid composition	15.0	42.4	58.9	64.3	79.9	87.6

To understand the reactions taking place between lanthanum acrylate and cinnamic acid, UV-Visible spectroscopy was carried out as presented in Figure 7.7 (a-f).

As can be seen from Figure 7.7 (a-f), lanthanum acrylate-cinnamic acid composition exhibit a peak at 210 nm, characteristic of acrylic acid and 273 nm which is a characteristic peak of cinnamic acid, at all concentrations. The peak in UV-Visible spectra of cinnamic acid appears at λ_{max} = 273 nm. This shows that the reaction between cinnamic acid and lanthanum acrylate composition do not take place at the vinyl group of cinnamic acid or lanthanum acrylate; the vinyl group remains intact.

Infrared spectroscopy was studied (Figure 7.8) to understand the interactions between lanthanum acrylate and cinnamic acid.

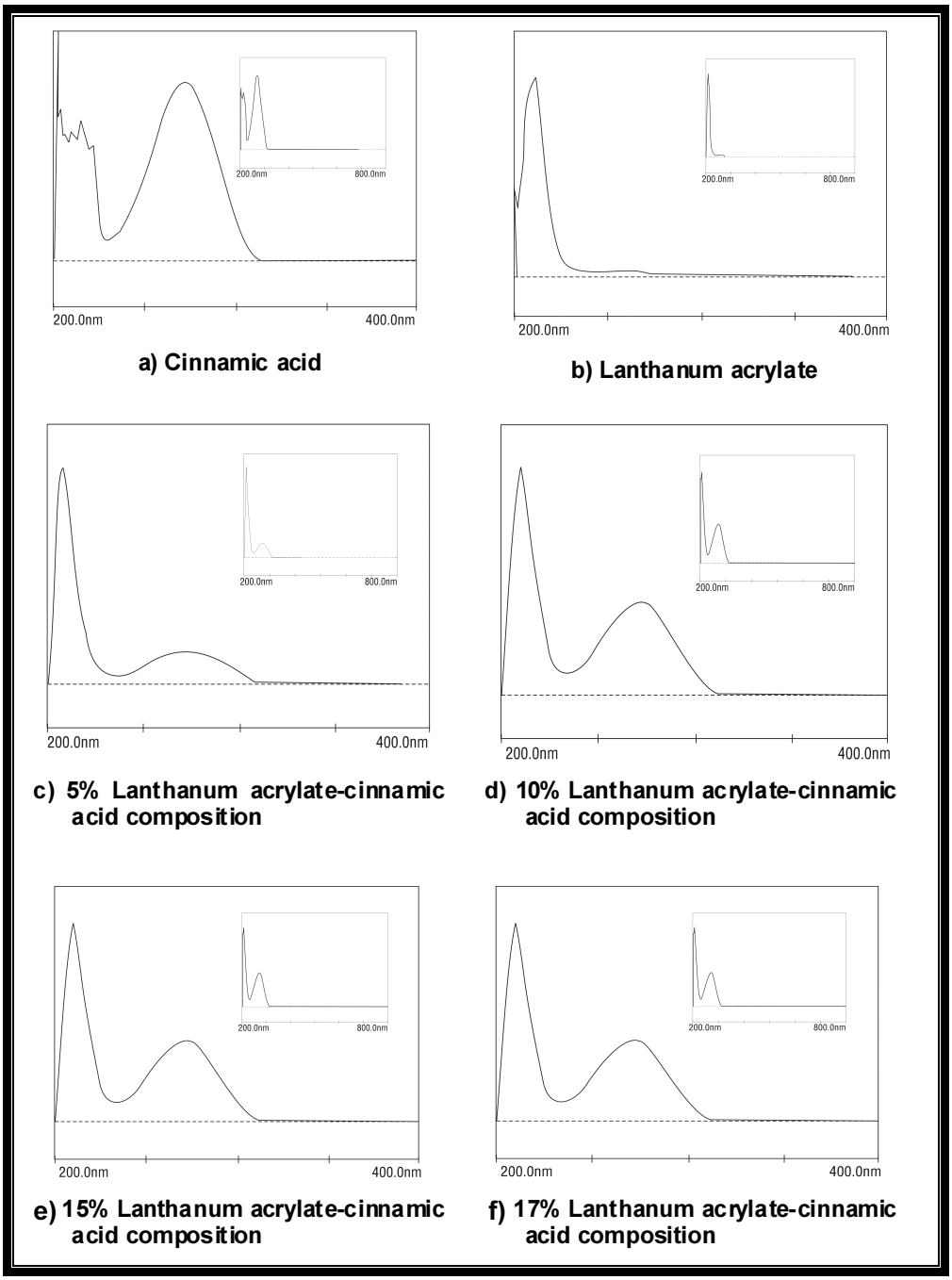

Figure 7.7 (a-f): UV-Visible spectra of cinnamic acid and lanthanum acrylate-cinnamic acid compositions. Cinnamic acid exhibits λ_{max} at 273 nm. In the case of lanthanum acrylate-cinnamic acid compositions, 2 peaks are observed; at 210 nm (characteristic of acrylic acid) and 273 nm (characteristic of cinnamic acid). Presence of peak at λ_{max} : 273 nm indicates that vinyl group of the cinnamic acid is intact.

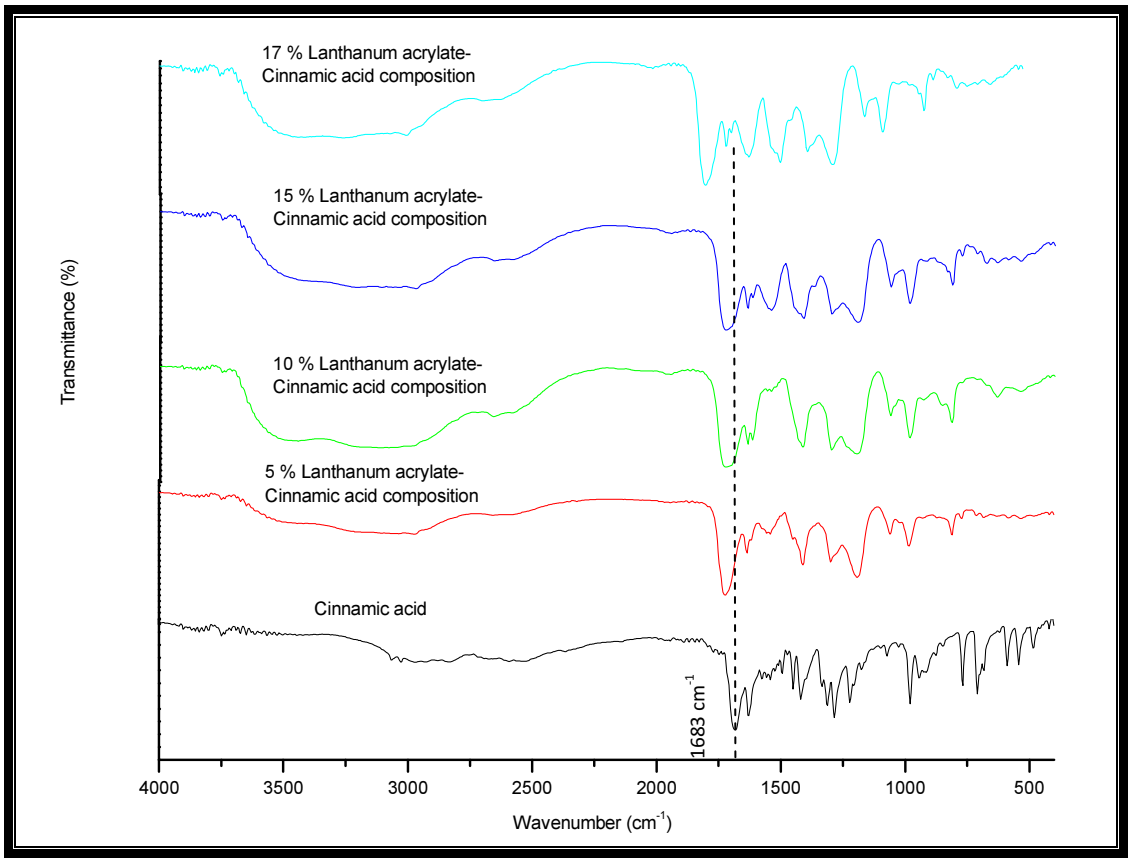

Figure 7.8: Infrared spectra of lanthanum acrylate-cinnamic acid compositions. The band pertaining to C=O stretch in -C=C-COOH at 1683 cm^{-1} is present in the spectra of cinnamic acid. In the case of lanthanum acrylate-cinnamic acid compositions, band at 1683 cm^{-1} has shifted towards higher frequency.

It can be seen from Figure 7.8 that the reaction between cinnamic acid and lanthanum acrylate is indicated by the shift of characteristic band of conjugated C=O stretch at 1683 cm^{-1}. The shift of band at higher frequency indicates the changes taking place in the composition.

Styrene, a co-monomer, was used for polymerization of cinnamic acid dispersed lanthanum acrylate compositions. Styrene was added in different percentages by weight to lanthanum acrylate-cinnamic acid compositions and stirred continuously to produce transparent and clear lanthanum acrylate-cinnamic acid-styrene compositions.

Cast polymerization of lanthanum acrylate-cinnamic acid-styrene composition

The high refractive index lanthanum acrylate-cinnamic acid-styrene compositions were cast polymerized into lenses using gamma irradiation technique. The effect of varying styrene (% by weight) was observed by evaluating the shore-D hardness of the polymerized lenses. The results are tabulated in Table 7.9.

Table 7.9: Effect of styrene (% by weight of lanthanum acrylate-cinnamic acid) on polymerization of lanthanum acrylate-cinnamic acid compositions

S. No.	Styrene (% by weight)	Observations	Shore-D hardness
1.	25	Soft, sticky sample, could not be released from the mold	40
2.	50	Soft, sticky sample, could not be released from the mold	50
3.	65	Brittle and semi-hard sample, could not be released from the mold	75
4.	85	Transparent sample, released easily from the mold	91
5.	100	Semi-transparent sample, released easily from the mold	90
6.	120	Slightly hazy sample, released easily from the mold	90

It may be seen that with 25-65 % (by weight of lanthanum acrylate-cinnamic acid composition) of styrene, the polymer is soft, sticky and brittle due to insufficient amount of styrene for polymerization. The shore-D hardness of the polymer is 40 for 25% (by weight of lanthanum acrylate-cinnamic acid composition) of styrene, 50 for 50% (by weight of lanthanum acrylate-cinnamic acid composition) of styrene and 75 for 65% (by weight of lanthanum acrylate-cinnamic acid composition) of styrene. The polymer could not be released from the mold, which limits the processing characteristics of the polymer. With 85% (by weight of lanthanum acrylate-cinnamic acid

composition) of styrene, shore-D hardness increased to 91 and the polymers were easily released from the mold. This indicates that 85% (by weight of lanthanum acrylate-cinnamic acid composition) of styrene is sufficient for polymerization of lanthanum acrylate polymers. Clear and transparent polymers were obtained. Styrene if used at 100% (by weight of lanthanum acrylate-cinnamic acid composition) or above with lanthanum acrylate, gave colored and hazy polymer. From these observations, it is clear that 85% (by weight of lanthanum acrylate-cinnamic acid composition) of styrene is required for the complete polymerization to form transparent lanthanum acrylate polymers.

Polymerization was carried out at various doses of gamma irradiation from 2-15 kGy. The optimum dose required for complete polymerization was arrived at by evaluating the cross-link density of the polymers at each dose. The results of cross-link density are tabulated in Table 7.10.

Table 7.10: Cross-link density results of lanthanum acrylate-cinnamic acid-styrene polymers indicate that 10 kGy is the optimum dose required for the polymerization

S. No.	Dose (kGy)	Observations	Cross-link density (%)
1.	2	Soft and sticky, not released from the mold	64
2.	4	Soft and sticky, not released from the mold	75
3.	8	Hard, easily released from the mold	97
4.	10	Hard and transparent, easily released from the mold	97
5.	15	Dark yellow coloured transparent, easily released from the mold	95

From the results of cross-link density, it can be seen that 10 kGy is the optimum dose required to achieve complete polymerization of lanthanum acrylate-cinnamic acid-styrene polymers. Above 10 kGy, colour of the polymer turns to dark yellow.

Having cast polymerized the lenses using various compositions of lanthanum acrylate-cinnamic acid plus styrene, the lenses were evaluated for various parameters. The results are discussed in the following section.

High refractive index lanthanum acrylate-cinnamic acid-styrene nanocomposites were evaluated for optical properties such as refractive index and Abbe number. The data is presented in Figures 7.9-7.10.

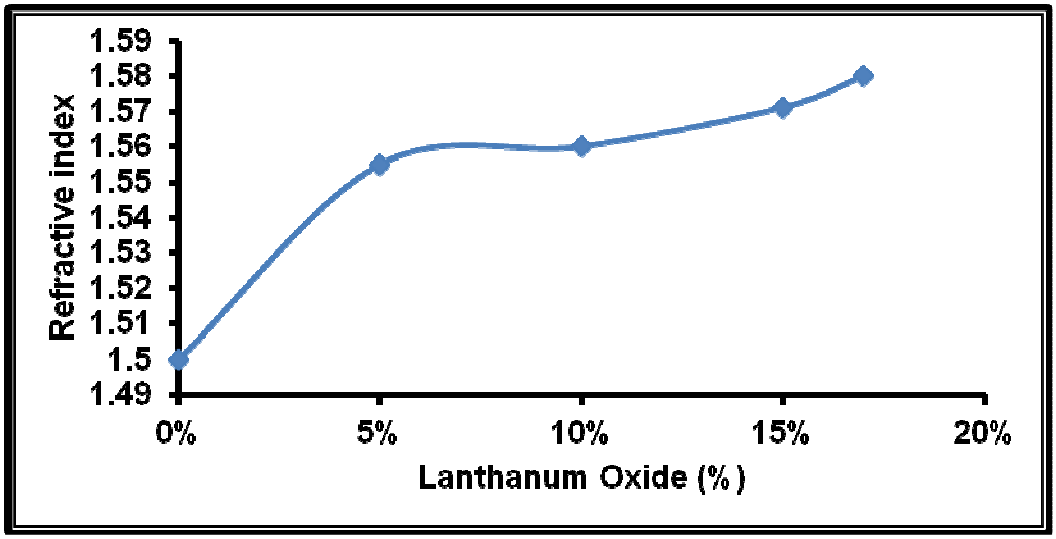

Figure 7.9: Effect of lanthanum oxide on refractive index of lanthanum acrylate-cinnamic acid-styrene nanocomposites. Refractive index increases with the increase in amount of lanthanum oxide in the nanocomposite. The refractive index increases to 1.58 from 1.50 (acrylic acid-styrene polymer) to start with.

As can be seen from Figure 7.9, there is an increase in the refractive index as lanthanum content is increased. The refractive index increases significantly from 1.50 (without lanthanum oxide) to 1.58 with 17% of lanthanum oxide. By varying the amount of lanthanum oxide, the refractive index can be increased to 1.58 indicating the possibility of tailor making, which is a novelty of lanthanum acrylate nanocomposites. The increase in refractive index from 1.42 (acrylic acid) to 1.58 (lanthanum acrylate-cinnamic acid-styrene nanocomposite) by varying the concentration of lanthanum oxide shows the possibility of tailor-making of optical properties as per the requirements of the user. It is found to be better than even commercially available polyacrylate i.e. polymethyl methacrylate which has a refractive index of 1.491. Lanthanum

acrylate-cinnamic acid-styrene nanocomposites are therefore ideal materials for optical applications.

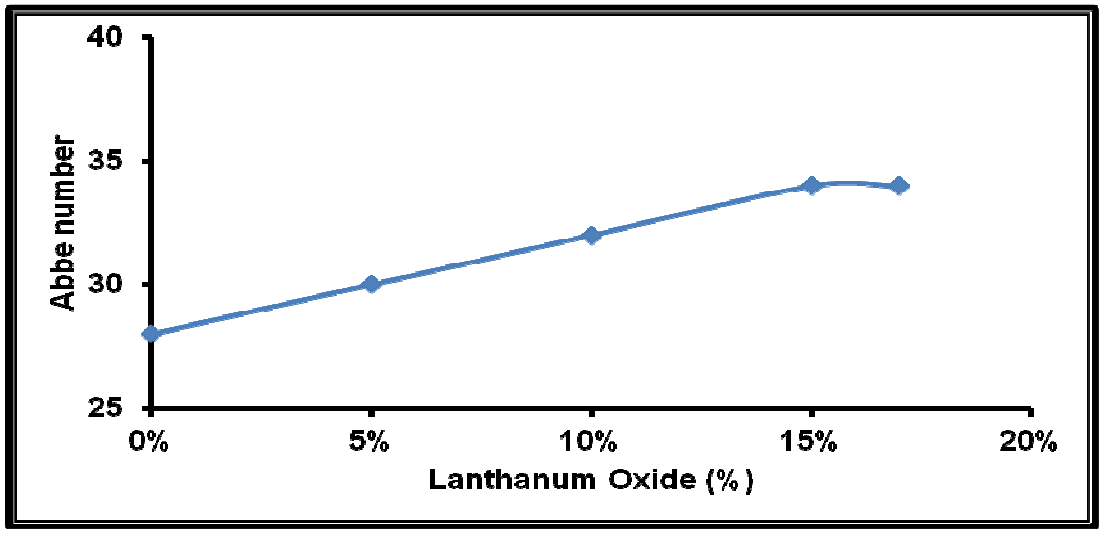

Figure 7.10: Effect of lanthanum oxide on Abbe number of lanthanum acrylate-cinnamic acid-styrene nanocomposites. Abbe number increases with increase in the amount of lanthanum oxide in the nanocomposite

Abbe number of lanthanum acrylate-cinnamic acid-styrene nanocomposites was determined on an Abbe refractometer. Abbe number was 30 in the case of 5% dispersion of lanthanum oxide in the polymer, 32 with 10% dispersion of lanthanum oxide in the polymer, 34.5 in the case of 15% and 17% dispersion of lanthanum oxide in the final polymer. Tailor-making of Abbe number has also been made possible by varying the concentration of lanthanum oxide in polymers. Thermal stability of lanthanum acrylate-cinnamic acid-styrene nanocomposites was evaluated and is presented in Figure 7.11 a) - c).

Acrylic acid-styrene polymer shows decomposition pattern as described earlier in Chapter 6. Lanthanum acrylate-cinnamic acid-styrene nanocomposite show a two step thermal decomposition supported by two sharp DTG peaks. The decomposition of lanthanum-containing acrylate nanocomposites starts immediately after 60 ºC with a well-defined weight loss of 40% till 312 ºC; maximum rate of loss in weight being at 216 ºC as is evident from a DTG peak.

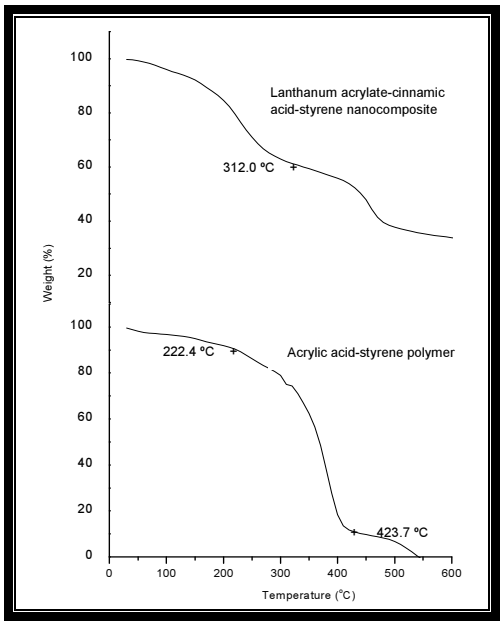

Figure 7.11a): TGA thermograms of lanthanum acrylate-cinnamic acid-styrene nanocomposite indicates higher thermal stability than acrylic acid-styrene polymer due to the formation of cross-linked matrix due to the presence of lanthanum

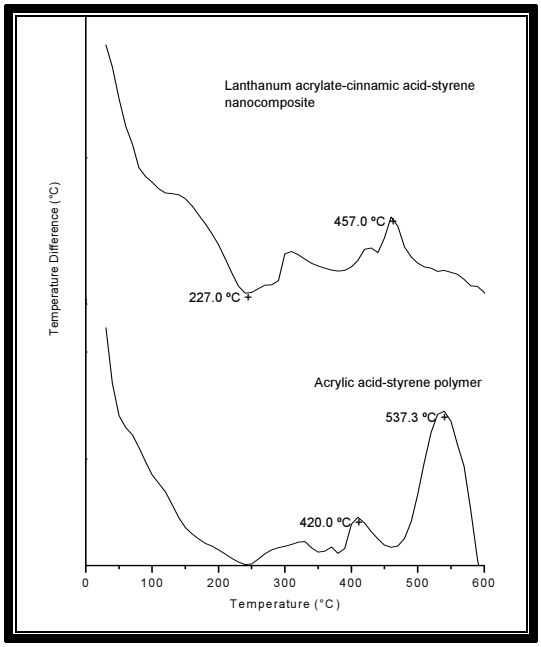

Figure 7.11b): DTA thermograms of acrylic acid-styrene polymer and lanthanum acrylate-cinnamic acid-styrene nanocomposites. The acrylic acid-styrene polymer shows an exotherm at 520 ºC which is not present in the case of lanthanum-containing polymer.

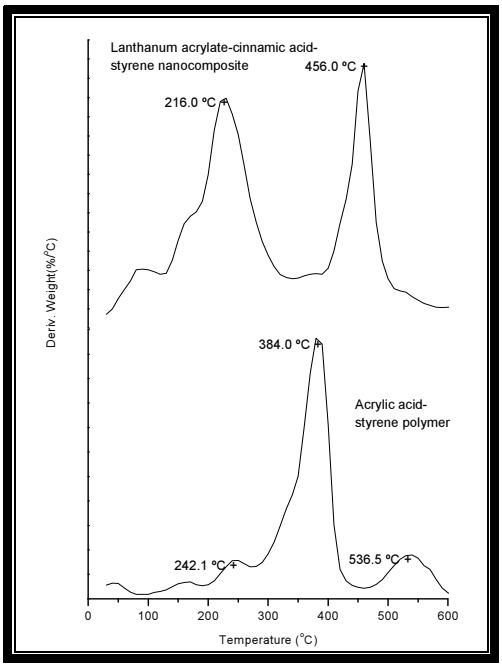

Figure 7.11c): DTG thermograms of lanthanum acrylate-cinnamic acid-styrene nanocomposite shows presence of new peaks due to the formation of new cross-links as compared to acrylic acid-styrene polymer

Corresponding DTA peak at 227 ºC supports the fact that decomposition is taking place and may be attributed to the loss of volatiles followed by chain scissioning of the lanthanum-containing acrylate nanocomposite. Next decomposition occurs up to 516 ºC with weight loss of 25%. A sharp DTG peak at 456 ºC indicates that maximum rate of loss in weight in this decomposition step takes place at this temperature. In the DTA thermogram, a small exotherm is observed at 457 ºC which is ascribed to the release of gases such as CO_2.

As can be seen from the weight loss data of the polymers with and without lanthanum, it is very clear that polymer without lanthanum undergoes complete decomposition by 600 ºC. In the case of lanthanum-containing nanocomposite, ~ 66% of weight loss is observed upto 600 ºC after which no loss in weight is observed. This is a clear indication of the fact that the stability of acrylic acid-styrene polymer is improved by the dispersion of lanthanum oxide.

Table 7.11 lists the weight loss (%) during thermal decomposition of polymer; with and without lanthanum.

Table 7.11: Weight loss (%) due to thermal decomposition of polyacrylate and lanthanum acrylate-cinnamic acid-styrene nanocomposite

Product	Weight loss (%)					
	100 °C	200 °C	300 °C	400 °C	500 °C	600 °C
Acrylic acid-styrene polymer	3.2	8.1	21	81.6	93.3	100
Lanthanum acrylate-cinnamic acid-styrene nanocomposite	3.9	15.4	37.1	44.1	62.3	66.1

Machinability of lanthanum acrylate-cinnamic acid-styrene nanocomposites was checked by subjecting the samples to grinding and machining. The hardness of the lenses was checked by determining the shore-D hardness and scratch resistance. Shore-D hardness of lanthanum-containing nanocomposites was found to be 91 while that of PMMA is 85. It was found to be better than even the commercially available polymethyl methacrylate, PMMA which has a scratch resistance of “C” grade and a pencil hardness of 4H while lanthanum-containing nanocomposites have a scratch resistance of “B” and pencil hardness of 6H. Lanthanum-containing nanocomposites are superior in hardness to PMMA due to the presence of lanthanum.

Vicat softening temperature was determined for lanthanum-containing nanocompsoites. Vicat softening temperature was determined to be 120 °C indicating that the working temperature of lanthanum-containing nanocomposites is higher than PMMA which has a working temperature of 109 °C.

To determine whether lanthanum is present in the bound or free form, leachability studies were carried out. Leachability was determined as per

method described in Chapter 3. Leachability of the polymers was studied in concentrated nitric acid and concentrated hydrochloric acid and evaluated by ICP-OES analysis. The results indicate that no lanthanum was leached out from the polymer in concentrated hydrochloric acid and in concentrated nitric acid.

Transmittance of lanthanum-containing nanocomposites was evaluated to be 90%. The polymers which were cast into lenses were found to be impact resistant (method described in Chapter 3) as per FDA regulations.

7.4 CONCLUSIONS

In this chapter, novel lanthanum acrylate nanocomposites using lanthanum oxide have been prepared. The achievements of these nanocomposites are as follows:

1. A novel approach for the in-situ synthesis and dispersion of metal nanoparticles has been adopted
2. It is possible to incorporate lanthanum in acrylic acid matrix. Lanthanum has been successfully incorporated in acrylate matrix for the first time.
3. Out of the many compounds of lanthanum tried for dispersion in acrylic acid, the most suitable was lanthanum oxide. The dispersion of upto 17% by weight of lanthanum oxide in acrylic acid was possible.
4. The modification of an important monomer, acrylic acid, for optical applications, has been done in a novel and cost-effective manner.
5. The effect of dispersion of lanthanum in acrylic acid was monitored by studying the changes taking place in the refractive index, acid value and thermal stability of acrylic acid.
6. The effect of dispersion of lanthanum oxide on the transmittance of acrylic acid was studied and was found be 99% in the visible range. Thus, the solutions obtained after the reaction of lanthanum oxide and

acrylic acid were transparent and clear in appearance and suitable for optical applications.

7. The formation of lanthanum oxide-acrylic acid compositions results in an increase in refractive index. After reaction of lanthanum oxide with acrylic acid at a particular concentration, it reaches a plateau. The refractive index of acrylic acid was increased from 1.424 to 1.466 with 17% by weight of dispersion of lanthanum oxide.

8. The acidity of acrylic acid decreases from 626 to 358 by the addition of lanthanum oxide. This fact was supported by the change in pH values from < 1 to 2.21 of acrylic acid. This clearly indicates that the reaction is taking place between lanthanum oxide and acrylic acid.

9. Particle size analysis of lanthanum oxide-acrylic acid compositions show that the particles are of the size of less than 0.8 nm confirming that the dispersion of lanthanum oxide in acrylic acid leads to the formation of homogeneous and clear solution.

10. The thermal analysis of the composition was carried out and the observed loss in weight of the composition was compared to the theoretical data. Acrylic acid as such looses its weight completely upto 300 $^{\circ}$C. It was found that the observed loss in weight was less as compared to the calculated one. This indicates high thermal stability of acrylic acid on addition of lanthanum.

11. In order to further confirm the interactions taking place between lanthanum oxide and acrylic acid, UV-Visible spectroscopy and infrared spectroscopy was performed. The results show that the vinyl group of acrylic acid remains intact during the dispersion of lanthanum oxide and that the reaction is taking place at the carboxylic acid group. It is evident by the presence of characteristic band of ester group (1550 cm^{-1}) due to the formation of lanthanum acrylate.

12. To further improve the properties of lanthanum acrylate, dispersion of cinnamic acid was done in lanthanum acrylate resulting in lanthanum

acrylate-cinnamic acid compositions. It was observed that upto 10% by weight of cinnamic acid could be added to lanthanum acrylate producing clear and transparent compositions.

13. The refractive index of lanthanum acrylate was determined to be in the range of 1.468-1.478 by the dispersion of 2% to 10% by weight of cinnamic acid.
14. Thermal analysis of lanthanum acrylate-cinnamic acid compositions was carried out to determine the thermal stability of the compositions. It was observed that the theoretical loss in weight matches very well with the observed thermal decomposition and hence, it can be said that there is a formation of new chemical bonds between lanthanum acrylate and cinnamic acid, as expected.
15. The UV-Visible spectroscopy and Infrared spectroscopy results show that the double bond in vinyl group of cinnamic acid remains intact and the reaction is taking place at the carboxylic acid group of the cinnamic acid.
16. The prepared compositions possessed improved optical and thermal properties as compared to acrylic acid as such. Polymerization of such compositions into transparent and clear lenses for optical applications would be a breakthrough in the optical industry.
17. To facilitate the cross-linking of the groups during polymerization, styrene as a co-monomer was added to lanthanum acrylate-cinnamic acid compositions. Styrene was added in varying percentages (by weight) to lanthanum acrylate-cinnamic acid composition to obtain clear and transparent solutions.
18. Gamma irradiation has been used as a novel technique for the polymerization of lanthanum acrylate compositions. Addition of 85% styrene (by weight of lanthanum acrylate-cinnamic acid composition) resulted in clear and transparent lenses with shore-D hardness of 91.

19. Optimization of irradiation dose was done based on cross-link density. Compositions were subjected to gamma irradiation from 2 kGy to 15 kGy. The dose of 10 kGy was found to be the optimum dose for complete polymerization as indicated by the cross-link density of 97%.
20. By varying the concentration of lanthanum oxide in nanocomposites, refractive index can be tailor-made from 1.424 to 1.580 and the Abbe number can be tailor-made from 30-35.
21. The developed acrylic nanocomposites are thermally stable having good machinability and impact resistance. They are hard and light-weight as compared to the conventional optical plastics in use
22. The studies pertaining to the leachability of lanthanum from the nanocomposites was carried out and it was found that the metal was tightly bound to the matrix.

At the end of this work, the process technology for making lanthanum acrylate nanocomposites of varying refractive index by employing in-situ dispersion of nanoparticles of lanthanum has been developed. The technology developed for the preparation of lanthanum acrylate nanocomposites for making optical plastics of high refractive index is an indigenous, cost effective and novel technology with good potential for commercialization. The present work has great relevance for the growth of optical plastics industry in India as much as for the society looking for an indigenous product with an affordable cost.

References

REFERENCES

1. D.E. Sharp and L .B. Ginther, “Effect of composition and temperature on the specific heat of glass”, Journal of the American Ceramic Society, 34, 260, 1951

2. E. Orowan, Z. Physik, 82, 235, 1933.

3. http://agamemnon.cord.org

4. H. A. Lorentz, Wied. Ann. Phys., 9, 641, 1880.

5. L. V. Lorenz, Wied. Ann. Phys., 11, 70, 1880.

6. I. D. Torbin and Y. F. Daminov, “Optical parts made from polymers”, 10, 72, 1974.

7. J. Lorkonski, “Plast and Kautschuk“, 23, 318, 1976.

8. H. Dislich, “Angewan Chemie. Inst.", 18, 52, 1976.

9. K. Nakasuka, K.Kamanta and K. Ivata, Kobunshi, 28, 105, 1979.

10. D. Hearer, Angewan. Macromol. Chem., 109-110, 267, 1982.

11. K. M. Dyumaev, Kvantovaya elecktronika, 10, 4, 810, 1983.

12. I. Svolstva, “Properties and Use of Optical and Transparent Polymers”, Leningrad, 80, 1984.

13. S. Kunikhiro, Koge Dzaire, 33, 6, 41, 1985.

14. E. I. Shepurev, Optiko-mekh, Prom-St’, 1, 51, 1986.

15. “Polymer optical materials”, Collection of articles, Institute of Chemical Physics, Academy of Sciences, USSR, 199, 1989.

16. Y. S. Lipatov, A. E. Nesterov, T. M. Gritsenko, “Polymer Chemistry Handbook”, 274, 1971.

17. Y. Zanka, T. Isaka, Y. Tamura, Jpn. Kokai Tokkyo Koho Japanese Patent 05,287,050 1994, 120, 177817

18. A.A. Askadskil and Y. I. Matveev, “Chemical Structure and Physical Properties of Polymers”, 24, 1983

19. J. C. Seferis, “Refractive Indices of Polymers” in Polymer Handbook, John Wiley & Sons, New York, 571, 1999

20. “Ophthalmic Optics, Uncut finished spectacle Lenses– Fundamental requirements for uncut finished lenses”, BS EN ISO 8980:2004, 2004

21. “Ophthalmic optics–Spectacle lenses–Fundamental requirements for uncut finished Lenses”, BS EN ISO 14889:2003, 2003

22. “Specification for complete spectacles”, BS 7394 Part 2:1994, 1994

23. M. Jalie, “Principle of Ophthalmic Lenses”, Ed. 5th, ABDO, London, 1984

24. C. Kittel, “Interpretation of the thermal conductivity of glasses”, Physical Review, 75, 6, 972, 1949.

25. E. B. Shand, “Glass Engineering Handbook”, 2nd Edition, McGraw – Hill Book Com., New York, 1958

26. H. Dislich, Angewandte Chemie International Edition in English., “Plastics as optical materials”, 18, 1, 49, 1979

27. C. J. Yang and A. Jenekhe, “Group contribution to molar refraction and refractive index of conjugated polymers”,Chemistry of Materials, 7, 7, 1276, 1995

28. J. D. Lytle, “Handbook of Optics”, McGraw Hill Inc., Ed 2, 1995

29. M. J. Minot, Journal of The Optical Society of America, 66, 515, 1976.

30. J. Wong and C.A. Angell, “Glass: Structure by Spectroscopy”, Marcel Dekker Inc., New York, 1976.

31. W. A. Wely, “Colored glass”, The Society of Glass Technology, Sheffield, 1951.

32. “Encyclopedia of Polymer Science & technology”, 3rd Ed. , John Wiley & Sons, ISBN: 0470046104, 2007

33. Standard Test Method for haze and luminous transmittance of transparent plastics, ASTM D-1003,1992

34. A. Masuno and H. Inoue, “High Refractive Index of 0.30 La_2O_3–0.70Nb_2O_5, Glass Prepared by Containerless Processing”, Applied Physics Express, 3, 102601, 2010

35. http://wikipedia.org/wiki/optical lens

36. R. K. Khandal, G. Seshadri and G. S. Jha, “A process for the synthesis of polythiol”, Indian Patent 248781, 2011

37. R. K. Khandal, G. Seshadri and G. S. Jha, “Polythiol”, Indian Patent 2342/DEL/2004

38. Y. Kato, M. Yuyama, M. Maritall, “A method for the preparation of polymers with good optical properties”, Japanese Patent Application 62-91507, 1988.

39. H. Takenosita, H. Takosi and H. Iosida, “Preparation of transparent co-polymers with high refractive index”, Japanese Patent Application 62-45604, 1988.

40. A. Sugio, T. Miki, S. Aoki, “Transparent resin with high refractive index”, Japanese Patent Application 62-79210, 1988.

41. I. Ito and K. Sibata, “Transparent material containing lead”, Japanese Patent Application 61-28542, 1987.

42. T. A. Speranskaya, and L. I. Tarutina, “Opticheskaya svolstva pollmerov”, 136, 1976.

43. D. B. Olson, B. C. Fong, S. Kang, D. S. Arney and Z. Bilkadi, “Ceramer containing a brominated polymer and inorganic oxide particles”, United States Patent 6261700, 2001

44. J. Kinkel, K. Marquard and L.Pohl, “Surface-modified oxide particles and their use as fillers and modifying agents in polymer materials”, United States Patent 5494949, 1996

45. S. Eguchi, N. Taketani, H. Asano and M. Wajima, “Transparent resin material containing metal atoms”, European Patent 0108985A1, 1984

46. R. K. Khandal, G. Seshadri and G. S. Jha, “Process of polymerization of diethylene glycol bis allyl carbonate”, United States Patent 7923484 B2, 2011

47. H. S. Nalwa, “Polymer Optic Fibers”, American Scientific Publishers, 2003

48. P. Prasad and D. Williams, “Introduction to Non-linear Optical Effects in Molecules and Polymers”, John Wiley and Sons, 1991

49. J. Brandrup, E. H. Immergut, E. A. Gruike, A. Abe and D. R. Bloch, “Polymer Handbook”, Ed 4th, John Wiley and Sons, 1999

50. J. Gaynor, G. Schueneman, P. Schuman and J. P. Harmon, “Effect of fluortinated substituents on the refractive index and optical resistance of methacrylates”, Journal of Applied Polymer Science, 50, 1645, 1993

51. P. Alexandrovich, F. E. Karasz and W. J. MacKnight, “Partialmiscibility in thes system poly (chlorostyrene-co-ortho-chlorostyrene)/poly(2,6-dimethyl-1,4-phenylene oxide)”, Polymer, 18, 10, 1022, 1977

52. A. R. Katrizky, U. Maran, M. Karelson and V. S. Lobanov, “Prediction of melting points for the substituted benzenes: A QSPR Approach”, Journal of Chemical Information and Computer Science, 37, 913, 1997

53. D. Nauti and S. Minami, “Method for the preparation of thermally hardened metal-containing polymers”, Japanese Application Patent 62-261305, 1987.

54. T. Abe, S. Eguti and N. Takotani, “Transparent polymers”, Japanese Application Patent 62-28618, 1988.

55. Y. Kato, F. Kanega, H. Kawai and S. Sagawara, “Heat and moisture resistant resins for getting optical materials with high refractive index”, Japanese Application Patent 62-201913, 1988.

56. H. Vehara and T. Shimiru, “Transparent polymers containing neodim and method for their manufacture”, United States Patent 4504616, 1985.

57. C. C. Batsanov, “Structural Refactometry”, Moscow: Vyssh.shk., 304, 1976.

58. E.C. Leonard, “Vinyl and Diene Monomer”, Part 1, Wiley-Intersciences, New York 148, 1970.

59. E. Ohmori and H. Shokodo, “Acrylic Acid and its Polymers”, Tokyo, 1, 1975

60. E.H. Riddle, “Monomeric Acrylic Esters”, Reinhold. New York, 1954

61. M. L. Miller, “Acrylic acid polymers”, EPST, 1, 197, 1964

62. M. Sittig: “Vinyl Monomers and Polymers”, Noyes Dev. Corp., Park Ridge, N.J. , 1966

63. L.S. Luskin, High Polymers, 24, 105,1970

64. S. Suzuki and G. K. Yuki, Kyokaishi, 12, 28, 1272, 1970

65. N. Grassie, J.G. Speakman and T.I. Davis, “Thermal degradation of poly (alkyl acrylates). II. Primary esters: Ethyl, n-propyl, n-butyl and 2-ethyl hexyl”, Journal of Polymer Science Part A-1: Polymer Chemistry, 9, 4, 931, 1971

66. R.F.B. Davies and G.E.J. Reynolds, “Alkaline hydrolysis of aqueous polymer dispersions, particularly vinyl acetate copolymers”, Journal of Applied Polymer Science, 12, 1, 47, 1968

67. B. B. George and J.R. Grawe, “Survey of the applications, properties and technology of crosslinking emulsions-3”, Journal of Coatings Technology, 50, 644, 83, 1978

68. K. Weimann, Farbe Lack 93, 447, 1987

69. E. Wistuba, Fatipec Congress, “Varnishes-Paints-Inks: Present and future”, 17, 209, 1984

70. K.A. Safe, Journal of Oil Colour Chem. Association, 53, 599,1970

71. K.A. Safe, Paint Manufacturers, 30, 249,1960

72. E.V. Schmid. Fatipec Congress, “Recent progress in the production, processing and control of varnishes and paints”, 14, 83, 1978

73. R. Dhein, L. Fleiter and R. Kuchenmeister, Fatipec Congress, “Recent progress in the production, processing and control of varnishes and paints”, 14, 195, 1978

74. L.A. Simpson, Fatipec Congress, “Recent progress in the production, processing and control of varnishes and paints”, 14, 623, 1978

75. K. Zimmerschied, Fatipec Congress, “Present and Future in Science and technology of coatings and their components”, 19, 105, 1988

76. H.U. Schenck, H. Spoor, M. Marx, “The chemistry of binders for electrodeoposition”, Progress in Organic coatings, 7, 1, 1, 1979

77. R. Zimmermann, Farbe Lack 82, 383,1976

78. W. Brushwell, Farbe Lack 90, 924, 1284

79. W.C. Wake, “Adhesion and the Formulation of Adhesives”, Applied Science, London, 1976

80. K. Eisentrager and W. Druschk, “Handbook of Adhesives”, 2nd Ed., Van Nostrand Reinhold, London Chapter 32, 1977

81. A. Zosel, “Adhesion and tack of polymers: Influence of mechanical properties and surface tensions”, Colloid Polymer Science, 263, 7, 541,1985

82. V.E. Basin, “Advances in understanding the adhesion between solid substrates and organic coatings”, Progress in Organic Coatings, 12, 3, 213,1984

83. B. B. Kine and R. W. Novak, “Acrylic ester polymers”, ECT, 1, 386, 1978

84. A.E. Alexander and D.H Napper, “Emulsion Polymerization”, Progress inn Polymer Science, 3, 145, 1971

85. F. W. Billmeyer, “Textbook of polymer science”, John Wiley and Sons, ISBN: 978-81-265-1110-5, 2009

86. J.A. Brydson, “Plastics Materials”, 7th Ed., ISBN 0750641320, 1999

87. M.B. Horn, “Acrylic Resins”, Reinhold New York, 1960

88. L.S. Luskin, R.J. Myers, J.P. Bruise, H. W. Coover and T.H. Wicker, “Acrylic ester polymers”, 1, 246, 1964

89. B. B. Kine and R. W. Novak, “Encyclopedia of Polymer Science and Engineering”, John Wiley & Sons Inc., 1, 257, 1985

90. H. Uehara and T. Shimizu, “Transparent resin containing neodymium and lead and production thereof”, Japanese Patent 60-65050A, 1985

91. R. K. Khandal, G. Seshadri and M. Tyagi, “Lead containing novel polyacrylate for optical applications”, United States Patent 2010/ 0029805 A1, 2010

92. T. Abe, I. Okabe and H. Terao, “Method for getting a transparent copolymer”, Japanese Patent 62-26518, 1988

93. H. Seisakusho and K. Eguchi, “Transparent Metal Containing resin with high refractive index used for the manufacture of lens”, Japanese Patent 60-94410, 61, 6, 76,1987

94. H. Selsakashi and E. Eguchi, “Resin with high refractive index and heat resistance obtained by radical co-polymerization of metal containing mono functional and poly functional monomer and its application for the manufacture of lens”, Japanese Patent 60-92306, 61, 5 89. 1987.

95. E. B. Hitachi, “Transparent resin containing metal atoms”, Japanese Patent 01-08985, 58, 3,22, 1985.

96. I. Manners, “Synthetic Metal Containing Polymers”, Willey VCH, ISBN : 3-527-29463-5, 2004

97. S. Eguchi, N. Taketani, H. Asano and M. Wajima, “Transparent resin material containing metallic atoms bonded to pendent carboxylic acid groups” United States Patent 4585841, 1986

98. S. Eguchi, N. Taketani, S. Tanno, Y.Okabe, H. Terao, H. Asano, M. Wajima and T. Abe, “Plastic Optical fibers from polymers derived from metallic salts of ethylenic carboxyl monomers”, United States Patent 5113477, 1992

99. L. T. Chang and C. C. Yen, “Studies on the preparation and properties of conductive polymers. VIII Use of heat treatment to prepare metallized films from silver chelate of PVA and PAN”, Journal of Applied Polymer Science, 55, 2, 371, 1995.

100. D. Y. Godovsky, “Electron behaviour and magnetic properties of polymer nanocomposites”, Advances in Polymer Science, 119, 79, 1995

101. G. Fu and S. M. Augustine, “Nanocomposite particle and process of preparing the same”, United States Patent 8075859, 2011

102. C. Sanchez, G. J. de A. A. Soler-Illia, F. Ribot, T. Lalot, C. R. Mayer and V. Cabuil, “Designed hybrid organic-inorganic nanocomposites from functional nanobuilding blocks”, Chemistry of Materials, 13, 10, 3061, 2001

103. N. Aihara, K. Torigoe and K. Esumi, “Preparation and characterization of gold and silver nanoparticles in layered laponite suspensions”, Langmuir, 14, 17, 4945, 1998.

104. Y. Shiraishi and N. Toshima, “Colloidal silver catalysts for oxidation of ethylene”, Journal of Molecular Catalysis A: Chemistry, 141, 187, 1999.

105. D. G. Duff, A. Baiker and P. P. Edwards, “A new hydrosol of gold clusters.1. Formation and particle size variation”, Langmuir, 9, 9, 2301, 1993.

106. R. M. Bright, m. D. Musick and M. J. Natan, “Preparation and characterization of Ag colloid monolayers”, Langmuir, 14, 20, 5695, 1998.

107. W. Wang, S. Efrima and O. Regev, “Directing oleate stabilized nanosized silver colloids into organic phases”, Langmuir, 14, 3, 602, 1998

108. N. Satoh, T. nakashima, K. Kamikura and K. Yamamoto, “Quantum size effect in TiO2 nanoparticles prepared by finely controlled metal assembly on dendrimer templates”, Nature nanotechnology, 3, 106, 2008

109. G. Suri, D. Khandal, R. Gupta, P. Kapoor, M. Tyagi, J. P. Singh, R. Singh, G. Seshadri, U. K. Niyogi, G. L. Verma and R. K. Khandal, “Radiation processing technology applications”, Chapter 21, ISBN: 978-81-910772-1-6, 2010

110. M.Hosokawa, K. Nogi, M. Naito and T. Yokoyama, Nanoparticle Technology Handbook, Elsevier B.V., ISBN 978-0-441-53122-3, 2007

111. H. Yanagida, “Engineering system for fine particles”, Fujitec Co.,1, 2001

112. H. S. Nalwa, “Encyclopedia of nanoscience and nanotechnology”, ISBN 158830624, 6, 2004

113. A.D.Pomogailo, V.N. Kestelman, “Metallopolymer nanocomposites”, Springer Series in Material Science, ISBN 978-3-540-20949-2, 2005

114. M. F. Ashby, P. J. Ferreira, and D. L. Schodek, “Nanomaterials Nanotechnologies and Design” An Introduction to Engineers and Architects”, Elsevier Ltd., ISBN 978-0-7506-8149-0, 2009

115. F. Kajzar and R. Reinisch, “Beam shaping and control with nonlinear optics”, Springer, 1998

116. Y. Sun, S. K. Gray and S. Peng, “Surface Chemistry: a non-negligible parameter in determining optical properties of small colloidal metal nanoparticles”, 13, 11814, 2011

117. S. Link, M. A. El-Sayed, T. G. Schaaff and R. L. Whetten, “Transition from nanoparticles to molecular behavior: a femtosecond transient absorption study of a size-selected 28 atom gold cluster”, Chemical Physics Letters, 356, 3-4, 240, 2002

118. R. K. Khandal, G. Seshadri and M. Tyagi, “A process for the synthesis and preparation of polymeric materials for use in optical applications such as plastic lenses”, Chinese Patent 200780027467.3

119. R. K. Khandal, M. Tyagi and G. Seshadri, “Metal Containing Polymers for optical applications”, Lambert Academic Publications (LAP), ISBN 978-3-838-36238-0, 216 , 2010

120. J. E. Mark, C. Y. C. Lee and P. A. Bianconi, “Hybrid Organic-Inorganic composites”, American Chemical Society, Washington DC, 585,1995

121. S.Komarneni, J.C. Parker and G.J. Thomas, “Nanophase & Nanocomposite Materials”, Materials Research Society: Pittsburg, PA, 286,15,1993

122. M. Weibel, W. Caseri, U. W. Suter, H. Keiss and E. Wehrli, “Preparation of polymer nanocomposites with “ultrahigh” refractive index”, Polymers for Advanced Technologies, 2, 2, 75, 1991

123. T. Selvan, J. P. Spatz, H. A. Klok and M. Moller, “Gold-polypyrrole core-shell particles in diblock copolymer micelles”, Advanced Materials, 10, 2, 132, 1998

124. H. J. Chen, P. C. Jian, J. H. Chen, L. Wang and W. Y. Chiu, “Nanosized-hybrid colloids of poly(acrylic acid)/titania prepared via in-situ sol-gel reaction”, Ceramics International, 33, 4, 643, 2007

125. L. Pang, Y. Shen, K. Tetz, and Y. Fainman, “PMMA quantum dots composites fabricated via use of pre-polymerization”, Optical Express, 13, 1, 44, 2005

126. C. H. Hung and W. T. Whang, “Effect of surface stabilization of nanoparticles on luminescent characteristics in ZnO/poly (hydroxyethyl methacrylate) nanohybrid films”, Journal of Materials Chemistry, 15, 267, 2005

127. M. Tamborra, M. Striccoli, R. Comparelli, M. L. Curri, A. Petrella and A. Agostiano, “Optical properties of hybrid composites based on higly luminescent CdS nanocrystals in polymer”, Nanotechnology, 15, 4, S240, 2004

128. M. Tamborra, R. Comparelli, M. L. Curri, M. Striccoli, A. Petrella and A. Agostiano, “Microtechnology for the New Millenium”, Sevilla, SPIE Proceedings, Spain, 5838, 236, 2005

129. C. Carotenuto and L. Nocolais, “Encyclopedia of Polymer Science and Technology”, 2003

130. L. Nicolais and G. Carotenuto, “Metal-Polymer Nanocomposites”, Wiley Interscience Publications, 2005

131. R. T. Clay and R. E. Cohen, “Synthesis of Cu and CuO nanoclusters within microphase separated diblock copolymers” New Journal of Chemistry, 22, 745, 1998

132. L. Troeger, H. Huennefeld, S. Nunes, M. Oehring and D. Fritsch, “Structural characterization of catalytically active metal nanoclusters in poly(amide imide) films with high metal loading”, Journal of Physical Chemistry B, 101, 8, 1279, 1997

133. S. Matsuda, S. Ando and T. Sawada, “Thin flexible polarizer of Ag-nanoparticle-dispersed fluorinated polyimide”, Electronics Letters, 37, 706, 2001

134. J. C. Huang, X. F. Qian, J. Yin, Z. K. Zhu and H. J. Xu, “Preparation of soluble polyimide-silver nanocomposites by a convenient ultraviolet irradiation technique”, Materials Chemistry and Physics, 69, 1-3, 172, 2001

135. L. A. Smirnova, A. P. Aleksandrov, N. O. Yakimovich, N. V. Sapogova, A. V. Kirsanov and L. V. Soustov, “UV-induced formation of gold nanoparticles in apoly (methyl methacrylate) matrix”, Doklady Physical Chemistry, 400, 5-6, 19, 2005

136. M. S. El-Shall and W. Slack, “Ultrafine metal particles in polymers and the formation of periodic polymer stripes”, Macromolecules, 28, 24, 8456,1995

137. A. Heilmann, C. Hamann, G. Kampfrath and V. Hopfe, “Preparation and optical properties of plasma polymer silver composite films”, Vacuum, 41, 4-6, 1472, 1990

138. S. Qi, Z. Wu, D. Wu, W. Wang and R. Jin, “Double-surface-silvered polyimide films prepared via a direct ion-exchange self-metallization process”, Chemistry of Materials, 19, 3, 393, 2007

139. A. L. Stepanov, S. N. Abdullin, V. Y. Petukhov, Y. N. Osin, R. I. Khaibullin and I. B. Khaibullin, “Formation of metal-polymer composites by ion implantation” Philosophical Magazine Part B, 80, 1, 23, 2000

140. S. Koizumi, S. I. Matsuda and S. Ando, “Synthesis, characterization and optical properties of uniaxially drawn and gold nanoparticles dispersed fluorinated polyimide films”, Journal of Photopolymer Science and Technology, 15, 1, 231, 2002

141. S. Porel, S. Singh, S. S. Harsha, D. N. Rao, and T. P. Radhakrishnan, “Nanoparticle embedded polymer: In-situ synthesis, free standing films with highly monodisperse silver nanoparticles and optical limiting”, Chemistry of Materials, 17, 9, 2005

142. G. Kickelbick, “Concepts for the incorporation of inorganic building blocks into organic polymers on a nanoscale”, Progress in Polymer Science, 28, 1, 83, 2003

143. W. Caseri, “Nanocomposites of polymers and metals or semiconductors: Historical background and optical properties”, Macromolecular Rapid Communications, 21, 11, 705, 2000

144. J. E. Mark and S. J. Pan, “Reinforcement of polydimethylsiloxane networks by in-situ precipitation of silica: A new method for preparation of filled elastomers”, Macromolecular Rapid Communications, 3, 10, 681,1982

145. H. H. Huang, B.Orler and G.L. Wilkes, “Ceramers: Hybrid materials incorporating polymeric/ oligomeric species with inorganic glasses by a sol-gel process”, Polymer Bulletin, 14, 6, 557, 1985

146. A. Sellinger, P. M. Weiss, A. Nguyen, Y. Lu, R. A. Assink, W. Gong and C. J. Brinker, “Continuous self-assembly of organic-inorganic nanocomposites coatings that mimic nacre”, Nature, 394, 256, 1998

147. B. M. Novak, “Hybrid nanocomposites materials-between inorganic glasses and organic polymers”, Advanced Materials, 5, 6, 422, 1993

148. A. Cartwright, “Organic & nanocomposite optical materials”, Mater Res Soc Symp, 846, Materials Research Soc, Warrendale, 2005

149. M.A. Otooni, “Grain size and mechanical properties: Fundamental and applications”, Materials, Materials Research Society: 362, 1995

150. H. K. Schmidt, “Synthesis and application of inorganic/organic composite materials”, Macromolecular Symposia, 101, 1, 333,1996

151. R. Clement, “Hybrid Organic Inorganic Composites”, American Chemical Society: DC, 585, 29,1995

152. P.H. Hess and P.H. Parker, “Polymers for stabilization of colloidal cobalt particles”, Journal of Applied Polymer Science, 10, 12, 1915,1966

153. T. Ogavwa and Y. Kanemitsu, “Optical properties of low dimensional materials”, World Scientific: River Edge, NJ, 1995

154. R. Alcala and R. Cases, “Optical properties of Pr^{+3} ions in fluoride glasses”, Advanced Materials, 7, 2, 190, 1995

155. M.G. Kanatzidis, C. Wu, H. O. Marcy and C. R. Kannewurf, “Conductive-polymer bronzes. Intercalated polyaniline in vanadium oxide xerogels”, Journal of The American Chemical Society, 111, 11, 4139, 1989

156. S. Srivastava, M. Haridas and J. K. Basu, “Optical properties of polymer nanocomposites”, Bulletin of Material Science, 31, 3, 213, 2008

157. L. L Beecroft and C. K. Ober, “Nanocomposite materials for optical applications”, Chemistry of Materials, 9, 6, 1302,1997

158. M. A. Olshavsky and H. R. Allcock, “Polyphosphazenes with high refractive indices: Synthesis, characterization and optical properties”, Macromolecules, 28, 18, 6188, 1995

159. C. L. Lu, Z. C. Cui, Z. Li, C. Guan, B.Yang and J.Shen, “High refractive index thin films of ZnS/polythiourethanes nanocomposites”Journal of Materials Chemistry, 13, 526, 2003

160. K. Nihara, “New design concept of structural ceramics”, Journal of the Ceramic Society of Japan, 99, 1154, 974,1991

161. I. Javni, K. Song, J. Lin and Z. S. Petrovic, “Structure and properties of flexible polyurethane foams with nano- and micro- fillers”, Journal of Cellular Plastics, 47, 357, 2011

162. F. Wakai, Y. Kodama, S. Sakaguchi, N. Murayama, K. Izaki and K. Niihara, “A superplastic covalent crystal component”, Nature, 344, 6265, 421,1990

163. A. Heilmann, “Polymer films & embedded metal nanoparticles”, Springer: New York, 2002

164. D. C. Bradley, “Metal alkoxides and dialkylamides”, Advances in Inorganic Chemistry and Radiochemistry, 15, 259, 1972.

165. A. J. Kinloch, “Adhesion and adhesives”, Chapman and Hall, London, 1987

166. H. Salmang and H. Scholze, “Keramik,” Part 1, Springer, Berlin, 1982.

167. A. Carre and J. Vial, Preprints EURADH 92 (J. Schultz and W. Brockmann, Eds.) DECHEMA Frankfurt am Main, 90, 1992

168. R. Roy, “Ceramic Microstructures ‘86”, Plenum Press, New York, 25, 1987.

169. P. D. Calvert and R. A. Broad, “Contemporary Topics in Polymer Science”, Plenum Press, New York, 6, 1989.

170. G. Carotenuto, Y.S. Her and E. Matijevic, “Preparation and characterization of nanocomposite thin films for optical devices”, Industrial and Engineering Chemistry Research, 35, 2929, 1996

171. M. Hawe and D. Farrar, “Dispersing agents”, United States Patent 4792343, 1988

172. M. Hiew and P. Chegwidden, “Coated titanium dioxide pigments and processes for production and use”, United States Patent 6342099, 2002

173. H. Su, J. Han, N. Wang, Q. Dong, D. Zhang and C. Zhang, “In situ synthesis of lead sulfide nanoclusters on eggshell membrane fibers by an ambient bio-inspired technique”, Smart Materials and Structures, 17, 1, 015045, 2008

174. E.D. Palik, “Handbook of optical constants of solids”, Academic Press, Orlando, 1985

175. B. Liu, H. Li, C. H. Chew, W. Que, Y. L. Lam, C. H. Kam, L. M. Gan, and. G. Q. Xu, “PbS-polymer nanocomposites with third-order nonlinear optical response in femtosecond regime”, Materials Letters, 51, 6, 461, 2001

176. J. M. Jethmalani and W. T. Ford, “Diffraction of visible light by ordered monodisperse silica-poly (methyl acrylate) composite films”, Chemistry of Materials, 8, 8, 2138, 1996

177. H. B. Sunkara, J. M. Jethmalani and W. T. Ford, “Composite of Colloidal crystals of silica in poly (methyl methacrylate)”, Chemistry of Materials, 6, 4, 362, 1994

178. J. Liu, Y. Gao, F. Wang, D. Li and J. Xu, “Preparation and characteristic of a new class of silica/polyimide nanocomposites”, Journal of Materials Science, 37, 3085, 2002

179. D. Y. Godovsky, A. E. Varfolomeev, D. F. Zaretsky, R. L. N. Chandrakanthi, A. Kündig, C. Weder and W. Caseri., “Preparation of nanocomposites of polyaniline and inorganic semiconductors”, Journal of Materials Chemistry, 11, 2465, 2001

180. S. Spiegelberg, A. Alteheld, X. Zhu, K. Peter and M. Moller, “Method for producing composite materials”, United States Patent 8012578, 2011

181. E. Marutani, S. Yamamoto, T. Ninjbadgar, Y. Tsujii, T. Fakuda and M. Takano, “Surface initiated atom transfer radical polymerization of methyl methacrylate on magnetite nanoparticles”, Polymer, 45, 7, 2231, 2005

182. S. W. Zhang, S. X. Zhou, Y. M. Wong and L. M. Wu, “Synthesis of SiO_2/Polystyrene nanocomposites particles via miniemulsion polymerization”, Langmuir, 21, 6, 2124, 2005

183. S. Joly, R. Kane, L. Radzilowski, T. Wang, A. Wu, R.E.Cohen, E. L. Thomas and M. F. Rubner, "Multilayer nanoreactors for metallic and semiconducting particles", Langmuir, 16, 3, 1354, 2000

184. S. S. Shiratori and M. F. Rubner, "pH-dependent thickness behavior of sequentially adsorbed layers of weak polyelectrolytes" Macromolecules, 33, 11, 4213, 2000

185. T. C. Wang, M. F. Rubner and R.E.Cohen, "Polyelectrolyte multilayer nanoreactors for preparing silver nanoparticles composites: controlling metal concentration and nanoparticles size", Langmuir, 18, 8, 3370, 2002

186. K. M. A. Haque, M. S. Hussain, S. S. Alam and S. M. S. Islam, "Synthesis of nano-nickel by a wet chemical reduction method in the presence of surfactant (SDS) and a polymer (PVP)", African Journal of Pure and Applied Chemistry, 4, 5, 58, 2010

187. S. Stankovich, D. A. Dikin, R. D. Piner, K. A. Kohlhaas, A. Kleinhammes, Y. Jia, Y. wu, S. T. Nguyen and R. F. Ruoff, "Synthesis of graphene-based nanosheets via chemical reduction of exfoliated graphite oxide", Carbon, 45, 1558, 2007

188. G. Carotenuto, "Synthesis and characterization of poly (N-vinylpyrrolidone) filled by monodispersed silver clusters with controlled sizes", Applied Organometallic Chemistry, 15, 5, 344, 2001

189. H. Nersisyan, "A new and effective chemical reduction method for preparation of nanosized silver powder and colloid dispersion", Materials Research Bulletin, 38, 6, 949, 2003

190. N. Herron, Y. Wang & H. Eckert, "Synthesis and characterization of surface-capped, size-quantized cadmium sulfide clusters. Chemical control of cluster size", Journal of The American Chemical Society, 112, 4, 1322, 1990

191. P. Yang, "The Chemistry of Nanostructured Materials", World Scientific Publishing Company Inc., ISBN: 978-9812384058, 2004

192. C. F. Bohren and D. R. Huffman, Absorption and scattering of light by small particles“, Wiley, ISBN: 0471293407, 1983

193. W. S. Taft, J. W. Mayer, R. Newman, P. Kuniholm and D. Stulik, “The Science of Paintings”, Springer, 2000

194. I. R. Kenyon, “The light fantastic: A modern introduction to classical and quantum optics”, Oxford University Press, 2008

195. R. O. Gumprecht and C. M. Sliepcevich, “Scattering of light by large spherical particles”, Journal of Physical Chemistry, 57, 1, 90, 1953

196. R. Rosetti, J. L. Ellison, J. M. Gibson and L. E. Brus, “Size effects in the excited electronic states of small colloidal CdS crystallites”, The Journal of Chemical Physics, 80, 9, 4464, 1984

197. D. D. Chung, “Composite material: Science and Applications”, Springer, 2003

198. F. Papdimitrakopoulos, P. Wisniecki and D. E. Bhagwagar, “Mechanical attrited silicon for high refractive index nanocomposites”, Chemistry of Materials, 9, 12, 2928, 1997

199. E. J. Meehan and D. J. Erdmann, “Light scattering studies on colloidal lead sulfide”, Journal of Colloid and Interface Science, 62, 1, 8, 1977

200. H. Altheus, J. Henle and S. Kaskel, “Functional inorganic nanofillers for transparent polymers”, Chem. Soc. Rev., 36, 1454, 2007

201. E. Arpac, H. Krug, P. Mueller, P. W. Oliveira, W. Peter , H. Schmidt, S. Sepeur and B.Werner, “Nanostructured moulded bodies and layers and methods of producing same”, United States Patent 6291070, 2001

202. A. D. Mcquillan and M.K. Mcquillan, “Metallurgy of the Rarer Metals”, Academic Press Inc., New York, 335, 1956

203. R. A. Wood, “The Titanium Industry in the Mid-1970s”, Batelle Report, Batelle Memorial Institute, Columbus, Oh, 1975.

204. H. B. Bomberger, “Titanium Technology Present Status and Future Trends”, The Titanium Development Association, 3, 1985

205. F. H. Froes and I. L. Caplan, “Titanium 92 Science & Technology”, TMS, Warrendale, Pa., 1993.

206. S. S. Joseph and F. H. Froes, “Light Metal Age”, 4, 11, 5, 1998

207. J. B. Goodenough and A. Hamnett, “Landolt Bornstein Semiconductors Group 3”, Springer-Verlag Berlin, Germany, 17, 133, 1984

208. T. A. Egerton and A. Tetlow, “Industrial Inorganic Chemicals Production and Uses”, The Royal Society of Chemistry Cambridge, U.K., Chapt. 13.

209. M. W. Chase, C. A. Davies, J. R. Downey, D. J. Frurip, R. A.M. Donald, and A. N. Syverud, “JANAF Thermochemical Tables”, 3rd. Ed., Journal of Physical Chemistry, Ref. Data, 14, 1985.

210. H. J. Kotzch, H. G. Srebny and H. J. Vahlensieck, “Method for the preparation of orthoesters of titanium, zirconium or hafnium”, United States Patent 4789752, 1988.

211. U. Diebold, “The surface science of titanium dioxide”, Surface Science Reports, 48, 5-8, 53, 2003

212. D. M. Scott, C. Torardi and V. Grushin, “Suspensions of titanium (IV) oxide particles and process for their production”, United States Patent 7998453, 2011

213. S. Ahmad, S. Ahmad and S. A. Agnihotry, “Synthsis and characterization of in situ prepared poly (methyl methacrylate) nanocomposites” Bulletin of Materials Science, 30, 1, 31, 2007

214. D. S. Arney and T. E. Wood, “Nanosize metal oxide particles for producing transparent metal oxide colloids and ceramers”, United States Patent 6329058, 2001

215. T. Yoshioka, H. Masuda and H. Tanaka,"Cosmetics having photoprotection properties", European Patent 0503922, 1992

216. H. Isabelle, D. Ribery and L. Guillemot, "Anhydrous TiO_2 containing nanopigments cosmetic compositions and hollow, transformable microspheres" European Patent 0755670A1, 1997

217. T. Maki and S. Idei, "Paraffin hydrocarbon dispersion of titanium dioxide-fine particles", European Patent 0523294 A1, 1993

218. Marchi-lemann, A. Collette and M. Mellul, "Cosmetic compositions comprising nanopigments", United States Patent 6132745, 2000

219. M. Chiming and Y. Xia, "Mixed adsorption of sodium dodecylsulfate and ethoxylated nonylphenol on TiO_2 and the stability of TiO_2 dispersions in sodium dodecylsulfate-ethoxylated nonylphenol mixed solutions", Colloids and Surfaces, 68, 3, 171, 1992

220. S. Fukushima and S. Kumangai, "The adsorption of nonionic ethoxylated surfactants on titanium dioxide and their dispersion effect in water", Journal of Colloid and Interface Science, 42, 3, 539, 1973

221. S. Kumangai and S. Fukushima, "Adsorption of nonionic ethoxylated surfactants on titanium dioxides and their dispersion effect in water. II. Differences by the functional group in surfactant molecule", Journal of Colloid and Interface Science, 56, 2, 227, 1976

222. J. L. Collins, "Method for preparing hydrous titanium oxide spherules and other gel forms thereof", United States Patent 5821186, 1998

223. C. C. Wang and J. Y. Ying, "Sol-gel synthesis and hydrothermal processing of anatase and rutile titania nanocrystals", Chemistry of Materials, 11, 11, 3113, 1999

224. A. Latifi, A. Afshar, A. Behnamghader and S. Joughehdoust, "Sol-gel derived titania coating on titanium substrate", Iranian Journal of Pharmaceutical Sciences, 4, 1, 17, 2008

225. K. Ozawa, Y. Sakka and M. Amano, “Preparation of polycrystalline antimonic acid films by electrophoretic deposition”, Journal of Sol-Gel.Science and Technology, 19, 1-3, 595, 2000

226. B. Wang and G. L. Wikes, “New Ti-PTMO and Zr-PTMO creamer hybrid materials prepared by the sol gel method: Synthesis and characterization” Journal of Polymer Materials Part A: Polymer Chemistry, 29, 29, 905, 1991

227. L. Brus, “Quantum crystallites and nonlinear optics”, Applied Physics A, 53, 6, 465,1991

228. C. B. Murray, C.R. Kagan and M.G. Bawendi, “Self organization of CdSe Nanocrystallites into three-dimenional quantum dots superlattices”, Science, 270, 1335, 1995

229. J. Hu, T.W. Odom and C.M. Lieber, “Chemistry and physics in one dimension: Synthesis and properties of nanowires and nanotubes”, Accounts of Chemical Research, 32, 435,1999

230. C. J. Murphy, Science, “Nanotubes and nanoboxes”, 298, 2139, 2002

231. L. R. Dalton, A.W. Harper, R. Ghosn, W.H. Steier, M. Ziari, H. Fetterman, Y. Shi, R. V. Mustacich, A. K. Y. Jen and K. J. Shea, “Synthesis and processing of improved organic second-order nonlinear optical materials for applications in photonics”, Chemistry of Materials, 7, 6, 1060,1995

232. W. U. Huynh, J.J. Dittmer and A. P. Alivisatos, “Hybrid nanorod-polymer solar cells”, Science, 295, 2425, 2002

233. J.Y. Bigot, V. Halte, J.C. Merle and A. Daunois, “”Electron dynamics in metallic nanoparticles”, Chemical Physics, 251, 1-3, 181, 2000

234. J. B. Khurgin and G. Sun, ”Enhancement of optical properties of nanoscaled objects by metal nanoparticles”, Journal of The Optical Society of America B, 36, 12, B83, 2009

235. G. V. Plessen, M. Perner and J. Feldmann, “Ultrafast relaxation dynamics of electronic excitations in noble-metal clusters”, Applied Physics B, 71, 3, 381, 2000

236. C. Guillon, P. Langot, N. D. Fatti and F. Vallee, “Non-equilibrium electron energy-loss kinetics in metal clusters”, New Journal of Physics, 5, 13, 2003

237. J. Eastoe, M. J. Hollamby and L. Hudson, “Recent advances in nanoparticles synthesis with reversed micelles”, Advances in Colloid and interface Science, 128, 5, 2006

238. N. Dhanam, B. Kavitha, N. Jose and D. P. Devasia, “Analysis of ZnS nanoparticles prepared by surfactant micelle-template inducing reaction”, Chalcogenide Letters, 6, 12, 713, 2009

239. V. Thomas, M. Namdeo, Y. M. Mohan, S. K. Bajpai and M. Bajpai, “Review of polymer, Hydrogel and microgel metal nanocomposites: A facile nanotechnological approach”, Journal of Macromololecular Science, Part A: Pure and Applied Chemistry, 45, 107, 2008

240. T. Okubo, S. Kohmoto, M. Yamamoto and T. Nakahira, “Preparation, characterization and optical properties of disulfide-comprising oligo [2, 5-bis(thiomethyl)-1,4-dithiane] and its poly [S-alkylcarbamate]”, Journal of Material Science, 34, 337, 1999

241. C. Lu, Z. Cui, Y.Wang, B. Yang and J. Shen, “Studies on syntheses and properties of episulfide-type optical resins with high refractive index”, Journal of Applied Polymer Science, 89, 9, 2426, 2003

242. Q. Wang, J. Xu and R. Xie, “Encyclopedia of Nanoscience and Nanotechnology”, 8, 101, 2004

243. H. Altheus, P. Simon and S. Kaskel, “Transparent and luminescent YVO4: Eu/polymer nanocomposites prepared by in situ polymerization”, Journal of Materials Chemistry, 17, 8, 758, 2007

244. H. Altheus, R. Palkovits, A. Rumplecker, P. Simon, W. Sigle, M. Bredol, U. Kynast and S. Kaskel, “Synthesis and characterization of transparent luminescent ZnS:Mn/PMMA nanocomposites”, Chemistry of Materials, 18, 4, 1068, 2006

245. M. Bredol and H. Altheus, “Luminescent Nano-Sized ZnS and ZnO Particles", Solid State Phenomena, 99-100, 19, 2003

246. H. X. Zhao and R. K. Y. Li, “A study on the photo-degradation of zinc oxide (ZnO) filled polypropylene nanocomposites”, Polymer, 47, 9, 3207, 2003

247. H. Altheus, P. Simon, F. Philipp, and S. Kaskel, “Integration of zinc oxide nanoparticles into transparent poly (butanediolmonoacrylate) via photopolymerization”, Journal of Nanoscience & Nanotechnology, 6, 2, 409, 2006

248. A. Ammala, A. J. Hill, P. Meakin, S. J. Pas and T. W. Turney, “Degradation studies of polyolefins incorporating transparent nanoparticulate zinc oxide UV stabilizers”, Journal of Nanoparticle Research, 4, 1, 167, 2002

249. N. S. Allen, M. Edge, A. Ortega, G. Sandoval, C. M. Liauw, J. Verran, J. Stratton and R. B. McIntyre, “Degradation and stabilization of polymers and coatings: nano versus pigmentary titania particles”, Polymer Degradation and Stability, 85, 3, 927, 2004

250. M. Tyagi, G.Suri, P. Chhabra, G.Seshadri, A. Malik, S. Aggarwal and R.K. Khandal, “Novel way of making high refractive index plastics; metal containing polymers for optical applications”, e-Polymers, 2009, no. 100, ISSN 1618-7229

251. Ullmann’s Encyclopedia of Industrial Chemistry, VCH publishers, A9, 1987.

252. A. R. Katritzky, S. Sild and M. Karelson, “General quantitative structure-property relationship treatment of the refractive index of organic compounds”, Journal of The Chemical Information and Modeling, 38, 5, 840, 1998

253. G. Elert, “Refraction: The Physics Hypertextbook”, 1998

254. Y. Nakao, “Noble metal solid sols in poly (methyl methacrylate)”, Journal of Colloid and Interface Science, 171, 2, 386,1995

255. G. Suri, M. Tyagi, G. Seshadri, , G. L. Verma and R. K. Khandal, “Novel nanocomposites optical plastics: Dispersion of titanium in polyacrylates”, Journal of Nanotechnology, 2010, Article ID 531284, 2010

256. M. Tyagi, M. Verma, G. Seshadri, A. Malik, S. Aggarwal and R. K. Khandal, “Development of metal containing polymers for optical applications”, Journal of Polymer Materials, 23, 1, 21, 2006

257. M. Tyagi, G. S. Jha, G. Seshadri, A. Malik, S. Aggarwal and R. K. Khandal, “Metal containing polymers for optical applications : Part II”, Journal of Polymer Materials, 2, 24,135, 2007.

258. G. S. Jha, G. Seshadri, A. Mohan and R. K. Khandal, “Development of high refractive index plastics”, e-polymers,120, 1, 2007

259. G. Suri, P. Chhabra, R. Gupta, S. Saxena, M. Tyagi, G. Seshadri, G. L. Verma and R. K. Khandal, “Challenges in preparartion of metal containing nanocomposites; dispersion of titanium into plastics”, e-Polymers, ISSN 1618-7229, 106, 2010

260. B. E. Yoldas and T. W. O. Keefe, “Antireflective coatings applied from metal-organic derived liquid precursors”, Applied Optics, 18, 18, 3133, 1979

261. R.A. Gaudiana and R.A. Minns, “High refractive index polymers”, Journal of Macromolecular Science: Part A, 28, 9, 831, 1991

262. L. L. Beecroft and C.K. Ober, “High refractive index plastics for optical applications”, Journal of Macromolecular Science Part A, 34, 4, 573, 1997

263. K. S. Anseth, C. N. Bowman and N. A. Peppas, “Polymerization kinetics and volume relaxation behavior of photopolymerized multifunctional monomers producing highly cross-linked networks”, Journal of Polymer Science, Part A: Polymer Chemistry, 32, 1, 139,1994

264. L. Song, W. Hu, G. Wang, G. Niu, H. Zhang, H. Cao, K. Wang, H. Yang and S. Zhu, “Tailored (Meth)acrylate shape-memory polymer networks for ophthalmic applications”, Macromolecular Bioscience, 10, 1194, 2010

265. E. I. Assia, M. Blumenthal and D. J. Apple, “Effect of expandable full-size intraocular lenses on lens centartion and capsule opacification in rabbits”, Journal of Cataract and Refractive Surgery., 25, 3, 347,1999

266. N. Sultanova, I. Nikolov and C. Ivanov, “Measuring the refractometric characteristics of optical plastics”, Optical and Quantum Electronics. 35, 1, 21, 2003

267. S. N. Kasarova, N. G. Sultanova and I. D. Nikolov, “Temperature dependence of refractive characteristics of optical plastics”, Journal of Physics: Conference Series, 253, 012028, 2010

268. J. Yang, T. Hasell, W. Wang and S. M. Howdle, “A novel synthetic route to metal-polymer nanocomposites by in situ suspension and bulk polymerizations”, European Polymer Journal, 44, 5, 1331, 2008

269. D.K. Avasthi, Y.K. Mishra, D. Kabiraj, N.P. Lalla and J.C Pivin, “Synthesis of metal-polymer nanocomposites for optical applications”, IOP Publishing, Nanotechnology, 18, 125604, 2007

270. U. Kreibig and M. Vollmer, “Optical Properties of Metal Clusters”, Berlin Springer, 1995

271. C. F. Bohren and D. R. Huffman, “Absorption & Scattering of Light by Small Particles”, New York Wiley, 1983

272. V. V. Vodnik, D. K. Bozanic, E. Dzunuzovic, J. Vukovic and J. M. Nedeljkovic, “Thermal and optical properties of silver-poly (methylmethacrylate) nanocomposites prepared by in-situ radical polymerization”, European Polymer Journal, 46,137, 2010

273. A.L. Volynskii, N. I. Nilkonorova, A. V. Volkov, M. A. Moskvina, A.A. Tunyan, N.G. Yaryshev, O.V. Arzhakova, A.A. Dolgova, E. S. Trofimchuk, S. S. Abramchuk, L. M. Yarysheva and N.F. Bakeev, “Preparation method for noble metal-polymer matrix nanocomposites”, Colloid Journal, 72, 4, 464, 2010

274. M. C. Tan, S. D. Patil and R. E. Riman, “Transparent infrared-emitting CeF_3:Yb-Er polymer nanocomposites for optical applications”, Applied Material Interfaces, 2, 7, 1884, 2010

275. T. Wan, et al., Journal of Applied Polymer Science, 102, 5105, 2006

276. G.S. Liou, P.H. Lin, H.J. Yen, Y.Y. Yu and W.C. Chen, “Flexible nanorystalline-titania/polyimide hybrids with high refractive index and excellent thermal dimensional stability”, Journal of Polymer Science Part A : Polymer Chemistry, 48, 6, 1433, 2010

277. W. Tao, F. Fei and W. Y.Chuan, “Structure and thermal properties of titanium dioxide-polyacrylate nanocompsites”, Polymer Bulletin, 56, 413, 2006

278. C.Ye, H.Li, A. Cai, Q. Gao and X. Zeng, “Properties and characterization of organic nano-titanium dioxide/acrylate composite emulsiooon by in-situ emulsion polymerization”, Journal of Macromolecular Science, Part A: Pure and Applied Chemistry 48, 309, 2011

279. J. Zhang, S. Luo and L. Gui, “Polymethyl methacrylate-Titania hybrid materials by sol gel processing”, Journal of Materials Science 32, 1469,1997

280. D. G. Yu, J. H. An, J. Y. Bae, S. D. Ahn, S. Y. Kang and K. S. Suh, “Preparation of titania/poly(methylmethacrylate-co-n-butyl acrylate-co-methacrylic acid) hybrid composite particles via emulsion polymerization”, Journal of Applied Polymer Science, 97, 72, 2005

281. J. Zhang, F. H. J. Maurer and M. Yang, “In-situ formation of TiO_2 in electrospun poly (methyl methacrylate) nanohybrids”, The Journal of Physical Chemistry C, 115, 10431, 2011

282. M. Gopal, W. J. M. Chan and L.C.J. Dejonghe, “Room temperature synthesis of crystalline metal oxides”, Journal of Materials Science, 32, 6001,1997

283. L. L. Hench, J.K. West, “The sol-gel process”, Chemical Reviews, 90, 1, 33,1990

284. R. Mueller, H.K. Kammler, K. Wegner and S. E. Pratsinis, “OH surface density of SiO_2 and TiO_2 by thermogravimetric analysis”, Langmuir,19, 1, 160, 2003

285. E. Ritzhaupt-Kleissl, J. Böhm, J. Hauelt and T. Hanemann, “Process chain for tailoring the refractive index of thermoplastic optical materials using ceramic nanoparticles”, Advanced Engineering Materials 7,6, 540, 2005

286. C. Lu, Z. Ciu, Y. Wang, Z. Li, C. Guan, B. Yang and J. Shen, “Preparation and characterization of ZnS-polymer nanocomposites films with high refractive index”, Journal of Materials Chemistry, 13, 2189, 2003

287. L. Zimmermann, M. Weibel, W. Caseri, U. W. Suter and P. Walther, “Polymer nanocomposites with ultralow refractive index”, Polymers for Advanced Technologies, 4, 1, 1, 1993

288. S.C. Wong, E. M. Wouterson and E. M. Sutherland, “Dielectric properties of graphite nanocomposites”, Journal of Vinyl & Additive Technology, 12, 127, 2006

289. L. S. Montagna, F. de C. Fim, G. B. Galland and R. R. de S. Basso, “Synthesis of poly(propylene)/graphite nanocomposites by in situ polymerization”, Macromolecular symposia, 299-300, 1, 48, 2011

290. B. Tryba, R.J. Kalenczuk, F.Y. Kang, M. Inagaki, and A.W. Morawski, “Studies of exfoliated graphite (EG) for heavy oil sorption”, Molecular Crystals and Liquid Crystals, 340,1, 113, 2000

291. A. Yasmin, J. J. Luo and I. M. Daniel, “Processing of graphite reinforced polymer nanocomposites”, Composites Science and Technology, 66, 1179, 2006

292. K. Wakabayashi, C. Pierre, D. A. Dikin, R. S. Ruoff, T. Ramanathan, L. C. Brinson and J. M. Torkelson, “Polymer-graphite nanocomposites: Effective dispersion and major property enhancement via solid-state shear pulverization”, Macromolecules, 41, 1905, 2008

293. G. H. Chen, D. J. Wu, W. G. Weng and W. L. Yan, “Preparation of polymer/graphite conducting nanocomposites by intercalation polymerization”, Journal of Applied Polymer Science, 82, 10, 2506, 2001

294. Y.X. Pan, Z.Z. Yu, Y.C. Ou and G.H. Hu, “A new process of fabricating electrically conducting nylon 6/graphite nanocomposites via intercalation polymerization”, Journal of Polymer Science Part B: Polymer Physics, 38, 12, 1626, 2000

295. W. Zheng and S.C. Wong, “Electrical conductivity and dielectric properties of PMMA/expanded graphite composites”, Composites Science and Technology, 63, 2, 225, 2003

296. W. Zheng, S.C. Wong and H.J. Sue, “Transport behavior of PMMA/expanded graphite nanocomposites”, Polymer, 43, 25, 6767, 2002

297. A. Gronowski and Z. Wojtczak, “The thermal decompositions of some transition metal acrylates and polyacrylates”, Journal of Thermal Analysis, 26, 233,1983

298. Z. Wojtczak and A. Gronowski, “Study of the thermal behavior of several metal acrylates and methacrylates”, Journal of Thermal Analysis, 36, 2357,1990

299. W. Balcerowiak, J. Hepter, J. Beres and J. Olkowska, “Study of thermal behaviours of some metal acrylates”, Journal of Thermal Analysis and Calorimetry, 11, 101,1977

300. I.C. McNeill and M. Zulfiqar, “Preparation and degradation of salts of poly (methacrylic acid). I. Lithium, sodium, potassium and caesium salts”, Journal of Polymer Science: Polymer Chemistry Edition, 16, 12, 3201,1978

301. G. I. Dzhardimalieva, S. I. Pomogailo, N. D. Golubeva and A. D. Pomogailo, “Refractory metal-containing polymers and nanocomposites: Preparation and properties”, Macromol. Symp., 304, 101, 2011

302. F. Bauer, and R. Mehnert, “UV-Curable acrylate nanocomposites: Properties and appplications”, Journal of Polymer Research, 12, 6, 483, 2005

303. R. P. Bagwe, L. R. Hilliard and W. Tan, “Surface modification of silica nanoparticles to reduce aggregation and non-specific binding”, Langmuir, 22, 9, 4357, 2006

304. F. Beari, M. Brand, P. Jenker, R. Lehnert, H.J. Metternich, J. Monkiewicz and H.W. Siesler, “Organofunctional alkoxysilanes in dilute aqueous solution: new accounts on the dynamic structural mutability”, Journal of Organometallic Chemistry., 625, 2, 208, 2001

305. M.W. Daniels and L.F. Francis, “Silane adsorption behavior, microstructure and properties of glycidoxypropyltrimethoxysilane-modified colloidal silica coatings”, Journal of Colloid and Interface Science, 205, 1, 191, 1998

306. G. O. Mueller, R. Mueller Mach, D. Bertram, T. Juestel, P. Schmidt and J. Optiz, “Light emitting devices utilizing nanoparticles”, European Patent 1369935 A1, 2003

307. N. Kato, T. Yamada, E. Koshiishi and S. Yoshida, “Optical lens”, United States Patent 8013106, 2011

308. J. Solcnee Hajna, “Colloidal size hydrophobic polymers particulate having discrete particles of an inorganic material dispersed therein”, United States Patent 4421660, 1983

309. A. Chandra, L. S. Turng, S. Gong, D. C. Hall, D. F. Caulfield and H. Yang, “Study of polystyrene/titania nanocomposites via melt compounding for optical applications”, Polymer Composites, 28, 2, 341, 2007

310. J. H. Adair, S. M. Rouse, J. Wang, M. Kester, C. Siedlecki, W. B. White, E. Wogler, A. Snyder, C. G. Pantano, V. Ruiz-Velasco and L. Sinoway, “Unagglomerated core/shell nanocomposites particles”, United States Patent 8071132, 2011

311. P. A. Dickinson, I. W. Kellaway and S. W. Howells, “Particulate composition”, United States Patent 7018657, 2006

312. W. C. Chen, L. H. Lee, B. F. Chen and C. T. Yen, “Synthesis and characterization of poly (methyl silsesquioxane)-titania optical thin films“, Journal of Materials Chemistry, 12, 3644, 2002

313. S. Wu, G. Zhou and M. Gu, “Synthesis of high refractive index composites for photonic applications”, Optical Materials, 29, 12, 1793, 2007

314. S. Kang, F. J. Rouser, S. K. Rowen, S. J. Martin, M. S. Terrazas, S. G. Norquist and J. L. Sadlo, “Sporting goods having creamer coatings” United States Patent 6458462, 2002

315. B. K. Coltrain, C. J. T. Landry, J. M. Oreilly, A. M. Chamberlain, G. A. Rakes, J. S. Sedita, L. W. Kelts, M. R. Landry and V. K. Long, “Role of trialkoxy functionalization in the preparation of organic-inorganic composites”, Chemistry of Materials, 5, 10, 1445,1993

316. S. Edelstein and R. C. Cammarata, “Nanomaterials: Synthesis, properties and applications”, Institute of Physics, ISBN 0-8503-0588.9, 1996

317. Gogotsc, “Nanomaterials Handbook”, CRC/Taylor and Francis, ISBN 13: 988.0-8493-2308.9, 2006

318. C. K. Chan, S. J. Peng, I. M. Chu & S. H. Ni, “Effects of heat treatment on the properties of poly(methyl methacrylate)/ silica hybrid materials prepared by sol-gel process”, Polymer, 42, 9, 4189, 2001

319. F. Mei, C. Liu, L. Zhou, W. K. Zhao, Y. L. Fang, J. B. Wang and Y. Y. Ren, “Effect of annealing temperature on binary TiO2: SiO2 nanocrystalline thin films”, Journal of The Korean Physical Society, 48, 6, 1509, 2006.

320. C. Wang, Z. X. Deng and Y. Li, “The synthesis of nanocrystalline anatase and rutile titania in mixed organic media”, Inorganic Chemistry, 40, 20, 5210, 2001

321. S. M. Klein, J. H. Choi, D. J. Pine and F. F. Lange, “Synthesis of rutile titania powders: Agglomeration, dissolution and reprecipitation phenomena”, Journal of Materials Research, 18, 6, 1457, 2003

322. A. Convertino, G. Leo, M. Tamborra, C. Sciancalepore, M. Striccoli, M. L. Curri and A. Agostiano, “TiO_2 colloidal nanocrystals functionalization of PMMA, A tailoring of optical properties and chemical adsorption”, Sensors and Actuators B: Chemical, 126, 1, 138, 2007

323. R. J. Nussbaumer, W. Caseri, T. Tervoort and P. Smith, “Synthesis and characterization of surface-modified rutile nanoparticles and transparent polymer composites thereof”, Journal of Nanoparticle Research, 4, 4, 319, 2002

324. R. J. Nussbaumer, W. Caseri, P. Smith and T. Tervoort, “Polymer TiO2 nanocomposites: A route towards visually transparent broadband UV filters and high refractive index materials”, Macromolecular Materials and Engineering, 288, 1, 44, 2003

325. W. L. Chang, H. W. Su and W. C. Chen, “Synthesis and properties of photo-sensitive polyimide-nanocrystalline titania optical thin films”, European Polymer Journal, 45, 10, 2749, 2009

326. Y. Liu, C. Lu, M. Li, L. Zhang and B. Yang, “High refractive index organic-inorganic hybrid coatings with TiO_2 nanocrystals”, Colloids and Surfaces A, 328, 1-3, 67, 2008

327. C. C. Chang and W. C. Chen, “High refractive index thin films prepared from aminoalkoxysilane-capped pyromellitic dianhydride-titania hybrid materials”, Journal of Polymer Science Part A: Polymer Chemistry, 39, 3419, 2001

328. N. Nakayama and T. Hayashi, “Preparation and characterization of titania and polymer nanocomposites films with high refractive index”, Journal of Applied Polymer Science, 105, 6, 3662, 2007

329. Y. Imai, A. Terahara, Y. Hakuta, K. Matsui, H. Hayashi and N. Ueno, “Transparent poly (bisphenol A carbonate)-based nanocomposite with high refractive index nanoparticles”, European Polymer Journal, 45, 630, 2009

330. H. W. Su and W. C. Chen, “High refractive index polyimide-nanocrystalline-titania hybrid optical materials”, Journal of Materials Chemistry, 18, 1139, 2008

331. J. K. Fink, “Handbook of Engineering and specialty thermoplastics, water soluble polymers”, John Wiley and Sons, 2011

332. A. Antonello, G. Brusatin, M. Guglielmi, V. Bello, G. Perotto, G. Mattei, M. Maiwald, V. Zollmer, A. Chiasera, M. Ferrari and A. Martucci, “Novel multifunctional nanocomposites from titanate nanosheets and semiconductor quantum dots”, Optical Materials, 33, 12, 1839, 2011

333. T. Ohya, A. Nakayama, T. Ban, Y. Ohya & Y. Takahashi, “Synthesis and characterization of halogen-free, transparent, aqueous colloidal titanate solutions from titanium alkoxide”, Chemistry of Materials, 14, 7, 3082, 2002

334. T. Sasaki, M. Watanabe, H. Hashizume, H. Yamada and H. Nakazawa, “Macromolecule-like aspects for a colloidal suspension of an exfoliated titanate. Pairwise association of nanosheets and dynamic reassembling process initiated from it”, Journal of The American Chemical Society, 118, 8329,1996

335. R. Abe, K. Shinohara, A. Tanaka, M. Hara, J. N. Kondo & K. Domen, "Preparation of thin films of a layered titanate by the exfoliation of $Cs_xTi_{(2-x/4)x/4}O_4$", Chemistry of Materials, 10, 1, 329, 1998

336. T. Sasaki, Y. Ebina, Y. Kitami, M. Watanabe and T. Oikawa, :Two dimensional diffraction of molecular nanosheet crystallites of titanium oxide", The Journal of Physical Chemistry B, 105, 26, 6116, 2001

337. D. Portehault, C. Giordano, C. Sanchez and M. Antonietti, "Nonaqueous route toward a nanostructured hybrid titanate", Chemistry of Materials, 22, 6, 2125, 2010

338. K. J. Jiang, K. Manseki, Y. H. Yu, N. Masaki, K. Suzuki, Y. I. Song and S. Yanagida, "Photovoltaics based on hybridization of effective dye-sensitized titanium oxide and hole-conductive polymer P3HT", Advanced Functional Materials, 19, 15, 2481, 2009

339. J. Wang, D. Montville and K. E. Gonsalves, "Synthesis of polycarbonate-co-poly(p-ethylphenol) and CdS nanocomposites", Journal of Applied Polymer Science, 72, 14, 1851, 1999

340. G. Teowee, P-Marc Allemand, J. P. Cronin, J. C. L. Tonazzi and A. Agrawal, "Photochromic devices", United States Patent 6246505, 2001

341. B. Craig, B. U. Kolb, J. D. Oxman, R. F. Peez and S. A. Frank, "Use of nanoparticles to adjust refractive index of dental compositions", United States Patent 7090721, 2006.

342. G. Chen, R. Rapaport, E. Reichmanis and S. Yang, "Process for making crystalline structures having interconnected pores and high refractive index contrasts", United States Patent 7168266, 2007

343. N. Nakayama and T. Hayashi, "Preparation and characterization of titania-zirconia and thiol-acrylate resin nanocomposites with high refractive index via UV-induced cross-linked polymerization", Composites Part A, 38, 1996, 2007

344. J. L. H. Chau, C. T. Tung, Y. M. Lin and A. K. Li, “Preparation and optical properties of titania/epoxy nanocomposites coatings”, Materials Letters, 62, 19, 3416, 2008

345. B. Erdem, E. D. Sudol, V. L. Dimonie and M. S. El-Aasser, “Encapsulation of inorganic particles via miniemulsion polymerization. I. Dispersion of titanium dioxide particles in organic media using OLOA 370 as stabilizer”, Journal of Polymer Science Part A: Polymer Chemistry, 38, 4419, 2000

346. B. Erdem, E. D. Sudol, V. L. Dimonie and M. S. El-Aasser, “Encapsulation of inorganic particles via miniemulsion polymerization. II. Preparation and characterization of styrene miniemulsion droplets containing TiO_2 particles”, Journal of Polymer Science Part A: Polymer Chemistry, 38, 4431, 2000

347. B. Erdem, E. D. Sudol, V. L. Dimonie and M. S. El-Aasser, “Encapsulation of inorganic particles via miniemulsion polymerization. III. Characterization of encapsulation”, Journal of Polymer Science Part A: Polymer Chemistry, 38, 4441, 2000

348. M. Zhang, G. Gao, C. Q. Li and F. Liu, “Titania-coated polystyrene hybrid microballs prepared with miniemulsion polymerization”, Langmuir, 20, 1420, 2004

349. Y. Wu, Y. Zhang, J. Xu, M. Chen and L. Wu, “One-step preparation of PS/ TiO_2 nanocomposite particles via miniemulsion polymerization”, Journal of Colloid Interface Science, 343, 18, 2010

350. J. Hu, M. Chen and L. Wu, “Organic-inorganic nanocomposites synthesized via miniemulsion polymerization”, Polymer Chemistry, 2, 760, 2011

351. M. Amiji, R. Tailor, M. K. Ly andJ. Goreham, “Gelatin-PEO-semi-interpenetrating polymer network with pH-sensitive swelling and enzyme degradable properties for oral drug delivery”, Drug Development and Industrial Pharmacy, 23, 6, 572, 1997

352. Y. Zhao, F. Wang, Q. Fu and W. Shi, “Synthesis and characterization of ZnS/ hyperbranched polyester nanocomposites and its optical properties”, Polymer, 48, 2853, 2007

353. S. Schmitt-Rink, D. A. B. Miller and D.S. Chemla, “Theory of the linear and non-linear optical properties of semiconductor microcrystallites”, Physical Review B, 35, 8113,1987

354. T. K. Leodidou, H.J Althaus, Y. Wyser. D. Vetter, M. Buchler, W. Caseri and U.W. Suter, “High refractive index materials of iron sulfide and polyethylene oxide”, Journal of Materials Research, 12, 2198, 1997

355. J. Kuljanin, M. I. Cornor, V. Djokovic and J. M. Nedeljkovic, “Synthesis and characterization of nanocomposites of polyvinyl alcohol and lead sulfide nanoparticles”, Material Chemistry and Physics, 95, 1, 67, 2006

356. T. Druffel, O. Buazza, M. Lattis, S. Farmer, M. Spencer, N. Nandzy and E. A. Grulke, “The role of nanoparticles in visible transparent nanocomposites”, Proc SPIE: Synthesis and Fabrication II, 7030, 2008

357. M. K. Corbierre, N. S. Cameron, M. Sutton, K. Laaziri and R. B. Lennox,”Gold nanoparticles/polymer nanocomposites: Dispersion of nanoparticles as a function of capping agent molecular weight and grafting density”, Langmuir, 21, 6063, 2005

358. A. B. R. Mayer, “Colloidal metal nanoparticles dispersedin amphiphilic polymers”, Polymers for Advanced Technologies, 12, 1-2, 96, 2001

359. V. Abdelsayed, Y. Abrahim, M. S. El-Shall and S. Deevi, “Polymerization of butadiene on naoparticles’ surfaces and formation of metal/polymer nanocomposites”, Applied Surface Science, 252, 3774 , 2006

360. L. Balan and D. Burget, “Synthesis of metal/polymer nanocomposites by UV-radiation curing”, European Polymer Journal, 42, 3180, 2006

361. Y. Dirix, C. Darribere, W. Haffels, W. Caseri & P. Smith, “Optically anisotropic polyethylene-gold nanocomposites”, Applied Optics, 38, 658,1999

362. J. G. C. Veniot, J. Galloro, L. Pugliese, R. Pestrin and W. J. Pietro, “Surface functionalization of cadmium sulfide quantum confined nanoclusters 5. Evidence of facile surface-core electronic communication in the photodecomposition mechanism of functionalized quantum dots”, Chemistry of Materials, 11, 642,1999

363. Y. Dirix, C. Bastiaansen, W. Caseri and P. Smith, ”Preparation, structure and properties of uniaxially oriented polyethylene-silver nanocomposites”, Journal of Material Science, 34, 3859, 1999

364. J. J. Schwab, “Metal-containing compositions”, US Patent Application 20110092653, 2011

365. Z. Lin, Y. Cheng, H. Lu, L. Zhang and B. Yang, “Preparation and characterization of novel ZnS/sulfur-containing polymer nanocomposites optical material with high refractive index and high nanophase contents”, Polymer, 51, 5424, 2010

366. C. Lu, Y. Cheng, Y. Liu, F. Liu and B.Yang, “A facile route to ZnS-polymer nanocomposites optical materials with high nanophase content via gamma ray irradiation initiated bulk polymerization”, Advanced materials, 18, 9, 1188, 2006

367. J. K. Kim, W. J. Koros and D. R. Paul, “Physical aging of thin 6FDA-based polyimide membranes containing carboxylic acid groups, Part II: Optical properties”, Polymer, 47, 3104, 2006

368. A. C. Balazs, T. Emrick and T. P. Russell, “Nanoparticle polymer composites: Where two small worlds meet”, Science, 314, 1107, 2006

369. Standard Test Method for Index of Refraction of Transparent Organic Plastics ASTM D-542, 1990.

370. Standard Practice for Computing the Colors of Objects by using the CIE system –ASTME-308, 1994.

371. Determination of Yellowness Index BS-2782; Part 5, 1976.

372. Standard Test Method for Vicat Softening Temperature of Plastics ASTM D-1525, 1991.

373. Code of Federal Regulations Food and Drugs, "Use of impact – resistant lenses in eyeglasses and sunglasses", FDA-21CFR 801.410

374. "Standard test method for film hardness by pencil test", ASTM D – 3363, 1992.

375. "Standard Test Method for Rubber Property –Durometer Hardness", ASTM D-2240, 2005.

376. "Standard Test Methods For Determination of Gel Content and Swell Ratio Of Cross-linked Ethylene Plastics", ASTM D-2765, 2005

377. "Acid values", IS 548(Part): 1964

378. W. Lewandowski, M. Kalinowska and H. Lewandowaska, "The influence of metals on the electronic system of biologically important ligands. Spectroscopic study of benzoates, salicylates, nicotinates and isoorotates", Journal of Inorganic Biocemistry, 99, 7, 1407, 2005

379. G. Swiderski, M. Kalinowska, S. Wojtulewski and W. Lewandowski, "Experimental (FT-IR, FT-Raman, ^{1}H NMR) and theoretical study of magnesium, calcium, strontium and barium picolinates", Spectrochimica Acta Part A: Molecular and Biomolecular Spectroscopy, 64, 1, 24, 2006

380. M. Kalinowska, R. Swislocka and W. Lewandowski, "The spectroscopic (FT-IR, FT-Raman and ^{1}H, ^{13}C NMR) and theoretical studies of cinnamic acid and alkali metal cinnamates", Journal of Molecular Structure, 834-836, 572, 2007

381. J.R Allan, B.R. Carson, D.L.Gerrard and S. Hoey, "Thermal, spectral and magnetic studies of some compounds of cobalt (II), nickel (II) and copper (II) with cinnamic acid", Thermochimica Acta, 154, 315, 1989

382. S. Roller & P. Seedhar, "Carvacrol and cinnamic acid inhibit microbial growth in fresh-cut melon and kiwifruit at 4° and 8 °C", Letters in Applied Microbiology, 35, 5, 390, 2002

383. J. S. Chamberlain, “A textbook of organic chemistry”, 1921

384. E. H. Riddle, “Monomeric acrylic esters”, Reinhold, New York, 1954

385. E. C. Leonard, “Vinyl and Diene Monomer”, Part 1, Wiley Interscience, New York, 148, 1970

386. E. Ohmori, “Acrylic acid and its polymers”, Shokodo, Tokyo, Vol. 1& 2, 1973 &1975

387. P. S. Kalsi, “Spectroscopy of Organic compounds”, Ed. 5th, New Age International Ltd. Publishers

388. “Acrylate esters-A guide to safety and Handling” compiled by Badiesche Corporation, Cleanse Chemical, Rohm and Hass Union Carbide Corp., Willianburg, 1989

389. M. Gordon and J. S. Taylor, “Ideal co-polymers and the second-order transitions of synthetic rubbers.i. non-crystalline co-polymers ”, Journal of Applied Chemistry, 2, 493, 1952

390. A. Eisenberg and M. Shem, “Recent advances in glass transition in polymers”, Rubber Chemistry and Technology, 43, 1, 156, 1970

391. L. S. Luskin, “Modern Plastic Encyclopedia”, 196, 1984

392. Titanium, Encyclopedia Britannica, 2006, Retrieved 2006

393. Titanium, Los Alamos National Laboratory, 2004, Retrieved 2006

394. American Welding Society Guide for the fusion welding of Ti & Ti alloys, Miami

395. Emsley, J. Nature’s building blocks: An A-Z guide to the elements. Oxford: Oxford University Press, 451, ISBN: 0198503415

396. H.H. Beacham, “Properties and uses of Organic titanates, Advances in Chem. Properties, Metal Organic Compounds”, Chap-26, 282.

397. A. F. Wells, “Structural Inorganic Chemistry”, Ed 4th, Oxford University Press, Oxford, 1975.

398. R. J. H. Clark, “The Chemistry of Titanium and Vanadium”, Elsevier, Amsterdam, 1968.

399. R. Colton, J.H. Conterford, “Halides of the First Row Transition Metals”, Wiley, London, 1969.

400. M. Rehan, X. Lai and G. M. Kale, “Hydrothermal synthesis of titanium dioxide nanoparticles studied employing in situ energy dispersive X-ray diffraction”, CrystEngComm, 13, 3725, 2011

401. Y. Tao, J. Pan, S. Yan, B. Tang and L. Zhu, “Tensile strength optimizationand characterization of chitosan/TiO_2 hybrid film”, Materials Science and Engineering B, 138, 1, 84, 2007

402. W. C. Chen, S. J. Lee, L. H. Lee, and J. L. Lin, “Synthesis and characterization of trialkoxysilane-capped poly (methyl methacrylate)-titania hybrid optical thin films”, Journal of Materials Chemistry, 9, 12, 2999, 1999.

403. N. Grassie, Chemistry of high polymer degradation processes. London: Butterworths, 1956.

404. H. H. G. Jellinek, “Encylopedia of Polymer Science and Technology”, 4, 1966

405. L. A. Wall, “High Polymers XII”, 1962

406. M. Coşkun and K. Demirelli, Polymer Degradation and Stability, “Thermal degradation of poly [2-(3-chloro-3-methylcyclobutyl)-2-hydroxyethyl methacrylate]”, 58 , 1-2, 187, 1997

407. M. Coşkun and K. Demirelli, “Thermal degradation of sulphonylated polystyrene”, Polymer Degradation and Stability, 51, 2, 173, 1996

408. K. Demirelli and M. Coşkun, “Synthesis, characterization and thermal degradation of poly[2-{3-p-bromophenyl-3-methylcyclobutyl}-2-hydroxyethylmethacrylate]”, Polymer International, 48, 12, 1999

409. M. Coşkun, K. Demirelli, İ. Erol and M. Ahmedzade, “Thermal degradation of poly [2-(3-aryl-3methylcyclobutyl)-2-hydroxyethyl methacrylate]”, Polymer Degradation and Stability, 61, 3, 493, 1998

410. O. Whichterle, “Encylopedia of Polymer Science and Technology”, 15, 273, 1971

411. M. Miyata, S. Senda and K. Takemoto, “Functional monomers and polymers, 115. Permeability of hydrogel membranes consisting of copolymers containing pendant nucleic acid bases”, Die Makromolekulare Chemie, 185, 4, 647, 1984

412. T.A. Horbett, “Advanced Biomaterials”, 3, 283, 1982

413. M. Kumakura and I. Kaetsu, “Radiation polymerization of 2-hydroxyethyl methacrylate in the presence of biological substances”, Journal of Polymer Science: Polymer Letters Edition, 21, 8, 609, 1983.

414. H.N. Vale and T.R. Greer, “Ex vivo shunt testing of hydrogel-silicone rubber composite materials”, Journal of Biomedical Materials Research, 16, 4, 471, 1982

415. M. Shimada, M. Unoki, N. Inaba, H. Tahara and I. Shinohara, T. Okano, Y. Sakurai and K. Kataoka, “Effect of absorbed protein on the adhesion behavior of platelet to the microdomain surface of 2-hydroxyethyl methacrylate-styrene block copolymer”, European Polymer Journal, 19, 929, 1983

416. J. Razga and J. Petranek. “Thermal degradation of poly-2-hydroxyethyl methacrylate by pyrolysis gas chromatography”, European Polymer Journal, 11, 12, 805, 1975

417. D. Braun and R. Steffan, “Gas chromatographic determination of pyrolysis products from poly (2-hydroxyethyl methacrylate)”, Polymer Bulletin, 3, 1-2, 111, 1980

418. J. D. Lee, “Concise Inorganic Chemistry”, Chapman and Hall, 1991

Publications

Hindawi Publishing Corporation
Journal of Nanotechnology
Volume 2010, Article ID 531284, 5 pages
doi:10.1155/2010/531284

Research Article

Novel Nanocomposite Optical Plastics: Dispersion of Titanium in Polyacrylates

Gunjan Suri,[1] Mukti Tyagi,[1] Geetha Seshadri,[1] Gurcharan Lal Verma,[2] and Rakesh Kumar Khandal[1]

[1] *Shriram Institute for Industrial Research, 19, University Road, Delhi 110007, India*
[2] *Department of Chemistry, Delhi College of Engineering, Bawana Road, Delhi 110042, India*

Correspondence should be addressed to Rakesh Kumar Khandal, rkhandal@shriraminstitute.org

Received 5 December 2009; Accepted 17 January 2010

Academic Editor: Apparao M. Rao

Copyright © 2010 Gunjan Suri et al. This is an open access article distributed under the Creative Commons Attribution License, which permits unrestricted use, distribution, and reproduction in any medium, provided the original work is properly cited.

Polyacrylates have become the preferred materials for optical applications replacing the conventionally used glass due to their superior optical clarity. The major disadvantage with polyacrylates is their low (1.40–1.50) refractive index besides their poor impact resistance. The improvements in refractive index as well as mechanical properties can be achieved by way of incorporation of metals or metal compounds in the matrix. A novel methodology for the incorporation of high refractive index metals into low refractive index polymeric materials to improve the refractive index and impact resistance of the latter has been developed. With the in-situ formation of nanoparticles of TiO_2, the refractive index of polyacrylates improved from 1.45 to 1.53 and the Abbe number increased from 40 to 57. One of the interesting dimension of this study pertains to the possibility of tailor-making of the two key optical properties of materials by way of varying the amount of TiO_2 being formed in-situ. Thermal stability and impact resistance of nano dispersed (4.3% by wt. of Ti) polyacrylates are found to be better than the neat polyacrylates. Moreover, TiO_2-containing polyacrylate is of light weight. TEM, SEM, and IR analysis confirms the in-situ formation of nanoparticles of TiO_2. Gamma irradiation has been used as an eco-friendly technique for polymerization. The developed compositions can be cast polymerized into clear and bubble free material for optical applications.

1. Introduction

Amongst the conventional materials used for optical applications, glass has been the most popular and till recently considered as the preferred candidate material. Glass, besides being a brittle and heavy material, is also prone to scratches. Plastics with optical properties as good as glass, if not better, have been found to be a better material than glass for various optical applications [1–7].

Apart from being light weight, optical plastics exhibit optical properties like refractive index, Abbe number, and transmittance superior to glass. These days, it has become possible to maneuver all of these properties by designing suitable optical plastics. However, it has been a challenge to manufacture optical plastics with high refractive index and high Abbe number. The other big challenge pertaining to the development of optical plastics concerns the tailor-making of properties. It has not been possible so far to have chemistries that can produce materials of varying properties as per requirements. For this, composite materials in devices such as lenses, coatings and filters are being extensively studied [8–11]. Organic-inorganic composite materials are being considered as the potential candidates for optical devices due to their properties of improved hardness, high refractive index and high Abbe number. The inorganic component such as metals and metal salts provide physico-mechanical properties to the matrix whereas the organic part or continuous phase such as plastics binds them together providing a uniform distribution of reinforced material, that is, metals. One of the approaches found [12] feasible and possible by the authors pertains to the in-situ synthesis and dispersion of nanoparticles of metals or metallic salts for the preparation of metal containing compositions. Incorporation of titanium in plastic matrices to form homogeneous and optically clear compositions was a challenge till recently.

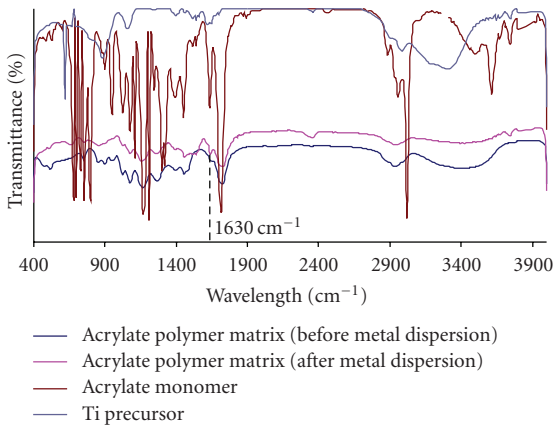

Figure 1: FTIR-Analysis of (a) Acrylate monomer, (b) Titanium precursor, (c) Acrylate polymer matrix (without metal dispersion), (d) Acrylate polymer matrix (with metal dispersion).

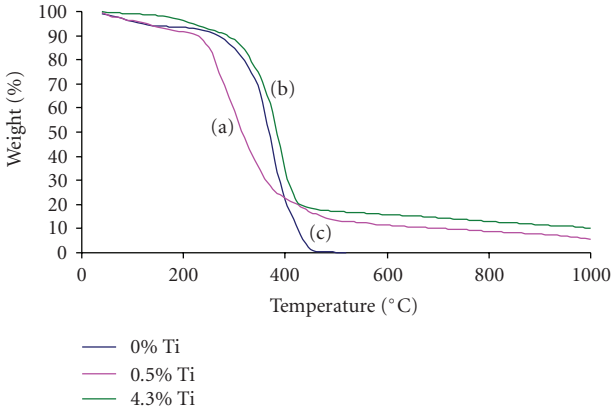

Figure 2: Thermogravimetric analysis of titanium containing nanocomposites and reference material.

Polyacrylates have been recognized as an obvious choice for optical applications, for example, spectacle lens [13]. The refractive index of polyacrylates is limited between 1.42 to 1.49 and to increase the refractive index further, dispersion of high refractive index metal compounds is one of the available options. The high refractive index and high hardness of titanium makes it a desirable metal for dispersion in optical plastics. It would be interesting to prepare high refractive index polymers based on acrylate as a base material.

In the present study, an attempt has been made to disperse titanium in different percentages in acrylate matrix and subsequently cast polymerized into lenses. Gamma radiation has been adopted for polymerization. By using gamma irradiation, the authors have been successful in creating a new range of acrylate polymers with unique features of high refractive index and high Abbe number.

2. Materials and Methods

2.1. Raw Materials. Acrylate monomer (99.9%) was procured from ACROS Chemicals, USA. Titanium precursor of industrial grade was procured from a local source. All the raw materials were used as such without further purification.

2.2. Methodology

(a) Dispersion of Titanium. Titanium precursor was added to the hydroxy alkyl acrylate monomer under vigorous stirring at room temperature for the formation of nanoparticles. The maximum possible amount of titanium that can be dispersed without adversely affecting the optical clarity of the acrylate monomer was determined and studied further.

(b) Cast Polymerization. The compositions were degassed under vacuum and injected into glass molds fitted in a gasket. They were then cast polymerized into lenses using gamma irradiation at dose rate of 25 kGy/12 hrs.

2.3. Characterization

(1) FTIR Analysis. The metal containing polymers were evaluated by FTIR for structural elucidation. The FTIR Spectrophotometer FTIR-ATR BOMEM (FTLA 2000) in transmittance mode from 4000–400 cm^{-1} was used.

(2) Thermal Analysis. Thermogravimetric analysis (TGA) was performed using SDT 2960 of TA Waters Instruments, USA. TGA was used to measure the thermal stability of the metal containing acrylate and to evaluate the residue content. The studies were carried out in nitrogen atmosphere at a heating rate of 10°C/min, from room temperature to 1000°C.

(3) Particle Size and Surface Morphology and Homogeneity. Transmission Electron Microscopy (TEM) was performed on Morgagni 268D to determine the dispersion and particle size of the nanoparticles in the polymer matrix.

Scanning Electron Microscopy (SEM) was performed on LEO 435 VP to study the particle shape of the dispersed material and surface morphology of the polymer.

Homogeneity of the cast polymerized lenses were evaluated with Polariscope Model 243, PTC Instruments, USA for the presence of bubbles in the lenses.

(4) Refractive Index and Abbe Number. Atago Refractometer DRM4 was used to determine the refractive index and Abbe number of the titanium nanocomposites [14].

(5) Transmittance (%). UV-Vis Spectrophotometer (Shimadzu 1700) was used to determine transmittance of the titanium containing polymer nanocomposites.

(6) Specific Gravity. Specific gravity of the polymer was determined as per ASTM D-792-00 [15].

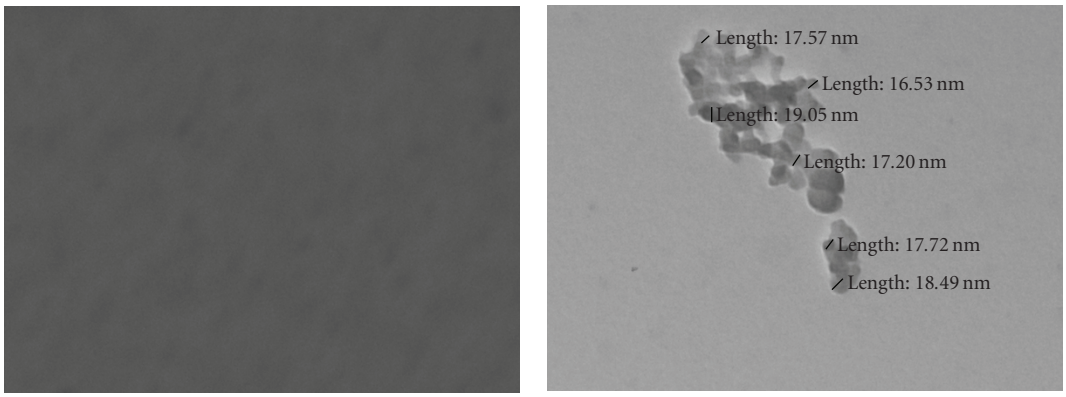

(a) (b)

Figure 3: TEM images of (a) Acrylate matrix (without metal dispersion) (b) Acrylate matrix (with metal dispersion). The images confirm the dispersion of particles of size <20 nm.

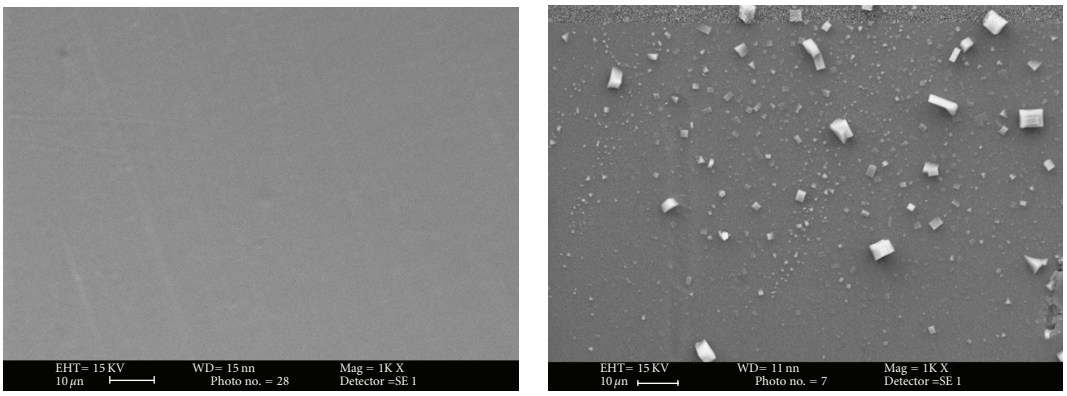

(a) (b)

Figure 4: SEM images of (a) Acrylate matrix (without metal dispersion), (b) Acrylate matrix (with metal dispersion). The images confirm the presence of nanoparticles in the polymer matrix.

(7) Inductively Coupled Plasma (ICP). Inductively Coupled Plasma technique was used to determine the amount of titanium present in the matrix. The studies were carried out using ICP-OES (VISTA-MPX EL06033904) of Varian Instruments, Australia.

(8) Ash Content. Muffle furnace maintained at 600°C was used for evaluating the ash content of metal containing polymers. The residue was then weighed and ash percentage was calculated using the following formula:

$$\text{Ash } (\%) = \frac{(W_3 - W_1)}{(W_2 - W_1)} \times 100, \quad (1)$$

where W_1 = weight of empty crucible, W_2 = weight of crucible + sample, and W_3 = weight of ash + crucible (after heating).

3. Results and Discussion

(1) *FTIR Analysis.* FTIR spectra (Figure 1) of acrylate-titanium composite confirms the formation of titanium-acrylates.

The stretching vibration bands at 1730 and 2950 cm^{-1} are ascribed to C=O and C–H bonds, respectively, [16]. The presence of absorption band at 1630 cm^{-1} is due to TiO_2 and a broad absorption band at 3400–3500 cm^{-1} may be attributed to the Ti–OH bond [12]. It can infact, be said that the IR studies confirm the simultaneous formation and dispersion of TiO_2 by the formation of intermediates in the acrylate matrix during the dispersion of the titanium precursor besides the formation of titanium-acrylate monomer. The mechanism is described (2)

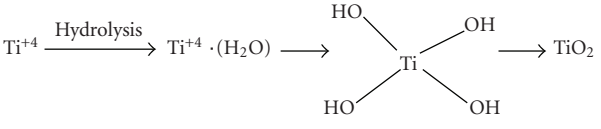

(2)

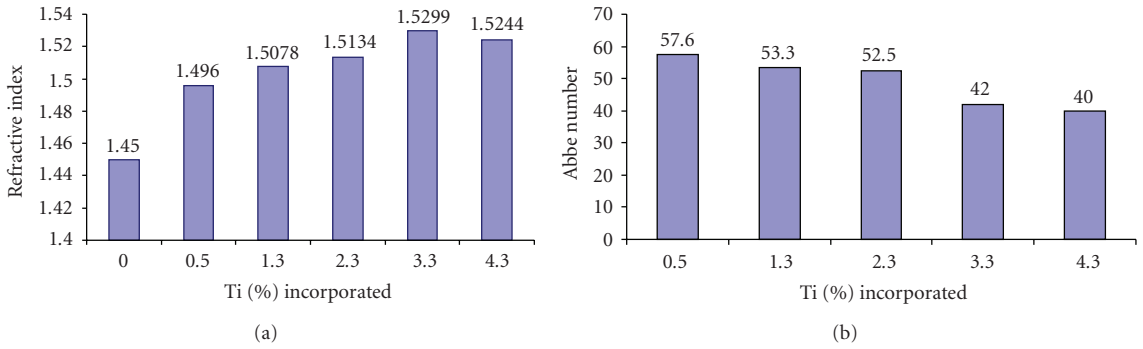

Figure 5: (a) Refractive index increases with increase in titanium content and (b) Abbe number decreases with increase in titanium content.

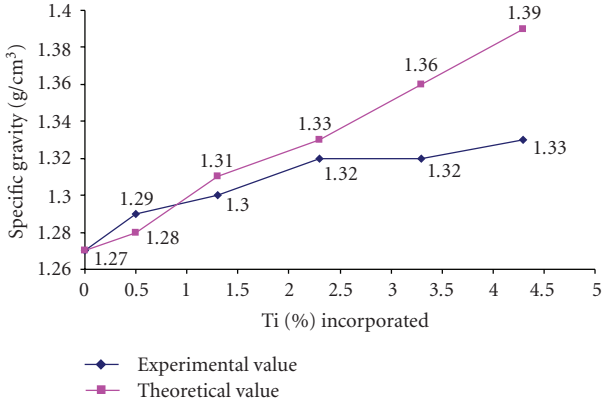

Figure 6: Specific gravity of the polymer increases with increase in titanium content.

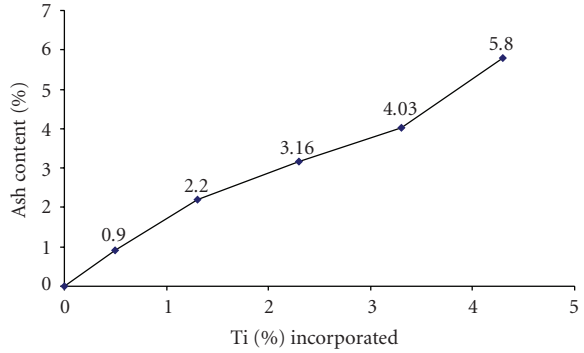

Figure 7: Ash content increases with increase in titanium content confirming the dispersion of titanium in the acrylate matrix.

(2) *Thermal Analysis.* TGA analysis shows the thermal stability of the acrylate polymer and metal containing polymers. The TGA graphs in Figure 2 shows that the neat polymer decomposes completely without any residue at ~500°C while the metal dispersed polymer shows a residual content of ~5% in (a) and 10% in (b).

The thermal stability of metal dispersed polymer is increased significantly as the content of the metal increases; the initial decomposition of the polyacrylate matrix without dispersion is at 120°C which increases to ~220°C in the case of 0.5% dispersion of titanium (a) and to ~240°C in the case of 4.3% dispersion of titanium (b).

(3) TEM and SEM Analysis. TEM images indicate a particle size <20 nm as shown in Figure 3(a) and 3(b).

The SEM images (Figure 4) confirms the shape of titanium particles to be cuboidal. The lenses were evaluated through polariscope and were found to be bubble free.

(4) Refractive Index and Abbe Number. The effect of titanium content on the refractive index of the acrylate matrix can be understood from Figure 5(a). As the incorporation of titanium in the acrylate matrix increases, the refractive index increases from 1.45 to 1.53. The effect of incorporation of titanium in the acrylate monomer on Abbe number can be seen from Figure 5(b). The Abbe number decreases from 57 to 40.

(5) Transmittance (%). Titanium containing acrylates were found to be clear and transparent having a transmittance of more than 90%. This confirms the formation of transparent and clear compositions due to the dispersion of nanoparticles in the acrylate matrix.

(6) Specific Gravity. Specific gravity of the titanium containing polyacrylates is depicted in Figure 6. The specific gravity of the samples increases with the increase in the titanium content. Even though titanium is a heavy metal of specific gravity of 4.54 g/cm^3, the specific gravity of the polymers is in the range of 1.29 to 1.33 which is similar to the specific gravity of optical polymers such as Polycarbonate (1.28), Polymethyl Methacrylate (1.26) and Polythiourethane (1.36) which supports the fact that metal composites are suitable for optical applications.

(7) Inductively Coupled Plasma (ICP). ICP analysis was carried out to determine the percentage dispersion of titanium in the metal containing polymers. The ICP results are found to agree closely with the theoretical value and falls in the range of 0.5% to 4.3% by wt.

(8) Ash Content. Ash content of the sample as evaluated from the furnace studies was used to indicate the residue (%) of the metal containing polymer. The polymer was burnt to ash and the residue (%) was calculated. The graph in Figure 7 shows the increase in ash content (%) with increase in content of titanium.

4. Conclusions

From the above studies, the following conclusions can be drawn:

(1) Metal containing polyacrylates with improved refractive index and desired Abbe number suitable for optical applications have been developed successfully.

(2) Microscopy studies indicate the formation of transparent and clear nanocomposites where the refractive index and Abbe number can be tailor made between 1.45–1.53 and 40–57, respectively.

(3) Novel nanocomposites of polyacrylates have been developed for the first time which paves the way for the use of hybrid materials for high refractive index applications.

Acknowledgments

The authors wish to express their sincere thanks to the Management of Shriram Institute for Industrial Research, India, for guidance and support. The authors also thank Department of Science & Technology, India for sponsoring the work.

References

[1] M. Tyagi, M. Verma, G. Seshadri, A. Malik, S. Agarwal, and R. K. Khandal, "Development of metal containing polymers for optical application," *Journal of Polymer Materials*, vol. 23, no. 1, pp. 21–28, 2006.

[2] H. Dislich, "Plastics as optical materials," *Angewandte Chemie International Edition*, vol. 18, no. 1, pp. 49–59, 1979.

[3] M. Tyagi, G. S. Jha, G. Seshadri, A. Malik, S. Aggarwal, and R. K. Khandal, "Metal containing polymers for optical applications; part II," *Journal of Polymer Materials*, vol. 24, no. 2, pp. 135–148, 2007.

[4] J. D. Lytle, *Handbook of Optics*, McGraw Hill, New York, NY, USA, 2nd edition, 1995.

[5] W. F. Frank, "Precision plastics optics for optical storage," in *Precision Plastic Optics for Optical Storage, Displays, Imaging, and Communications*, vol. 3135 of *Proceedings of the SPIE*, pp. 169–178, July 1997.

[6] M. Verma, G. S. Jha, G. Seshadri, and R. K. Khandal, "Optical plastics—a wonder material," *Journal of the Indian Chemical Society*, vol. 82, no. 12, pp. 1113–1118, 2005.

[7] G. S. Jha, G. Seshadri, A. Mohan, and R. K. Khandal, "Development of high refractive index plastics," *e-polymers*, no. 120, pp. 1–25, 2007.

[8] G. Philipp and H. Schmidt, "New materials for contact lenses prepared from Si- and Ti-alkoxides by the sol-gel process," *Journal of Non-Crystalline Solids*, vol. 63, no. 1-2, pp. 283–292, 1984.

[9] B. Wang, G. L. Wilkes, J. C. Hedrick, S. C. Liptak, and J. E. McGrath, "New high refractive index organic/inorganic hybrid materials from sol-gel processing," *Macromolecules*, vol. 24, no. 11, pp. 3449–3450, 1991.

[10] F. Papadimitrakopoulos, P. Wisniecki, and D. E. Bhagwagar, "Mechanically attrited silicon for high refractive index nanocomposites," *Chemistry of Materials*, vol. 9, no. 12, pp. 2928–2933, 1997.

[11] A. Ershad-Langroudi, C. Mai, G. Vigier, and R. Vassoille, "Hydrophobic hybrid inorganic-organic thin film prepared by sol-gel process for glass protection and strengthening applications," *Journal of Applied Polymer Science*, vol. 65, no. 12, pp. 2387–2393, 1997.

[12] W. C. Chen, S. J. Lee, L. H. Lee, and J. L. Lin, "Synthesis and characterization of trialkoxysilane-capped poly(methyl methacrylate)-titania hybrid optical thin films," *Journal of Materials Chemistry*, vol. 9, no. 12, pp. 2999–3004, 1999.

[13] H. A. Hornak, *Polymers for Lightwave and Integrated Optics*, Marcel Dekker, New York, NY, USA, 1992.

[14] "American Standard Test Method for Index of Refraction of Transparent Organic Plastics ASTM D-542," 2009.

[15] "American Standard Test Method for density and specific gravity (Relative density) of plastics by displacement ASTM D-792-00," 1995.

[16] A. Leaustic, F. Babonneau, and J. Livage, "Structural investigation of the hydrolysis-condensation process of titanium alkoxides $Ti(OR)_4$(OR = OPri,OEt) modified by acetylacetone. 1. Study of the alkoxide modification," *Chemistry of Materials*, vol. 1, no. 2, pp. 240–247, 1989.

e-Polymers **2010**, no. 106

http://www.e-polymers.org

ISSN 1618-7229

Challenges in preparation of metal-containing nanocomposites; dispersion of titanium into plastics

Gunjan Suri,[1] *Pranshu Chhabra,*[1] *Ruchi Gupta,*[1] *Shikha Saxena,*[1] *Mukti Tyagi,*[1] *Geetha Seshadri,*[1] *Gurucharan Lal Verma*[2] *Rakesh Kumar Khandal*[1*]

[1*]Shriram Institute for Industrial Research, 19, University Road, Delhi-110007, India; phone: +91-11-27667850; fax: +91-11-27667676; *e-mail: rkhandal@shriraminstitute.org*

[2] Delhi Technological University, Bawana Road, Delhi-110042, India.

(Received: 09 October, 2009; published: 09 October, 2010)

Abstract: Metal containing polymers are of great interest as they have proven to be the most promising materials for applications such as microelectronics, holography and magnetic recording of information. Metal containing polymers also provide an alternative to even the specialty glass materials conventionally used for optical applications.

Metals such as barium, lead and lanthanum have been used to improve the optical properties such as refractive index and mechanical properties such as hardness of optical plastics. The metal-containing optical plastic materials with improved refractive index of as much as 1.60 along with the Abbe number of more than 30 have been successfully designed using these metals by the authors of this paper.

To further increase the refractive index without any drop in Abbe number and to improve the hardness of the polymer matrix, titanium would be the most promising metal. Incorporation of titanium in plastic matrices to form homogeneous and optically clear compositions is a challenging task. This paper reviews the state-of-the-art by which titanium can be dispersed in polymer matrices to form metal containing composites as optical plastics.

Introduction

Plastics or polymers have already become the wonder material of modern times, replacing conventional materials in almost every field of application [1]. Even for applications where polymers could not be used due to their inherent drawbacks, the polymers are being modified to suit the needs of any given requirement. As a result, the conventional materials like metals, glass, wood, etc. are being replaced by plastics.

One of the high value applications for which plastics have been gaining preference over the conventionally used glass materials pertains to the optical devices like spectacle lenses. Efforts are being made to develop optical plastics for this purpose, as evident from the published literature [2]. The aim has been to improve the refractive index as well as the Abbe number besides the mechanical properties of well-known polymers like polycarbonates and polyacrylates. Incorporation of metals and metal salts in plastics to achieve the desired improvements has been the topic of interest in recent years.

Incorporation of metals in glass has been known for years for improving the properties of the glass as per the requirements of the end use applications. Examples of the metals like lanthanum, barium, lead, zirconium, zinc, niobium, etc. in

glass are the prominent ones amongst the many to achieve unique properties of glass. The metals like titanium and niobium have been known for the manufacture of specialty glasses [3].

If some of the characteristics exhibited by metals could be achieved in plastics by making metal-containing optical plastics, a novel material with best of both the organic polymer and the inorganic metal can be obtained. Incorporation of metals or metal salts in plastics has been done through Chemical Vapour Deposition (CVD) and by dispersion using chemical methods. [4].

The metals provide physico-mechanical properties to the matrix whereas the continuous phase i.e. plastic binds them together providing a uniform distribution of reinforced material i.e. metals. Such composite materials involving inorganic materials and organic polymers have become a subject of interest because of the fact that a composite exhibit better electrical, optical, catalytic and mechanical properties than the individual neat polymer [5-9]. The preparation of materials consisting of metals in plastics, yet retaining the optical properties is the challenge!

The studies reported on plastics have shown that incorporation of metals like lanthanum, barium and lead in plastics has resulted in an improved plastic material with desired optical as well as mechanical properties [10-11]. However, it has not been an easy task to incorporate titanium and niobium in plastics.

Titanium has found its niche in many industries owing to its unique properties of high corrosion resistance and good mechanical strength [12-16]. It is considered superior to materials such as aluminium and steel since it is about fourty times lighter than steel. The advantages of using titanium over the other metals are evident from the fact that titanium finds its use in almost all kinds of applications [17-20].

Titanium finds wide use in various industries in its many forms of existence, which are titanium metal, organic titanates and titanium dioxide [21-23]. Titanium metal due to its unique properties of being lightweight, temperature and corrosion resistant is a preferred material for applications in industries such as aerospace, marine, medical and manufacturing equipment. Organic titanates which include basic titanates, polymerized titanates and chelated titanates find wide applications in surface coatings, printing inks and paint industry [24]. The most abundant form (titanium dioxide) is the one preferably used to acquire the attributes of titanium in various products instead of using the pure metal, wherever possible, mainly due to the high cost of extraction of titanium.

The present paper deals with the review of the state-of-the-art on the methodologies of incorporation of titanium in plastics. The challenges involved in getting the dispersions of titanium dioxide in nano range in plastics have been presented to help develop the techniques for this purpose. The focus of research on the development of optical plastics has been to either design new monomers with improved optical properties or to modify the already established optical plastics in use as the base material for spectacle lenses. Homogeneous and transparent metal containing polymers or nanocomposites offer promising materials in the area of optical applications. Nanocomposites are the only way by which the limitations of refractive index and Abbe number of polymers can be overcome [25-26]. This paper also presents the methodologies involved in the dispersion of titanium (through its various forms) in plastic matrices, mainly for optical applications.

Applications of plastics can be divided into two diverse types: those in which the product is used in a transparent condition, and those in which complete opacity is required [27]. An important and challenging aspect of incorporating titanium in the form of titanium dioxide pigment in plastics is its dispersibility. A uniform dispersion of the oxide within the plastic matrix is needed to impart maximum opacity without causing loss of physical and mechanical properties. The high refractive index and hardness of titanium dioxide make it the most desirable material for dispersion. Thermodynamically stable dispersion of particles in a polymeric liquid is enhanced for systems where the radius of gyration of the linear polymer is greater than the radius of the particles. Even when the dispersed state is thermodynamically stable, it may be inaccessible unless the correct processing strategy is adopted. This is due to the fact that light directed at the polymer containing large metal oxide particles would be reflected back to the light source or deflected to the side, reducing the apparent transparency of the polymer.

Properties of titanium

Titanium is a lustrous, light and strongly metallic white colored metal recognized for its high strength to weight ratio [28], ductile nature [29], high melting point of 1650 °C and density of 4.05 g/cm^3. Though a number of inorganic & organic compounds of titanium are known, one of the most important compound of titanium finding applications in a wide range of industries is titanium dioxide or TiO_2. TiO_2 powder is chemically inert, resists fading in sunlight and is opaque. Pure TiO_2 has a very high refractive index; higher than diamond [30]. The pigment has UV resistant properties and is an opacifier.

Various properties of titanium that make it useful for different applications are listed in Table 1.

Tab. 1. Properties of titanium metal and its corresponding applications.

Properties	Applications
High melting point (~1649 ^oC)	Refractory metal
Resistance to corrosion	Coating material, propeller shafts, heat exchangers for desalination
High strength to weight ratio	Aircrafts, naval ships, fishing rods, golf rods, wheelchairs
Biocompatible	Surgical implants
Non-ferromagnetic	Biomedical instruments such as MRI
Inertness and colorability [31]	Jewellery, artworks, etc.

Origin & occurrence of titanium

Titanium owes its name to the “Titans”, the mythical Greek first sons of the earth, and the ore ilmenite has been named after it was discovered in the Mountain Ilem in Russia [32-33].

Titanium is found in nature mainly in inorganic ores and is extracted using different processes. Naturally occurring titanium is composed of five stable isotopes ^{46}Ti, ^{47}Ti, ^{48}Ti, ^{49}Ti, ^{50}Ti, out of which ^{48}Ti is the most abundant isotope found in minerals like anatase, rutile, ilmenite, perovskite and titanite [34-37]. Both inorganic and organic compounds are formed synthetically using various industrial processes.

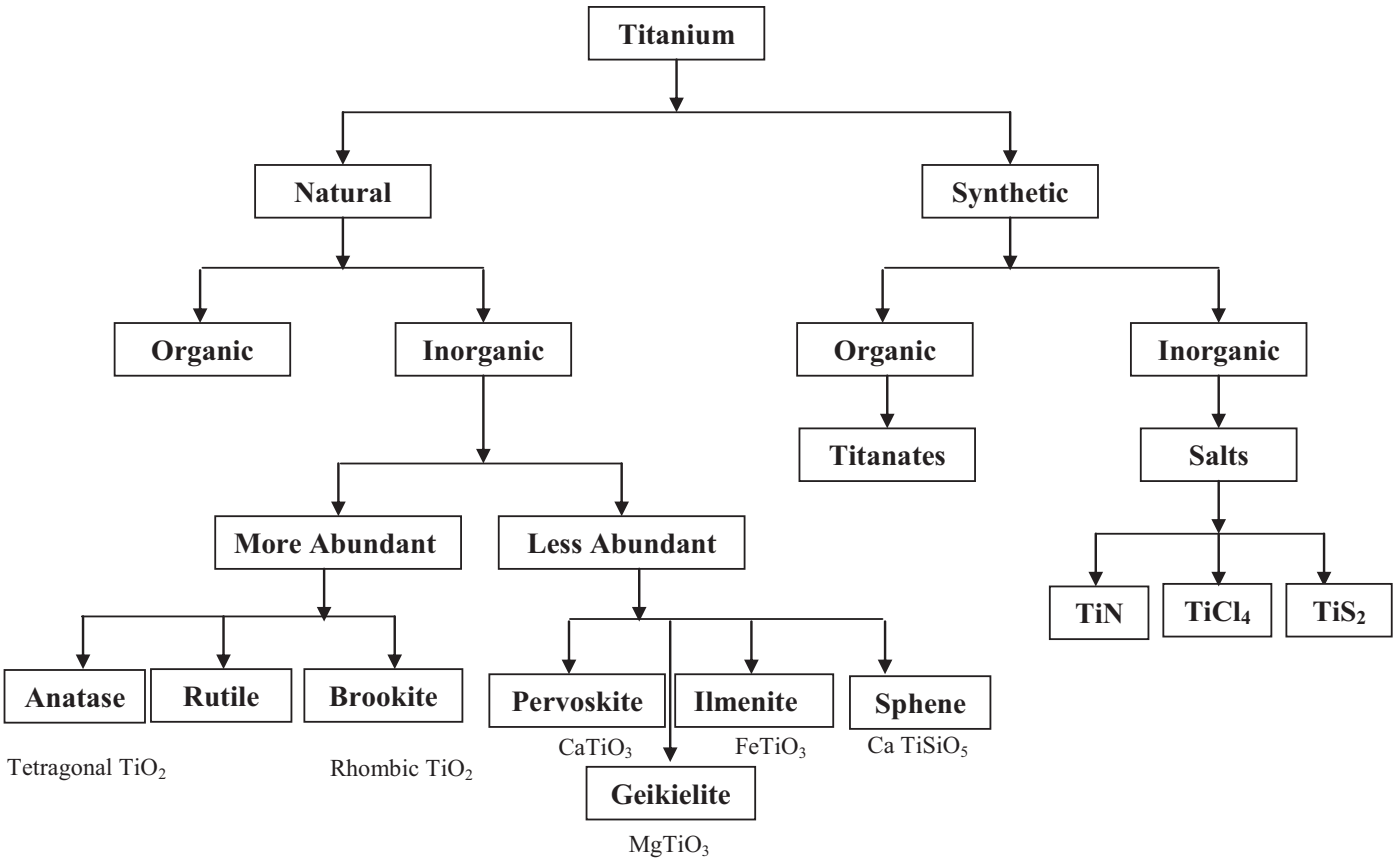

Fig. 1. Occurrence of titanium in its various forms, both natural and synthetic as organic or inorganic.

Titanates and salts of titanium are synthetic forms of titanium. The occurrence of titanium in its various forms is as depicted in Figure 1.

Ilmenite is the most common mineral [38] and rutile has been an important source of titanium. About 95% of titanium ore extracted from the earth is processed further or refined into titanium dioxide (TiO_2) used in various industries like paints, cosmetics, plastics, etc. [39]. Of that, 90%-95% is used as such and the rest is used for producing titanium metal.

Titanium dioxide is used for a variety of applications in photovoltaic cells, batteries, sensing, optical emissions, photonic crystals, catalysis and photocatalysis to perform many functions [40-46]. When titanium dioxide is used as a catalyst, it is required to have activity not only on the main reaction but also selectivity, mechanical strength, acid resistance, heat resistance and service durability. For applications involving catalytic activity, particle sizes of nano-range (< 10 nm) are ideal. For other applications, larger particles of 10-100 nm or 100 – 200 nm are desirable [47]. A compatible dispersion medium allows the particles to maintain a high electrostatic charge with no agglomeration. To prepare these types of dispersions, parameters such as pH, ion concentration, size of particles, temperature, etc. are to be controlled [48].

When titanium dioxide is used as a cosmetic material, it is required not only to have an ultraviolet shielding effect but also smoothness, texture and transparency. When it is used as a coating material, it is required to have excellent film forming properties, adhesive properties, hardness, mechanical strength and abrasion resistance in addition to transparency and high refractive index [49]. It is highly desirable to have homogeneously dispersed compositions of titanium dioxide in organic matrices to provide highly transparent coating materials, high refractive index materials, abrasion resistant coatings and UV resistant coatings [50].

Chemistry of titanium

Titanium metal is considered to be physiologically inert. This metal form a passive and protective oxide coating (leading to increased corrosion-resistance) when exposed to elevated temperatures in air, but at room temperature it resists tarnishing. When it first forms, this protective layer is only 1–2 nm thick but continues to slowly grow; reaching a thickness of 25 nm in four years. Titanium burns in air when heated to 1200 °C and in pure oxygen when heated to 610 °C or higher, forming titanium dioxide. This results in the fact that it is not possible to melt the metal in open air as it burns well before its melting point is reached, so melting is possible only in an inert atmosphere or in vacuum. It is also one of the few elements that burn in pure nitrogen gas (it burns at 800 °C and forms titanium nitride which causes embrittlement). Titanium is resistant to dilute sulfuric acid and hydrochloric acid along with chlorine gas, chloride solutions, and most organic acids. It is paramagnetic, weakly attracted to magnets and has fairly low electrical and thermal conductivity [51].

Experiments have shown that natural titanium becomes radioactive after it is bombarded with deuterons, emitting mainly positrons and hard gamma rays. The metal is dimorphic. At 880 ^{o}C, the hexagonal alpha form slowly changes to the cubic beta form. Metal combines with chlorine at 550 ^{o}C. It also reacts with the other halogens and absorbs hydrogen [52].

Organic salts [53-64]

Organic compounds of titanium, which are of commercial importance, are titanium alkoxides and titanium chelates.

Organic titanium compound are materials having a covalent bond between titanium and another atom which are also bonded to a carbon-based group prepared from $TiCl_4$ by reaction with main group organometallics. Although a Titanium (IV) atom strives to achieve a coordination number of six by sharing electron pairs of nearby ester molecule but this tendency is opposed due to steric crowding. This is the reason why only monomers, dimers and trimers of titanium are obtained such as tetra isopropyl titanates, tetramethyl titanates and tetra ethyl titanates.

Titanium alkoxides are excellent catalysts for esterification, transesterification and crosslinking of ester containing resins and epoxides. Titanium chelates are widely used in crosslinking of dilute polysaccharide solutions.

Organic Titanates perform three important functions for a variety of industrial applications, which includes (a) catalysis (b) polymer crosslinking and (c) surface modification.

Inorganic salts

The most widely known inorganic forms of titanium are the oxides and chlorides. The sulfide form of titanium known as titanium sulfide also exists.

-Oxides, chlorides & sulfides

Titanium dioxide or Titania is used in almost every field as a white pigment for manufacture of paint and paper, as a filler in rubber and plastics due to its exceptionally high refractive index higher than that of diamond in the visible region of the electromagnetic spectrum. While large crystals of Titanium dioxide are transparent and do not refract, fine particles scatter light very strongly [65].

There are three crystalline forms of TiO_2; rutile (the most common form), anatase and brookite. Both anatase and brookite get converted to rutile at elevated temperatures. All contain six- coordinated titanium atoms; in anatase and brookite, the octahedron is distorted. Natural forms of TiO_2 are often colored due to the presence of impurities. Synthetic TiO_2 is manufactured either by oxidizing $TiCl_4$ with oxygen or by the hydrolysis of Ti^{IV} sulfate. Rutile can be reduced to give a wide range of non-stoichiometric oxide phases such as the Magnelli-type phases Ti_nO_{2n-1} ($4 \leq n \leq 9$), the broad non-stoichiometric phases TiO_x ($0.7 \leq x \leq 1.3$), and the lower oxides Ti_3O_5 and Ti_2O_3 [66].

A large number of complex oxides or 'titanates' are known. They are produced by fusing TiO_2 at high temperatures with stoichiometric amounts of the appropriate metal oxide. Two main types of titanates exists; orthotitanates & metatitanates. Orthotitanates, $M_2^{II}TiO_4$ in which the M^{II} (M = Mg, Mn, Fe,Co, Ni) is of (approximately) same size as Ti^{IV} have the ilmenite structure, $FeTiO_3$. Metatitanates, $M^{II}TiO_3$, contain M^{II} (M= Ca, Sr, Ba) which is larger than Ti^{IV}; in these compounds the preferred structure is that of perovskite, $CaTiO_3$. Another important structural type of titanate is the spinal structure, $MgAl_2O_4$ which is possessed by the compounds $M^{II}{}_2TiO$ (M = Mg, Zn, Mn, Fe, Co) [67]. The most important sulfide is TiS_2, which has a CdI_2 layer structure in which the Ti atoms occupy octahedral sites between alternate layers of close-packed sulfur atoms. The adjacent sulfur layers are able to intercalate Lewis bases such as aliphatic amine [68].

Apart from the oxides & sulfides, titanium halides such as titanium chloride is also well known. titanium tetrachloride ($TiCl_4$) [69-70] is the basic raw material from which all the organic titanium compounds are made and are readily converted to titanium esters (tetra alkyl titanates) [71].

Need for titanium dispersions

Some of the challenges listed below make working with titanium in its purest form a huge challenge:

1. Rarity of the pure metal
2. Low thermal conductivity of titanium leading to high manufacturing cost.
3. Adhesion with other metals
4. Loss of strength at temperatures > 427 $^{\circ}$C

5. Titanium catches fire and causes severe damage where it rubs against other metals at elevated temperatures.

It is due to these reasons that titanium dispersions in polymers are achieved through the fine particles or nanoparticles of TiO_2. Organic dispersions are those in which both polar & non-polar organic fluids and non-ionic steric stabilizers or dispersants are used to prevent the particles from forming larger aggregate ions [72]. Generally the dispersion in polymeric materials has proven to be difficult and frequently results in phase separation due to agglomeration. The agglomerates act as larger particles that may scatter or reflect light. So for transparency, the small particles must be highly dispersed (non-agglomerated) in the polymer to avoid light scattering [73].

Dispersion of metal oxide particles in polymers is possible by the surface treatments such as a) coating of the metal oxide particles with an organic acid or a surfactant to create an organophilic surface and b) electrostatic stabilization by the creation of an aqueous colloid. To obtain transparent dispersions is a huge challenge where the transparency of a polymer depends on the size and refractive index of the metal oxide particles [74].

Challenges associated with dispersion of titanium

Composite materials having homogeneously dispersed inorganic nanoparticles in an organic phase have been used as protective coatings for various applications. Such materials have improved abrasion resistance and optical properties as compared to the corresponding organic binder not having nanoparticles dispersed therein. Nanocomposite materials containing various inorganic nanoparticles such as titania have been described. The rutile form is the most desirable form due to hardness and refractive index [75]. The major problems with titanium dioxide sols, particularly the rutile crystalline phase include: long process times, need to use additional stabilizing counter ions which must be laboriously removed prior to use, extreme pH conditions and limited stability [76].

It would be desirable to have quick and easy methods for preparing the stable colloidal dispersions of inorganic particles containing titanium where the particles have properties comparable to the rutile form of titanium dioxide. It would also be desirable to homogeneously incorporate such particles into an organic binder to provide high refractive index abrasion resistant coatings. Fine particles of titania having narrow particle size distribution and little aggregation have been produced by the hydrolysis of the metal halide in the presence of an organic solvent [77].

Dispersing aids have been used to disperse metal oxides particles in organic materials to form transparent colloids and ceramers. One method of ceramer preparation is to treat metal oxide particles with specific organic acids or surface active agents before combining the metal oxide particles with polymer precursors. Transparent polymer/metal oxide compositions having high refractive indices are desirable but difficult to obtain because the metal oxide particles, when combined with polymer precursors, may agglomerate and decrease the transparency of the resulting ceramers [78].

The major challenge with dispersion of titanium dioxide particles is the inability to suitably stabilize suspensions of the nanoparticles. It would be desirable to have stable suspensions of nanoparticles that could be used days later or preferably even weeks or months later. Existing titanium dioxide particles and solutions are often too unstable to be economically feasible for use in suspension form. Expensive drying and reconstituting steps are needed to use many existing titanium dioxide particles. The challenge is to use particles with controlled particle size, shape and stability and

methods for economic production. The use of dispersing agents give stable dispersion of nanoparticles of titanium dioxide with more uniform shape, size and more stability than titanium nanoparticles formed without the use of a dispersing agent. Dispersing agents are used to influence the average size of the titanium dioxide nanoparticles [79-82]. Dispersing agents can be alkoxyorganosilanes, carboxylic acids or combination of both. Examples of alkoxyorganosilanes are octyltriethoxysilane, octadecyltrimethoxy silane, hexadecyltrimethoxy silane or combination of all. Carboxylic acids having C_3-C_{18} carbon chain length is also preferred as dispersing aids.

It is challenging to disperse titanium dioxide as such into polymer matrices. It is preferable to use highly dispersed colloidal titanium dioxide or sols. The particles dispersed in a sol are spherical or pseudospherical agglomerates, non-uniform in particle diameter leading to opacity and poor transparency [83-84]. The sol is stable only in the acid region in a pH of less than 3; its limitations are that it forms precipitates or gels under neutral or alkaline conditions. When the sol is mixed with an organic solvent, it becomes unstable and precipitates out thus making it difficult to be used as a hard coating material to be applied to the surface of plastics [85-88].

Particles in a sol assume a spherical or pseudospherical configuration, when it is used as a coating, by mixing it with a base resin. The TiO_2 particles are not present densely in the coating and leave spaces among the particles. The density of the particles cannot be enhanced thus giving a coating, which is poor in characteristics and strength as coatings for optical plastics [89-90].

Titanium dioxide particles though can be made in very small particle sizes of 50 Å, they can seldom be applied as such due to the fact that the particles are always highly coagulated. Such nanoclusters appear to be indefinitely stable at room temperature in highly acidic solutions. Heating or dilution of such particles results either in flocculation, precipitation or formation of an elastic gel. Titanium dioxide based sols and gels in which the size of the nanoclusters is made much smaller than the wavelength of visible light are the characteristics of a good dispersion [91].

These characteristics of titanium dioxide have been utilized in cosmetic applications where certain types of ultraviolet radiation absorbing compositions have long been in use. Titanium dioxide has been approved for use in cosmetics and that it is known that amorphous titanium dioxide or oxyhydride will absorb short wavelengths. Thus, for particle sizes of titanium dioxide approaching the wavelength of visible light, the high extinction coefficients of titanium dioxide leads to a very high reflectivity for radiation that would normally be absorbed by nanosizes particles. However, titanium dioxide nanoclusters having superior UV absorbing properties are not satisfactorily used in sunscreen compositions because of their noted lack of stability [92].

Tried ways of incorporation of titanium as titania in different plastics

As a pigment

Titania pigments are the most commonly used form of titanium for incorporation into plastic matrices like polyethylene and polypropylene. They are incorporated into commodity plastics for the provision of better brightness, whiteness and opacity than the most commonly used pigments such as ZnO, ZnS. When properly chosen, titania pigments provide extensive protection of polymers from UV light. The common routes to pigmentation of plastics with TiO_2 are described in Table 3.

The methods whereby titania pigments are incorporated into plastic matrices are diverse. Multiple options exists for the plastic processor such as a) solid concentrates b) direct end use pigmentation c) simple dry blends or d) use of liquid colorants. While the use of concentrates is prevalent in most resin categories, nearly all the titanium dioxide used in finished products composed of polyethylene & polypropylene enters by the way of solid concentrates. These concentrates typically vary in pigmentation loading level between 30%-80% (by wt.). The manufacture of these solid concentrates is usually done in internal mixers, continuous mixers or multiple screw extruders [94].

Tab. 3. Common routes to pigmentation with titanium dioxide [93].

Polymers	Route	Manufacturing process
Polyolefins: Polyethylene, Polypropylene	Solid concentrates	Internal mixers, continuos mixers, multiple screw exruders
Poly vinyl chloride(rigid and plasticized)	Dry blends Liquid/paste dispersions	Intensive high speed mixers Roll mills/ disk impeller mixers
Engineering polymers: Polystyrene, Styrene Acrylo Nitrile, (SAN), Acrylonitrile Butadiene Styrene (ABS)	Solid concentrates, intensive blends	Internal mixers, continuos mixers, , high speed dry blenders
Others: Polyacetals, Polycarbonates, Polyacrylates, Polyesters	Melt compounding	Multiple screw exruders

Titanium dioxide is usually intensively mixed in high-speed blenders with rigid PVC resins. Incorporation of titanium dioxide plasticized PVC usually begins with the production of a liquid or paste dispersion of the pigment in monomeric plasticizers or low molecular weight polymers.

Incorporation of titanium dioxide into polystyrene, acrylonitrile, acrylonitrile butadiene styrene & other associated co-polymers and alloys is normally by the way of concentrates prepared on equipment similar to that used in polyethylene i.e. by premixing pigment, plasticizer & surfactant followed by high shear stress dispersion [95].

As transparent dispersions

Since India depends totally on import of optical materials, a need always exists to develop an indigenous technology, which not only serves the Indian stake-holders of the optical market but also to a common man for his daily ophthalmic requirements. Need for a technology to develop scratch resistant and improved refractive index plastics always remains a challenge for the researchers.

Incorporation of titanium to maintain transparency of the dispersed matrix is a big challenge. Transparency of the resultant matrix depends on the particle size of the

dispersant. Incorporation of nanosized titania pigments into polymeric materials has always been a challenge because of the following reasons:

1) High density in comparison to polymer matrices and 2) Agglomeration of nanoparticles due to high specific surface energy [96]

There are various chemical methods through which titania is incorporated into polymer matrices. These include a) ex-situ incorporation and b) in-situ incorporation. High density of titanium dioxide does not allow it to disperse homogeneously in the polymer matrix. This in turn leads to settling down giving an inhomogeneous matrix. The nanoparticles are so strongly adhered to each other that the breaking down of secondary particles into primary particles becomes difficult. This again, in turn, gives rise to non-homogeneity of the polymer matrix incorporated with titanium dioxide.

The high density of titanium dioxide (>4), makes it almost impossible to be dispersed in any organic material. Surface modification using coupling agents and dispersing aids can serve as an effective way of dispersing TiO_2 particles. There has been an increasing interest in the fabrication of TiO_2 thin films because of their useful optical, electrical and chemical properties such as high refractive index, high dielectric constant, remarkable solar energy conversion and photo catalysis [97-111].

Incorporation of titanium dioxide by ex-situ methods

Binding inorganic particles to organic molecules using a bi-functional coupling agent is a useful method for incorporation of TiO_2. Nanoparticles may be incorporated in a binder to form a nanocomposite or the nanoparticles may be taken in a binder precursor and then cured to form a binder [112].

The coupling agent links the organic and the inorganic phases by covalent bonding, hydrogen bonding or simple physical interactions that prevent phase separation. Coupling agents are used to bring about compatibility between inorganic nanoparticles and organic binder. Surface modified agents are used to modify the surface characteristics to achieve properties like compatibility, dispersion and optical clarity. Organo silanes have been used as coupling agents to prepare high refractive index coatings having a refractive index of 1.569. Mixed oxide (nanoparticles) of metals such as titanium/antimony have been prepared from peroxy titanic acid and hexahydroxy antimony and coated onto PMMA [113].

Preparation of acetic acid modified TiO_2 nanoparticles was done by sol gel method and the nanoparticles have been incorporated directly into the polymer matrix such as acrylates to form transparent high refractive index nanocomposite thin films. Increasing the titania content in the hybrid nanocomposite thin film has been found to increase the refractive index. An ultra high refractive index of 2.38 was obtained [114].

Titanium dioxide nanoparticles of the desired shape, size and uniformity are formed by hydrolysing titanium tetrachloride to form an aqueous titanium compound. Titanium dioxide nanoparticles are then precipitated to form a suspension, which is influenced by the presence of bonding of the dispersing agent. Size of the nanoparticles can be controlled by selecting the ratio of titanium precursor to the dispersing agent [115].

A coating composition has been prepared comprising of titanium dioxide having a high refractive index and good hardness. Fine particles of Titanium dioxide have been used in an amount of at least 10% by wt., below which significant increase in

refractive index is not seen. For the surface modification of the particles, organic silicon compounds such as methyl trimethoxysilane or glycidoxy propyltrimethoxysilane have been used which impart increased reactivity and affinity for the resin matrix. Curing catalysts such as ammonium perchlorate is used to cure the composition either before or after applying the coating. Fluidity of the coating composition can be improved using levelling agents such as silicone surface-active agents. The final coating composition was applied onto a plastic lens of urethane resin having a refractive index of 1.594 followed by curing at 120 °C. The cured film has a refractive index of 1.58 [116].

Incorporation of Titanium dioxide by in-situ methods

In-situ methods are more promising to obtain homogeneous dispersions. Hybrids of polyimide titanium dioxide with improved properties of good thermal stability, high optical transparency and good mechanical properties have been fabricated by in-situ methods involving sol-gel reaction of polyamic acid precursor with a modified titanium precursor. Another approach is dissolving the polymer in solvent and mixing with the dispersing media, while the third approach is of melt intercalation which involves heating the polymer upto its glass transition temperature and then mixing it with the dispersing media [117 -118].

Optically transparent polyimide titanium dioxide composite waveguide materials were prepared by the dispersion of nano-sized Titanium dioxide particles in polyimide. The particles were produced through reverse micelle technique using sol-gel method and were dispersed into the fluorinated polyimide solution. The solution was coated on a glass substrate and a polyimide titanium dioxide composite waveguide (4% titanium dioxide concentration) was successfully produced after heat treatment. Refractive index was increased from 1.550 to 1.560 by the incorporation of Titanium dioxide. Particle size was very small, no noticeable scattering loss was observed in the resultant slab waveguide [119].

Photocatalytic, transparent and aqueous titanium dioxide ceramic paint having a particle size between 1-200 nm has been produced for coating glass, metals and plastics. The coatings exhibit properties of being hydrophilic, photocatalytic and having excellent transmittance. Complexing agents such as lactic acid or oxalic acid are employed along with a surface-active agent as dispersing aids to promote dispersion of titanium dioxide [120-121].

Transparent ceramers having a refractive index of ≥ 1.9 have been prepared for optical applications. Conventional materials for optical parts of optical devices such as lenses are glass and plastics [122-123]. These materials have high light transmittance and can easily be processed into devices. Conventional materials such as glass has a refractive index of less than 1.9 and the resulting optical devices have limitations in miniaturization and slimming. Plastics having low moisture resistance and low refractive index, exhibit double refraction and efficiently transmit and condense light. The translucent ceramer can therefore improve the optical properties of optical devices such as lenses, prisms and can miniaturize the resulting optical device [124].

Lanthanum titanate prepared from lanthanum oxide and titanium dioxide in 1:2 ratio has a ultra-high refractive index of 2.3, is transparent to visible & near IR region therefore making it useful for photonic applications [125].

Anti-reflective layers of titanium dioxide prepared by the hydrolysis of tetra isopropoxide have been used for the coating on plastics such as polyesters, polyacrylates and polycarbonates [126]. Titanium dioxide is commonly used as a pigment in the paint industry. It is incorporated as an aqueous dispersion in water-based paints. Number of problems such as high viscosity, agglomeration and settling down of particles to the bottom of the container are associated with aqueous titanium dioxide slurries. To overcome this problem, dispersing agents are used; most common ones being polyacrylic acid. Polyacrylic acid, due to residual acrylic acid, has several disadvantages like risks related to health and safety and effectiveness in neutral conditions limits its use for various applications. Hence, alkyl polyglycoside surfactants are used as effective dispersing agents for aqueous titanium dioxide dispersion. This overcomes the difficulty of being non-toxic and very mild to eyes and skin [127].

Process and processing conditions leads to variations in structure, particle size and optical properties of titanium dioxide [128]. Composites with enhanced refractive index have been synthesized through a sol-gel method. A refractive index of approximately 1.70 has been achieved with 75-wt% titanium dioxide [129]. This has been found to be useful for coating applications.

One of the most important and emerging applications is the development of ferro electric materials. A solution of ferroelectric nanowires of titanium based compound like $BaTiO_3$ (at a high concentration) and polymer can be mixed together and placed in a small electric field to orient them in the desired direction. Such a combination also exhibits a liquid crystal phase [130]. A great deal of research is being carried out on the synthesis of high quality transparent films consisting of polymer-titanium dioxide hybrid nanocomposites and their optical properties.

Bismuth titanate nanoparticles have been dispersed in polyacrylate matrix to obtain composites having a high refractive index of 1.6, high dielectric constant and high optical transmission of 90% [131-134]. Ternary compound system $BaO\text{-}TiO_2\text{-}La_2O_3$ was prepared by solid state reaction technique at temperatures between 1300-1400°C using Ba, Ti, La oxides as starting materials. In another method, $BaTiO_3$ was reacted with the lanthanum titanates to obtain $BaO\text{-}TiO_2\text{-}La_2O_3$ that finds its use as ferrro electric materials [135].

In recent years, in the field of ceramics, fine particles of metal oxide having narrower particle size distribution with no aggregation is desirable, titanium dioxide particularly attracts attention as useful fine particle material in the field of photocatalysis, optical communication, cosmetics, etc [136].

Fine particles of metal oxide have been prepared in various ways, which involves the hydrolysis of metal alkoxide in organic solvents and hydrolysis of organometallic compounds. Particles produced by this method are apt to have wider particle size distribution [137].

Colloids of titanium dioxide, with 2.5 nm average particle diameter were synthesized by hydrolysis of titanium tetrachloride in acidic solution. The as prepared particles were incorporated in polymers such as polyvinyl alcohol, partially hydrolyzed polyvinyl acetate, polyvinyl pyrrolidone and poly(4- vinyl pyridine); nanocomposites transparent in the visible range were obtained. The highest titanium dioxide contents in such materials were achieved with PVAL and PVAC with titanium dioxide content ~35%. Incorporation of titanium dioxide in PVA upto 10.5 vol % enhanced the

refractive index of nanocomposites upto 2.38 compared to 1.521 for the pristine polymer [138].

In –situ synthesis and dispersion of titanium dioxide by sol-gel method has been used for the preparation of optical films where trialkoxy silane capped PMMA titania hybrid optical thin films have been prepared using spin coating and multi-step baking. Titanium butoxide was used for the preparation of titania network in acrylic monomers. FTIR shows good bonding between organic and inorganic moieties. DSC results show good dispersion of the PMMA segment in the titania network. Variation of titania content not only tune the refractive index but also the position of absorption maxima. Refractive indices of the prepared hybrid films were in the range of 1.505-1.553, which increases linearly with the titania content. Hybrid polymer films with Abbe number > 30 showed high transparency in the visible region [139-140].

Hybrid composites were synthesized using titanium tetrapropoxide and multifunctional acrylate or methacrylate. 3-(methacryloyloxypropyl)trimethoxy silane has been used as the dispersant. The organic and inorganic networks interpenetrate together to form a transparent composite. The composites with enhanced refractive index up to 1.68 and potential applications in photonics area by means of micro-explosion method has been reported [141].

Uniform dispersions of titanium dioxide are obtained by the use of organosilane coupling agents. Such dispersions have been used for the coating of polymer, wood and metal surfaces. Such ceramers have been used on articles for abrasion resistance and high gloss appearance for traffic signs, pavement markers, lenses for glasses & microwave oven doors [142 - 143].

UV curable, transparent acrylic resin/ titania organic-inorganic hybrid films were prepared by controlled hydrolysis of titanium tetrabutoxide in Span 85/ Tween 80 reverse micelles & the subsequent in-situ photo polymerization of acrylic monomer. The refractive index and UV shielding properties of the organic polymer increased with the increasing titania content [144].

By using sol-gel method, amorphous titania was introduced into epoxy matrix to prepare a series of high refractive index titanium resin nanocomposite films. To increase the refractive index of the hybrid films, triethoxy silane capped trimercapto thioethylamine was synthesized. Refractive index was tailor-made from 1.61 to 1.797 with the increasing content of TiO_2 from 0% to 65 % [145].

In Shriram Institute for Industrial Research, Delhi, India, a novel methodology for the incorporation of metals into polyacrylate has been developed. In this method, transparent, high refractive index metal containing polyacrylates having a refractive index of 1.60 have been developed. This has been regarded as a breakthrough for the in-situ preparation of metal-polymer nanocomposites.

Titanium dispersed polymers therefore prove to be promising materials for the preparation of high refractive index plastics.

Acknowledgements

The authors wish to express their sincere thanks to the Management of Shriram Institute for Industrial Research, India for the guidance & technical support on this interesting topic of research. The authors also acknowledge Department of Science & Technology for sponsoring the work.

References

[1] Khandal, R. K.; et al. *J. Indian Chem. Soc.,* **2005**, 82, 1, 1113.
[2] Khandal, R. K.; et al. *e-Polymers,* **2007**, 120, 1.
[3] Khandal, R. K.; et al. *e-Polymers*, **2009**, 100, 1.
[4] Eguchi, S.; et al. *United States Patent 5*,113,477, **1992**.
[5] Chang, L. T.; Yen, C. C. *J. App. Polym. Sci.,* **1995**, 55, 371.
[6] Godovsky, D. Y. *Adv. Polym. Sci.,* **1995**,119, 79 .
[7] Nakao, Y. *J. Colloid Interface Sci.,* **1995**, 117, 386.
[8] Aihara, N.; et al. *Langmuir,* **1998**, 14, 4945.
[9] Wang, W.; et al. *Langmuir,* **1998**, 14, 602.
[10] Khandal, R. K.; et al. *J. Polym. Mater.,* **2006**, 23, 21.
[11] Khandal, R. K.; et al. *J. Polym. Mater.,* **2007**, 24, 135.
[12] McQuillan, A. D. and McQuillan, M.K., in H. M. Finniston, ed. '*Metallurgy of the rarer metals'*, Academic Press Inc., New York, **1956**, 335.
[13] Wood, R. A. '*The Titanium Industry in the Mid-1970s*', Batelle Report, MCIC-75-26, Batelle Memorial Institute, Columbus, Oh, **1975**.
[14] Bomberger, H. B., eds., *'Titanium Technology: Present Status and Future Trends'*, The Titanium Development Association, **1985**, 3.
[15] Froes, F. H. and Caplan, I. L. *'Titanium 92 Science & Technology',* TMS, Warrendale, Pa., **1993**.
[16] Joseph, S. S.; Froes (Sam), F. H. *'Light Metal Age'*, **1998**, 4-6 (11-12), 5.
[17] Field, R.; Crowe, P. L. *'The organic chemistry of Titanium'*, Butterworth & Co., (Publishers) Ltd., London, U.K., **1965**.
[18] *Gmelins Handbech der Anorganischen Chemie*, 8th Ed., Springer-Verlag, Berlin, Germany, **1979**.
[19] Pascal, P.; et al. *Nouveau Traite de Chimie Minerale*, Tome IX, Paris, France, **1963**.
[20] Grant, F. A. *Rev. Mod. Phys*., **1959**, 31, 646.
[21] Goodenough, J. B.; Hamnett, A., in O., Medelung, ed*., Landolt Bornstein Semiconductors, Group 3*, Springer-Verlag Berlin, Germany, **1984**, 17, 133.
[22] Egerton, T. A.; Tetlow, A., in R. Thompson, ed., *Industrial Inorganic Chemicals Production and uses*, The Royal Society of Chemistry Cambridge, U.K., " Chapt. 13.
[23] Chase, M. W.; et al., *JANAF Thermochemical Tables-3rd. Ed*. J. Phys. Chem. Ref. Data, 1985, 14.
[24] Beacham, H.H. *Properties & uses of Organic titanates, Advances in Chem. Properties, Metal Organic compounds,* Chap-26, 282.
[25] Khandal, R.K. et al., *United States Patent 0209675 A1*, **2009**.
[26] Khandal, R.K. et al., *PCT/IN07/00097*
[27] Norris, J.R. and Ribbons, D.W. *Methods in Microbiology*, Acad. Press Inc. (London) Ltd., ISBN :12-5215010, **1969**, 1.
[28] *Titanium*, Columbia Encyclopedia, 6th Ed., New York, **2000**.
[29] *Titanium*, Encyclopedia Britannica, **2006**, Retrieved **2006**.
[30] *Titanium*, Los Alamos National Laboratory, **2004**, Retrieved **2006**.
[31] *American Welding Society Guide for the fusion welding of Ti & Ti alloys*, Miami **2006**.
[32] Emsley, J. *Nature's building blocks: An A-Z guide to the elements.* Oxford: Oxford University Press, 451, ISBN: 0198503415.
[33] *Origin of the elements names: Names derived from Mythology or Superstition.*
[34] Wells, A. F. Structural Inorganic Chemistry, 4th Ed., Oxford University Press, Oxford, **1975**.

[35] Greenwood, N. N.; Earnshaw, A. *Chemistry of the Elements*, 2nd Edition, Oxford: Bulterworth-Heinemann, ISBN: 0-7506-3365-4, **1997**.
[36] Hoffmann, M. R. ; et al*. Chem. Rev.,* **1995**, 95, 69.
[37] Cromer, D.T. *J. Am. Chem. Soc.,* **1955**, 77, 4708.
[38] Barksdale, J. *The Encyclopedia of the chemical elements*, Skokie, Illinois: Reinhold Book Corporation, Titanium, **1968**, 732.
[39] *National Mat. Advisory Board Commission on Eng. & Tech. Systems*, National Research Council, Titanium: Past, Present & Future, Washington D.C. **1983**.
[40] Zhang, M.; et al. *J. Mater. Res.,* **2001**, 16, 1408.
[41] Zhou, Y.; et al. *J. Electrochem. Soc.,* **2003**, 150, A1246.
[42] Ruiz, A. M.; et al. *Sens. Actuators B*, **2004**, 103, 312.
[43] Wang, H.; et al. *Optic. Mater.,* **2004**, 27, 161.
[44] Kavan, L.; et al. *J. Electrochem. Soc.,* **2004**, 151, A1301.
[45] Yadollahi, B.; et al. *Synth. Commun.* **2004**, 34, 2823.
[46] Lu, Z. X.; et al. *Langmuir,* **2003**, 19, 8765.
[47] Anpo, M., et al. *J. Phys. Chem.,* **1987**, 91, 4010.
[48] Bettler ; et al*. United States Patent 6,*783,586, **2004**.
[49] Clint, J. H.; et al. *Faraday Discuss. Chem. Soc.,* **1993**, 95, 219.
[50] Brand, J. R. and Story, P. M. *United States Patent 3,119,852*, **1988**.
[51] Krebs, R. E. *The History and Use of Our Earth's Chemical Elements: A reference Guide* (2nd edition), Westport CT: Greenwood Press ISBN : 0313334382, **2006**.
[52] Donachie, M. J. *Titanium: A technical guide,* Metals Park, OH: ASM International, **1988**, 11.
[53] Ibers, J. A. *Nature London*, **1963** 197, 686.
[55] Bradley, D. C.; Holloway, C. E. *J., Chem. Soc.,* **1968**, A21316.
[56] Lover, T.; et al. *J. Mater. Chem.* **1997**, 7(8), 1553.
[57] Hao , N; et al. *J. Magn. Reson.* **1982**, 50, 50.
[58] Gilsdorf, R.T. *United States Patent 3*,119,852, **1961**.
[59] H.J. Kotzch and Screnby, H.G. *United States Patent, 4,789,752*, **1988**.
[60] Kijama, I. *Jpn. Kokai Tokyo Koho, Oct. 31*, **1980**, 80-139, 392.
[61] Albizatti, E. ; et al*. Inorg. Chem. Acta,* **1986**, 120 (2), 197.
[62] Kraitzer, I.; et al. *J. Counc. Sci. Ind. Res.* **1948**, 21, 328.
[63] Tatsumi, T; et al. *J. Chem. Soc. Chem. Commun.,* **1996**, 19, 2281.
[64] Feld, R.; Cowe, P. L. '*The Organic Chemistry of Titanium'*, Butterworths, London, **1965**.
[65] Kotzch, H. J.; et al. *United States Patent 4*,789,752, **1988**.
[66] Pelton, R.; Geng, X*. Adv. Colloid Interface Sci.,* **2006**, 127, 1, 43.
[67] Diebold, U. *Surf. Sci. Rep.,* **2003**,48, 53.
[68] Marchand, R.; et al. *Mat. Res. Bull.,* **1980**, 15, 1129.
[69] Wells, A. F. *'Structural Inorganic Chemistry'*, 4th edn., Oxford University Press, Oxford, **1975**.
[70] Clark, R.J.H. *'The Chemistry of Titanium and Vanadium'*, Elsevier, Amsterdam, **1968**.
[71] Colton, R.; Conterford, J.H. *'Halides of the First Row Transition Metals'*, Wiley, London, **1969**.
[72] Bradley, D. C. *Adv. Inorg. Chem. Radiochem.,* **1972**, 15, 259.
[73] Hawe; et al. *United States Patent, 4,792,343,* **1988**.
[74] Hiew; et al. *United States Patent 6,342,099*, **2002**.
[75] Balfour, J. G. *J. of Oil & Color Chemists Assoc.,* **1990**.
[76] Zhou, B.; et al. *United States Patent 734,459,* **2008**.

[77] Ahmad, S.; et al. *Bull. Mater. Sci.,* **2007**, 30 -1.
[78] Monden; et al. *United States Patent 6,328,974*, **2001**.
[79] Arney; et al. *United States Patent 6,329,058,* **2001**.
[80] Yoshioka, T.; et al. *European Patent 0503922*, **1995**.
[81] Isabelle, H.; et al. *European Patent 0755670*, **1997**.
[82] *European Patent 523,294*, **1993**.
[83] Marchilemann ; et al. *United States Patent 6,132,745*, **2000**.
[84] Chiming, M.; Xia Y. *Colloids and Surfaces*, **1992**, 68, 171.
[85] Fukushima, S.; Kumangini, S. *Journal of Colloid and Interface Science,* **1973**, 42(3).
[86] Kumagini, S.; Fukushima, S. *Journal of Colloidal and Interface Science,* **1976**, 56(2).
[87] Collins, J. L. *United States Patent 5,821,186*, Lockheed Martin Energy Research Corporation, **1998**.
[88] Wang ; et.al. *Chem. Mater.,* **1999**, 11.
[89] Goldshtein; et al. *Izaxestiya Akademii Nank SSSR, Neorganicheskie Material*, **1974**, 10(1).
[90] Ozowa; et al. *Journal of Sol-gel Science and Technology*, **2000**, 19.
[91] Wang, B.; et al*. Journal of Polymer Science: Part A : Polymer Chemistry ,* 29: 905.
[92] Allard; et al. *United States Patent 6,004,567*, **1999**.
[93] Oshima, K.; et al. *WO/1995/009895,* **1995**.
[94] Dwight, A.H.; Austin, H. R. Jr. *Titanium Dioxide Pigments in Coloring of Plastics: Fundamentals, Ed.2nd*, Edited by Robert A. Charvat, ISBN: 0-471-13906-8, **2004**.
[95] Mackay, B. R. *Technological applications of dispersions, Surfactant Science Series,* ISBN: 0824791800, **1994**, 52.
[96] Miller; G.D.; et al. *European Patent 0461635*, **1991**.
[97] Schwarz, J. A. *Dekker Encyclopedia of Nanoscience & Nanotechnology,* ISBN: 0824750500, 4.
[98] Hoffmann, M. R.; et al. *Chem. Rev.,* **1995**, 95, 69.
[99] Moritz, T.; et al. *J. Phys. Chem. B,* **1997**, 101, 8052.
[100] Fox, M. A.; Dulay, M. T. *Chem. Rev.,* **1995**, 93, 341.
[101] Hagfeldt, M. *Chem. Rev.,* **1995**, 95, 49.
[102] Ollis, D. F. and Al-Ekabi, H. Eds. *Photocatalytic Purification and Treatment of Water and Air*, Elsevier : Amsterdam , **1993**.
[103] Fitzgibbons, E. T.; et al. *J. Electrochem. Soc.,* **1972**,119, 735.
[104] Samsonov, G. V. *The Oxide Handbook*, Plenum, New York, **1973**.
[105] Regan,B. O. and Gratzel, M. *Nature*, **1991**, 353, 737.
[106] Nazeruddin, M. K.; et al. *J. Am. Chem. Soc.,* **1993**, 115, 6382.
[107] Zhou; B.; et al. *Nanotechnology in Catalysis,* **2004**.
[108] Gonzalez I. D.; et al. *Catalysis Comm.,* **2008**, 1759.
[109] Rodriguez J. A.; et al. *Science* 318, **2007**, 1757.
[110] Valden, M.; et al. *Science 281*, **1998**, 1647.
[111] Wendt, S.; et al. *Science* 320, **2008**, 1755.
[112] Diwald, O.; et al. *J. Phys. Chem. B,* 108, **2004**, 52.
[113] Chen, H. J.; et al. *Ceramics International*, **2007**, 33, 643.
[114] Brady; et al. *United States Patent 7,304,106*, **2007**.
[115] Chau, J. L. H.; et al. *Mater. Lett.*, **2007**, 61(14-15), 2908.
[116] Zhou, B.; et al. *United States Patent 7,344,591*, **2008**.
[117] Kayanoki , H. *United States Patent 5,654,090*, **1997**.

[118] Buretea; et al. *United States Patent 7,228,050*, **2007**.
[119] Ahmed, S.; et al. *Bull. Mater. Sci.,* **2007**, 30, 1, 31.
[120] Yashida, M.; et al. *J. of Mat. Sci.,* **1997**, 32, 4047.
[121] Nakamura, M.; et al. *United States Patent 5,759,251*, **1998**
[122] Jackson, N.B.; et al*. J. Electrochem. Soc.,* **1991**, 138, 3660.
[123] Jorgensen; et al. *Japanese Patent 5,107,467,* **1992**.
[124] Miyauchi; et al. *United States Patent 4,019,915*, **1977**.
[125] Tanaka; et al. *United States Patent 7,378,050,* **2008**
[126] Kimura; et al. *United States Patent 3,900,246,* **1975**.
[127] Yan; et al. *United States Patent 5,948,481,* **1999**.
[128] Smith. *United States Patent 5,279,662*, **1994**.
[129] Almquist, C. B.; Biswas, P. *J. Catal.,* **2006**, 212, 145.
[130] Wu, S.; et al. *Optical Materials*, **2005**, 27, 1471.
[131] Turkevich, J.; et al. *Trans. Faraday Soc. Discuss*, **1951**, 11, 55.
[132] Ferns, G. *Nat. Phys. Sci.,* **1973**, 241, 20.
[133] Goodmann, S. L. *J. Microsoc.,* **1981**,123, 201.
[134] Heffels, W. *Recent Res. Devel. Macromol. Res.,* **1997**, 2, 143.
[135] Wei, F. S.; et al. *Bulletin of the College of Eng. NTU*, **2003**, 89, 29.
[136] Guha J. P*. J. of the Am. Ceramic Soc.,* **1991**, 74, 4, 878.
[137] Duyvesteyn; et al. *United States Patent 6,440,383*, **2002**.
[138] Monden; et al. *United States Patent 6,328,947*, **2001**.
[139] Nussbauner, R. J.; et al. *Macromolecular Materials and Engineering,* **2003**, 288, 44.
[140] Chen, W. C.; et al. *Journal of Mater. Chem.,* **1999**, 9, 2999.
[141] Chen, W. C.; et al. *Journal of Mater. Chem.,* **2002**, 12, 3644.
[142] Shuhui, W.; et al. *Optical Materials,* **2007**, 29(12), 1793.
[143] Kang, et al. *United States Patent 6,458,462,* **2002**.
[144] Hua, L. L.; Chang, C. W. *Chem. Mat.,* **2001**, 13, 1137.
[145] Wan, T.; et al. *J. App. Polym. Sci.,* **2006**, 102, 5105.
[146] Guan, C.; et al. *J. App. Polym. Sci.,* **2006**, 102, 1631.

Chapter-21

Radiation Processing for Development of Novel Materials

Gunjan Suri[1], Dhriti Khandal[3], Ruchi Gupta[1], Pranshu Kapoor[1], Mukti Tyagi[1], Jay Pal Singh[1], Rakhi Singh[1], Geetha Seshadri[1], U. K. Niyogi[1], G.L. Verma[2], Xavier Coqueret[3] and R. K. Khandal[1]

[1]Shriram Institute for Industrial Research, India
[2]Delhi Technological University, India
[3]Université de Reims Champagne-Ardenne, France

Abstract

During the last century, there have been many technological developments, leading to the demand for new materials and technologies to produce novel materials. The moment a material is brought in the market, need for its improvement and value-addition comes up. The challenges faced by the research scientists, today, pertain to the sustainability and viability of the material. Thus, for the long life of a material in the market, novelty is a key factor that one has to keep in mind before its designing. The emphasis while designing a material for any given application involves achieving maximum output from minimum input.

The development of novel materials involves novel approaches and novel processing techniques. Irradiation processing, is gradually gaining importance as a niche processing technology for various industrial products. It holds a lot of scope in the development of such novel materials for varied applications.

The present chapter describes the experiences of Shriram Institute in the utilization of gamma irradiation for the development of novel materials such as optical plastics and nanocomposites. Case studies pertaining to the development of spectacle lenses, contact lenses and foldable intraocular lenses, metal containing nanocomposites including in-situ dispersion of titanium in polyacrylates are described. Comparison with conventional

techniques such as thermal polymerization has been carried out.

It is evident from the results presented that radiation processing can be taken up as a viable, cost-effective and green alternative with a lot of commercial potential especially for biomedical applications involving optical plastics.

Introduction

Technological progress and demands of modern society have always been the driving forces for innovation. Innovative products and processes have led to the development of materials with novel properties different from the existing ones. The concept of development of novel materials in the present times is quite diverse. How one can maneuver various properties of input materials to create novelty is the key to decide about the appropriate concept and methodology for the purpose. Let us talk about the requirements.

i. The materials are required to last longer under all sorts of natural and man-made conditions. For this, the materials would have to be highly stable.

ii. The other requirement to be met by novel materials pertain to the performance besides the reduced cost and environment-friendliness. Such requirements are never ending and the need for materials with one novelty or the other,has been ever rising.

Development of materials with unique properties and novelty is the key to the introduction of a new device or a new product. In order to deal with the challenges of the future, the advent of new materials has become imminent. In almost all sectors, there would be a demand for novel materials; efficient as also environment-friendly. Unlike the past, the requirements for new materials have changed a lot. The emphasis today is on the protection of environment and ecology. The aim is to look for alternative (preferentially renewable) sources of materials. The development concepts centered on the exploitation of the available resources to the maximum possible extent no longer holds good. Today, the concepts should be based on the maximum output from minimum input, keeping the sustainability of the process as well as the product and the basic guidelines in mind. As a result, the development of processing technologies that produce new materials or the development of processing methodologies to transform the existing materials into novel materials are the need of the present day situation.

Conventional materials are based on basic raw materials like metal, glass, ceramic, wood, polymer, etc. as a result of which there are products of the type called metallic, ceramic and polymeric.The novelty isof the metal acquiringthe attributes of a polymer and vice-versa, &a ceramic material acquiring the characteristics of a metal, and vice-versa.These are going to be the challenges of the future for the material scientists.

The designing of materials involves the following:

(a) Bulk modification of existing matrix
(b) Surface modification of existing materials
(c) All-together new materials

Conventional methods used for the above modifications include casting, sintering, plasma spraying, surface alloying and plasma alloying in the case of metals and ceramics; for polymers, modification methods include physical and chemical processes such as sulfonation, alkylation, acid/base hydrolysis, hydrogenation, stress orienting, annealing, crystallization,etc.

For creating novel materials, this chapter describes some of the innovative approaches such as radiation processing technologies adopted by the authors.

Polymeric and organic materials are characterized by the presence of functional groups, unsaturation, etc. which are modified by conversion of the existing functional groups into new groups which in turn result in the formation of novel materials. In the case of acrylic acid, for example, this simple molecule can be modified by attaching a hydroxyl group in its structure to form a highly hydrophilic material such as 2-hydroxy ethyl methacrylate (HEMA); the same material can be made hydrophobic by esterification of the carboxyl group reacting it with an alcohol like methanol to obtain methyl acrylate (MA). This has resulted in materials that can be used as the base materials for producing novel materials. By functionalization of the carboxyl group, novel materials useful for the designing of ophthalmic materials is a well-known phenomenon. Soft and flexible materials with low glass transition temperature and foldability for specialized applications of eye care are

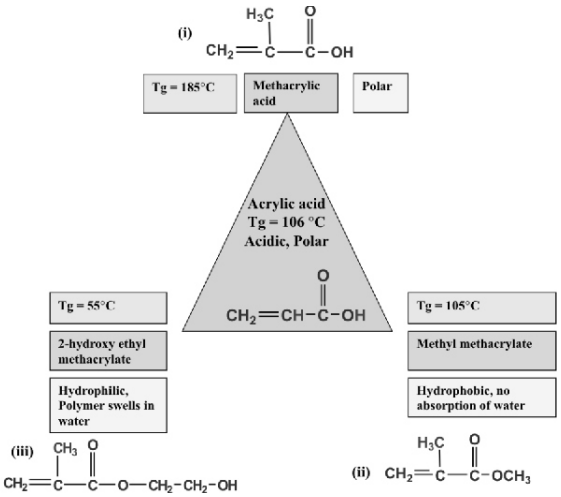

Figure 1 a) Schematic representation of base monomers. Acrylic acid can be converted into hydrophobic as well as hydrophilic monomers to produce a range of polymers.

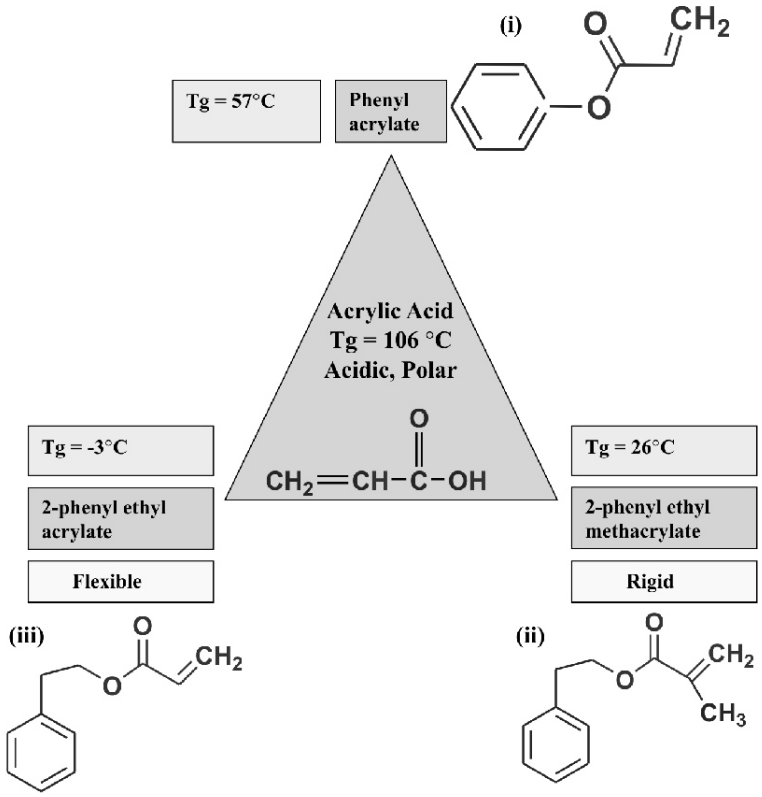

Figure 1 b). Schematic representation of base monomers. Acrylic acid can be converted into various acrylates having aryl group in the structure making them the base material for optical plastics.

desired. Aryl alkyl acrylates and aryl alkyl methacrylates are some of the novel materials already being used for foldable intraocular lenses (Figures 1 a - b).

Synthesizing all together new chemistries and products from a single base material is something, which is unique. The change of properties with change in the functional groups provides a material with a new direction for further exploitation. Such materials are used in various high-end applications like ophthalmic and other industrial processes.

Radiation processing technology for development of materials

Radiations or ionizing radiations such as accelerated electrons and X-rays emitted by energetic electrons, gamma rays by radioactive nuclides are used for the development of novel materials with improved physical, chemical or biological characteristics, to increase their usefulness or value and to reduce their impact on the environment. UV, X-rays and magnetic radiations cause transitions at the atomic level; Ultraviolet radiations make electronic transitions from one level to another while Infrared radiations having the least energy creates vibrations of a material at the molecular level.

Irradiation processing provides significant advantages in comparison to typical thermal and chemical processes such as high throughput rates, reduced energy consumption, less environmental pollution, more precise control over the process and the production of products with superior qualities. The prominent drawbacks of chemical cross-linking typically involve the generation of noxious fumes and by products of peroxide degradation.

Interaction between ionizing radiation and matter gives rise to ions and excited molecules . Ionizing radiations can alter the molecular structure and macroscopic properties of materials such as polymers. In the case of polymers, the effective radiation dose required to bring about changes in the polymers is much less than that required by glass, ceramics and metals.

Changes in a material due to radiations are brought about by the interaction of high-energy radiation with matter. The interaction leads to the formation of ions and excited state molecules via the formation of the intermediate, which is the free radical. The effects of irradiation depend on the quantity of energy deposited on the material regardless of the nature of the incident ionizing photons or particles.

The radiation-induced reactions are brought about by free-radical intermediates. By using ionizing radiations, it is possible to synthesize, modify, cross-link and degrade polymers. The effects of ionizing radiation on polymeric materials can be manifested in one of three ways:

a) Increase in molecular weight of polymer or cross-linking
b) Decrease in molecular weight of polymer or chain-scissioning
c) No change in molecular weight of polymer due to the presence of radiation resistant additives

During irradiation, chain scissioning occurs simultaneously and competitively with cross-linking. The ratio of cross-linking to scissioning depends on factors including irradiation dose, dose rate, presence of stabilizers, radical scavengers and steric hindrances derived from structural or crystalline forces.

While some polymeric materials are degraded, others such as polyethylene, exhibit improved thermal and mechanical properties after controlled irradiation. The improved properties result from cross-links formed between adjacent polymer chains. Polymerization by radiation occurs via addition mechanism for polymers such as polyethylene, polypropylene, poly (vinyl chloride), and polystyrene which are well established.

Advantages of gamma irradiation for polymerization

Radiation processing can be used as a promising and alternative technology to conventional methods of processing. Besides, in many cases it has been established as the only means of

processing some novel materials. This has resulted in novel materials with unique properties. Shriram Institute has experience in the development of novel materials, which have been processed by radiations such as gamma rays.

The case studies involve the development of novel materials for the following fields of application:

(a) Optical plastics
- Diethylene glycol bisallyl carbonate (DEGBAC)
- Hydrophobic and hydrophilic compositions for contact lenses and intraocular lenses

(b) Metal containing nanocomposites

Optical Plastics using Radiation Processing

Optical plastics have already become popular and the most preferred materials replacing conventional inorganic materials (mostly glass) for different applications. The use of optical plastics for ophthalmic applications, like spectacle lenses, contact lenses, intraocular lenses, and so forth, has been the subject of interest for material scientists over the world. During the past two decades, several types of polymers for optical applications have been tried and as a result, a number of products have been successfully launched in the market. However, this does not mean that the search for a suitable polymeric material for a given application is over. In fact, the demand for newer and affordable materials has increased more than ever before. This is true, more so for the developing world where the number of patients with ophthalmic defects have been increasing with a higher rate than their capacity to afford optical plastics. The technologies for the manufacture of optical plastics exist mostly with a select few manufacturers in the developed countries. Moreover, the base materials for optical plastics is also a cause of concern, since they are either costly or are not available locally. Hence, there is a need for development of technologies using locally available or easily available raw materials for making optical plastics. The development of the desired polymer materials for optical applications is done based on the design parameters and criteria for selection as per the desired application. The properties such as refractive index, transmittance, Abbe number, and physico-mechanical properties are essential. A list of selected monomers is already available based on the research conducted so far. Even though the candidate monomers are many, only a few have been found to be commercially viable. For spectacle lenses, the market leadership lies mainly with a couple of monomers. Similarly, for contact lenses and intraocular lenses, only five monomers have been used commercially. The need for new materials thus,remains a top priority even today.

Optical plastics are used for a variety of applications such as prescription and nonprescription lenses, sport masks, goggles, visors, camera lenses, windows, windshields, aircraft and automotive applications. In fact, optical plastics have proven to be a good

replacement for conventionally used glass materials, providing useful optical properties and light weight to the finished product as compared to glass. Optical plastics are based on various functional monomers. Generally, the monomers are cast polymerized by thermal processing to manufacture optical plastics suitable for any desired application. In the presence of initiators, the monomers get polymerized by free radical polymerization to result in polymeric materials with the targeted physico-mechanical, optical and other related properties. Conventionally, polymerization is done using thermal energy, by subjecting the composition consisting of monomers to heat. The other well-established method involves the use of UV-radiations as well as other types of radiations for producing polymer.

The thermal method involves a long polymerization cycle and the use of initiators, which makes the process cumbersome and results in a significant amount of rejections. Thus, there exists a need for an alternative polymerization process. Gamma irradiation has been used as a novel technology for the development of optical plastics. Optically clear, transparent and colorless lenses with the required refractive index can be obtained by gamma radiation. Based on the initial encouraging results with radiation processing, the present studies were planned.

The designing of optical plastics involves three approaches, that is,

(i) developing a new chemistry with molecular bonds of unique optical properties as well as physico- mechanical behavior,

(ii) trying combinations of several homopolymers or copolymers with synergistic properties and

(iii) combining inorganics with organics to achieve properties derived from the complementary effects of two different (organic and inorganic) base materials.

Each of these approaches has resulted in unexpected success with the advent of newer materials, besides providing various leads for researchers to pursue further for improved products.

The manufacture of optical plastics is mostly by the process of thermal polymerization. It has been studied that radiation processing leads to polymers of desired properties with greater efficiency. The use of radiation processing to develop a series of candidate polymers with varying properties, would be a practical approach.

The different monomers have been polymerized using gamma radiations and studied for their capacity to absorb and retain water. For applications such as contact lenses and IOL lenses of the foldable type, optical plastics are supposed to be hydrophobic in nature with no

water absorption. On the other hand, IOLs of the rigid type require materials with controlled capacity to absorb water. Similarly, for contact lenses, materials of varying water absorption capacity are needed.

Glass has been the natural inorganic material of choice for optical applications due to its excellent clarity and hardness. The limits of glass for optical applications in terms of processability, fragility and heavy weight raised the need for alternative materials such as polymeric materials or optical plastics. Optical plastics are superior in shock resistance, lightness, processability and is more commonly used in the field of optical applications in place of glass. For manufacture of polymers, the monomers are subjected to different forms of energy i.e. thermal, electronic, nuclear,etc. in the presence of different initiators, catalysts, cross-linkers, etc. The degree of polymerization, final molecular weight of the polymer, distribution of molecular weight of the polymer, etc. are some of the major parameters which are governed by the process of polymerization adopted, besides the conditions and type of catalyst used for polymerization.

The possibility of using gamma irradiations has been studied as an alternative to the popularly used technique of thermal polymerization for the manufacture of optical plastics. The results demonstrated that polymerization by gamma radiation leads to a better product compared to the one produced by thermal polymerization. Based on this study, it is expected that the industry will use radiation processing as a cost- effective and environment-friendly process for producing optical plastics.

Case I

Spectacle lenses based on Diethylene glycol bis allyl carbonate (DEGBAC) using gamma irradiation

Allyl carbonate is a liquid monomer, which hardens on polymerization under the effect of heat and in the presence of a catalyst. The presence of allyl groups allows the polymer to form cross-links. A refractive index of 1.49, density of 1.32, Abbe number (>50), high impact resistance and excellent transparency are some of the key features responsible for making poly (allyl) carbonate as the most preferred optical plastic. Further, additional advantages such as multiple tinting and coating possibilities are other features associated with the processing and usage of optics based on allyl carbonate. The commercially available optical plastics based on allyl carbonate, at present, are being widely produced following thermal polymerization technique. Even though, thermal polymerization is a useful technique for this purpose, there has always been a need for an alternative technique, which is not only cost effective but also minimizes the rejections of the polymerized product. Conventional and industrial methods of production of optical plastics involve using free radical initiators such as benzoyl peroxide, lauryl peroxide and di-isopropyl peroxyper-carbonate (DIPP).

Mechanism of polymerization of DEGBAC

Process of polymerization of monomers is determined mainly by the chemistry of the monomers. Depending upon the mechanism involved, there exist two major processes for obtaining polymers i.e. addition and condensation of monomers. While the condensation polymerization is accompanied by the release of a small molecule like water, carbon dioxide etc., in the case of addition polymerization,there is complete addition of monomers without any loss of small entities. Addition polymerization process basically involves free radical mechanism taking place in three steps: (i) chain initiation (ii) chain propagation and (iii) chain termination. For the initiation reaction, it is essential that the energy be supplied to the system. Different types of energy used for polymerization will have ultimate bearing on these three steps involved in the polymerization process. For the manufacture of polycarbonates used as optical plastics, thermal polymerization is the commonly used process. In thermal polymerization process, the formation of free radicals is initiated by diisopropyl peroxy dicarbonate (DIPP). The free radicals formed by the dissociation of peroxy dicarbonate (Figure 2) interacts with the monomer resulting in the formation of alkyl radicals which further react with the monomer resulting in chain propagation as shown in Figure 3. Chain termination occurs by combination of two growing chains with mutual extinction of radicals. Chain termination by disproportion occurs when the radical of a propagating chain abstracts a H-atom from another propagating polymer chain to achieve mutual extinction of radicals. In this case, the two polymer chains do not continue, but remain as separate entities, one chain containing an unsaturated end unit and the other, a saturated end unit as presented in Figure 3. In the case of the process of polymerization by gamma irradiations, the chain initiation takes place as a result of irradiation by gamma rays. Random destruction of allyl carbonate (monomer) by the gamma rays leads to the formation of free radicals responsible for chain initiation. The free radicals, then, react with non-radical species leading to chain propagation. Chain termination occurs when two growing chains react by dimerization or disproportionation to give stable products. Polymerization by gamma radiation depends on a number of factors, which include the nature of the monomer, absorbed dose of gamma radiation and temperature. The reaction mechanism of polymerization of allyl carbonate by gamma radiation is shown in Figure 4. Different features of polymerization by thermal process and by gamma radiation are presented in Figure 5 for better understanding of the two processes. Radiation processing is expected to produce a better product than the thermal process due to the following reasons:

(a) Formation of pure product since contamination resulting from initiator residues does not arise.

(b) Radiation processing can be carried out at low temperature resulting in lower energy costs and less thermal damage to the system.

(c) Intensity of the ionizing radiation can be controlled.

(d) Radiations have greater penetrating power resulting in a more uniform product.

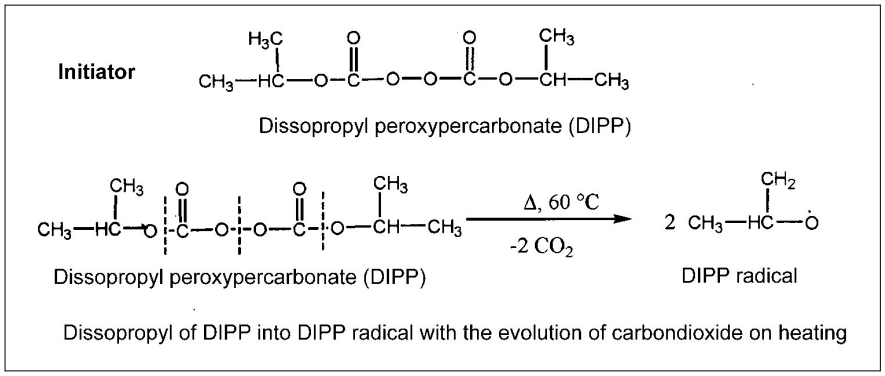

Figure 2. Diisopropyl peroxypercarbonate (initiator) and formation of a free radical on dissociation because of heating. The DIPP radical, then, plays the role of an initiator to help achieve chain initiation.

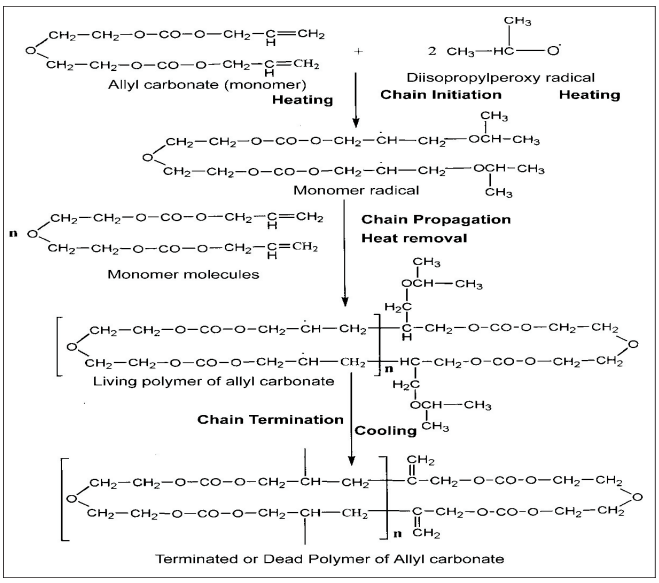

Figure 3. Reaction mechanism of polymerization of allyl carbonate by thermal process. The chain initiation step involves the reaction between the free radicals of the DIPP initiator and the monomer molecules of allyl carbonate. The chain propagation takes place with the reaction between monomer radicals and the 'n' number of monomer molecules leading to the living polymer capable of further addition of monomers. The final step of chain termination is achieved by stopping the heat cycle leading to the dead or terminated polymer.

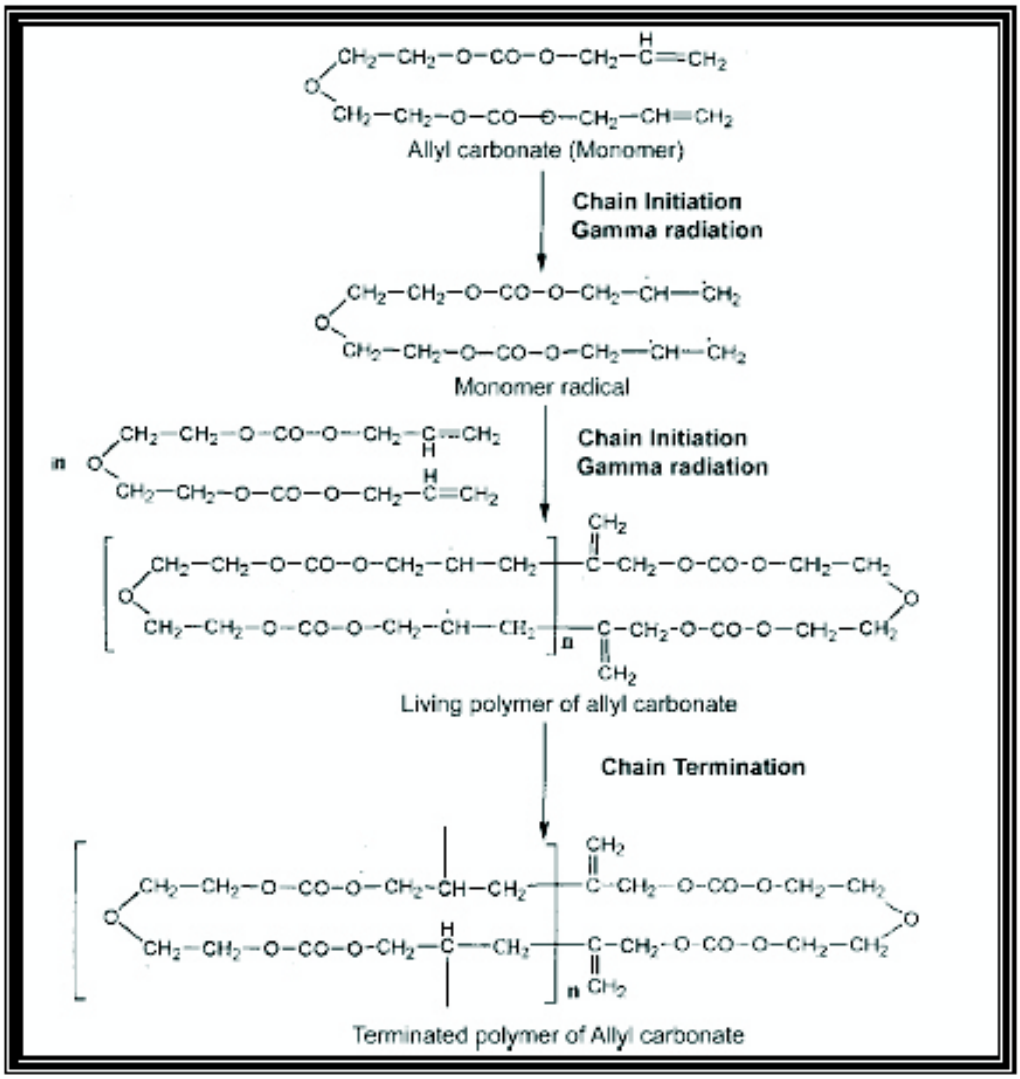

Figure 4. Reaction mechanism of polymerization of allyl carbonate by gamma radiation. Here, no chain initiator is used. Gamma radiation causes the initiation as well as the propagation of the chain. The termination of the chain occurs as soon as the exposure to radiation is stopped.

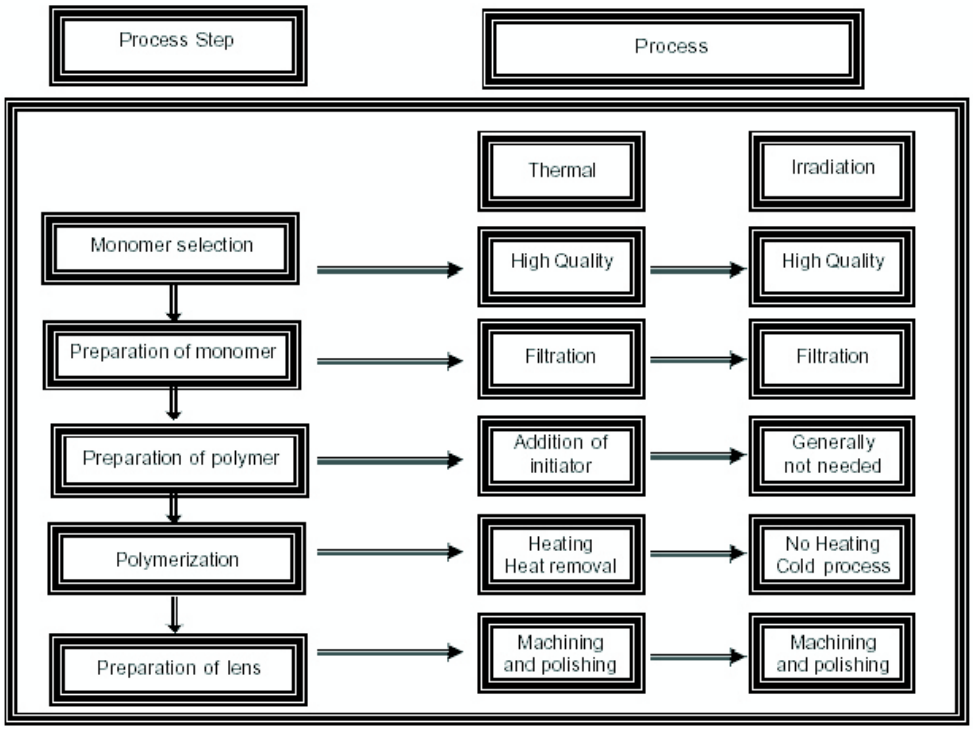

Figure 5: Various process steps and processes involved in the polymerization of allyl carbonate for making lenses by thermal and radiation processing

Effect of irradiation dose on various properties of P(DEGBAC)

(a) Clarity and transparency: UV-Visible spectroscopy for light transmittance (%) is used to assess the clarity and transparency of the lens. From the results presented in Figure 6, it can be seen that lenses irradiated at 25 kilogray (kGy) and above exhibited 95% transmittance and high optical clarity exactly matching with that of the thermally cured lens. There is no change in transmittance and clarity upto 75 kGy. However, on increasing the radiation dose beyond 75 kGy, there is a loss of transmittance, which is ascribed to the degradation of the polymer, and to the formation of free radicals. The results clearly show that polymerization with desired optical clarity and acceptable color can be obtained if cast polymerization is done at a radiation dose range of 25 kGy-75 kGy.

(b) Shore-D Hardness: The effect of radiation dose on the hardness can be understood from the data presented in Figure 7. The lenses were soft at lower doses of 25 kGy and 50 kGy, indicating incomplete polymerization. Complete polymerization has taken place at the dose rate between 50 kGy and 75 kGy as indicated by the hardness of the lenses

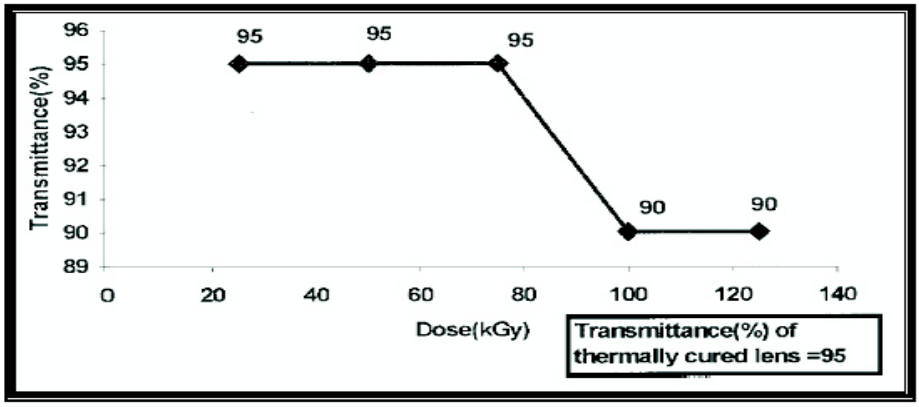

Figure 6. Effect of gamma radiation dose on transmittance of irradiated lens. The maximum transmittance of 95% as achieved by thermal polymerization process could be obtained for a gamma radiation dose of 75 kGy. Beyond 75 kGy, the transmittance decreases sharply, indicating polymer degradation.

comparable to those obtained by thermal polymerization. This shows that in order to achieve the desired hardness, the polymerization needs to be carried out at a radiation dose of more than 50 kGy. The results of hardness suggest that at 75kGy, the polymerization is almost complete leading to the formation of a highly crosslinked structure.

(c) Gel content (%): Results of gel content (%) vs irradiation dose (kGy) are presented in Figure 8.The extent of crosslinking increases with the increase in the dose of radiation. At 25 kGy and 50 kGy, a gel content of 85.2 % and 91.1% respectively, indicates the presence of significant amounts of unreacted monomer. This could be due to the fact that at these doses, chain propagation is slowed down. At 75kGy, gel content of 99.7 %

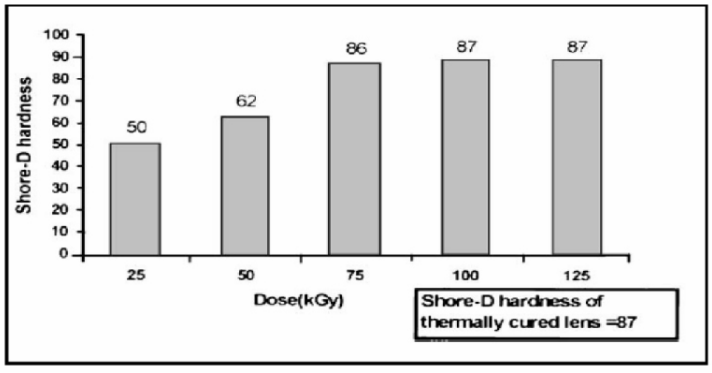

Figure 7. Effect of radiation dose on hardness of irradiated lens. The maximum hardness of 87 as achieved by thermal polymerization process could be obtained for a gamma radiation dose of 75 kGy. Beyond 75 kGy, the hardness remains the same

indicates that the polymer is completely cross-linked. Beyond 75 kGy, there is a decrease in the values of gel content, indicating the on-set of degradation of the polymer. The lenses irradiated at a dose of 75kGy exhibit better cross-linking than the thermally cured product. The better crosslinking could be attributed to the fact that at a dose of 75kGy, initiation and chain transfer reactions predominate leading to a higher degree of crosslinking than the conventional (thermal) methods.

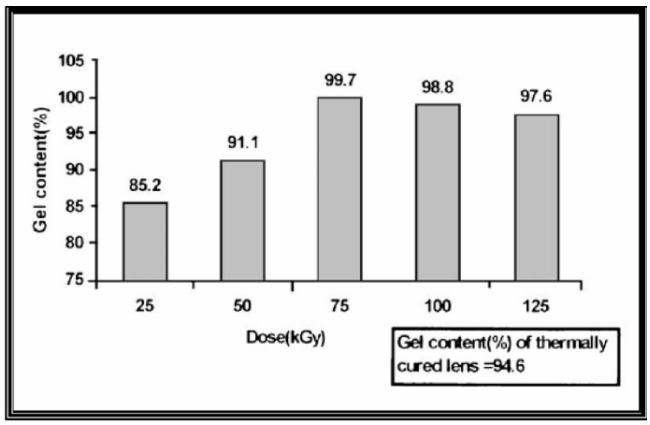

Figure 8. Effect of radiation dose on gel content (%) of irradiated lens. The maximum gel content of 99.7% is achieved by a gamma radiation dose of 75 kGy whereas 94.6% gel content is achieved in the case of thermal polymerization. Beyond 75 kGy, the gel content decreases indicating polymer degradation.

(d) Color: From the results presented in Figure 9, it can be seen that at lower doses of gamma radiations, the lenses are colorless as indicated by the Lab values that are closely similar to the Lab values of the thermally cured lens. As the dose of gamma radiation is increased beyond 75 kGy, the yellow color also increases as indicated by the increase in value of "b". The presence of color maybe attributed to the formation of colored by-products by the radical formation during gamma irradiation.

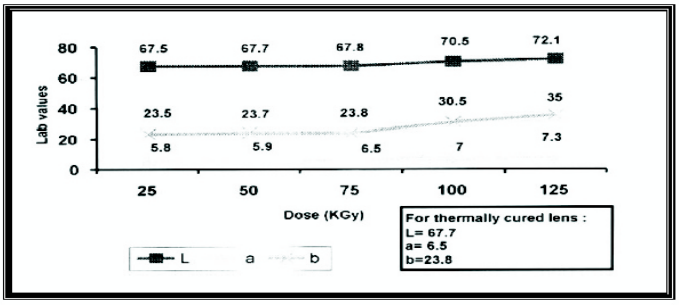

Figure 9. Effect of radiation dose on color of irradiated lens. The "L", "a", "b" values as achieved by thermal polymerization could be obtained for a gamma radiation dose of 75 kGy

(e) Yellowness index: The yellowness index (Figure 10) of the irradiated material upto 75 kGy is found to be 0.0074 which is comparable to that of the thermally cured lenses having a yellowness index of 0.0075. At doses beyond 75 kGy, yellowness index increases considerably. This maybe attributed again to the formation of by products during gamma irradiation.

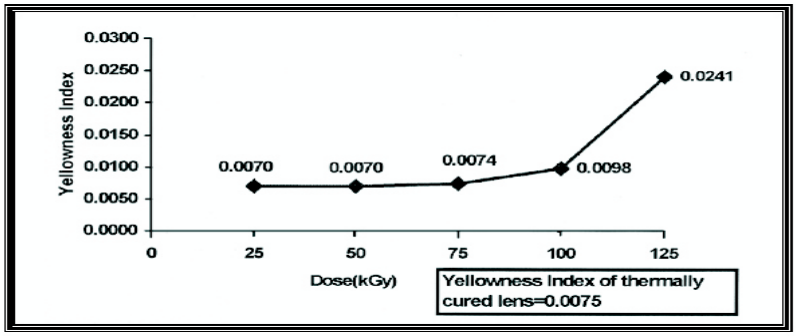

Figure 10. Effect of radiation dose on yellowness index of irradiated lens. The value of yellowness index as achieved by thermal polymerization process could be obtained for a gamma radiation dose of 75 kGy.

(f) Thermal stability: From the thermogravimetric analysis, the temperature at which the complete degradation of the material takes place is taken as the indicator of thermal stability and the results are presented in Figure 11. It maybe noted that the radiation dose at 75 kGy provides the maximum thermal stability. When compared with the stability (461°C) of the lens cured by thermal process, it is evident that the lenses irradiated at 75 kGy were more stable. The higher thermal stability could be attributed to the fact that at a dose of 75kGy, chain propagation takes place leading to the formation of more crosslinks resulting in a highly cross-linked product with high thermal stability.

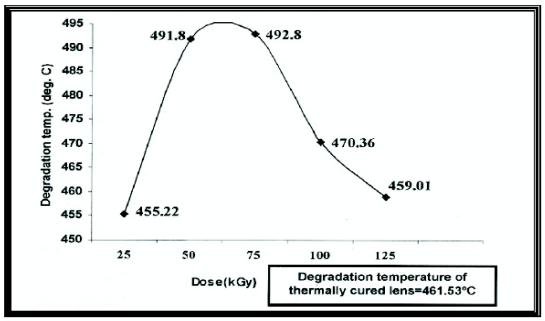

Figure 11. Effect of radiation dose on the thermal stability (100% degradation) of irradiated lens. The thermal stability of the irradiated lens as achieved in the case of 75 kGy is more than that achieved by thermal process. Beyond 75 kGy, the thermal stability decreases, indicating polymer degradation.

(g) Specific gravity: The results indicate that the gamma-irradiated lenses are similar to the thermally cured product having specific gravity value of 1.3. Based on the results of the experiments, it is evident that 75 kGy is the optimized radiation dose to obtain optical plastics based on DEGBAC with desired properties.

Thus, gamma irradiation is found to be more efficient than thermal processing. While radiation processing is a cold process and helps in eliminating the step of subjecting the monomer composition etc., to heating which in turn requires thermal energy, it helps in getting the uniform structure of the polymer as has been observed during the characterization of the polymer. This finding would certainly pave way for the development of a range of optical plastics using radiation processing. Faster processing and therefore better output for plastic lenses plus minimum wastage would attract the manufacturers to adopt this technology.

Case II

Contact lens materials using gamma irradiation

For the development of materials for contact lenses and intraocular lenses, the selection criteria is based on the (i) capacity to absorb and retain water, (ii) hydrophilicity and hydrophobicity, (iii) refractive index and (iv) hardness besides the other essential properties. Various monomers are being studied to develop suitable materials for such applications. Authors of this chapter have carried out extensive studies in this field and they are being described here.

Selection of suitable monomers that can be converted into optical materials of desired characteristics is the most essential step. In the present paper, an attempt has been made to develop suitable optical polymers based on 2-hydroxy ethyl methacrylate (HEMA), N-vinyl pyrrolidone (NVP), methyl methacrylate (MMA), methacrylic acid (MAA), and styrene. Compositions are prepared in such a way that polymers of varying hydrophilicity or hydrophobicity could be obtained keeping HEMA as the base (main) monomer. For polymerization, gamma irradiation (Co-60 as a source) is used. The results of the studies show that: (i) an increase in NVP and MAA content brings an increase in hydrophilicity of polymerized HEMA (pHEMA), while the addition of styrene and MMA decreases hydrophilicity of polymerized HEMA (pHEMA), (ii) polymers for contact lenses with water retention capacity as high as >50 wt% and as low as <10 wt% with varying content of suitable co-monomers can be designed, (iii) polymeric materials for contact lenses can be made by using radiation processing such as Co-60 and (iv) a dose of 40 kGy is found to be ideal for the purpose.

Water absorption behaviour of irradiated materials

The results of water absorption capacity of HEMA polymerized by gamma irradiation at a dose of 40 kGy are presented in Table 1. From the results, it is evident that HEMA gets polymerized in the solution form in water at all concentrations starting from 10 wt.% to 90 wt.% of water. The following notable observations were made: (i) the polymer is hard and transparent upto compositions with less than 50 wt.% of water. Beyond 50 wt.% of water content, the material turns opaque and remains hard; (ii) the polymer retains the water added to the monomer upto an extent of 40 wt.% (for compositions with more than 40 wt.% of water, the excess of water is released from the polymer); (iii) in the case of compositions containing 90 wt.% of water and 10 wt.% of HEMA, more than 40 wt.% of water is found to get released from the polymer (a soft solid). Based on the above observations, it is understood that the water absorption capacity of polymerized HEMA (pHEMA) is 40% and any excess water present during polymerization would remain unused. This is as expected. However, the material turning opaque in cases where the percentage of water is more than 40% is something unusual. The results of the studies involving the polymerization of HEMA as such show the following properties:

(i) pHEMA, when immersed in water absorbs a maximum (approximately 40% by wt.) of water and remains transparent; (ii) material remains transparent throughout the absorption studies contrary to the opaque material obtained in the case when polymerization was conducted in the presence of excess amount (>50wt.%) of water.

Table 1. HEMA polymerized in the presence of water

Composition HEMA:WATER	Shore-D Hardness	Transmittance (%)	Ref. Index	Appearance
100: 0	80	90	1.453	Transparent, clear & hard
90 : 10	80	90	1.439	Transparent, clear & hard
80 : 20	80	90	1.423	Transparent, clear & hard
70 : 30	80	90	1.417	Transparent, clear & hard
60 : 40	70	90	1.383	Transparent, clear & hard
50 : 50	60	0	1.383	Transparent, clear & hard
40 : 60	60	0		Opaque & hard
30 : 70	60	0		Opaque & hard
20 : 80	50	0		Opaque & hard
10 : 90	50	0		Opaque & hard

This demonstrates that HEMA when polymerized in the presence of water is able to retain more amounts of water than the case where the polymerization is carried out in the absence of water. This behavior can be explained on the basis of the manner in which the polymer arranges itself during the process of polymerization in water (Please see Figure 12).

While the monomers start interacting with each other by the mechanism of free radical polymerization, the solvation of the monomer is affected. As a result, the water molecules detach from the monomer every time the polymerization proceeds in the right direction. In this process, however, some amount of water remains entrapped within the polymer molecule. It is due to this reason that the polymer appears opaque. On removal of both types of water, that is, associated as well as entrapped, the polymer turns transparent. When the dehydrated polymer is re-immersed in water, it does not turn opaque which confirms the proposed reason for obtaining an opaque material when polymerization is done in the presence of water, as depicted in Figure 12.

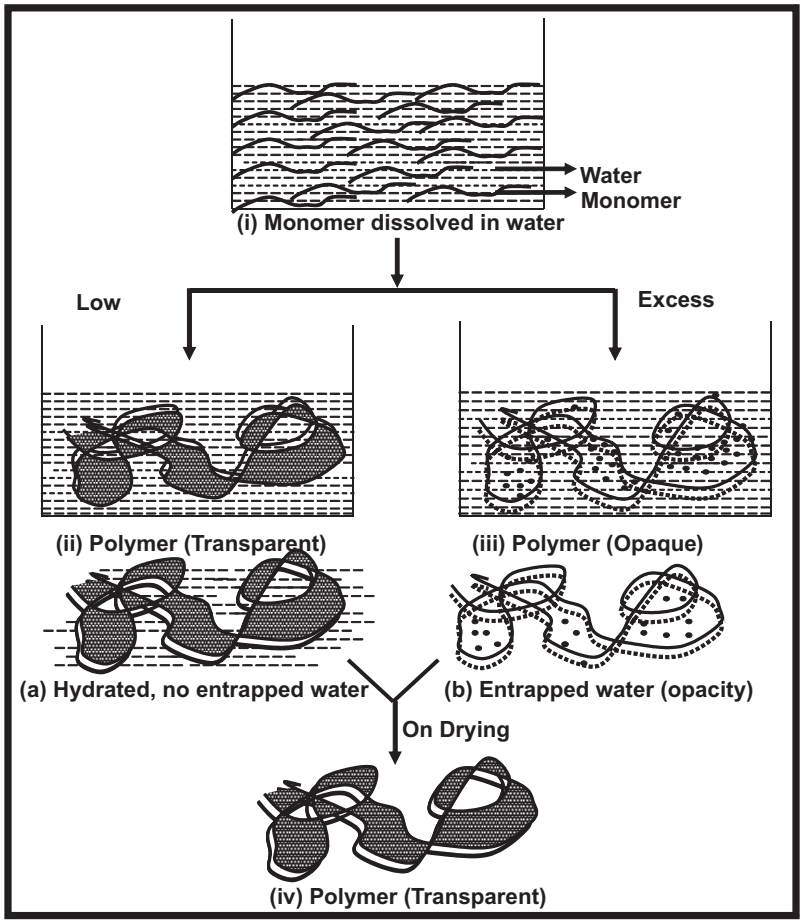

Figure 12: Polymerization of HEMA and mixtures of HEMA with other monomers in the presence of water (i) solution of monomer or monomer mixture in water (ii) hydrated polymer without entrapped water remains transparent (iii) hydrated polymer with entrapped water appears opaque (iv) dehydrated polymer from both the hydrated, transparent and opaque polymers.

(1) Monomer dissolved in water remains as a clear solution where each monomer chain is solvated.

(2) With polymerization, monomer-monomer interactions occur in place of monomer-water interaction.

(3) As long as the amount of water is within the range of the maximum possible amount for hydration, the polymer remains transparent with the hydrophilic part hydrated completely. The excess water may be entrapped causing it to be opaque.

Effect of different monomers on water absorption of HEMA: The results of the effect of different monomers on water absorption and water desorption at room temperature and at 100^0C, on HEMA are presented in Figure 13–16. The properties of the various compositions obtained on polymerization are described in the following sections and in Tables 2–5.

MMA and HEMA: The results of the effect of methyl methacrylate on water absorption and water desorption at room temperature and at 100^0C on HEMA-MMA are shown in Figure 13. The properties of the various compositions of HEMA: MMA obtained on polymerization are presented in Table 2.

Table 2: Properties of HEMA: MMA of varying ratios.

Composition HEMA:MMA	Shore-D Hardness	Transmittance (%)	Ref. Index	Appearance
100: 0	80	90	1.453	Transparent, clear & hard
90 : 10	80	90	1.446	Transparent, clear & hard
80 : 20	80	90	1.442	Transparent, clear & hard
70 : 30	80	90	1.439	Transparent, clear & hard
60 : 40	80	90	1.435	Transparent, clear & hard
50 : 50	80	90	1.432	Transparent, clear & hard
40 : 60	80	90	1.428	Transparent, clear & hard
30 : 70	80	90	1.423	Transparent, clear & hard
20 : 80	80	90	1.419	Transparent, clear & hard
10 : 90	80	90	1.415	Transparent, clear & hard
0 : 100	80	90	1.412	Transparent, clear & hard

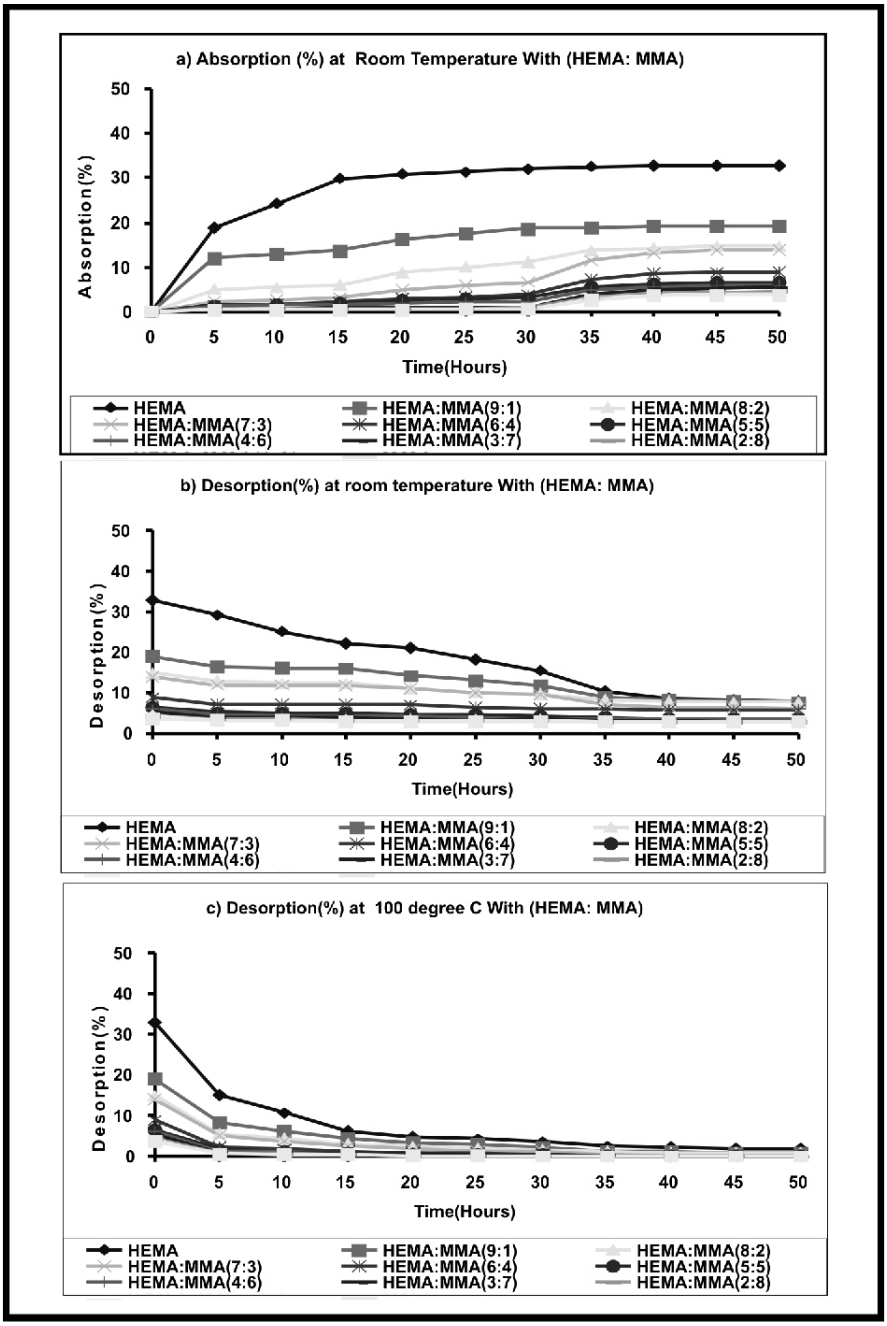

Figure 13. Studies of water absorption and desorption of HEMA: MMA. Co-polymerization of HEMA with MMA, a hydrophobic monomer results in decrease in water absorption capacity of HEMA. Water that is absorbed is completely lost on desorption

The following observations were noted:

(1) Water absorption capacity of pHEMA is reduced from 32.82% to 4.42% with an increase in the concentration of MMA. Initial resistance to the uptake of water upto 30 hours indicates hydrophobic nature of MMA.

(2) As the amount of MMA increases, refractive index of the composition decreases due to low molar refraction of MMA.

(3) With varying ratios, transparency and hardness of polymers do not change due to good compatibility of MMA with HEMA

(4) On absorption of water, all the samples retain their transparency.

(5) The water that is absorbed is completely lost on dehydration.

From the fact that the absorption of water by the copolymer is reversible and leads to complete transparency, it can be said that the absorption takes place due to the hydrophilic nature of the copolymer without any entrapment of water.

MAA and HEMA: The results of the effect of methacrylic acid on water absorption and water desorption at room temperature and at 100^0C, on HEMA are shown in Figure 14. The properties of the various compositions of HEMA : MAA obtained on polymerization are presented in Table 3.

Table 3. Properties of HEMA: MAA Co- Polymers of varying ratios

Composition HEMA:MAA	Shore-D Hardness	Transmittance (%)	Ref. Index	Appearance
100: 0	80	90	1.453	Transparent, clear & hard
90 : 10	80	90	1.449	Transparent, clear & hard
80 : 20	80	90	1.447	Transparent, clear & hard
70 : 30	80	90	1.445	Transparent, clear & hard
60 : 40	80	90	1.444	Transparent, clear & hard
50 : 50	80	90	1.442	Transparent, clear & hard
40 : 60	80	90	1.439	Transparent, clear & hard
30 : 70	80	0	★	Opaque & hard
20 : 80	80	0	★	Opaque & hard
10 : 90	80	0	★	Opaque & hard
0 : 100	80	0	★	Opaque & hard

★ Not measurable due to opacity of sample

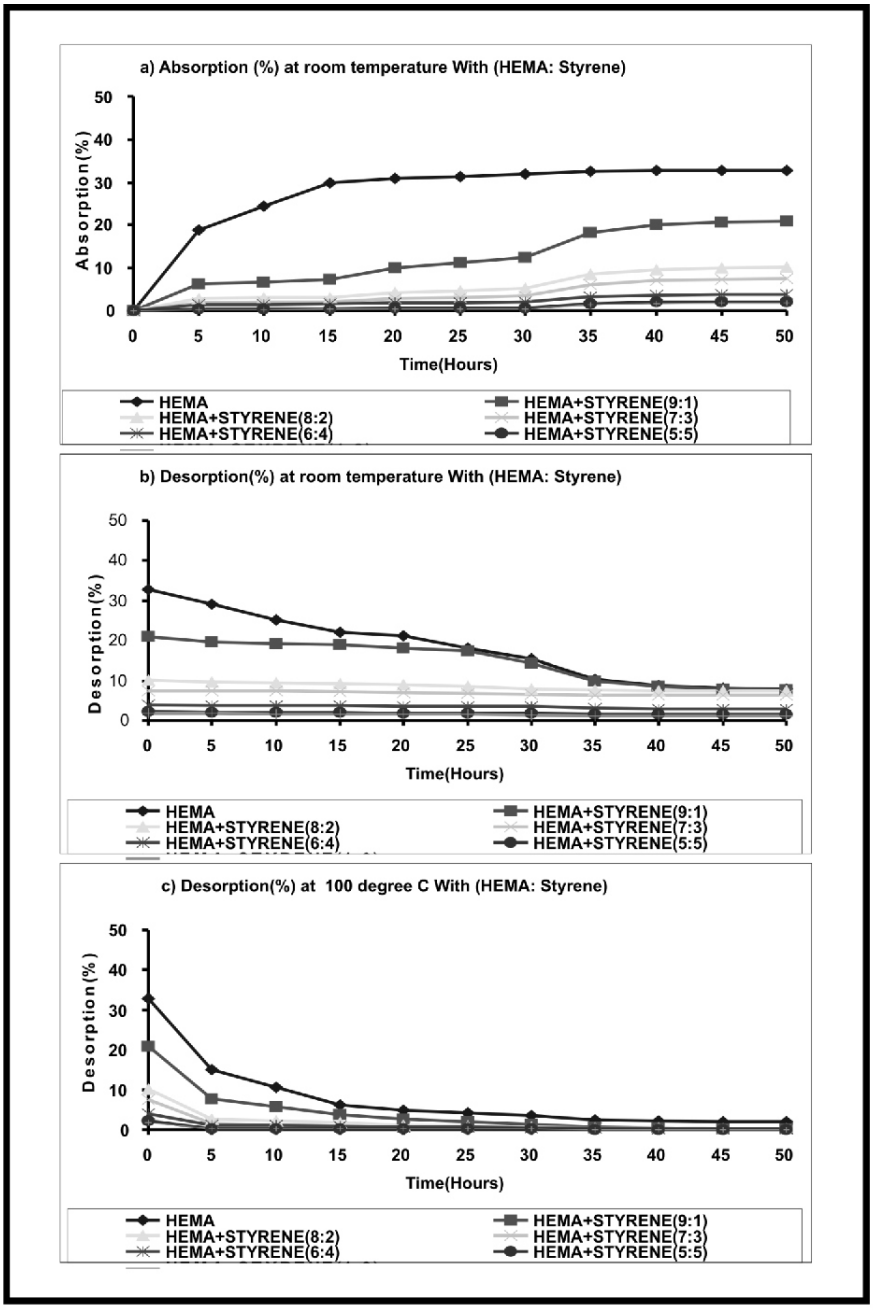

Figure 14. Studies on water absorption and desorption of HEMA: MAA. Water absorption capacity of HEMA decreases on co-polymerization with MAA which is less hydrophilic than HEMA, The absorbed water is attached with the hydrophilic part of the co-polymer. The amount of water that is absorbed is completely lost on desorption

The following observations were noted:

(1) Water absorption capacity of pHEMA decreases from 32.82% to 28.02% with increase in the amount of MAA. This indicates lower hydrophilicity of MAA as compared to HEMA.

(2) As the ratio of MAA increases, refractive index of the composition decreases due to low molar refraction of MAA.

(3) Copolymerization of HEMA with MAA leads to transparent and hard polymers for ratios of HEMA: MAA upto 60% by wt. while ratios beyond 60wt.% of MAA leads to opacity of polymer.

(4) The copolymer remains transparent and the water is attached with the hydrophilic part of the copolymer.

(5) The amount of water that is absorbed is completely lost on dehydration.

Styrene and HEMA. The results of the effect of Styrene on water absorption and water desorption at room temperature and at 100 C, on HEMA are shown in Figure 15. The properties of the various compositions of HEMA : Styrene obtained on polymerization are presented in Table 4.

Table 4. Properties of HEMA : STYRENE of varying ratios

Composition HEMA:STYRENE	Shore-D Hardness	Transmittance (%)	Ref. Index	Appearance
100: 0	80	90	1.453	Transparent, clear & hard
90 : 10	80	90	1.460	Transparent, clear & hard
80 : 20	80	90	1.470	Transparent, clear & hard
70 : 30	80	90	1.480	Transparent, clear & hard
60 : 40	80	90	1.490	Transparent, clear & hard
50 : 50	80	90	1.500	Transparent, clear & hard
40 : 60	80	0	1.506	Transparent, clear & hard
30 : 70	80	0	-	Opaque & hard
20 : 80	80	0	-	Opaque & hard
10 : 90	80	0	-	Opaque & hard
0 : 100	N.A	N.A	N.A	Transparent liquid

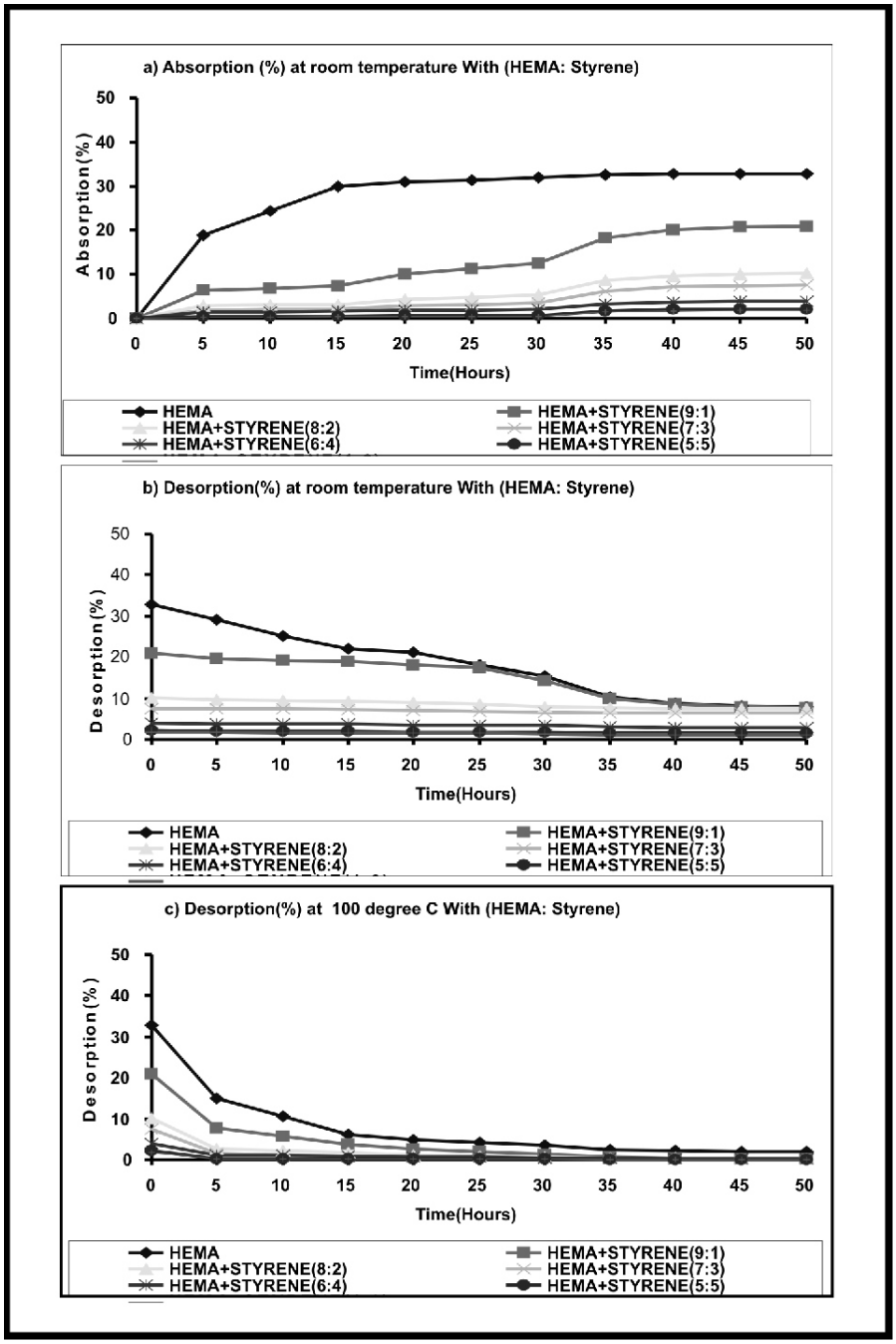

Figure 15. Studies on water absorption and desorption of HEMA : Styrene. Water absorption capacity of HEMA decreases on co-polymerization with styrene, a hydrophobic monomer. Absorption of water takes place by solvation of the hydrophilic portion of the co-polymer. The water that is absorbed is lost on desorption.

The results of copolymerization of styrene and HEMA apparently show that the following observation holds true.

(1) Addition of styrene to HEMA brings reduction in the water absorption capacity of HEMA from 32.82% to 0.08%. This indicates the hydrophobic nature of styrene.

(2) As the ratio of styrene increases, refractive index of the composition increases due to a high molar refraction of the phenyl ring present in styrene.

(3) Copolymerization of HEMA with styrene leads to hard and transparent polymers for ratios of HEMA: Styrene upto 60 wt.% while ratios beyond 60 wt.% of styrene leads to opacity.

(1) Absorption of water is reversible with complete loss of water on dehydration and vice versa.
(2) Transparency of hydrated copolymers show that the absorption of water is by the solvation of the hydrophilic part of the copolymer.

NVP and HEMA. The results of copolymerization of HEMA with varying amounts of NVP are shown in Table 5 and Figure 16.

Table 5: Properties of HEMA: NVP of varying ratios.

Composition HEMA:NVP	Shore-D Hardness	Transmittance (%)	Ref. Index	Appearance
100: 0	80	90	1.453	Transparent, clear & hard
90 : 10	80	90	1.458	Transparent, clear & hard
80 : 20	80	90	1.465	Transparent, clear & hard
70 : 30	80	90	1.470	Transparent, clear & hard
60 : 40	80	90	1.475	Transparent, clear & hard
50 : 50	80	90	1.486	Transparent, clear & hard
40 : 60	80	90	1.487	Transparent, clear & hard
30 : 70	80	90	1.490	Transparent, clear & hard
20 : 80	80	90	1.491	Transparent, clear & hard
10 : 90	80	90	1.497	Transparent, clear & hard
0 : 100	80	90	1.508	Transparent, clear & hard

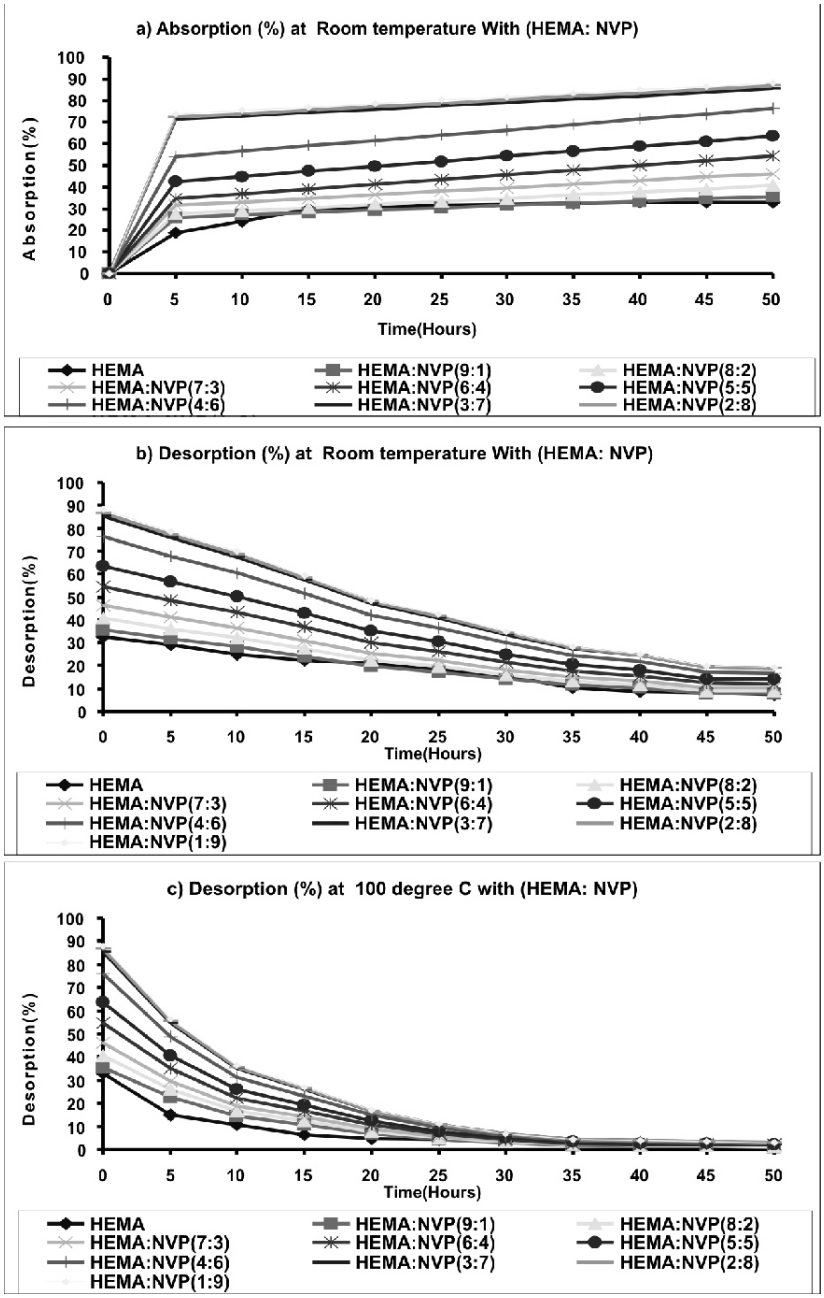

Figure 16. Studies on water absorption and desorption of HEMA: NVP. Co-polymerization of HEMA with NVP, a hydrophilic monomer results in an increase in the water absorption capacity of HEMA. Absorption of water takes place by solvation of the hydrophilic portion of the co-polymer. The water that is absorbed is lost on desorption.

The results show that the following reasons hold true:

(1) NVP brings a positive effect as far as the absorption of water is concerned. It is due to higher hydrophilicity of NVP as compared to HEMA.

(2) As the ratio of NVP increases, refractive index of the composition increases due to high molar refraction of pyrrolidone ring present in NVP.

(3) With varying ratios, transparency and hardness of polymers do not change due to good compatibility of NVP with HEMA

(4) The water absorption is completely reversible meaning that the amount of water that is absorbed can be removed on dehydration.

(5) Transparency of the hydrated copolymers obtained shows that the water remains absorbed in the polymer as a result of solvation of the hydrophilic part of the copolymer.

From the studies (Tables 2-5), it is evident that all the polymers are found to be transparent upto a particular compositions, HEMA : MMA is transparent for all compositions; HEMA : MAA and HEMA : styrene is transparent upto 60% of MAA and styrene, respectively. In case of HEMA : NVP, transparent polymers at all compositions were obtained. This is an interesting observation, keeping in view the fact that all the monomers used in the study are otherwise known to form transparent polymers when polymerized as such. The reason as to why HEMA : Styrene and HEMA : MAA are opaque when the concentration of HEMA is brought down to less than 40% is that the copolymer does not form at low concentrations of HEMA. The present work of polymerizing styrene and MAA by gamma irradiation has shown that polystyrene as well as polymethacrylic acid do not form easily. In fact, the transparency achieved with polystyrene as well as polymethacrylic acid by gamma irradiation at the dose rate studied in this paper is found to be poor. The findings of the present study, therefore, have significance in the sense that the copolymers using styrene as well as MAA with HEMA could be made transparent upto a given ratio of monomers. The transparency achieved for all compositions of HEMA with NVP as well as MMA are as per the expected lines; poly (N-vinyl pyrrolidone) and poly (methylmethacrylate) as obtained by gamma irradiation are also transparent. Taking the water absorption capacity of HEMA as directly proportional to the content of HEMA, it is possible to assess the hydrophilic or hydrophobic behavior of the added monomer.

It is evident from the results that the hydrophobicity of the monomers added falls in the following decreasing order:

Styrene > MMA > HEMA > MAA > NVP

In the case of MAA, however, the trends of change in water absorption are different from all other monomers. The presence of a phenyl ring in the molecular structure of styrene makes it more hydrophobic than MMA, HEMA, and MAA, which are characterized by the presence of a linear bond structure. Moreover, the functional groups in MAA and MMA have more hydrophilic character than styrene beside the presence of aromatic ring in the latter. This is the reason as to why the water absorption capacity of HEMA drops down from 32.82 % to 0.08% on the addition of even 10 wt.% of styrene. Further, with the comonomers of HEMA with MAA and NVP, it is evident that the water absorption capacity of HEMA increases with increase in concentration of comonomer. It may be noted, however, that in the case of MAA, the trend is different from what is observed for NVP. Here, there is an initial drop in water absorption capacity when MAA is increased from 0% to 40% by wt. Beyond 40 wt.% of MAA, the absorption capacity rises, reaching well above the value (32.82%) obtained for HEMA alone. The water absorption capacity data for HEMA : MAA, inspite of the fact that the polymer is opaque, suggest that it is possible to develop polymers based on HEMA : MAA with varying water absorption capacity which can be used for other applications. Based on these results it can be said that :

(I) While the addition of a hydrophobic monomer brings about a reduction in capacity to absorb water, the presence of a more hydrophilic component, increases the capacity to absorb water.

(ii) The absorption of water takes place in two stages; upto 30 hours with a low rate and beyond 30 hours with a higher rate of absorption. This is true mainly for copolymers having a significant amount of hydrophobic portion, for example, MMA and styrene. Such behavior is not seen with NVP and MAA. In all the cases, the transparency of the copolymer remains unchanged even with the water absorbed. This shows that materials of varying optical properties like refractive index with different capacities of water absorption can be obtained by the use of different co-monomers with HEMA. This is a notable achievement of this study. Further, the use of irradiation using gamma rays for polymerization is established with this research work. Since the polymerization is carried out at ambient conditions, this would be a preferred option for polymerization compared to conventional methods like thermal polymerization.

HEMA can be polymerized easily using gamma rays at a dose of 40 kGy. The polymerization is possible even in the presence of water. The use of co-monomers of different hydrophilicity and hydrophobicity results in enhanced and reduced capacity of water absorption, respectively. Optical plastics of varying optical properties and water absorption capacities can be developed based on HEMA, a well-known monomer for optical plastics.

Materials with the capacity to contain various hydrophilic as well as hydrophobic substances can be obtained based on the data presented here. Here, it may be noted that the absorption of

water in the case of combination of HEMA with various monomers follows a set pattern of initial resistance to absorb water. As evident from the fact that after an initial uptake of water upto 5 hours, there appears to be a plateau upto 30 hours. Beyond 30 hours, the water uptake increases and this is apparent in almost all the cases except MAA and NVP. This could be ascribed to the hydrophilic barrier created due to the incorporation of the hydrophobic segment in the co-polymer. This barrier appears to be only kinetic in nature. The observations would help in designing combination of copolymers for intraocular and contact lenses for which water absorption and retention in the life cycle of the lenses are key factors.

Case III

Foldable Intraocular lenses (IOLs)

Aryl alkyl acrylates and aryl alkyl methacrylates are preferred raw materials for applications such as foldable intraocular lenses where flexibility/ foldability is the major criterion. They are characterized by the presence of a double bond, an aromatic ring in the case of aryl alkyl acrylates and methacrylate group in the case of aryl alkyl methacrylates. For the designing of IOLs, the glass transition temperature which in turn affects the flexibility/rigidity of a material is to be kept in mind. For foldable IOLs, glass transition temperature of 13-15^0 C is desirable. The materials that are suitable for foldable IOLs are modified silicones and acrylates. The authors have used acrylate based materials for their studies. The schmetic structure of the base materials used for the studies is given in Figures 17 a - b.

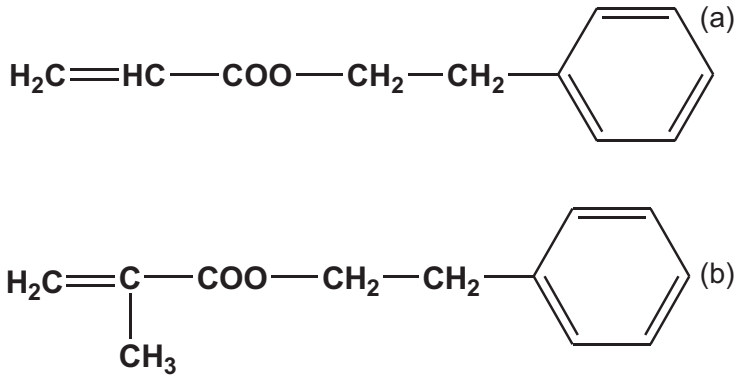

Figure 17. Structure of (a) aryl alkyl acrylate (b) aryl alkyl methacrylate

The presence of double bonds in acrylate and methacrylate monomers make it susceptible to cross-linking. Crosslinking of the monomers is brought about by gamma irradiation by free radical mechanism Schematic representation of the polymer obtained after polymerization is depicted in Figure 18.

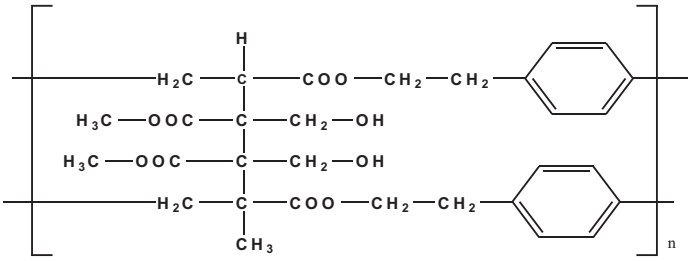

Figure 18: Schematic structure of the crosslinked polymer

The conventional methods for the preparation of foldable IOLs involves the thermal polymerization technique. Crosslinking of the monomers takes place in the presence of free radical initiators such as benzoyl peroxide and a cross-linking agent such as Butane diol diacrylate (BDDA). Thermal polymerization techniques for intraocular lenses are cumbersome and time consuming,requiring a number of post-polymerization processes such as removal of residual monomers etc. An alternative technique with less amount of rejections is desirable.

The authors have studied the effect of gamma irradiation on the polymerization of foldable intraocular lenses. Polymerization by gamma radiation is found to be more advantageous due to the fact it eliminates the need for initiators and also the need for post–polymerization steps,involved in the conventional techniques. Further, it is a cost –effective and quicker process providing better output than conventional techniques. The effect of gamma irradiation on the various properties of the polymers has been studied. Acrylate and methacrylate monomers are taken in different ratios ranging from 100:0 of acrylate:methacrylate upto 0:100 of acrylate:methacrylate.

The effect of gamma irradiation on polymerization was studied by subjecting the acrylate: methacrylate monomers in the ratio of 0 : 100 in the presence of BDDA as crosslinking agent.25 kGy was found to be sufficient for polymerization. The effect of gamma irradiation on the polymers was studied by evaluating the properties of the foldable intraocular lens compositions at 25kGy.

Effect of gamma irradiation on properties of IOLs

a) Gel content: The results of gel content of the various ratios of acrylate and methacrylate monomers polymerized by gamma irradiation and thermal methods are presented in Figure 19. Gel content of 97-98% is obtained at 25Kgy while a gel content of 95% is obtained by thermal methods. This indicates better crosslinking through radiation processing. Polymerization by gamma irradiation results in a highly crosslinked structure than the conventional method. Gel content obtain by gamma radiation is comparable to thermal polymerization indicating that gamma radiation is viable option for polymerization of IOL's

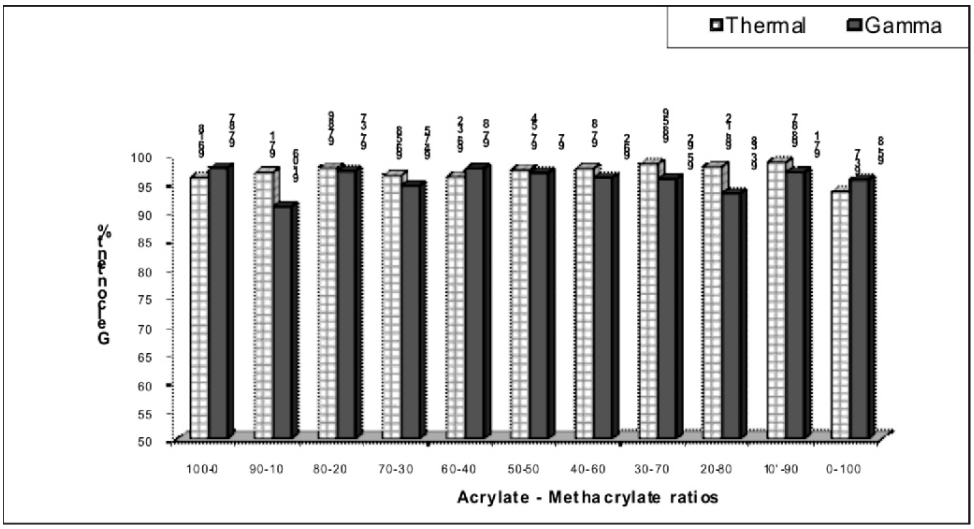

Figure 19. Effect of gamma irradiation on the gel content of various acrylatemethacrylate monomer ratios polymerized by thermal methods and by gamma irradiation.

b) Glass transition: The results of glass transition temperature of various ratios of acrylate:methacrylate monomers polymerized by thermal methods and by gamma irradiation are presented in Figure 20. As the acrylate content increases, glass transition temperature decreases.

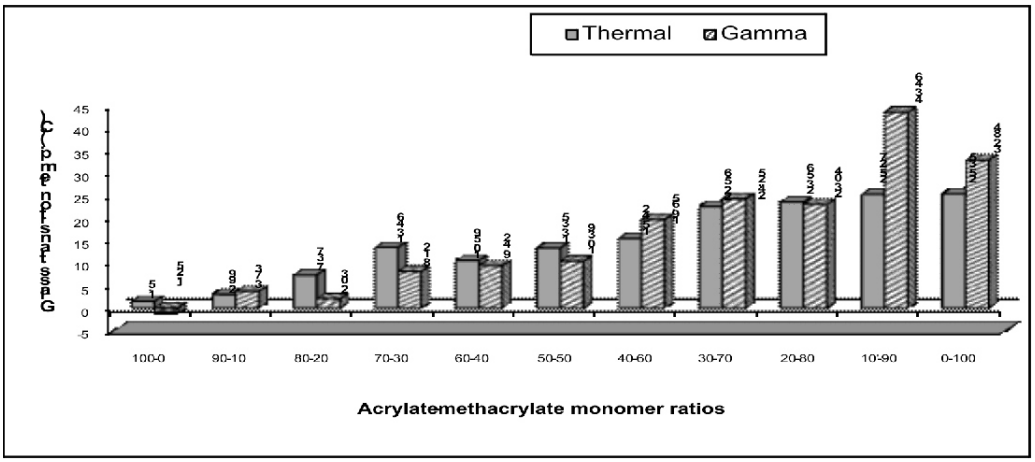

Figure 20 Effect of gamma radiation on glass transition temperature of acrylate – methacrylate monomer ratios polymerized by thermal methods and by gamma irradiation

The low glass transition temperature required for flexibility is achievable by gamma irradiation. From the results it can be seen that the glass transition temperature of the compositions polymerized by gamma irradiation are similar to the glass transition temperature obtained by thermal methods. It can also be seen that as the ratio of the methacrylate monomer increases, the glass transition temperature increases upto 32.84 ^{0}C in the case of polymerization by gamma irradiation and upto 25.35 ^{0}C in the case of thermal methods.

The results show that gamma irradiation can be a useful tool for:

a) Designing of polymer materials of desired hardness, softness, flexibility, and rigidity.

b) Polymer materials with a range of glass transition temperature ranging from 2.00 ^{0}C to 45.00 ^{0}C can be designed using gamma irradiation.

c) Radiation processing has been found to be ideal for the designing of materials for intraocular lenses.

Case IV

Metal containing polymers prepared by gamma irradiation

Polyacrylates are the cheapest optical materials having excellent optical clarity as well as easy moldability. The drawbacks associated with Polyacrylates such as low refractive index, poor heat stability, poor impact resistance and hardness are some of the features, which limit the widespread use of Polyacrylates as optical plastics. These drawbacks can be overcome by modifying either the structure or the constitution of polyacrylates.The scope of the applications of Polyacrylates can be widened, by suitable modifications to take care of drawbacks.

The authors have carried out studies on the feasibility of exploiting acrylic acid as a monomer for optical applications by overcoming the drawbacks of polyacrylates by dispersing metal salts and certain other additives in it. The use of metal salts such as barium hydroxide and lead monoxide is established so, that metal salts can be dispersed to a significant level in acrylic acid without causing any loss in transparency. The added feature is also the fact that tailor making of optical properties, unachievable with conventional materials is possible.

The development of metal containing polymers involve the following steps:

Step I : Dispersion of metal salts

Barium hydroxide, lead monoxide and lanthanum oxide are dispersed gradually at room temperature in acrylic acid : effect of addition was monitored on refractive index. The refractive index increases with the increase in addition of the metal salt till precipitation takes place

Step II: Preparation of monomer mixture

A monomer mixture is prepared by the slow addition of an aryl carboxylic acid to different metal-containing acrylic acid solution The addition of the aryl carboxylic acid is continued till the solution remains clear and transparent.

Step III: Cast polymerization of monomer mixture

The monomer mixtures consisting of acrylic acid, aryl carboxylic acid and different metal salts thus prepared are subjected to polymerization along with a comonomer. Lenses are cast by polymerization of the monomer mixture with a co-monomer using gamma irradiation. Casting of lenses is carried out by injecting the monomer mixture and comonomer into a mold, which is assembled by fitting glass molds in rubber gaskets.

The polymerization of monomer mixture into lenses was carried out by subjecting them to gamma irradiation. During polymerization, an aromatic vinyl group is added which not only acts as a copolymer but also as a crosslinking agent.

Effect of gamma irradiation on the properties of metal containing polymers

Polymerization studies have been carried out with varying concentrations of an aromatic vinyl group in order to finalize the optimum concentration required for polymerization. The transparency, as indicated by transmittance (%), was found to be improved since samples prepared without the vinyl group were found to be opaque.

This confirms the necessity of vinyl group in the structure for crosslinking. The co-monomers mixed with various concentrations of the aromatic vinyl system when cast polymerized shows an improvement in desired properties of the cast lenses. The mixture was polymerized into transparent lenses by gamma irradiation. The lenses were evaluated for optical and mechanical properties and compared with the reference material of polymethyl methacrylate (PMMA). The results are tabulated in Table 6.

The metal containing polymers as can be seen, have higher refractive index and better impact resistance than PMMA.

Table 6. Properties of metal containing polymers vis-a -vis PMMA. The standard metal containing polymers are found to be superior to PMMA. Metal containing polymers are found to be superior to PMMA in scratch resistance and hardness due to the dispersion of metal atoms

Properties	Barium	Lead	Lanthanum	PMMA
Color	Light Yellow	Dark Yellow	Light Yellow	Colorless
Refractive index	1.56	1.59	1.58	1.495
Abbe No.	35	34	34	57
Hardness(Shore-D)	85-86	85-86	85-86	65
Scratch resistance	Grade B	Grade B	Grade B	Grade-C
Haze number	8.00-8.50	10.0-10.5	6.0-7.0	>2.0
Pencil hardness	6H	6H	6H	4H
Impact resistance	Pass	Pass	Pass	Fail
Machinability	Good	Good	Good	Good
Specific gravity	1.31	1.30	1.28	1.24
Transmittance (%)	90	90	90	90
Yellowness Index	1.044	1.218	1.158	0.030
Service temperature	-60^0C to 90^0C	-60^0C to 90^0C	-60^0C to 90^0C	-60^0C to 90^0C

Image analysis: Image analysis of the lenses cast from metal containing compositions indicates a homogeneous dispersion of metal atoms in the polymer matrix. (Figure 21a - c)

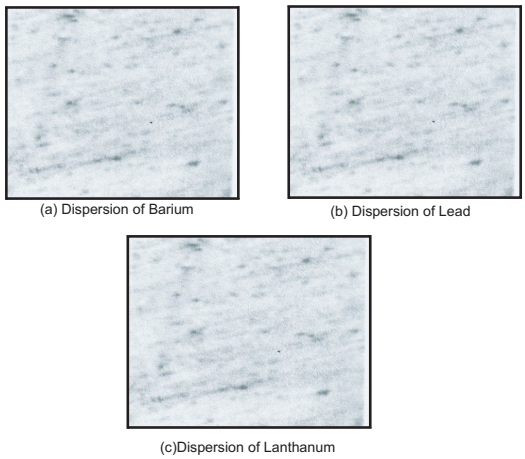

Figure 21 a-c. Image Analysis of polymer indicating a homogeneous dispersion of metal atoms in polymer matrix

b) Thermal analysis: Interactions between the polymer matrix and metal salts due to gamma irradiation have been studied by TGA- DTA analysis (Figures 22-23). The differential thermogram of the individual monomers such as metal dispersed acrylic acid, aryl carboxylic acid and aromatic vinyl group clearly indicate major decompositions below 200^0C before polymerization which increases to > 400^0C after polymerization. The increase in thermal stability of the polymer is attributed to the formation of strong crosslinkages formed by the chemical interaction between the components.

The presence of a crosslinked structure is further confirmed by a solubility test of the polymers in chloroform. No change in weight and appearance confirms the presence of a crosslinked structure. The presence of a cross-linked structure is further confirmed by no change in weight and appearance.

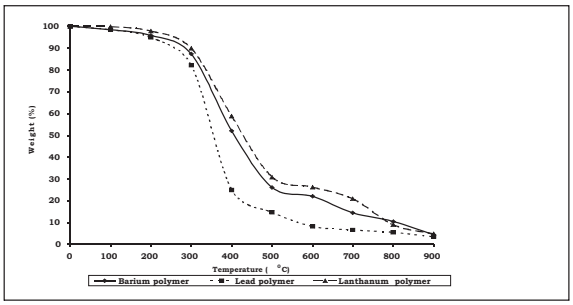

Figure 22. Thermogravimetric analysis (TGA) showing interaction between the different components of the metal containing polymers.

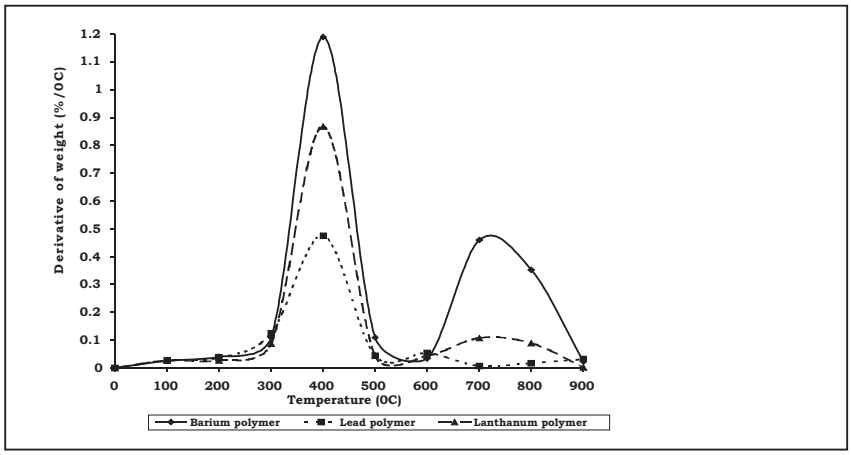

Figure 23. Differential thermograms (DTA) of metal containing polymers indicate the formation of a highly crosslinked structure.

The TGA studies of the system indicate the formation of a highly crosslinked, thermally stable structure with no free acrylic acid and aryl carboxylic acid.

On gamma irradiation, free radicals are formed by the metal acrylate which add onto the unsaturated, active sites leading to the formation of a highly crosslinked structure.

The mechanism for the formation of the crosslinked structure by gamma radiation, involves the formation of free radicals of the aryl carboxylic system, unsaturated aromatic system and metal acrylate, which results in the formation of a cross-linked structure (Figure 24).

Through these studies, it can be concluded that radiation processing is a useful tool for the modification of polyacrylates. The refractive index of Polyacrylates can be improved by dispersing metal salts. It has been possible to incorporate metal salts such as lead and lanthanum to the extent of ~30% by weight with no loss in transparency etc. Polymers of the monomers incorporated with metals have shown improvements in various properties such as refractive index and impact resistance. Tailor making of optical properties has been made possible by changing the concentration of the dispersed salts. The incorporation of cross-linking agent as well as co-monomer has resulted in polymer materials that can be used for optical applications.

(a)Free radical formation

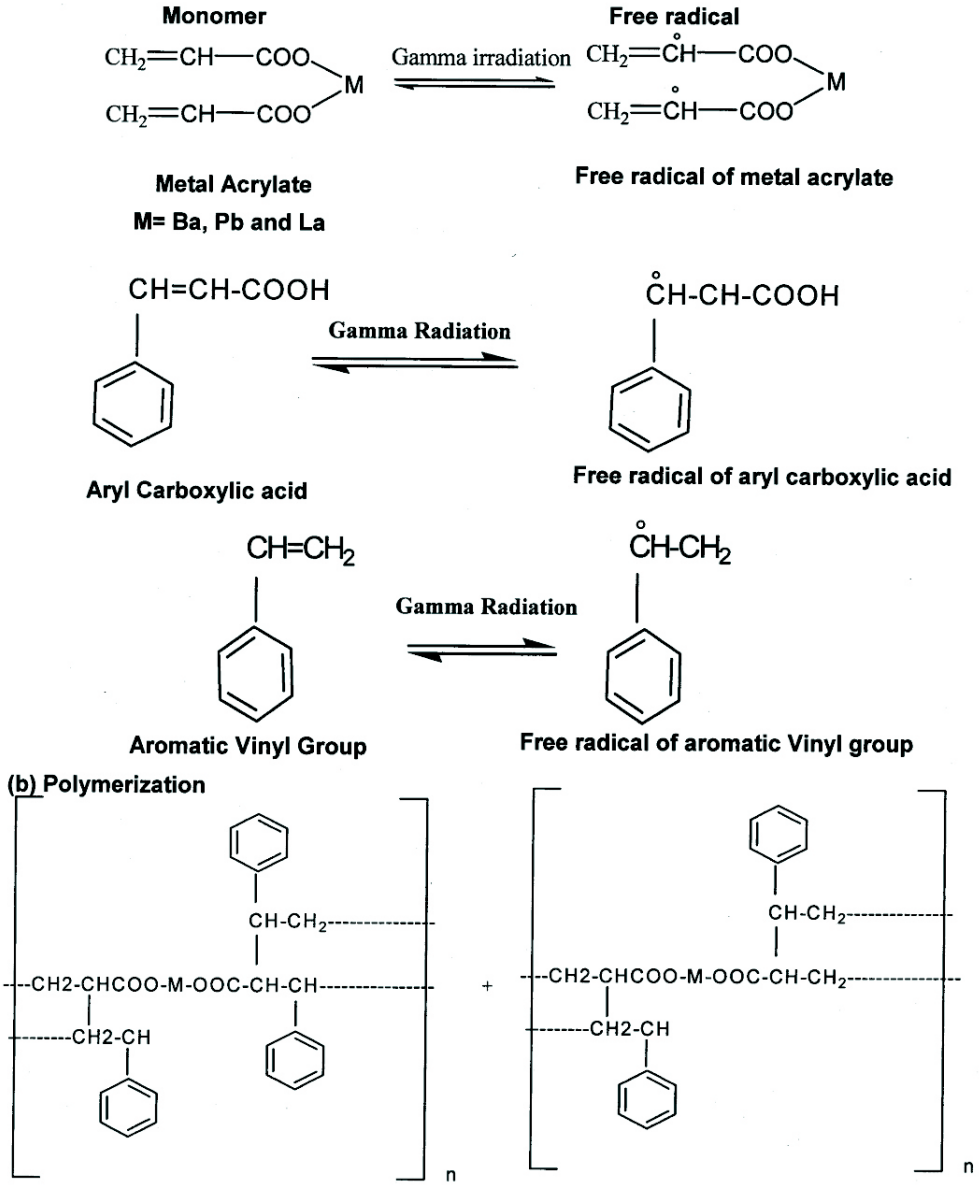

Figure 24 Schematic representation of cross linked structure of metal containing polymers prepared by gamma irradiation. The components used for the preparation of metal containing polymers generate free radicals by gamma irradiation. The sites available for polymerization and the likelihood of getting a particular polymer are depicted here.

Case V

Metal containing nanocomposites of Titanium

It has not been possible so far to have chemistries that can produce materials of varying properties as per requirements. For this, composite materials in devices such as lenses, coatings and filters are being extensively studied. Organic-inorganic composite materials are being considered as the potential candidates for optical devices due to their properties of improved hardness, high refractive index & high Abbe number. The inorganic component such as metals and metal salts provide physico-mechanical properties to the matrix whereas the organic part or continuous phase such as plastics binds them together providing a uniform distribution of reinforced material i.e. metals. One of the approaches found feasible and possible by the authors pertains to the in-situ synthesis & dispersion of nanoparticles of metals or metallic salts for the preparation of metal containing compositions. Incorporation of titanium in plastic matrices to form homogeneous & optically clear compositions was a challenge till recently.

Polyacrylates have been recognized as an obvious choice for optical applications e.g. spectacle lens. The refractive index of polyacrylates is limited between 1.42 to 1.49 and to increase the refractive index further, dispersion of high refractive index metal compounds is one of the available options. The high refractive index & high hardness of titanium makes it the desirable metal for dispersion in optical plastics. It would be interesting to prepare high refractive index polymers based on acrylate as a base material.

In the present study, an attempt has been made to disperse titanium in different percentages in acrylate matrix and subsequently cast polymerized into lenses. Gamma radiation has been adopted for polymerization. By using gamma irradiation, the authors have been successful in creating a new range of acrylate polymers with unique features of high refractive index and high Abbe number.

Mechanism of in-situ formation of nanocomposites using gamma irradiation

The formation of novel nanocomposites can be attributed to the simultaneous formation and dispersion of Titania (TiO_2) by the formation of intermediates in the acrylate matrix during the dispersion of the titanium precursor besides the formation of titanium-acrylate monomer.

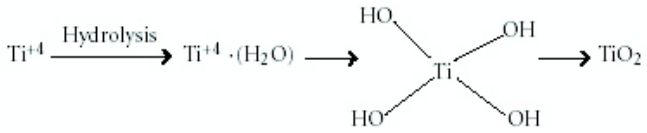

Figure 25 Schematic representation of the formation of TiO_2

Characterisation of Titanium composites

The nanocomposites of titanium were evaluated for various properties

a) FTIR Analysis: FTIR spectra (Figure 26) of acrylate-titanium composite confirms the formation of titanium- acrylates. The stretching vibration bands at 1730 cm^{-1} and 2950 cm^{-1} are ascribed to C=O and C-H bonds respectively. The presence of absorption band at 1630 cm^{-1} is due to TiO_2 and a broad absorption band at 3400-3500 cm^{-1} is attributed to Ti-OH bond. It can infact, be said that the IR studies confirm the simultaneous formation and dispersion of TiO_2 by the formation of intermediates in the acrylate matrix during the dispersion of the titanium precursor besides the formation of titanium-acrylate monomer.

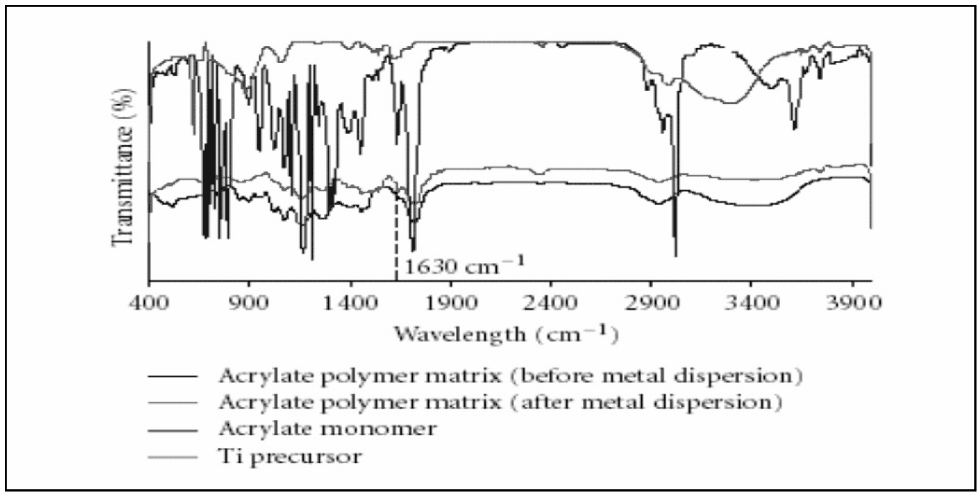

Figure 26. FTIR analysis of metal acrylate nanocomposites. The presence of the peak at 1630cm, confirms the simultaneous formation and dispersion of Titanium as TiO_2 in the polyacrylate matrix.

b) Thermal Analysis: TGA analysis shows the thermal stability of the acrylate polymer and metal containing polymers. The TGA graphs in Figure 27 shows that the neat polymer decomposes completely without any residue at 500°C while the metal dispersed polymer shows a residual content of ~ 5 % in (a) & 10 % in (b). The thermal stability of metal dispersed polymer is increased significantly as the content of the metal increases; the initial decomposition of the polyacrylate matrix without dispersion (c) is at 120° C which increases to ~ 220 C in the case of 0.5% dispersion of titanium (a) and to ~ 240 °C in the case of 4.3 % dispersion of titanium (b).

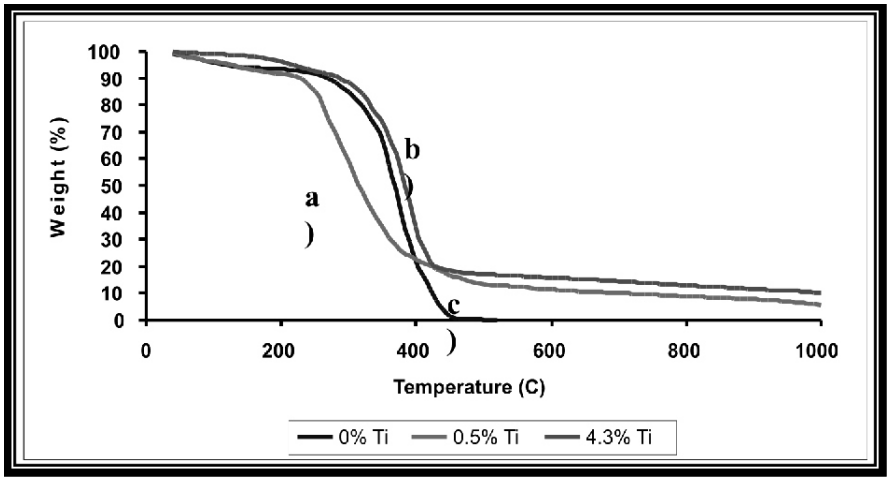

Figure 27: Thermogravimetric analysis of polyacrylate with and without dispersion of TiO_2. The thermal stability of the polyacrylates increases with increase in the content of TiO_2

c) TEM & SEM analysis: TEM image analysis indicates a particle size <20 nm as shown in Figure 28 a. The SEM images (Figure 28 b) given below confirms the shape of titanium particles to be cuboidal. These results are a further confirmation of the fact that the methodology adopted the authors is successful for the in-situ formation and dispersion of TiO_2

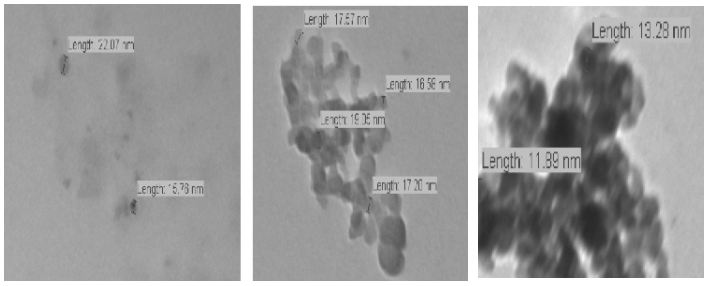

(a) *TEM Analysis.*

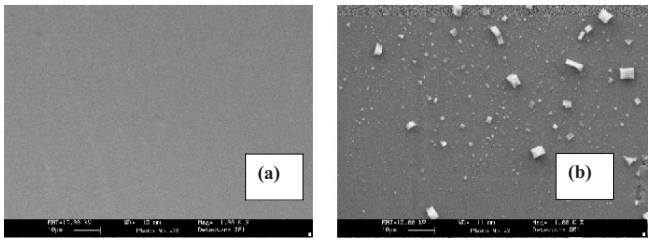

(b) *SEM Analysis*

Figure 28 : TEM and SEM analysis confirms the In-situ formation and dispersion of cuboidal nanoparticles of TiO2 of < 20nm .

d) Refractive Index & Abbe number: The effect of titanium content on the refractive index of the acrylate matrix can be understood from Figure 29 (a). As the incorporation of titanium in the acrylate matrix increases, the refractive index increases from 1.45 to 1.53. The effect of incorporation of titanium in the acrylate monomer on Abbe number can be seen from Figure 29 (b). The Abbe number decreases from 57 to 40. The refractive index and the Abbe number values obtained by the dispersion of TiO_2 in polyacrylates are the desired values for optical applications such as spectacle lenses

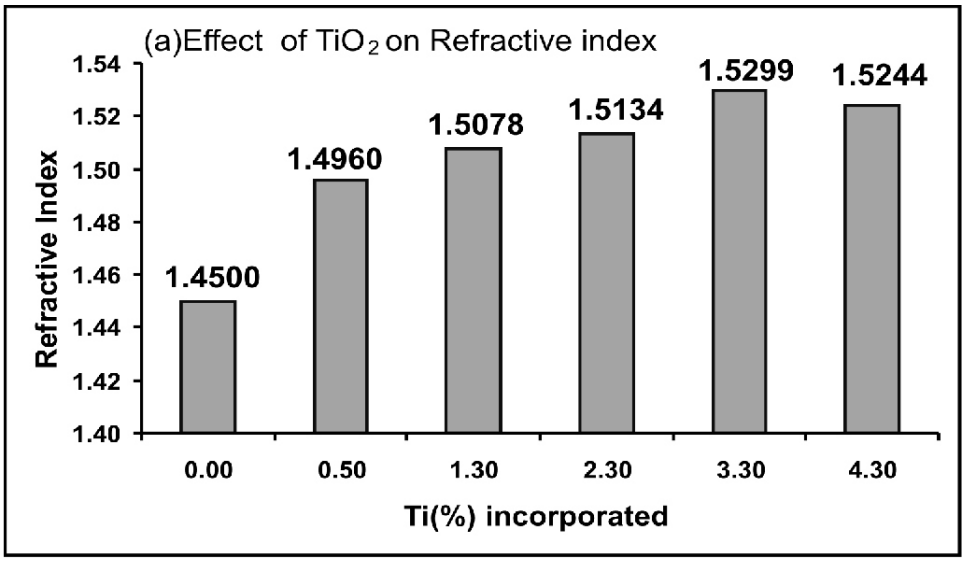

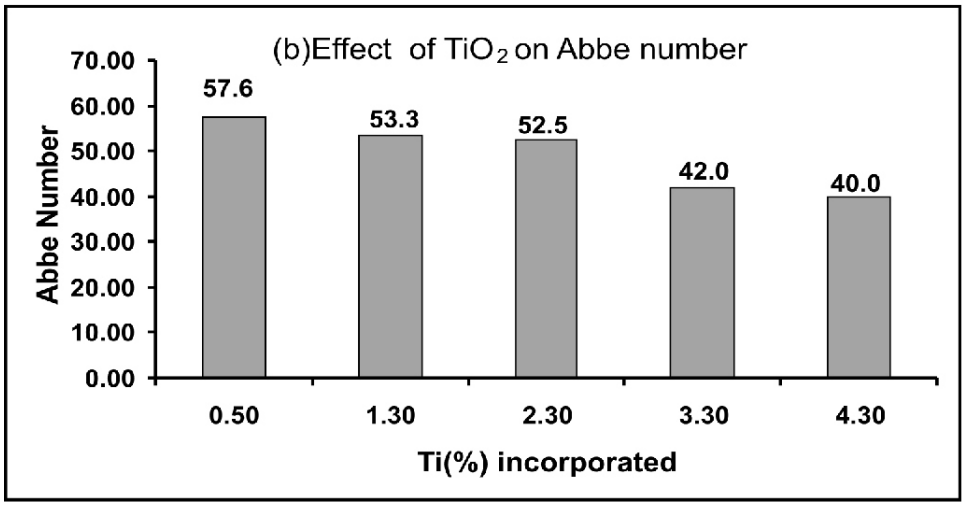

Figure 29 a- b As the concentration of Titanium increases in the polyacrylate matrix, the essential optical properties such as , refractive index increases from 1.4500 to1.5244 and the Abbe number decrease from 57 to 40

e) Transmittance (%): Titanium containing acrylate are found to be clear and transparent having a transmittance of more than 90%. This confirms the formation of transparent & clear compositions by the dispersion of titanium in the acrylate matrix. This also confirms the dispersion of nanoparticles in the acrylate matrix.

f) Specific gravity: Specific gravity of the titanium containing polyacrylates is depicted in Figure 30. The specific gravity of the samples increases with the increase in the titanium content. Even though titanium is a heavy metal of specific gravity of 4.05 g/cm^3, the specific gravity of the polymers is in the range of 1.29 to 1.33 g/cm^3 which is similar to the specific gravity of optical polymers such as polycarbonates (1.28), Polymethyl methacrylate (1.26) and Polythiourethane (1.36) which supports the fact that metal composites are suitable for optical applications.

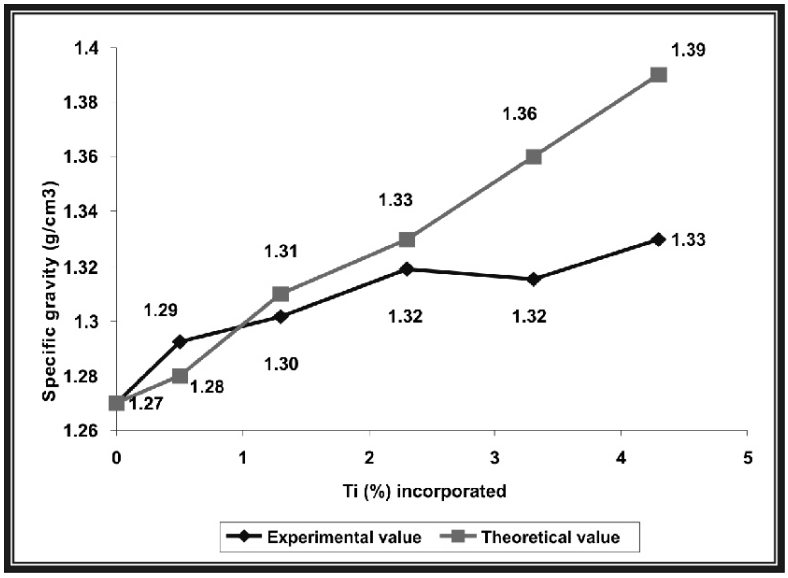

Figure 30. Effect of Titanium on the specific gravity of Polyacrylates. Change in specific gravity with incorporation of Titanium in polyacrylates. Specific gravity increases with increase in titanium content

g) Inductively coupled plasma (ICP): ICP analysis was carried out to determine the percentage dispersion of titanium in the metal containing polymers. The ICP results are found to agree closely with theoretical value and falls in the range of 0.5% to 4.3% by wt.

h) Ash Content: Ash content of the sample as evaluated from the furnace studies was used to indicate the residue (%) of the metal containing polymer. The polymer was burnt to ash and the residue (%) was calculated. The graph in Figure 31 shows the increase in ash content (%) with increase in content of titanium.

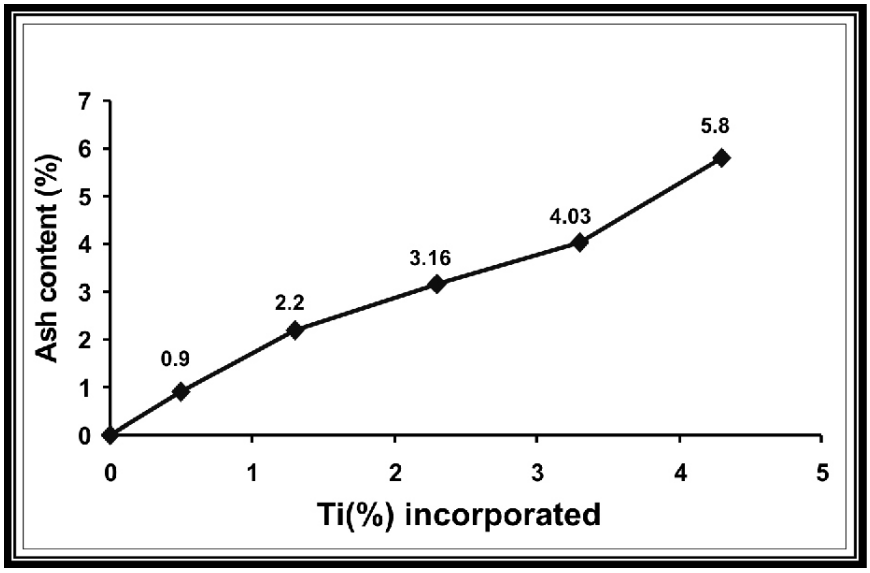

Figure 31. Ash content of Titanium containing polymer. Ash content increases with increase in titanium content confirming the dispersion of Titanium in the acrylate matrix.

From the above studies, the following conclusions can be drawn:

1. Metal containing polyacrylates with improved refractive index and desired Abbe number suitable for optical applications have been developed successfully.

2. Microscopy studies indicate the formation of transparent & clear nanocomposites.

3. Tailor making of the refractive index and Abbe number between 1.45-1.53 & 40-57 are novel features which have been achieved successfully.

The use of gamma radiation processing technology has proven to be ideal for development of such novel nanocomposite materials.

Path Forward

The past two decades has seen the emergence of several technologies arising out of the need for better, newer and affordable materials. Metals, ceramics and polymers have been exploited to the maximum limit. However, this does not mean that the search for a suitable material for a given application is over. The demand for alternative materials and technologies to the existing ones has been increasing where sustainability is most sought after .

Plastics has proven to be one of the most cost effective alternatives to existing materials

especially in the field of optical applications. where plastics have almost completely replaced glass. Plastics are light in weight, easy to manufacture and process and have better aesthetics. They however have an inherent limitation of being extremely soft. Combination of plastics with metals or nanocomposites are novel materials which can overcome this. Though nanocomposites are promising materials, the methods of preparation of nanocomposites are quite cumbersome.

Radiation processing technology has been found to be an efficient technique for the preparation of novel nanocomposites. It not only provides a green and environment friendly alternative to produce nanocomposites but also helps in the creation of unique features such as tailor making of essential properties which are not possible with conventional materials.

References

1. S.Mach, Radition Physics and Chemistry,1995,46,1,399
2. J.Kohi, Journal of Nuclear Energy ,1971,25,11,568
3. C.H.Jones, Journal of Applied Radition and isoptope,1968,19,10,777
4. E.I.Hamilton ,Science of the Total Environment ,1977,7, 2,195
5. W.G.Waston,Amercian Journal of Orthodonitics, 1982,82,3,257
6. H.Dislich,Angew.Chem.Int,Ed.Engl.18,1979,49
7. J.M.Young, Opt.World, 1989, 18, 124
8. G.Suri, et al, Journal of polymer material, 2009, 26,1,21
9. P.J. Flory, J.Am.chem.Soc.1937, 59, 241.
10. S.G.Cohen and D.B.Sparrow, J.Am.Chem.Soc.1950, 72,611
11. C.Darraud, et al., 1995, polymer,1995 36, 325
12. S.G.Cohen and D.B.Sparow, J.Am.Chem.Soc. 1950,72,611
13. G.S.Jha, et al.,e-polymer, 2007, 120.
14. O. Wichterle and D.Linn, ”hydrophilic gels for biological use“, Nature, 1960, 185,9,117.

15. P.Chhabra, et al., International Journal of Polymer Science , volume 2009, Article ID 906904

16 I.Tranoudis and N.Efron ," Parameter stability of soft contact lenses made from different materials ," Contact lens & Anterior Eye, 2004, 27,3,115 18.

17 P.D.Dalton , et al., Biomaterials, 2002, 23,18, 3843

18 L.Li and L.J.Lee, " Photopolymerization of HEMA/DEGDMA hydrogels in solution," Polymer ,2005, 46,25,11540

19 I.Tranoudis and N.Efron, " tensile properties of soft contact lens materials," contact Lens & anterior Eye, 2004, 27, 4,177

20 J.E.Kohler and G.W.Flangan, international Contact lens Clinic,1985,12,3.

21 N.A.Bernnan and N.Effron ,contact lens forum , 1987,12,28

22 H. Ridley, Intraocular Acrylics lenses, Trans Ophthalmol. Soc.UK, 1951,71, 617

23 Edward Maumenee,M.D,Intraocular lens implantation ,NIH Consens Statement ,1979,2, 7, 37

24 S. Wshalaby, in Thermal Characterization of Polymeric Materials , 1981,262,Academic Press,New York,

25 Wolter.J.R et al. ,Biomaterials in Ophthalmology,1990

26 C.D. Kelman, Phacoemulsification and aspiration,Am.J.Opthalmol,1967,64,23

27 Mackool,R.J,Decentration of plate hepatic lenses ,J.Cataraact RefractSurg,1996,22,396

28 Decker , Macromol. Symp. 1999, 45, 143

29 A. R. Le-boeuf and M. Karakelle, U.S.Pat., 5,922,821,1999

30 T. Kawai, et al., Eur. Pat.Appl. E.P., 661, 307, 1995

31 H. Seisakusho and K. Eguchi, Japan Pat 60-94410,1987

32 H. Terao, S. Eguchi and H. Asano,Chem.Lett., 1987, 6 , 1001

33 S. Eguchi, et al., U.S. Pat. 4,585,841,1986

34 M. Tyagi, et al. , Journal of Polymer Materials, 2006, 23, 1, 21

35 M.Tyagi,et al., Journal of Polymer Materials 2007, 24, 2, 135

36 S. Eguchi, et al., U.S. Pat. 5, 113, 477 ,1992

37 J. D. Lee, "Concise Inorganic Chemistry", 4th ed., Chapman &Hall, London, 1991, 336.

38 J.D. "Handbook of Optics", 2nd edition, McGraw Hill. New York, 1995

39 W.F. Frank, Precision Plastics Optics for Optical Storage, SPIE, July 30-31, 1997, 3135

40 G . Philip and H.J. Schmidt, Non-Cryst. Solids , 1984, 63, 283

41 B. Wang, et al., Macromolecules 1991, 24, 3449

42 A. Ershad-Langroudi, et al., .J. Appl. Polym. Sci., 1997, 65, 2387

43 Chen, W. C.; et al., Journal of Mater. Chem., 1999, 9, 2999

44 American Standard Test Method for Index of Refraction of Transparent Organic Plastics ASTM D-542, 1990.

45 American Standard Test Method D-792-00; Standard test method for density and specific gravity (Relative density) of plastics by displacement ,1995

46 A. Leaustic, et al., J. Chem. Mater. 1989, 1, 240.

Awards

SHRIRAM INSTITUTE FOR INDUSTRIAL RESEARCH (SRI)
19, University Road, Delhi - 110 007, India

SHRIRAM
ISO 9001

Certificate

This is to certify that **Ms. Gunjan Suri**
was adjudged as the Second Best Speaker by the
Technical Committee of the International Conference on

RADIATION PROCESSING :
Value addition for Food, Agro, Healthcare, Polymers and other Industrial Products

at *Shangri-La's - Eros Hotel*, New Delhi, India during Dec. 17-18, 2010

Dr. U. K. Niyogi
Jt. Director, SRI

Dr. V. K. Verma
Jt. Director, SRI

Dr. R. K. Khandal
Director, SRI

SHRIRAM INSTITUTE FOR INDUSTRIAL RESEARCH (SRI)
19, University Road, Delhi - 110 007, India

SHRIRAM
ISO 9001

Certificate

This is to certify that **Ms. Gunjan Suri** has been conferred with the **Best Poster Award** for her poster titled "Optical Plastics by Gamma Radiation" at the International Conference on

RADIATION PROCESSING :
Value addition for Food, Agro, Healthcare, Polymers and other Industrial Products

at *Shangri-La's - Eros Hotel*, **New Delhi, India during Dec. 17-18, 2010**

Dr. U. K. Niyogi
Jt. Director, SRI

Dr. V. K. Verma
Jt. Director, SRI

Dr. R. K. Khandal
Director, SRI

Asian Polymer Association

APA

APA 2009 Asian Polymer Association

Polymer Congress

APA-2009

POLYMER SCIENCE AND TECHNOLOGY : VISION & SCENARIO

December 17-20, 2009 | New Delhi, India

Certificate

Asian Polymer Association is pleased to Confer

Best Poster Award

to

Gunjan Suri

in the Polymer Congress 'APA-2009'

Polymer Science & Technology : Vision & Scenario

December 17-20, 2009

New Delhi, India

Bhuvanesh Gupta
Chairman, APA

Saiqa Ikram
Secretary, APA

Biodata of the Student

BIODATA

Name : Ms. Gunjan Suri

Date of Birth : February 28, 1983

Place of Birth : Delhi, India

Educational Qualification

Year	Degree	Course	Subjects	University	Division
2003	Graduation	B.Sc.	Chemistry, Physics, Mathematics	University of Delhi, India	Ist
2005	Post-Graduation	M.Sc.	Chemistry	University of Delhi, India	Ist
2006	Doctorate (In process)	Ph.D	Applied Chemistry	Delhi College of Engineering, University of Delhi, India	-

Job Details

Organization : Shriram Institute for Industrial Research

Total years of experience : 6 years 5 months

2005-2006 : Project Trainee, Shriram Institute for Industrial Research

2006-2008 : Analyst 'B', Shriram Institute for Industrial Research

2008-Till date : Assistant Scientist 'B', Shriram Institute for Industrial Research

Area of Expertise

I. Research & Development studies related to the areas of:

i. *Nanotechnology:* Applications of nanotechnology for the

a) Development of novel nanocomposites with unique optical properties

b) Development of recyclable nanophotocatalyst for industrial effluent treatment

ii. *Radiation processing technology:* Applications of radiation processing technology for the development of novel optical polymeric materials with enhanced properties.

iii. *Process modification for development of new products with improved characteristics*

II. Undertaking analytical studies for characterization of new polymeric materials using

- Particle Size Analyzer
- Rheometer
- Thermogravimetric Analyzer
- Differential Scanning Calorimeter
- UV Spectrophotometer
- IR Spectrophotometer

R&D projects undertaken at Shriram Institute for Industrial Research

1. Development of optical plastics using novel processing technology of gamma irradiation
2. Modification of low refractive index polycarbonates and conversion into high refractive index materials
3. Development of high refractive index polythiourethane for optical applications
4. Development of metal containing polyacrylates for optical applications
5. Development of nano-dispersed polyacrylates for optical applications
6. Development of polymeric materials for contact lenses and intraocular lenses
7. Development of energy efficient photocatalytic system

Contact details:

Address	:	*Shriram Institute for Industrial Research*
		19, University Road, Delhi-110007, India
Phone	:	*+91-11-27667267*
Fax	:	*+91-11-27667676*
E-mail	:	sridlhi@vsnl.com

Publications

Research papers	*:*	*8*
Chapters in Books and Handbooks	*:*	*4*

Papers Presented

1. "Metal Dispersed Nanocomposites Plastics; Novel Materials for Value Added Applications"; presented at 2nd Indo-Swiss Bonding International Symposium on "Bonding a key technology for progress Engineering & Structural Design, Nanotechnology and Polymeric nanocomposites", Sikkim Manipal Institute of Technology, Sikkim, February 11-13, 2010
2. “Development of Metal Dispersed Polymers; Novel Materials with Unique Properties“, Presented at Indian Science Congress Symposium January 3-7,2010 at Thirvananthapuram, Kerala.
3. “Development of Titanium based Nano optical plastics”, Presented at Indian Science Congress Symposium January 3-7,2010 at Thirvananthapuram, Kerala.
4. Novel Optical Nanocomposites by Radiation Processing”, Presented at International Conference on Radiation Processing, Shriram Institute for Industrial Research, Delhi, December 17-18, 2010.
5. “Optical Plastics by Gamma Irradiation; Studies to demonstrate feasibility”, Presented at International Conference on Radiation Processing, Shriram Institute for Industrial Research, Delhi, December 17-18, 2010.

Awards

- Second Best Oral Presentation Award on “Novel Optical Nanocomposites by Radiation Processing” at International Conference on Radiation Processing, Shriram Institute for Industrial Research, Delhi, December 17-18, 2010.
- Best Poster Presentation Award on “Optical Plastics by gamma Radiation; Studies to demonstrate Feasibility” at International Conference on Radiation Processing, Shriram Institute for Industrial Research, Delhi, December 17-18, 2010.
- Best Poster Presentation Award on "Development of High Refractive Index Nanocomposites for Optical Applications"; International Conference on Polymer Science & Technology: Vision & Scenario, Polymer Congress 'APA-2009', New Delhi, India, December 17-20, 2009

LIST OF PUBLICATIONS

Research papers

- "Novel Nanocomposite Optical Plastics: Dispersion of Titanium in Polyacrylates";
  Gunjan Suri, Mukti Tyagi, Geetha Seshadri, Gurucharan Lal Verma & Rakesh Kumar Khandal
  J. of Nanotechnology, Article ID 531284, Volume, 2010

- "Challenges In Preparation Of Metal-Containing Polymers; Dispersion of Titanium Into Plastics";
  Gunjan Suri, Pranshu Chhabra, Mukti Tyagi, Ruchi Gupta, Shikha Saxena, Geetha Seshadri, Gurucharan Lal Verma & Rakesh Kumar Khandal
  e-Polymers, 106, 2010

- "Understanding Interparticle interactions through viscosity of Guar surfactant aqueous systems"
  Meenu Talwar, Dhriti Khandal, *Gunjan Suri*, Pranshu Chhabra, Mukti Tyagi, Geetha Seshadri, Ajay Kumar, Saroj Aggarwal, U. K. Niyogi & Rakesh Kumar Khandal
  Trends in Carbohydrate Research, 2, 2, 2010

- "Studies on development of polymeric materials using gamma irradiation for Contact and Intraocular Lenses"
  Pranshu Chhabra, Ruchi Gupta, *Gunjan Suri*, Mukti Tyagi, Geetha Seshadri, S. Sabharwal, U. K. Niyogi and R.K. Khandal
  International Journal of Polymer Science, Article no. 906904, 2009

- "Modification of low refractive index polycarbonate for high refractive index applications"
  G. Suri, G. S. Jha, G. Seshadri, R. K. Khandal
  International Journal of Polymer Science, Article no. 836819, 2009

- “Properties of Optical Plastics Prepared by Gamma Radiation”
  G. Suri, P. Chhabra, M. Tyagi, S. Kaushik, G. S. Jha, G. Seshadri, A. Malik, U. K. Niyogi, R. K. Khandal
  J. Polymer Materials 26, 1, 33-44, 2009

- “Studies to design a sulfur containing bifunctional (diol) building block with improved refractive index”
  G. S. Jha, P. Chhabra, *G. Suri*, M. Tyagi, P. Arora, G. Seshadri, R. K. Khandal
  E-Journal of Chemistry, 6, 2, 399, 2009.

- “Novel way of making High Refractive Index Plastics; Metal Containing Polymers for Optical Applications”
  M. Tyagi, *G. Suri*, P. Chhabra, G. Seshadri, A. Malik, S.Aggarwal, R. K. Khandal
  e-Polymers, 100, 2009

LIST OF PUBLICATIONS

Chapters in Books and Handbooks

- "Radiation Processing for development of novel materials"
  Gunjan Suri, Dhriti Khandal, Ruchi Gupta, Pranshu Kapoor, Mukti Tyagi, Jay Pal Singh, Rakhi Singh, Geetha Seshadri, U.K.Niyogi, G.L.Verma, Xavier Coqueret and R.K.Khandal
  Radiation Technology Applications, SRI Publications, Volume 2, 2010

- "Modification of natural Polymers: Prospects of using radiation technology"
  Meenu Talwar, *Gunjan Suri*, Neeraj Verma, Prashansa Parmar, Geetha Seshadri, Ajay Kumar, U.K.Niyogi & R.K.Khandal
  Radiation Technology Applications, SRI Publications, 2010

- "Radiation processing for degradation and depolymerization"
  Meenu Talwar, Pushplata Gupta, Bhuvaneshwar Rai, Rakhi Singh, *Gunjan Suri*, Pranshu Kapoor, Dhriti Khandal, Geetha Seshadri, R.K.Diwan, Saroj Aggarwal, Xavier Coqueret, U.K.Niyogi & R.K. Khandal
  Radiation Technology Applications, SRI Publications, 2010

- "Role of Surfactants in paints, inks and polishes "
  Rakesh Kumar Khandal, Geetha Seshadri, *Gunjan Suri*, Dhriti Khandal
  Handbook of Detergents, Part E, CRC Press, 2008

DEVELOPMENT OF ACRYLIC NANOCOMPOSITES FOR OPTICAL APPLICATIONS

THESIS SUBMITTED TO THE
FACULTY OF TECHNOLOGY
UNIVERSITY OF DELHI
FOR THE AWARD OF THE DEGREE OF

DOCTOR OF PHILOSOPHY

BY

GUNJAN SURI

Under the supervision of

DR. R. K. KHANDAL & PROF. G. L. VERMA

DEPARTMENT OF APPLIED CHEMISTRY
DELHI COLLEGE OF ENGINEERING
UNIVERSITY OF DELHI
DELHI (INDIA)

Chapter 8
Conclusions

CHAPTER 8
CONCLUSIONS

Metal containing nanocomposites developed by the dispersion of metal salts in simple base materials involving simple chemistries such as acrylic acid are a good alternative to the currently existing optical plastics.

In this thesis, possibility of incorporation of various metals and their salts in simple base materials such as acrylic acid and 2-hydroxyethyl methacrylate has been established. Studies have been carried out pertaining to the feasibility of developing metal containing acrylates for optical applications. An attempt has been made to overcome the existing drawbacks of acrylates by dispersing metal salts and other additives. The metals which were, found almost impossible to be disperse in acrylates, have been successfully incorporated using in-situ approaches. The salts of metals such as barium, titanium and lanthanum have been dispersed in acrylic acid and 2-hydroxyethyl methacrylate in significant amounts. Clear and transparent metal containing polymers suitable for optical applications have been successfully developed.

It is worth-mentioning that gamma irradiations have been used as a tool for the development of metal-containing nanocomposites for optical applications. By the above studies, gamma irradiation technology has been established as a safe, eco-friendly and viable technique for the polymerization of metal containing nanocomposites. The metal containing nanocomposites have been cast into hard and clear lenses suitable for optical applications by gamma irradiation technology.

The work presented in this thesis can be concluded with the following notable outcome:

a) Metals such as barium, titanium and lanthanum can be dispersed in acrylic acid and 2-hydroxyethyl methacrylate to give transparent and clear acrylic nanocomposites suitable for optical applications.

b) Synthesis and dispersion of metal salts by adopting in-situ approach has been successful for the preparation of metal-containing nanocomposites.

c) Barium has been dispersed upto significant amounts of 14%, titanium has been dispersed upto 4% and lanthanum has been dispersed in upto amounts of 17% without any loss in optical clarity and transparency.

d) The dispersion of metals in the matrices was in nanometer range which led to optically clear and transparent compositions.

e) Further improvements in the properties of metal containing compositions have been made by the incorporation of aromatic carboxylic acids such as cinnamic acid. This leads to an improvement in key optical properties. The refractive index of acrylic acid was improved from 1.424 to 1.470 in the case of dispersion of barium, 1.463 in the case of dispersion of titanium and 1.466 in the case of dispersion of lanthanum. These unique properties provided by the co-monomer has been instrumental in transforming metal containing acrylates into compositions suitable for optical applications.

f) Styrene was found to be suitable for the polymerization of metal-containing compositions to yield transparent, hard, high refractive index metal containing acrylic nanocomposites.

g) The compositions have been cast polymerized into transparent, bubble free lenses by gamma irradiation technology. The dose of the gamma irradiation for the polymerization of metal containing compositions was optimized. A three-dimensional structure with the desired optical properties has been obtained.

h) The suitability of metal containing nanocomposites for lenses has been established by the cast polymerization of the nanocomposites

into bubble-free, clear and transparent lenses suitable for optical applications.

i) The refractive index and Abbe number within the desired limits for optical applications have been achieved successfully.

j) The refractive index of the cast lenses were evaluated to be 1.572 in the case of dispersion of barium, 1.530 in the case of dispersion of inorganic form of titanium, 1.563 in the case of dispersion of organic form of titanium and 1.580 in the case of dispersion of lanthanum.

k) By varying the type and percentage of metal salt, the key properties can be tailor-made to the desired level, a novel feature not available with conventional optical materials such as polycarbonate, polymethyl methacrylate, etc.

l) Apart from the optical properties, the metal-containing acrylic nanocomposites exhibit high thermal stability as compared to the conventional polymers without metals. This indicates that the developed metal-containing acrylic nanocomposites will be very useful for applications where high thermal stability of polymeric components is required.

Thus, it has been successfully established that the dispersion of metal salts in polymer matrices is possible by following in-situ approach. The outcome of the study will not only create a new range of materials but will also result in developing interest all over the world for nanocomposites or nanomaterials involving metals and polymers. It is also expected to generate a lot of possibilities for the development of novel materials and unique devices useful for optical applications such as optical waveguides , solar cells, etc.

The novel research work carried out by the student in this thesis work is also expected to benefit the optical industry looking for cost-effective and alternative technologies. This work would help the researchers to resolve many of the key issues pertaining to the development of metal-containing polymeric materials for optical applications.